

108-15

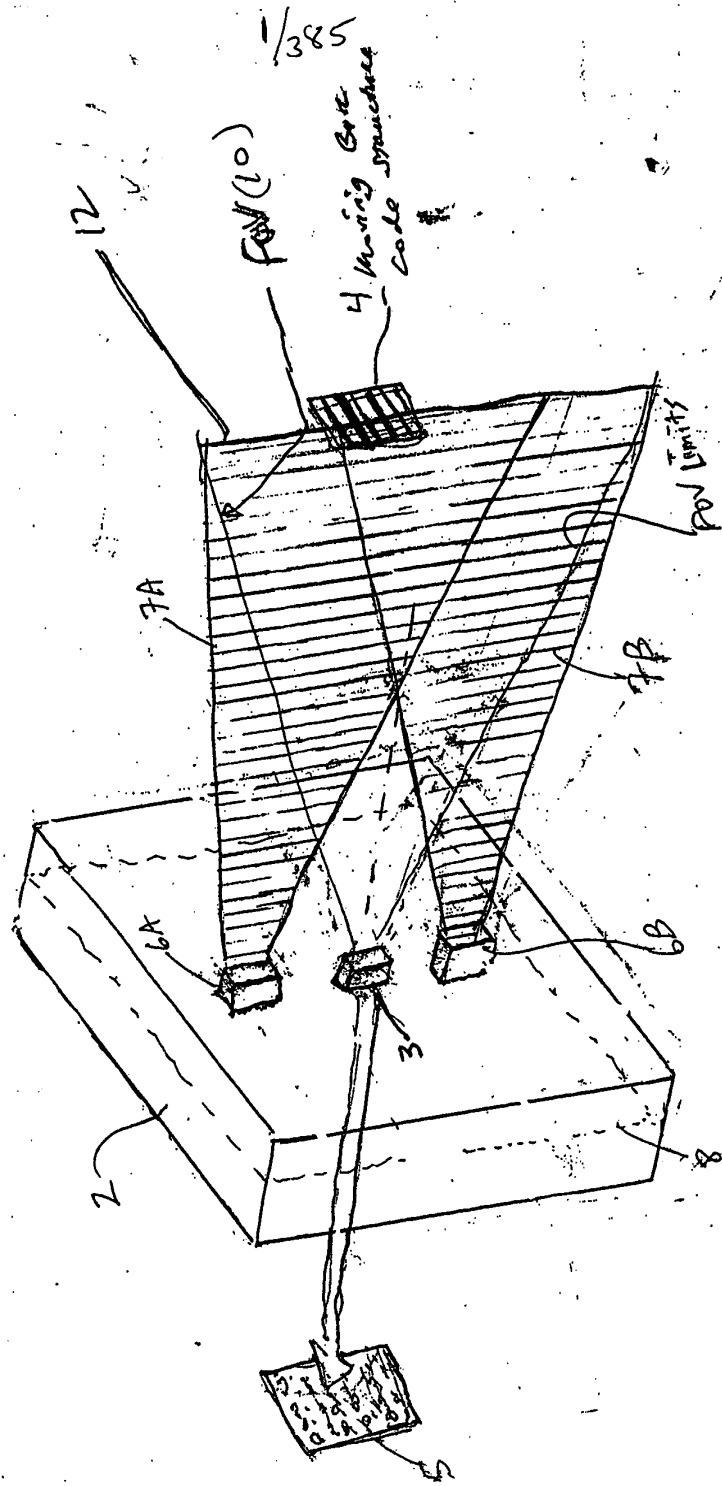
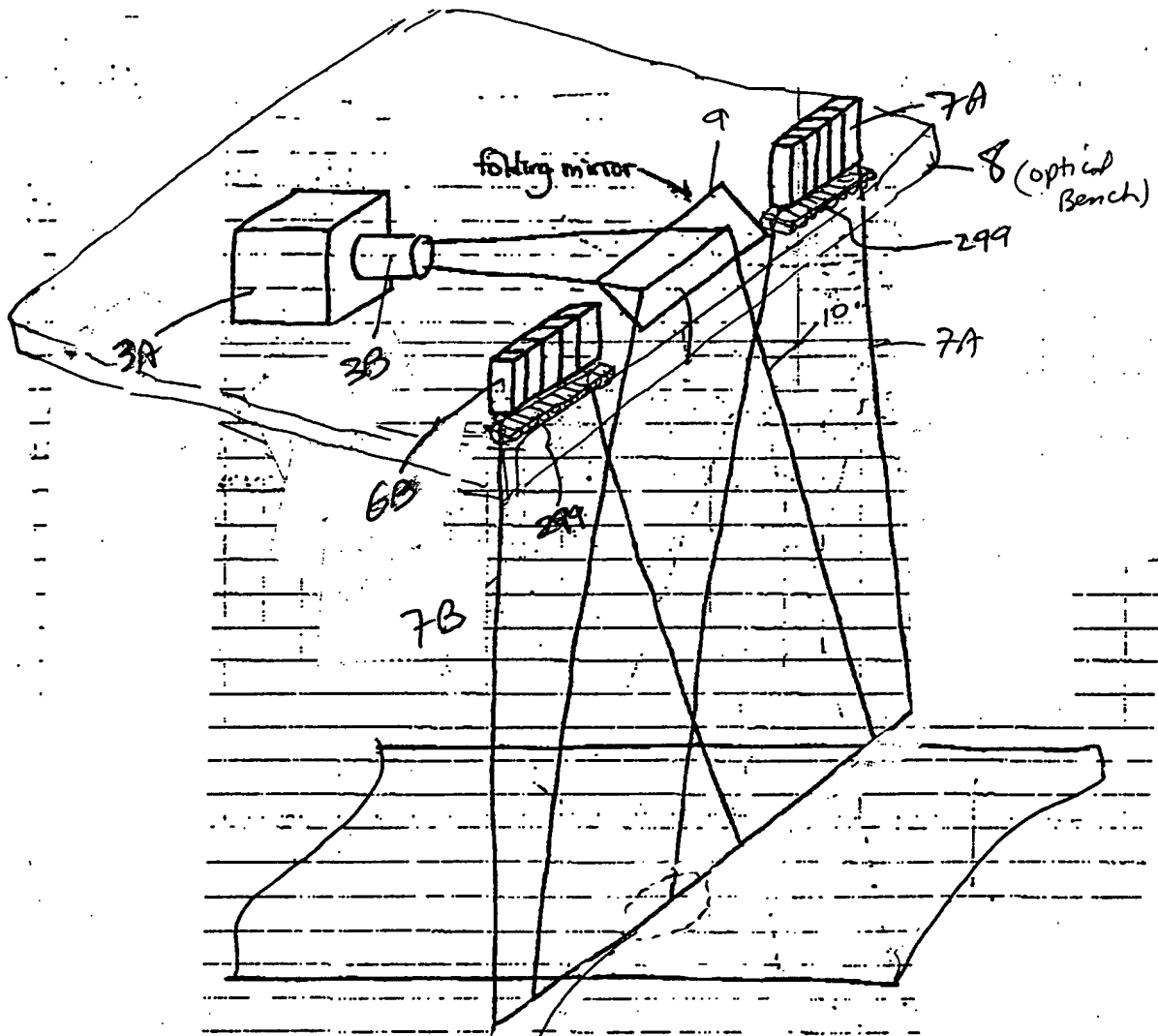


FIG 1A

2/385



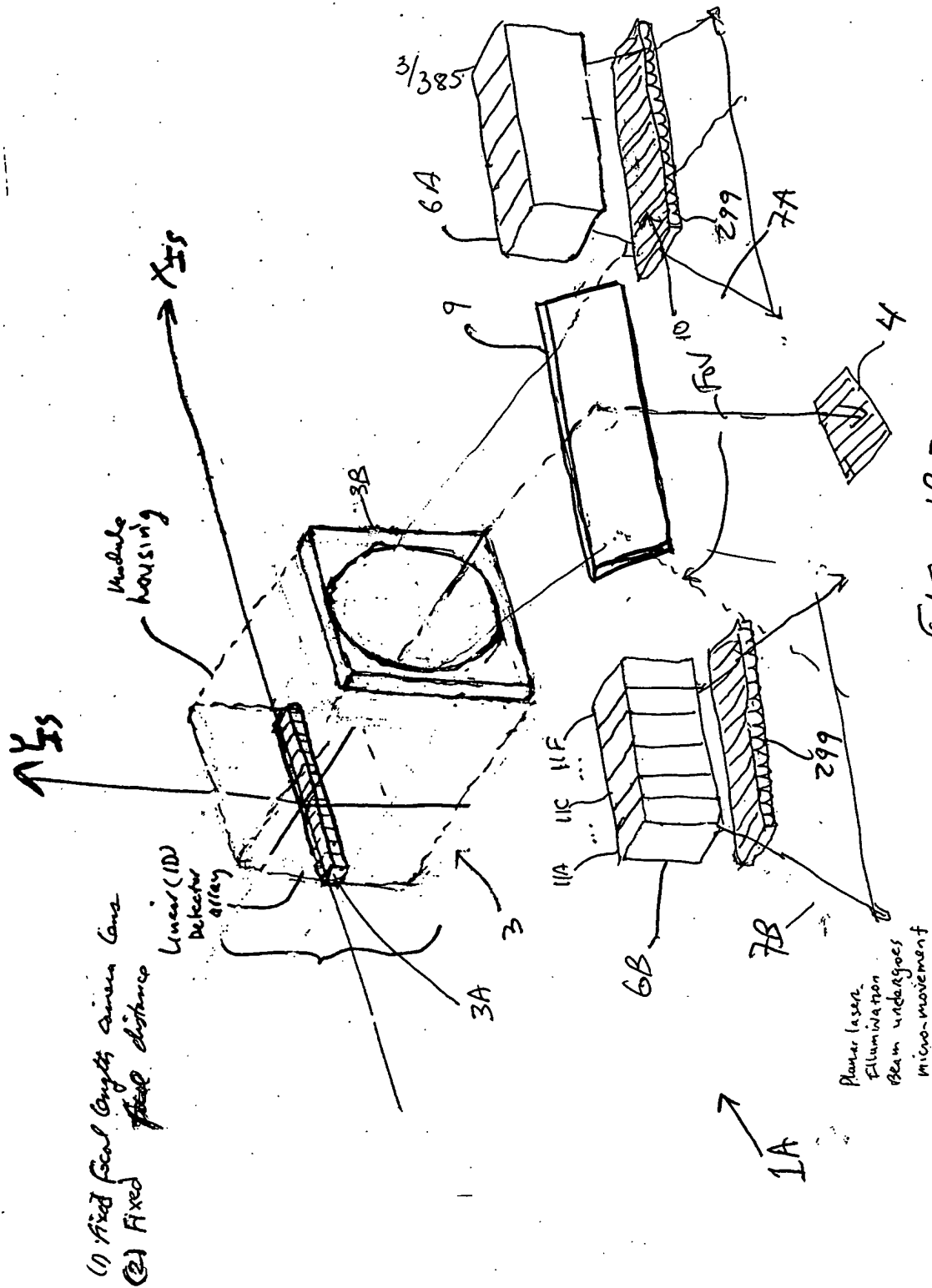
1A

FIG. 1B1

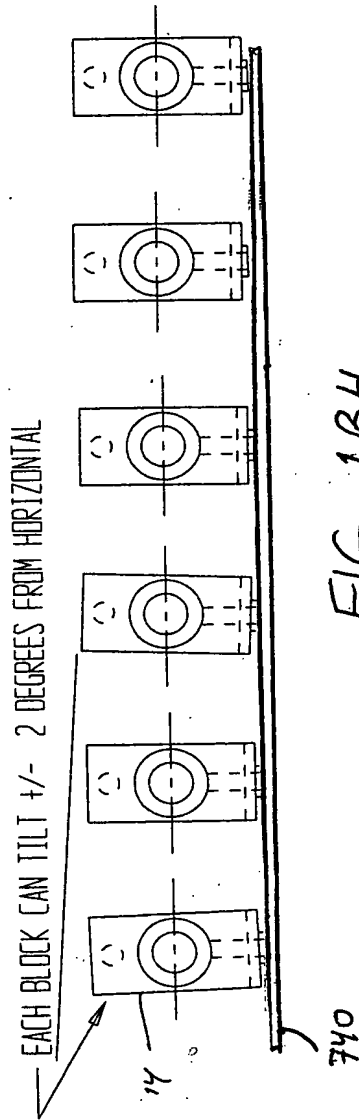
Magnified Field of View of
CCD Sensor element on
object
width of projected
Planar laser illumination
Beam on
object

FIG. 1B3

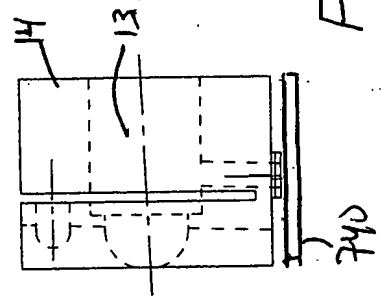
0000055-1101

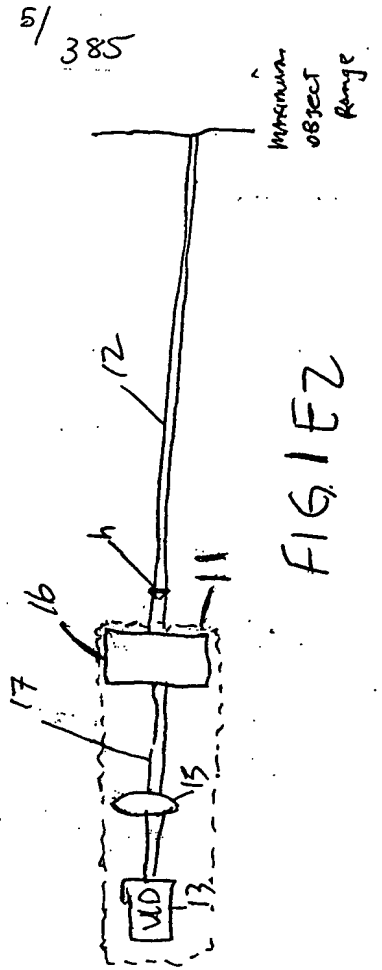
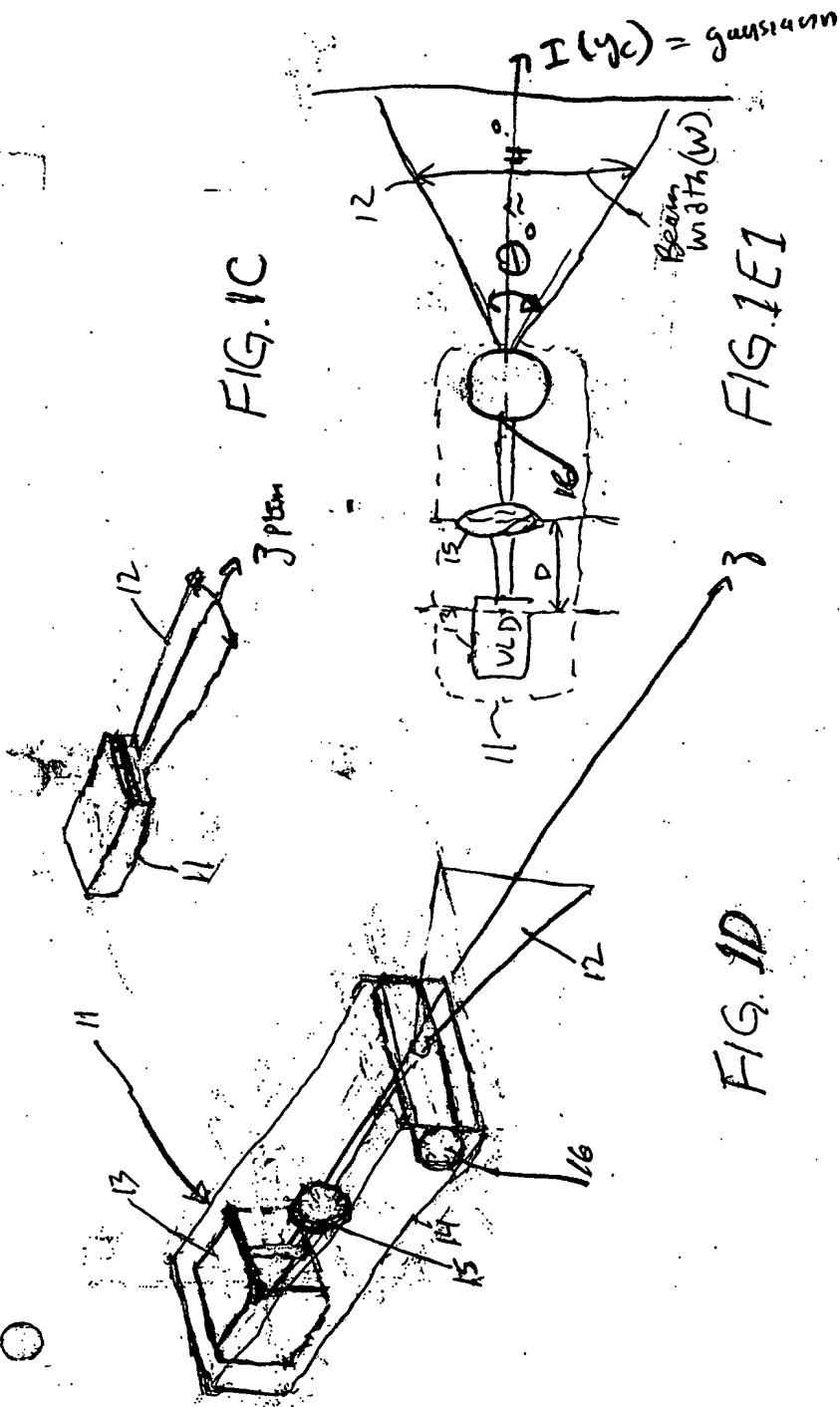


4/385



VLD BLOCK CAN PITCH FORWARD FOR ALIGNMENT WITH OTHER VLD BEAMS





| 1234567 | 89101112131415161718192021222324252627282930313233343536373839404142434445464748495051525354555657585960616263646566676869707172737475767778798081828384858687888990919293949596979899100 |
|---------|-------------------------------------------------------------------------------------------------------------------------------------------------------------------------------------------|
| 1234567 | 89101112131415161718192021222324252627282930313233343536373839404142434445464748495051525354555657585960616263646566676869707172737475767778798081828384858687888990919293949596979899100 |

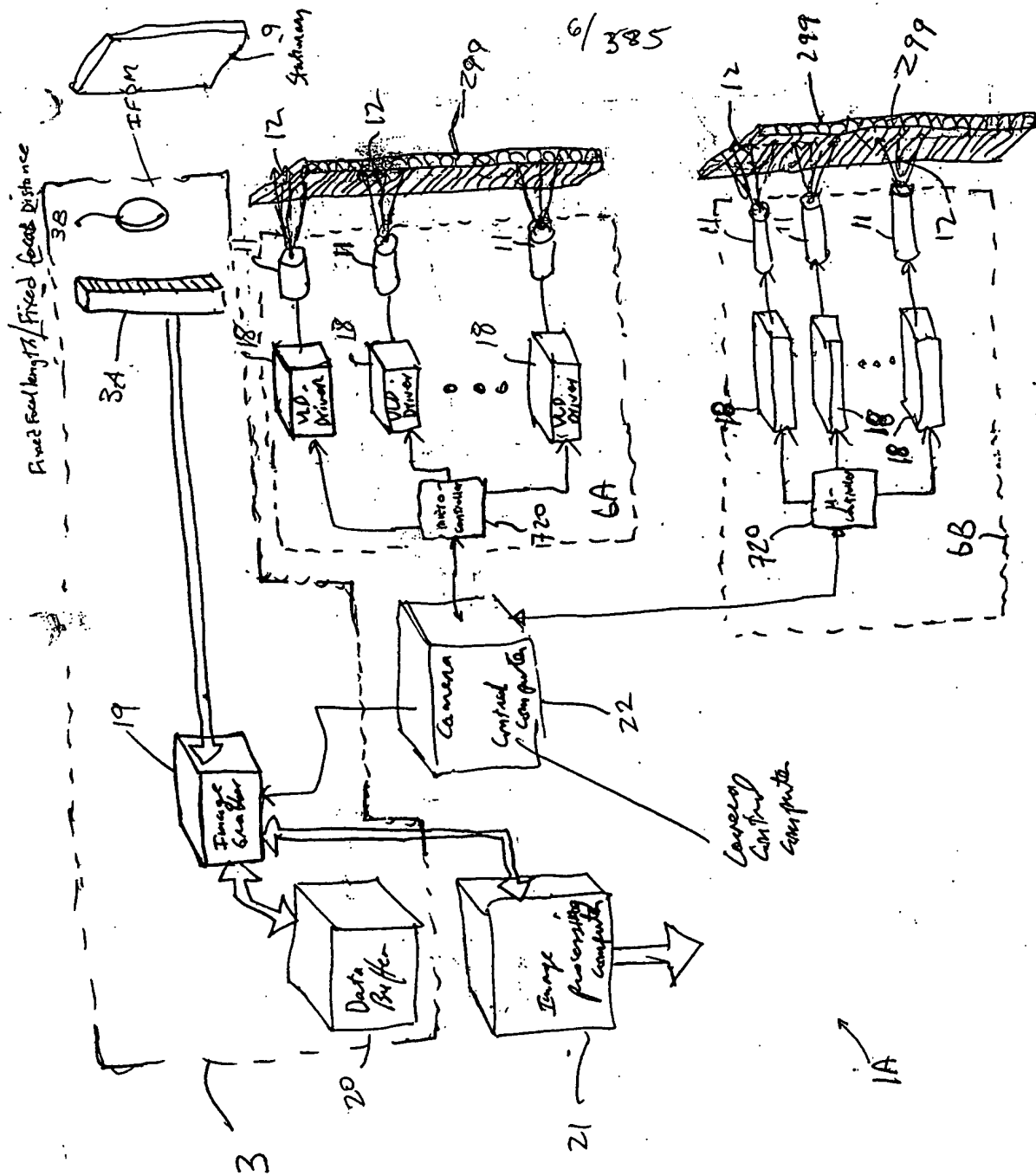
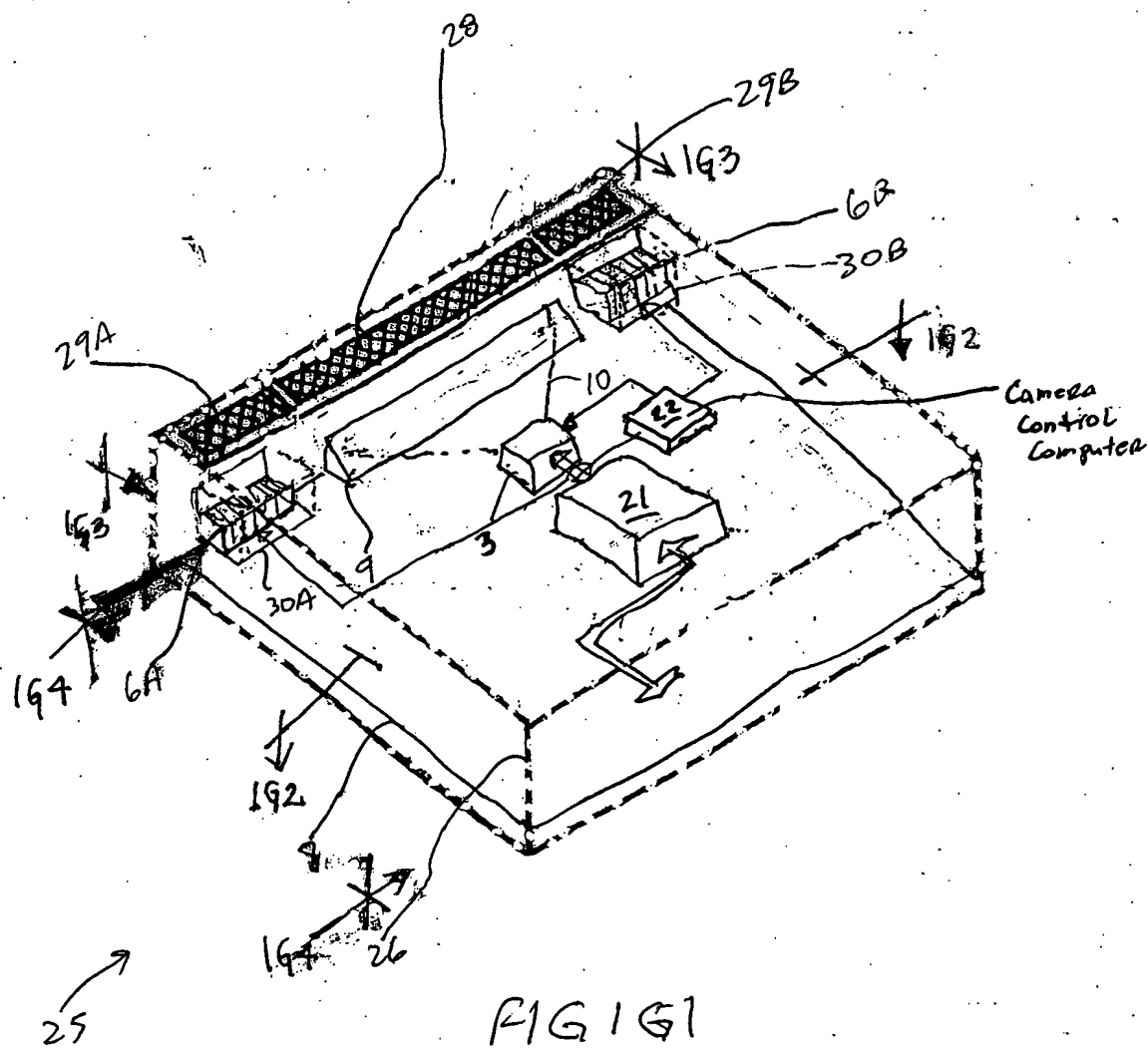


FIG. 1F

7/385



0000585 112101

8/ 385

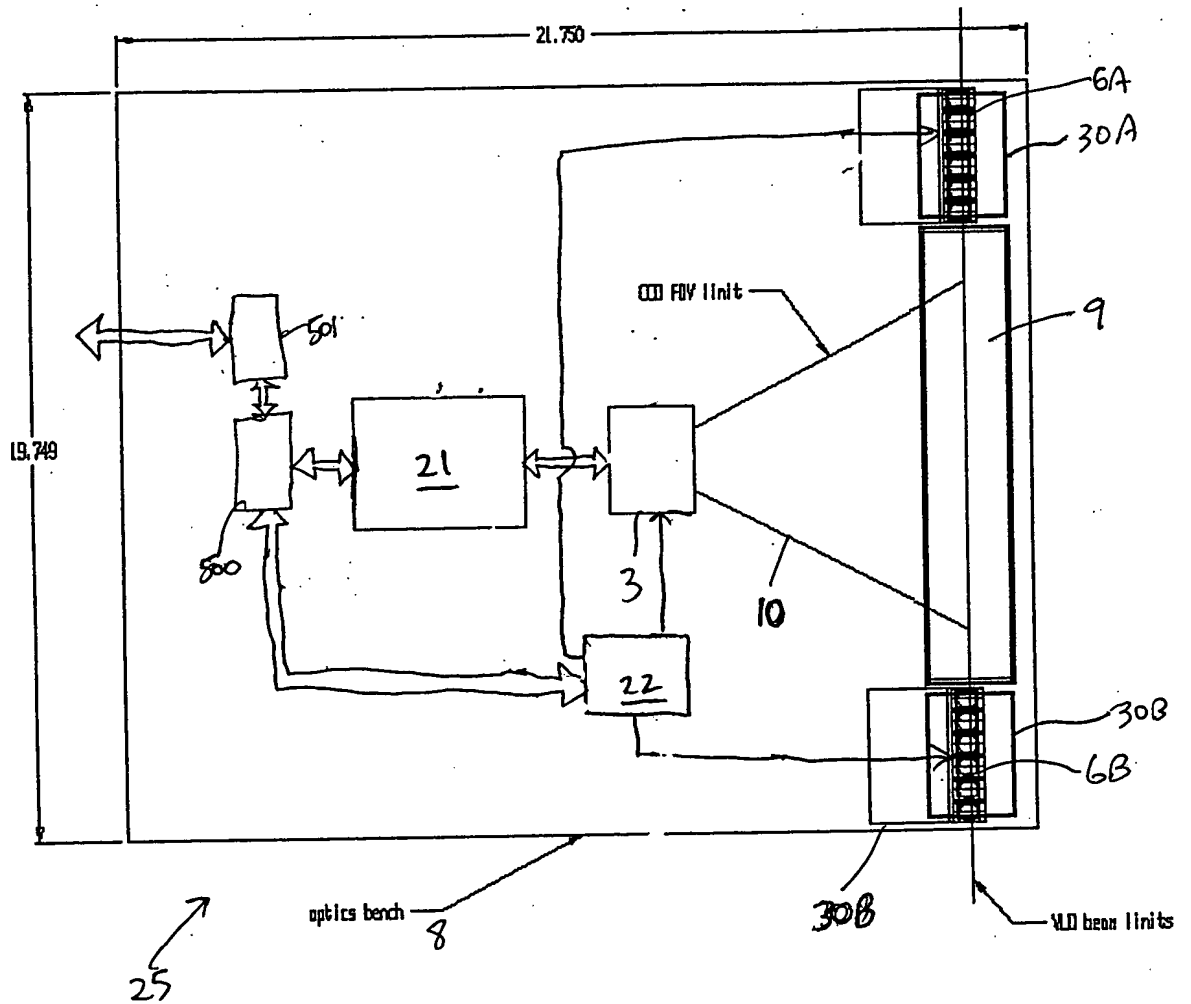
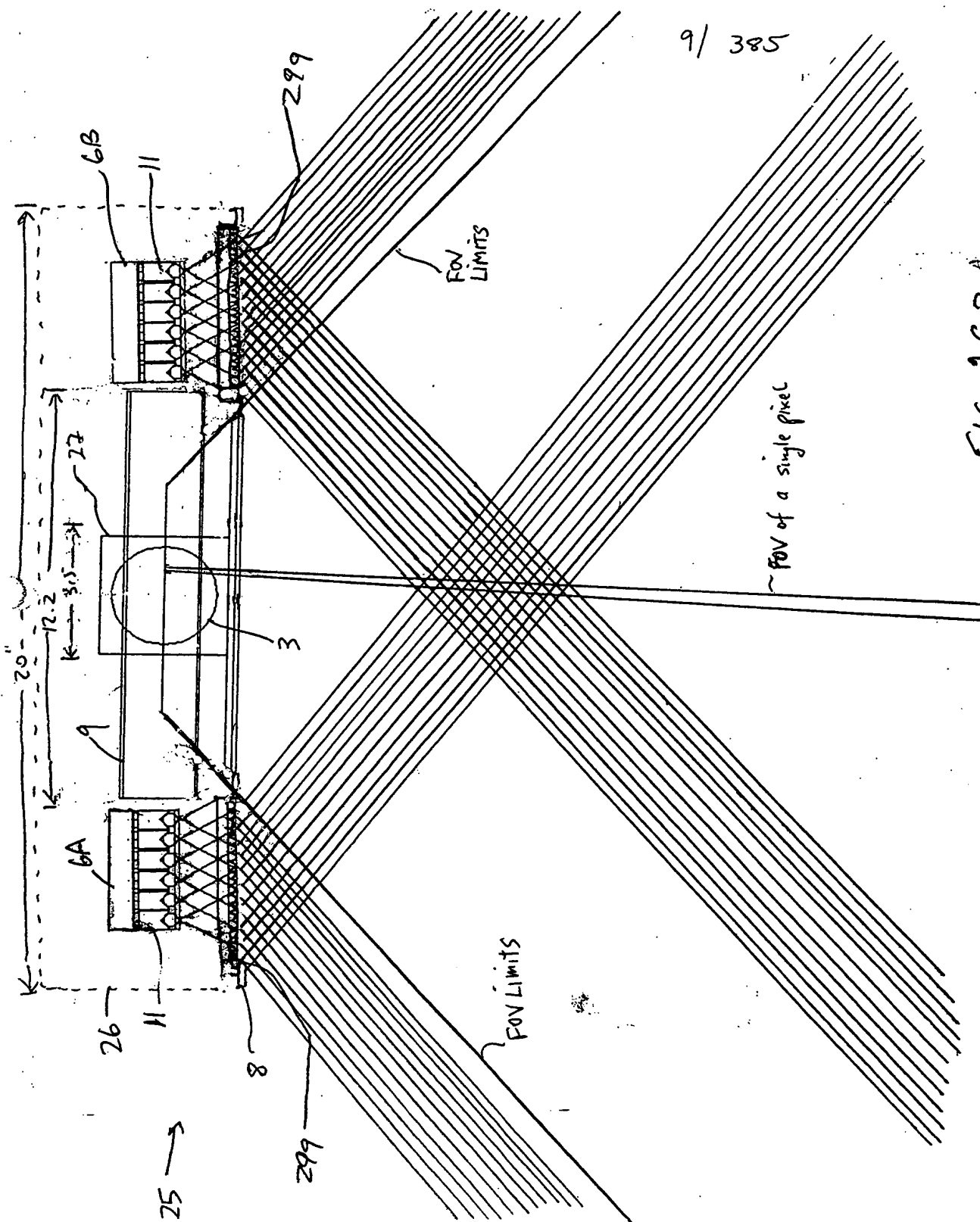


FIG. 1G2



10/385

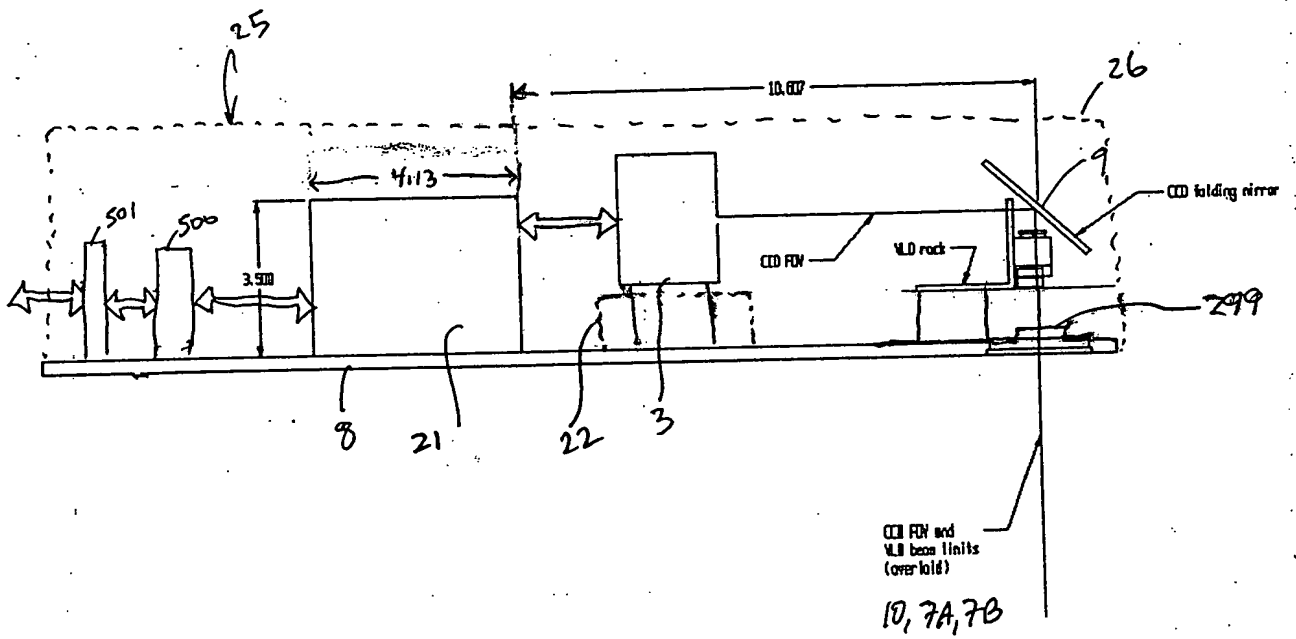
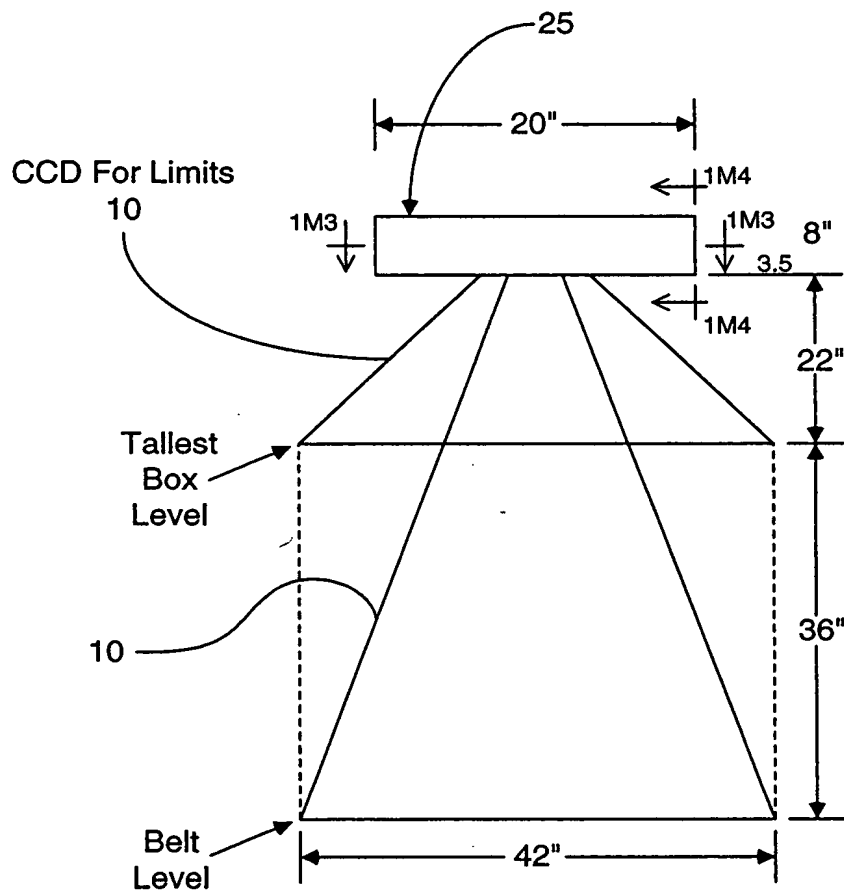


FIG. 164

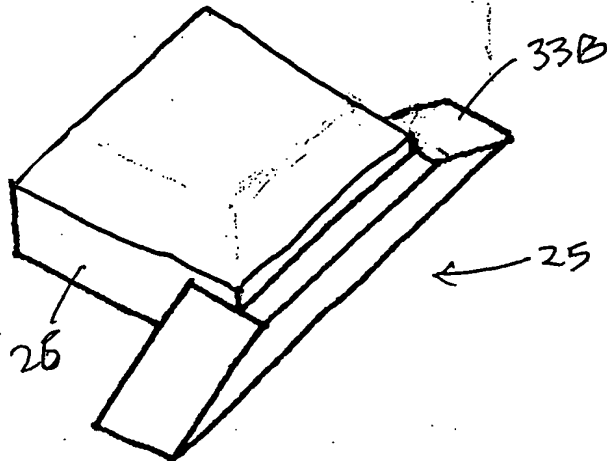
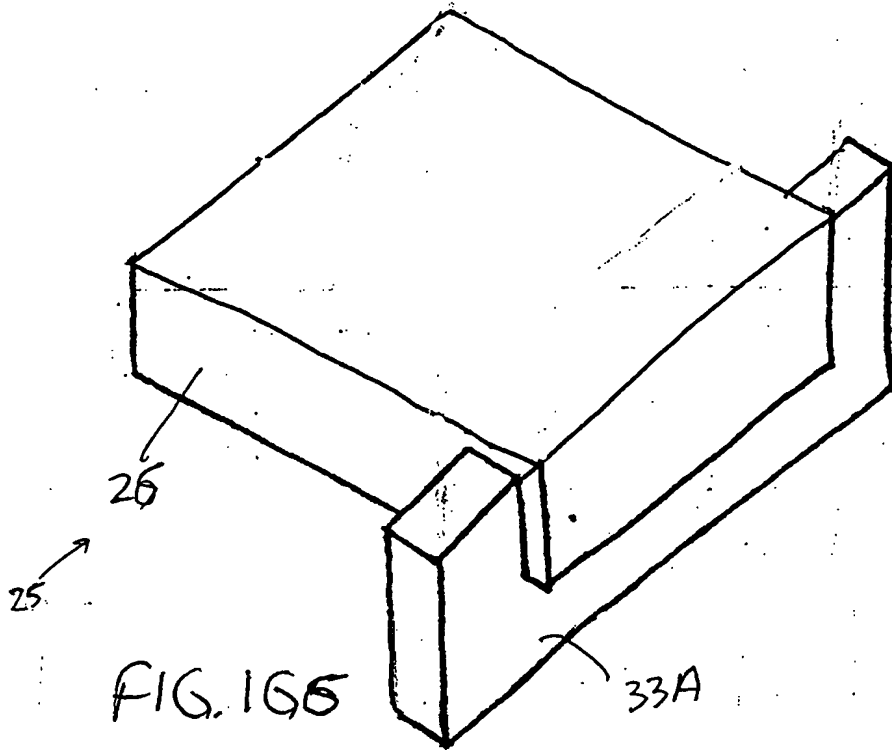
11/385

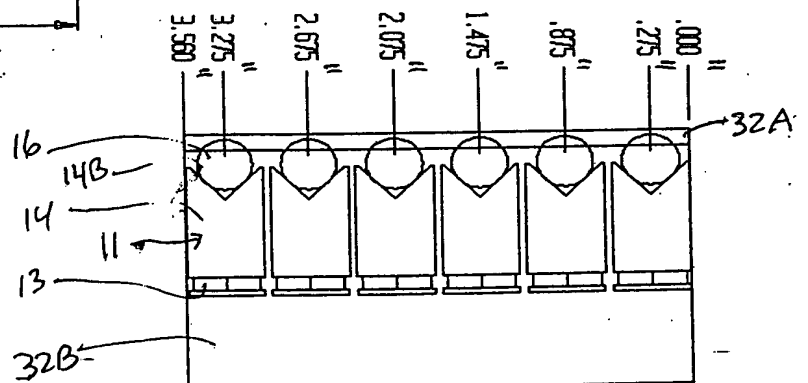
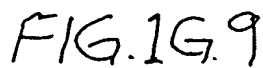
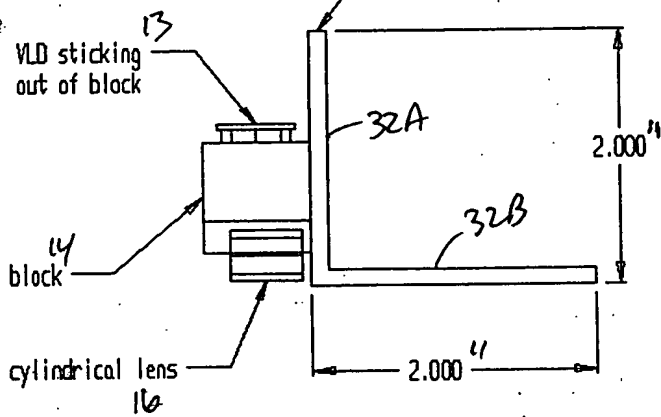


* Fixed Field Of Field

FIG. 1G5

12/385





14/ 385

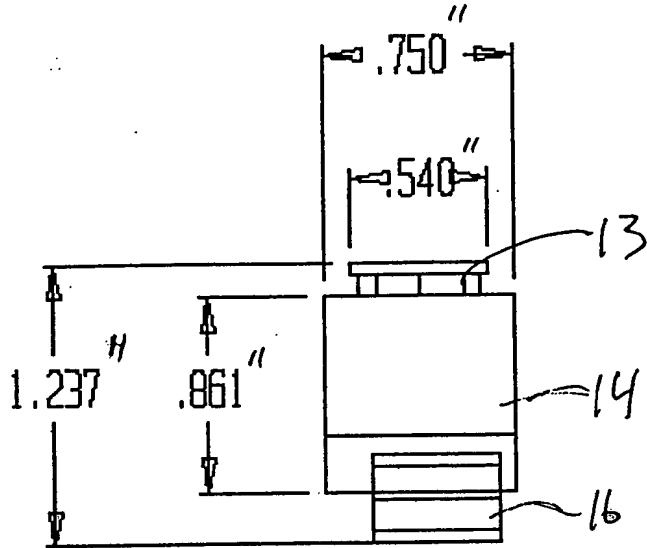


FIG. 1G11

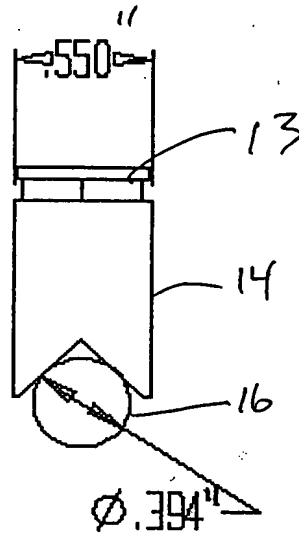
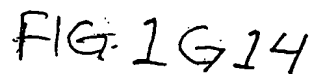
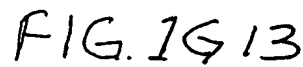


FIG. 1G12

00000000 112101



16/385

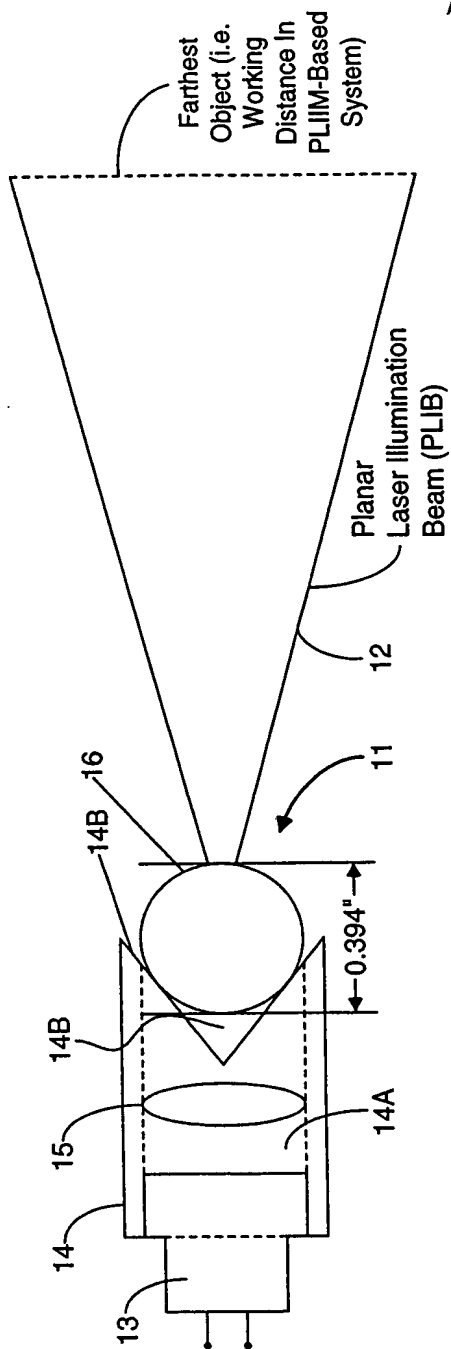


FIG. 1G15A

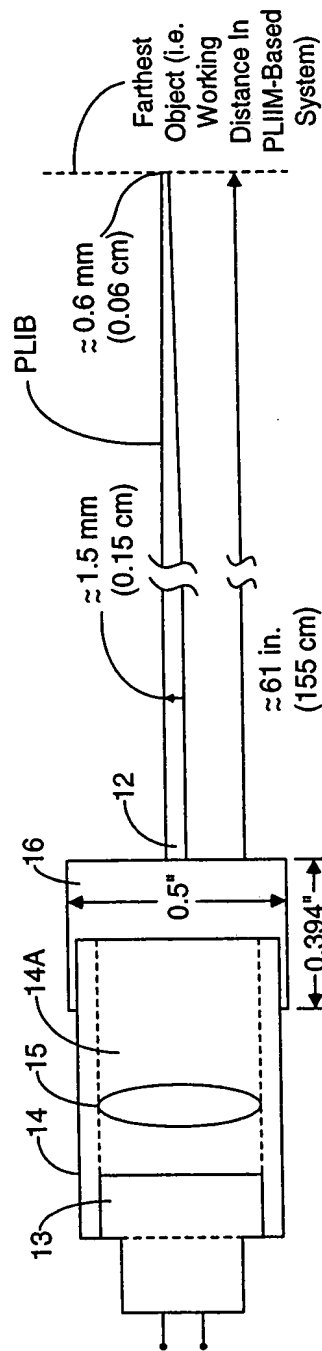


FIG. 1G15B

17/385

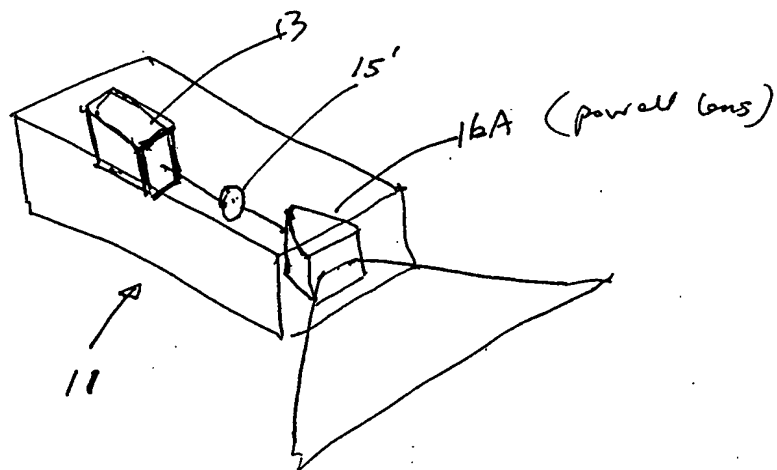


FIG. 1G.16A

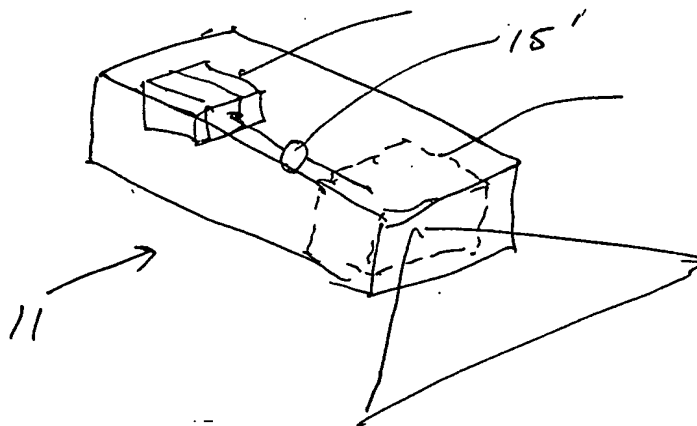
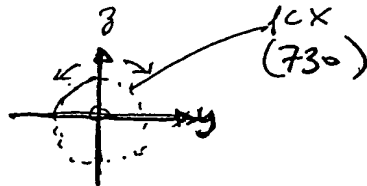


FIG. 1G.16B

• PLIM w/
powell lens

09990585-113101

[illegible]

A diagram showing a circle in the complex plane. The horizontal axis is labeled y and the vertical axis is labeled z . A circle is drawn with a dashed line, centered at the origin. A point labeled $PCV(731)$ is marked on the positive y -axis. A dashed arc indicates a radius of 3 from the origin to the circle's edge.

A diagram showing a 2D grid with a 3x3 sub-region highlighted. The sub-region is labeled $VLD(13)$. The grid is divided into four quadrants by a horizontal and vertical axis. The sub-region is centered in the top-left quadrant. The label $VLD(13)$ is written to the right of the sub-region, with a line pointing to it.

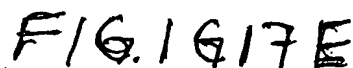


FIG. 16, 17F

19/385

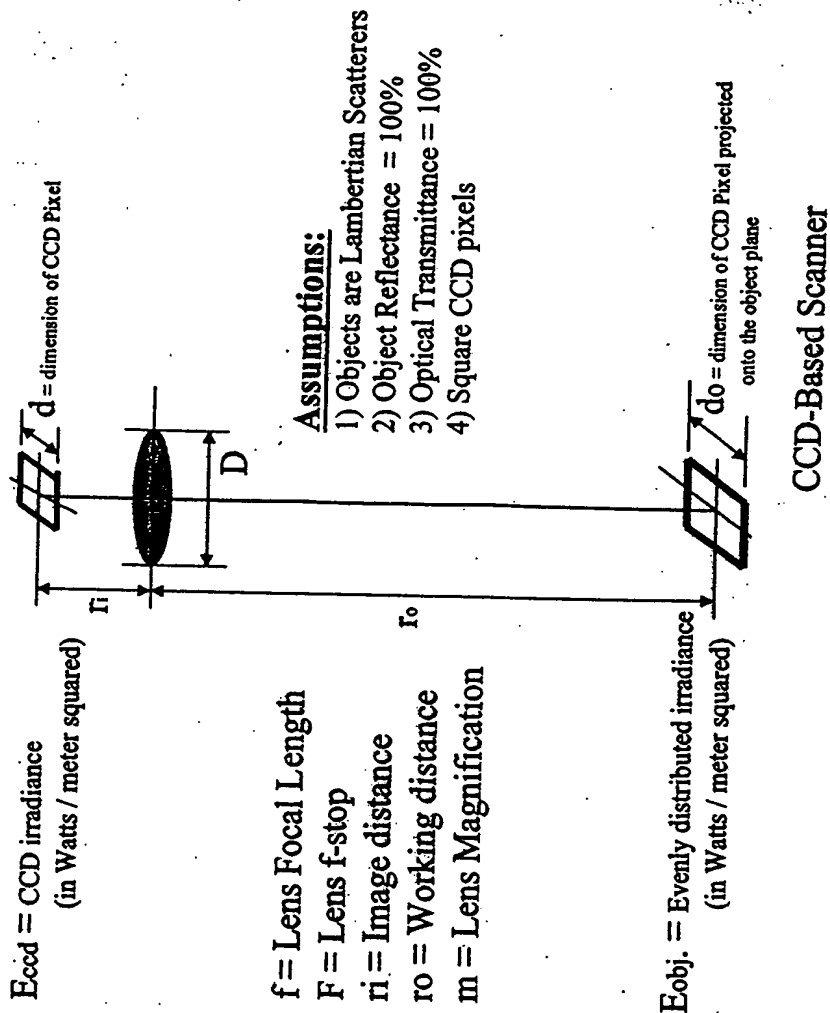


FIG. 1H6

FIRST GENERALIZED METHOD
OF REDUCING SPECKLE-NOISE
PATTERNS AT IMAGE
DETECTION array OF THE
FPD subsystem (3)

20/ 385

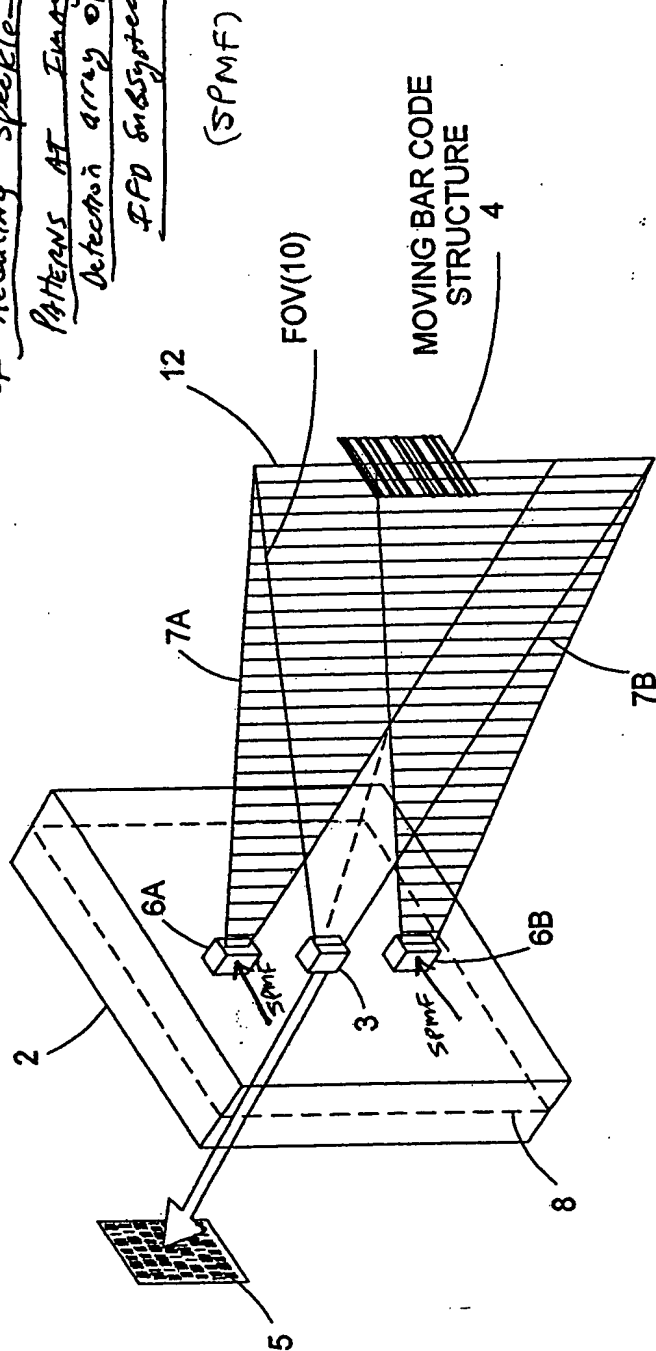


FIG. 1I1

22/ 385

The First Generalized Speckle-Noise Pattern Reduction Method
Of The Present Invention

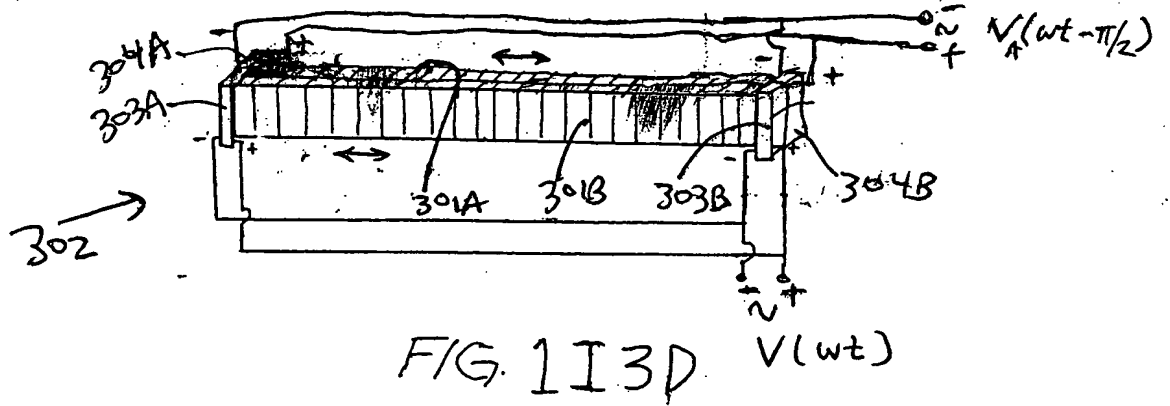
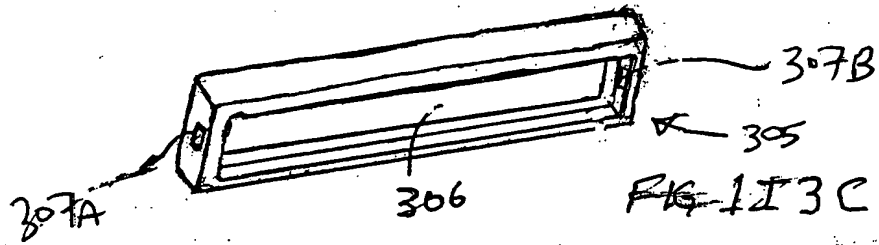
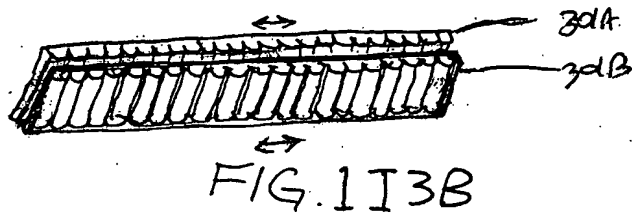
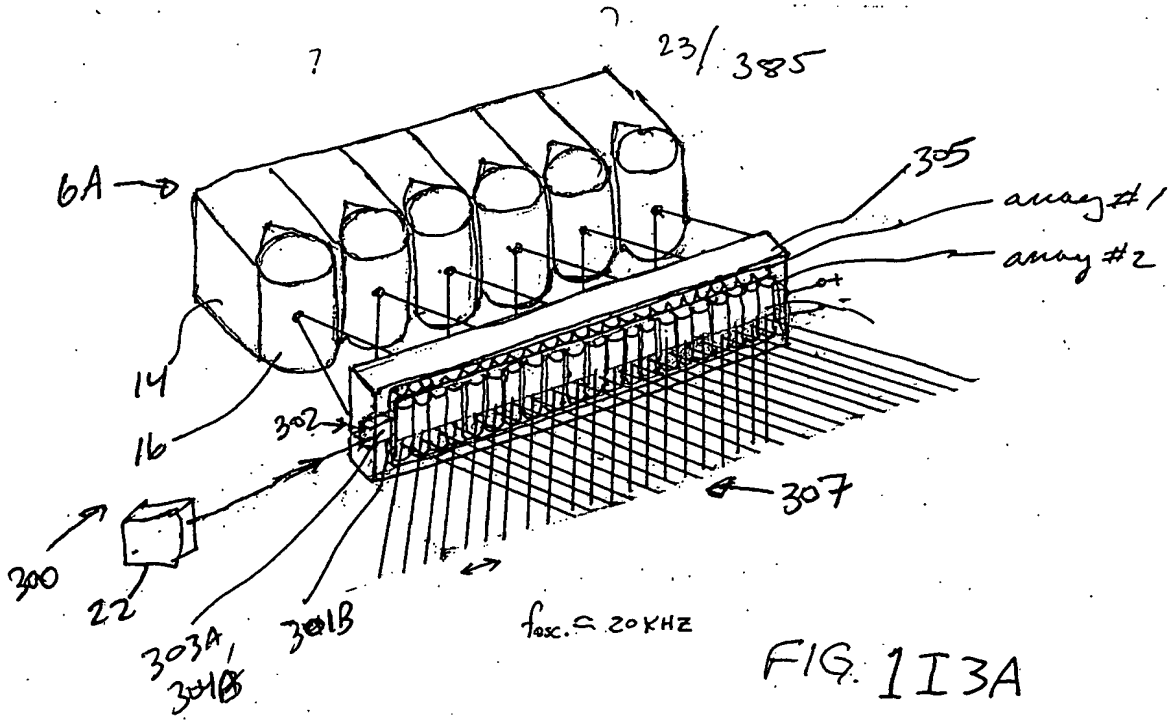
Prior to illumination of the target with the planar laser illumination beam (PLIB), modulate the spatial phase of the transmitted PLIB along the planar extent thereof according to a spatial phase modulation function (SPMF) so as to

produce numerous substantially different time-varying speckle-noise patterns at the image detection array of the IFD Subsystem during the photo-integration time period thereof.



Temporally average the numerous substantially different time-varying speckle-noise patterns produced at the image detection array in the IFD Subsystem during the photo-integration time period thereof, so as to thereby reduce the power of the speckle-noise pattern observed at the image detection array.

FIG. 1I2B



24/ 385

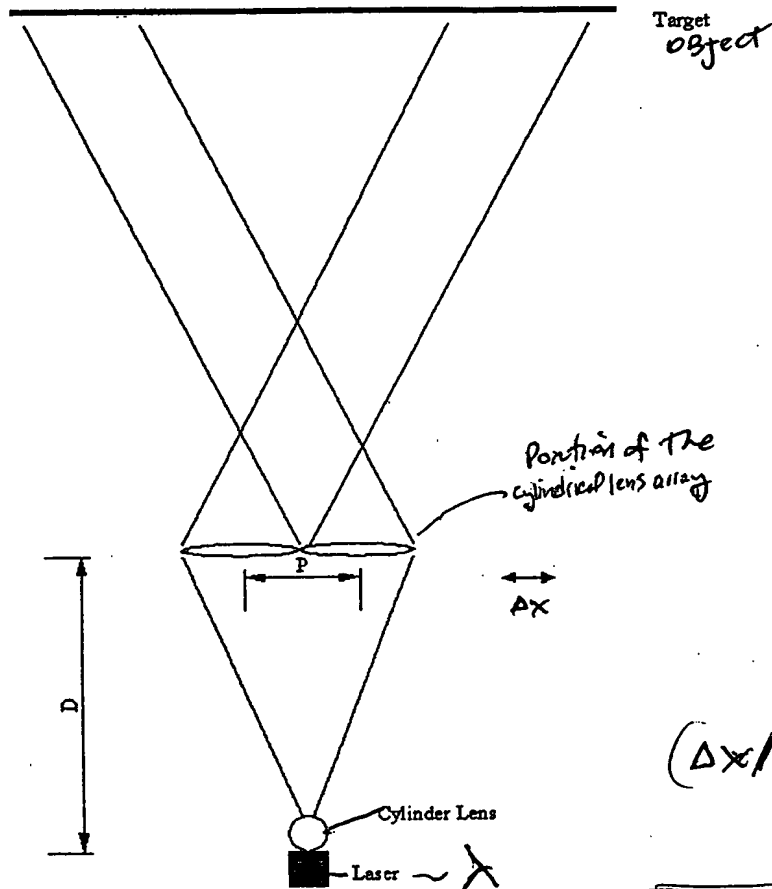


Figure 1

$$(\Delta x / D) P = \lambda$$

$$\Delta x \geq \frac{\lambda \cdot D}{P}$$

FIG. 1I3E

0000585 112101

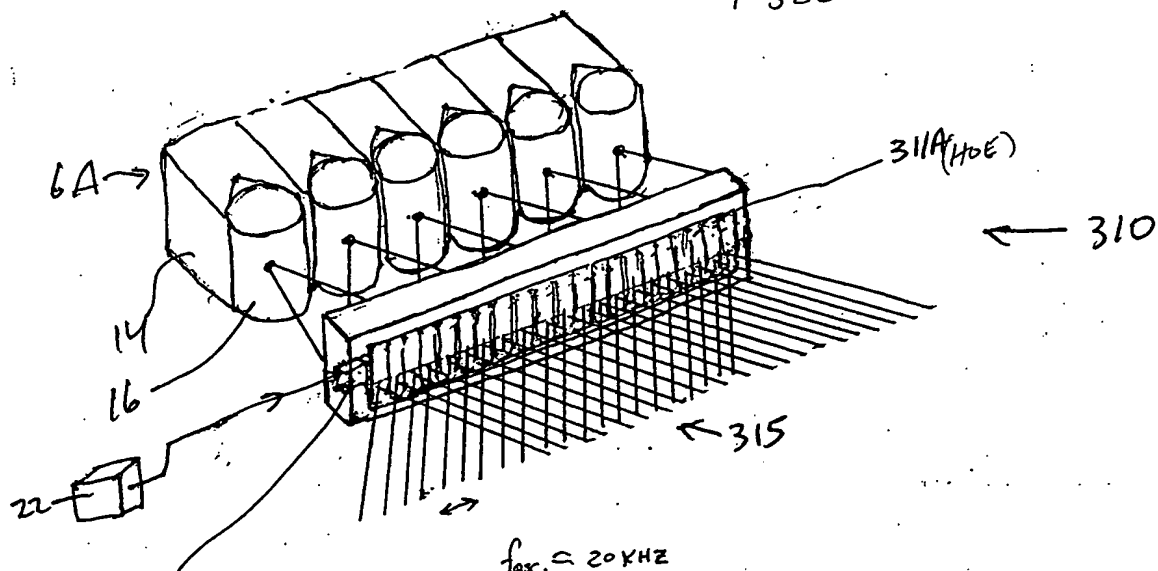

$$f_{osc.} = 20 \text{ KHz}$$

FIG 1I4A

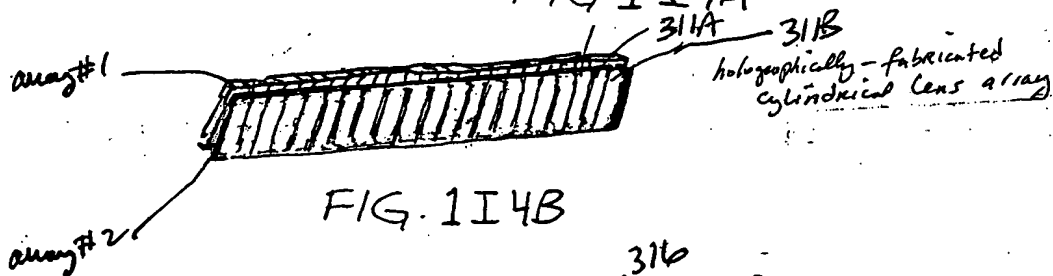


FIG. 1I4B

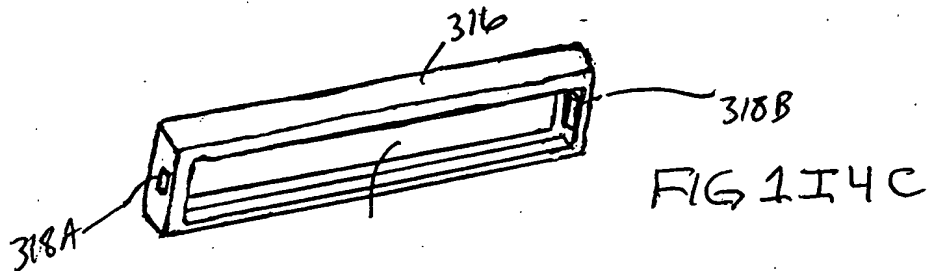
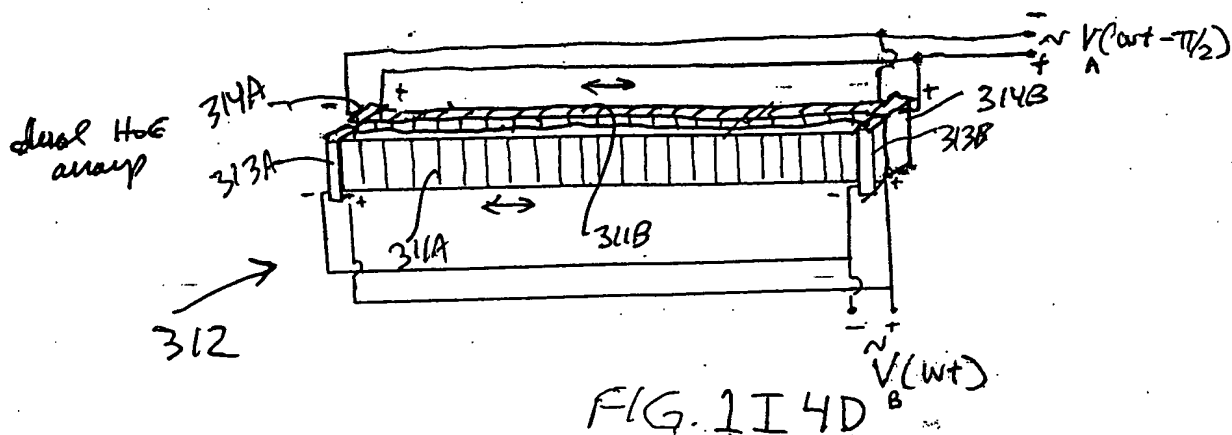
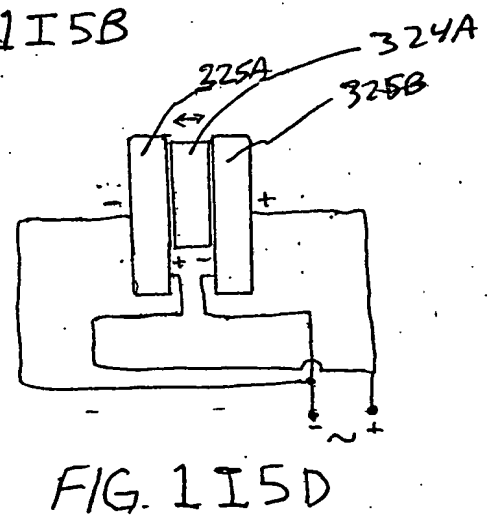
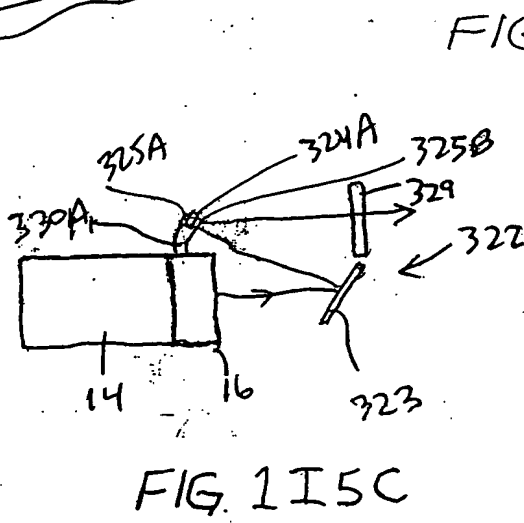
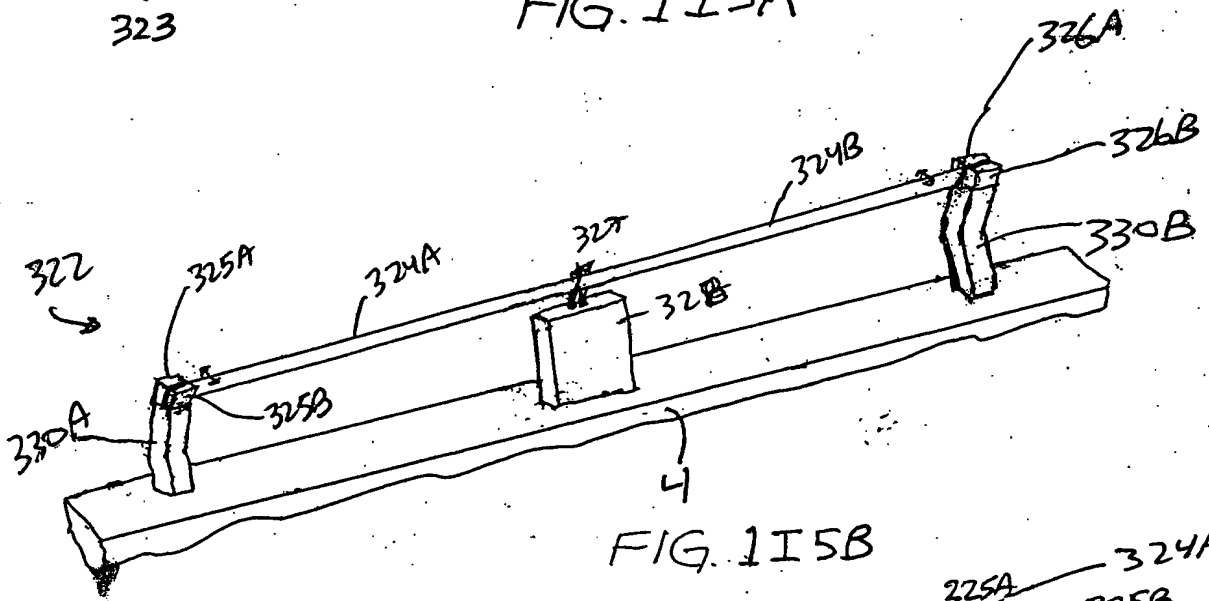
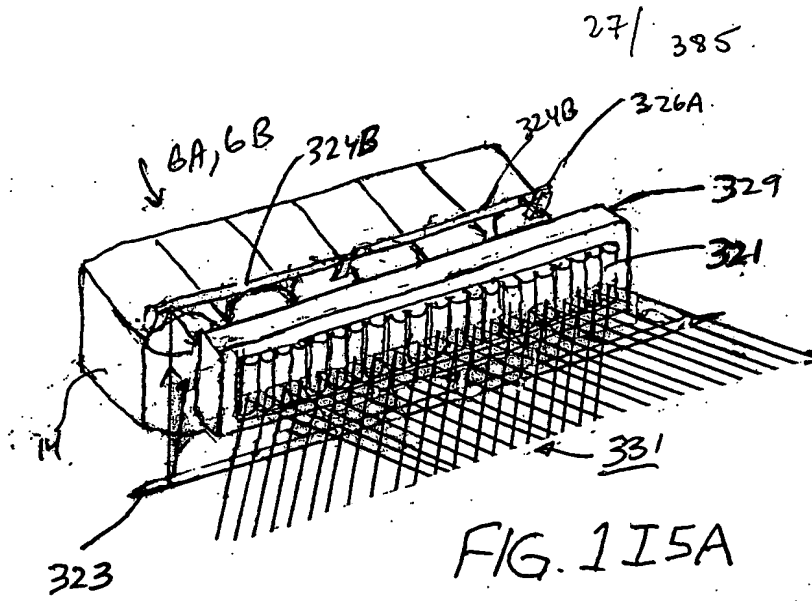


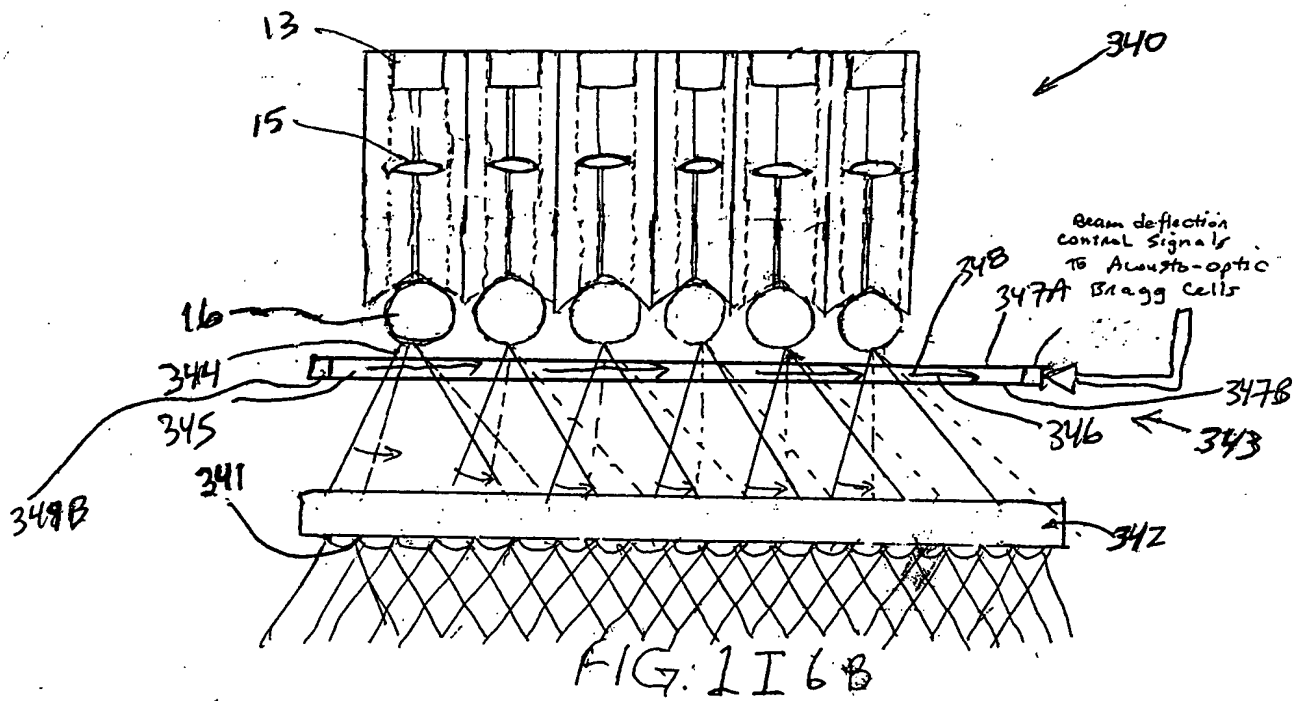
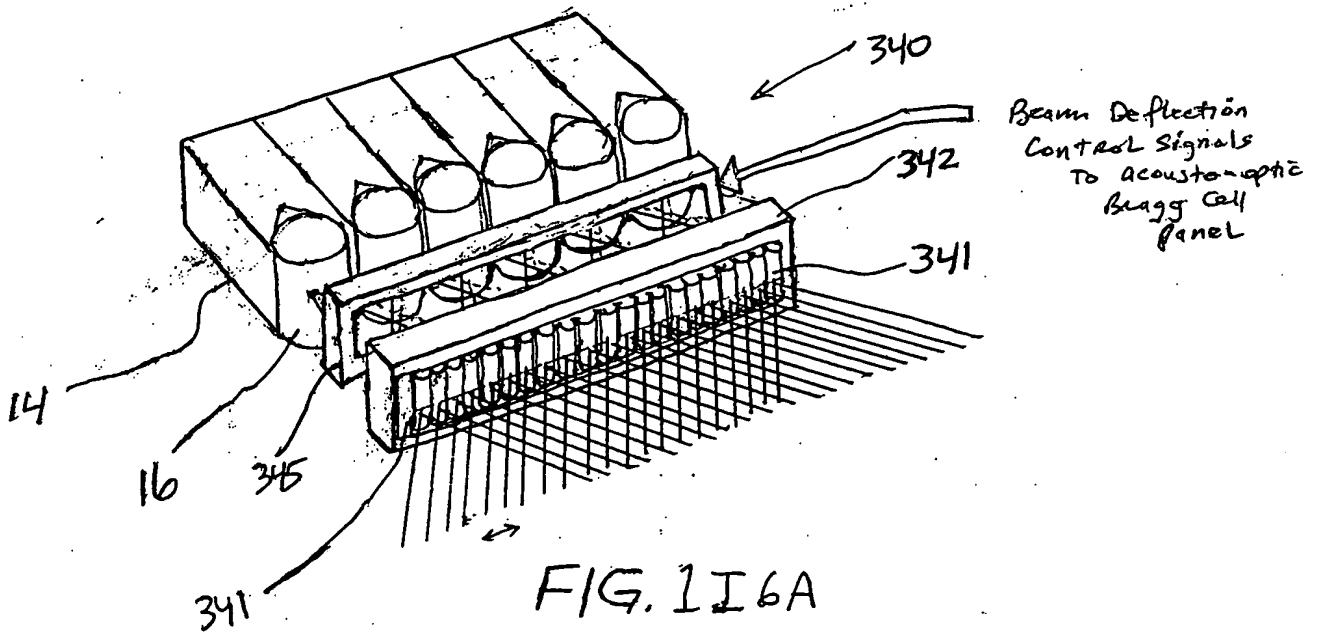
FIG 1I4C

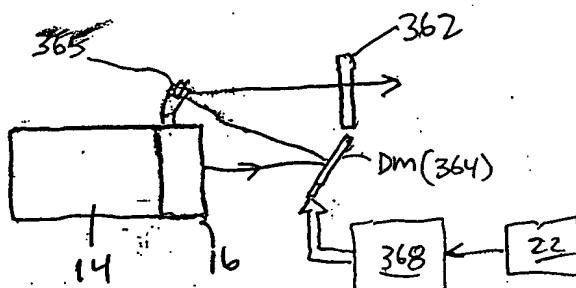
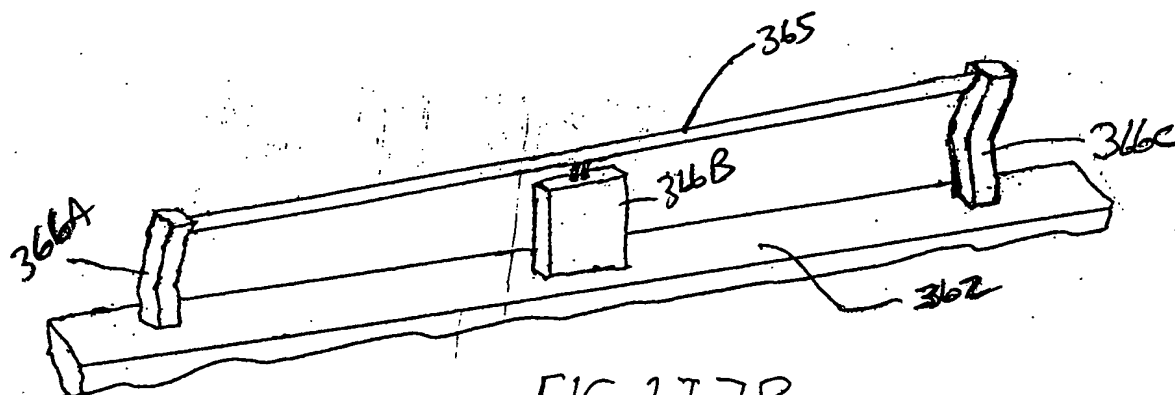
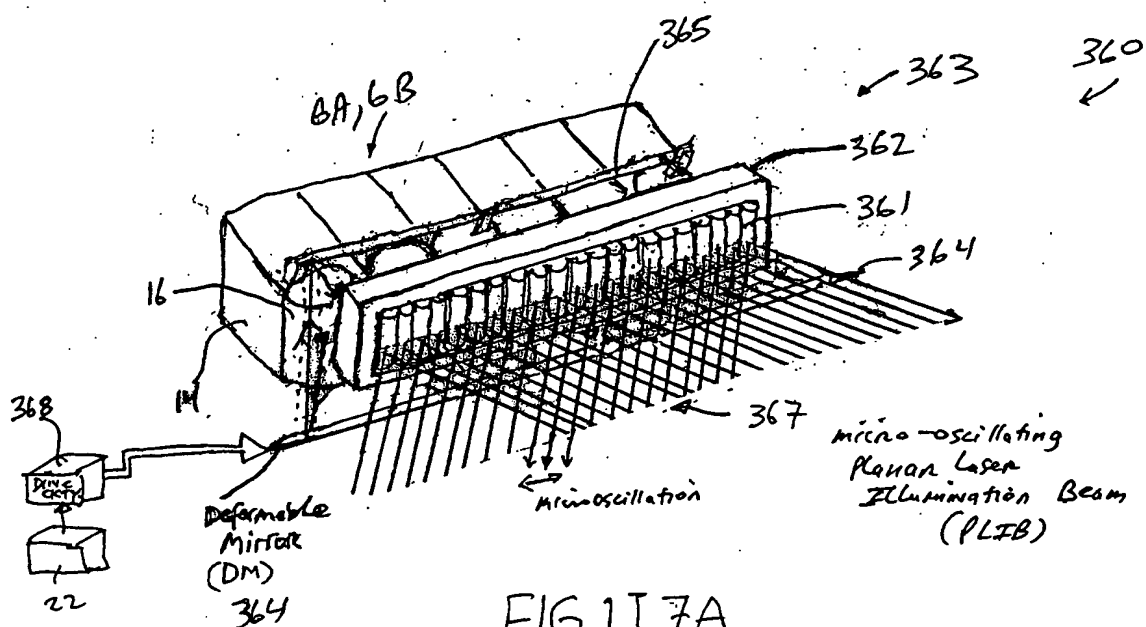


00990585 442404
TOTAL 58506660



28/ 385





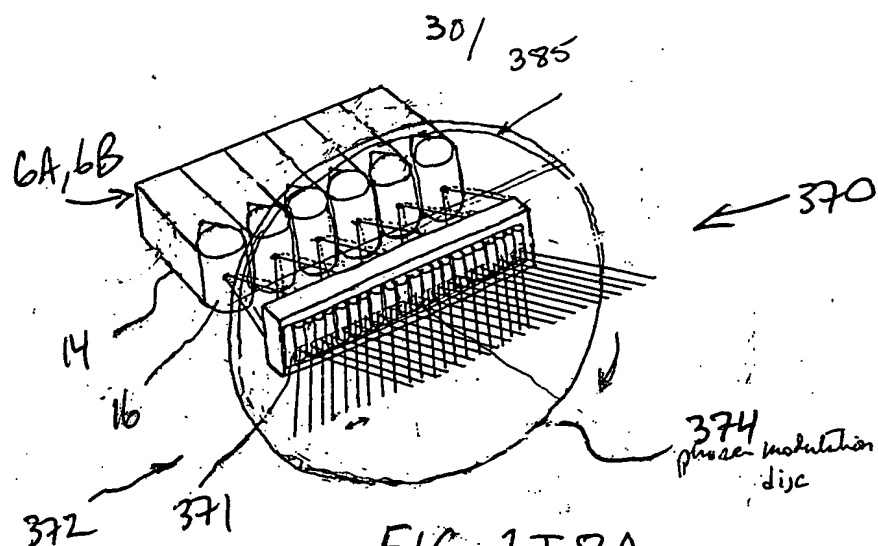
[illegible]

FIG. 1I8A

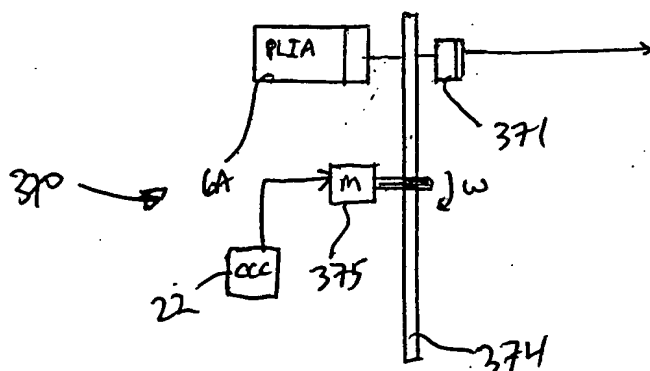


FIG. 118B

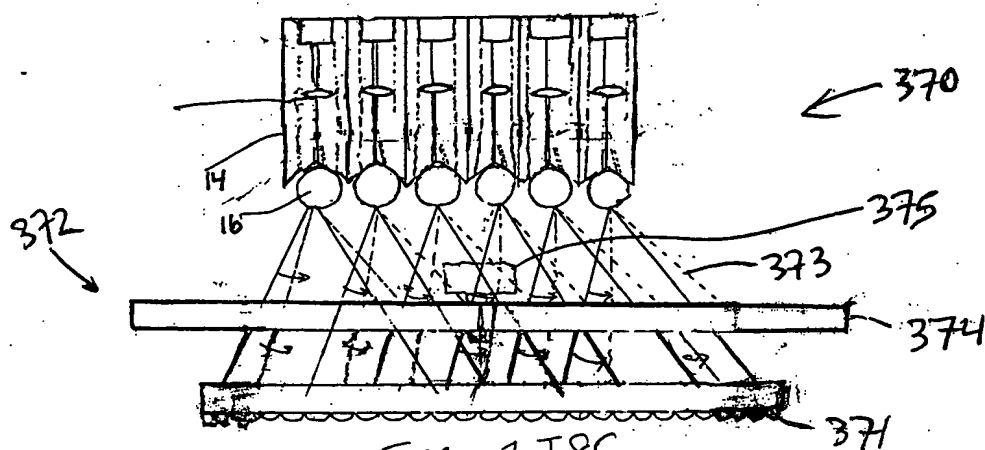
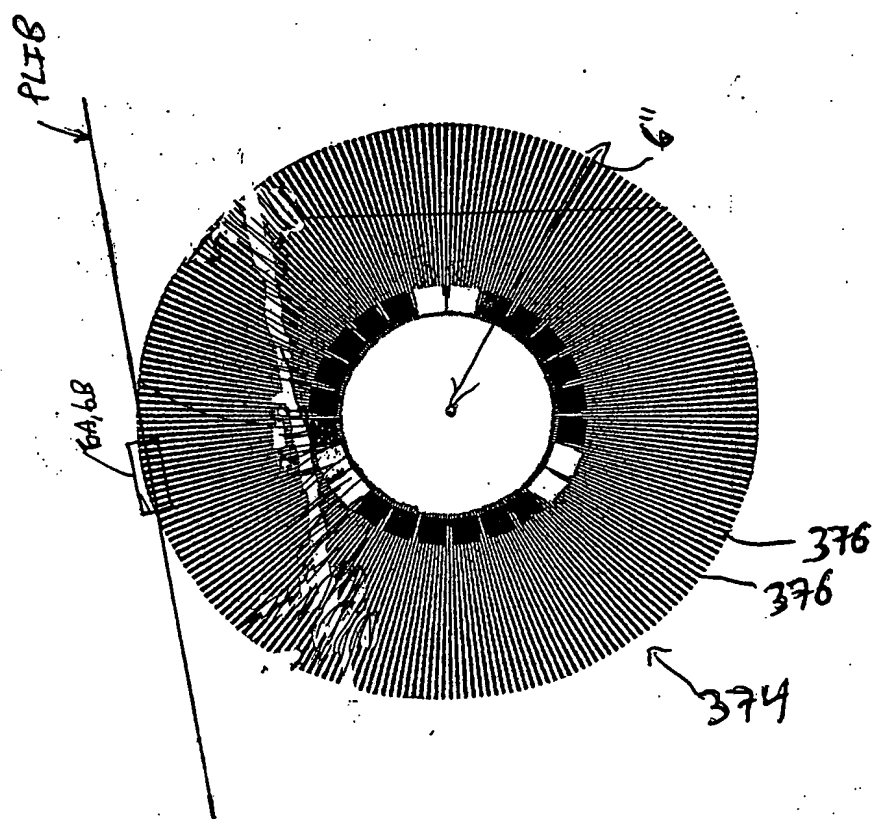
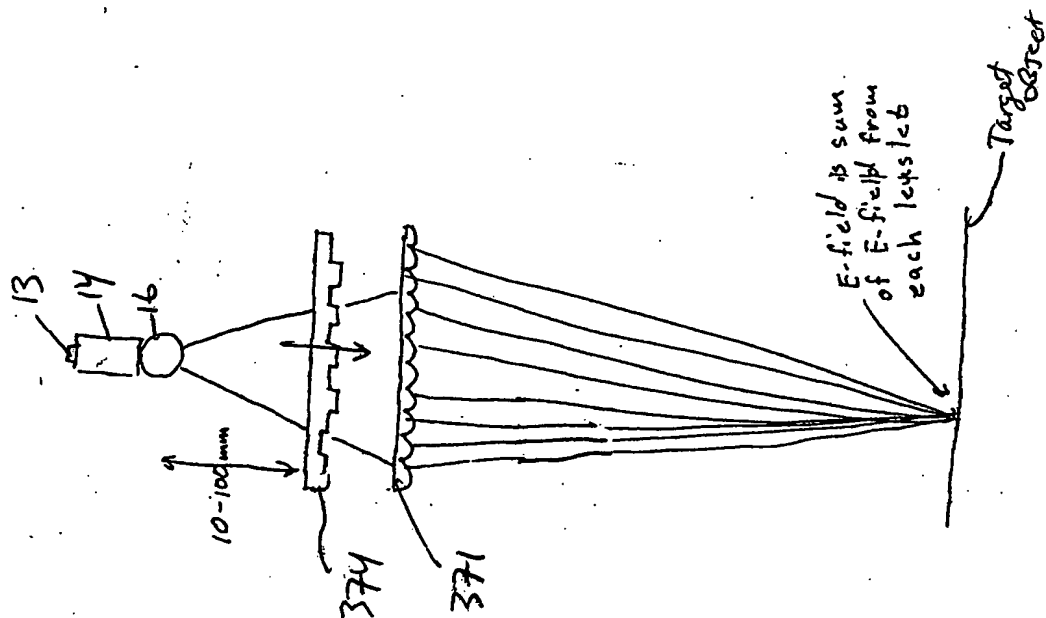
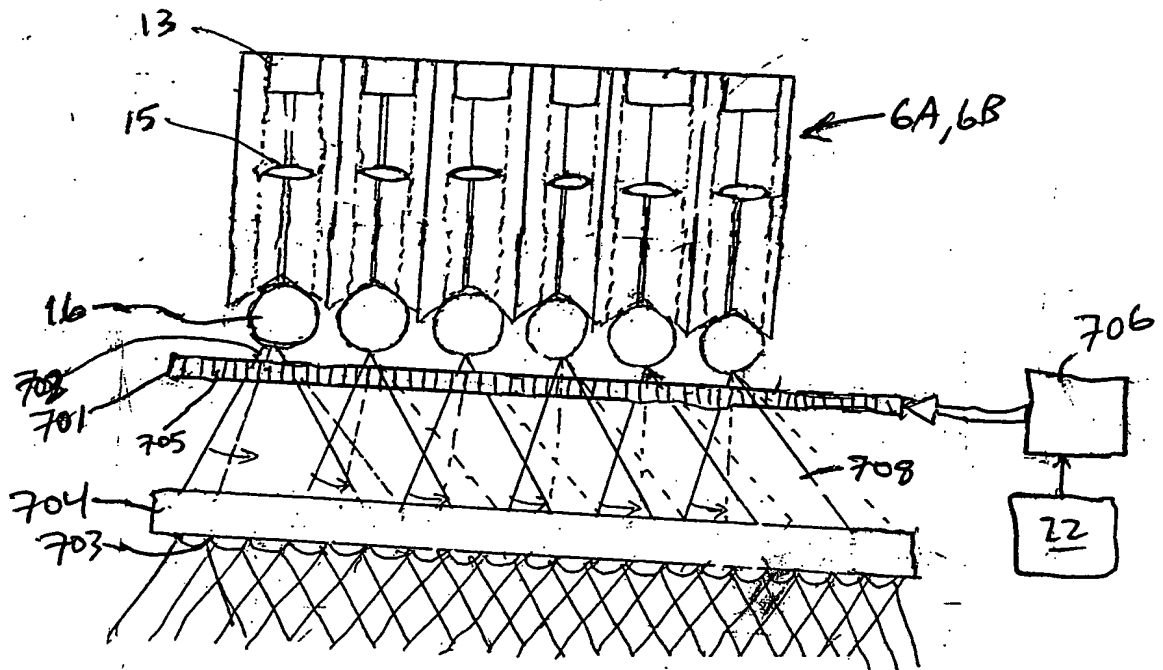
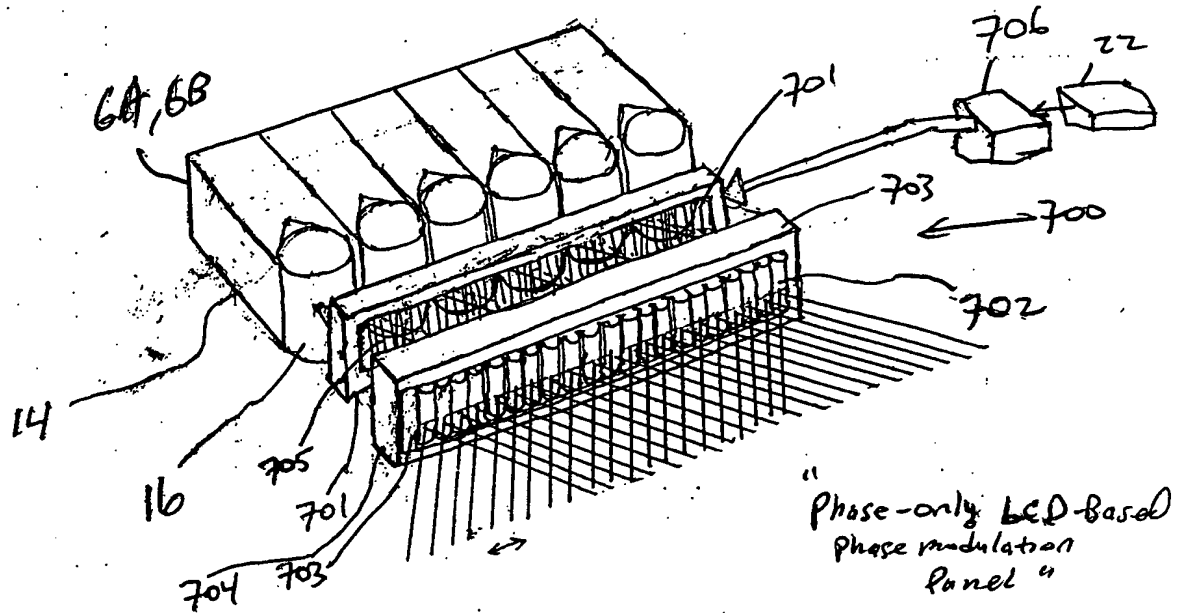


FIG. 1I8C

31 / 385





33/ 385

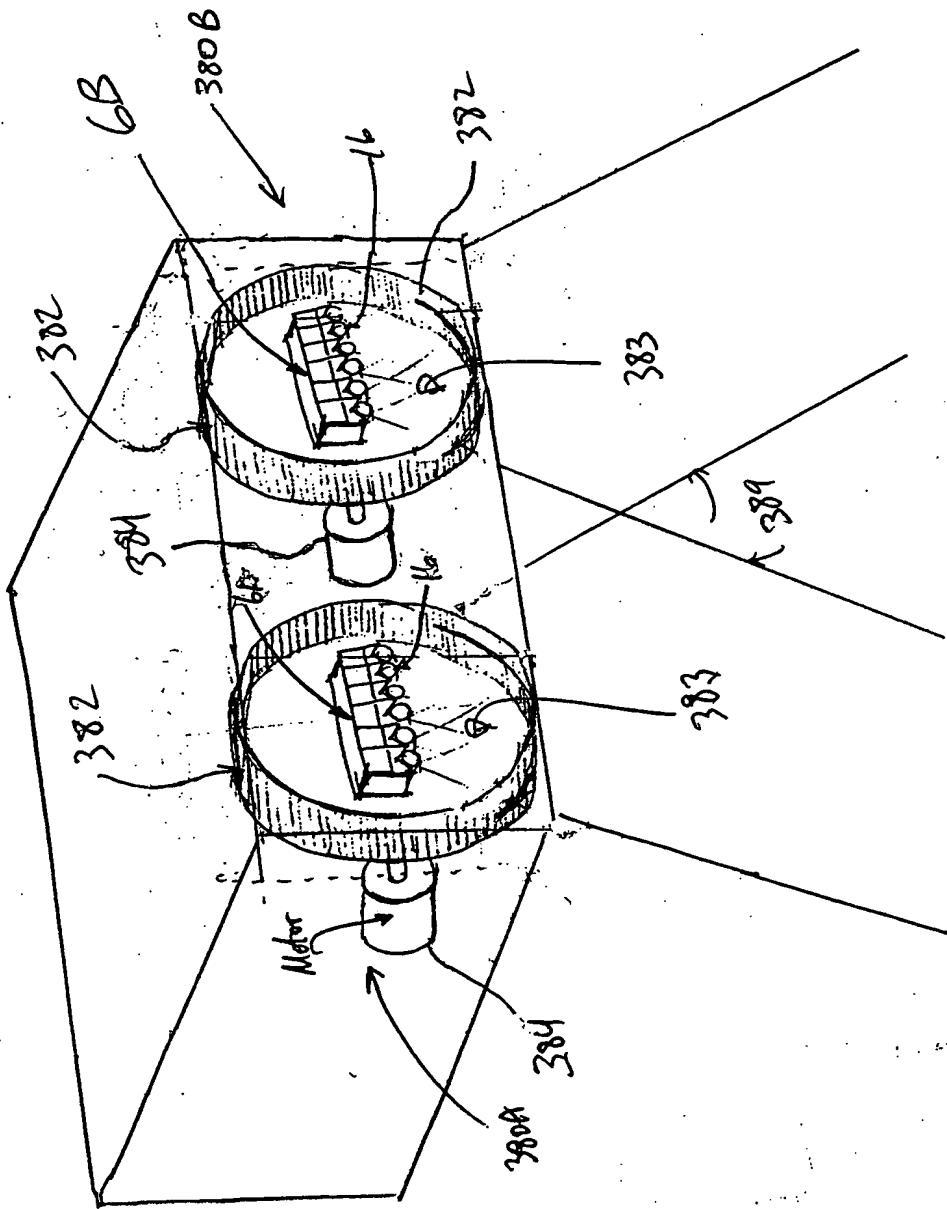
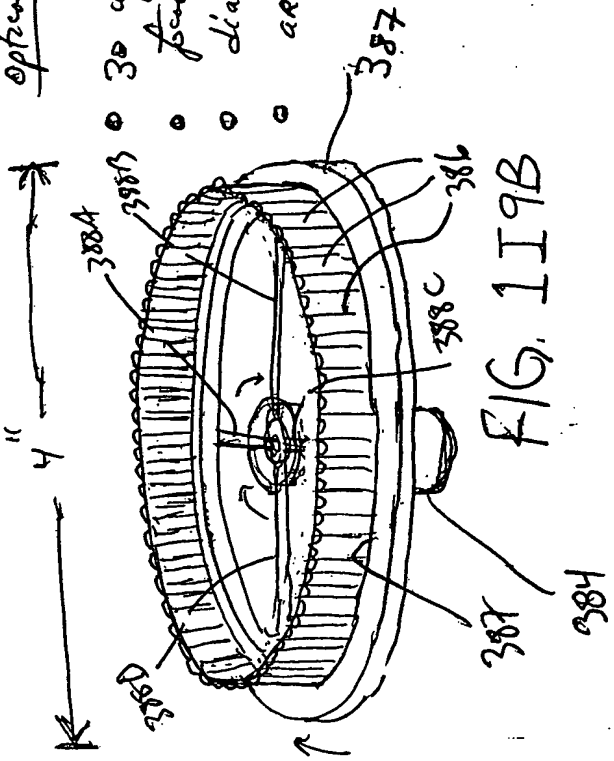


FIG. 11 9A

Optical specifications:

- 30 cylindrical lens (lens) per linear inch
- focal length: 2.0 millimeters
- diameter of cylindrical carousel ≈ 4 inches
- acrylic material



35/ 385

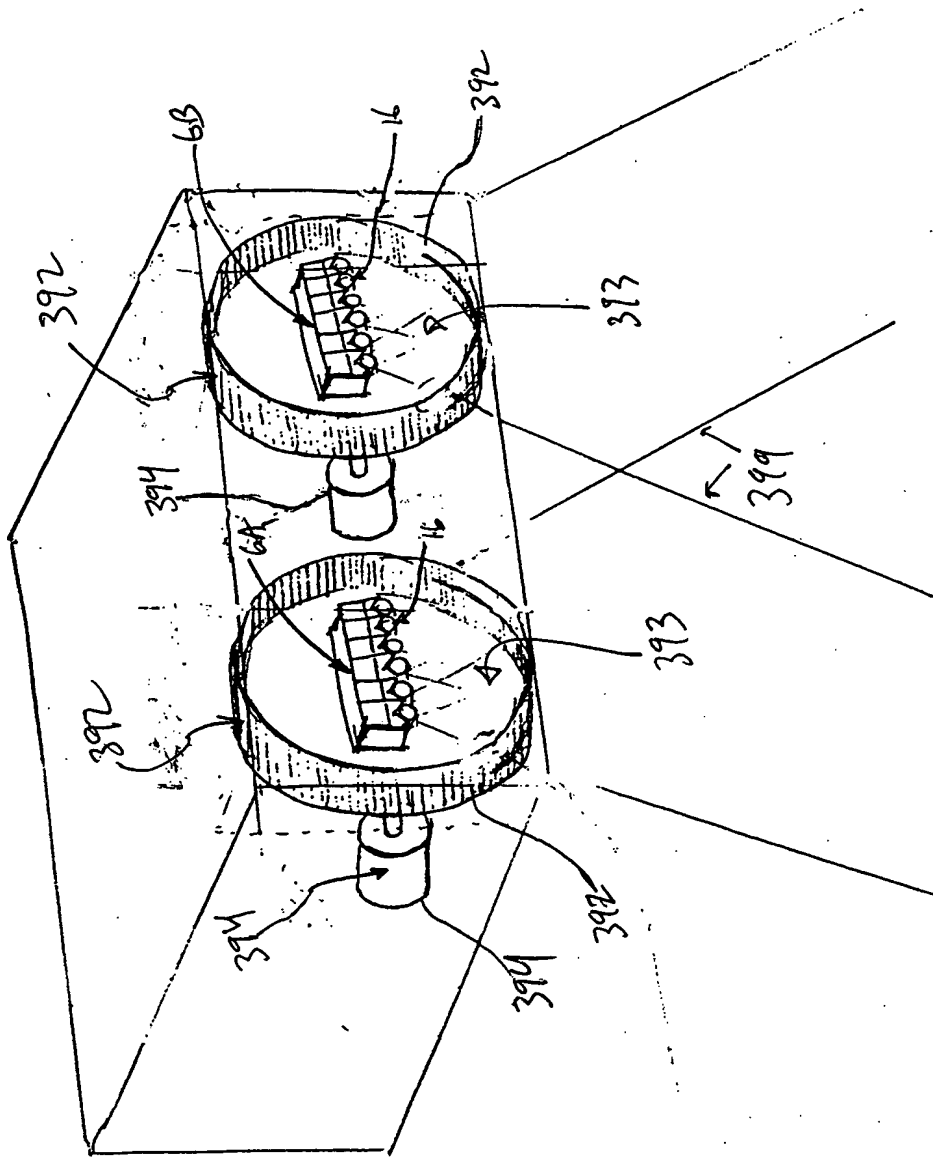
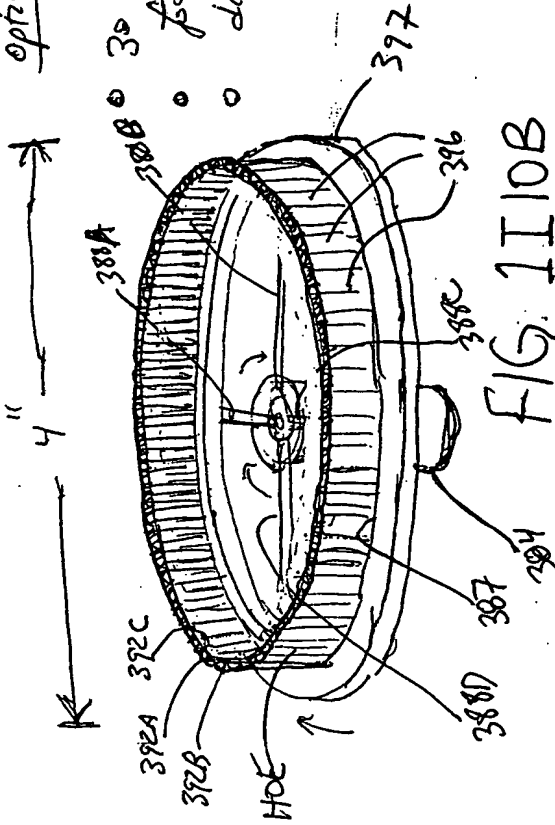


FIG. 1110A

Optical Specifications:

- 30 cylindrical lens (lines) per linear inch
- focal length: 2.0 millimeters
- diameter of cylindrical carousel ≈ 4 inches



[illegible]

37/ 385

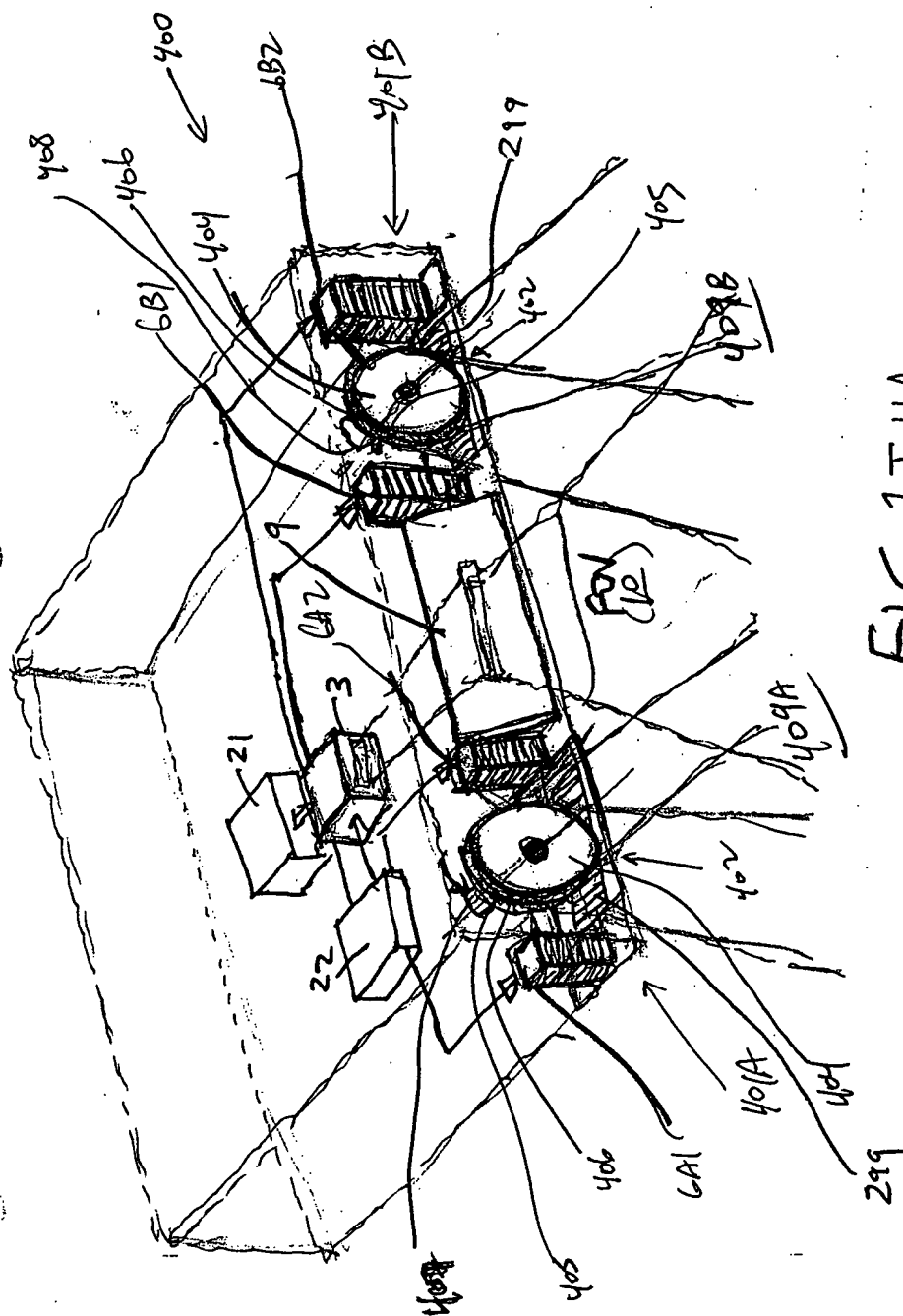


FIG. 1I11A

30/ 385

TOTAL: 53506660

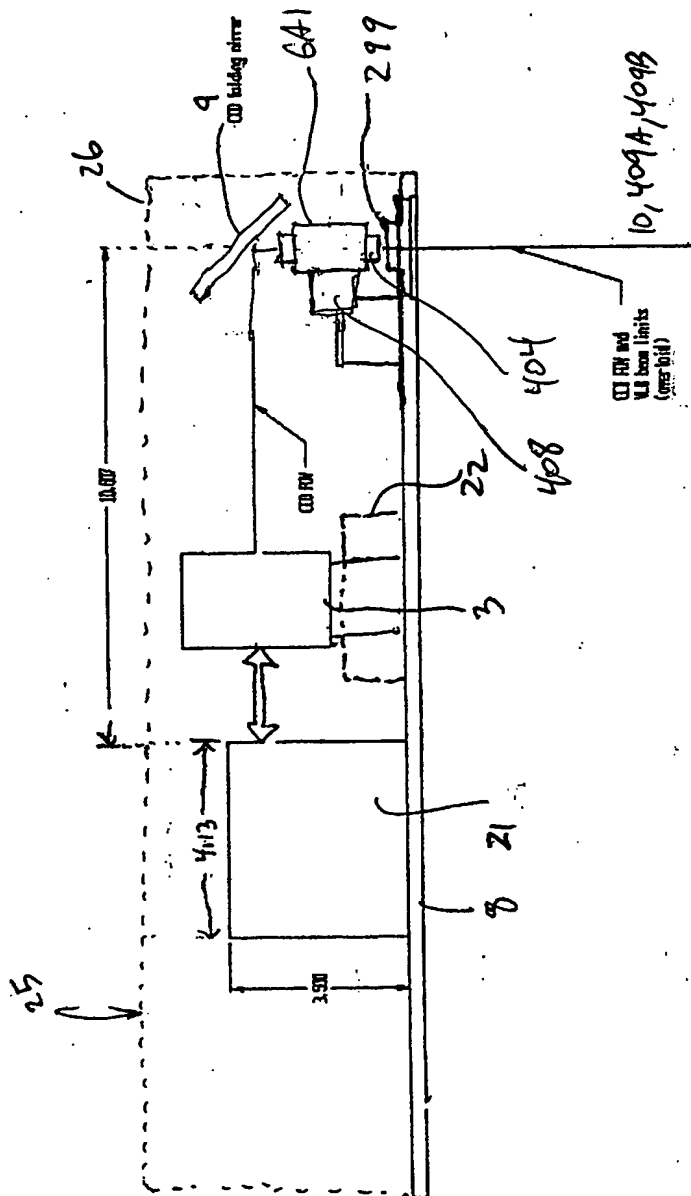


FIG 1I1/B

39/ 385

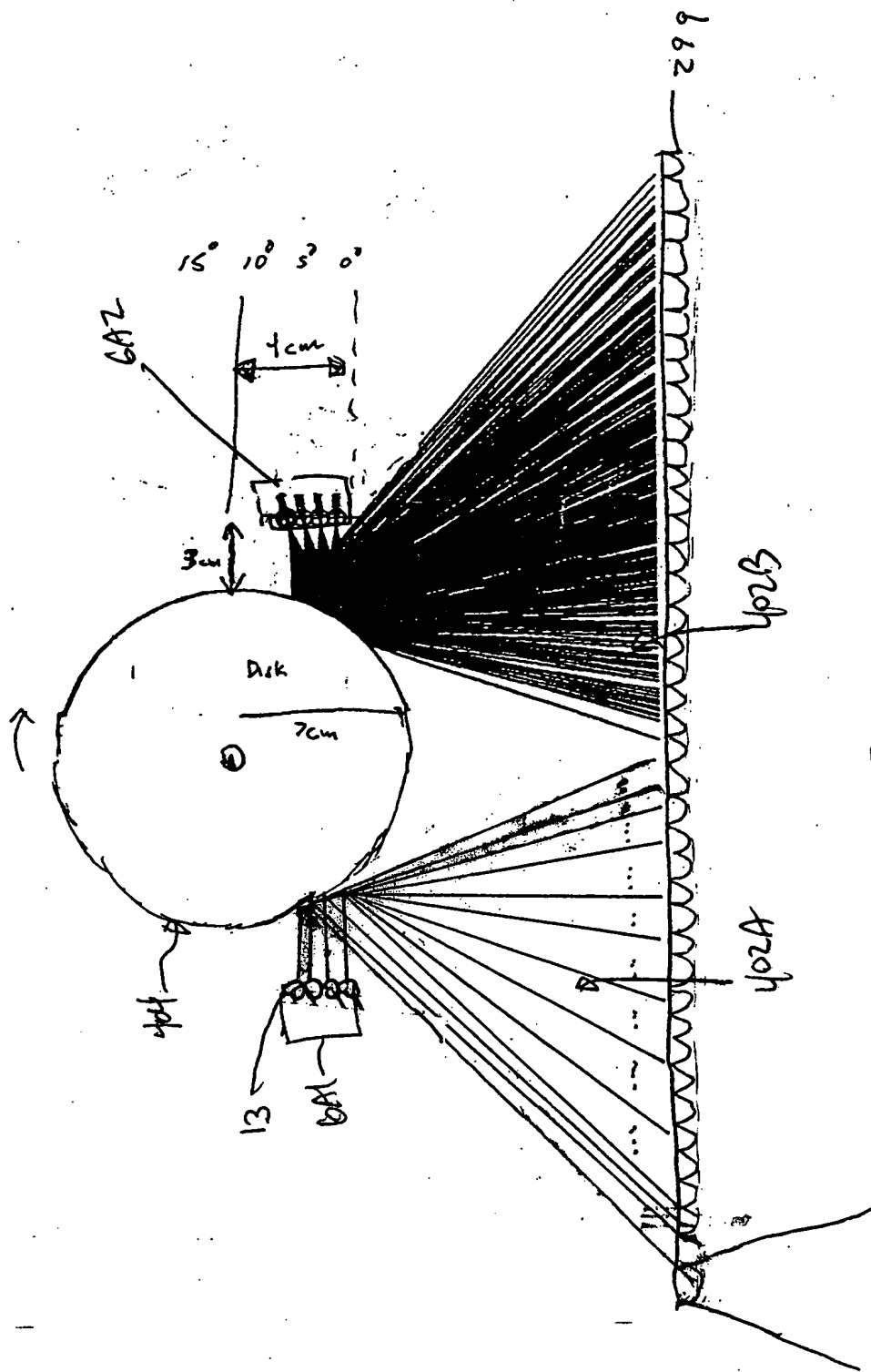
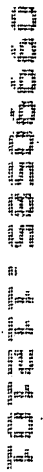
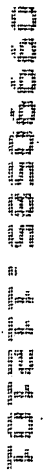


FIG. 1IIC

FOOTNOTES

[illegible][illegible]

Second Generalized Method of
Reducing Speckle-Noise Patterns
at Image Detection Array
of the FFD Subsystem (3)

42/ 385

(TIME)

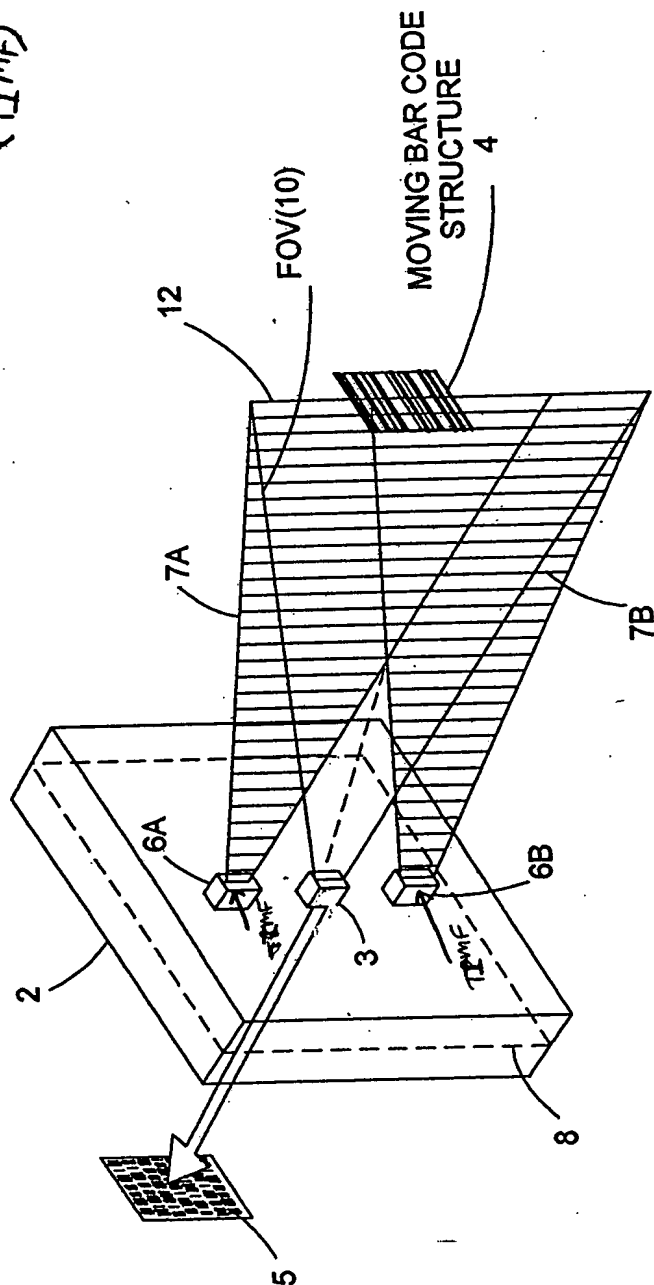


FIG. 1113

43/ 385

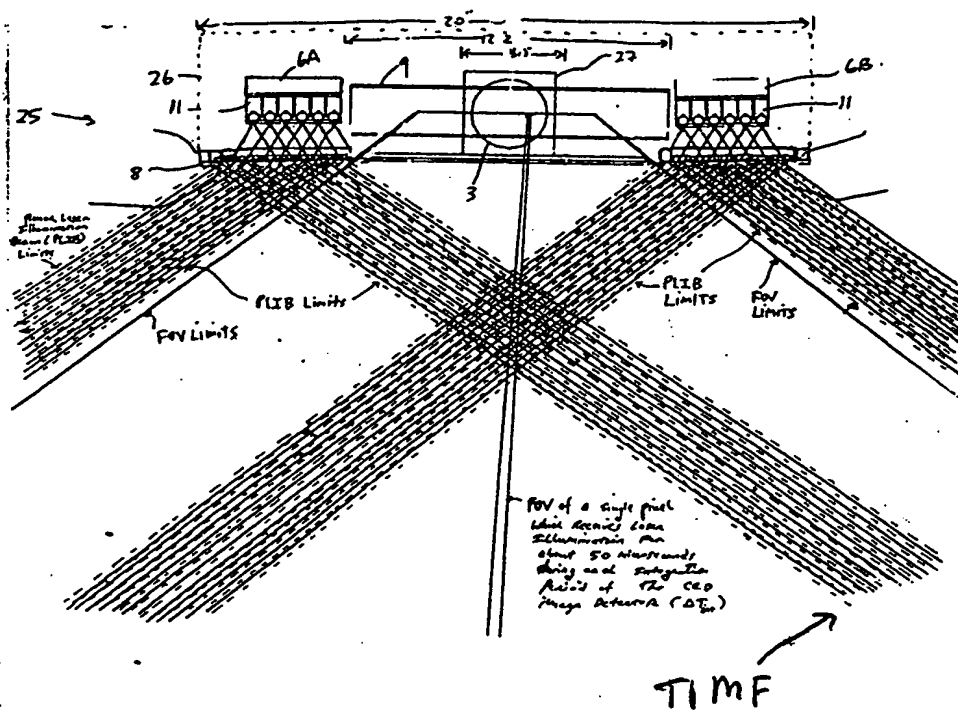


FIG. 1 I 13A

44/ 385

The Second Generalized Speckle-Noise Pattern Reduction Method
Of The Present Invention

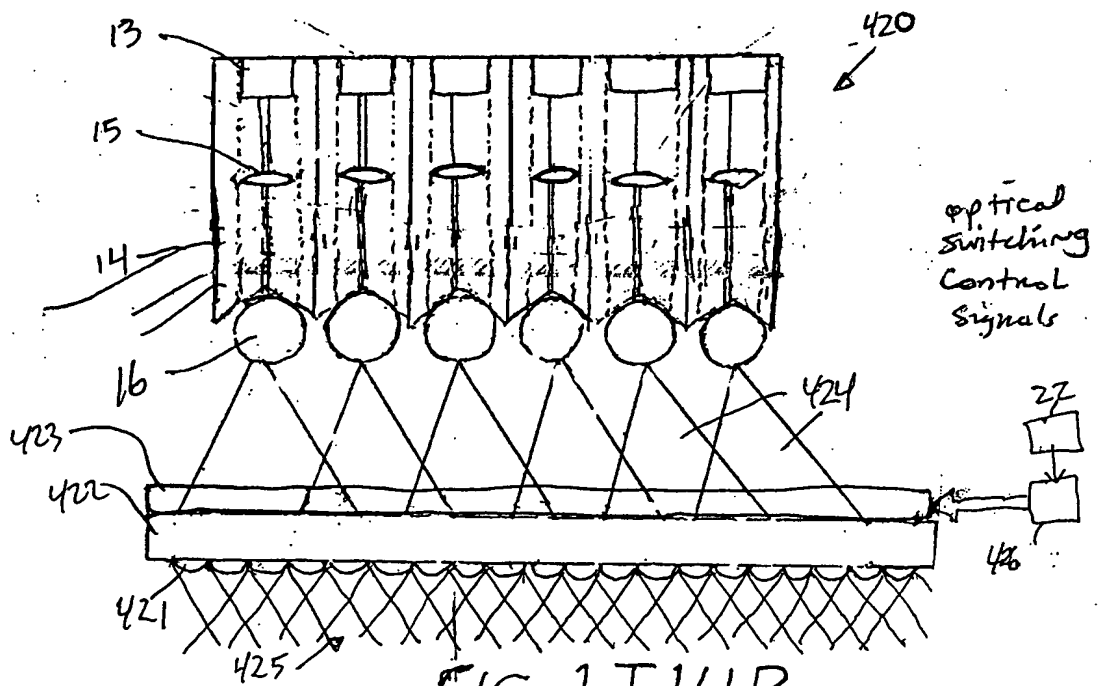
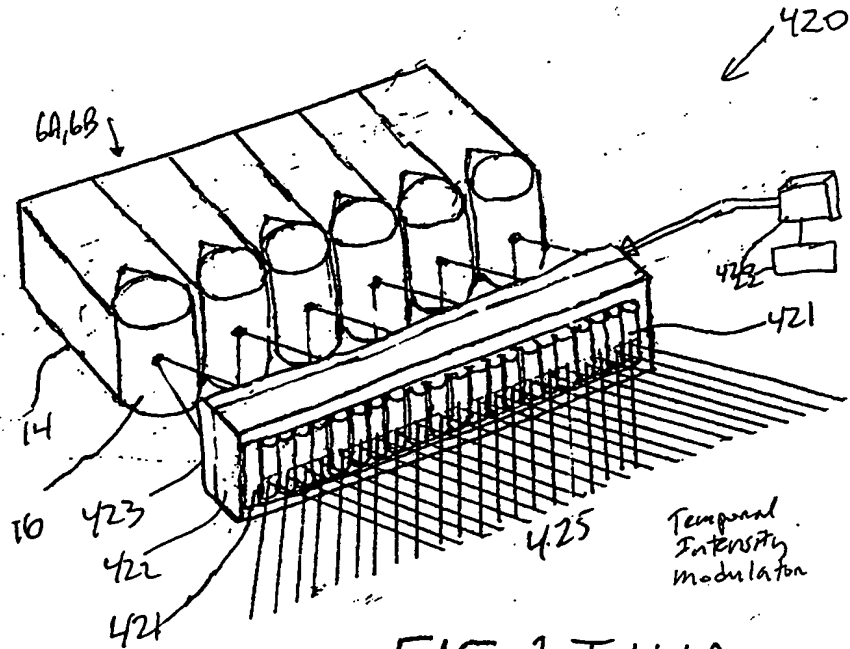
Prior to illumination of the target with the planar laser illumination beam (PLIB), modulate the temporal intensity of the transmitted PLIB along the planar extent thereof according to a temporal intensity modulation function (TIMF) so as to

produce numerous substantially different time-varying speckle-noise patterns at the image detection array of the IFD Subsystem during the photo-integration time period thereof.

Temporally average the numerous substantially different time-varying speckle-noise patterns produced at the image detection array in the IFD Subsystem during the photo-integration time period thereof, so as to thereby reduce power of the speckle-noise pattern observed at the image detection array.

FIG 1 I 13 B

45/ 385



00000585 112101

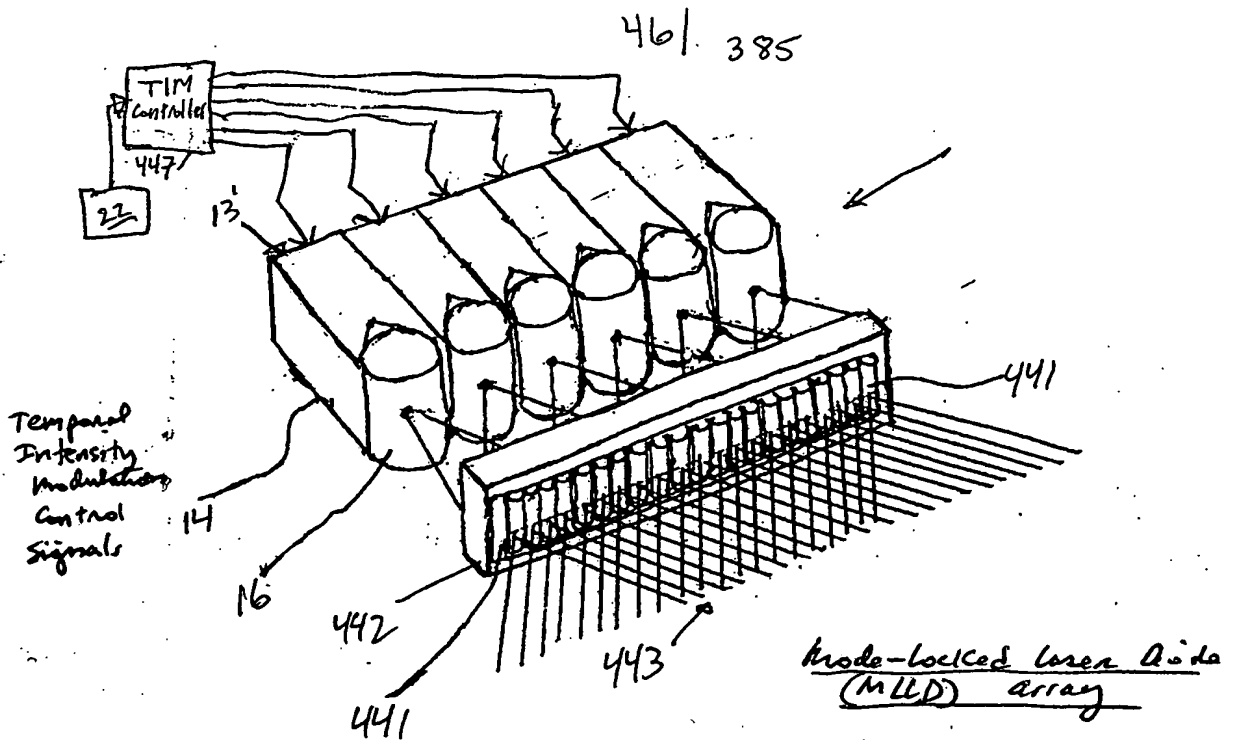


FIG. 1I15A

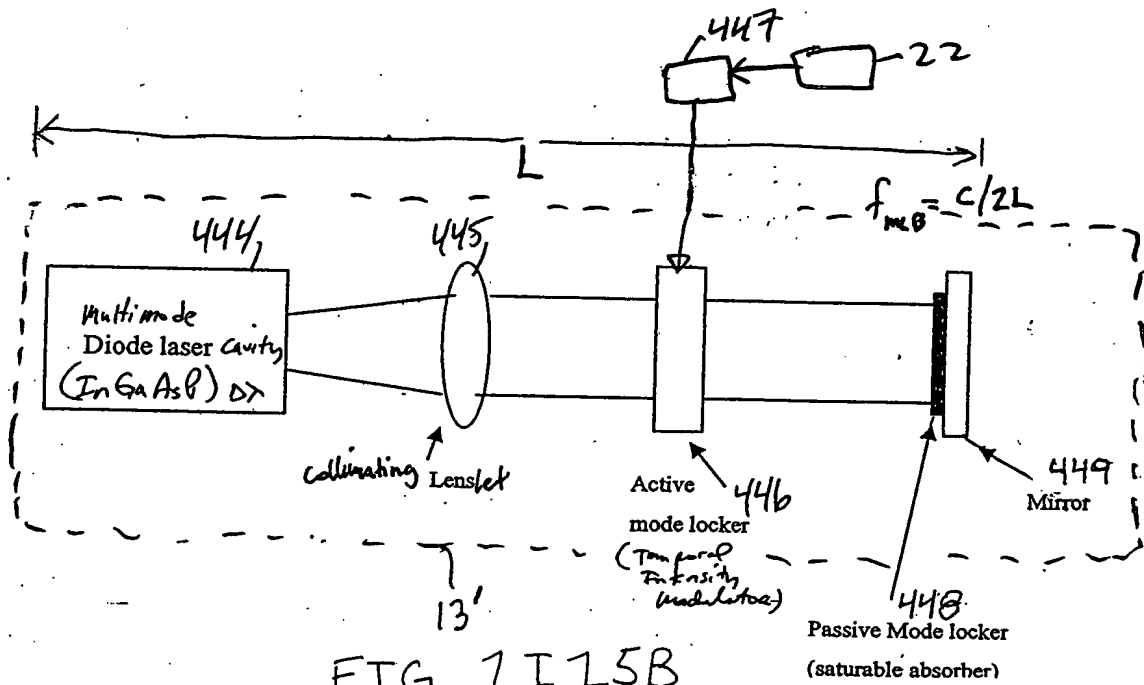


FIG. 1I15B

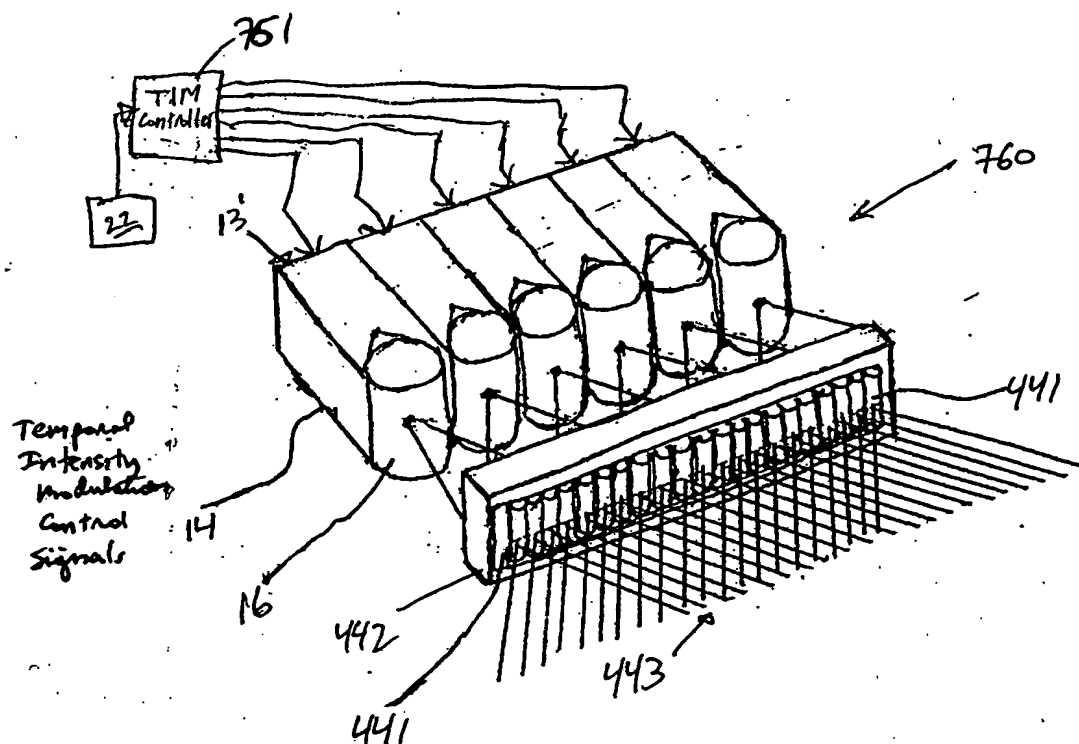


FIG. 1I 15C

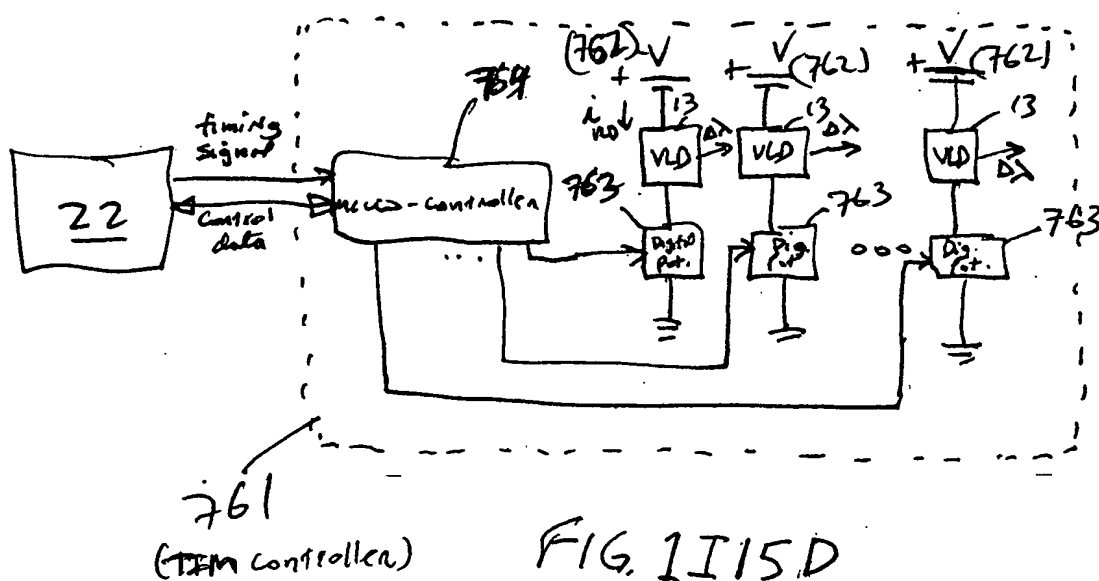


FIG. 1I15D

48/ 385

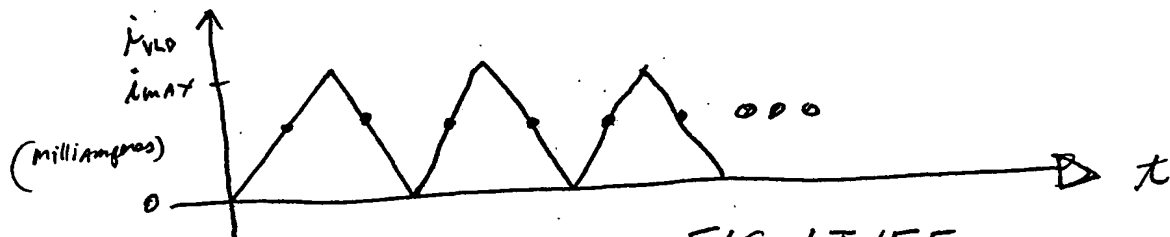


FIG. 1I15E

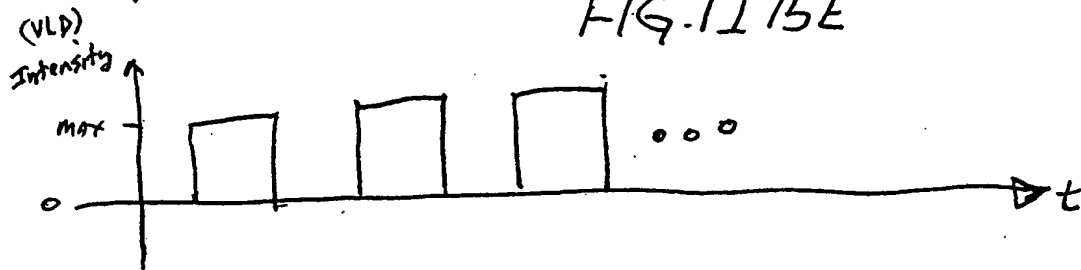


FIG. 1I15E

00000585 112101

49/ 385

Third Generalized Method of
Reducing Speckle-Noise Patterns
at Image Detection Array
of the FFD Subsystem (3)

(TIME)

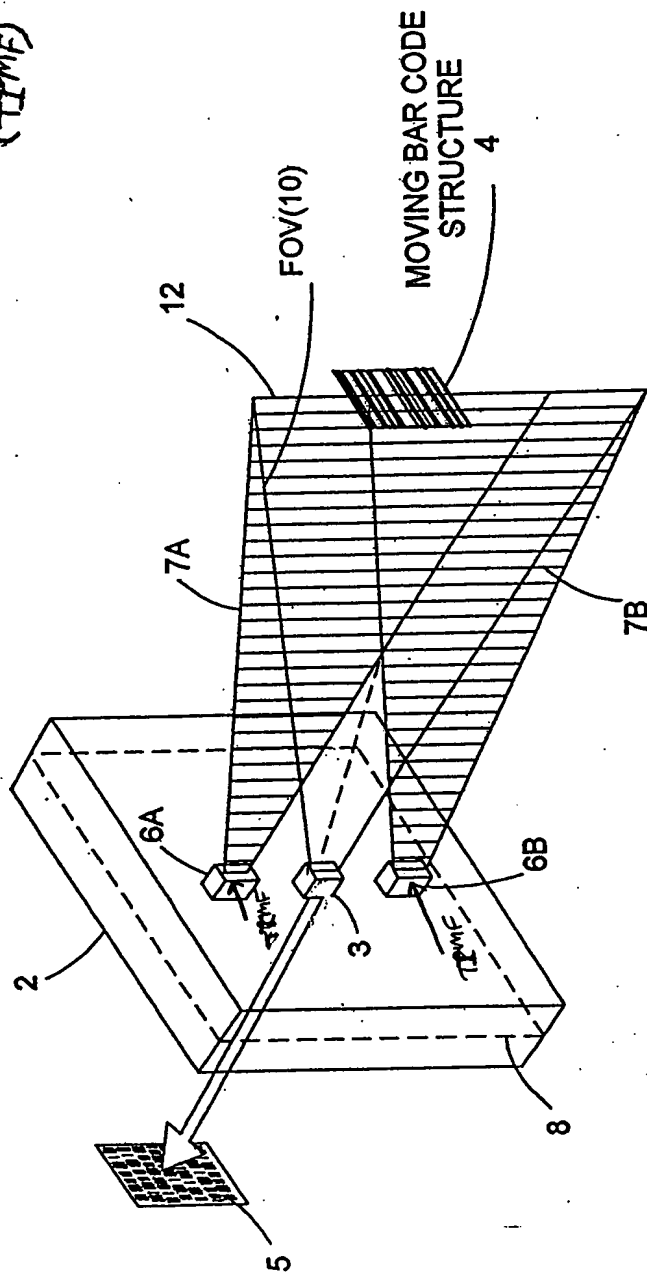
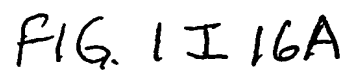


FIG. 1116

| Year | 1970 | 1971 | 1972 | 1973 | 1974 | 1975 | 1976 | 1977 | 1978 | 1979 | 1980 | 1981 | 1982 | 1983 | 1984 | 1985 | 1986 | 1987 | 1988 | 1989 | 1990 | 1991 | 1992 | 1993 | 1994 | 1995 | 1996 | 1997 | 1998 | 1999 | 2000 | 2001 | 2002 | 2003 | 2004 | 2005 | 2006 | 2007 | 2008 | 2009 | 2010 | 2011 | 2012 | 2013 | 2014 | 2015 | 2016 | 2017 | 2018 | 2019 | 2020 | 2021 | 2022 | 2023 | 2024 | 2025 | 2026 | 2027 | 2028 | 2029 | 2030 | 2031 | 2032 | 2033 | 2034 | 2035 | 2036 | 2037 | 2038 | 2039 | 2040 | 2041 | 2042 | 2043 | 2044 | 2045 | 2046 | 2047 | 2048 | 2049 | 2050 | 2051 | 2052 | 2053 | 2054 | 2055 | 2056 | 2057 | 2058 | 2059 | 2060 | 2061 | 2062 | 2063 | 2064 | 2065 | 2066 | 2067 | 2068 | 2069 | 2070 | 2071 | 2072 | 2073 | 2074 | 2075 | 2076 | 2077 | 2078 | 2079 | 2080 | 2081 | 2082 | 2083 | 2084 | 2085 | 2086 | 2087 | 2088 | 2089 | 2090 | 2091 | 2092 | 2093 | 2094 | 2095 | 2096 | 2097 | 2098 | 2099 | 2100 |
|------|------|------|------|------|------|------|------|------|------|------|------|------|------|------|------|------|------|------|------|------|------|------|------|------|------|------|------|------|------|------|------|------|------|------|------|------|------|------|------|------|------|------|------|------|------|------|------|------|------|------|------|------|------|------|------|------|------|------|------|------|------|------|------|------|------|------|------|------|------|------|------|------|------|------|------|------|------|------|------|------|------|------|------|------|------|------|------|------|------|------|------|------|------|------|------|------|------|------|------|------|------|------|------|------|------|------|------|------|------|------|------|------|------|------|------|------|------|------|------|------|------|------|------|------|------|------|------|------|------|------|------|
| 1970 | 1971 | 1972 | 1973 | 1974 | 1975 | 1976 | 1977 | 1978 | 1979 | 1980 | 1981 | 1982 | 1983 | 1984 | 1985 | 1986 | 1987 | 1988 | 1989 | 1990 | 1991 | 1992 | 1993 | 1994 | 1995 | 1996 | 1997 | 1998 | 1999 | 2000 | 2001 | 2002 | 2003 | 2004 | 2005 | 2006 | 2007 | 2008 | 2009 | 2010 | 2011 | 2012 | 2013 | 2014 | 2015 | 2016 | 2017 | 2018 | 2019 | 2020 | 2021 | 2022 | 2023 | 2024 | 2025 | 2026 | 2027 | 2028 | 2029 | 2030 | 2031 | 2032 | 2033 | 2034 | 2035 | 2036 | 2037 | 2038 | 2039 | 2040 | 2041 | 2042 | 2043 | 2044 | 2045 | 2046 | 2047 | 2048 | 2049 | 2050 | 2051 | 2052 | 2053 | 2054 | 2055 | 2056 | 2057 | 2058 | 2059 | 2060 | 2061 | 2062 | 2063 | 2064 | 2065 | 2066 | 2067 | 2068 | 2069 | 2070 | 2071 | 2072 | 2073 | 2074 | 2075 | 2076 | 2077 | 2078 | 2079 | 2080 | 2081 | 2082 | 2083 | 2084 | 2085 | 2086 | 2087 | 2088 | 2089 | 2090 | 2091 | 2092 | 2093 | 2094 | 2095 | 2096 | 2097 | 2098 | 2099 | 2100 | |



51/ 385

Third Generalized Speckle-Noise Pattern Reduction Method
Of The Present Invention

Prior to illumination of the target with the planar laser illumination beam (PLIB), modulate the temporal *phase* of the transmitted PLIB ~~along the planar extent thereof~~ according to a *temporal phase* modulation function (TPMF) so as to:

produce numerous substantially different time-varying speckle-noise patterns at the image detection array of the IFD Subsystem during the photo-integration time period thereof.

↓

Temporally average the numerous substantially different time-varying speckle-noise patterns produced at the image detection array in the IFD Subsystem during the photo-integration time period thereof, so as to thereby reduce power of the speckle-noise pattern observed at the image detection array.

FIG. 1I/6B

09990595-112101

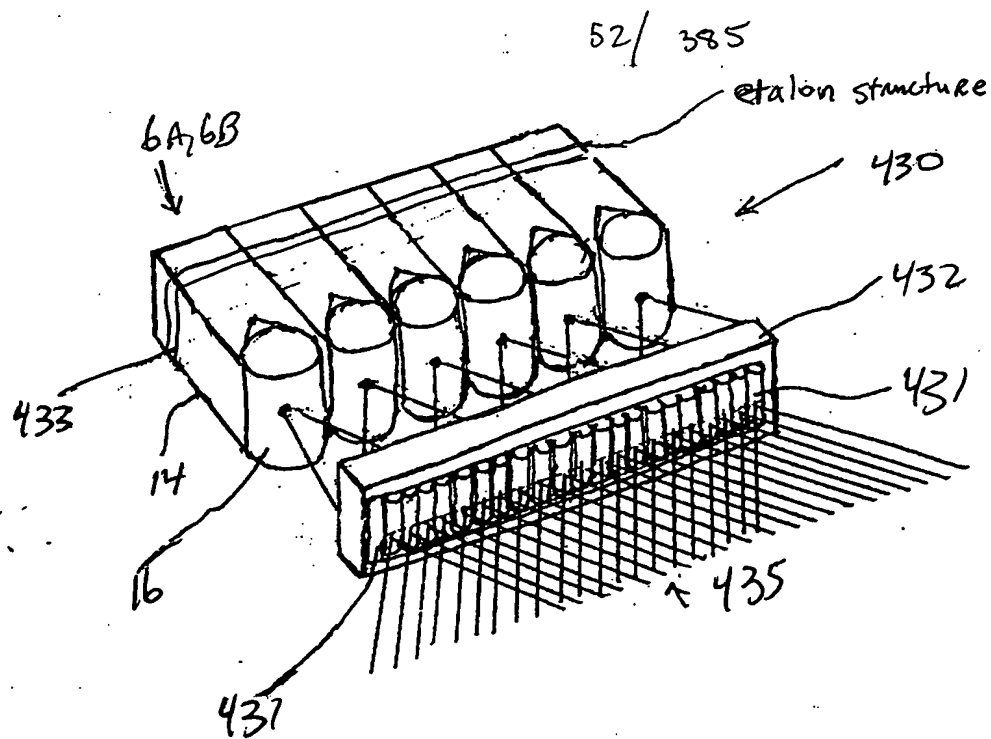


FIG. 1I17A

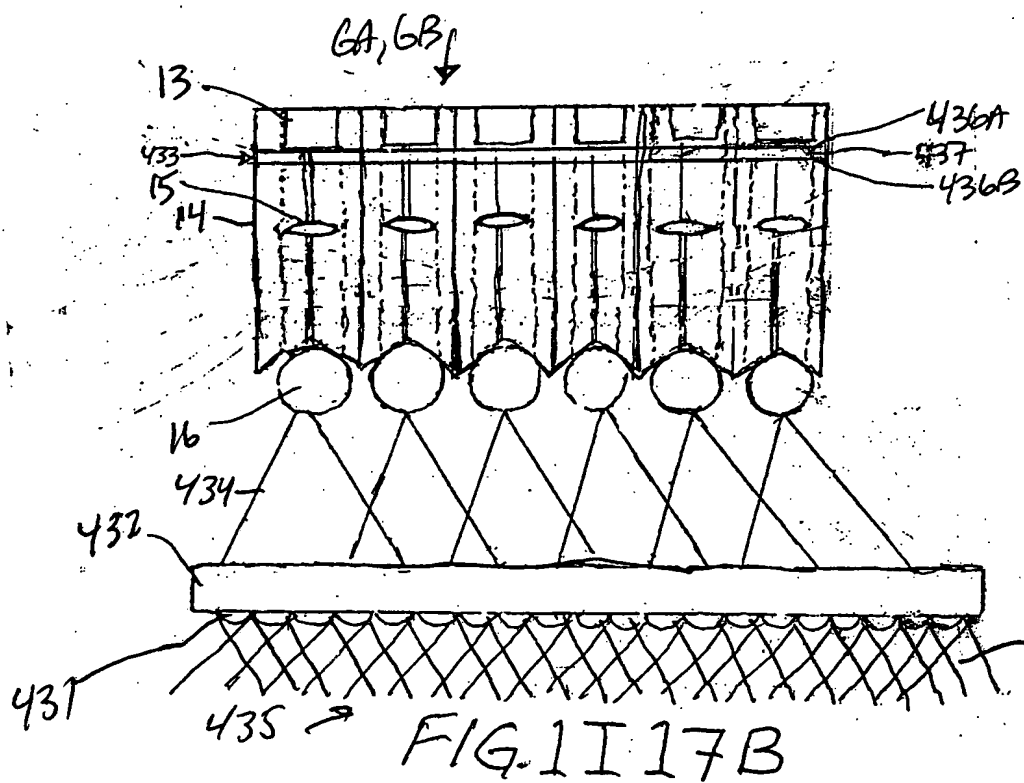


FIG. 1I17B

53/ 385

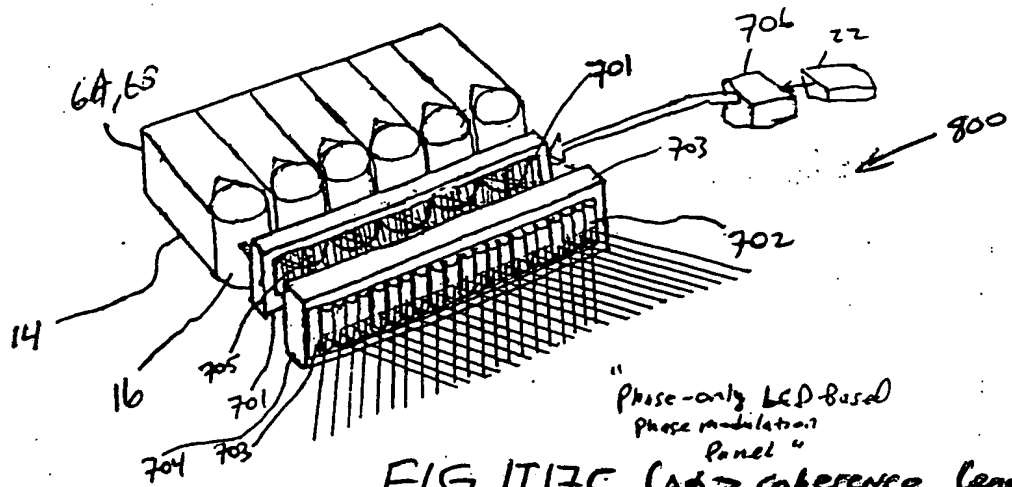


FIG. 1I17C ($\Delta\phi >$ coherence length
of VLD)

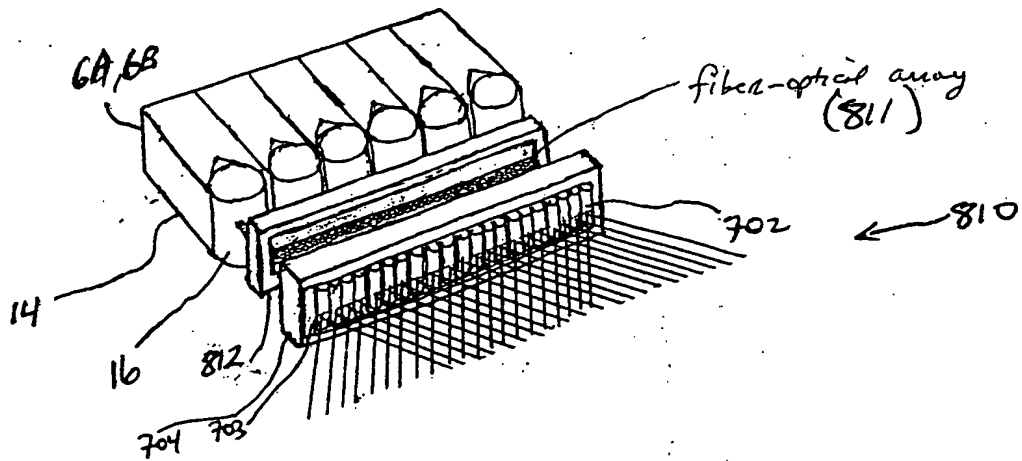


FIG. 1I17D

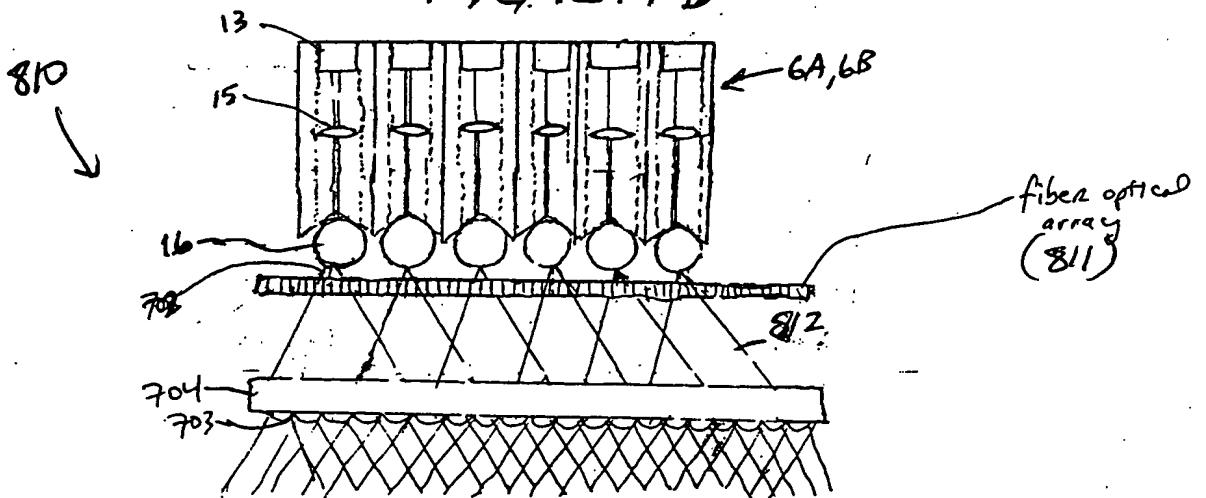


FIG. 1I17E

00000555 112101

Fourth Generalized Method of
Reducing Speckle-Noise Patterns
of Image Detection Array
of the FFD Subsystem (3)

(TFMP)

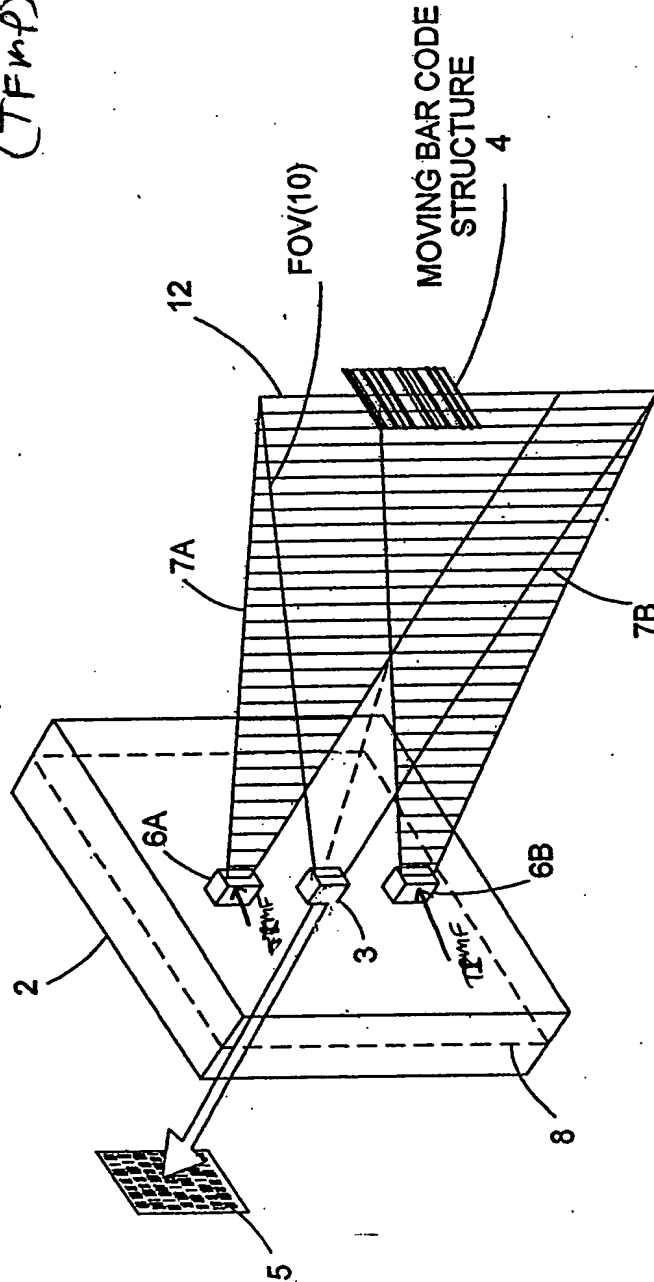
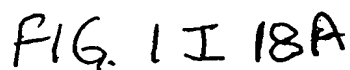


FIG. 1118



56/ 385

Fourth Generalized Speckle-Noise Pattern Reduction Method
Of The Present Invention

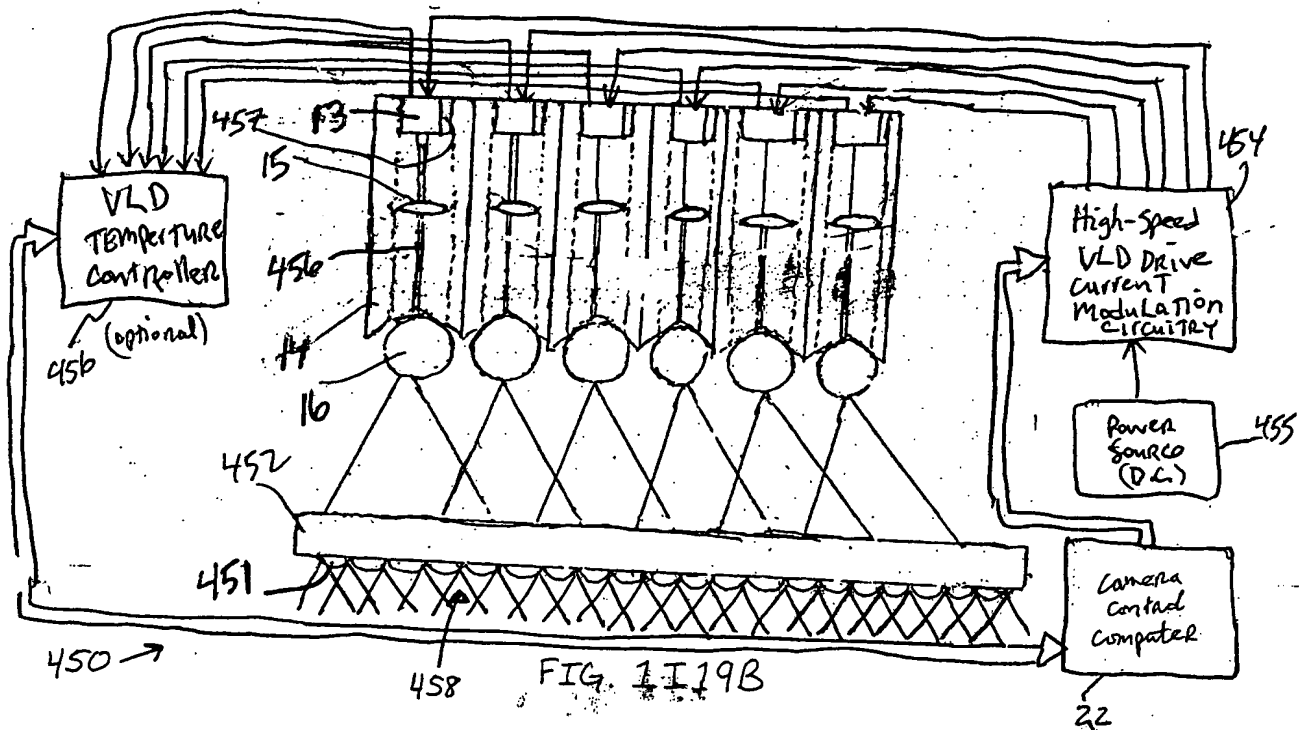
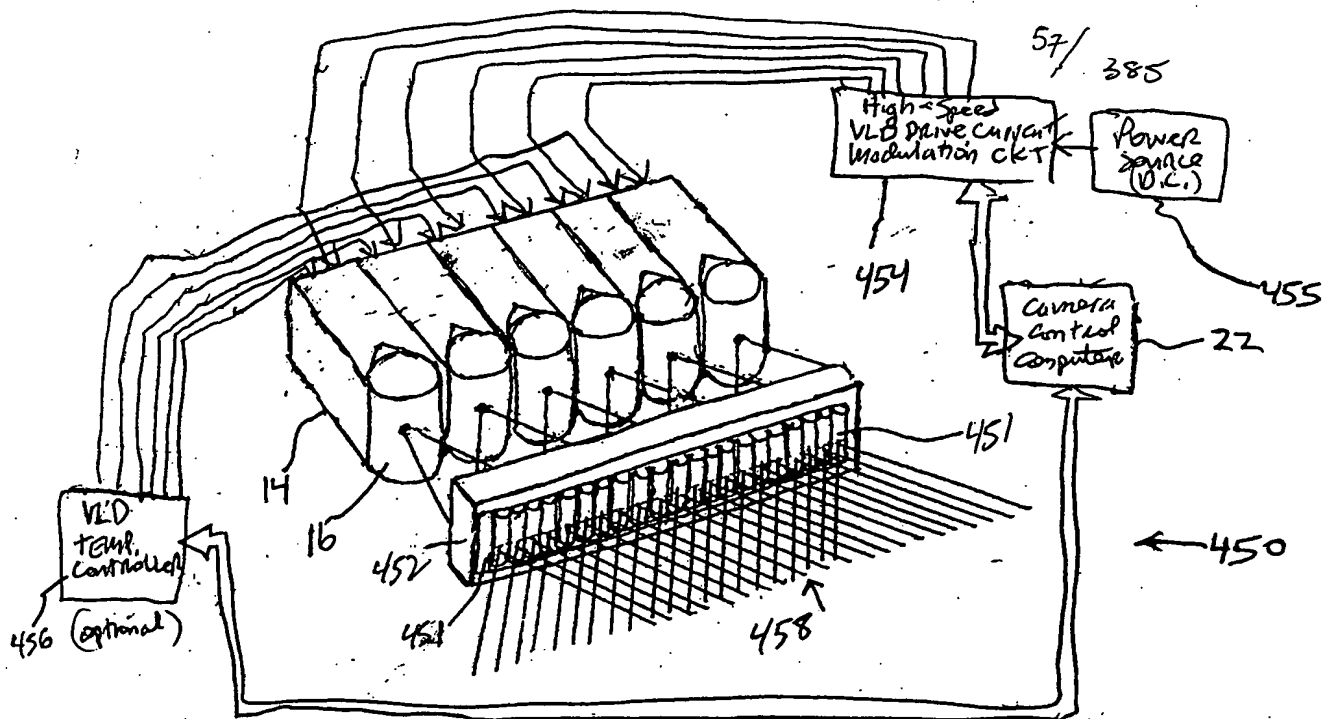
Prior to illumination of the target with the planar laser illumination beam (PLIB), modulate the temporal frequency of the transmitted PLIB according to a temporal intensity modulation function (T IMF) so as to :

produce numerous substantially different time-varying speckle-noise patterns at the image detection array of the IFD Subsystem during the photo-integration time period thereof.

Temporally average the numerous substantially different time-varying speckle-noise patterns produced at the image detection array in the IFD Subsystem during the photo-integration time period thereof, so as to thereby reduce power of the speckle-noise pattern observed at the image detection array.

FIG. 1I18B

0000585 112101



58/385

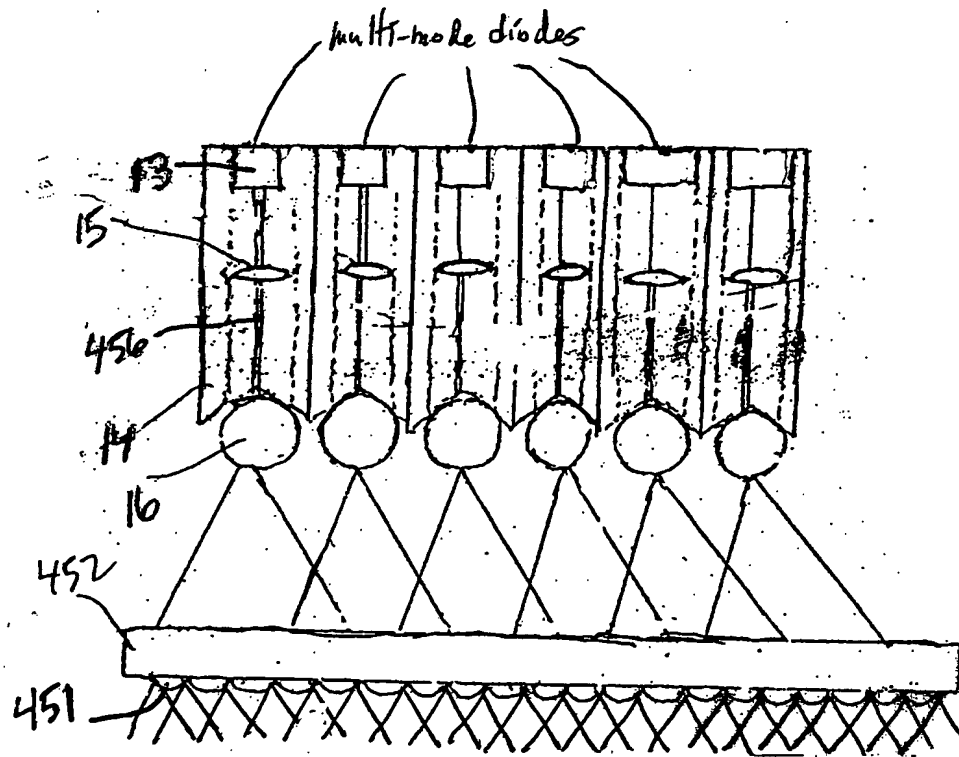


FIG 119C

59/ 385

Fifth GENERALIZED METHOD
of Reducing Speckle-Noise
PATTERNS AT IMAGE
Detection array OF THE
FPD subsystem (3)

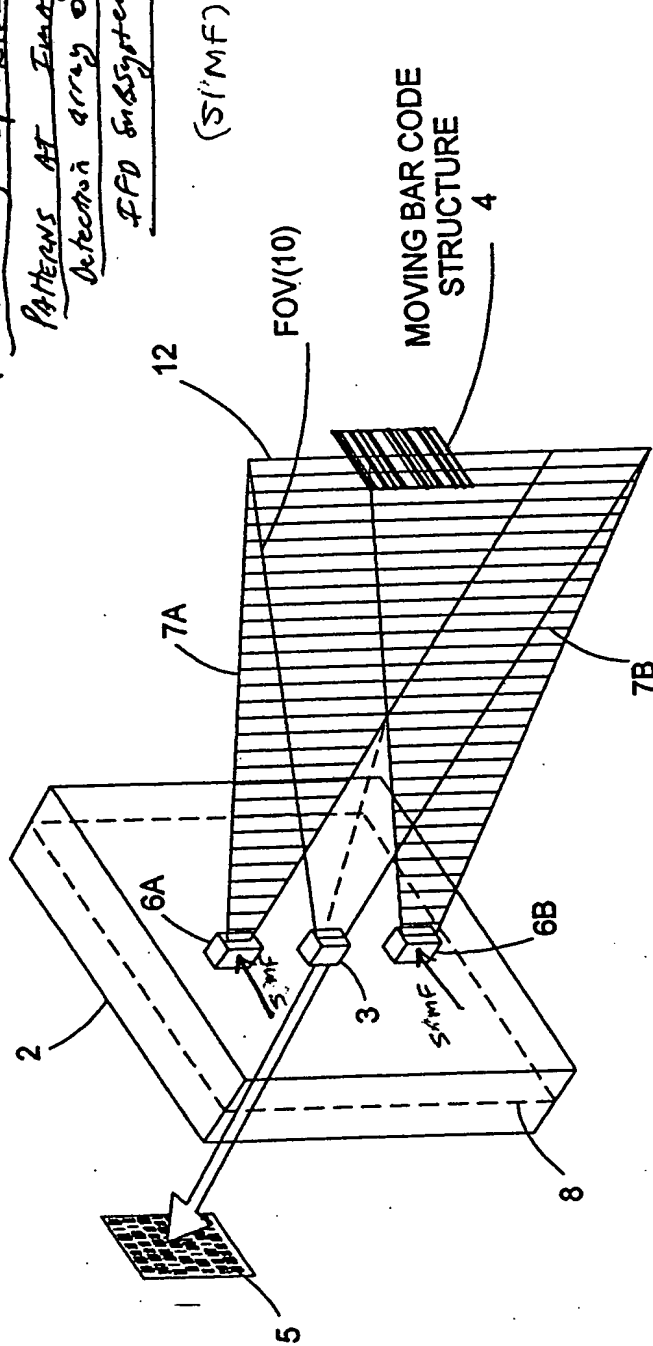


FIG 1E 20

61/ 385

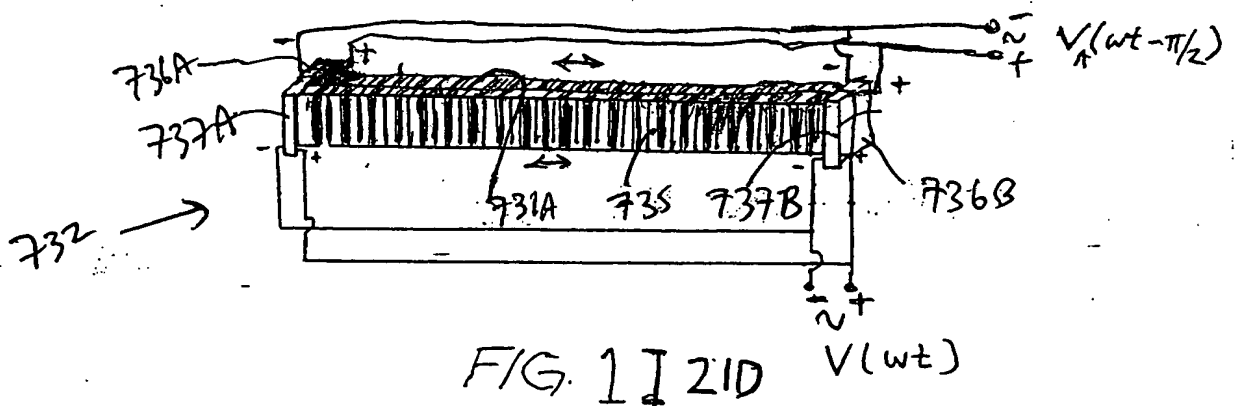
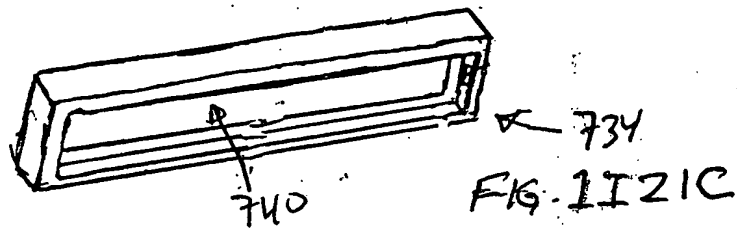
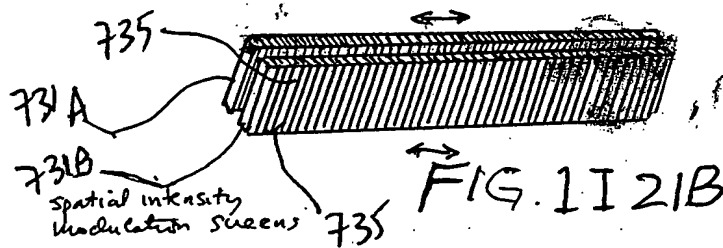
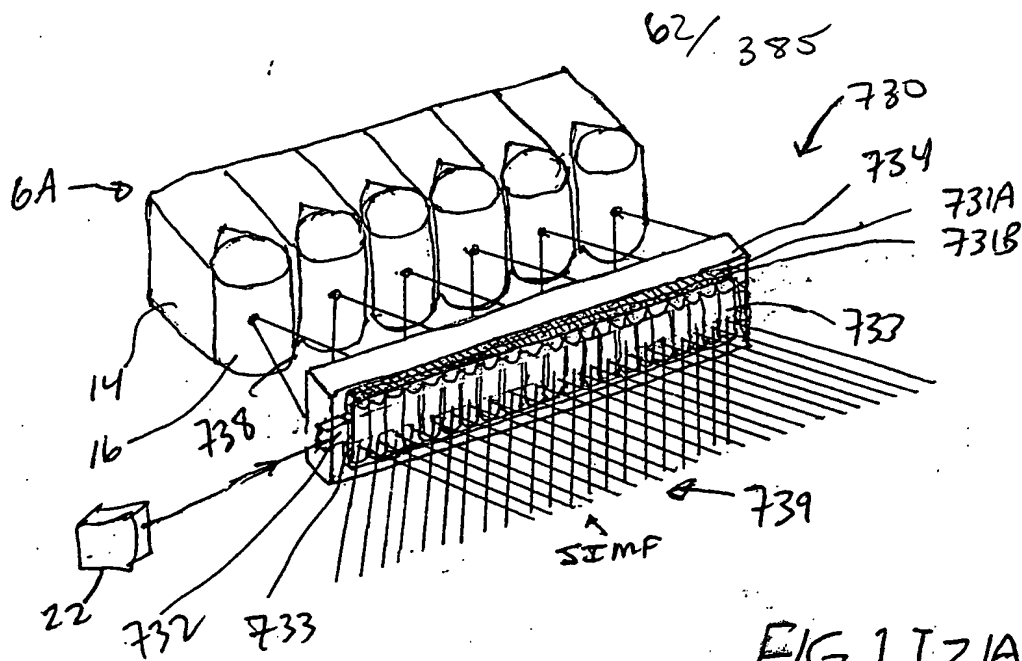
Fifth Generalized Speckle-Noise Pattern Reduction Method
Of The Present Invention

Prior to illumination of the target with the planar laser illumination beam (PLIB), modulate the spatial intensity of the transmitted PLIB along the planar extent thereof according to a spatial intensity modulation function (SIMF) so as to:

produce numerous substantially different time-varying speckle-noise patterns at the image detection array of the IFD Subsystem during the photo-integration time period thereof.

Temporally average the numerous substantially different time-varying speckle-noise patterns produced at the image detection array in the IFD Subsystem during the photo-integration time period thereof, so as to thereby reduce power of the speckle-noise pattern observed at the image detection array.

FIG. 1I20B



Generalized Method of
Reducing Speckle-Noise Patterns
at Image Detection array
of the IFD Subsystem

(SIMF)

63/ 385

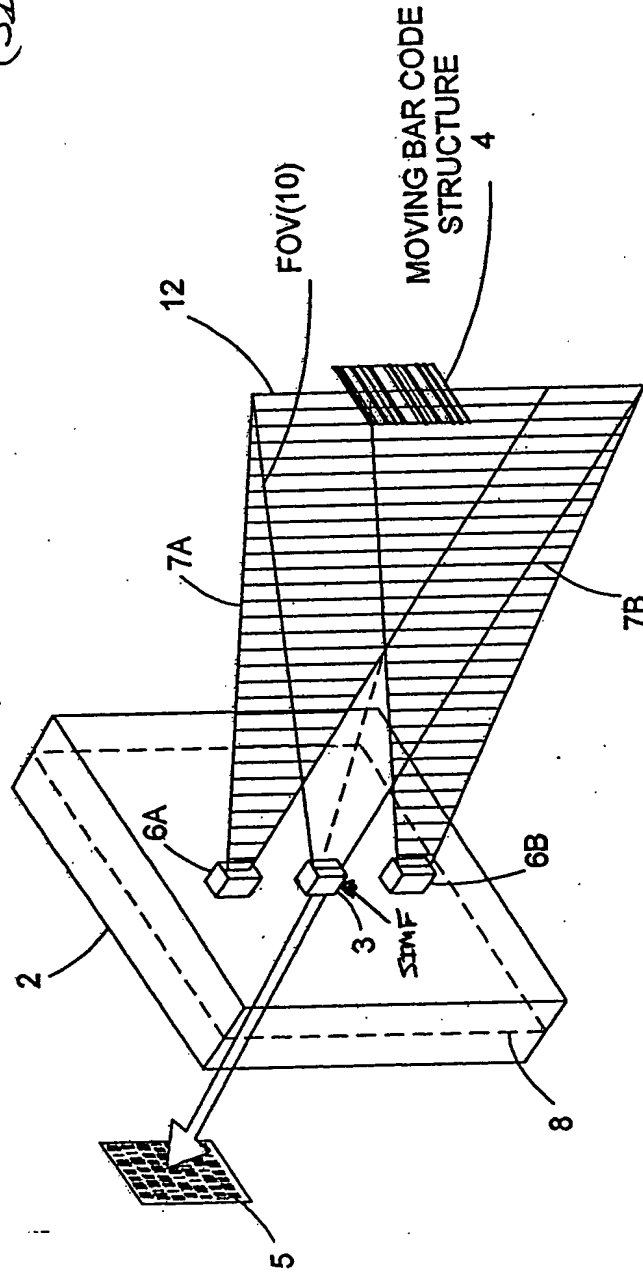


FIG. 1I 22

64/385

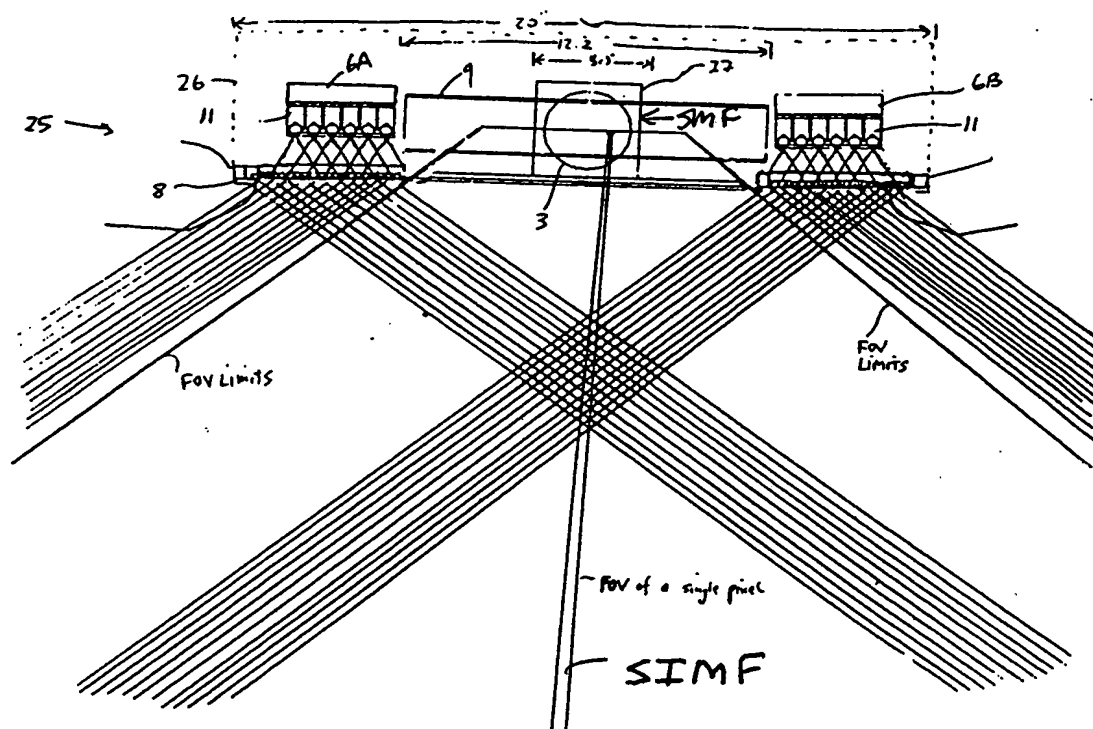


FIG. 1I 22A

00000585 112101

65/385

Sixth Generalized Speckle-Noise Pattern Reduction Method
Of The Present Invention

After illumination of the target with the planar laser illumination beam (PLIB), modulate the spatial intensity of the reflected/scattered (i.e. received) PLIB along the planar extent thereof according to a spatial intensity modulation function (SIMF) so as to :

produce numerous substantially different time-varying speckle-noise patterns at the image detection array of the IFD Subsystem during the photo-integration time period thereof.

Temporally average the many substantially different time-varying speckle-noise patterns produced at the image detection array in the IFD Subsystem during the photo-integration time period thereof, so as to thereby reduce the speckle-noise pattern observed at the image detection array.

FIG. 1I 22B

00000585 112101
TOTAL 58506660

66/ 385

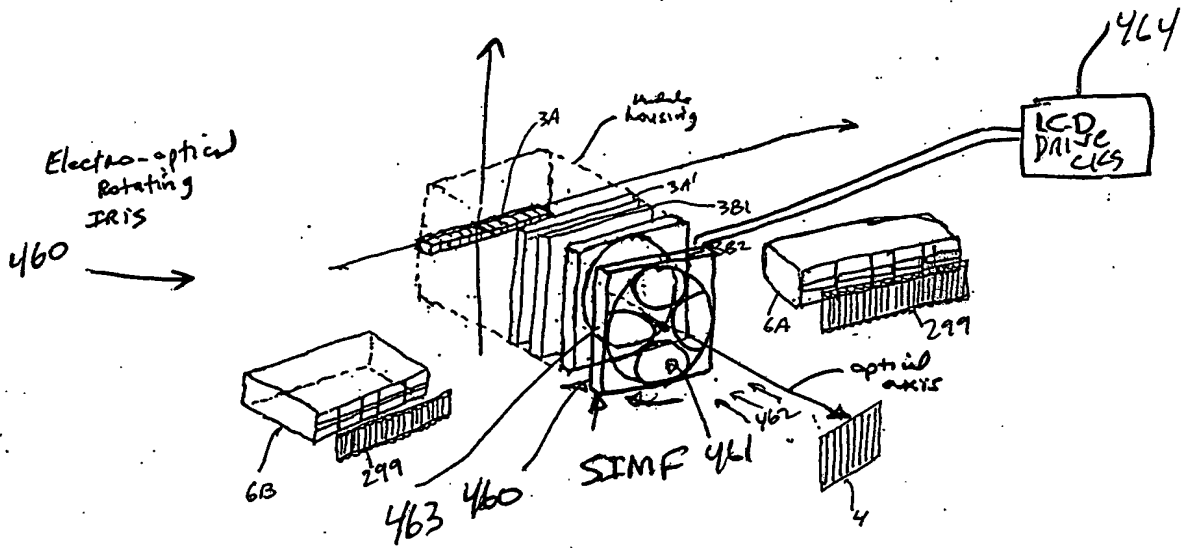


FIG. 1I 23A

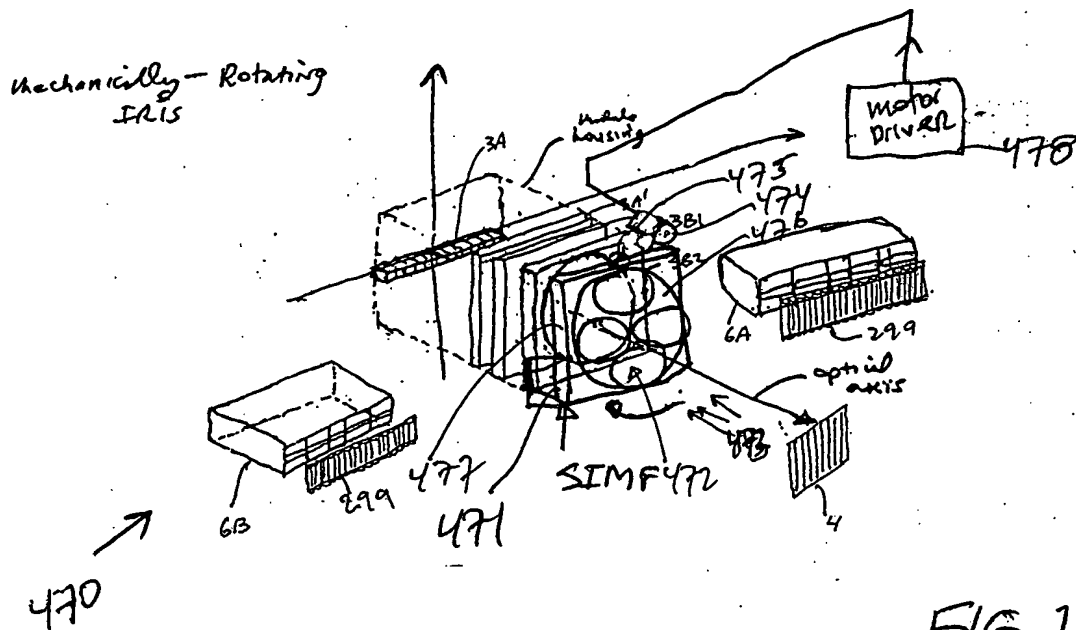


FIG. 1I 23B

Seventh Generalized Method of
Reducing Speckle - Noise Patterns
at Image Detection Array
of 76 IFD Subsystem

(TIME)

67/ 385

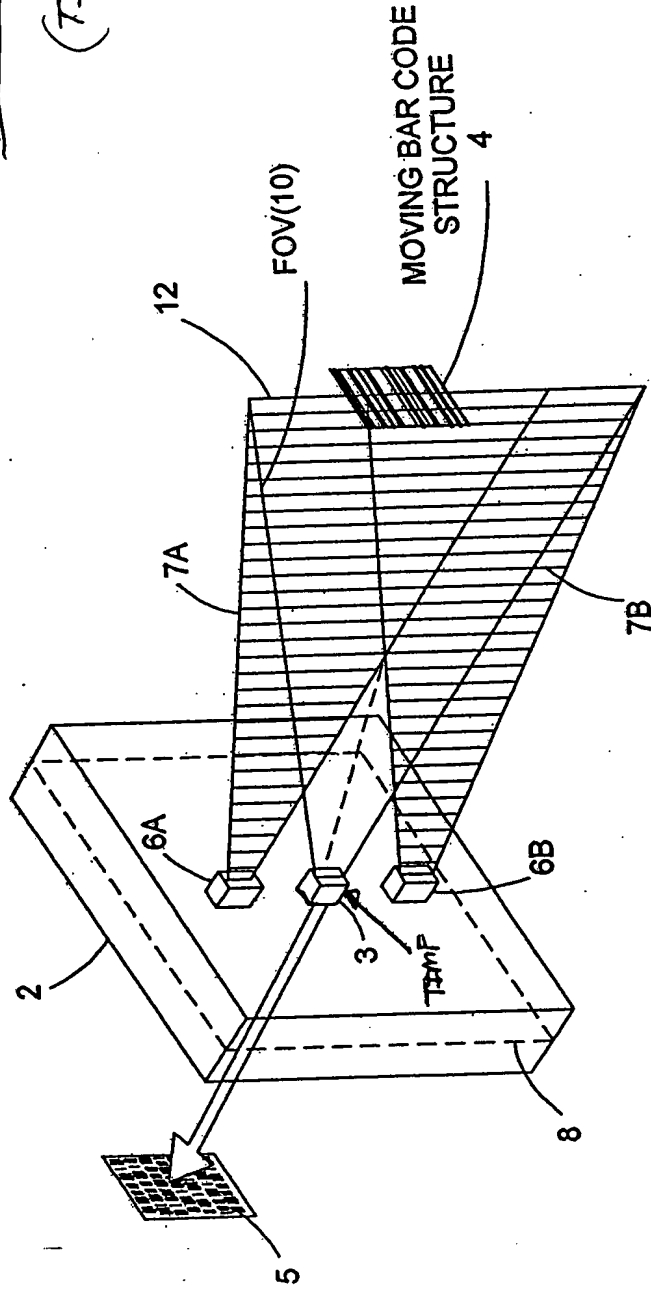


FIG. 11

[illegible]

© 2004 Blackwell Publishing Ltd

69/ 395

Seventh Generalized Speckle-Noise Pattern Reduction Method
Of The Present Invention

After illumination of the target with the planar laser illumination beam (PLIB), modulate the temporal intensity of the reflected/scattered (i.e. received) PLIB along the planar extent thereof according to a temporal intensity modulation function (TIMF) so as to :

produce many substantially different time-varying speckle-noise patterns at the image detection array of the IFD Subsystem during the photo-integration time period thereof.

Temporally average the many substantially different time-varying speckle-noise patterns produced at the image detection array in the IFD Subsystem during the photo-integration time period thereof, so as to thereby reduce the speckle-noise pattern observed at the image detection array.

FIG. 1I 24B

70/ 385

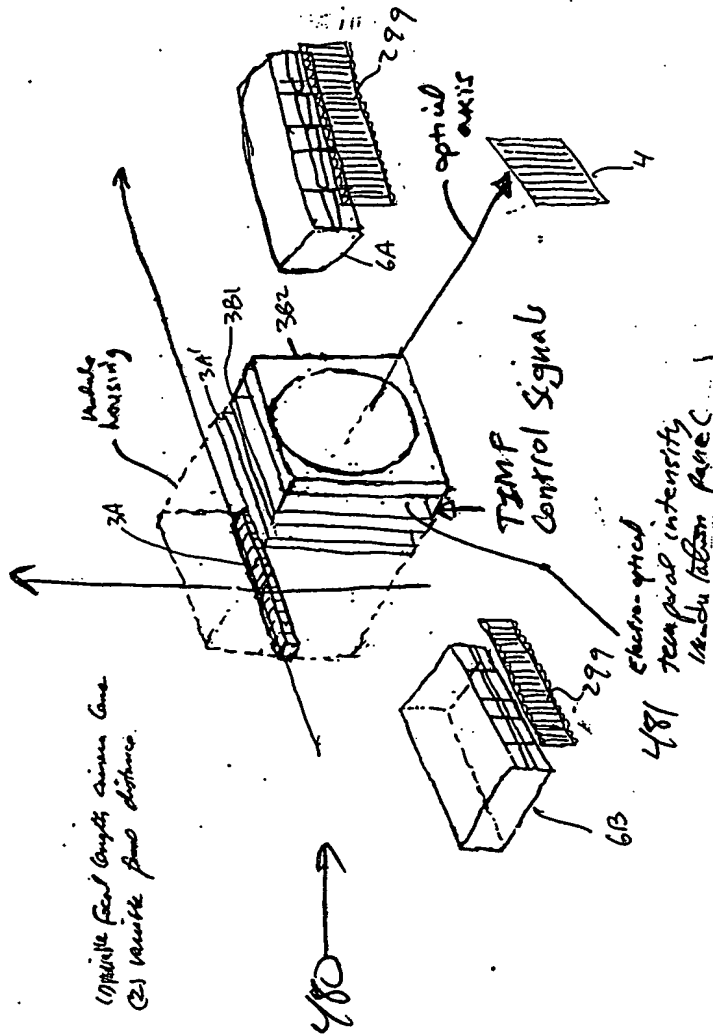


Fig. 11 z4c

7/1/85

EIGHT GENERALIZED METHOD OF REDUCING THE SPECKLE PATTERN
NOISE OBSERVED IN PLIIM-BASED IMAGING SYSTEMS

A

Use a PLIIM-BASED Imager to produce a series of consecutively captured digital images of an object over a series of photo-integration time periods of the PLIIM-Based Imager, wherein each digital image of the object includes a substantially different speckle noise pattern produced by natural oscillatory micro-motion and/or forced oscillatory micro-movement of the Imager relative to the object during operation of the PLIIM-Based Imager.

B

Store the series of consecutively captured digital images of the object in buffer memory within the PLIIM-Based Imager.

C

Add relatively small (e.g. 3x3) windowed image processing filters to the additively combine and average the pixel data in the series of consecutively captured digital images so as to produce a reconstructed digital image having a speckle noise pattern with reduced RMS power.

FIG. 1124D

FIG. 1124D

72/385

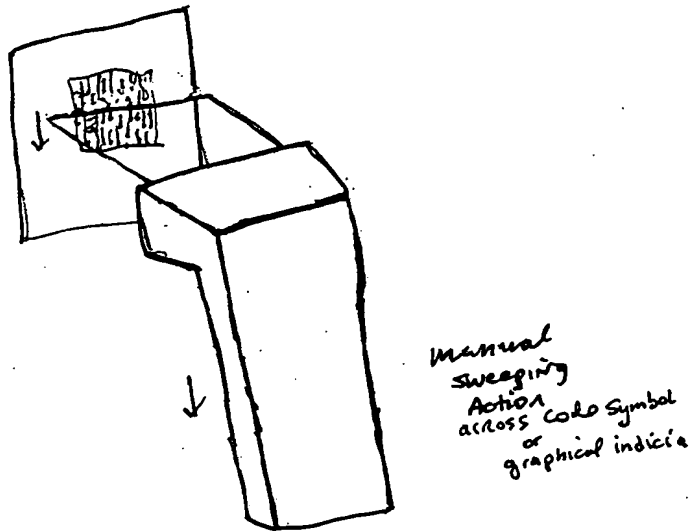
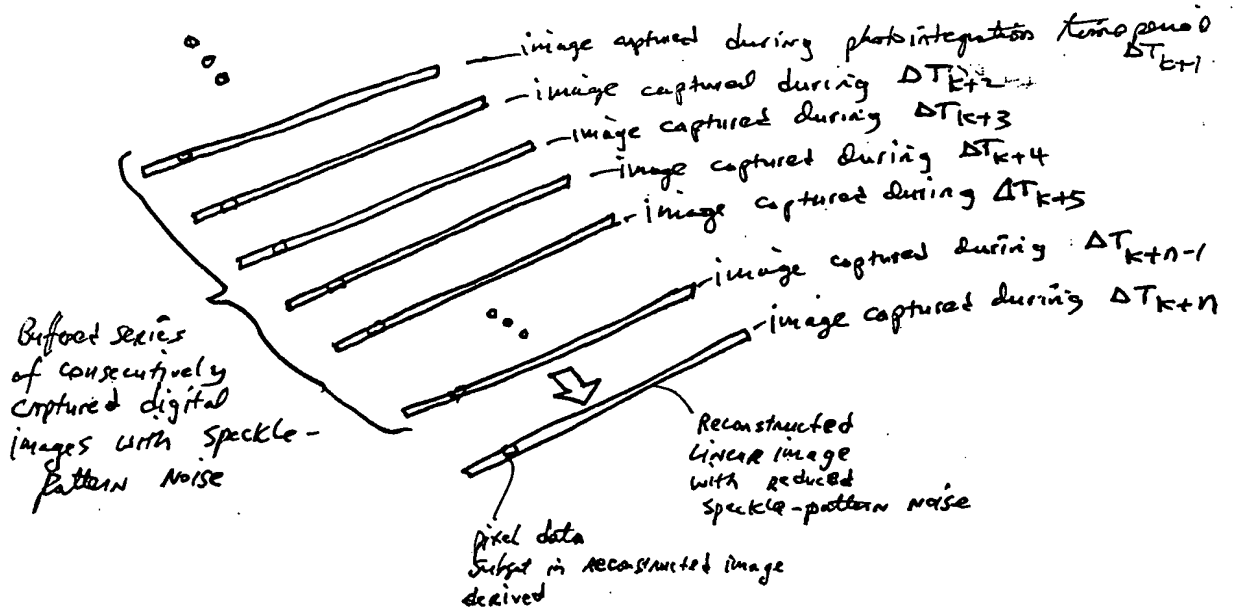


FIG. 1124E



Case: Linear image

FIG. 1124F

| 11134 | 11135 | 11136 | 11137 | 11138 | 11139 | 11140 | 11141 | 11142 | 11143 | 11144 | 11145 | 11146 | 11147 | 11148 | 11149 | 11150 | 11151 | 11152 | 11153 | 11154 | 11155 | 11156 | 11157 | 11158 | 11159 | 11160 | 11161 | 11162 | 11163 | 11164 | 11165 | 11166 | 11167 | 11168 | 11169 | 11170 | 11171 | 11172 | 11173 | 11174 | 11175 | 11176 | 11177 | 11178 | 11179 | 11180 | 11181 | 11182 | 11183 | 11184 | 11185 | 11186 | 11187 | 11188 | 11189 | 11190 | 11191 | 11192 | 11193 | 11194 | 11195 | 11196 | 11197 | 11198 | 11199 | 11200 |
|-------|-------|-------|-------|-------|-------|-------|-------|-------|-------|-------|-------|-------|-------|-------|-------|-------|-------|-------|-------|-------|-------|-------|-------|-------|-------|-------|-------|-------|-------|-------|-------|-------|-------|-------|-------|-------|-------|-------|-------|-------|-------|-------|-------|-------|-------|-------|-------|-------|-------|-------|-------|-------|-------|-------|-------|-------|-------|-------|-------|-------|-------|-------|-------|-------|-------|-------|
| 11134 | 11135 | 11136 | 11137 | 11138 | 11139 | 11140 | 11141 | 11142 | 11143 | 11144 | 11145 | 11146 | 11147 | 11148 | 11149 | 11150 | 11151 | 11152 | 11153 | 11154 | 11155 | 11156 | 11157 | 11158 | 11159 | 11160 | 11161 | 11162 | 11163 | 11164 | 11165 | 11166 | 11167 | 11168 | 11169 | 11170 | 11171 | 11172 | 11173 | 11174 | 11175 | 11176 | 11177 | 11178 | 11179 | 11180 | 11181 | 11182 | 11183 | 11184 | 11185 | 11186 | 11187 | 11188 | 11189 | 11190 | 11191 | 11192 | 11193 | 11194 | 11195 | 11196 | 11197 | 11198 | 11199 | 11200 |

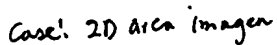
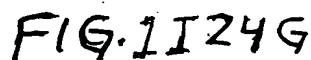


FIG 1I24H

74/385

NINTH GENERALIZED METHOD OF REDUCING SPECKLE PATTERN
NOISE IN PLIIM-BASED IMAGING SYSTEMS

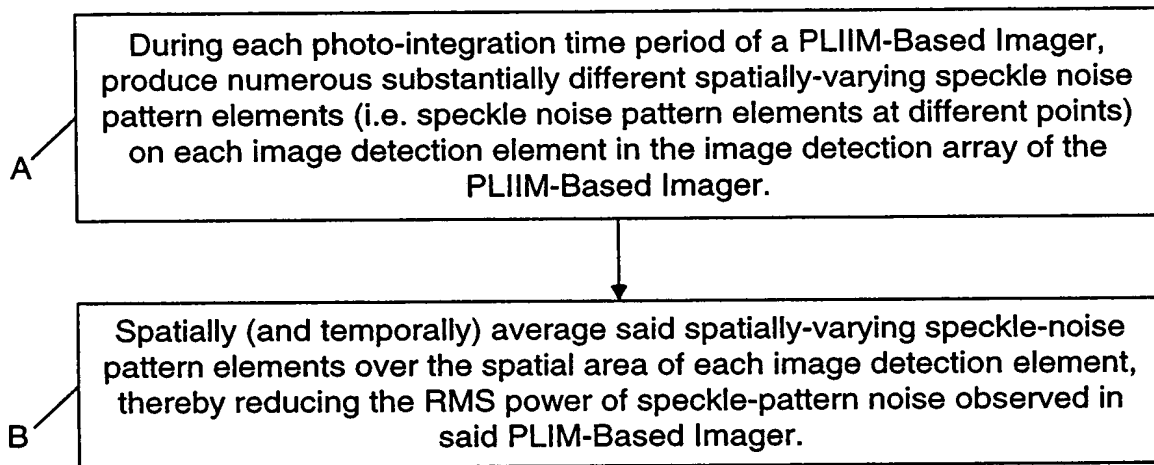


FIG. 1124I

75/385

860

861

862

863

864

865A

866

867

868

870

FOV of a magnified video detector element

Maximum working distance

FIG. 1I25A1

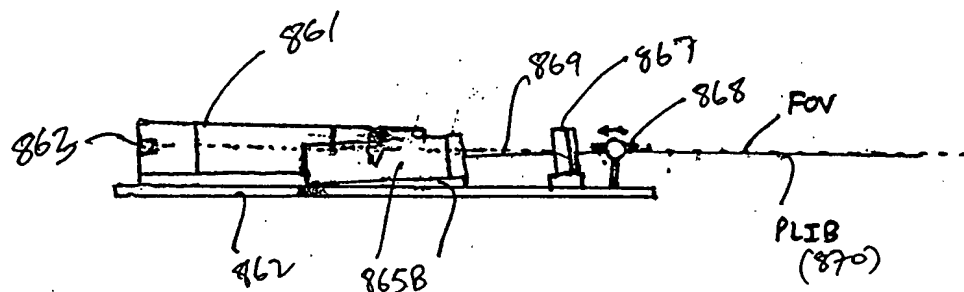


FIG. 1I25A2

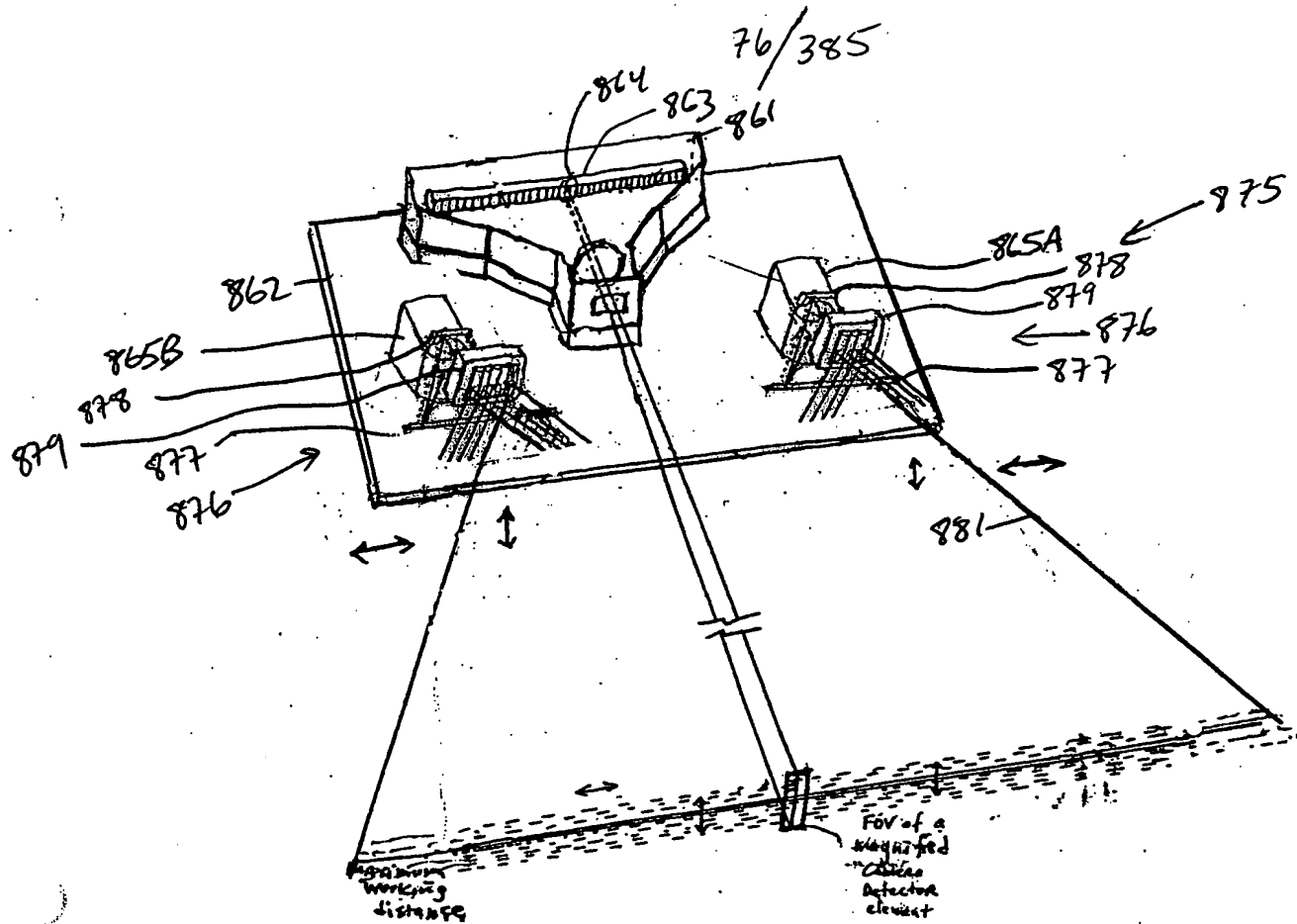


FIG. 1I25B1

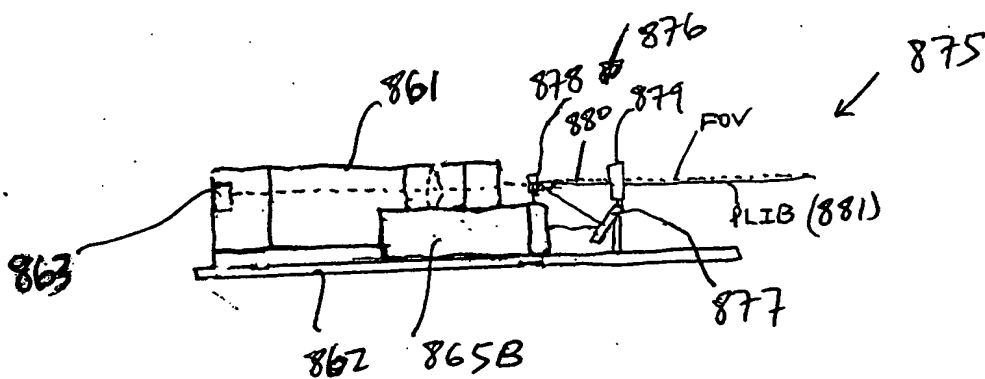
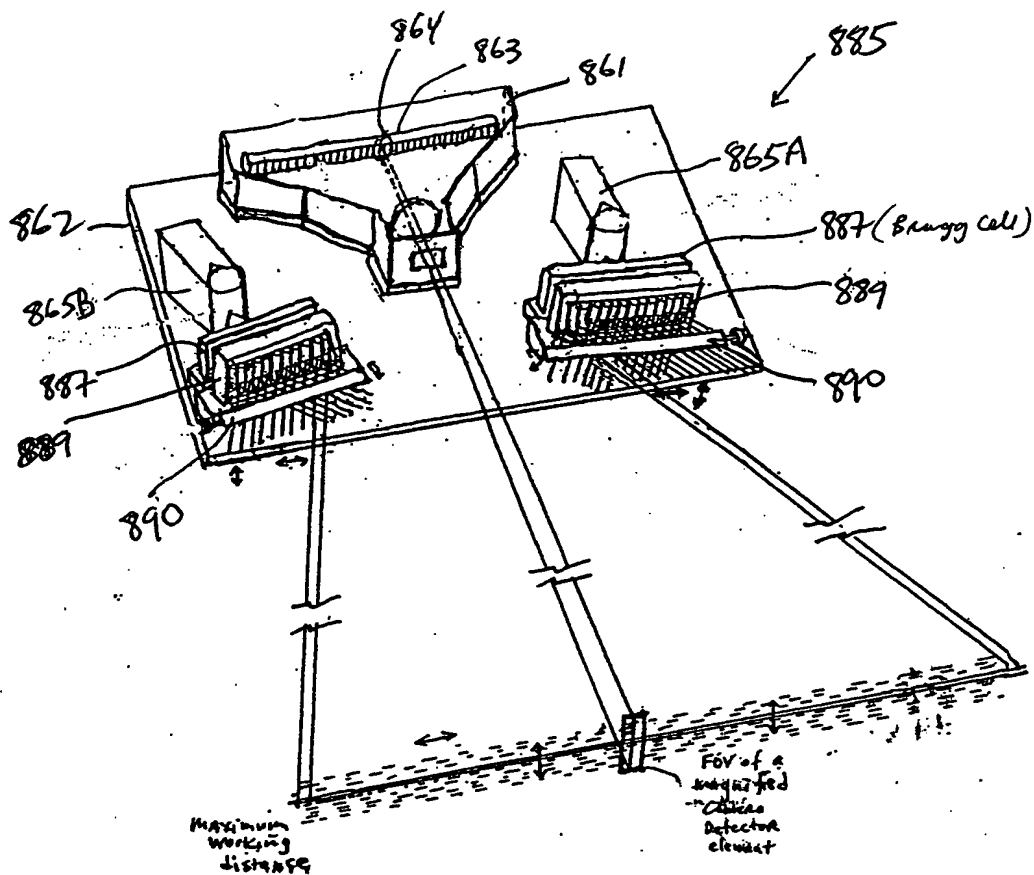


FIG. 1I25B2

0990555-11210

77/385



* Lateral and Transverse Microoscillation of PLIB

FIG. 1I25C1

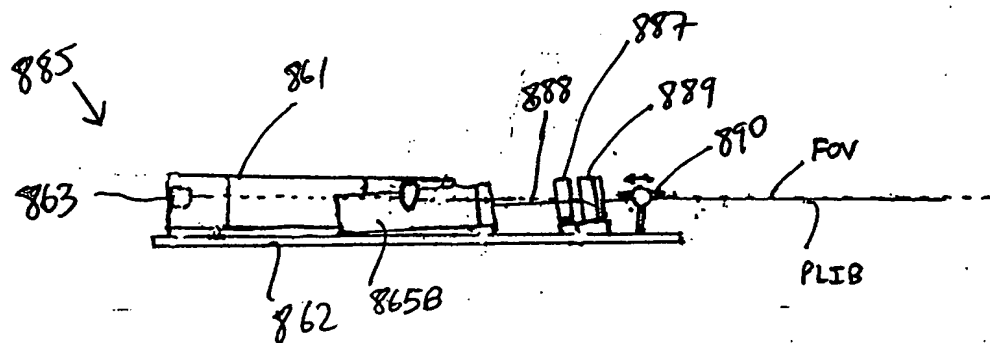


FIG. 1I25C2

09990585 112101

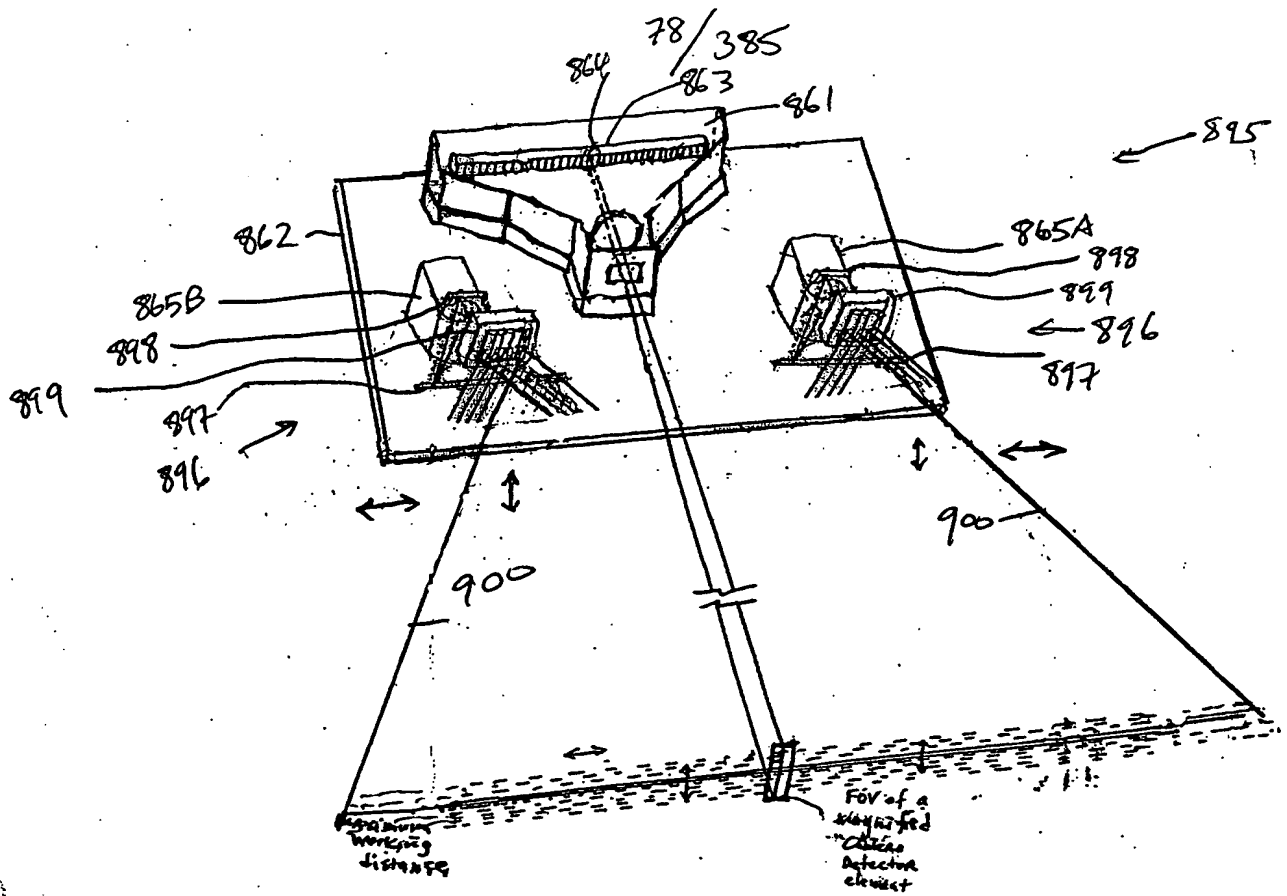


FIG. 1 I 25 D1

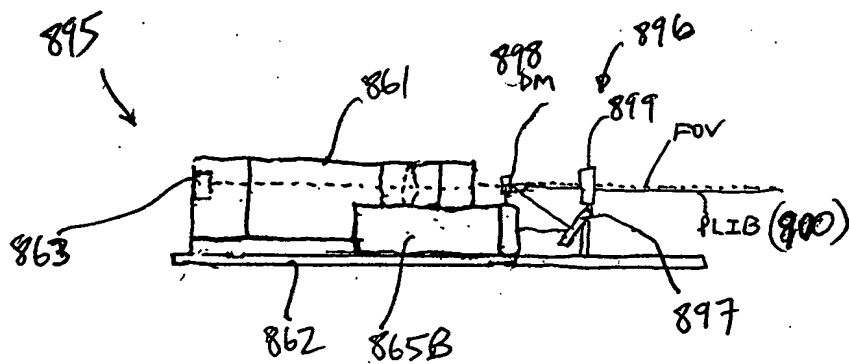


FIG. 1 I 25 D2

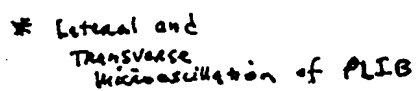
[illegible]

FIG. 1I 25E2

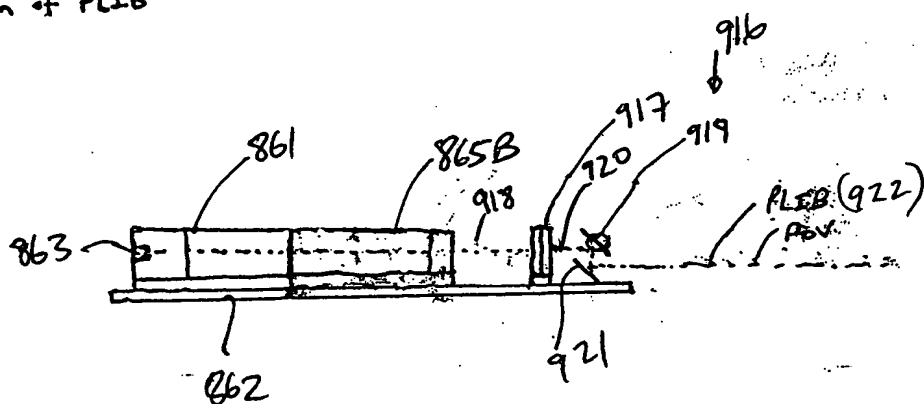
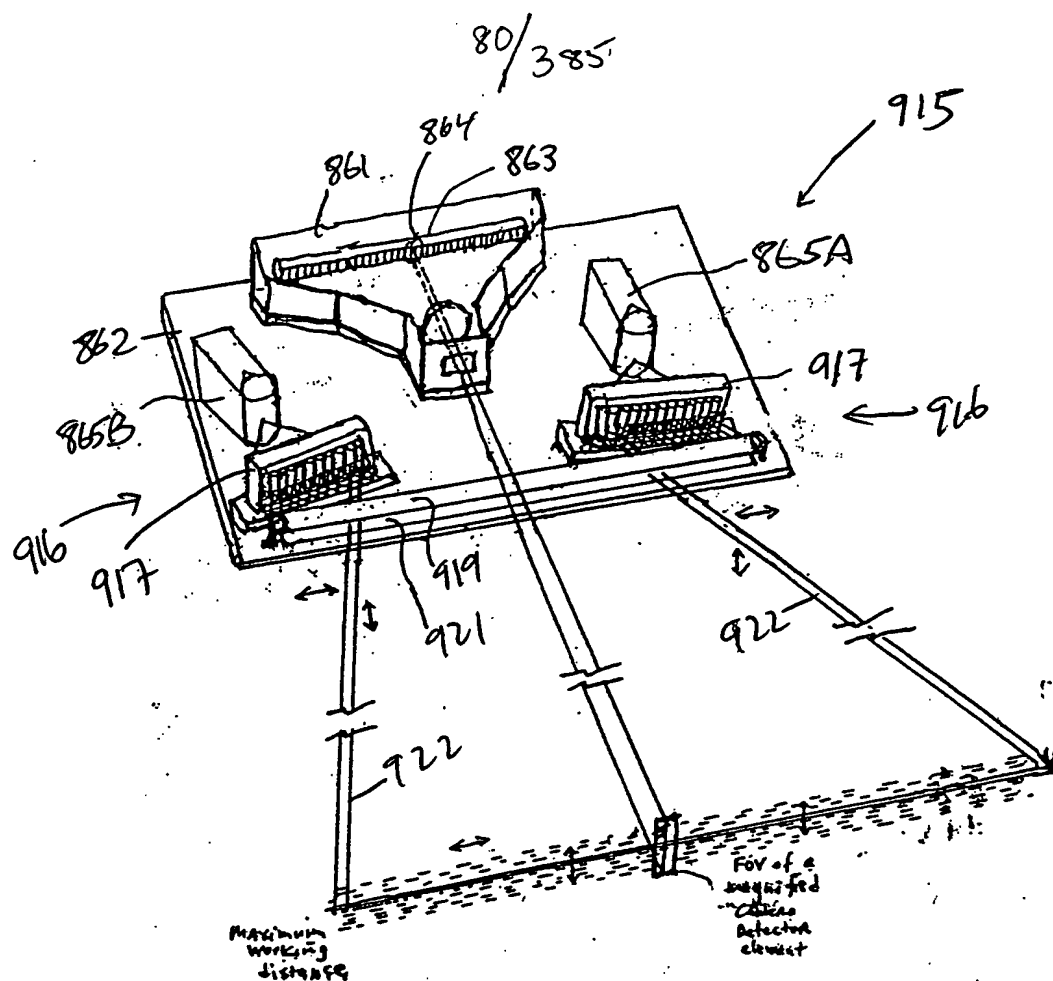
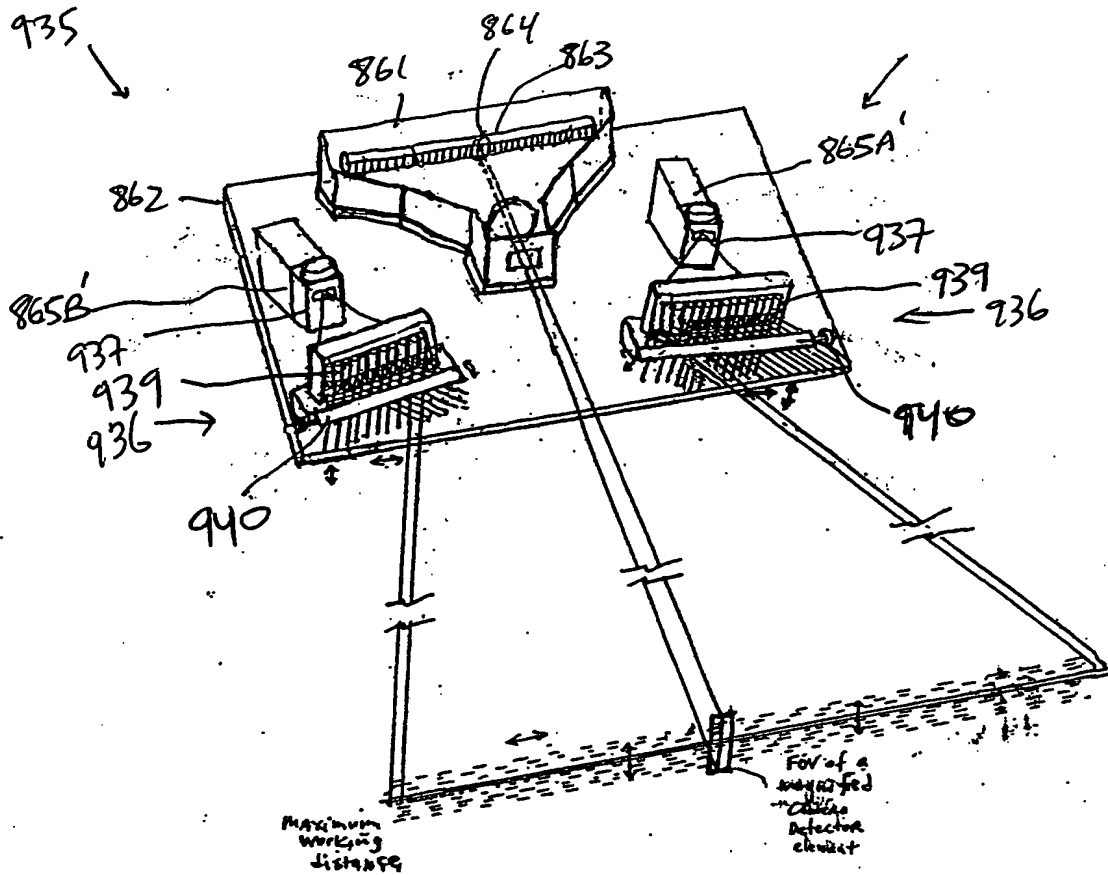


FIG. 1 is a perspective view of a system for detecting a target object. The system includes a base 925 with a sensor assembly 927 and a display 926. A target object 928 is positioned on a surface 930. A line of sight 929 is shown from the sensor assembly to the target object. A dashed line indicates the "Maximum working distance". A label "Fov of a magnified video detector circuit" points to a specific area on the surface 930.

925

FIG. 1I 25G2

82/385



* Lateral and Transverse Microoscillation of PLIB

FIG. 1I25H1

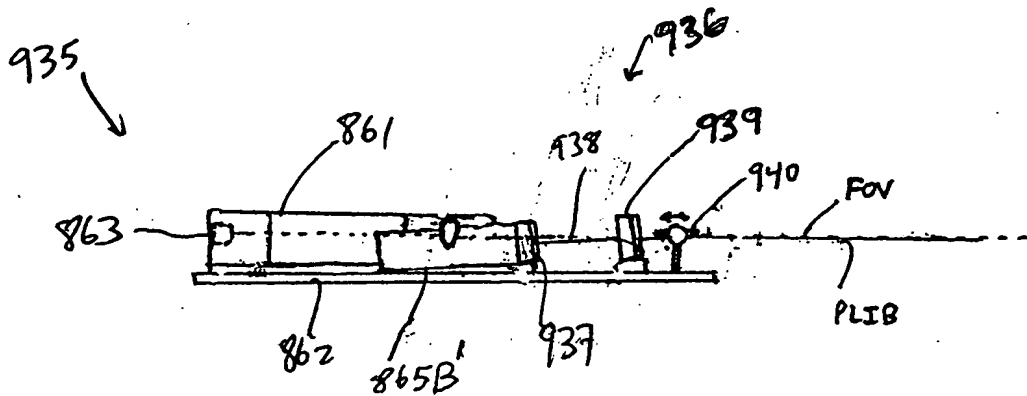
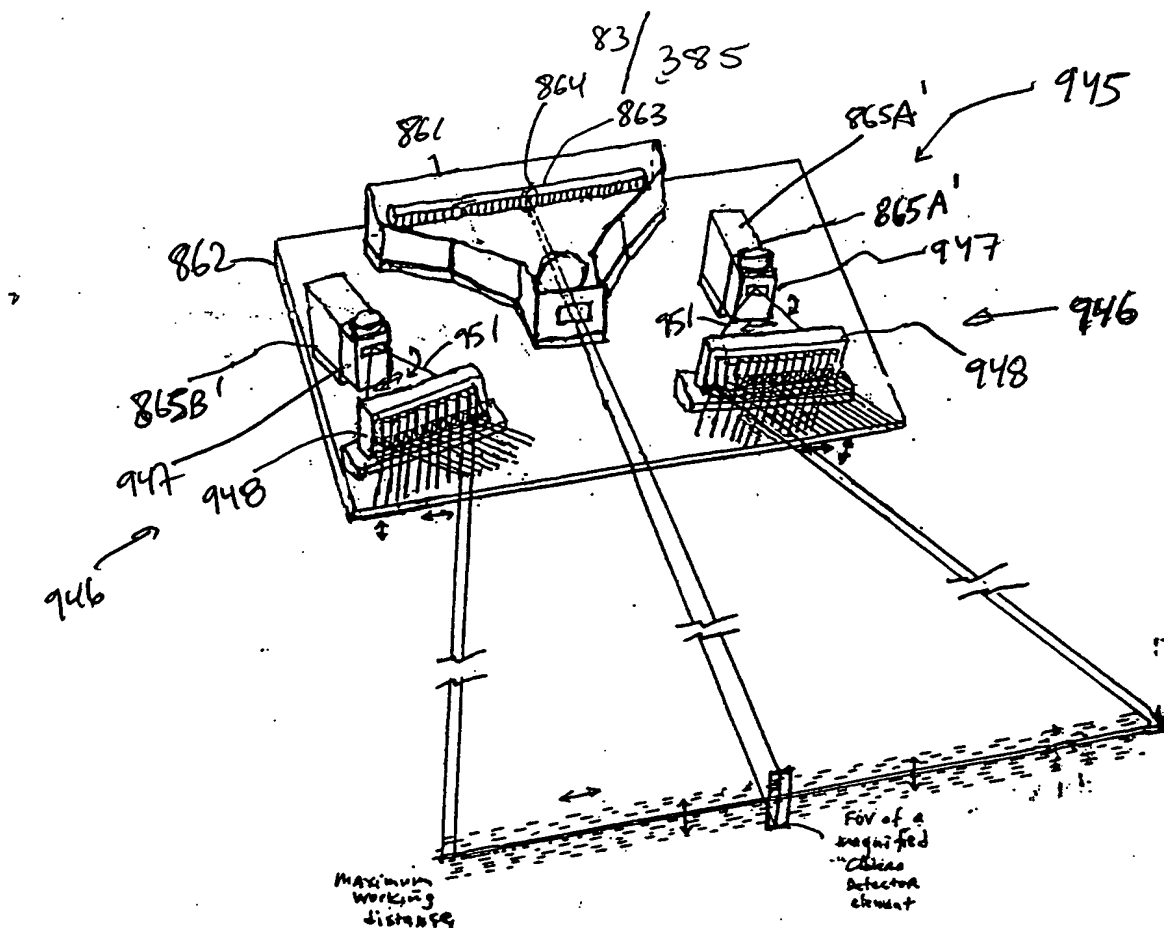


FIG. 1I25H2



Lateral and Transverse
Vibration of PLIB

FIG. 1 I 25 I 1

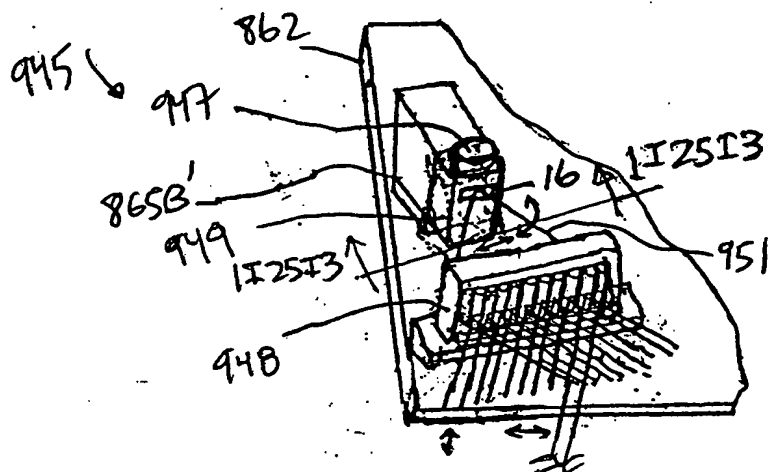


FIG. 1I25I2

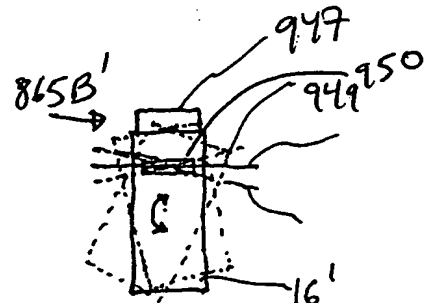


FIG. 1125I3

84/385

955

861

863

862

865B

865A

957 optical shutter

958

956

959

957

958

956

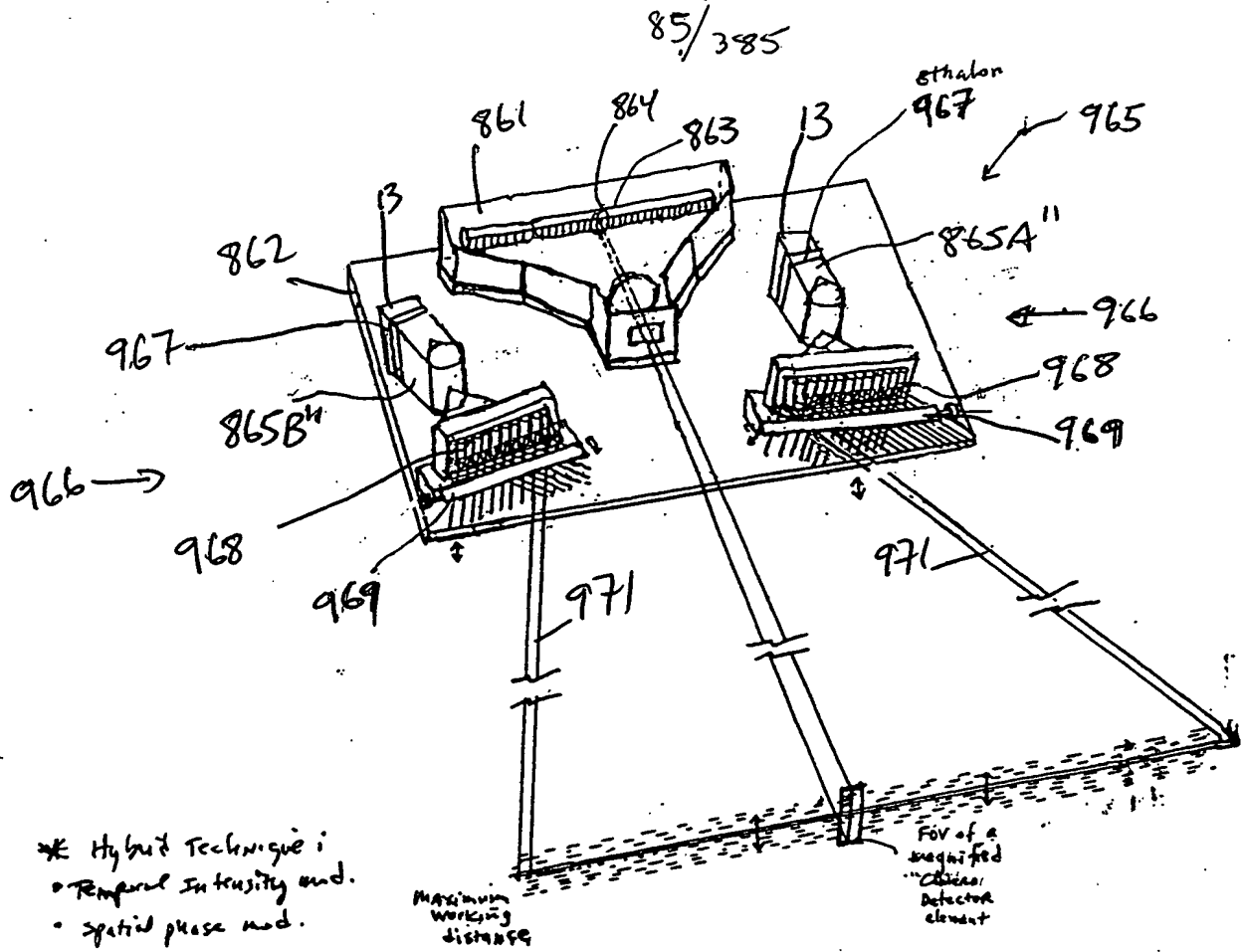
Maximum working distance

FOV of a magnified video detector element

* Hybrid Technique:

- Temporal intensity modulation
- Spatial modulation in transverse direction

FIG. 1 I 25 J 2



* Hybrid Technique i
• Temporal Intensity and.
• Spatial phase mod.

FIG. 1I25K1

* Transverse
vibration of PLIB

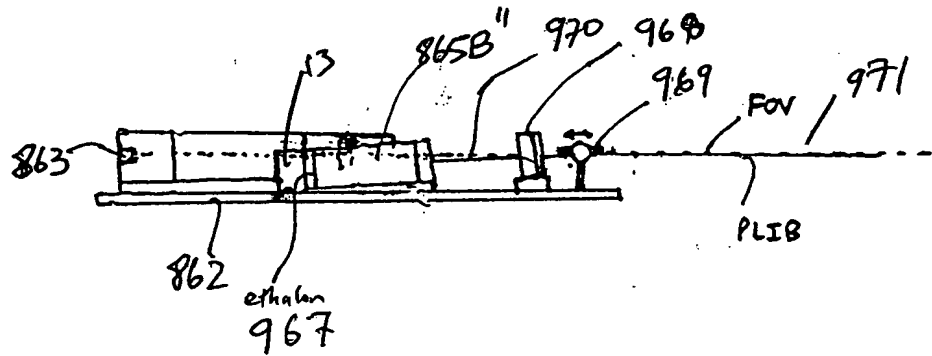
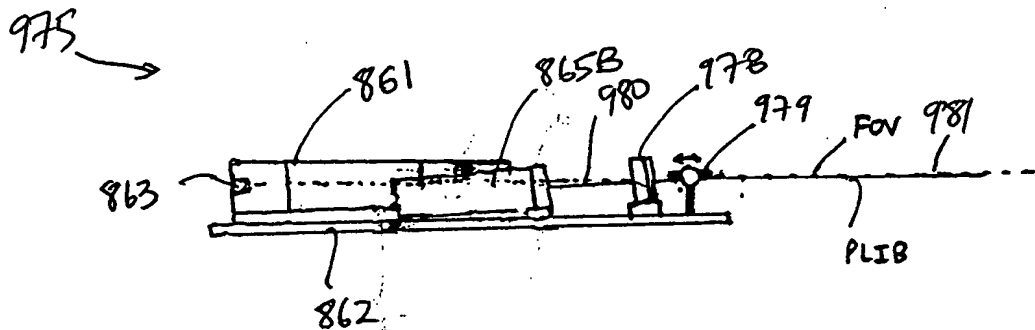
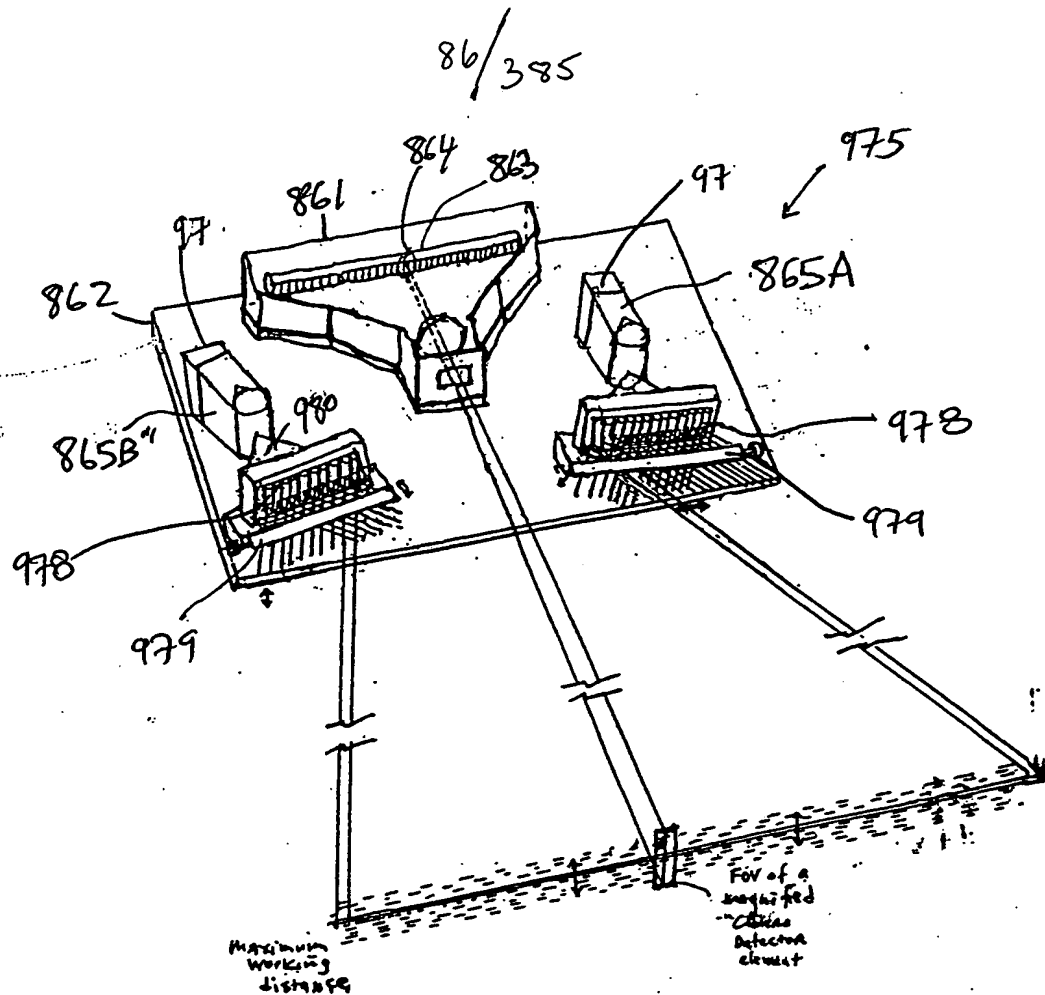
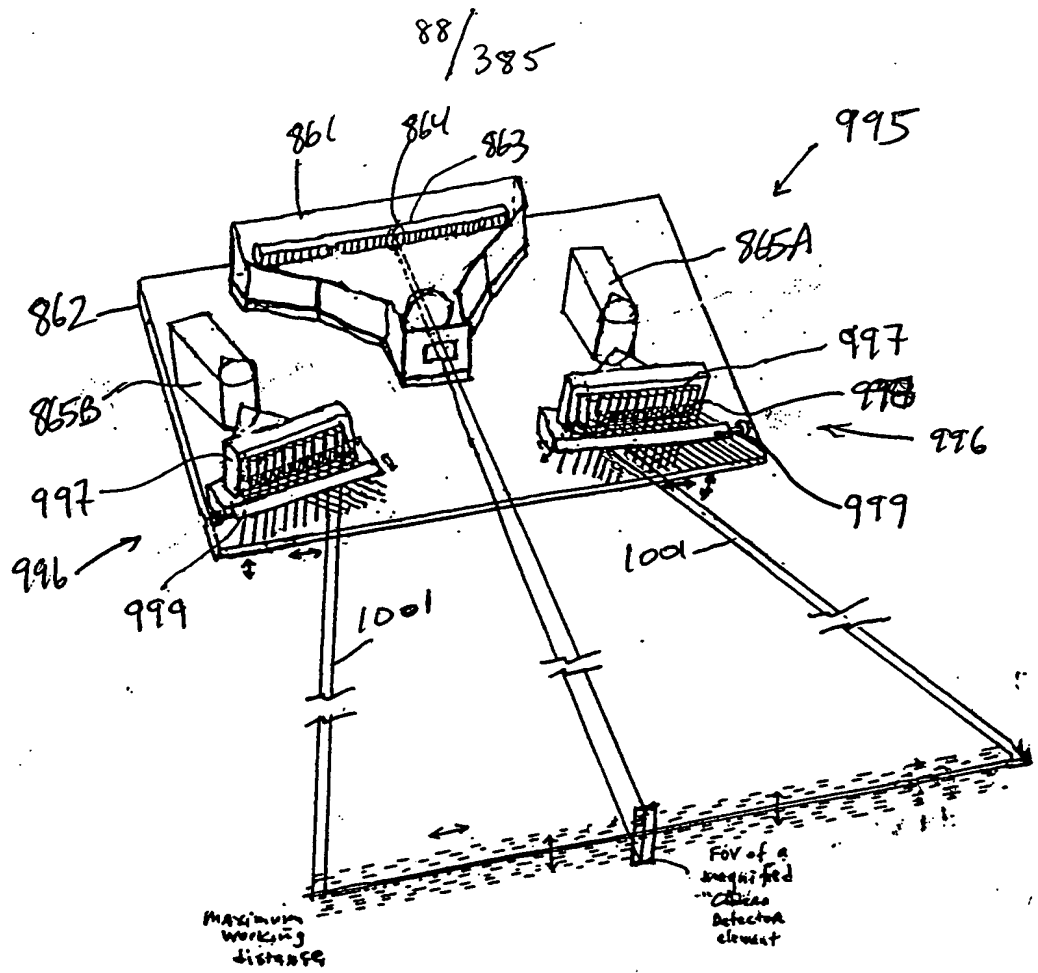


FIG. 1I25K2





hybrid:

- spatial intensity mod.
- spatial phase

* Lateral and Transverse Modulation of PLIB

FIG. 1I25N1

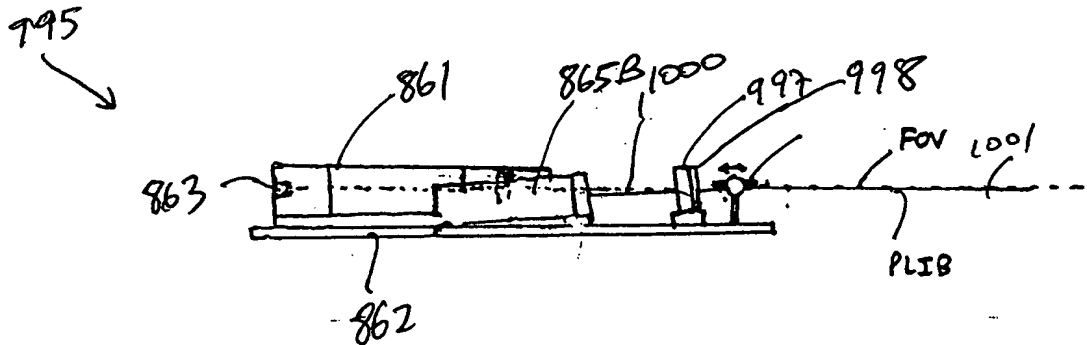


FIG. 1I25NZ

89/385

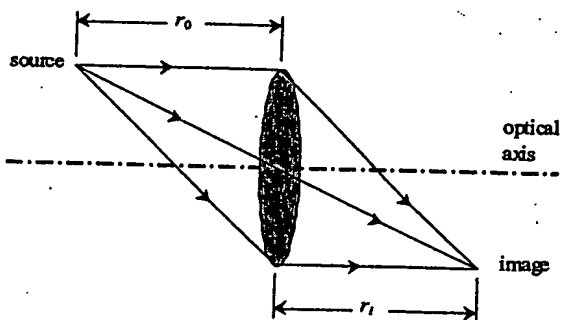


FIG. 1H1

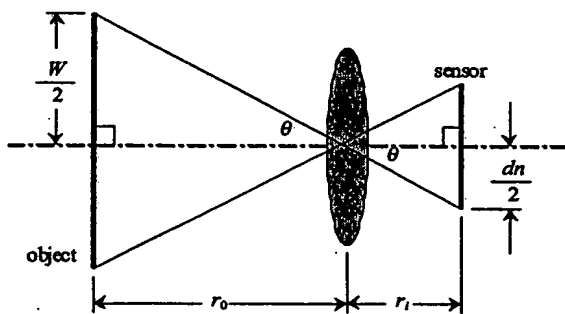


FIG. 1H2

09095-1101

90/385

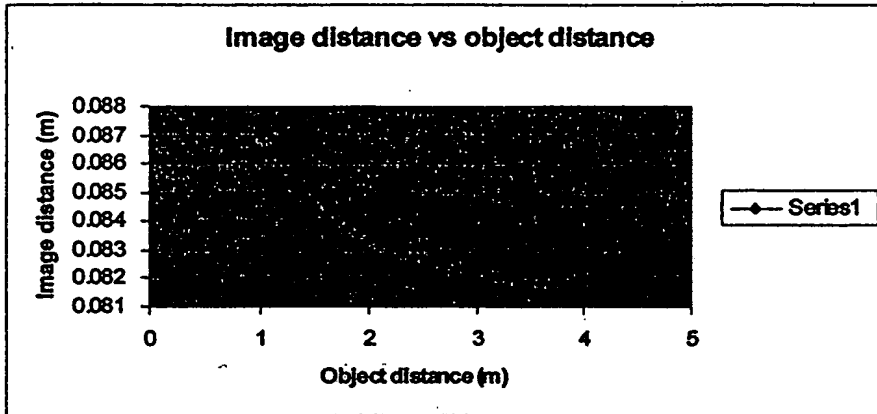


FIG. 1H3

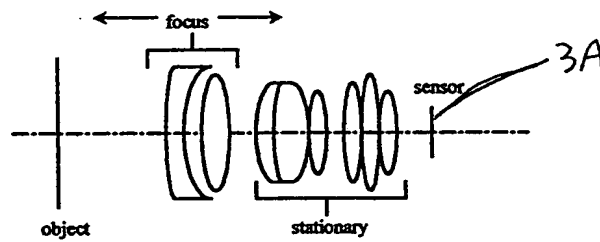


FIG. 1H4

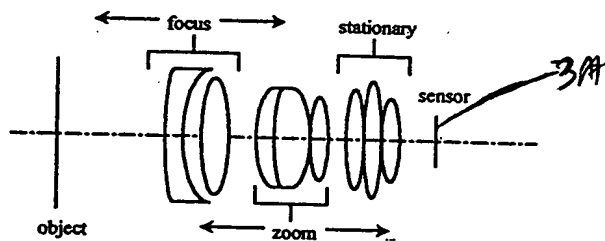
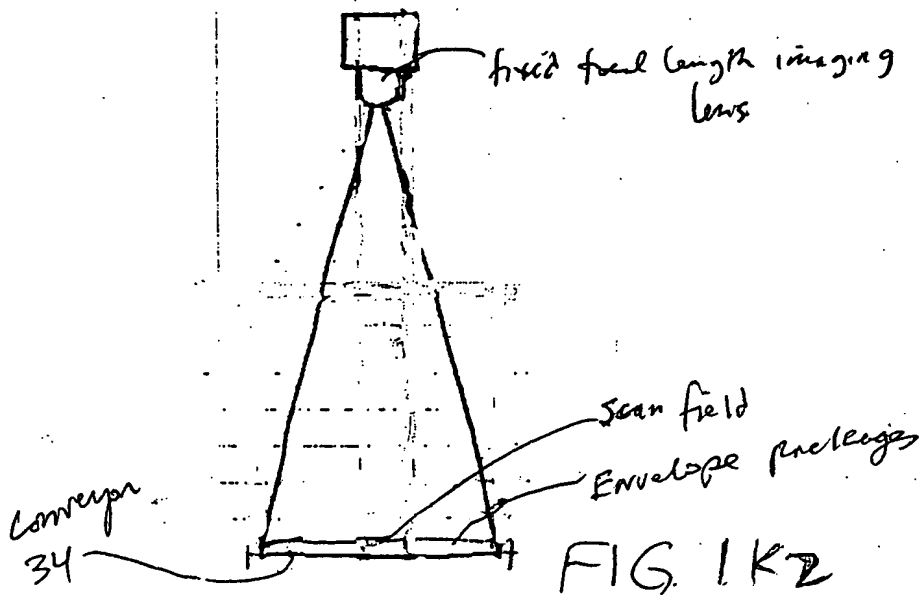
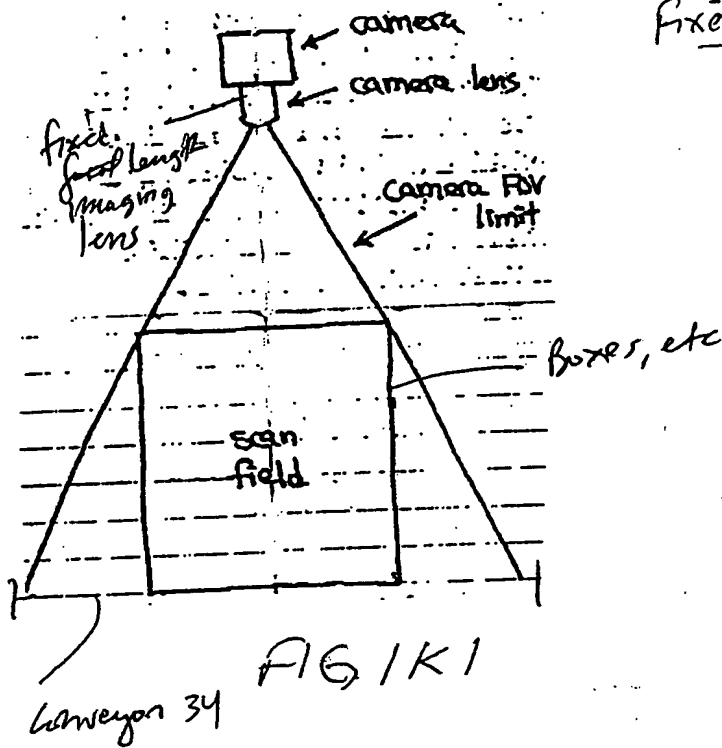


FIG. 1H5

91/385

Fixed focal length lens
cases



100

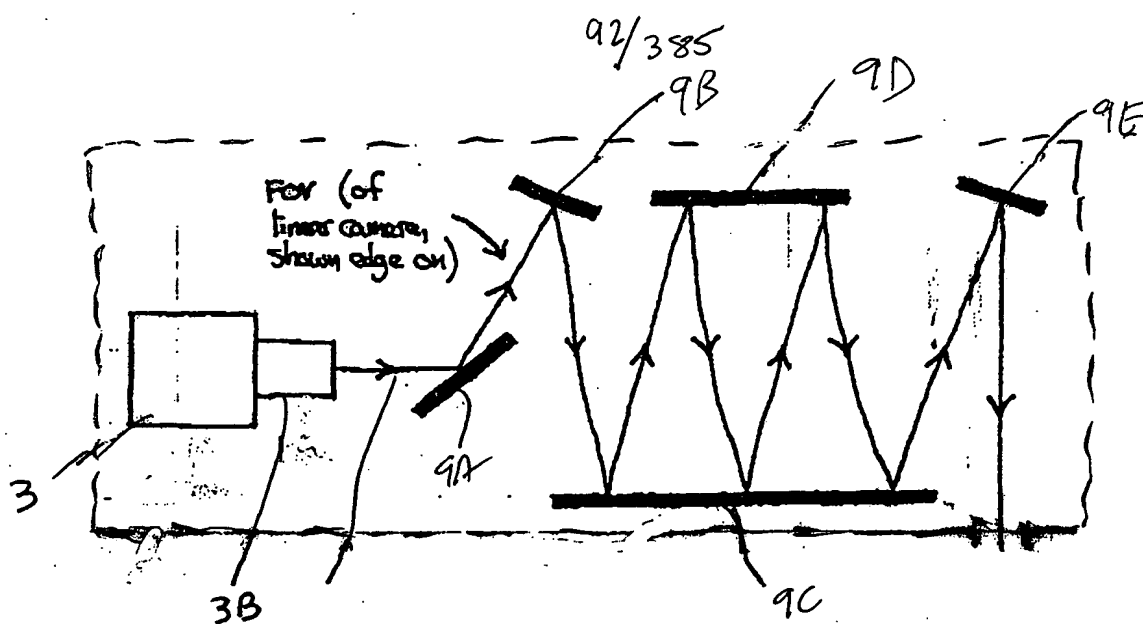


FIG. 1L1

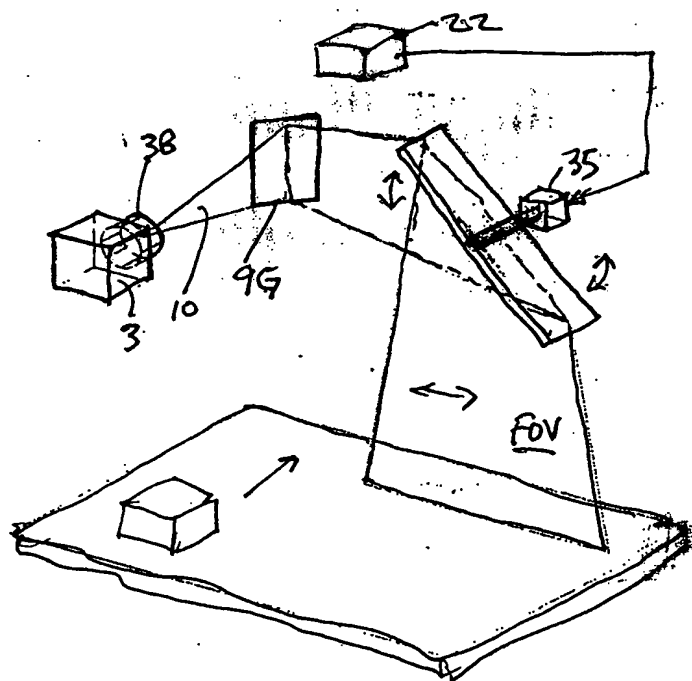


FIG. 1L2

93/385

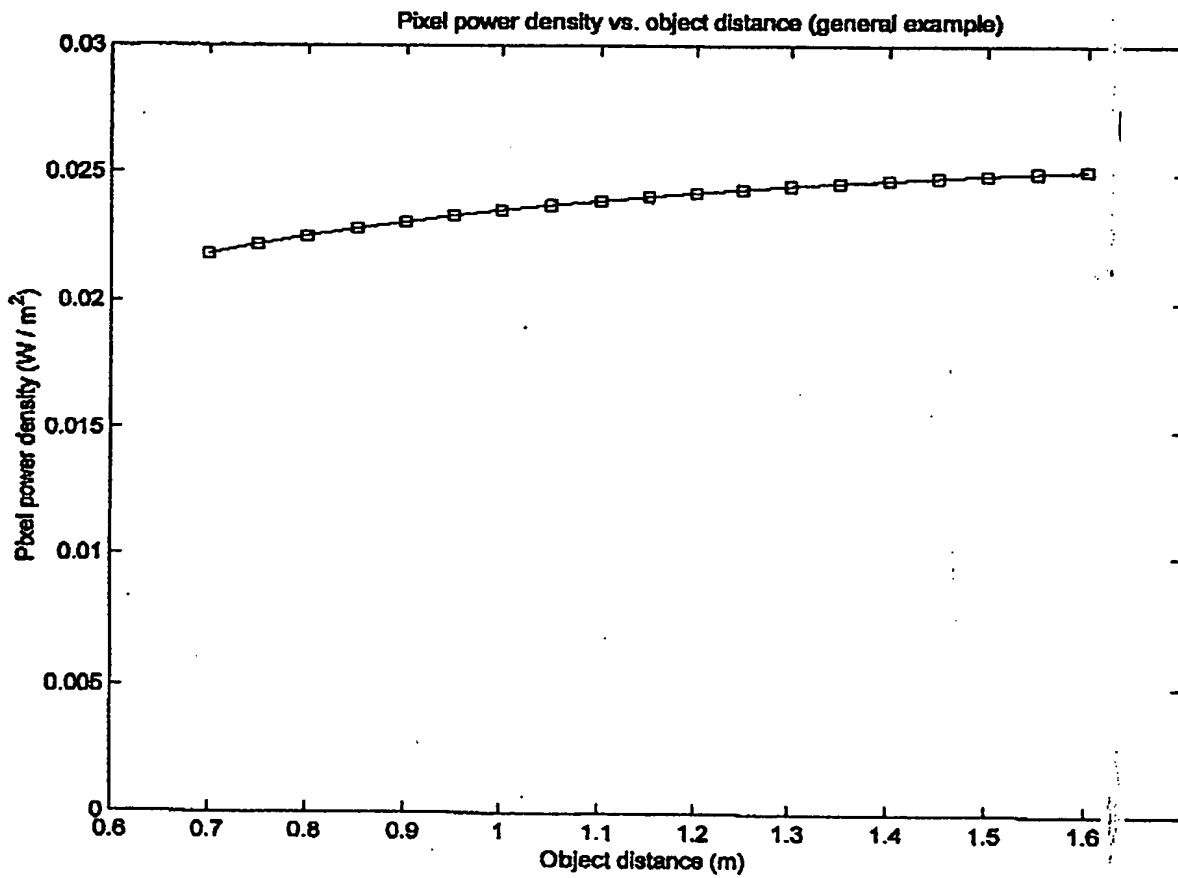


FIG-1M1

94/385

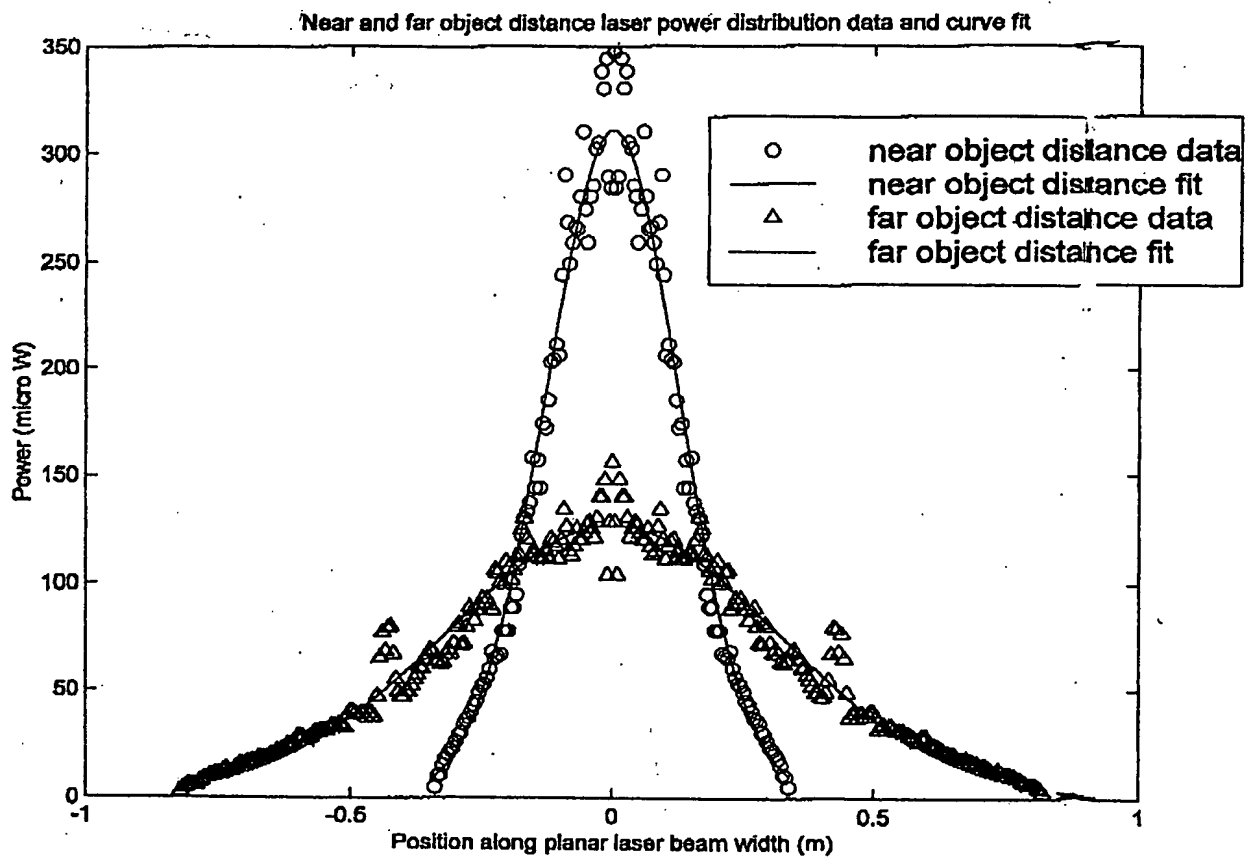


FIG. 1M2

95/385

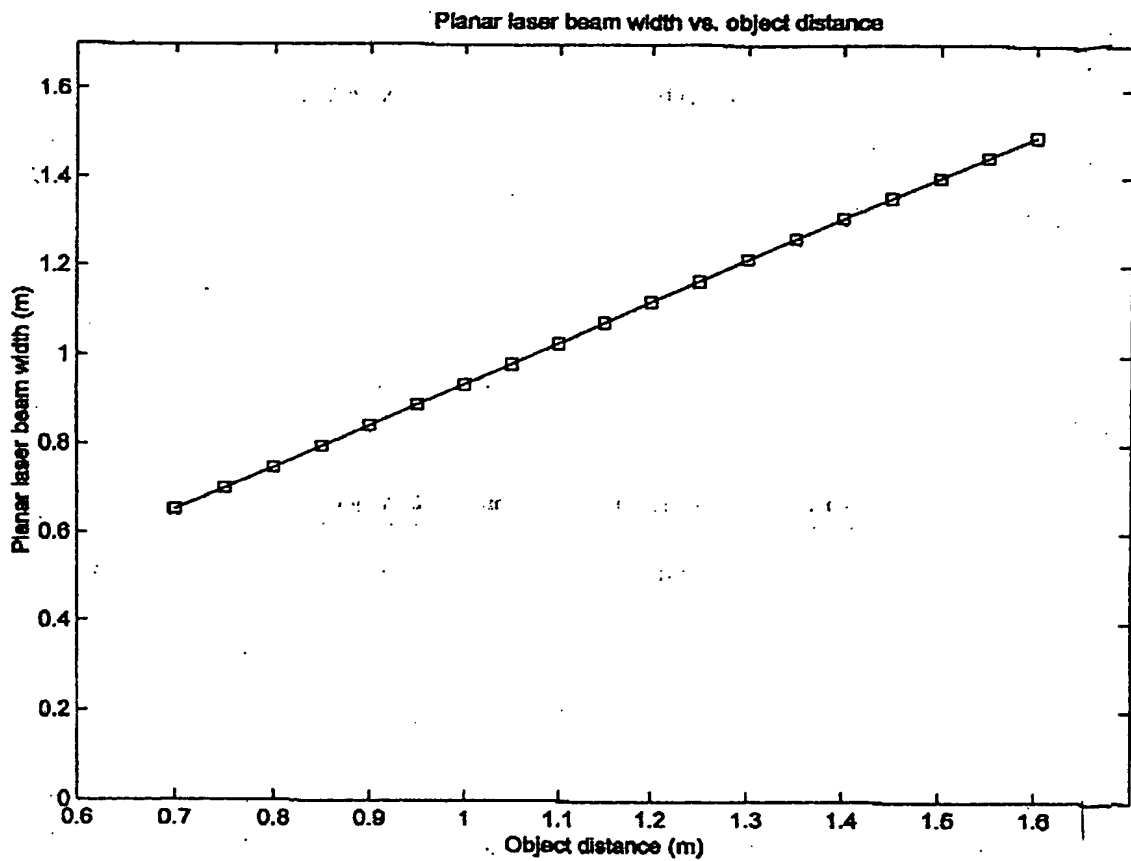


FIG. 1M3

96/385

Figure 4: Planar laser beam height vs. object distance (far object distance focus)

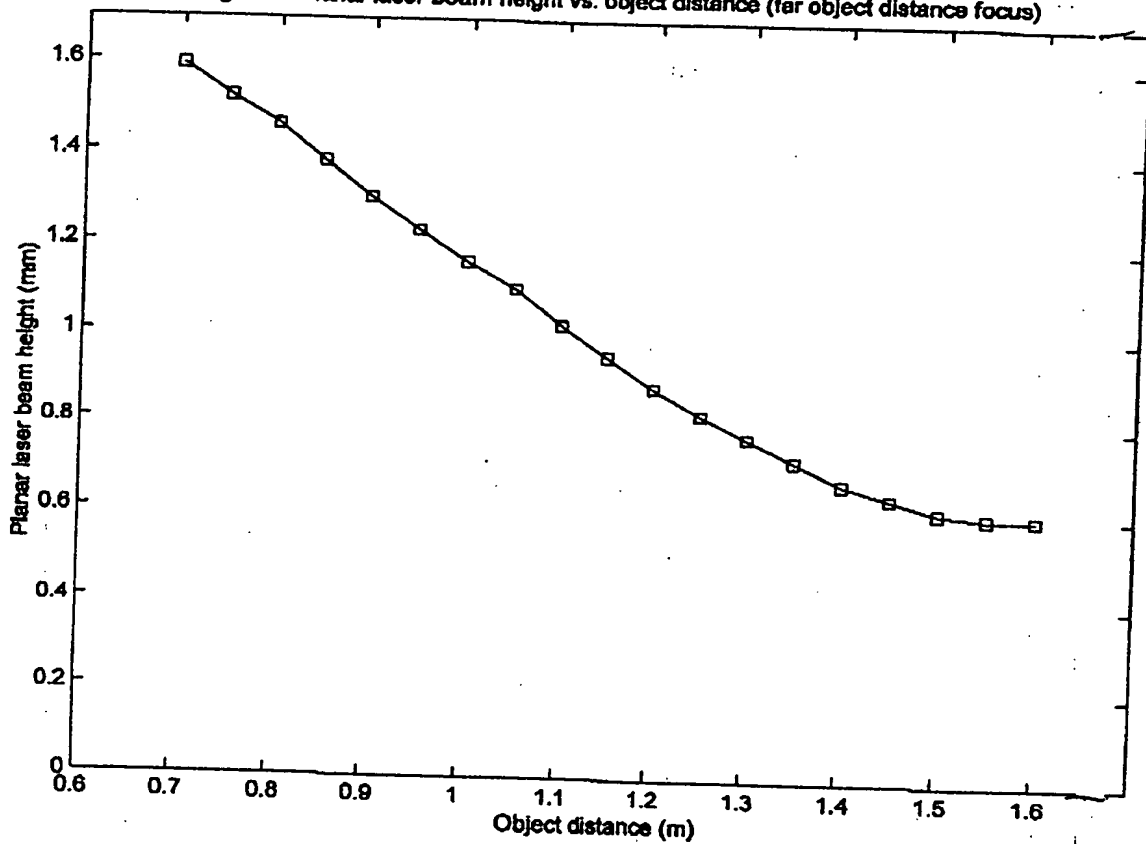


FIG 1M4

000055-140
TOTAL 5350660

97/385

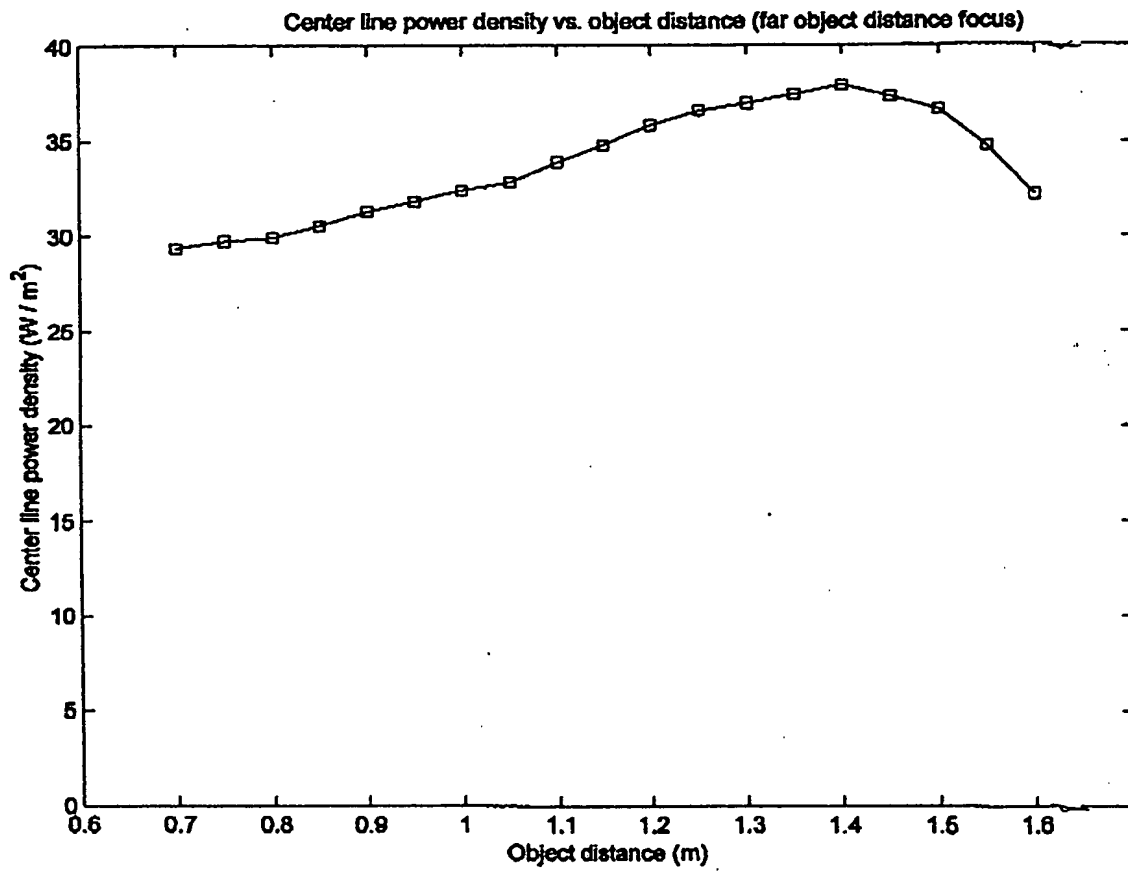


FIG. 1N

98/385

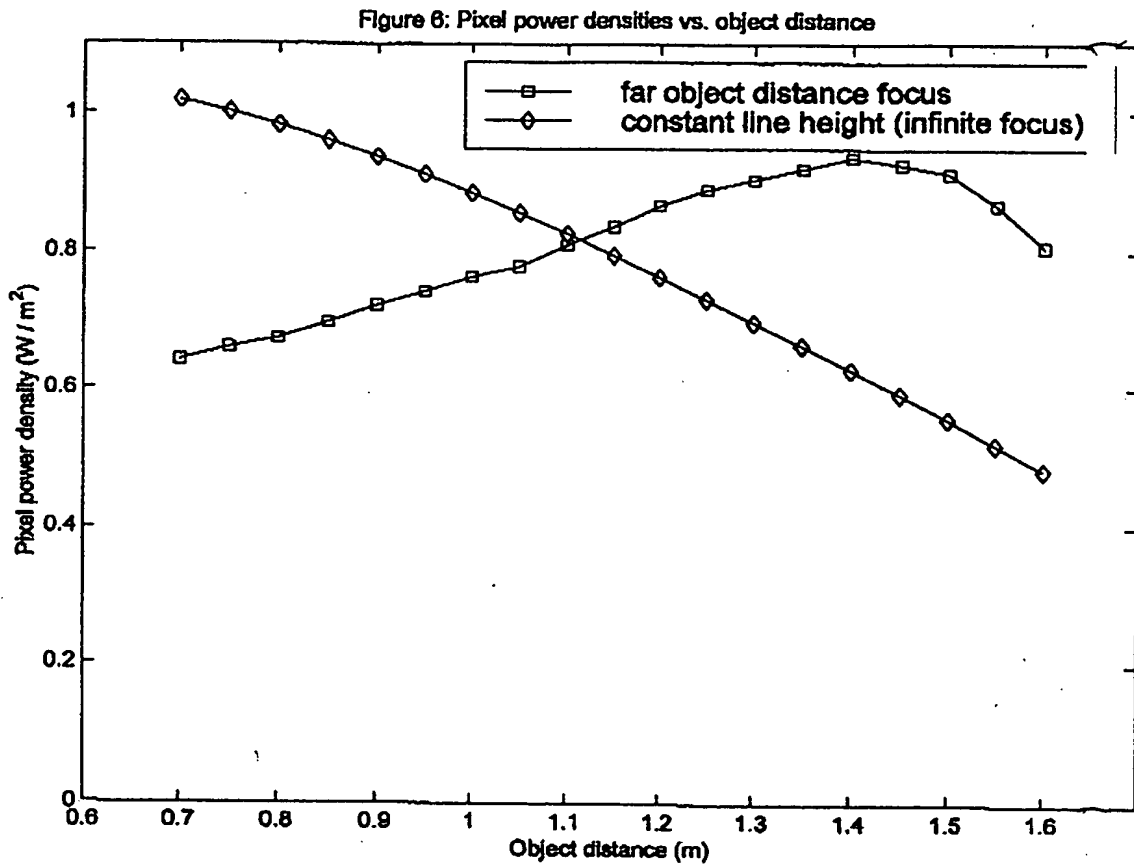


FIG. 10

FOUO 330660

99/385

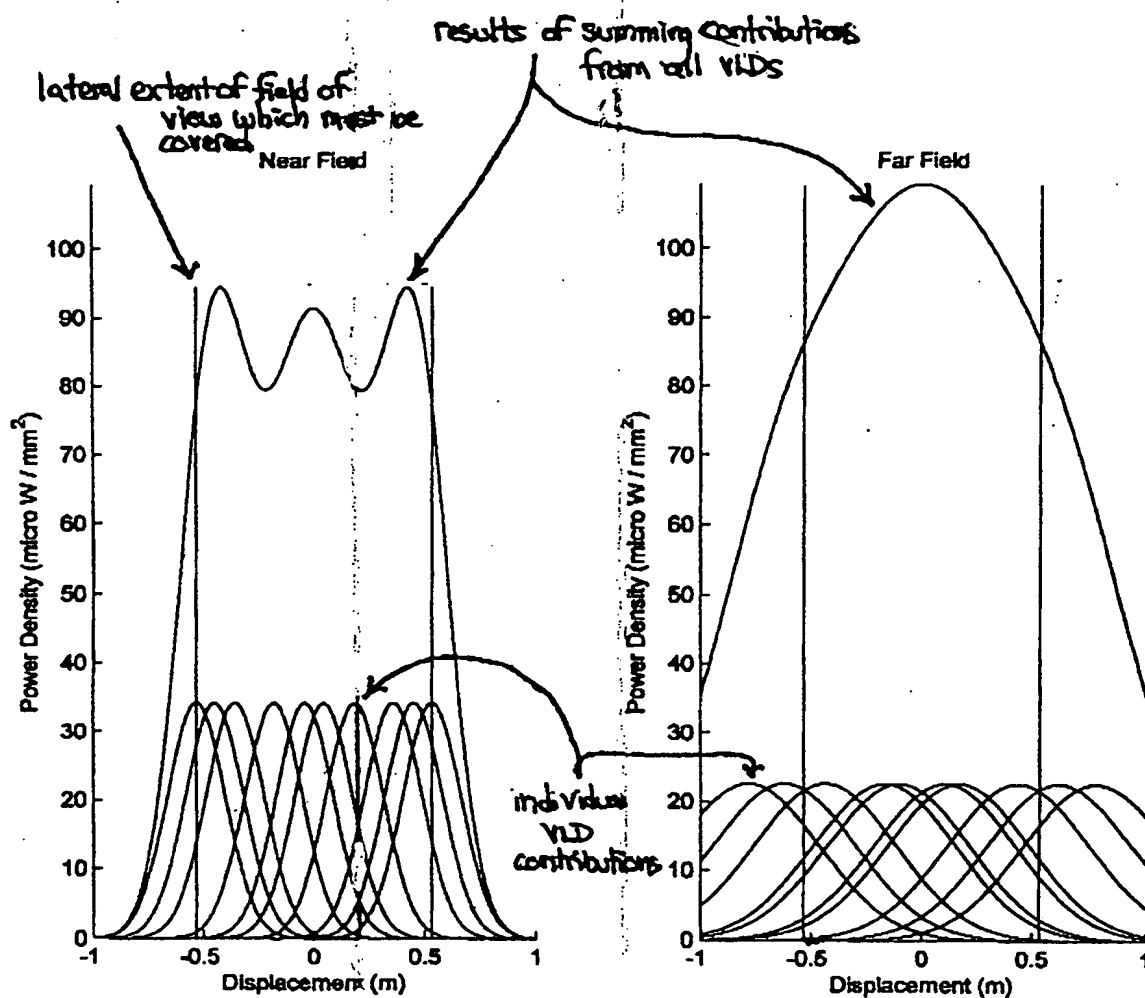


FIG 1P1

FIG 1P2

FIG. 100

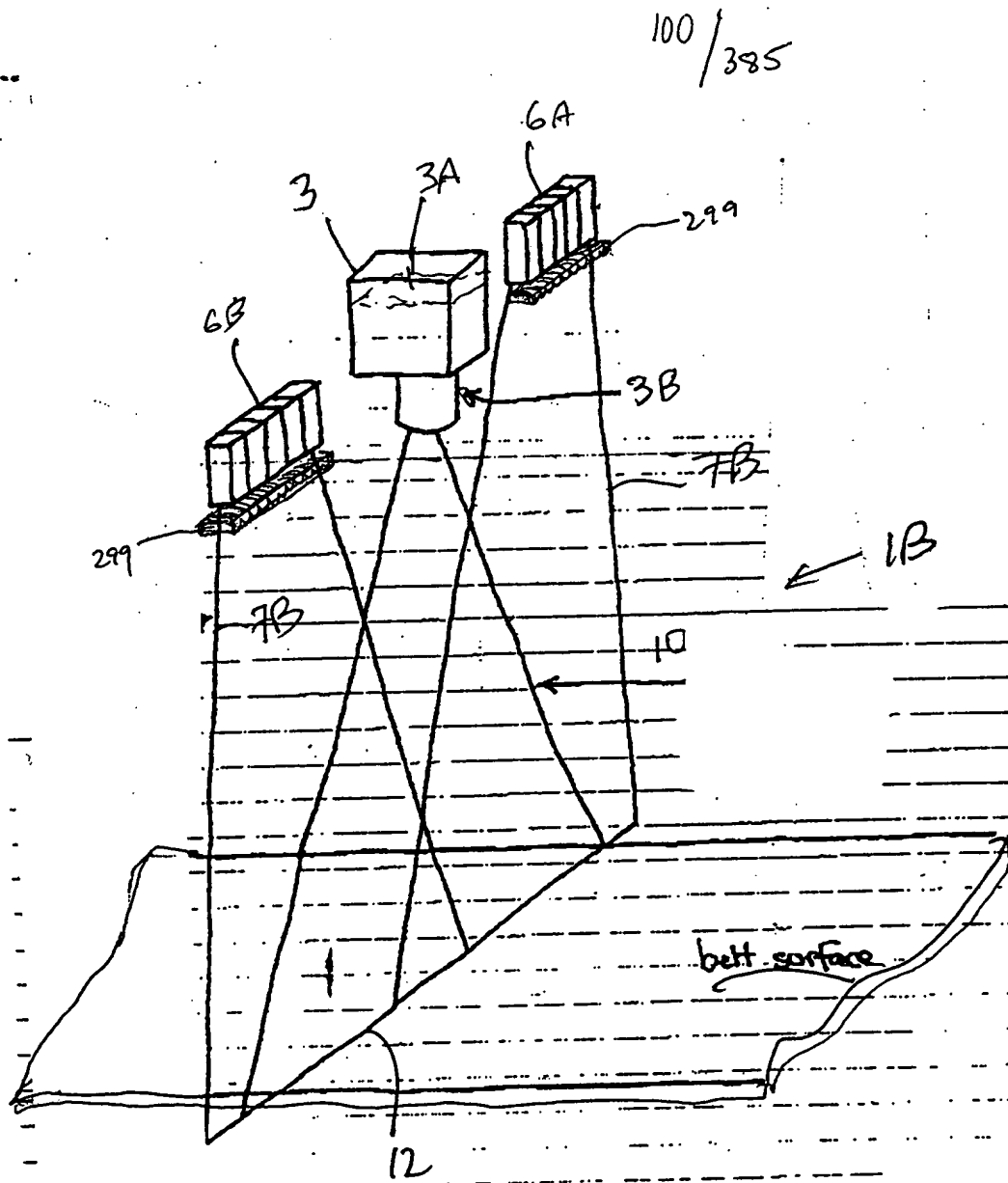


FIG. 101

101/385



Bob



TOTET 58506660

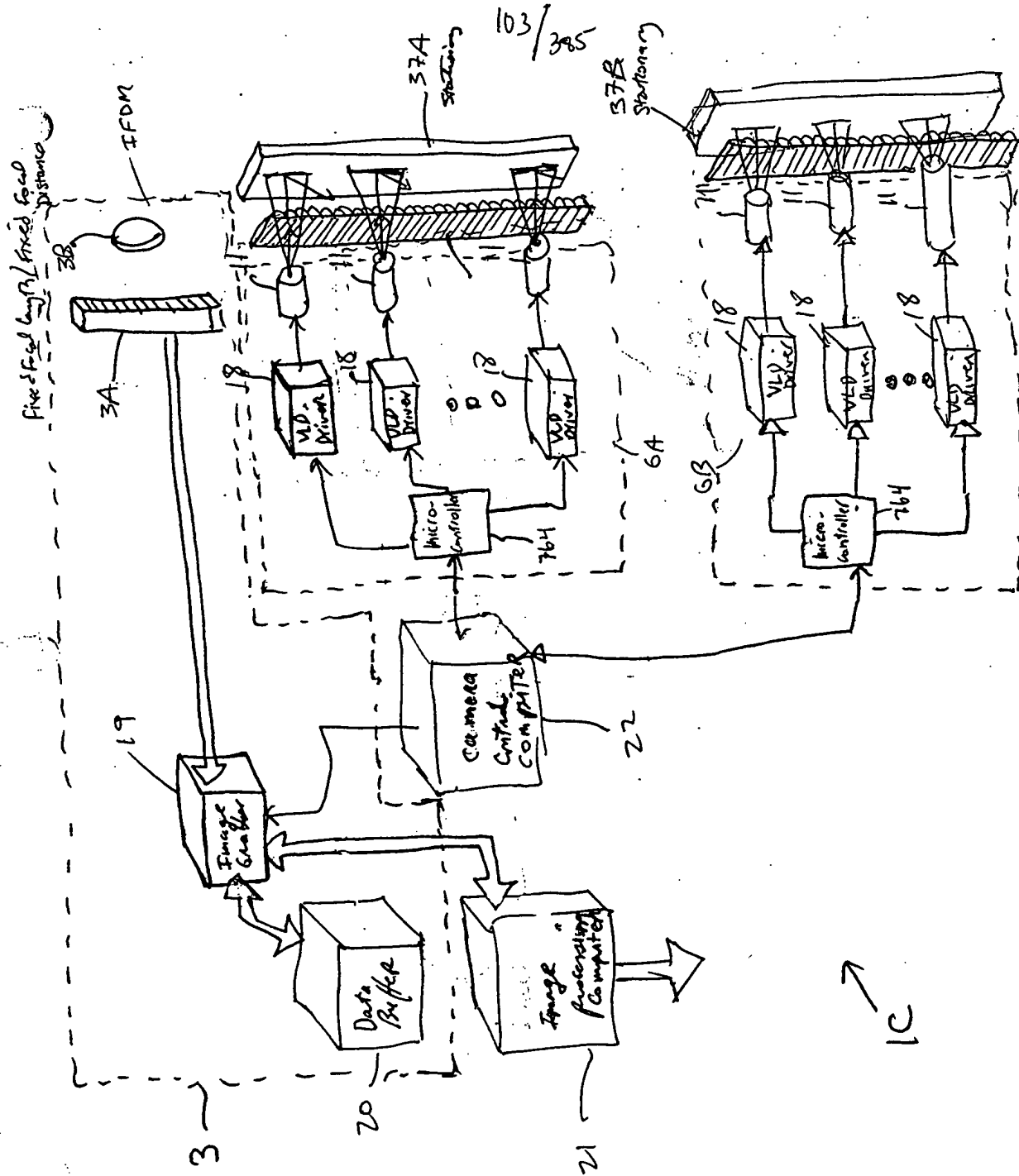


FIG. 1R2

104/385

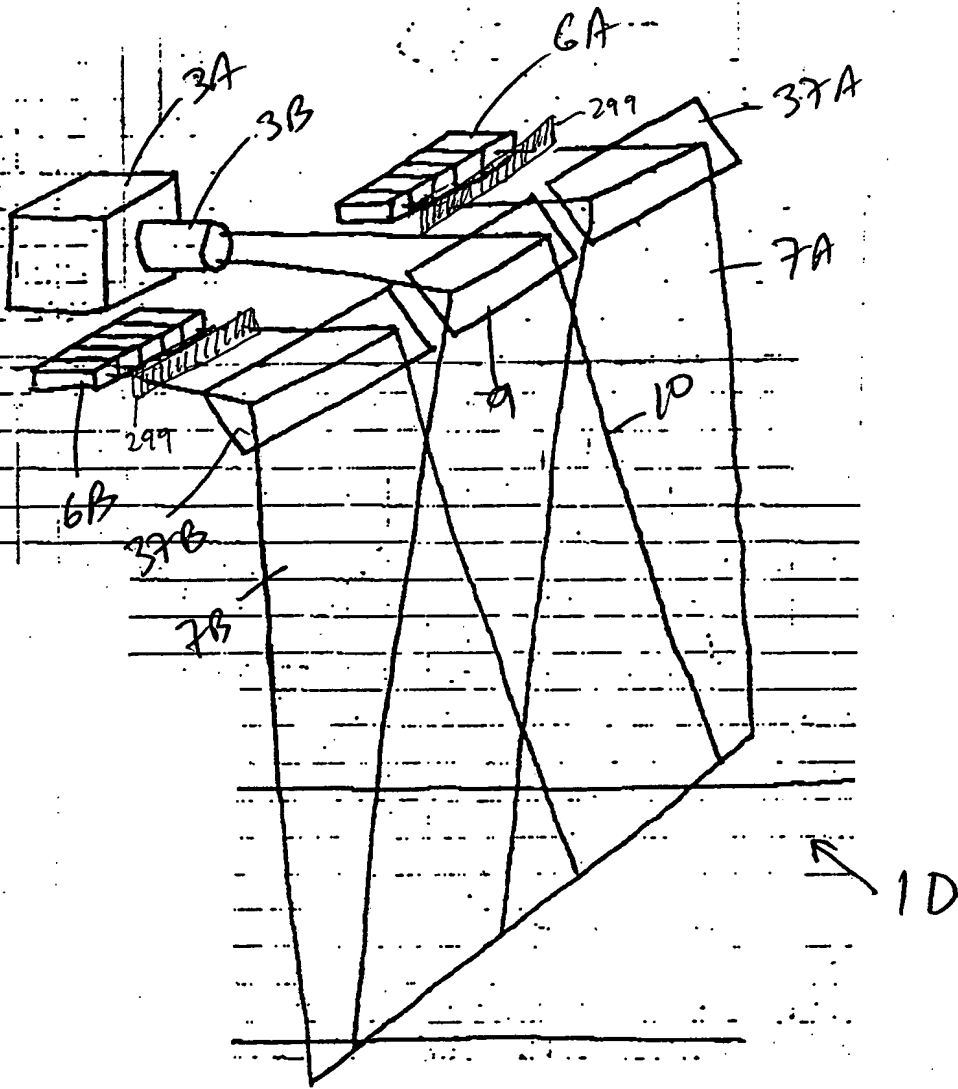


FIG. 1S1

FIG. 1S2

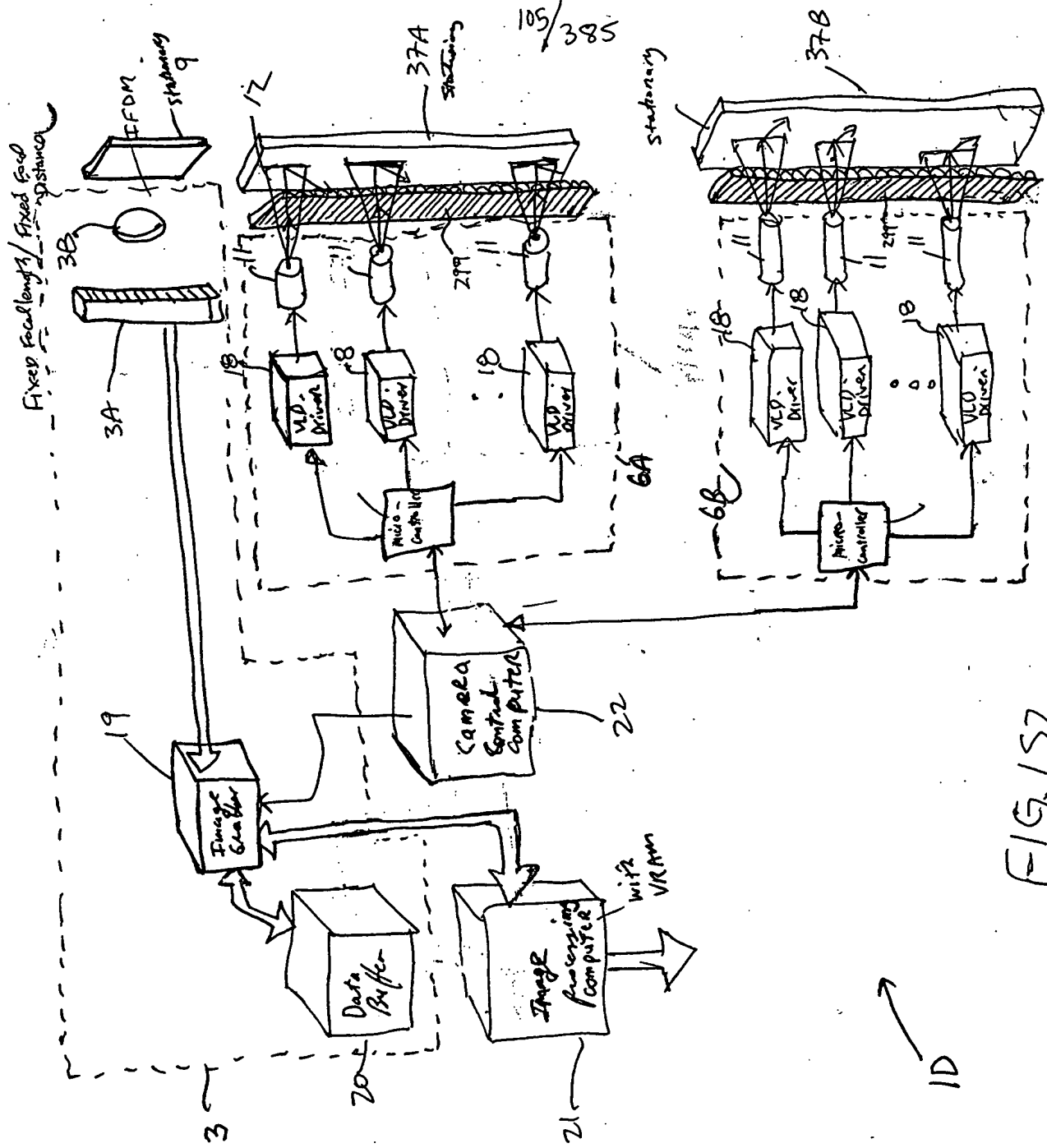


FIG. 1S2

106/385

09990585 112101

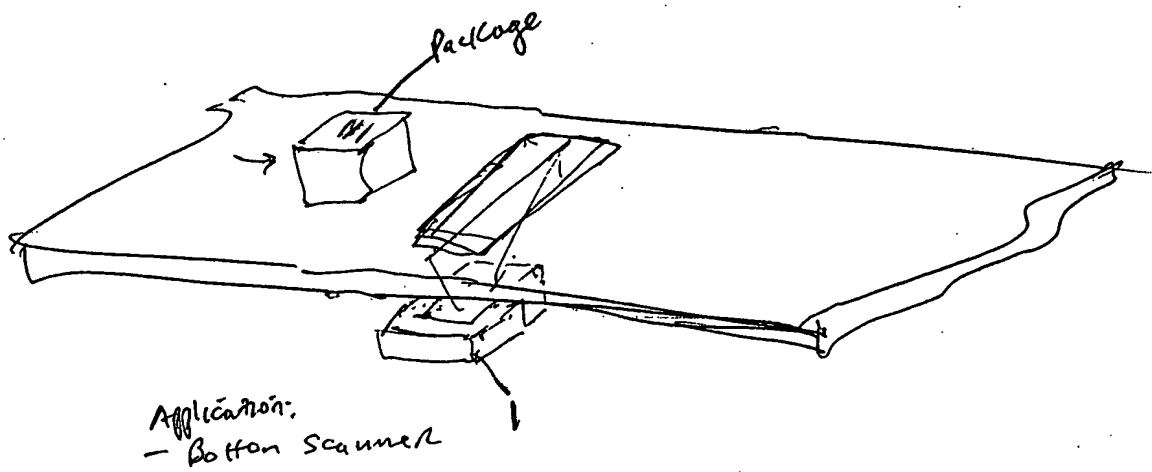
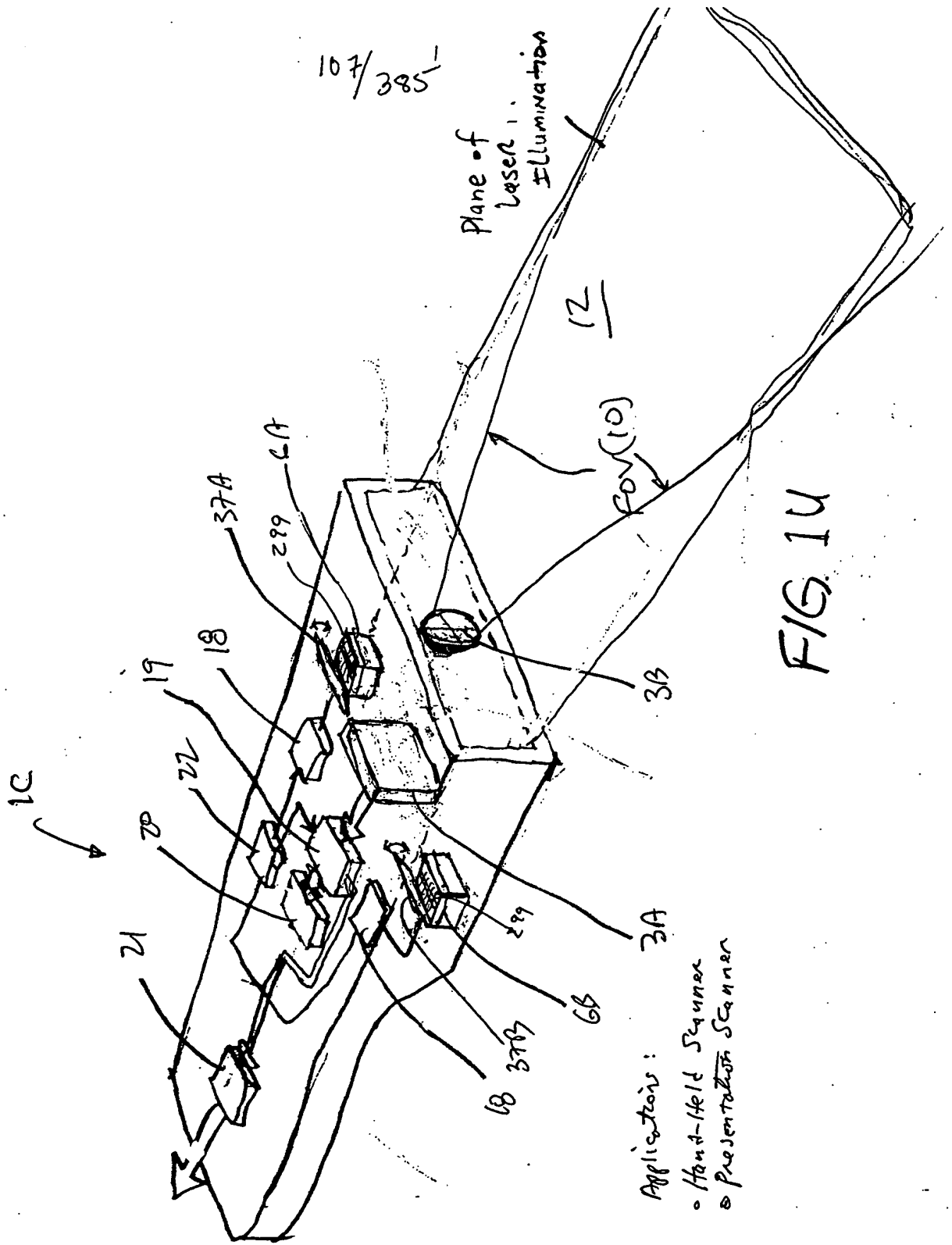


FIG 1T



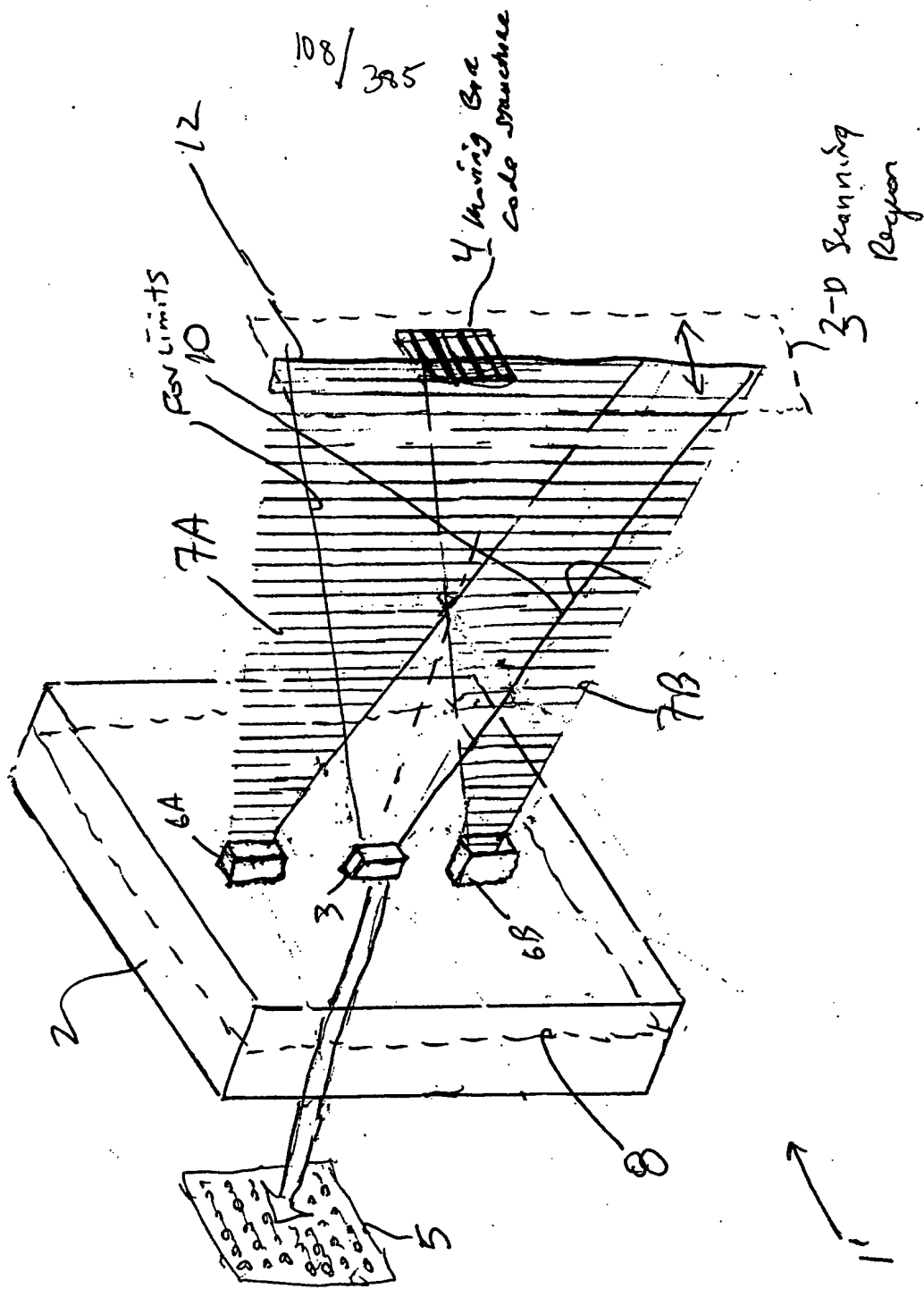


FIG. 1VI

109/385

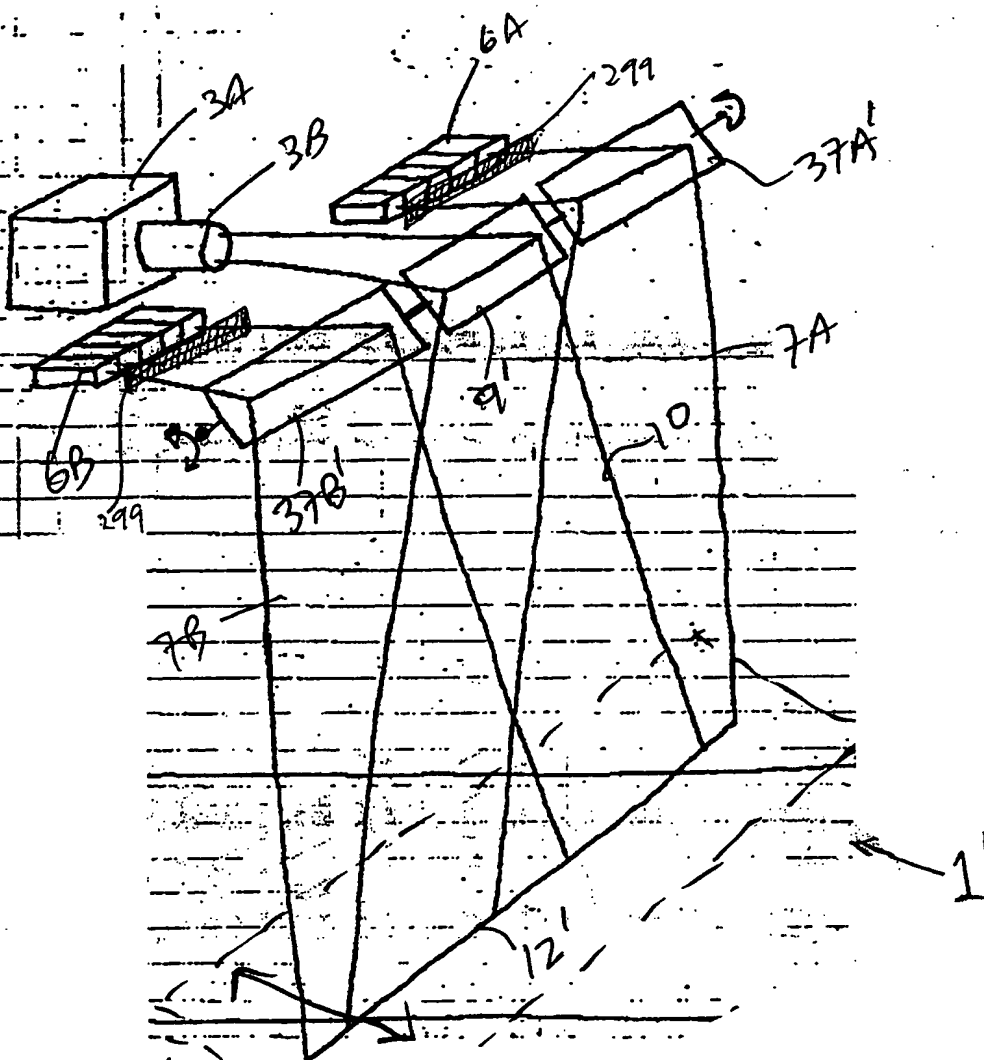


FIG. IV2

2-D
region
of
space

110 / 385



C)

TOTET-SS506660

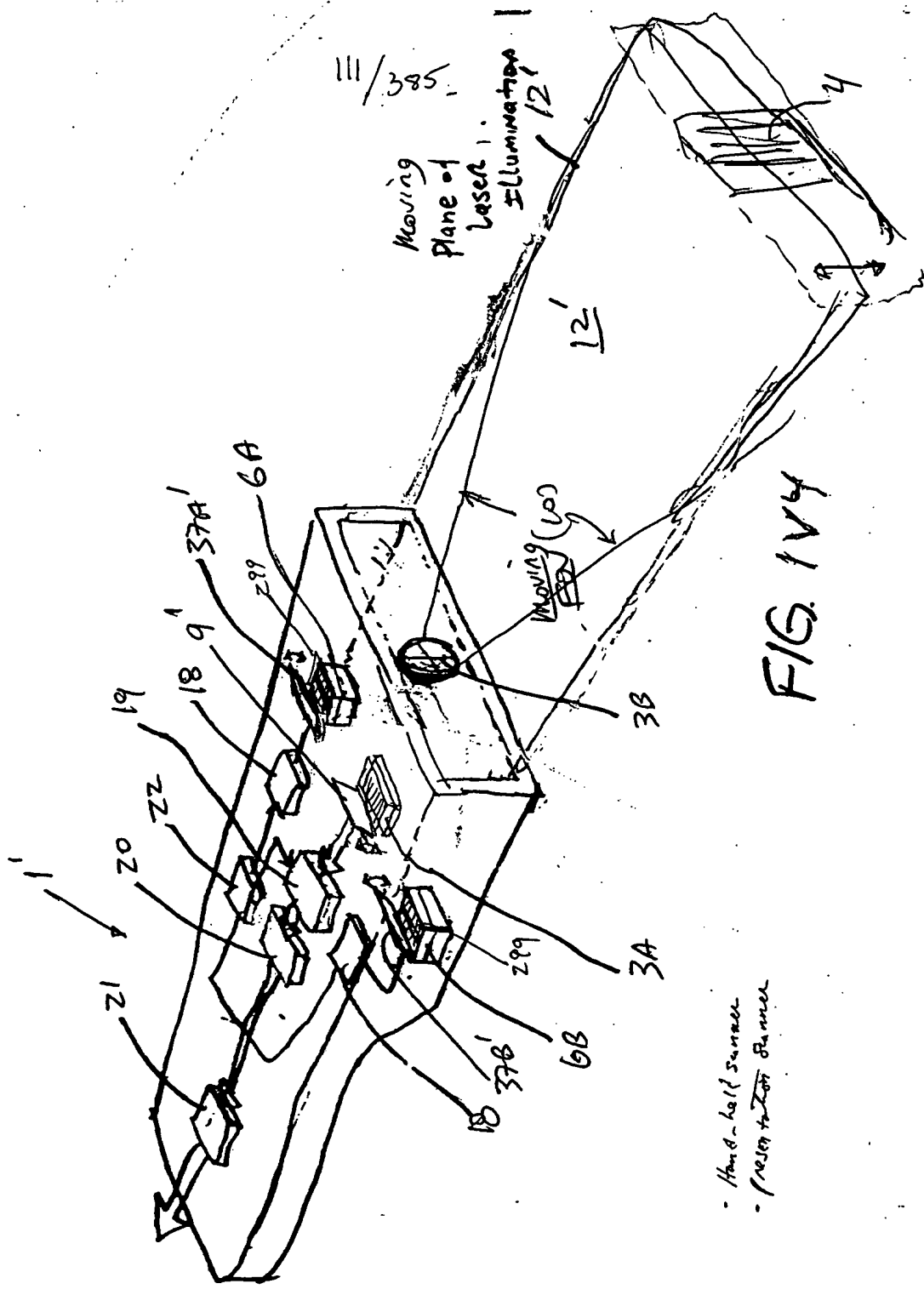


FIG. 1V4

- Hand-held scanner
- Projector to 200 ft

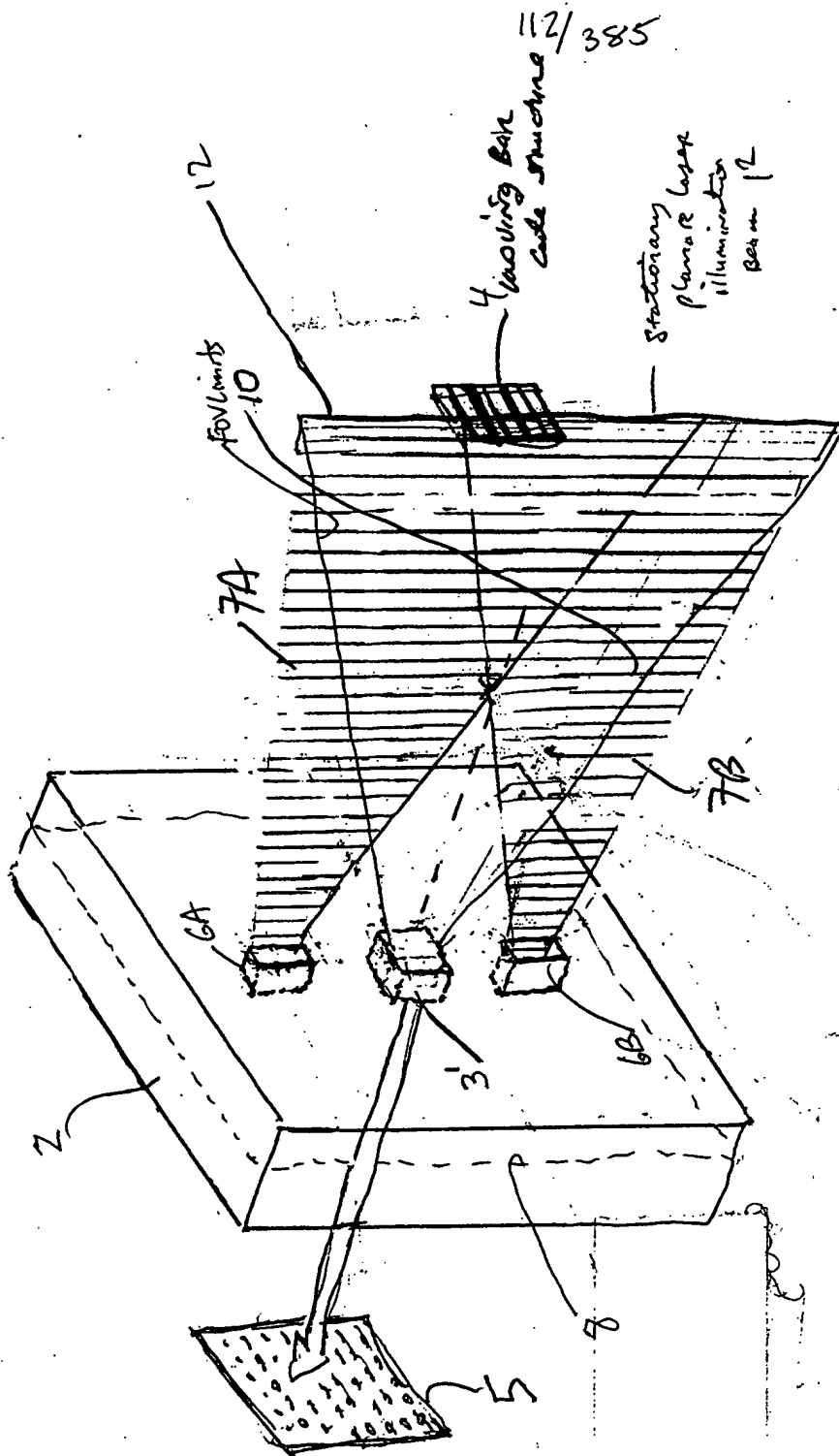


FIG. 2A

113/385

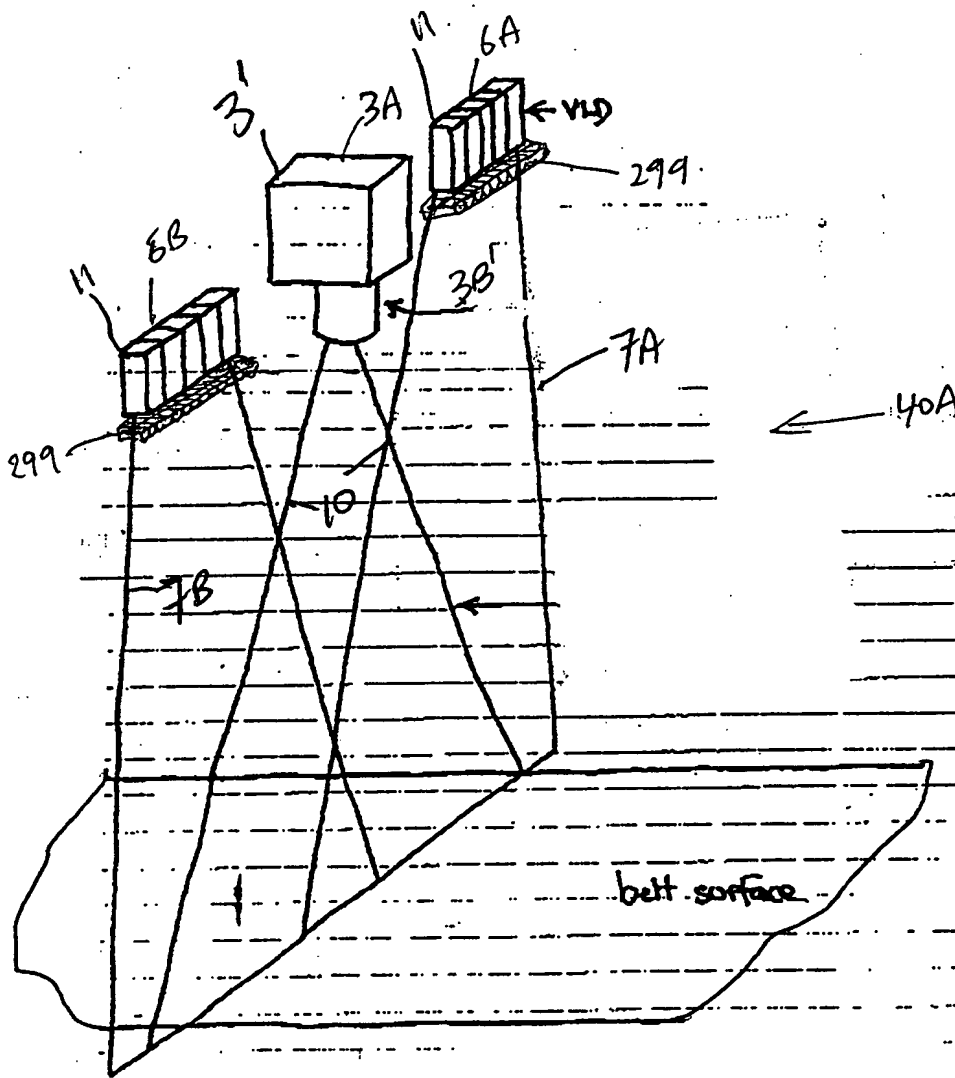


FIG. 2 B1



FIG. 2B2

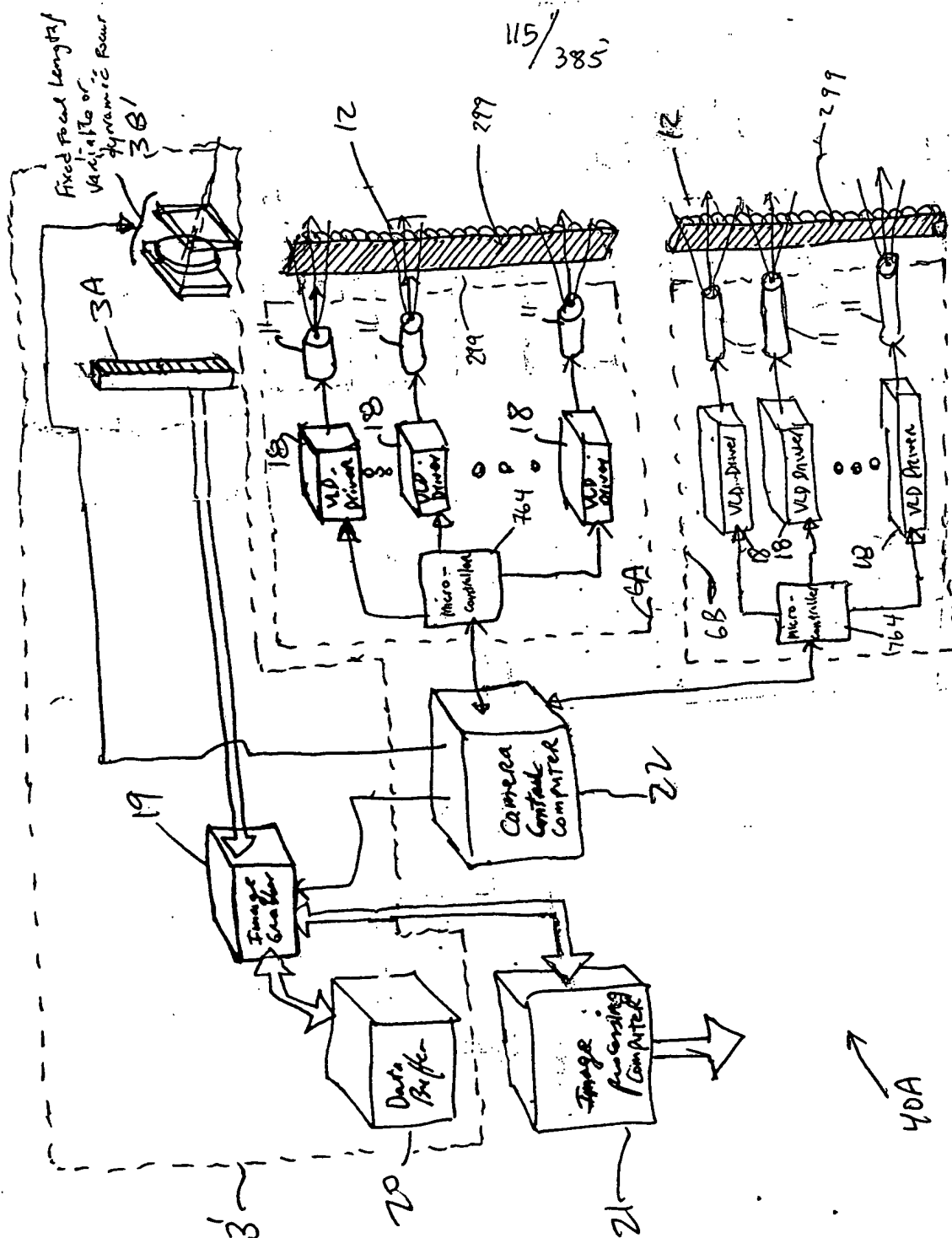
[illegible]

Fig. 2C1

TOP SECRET

116/385

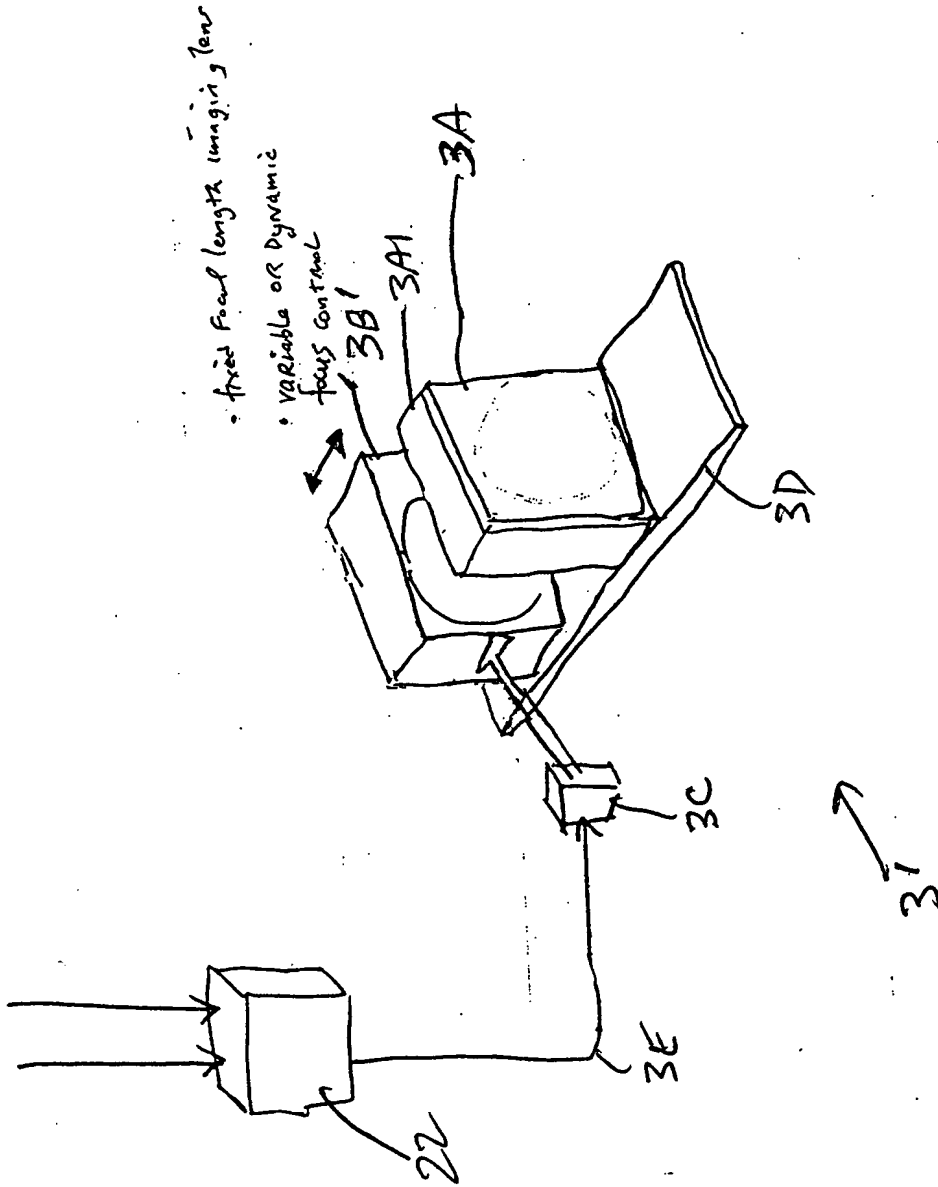


FIG. 2C2

117/385

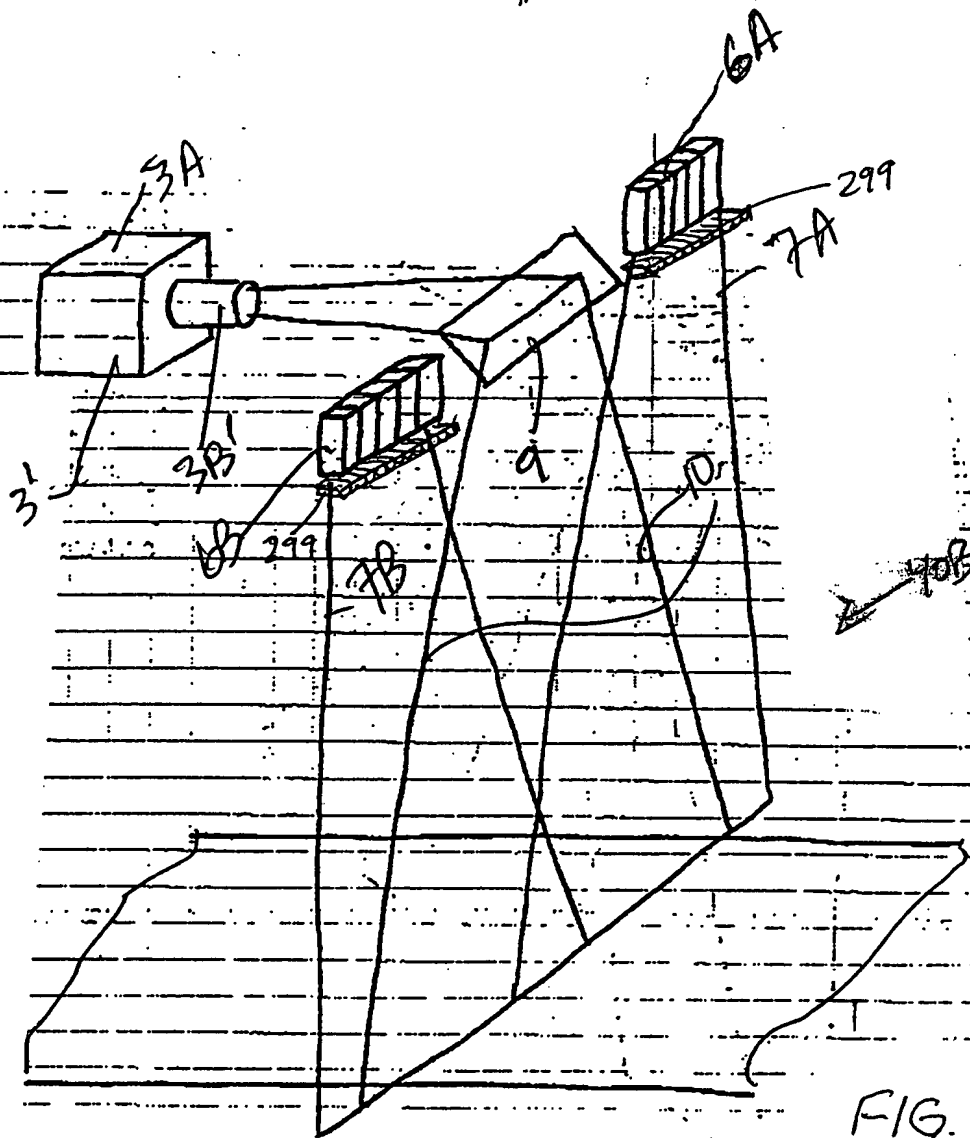
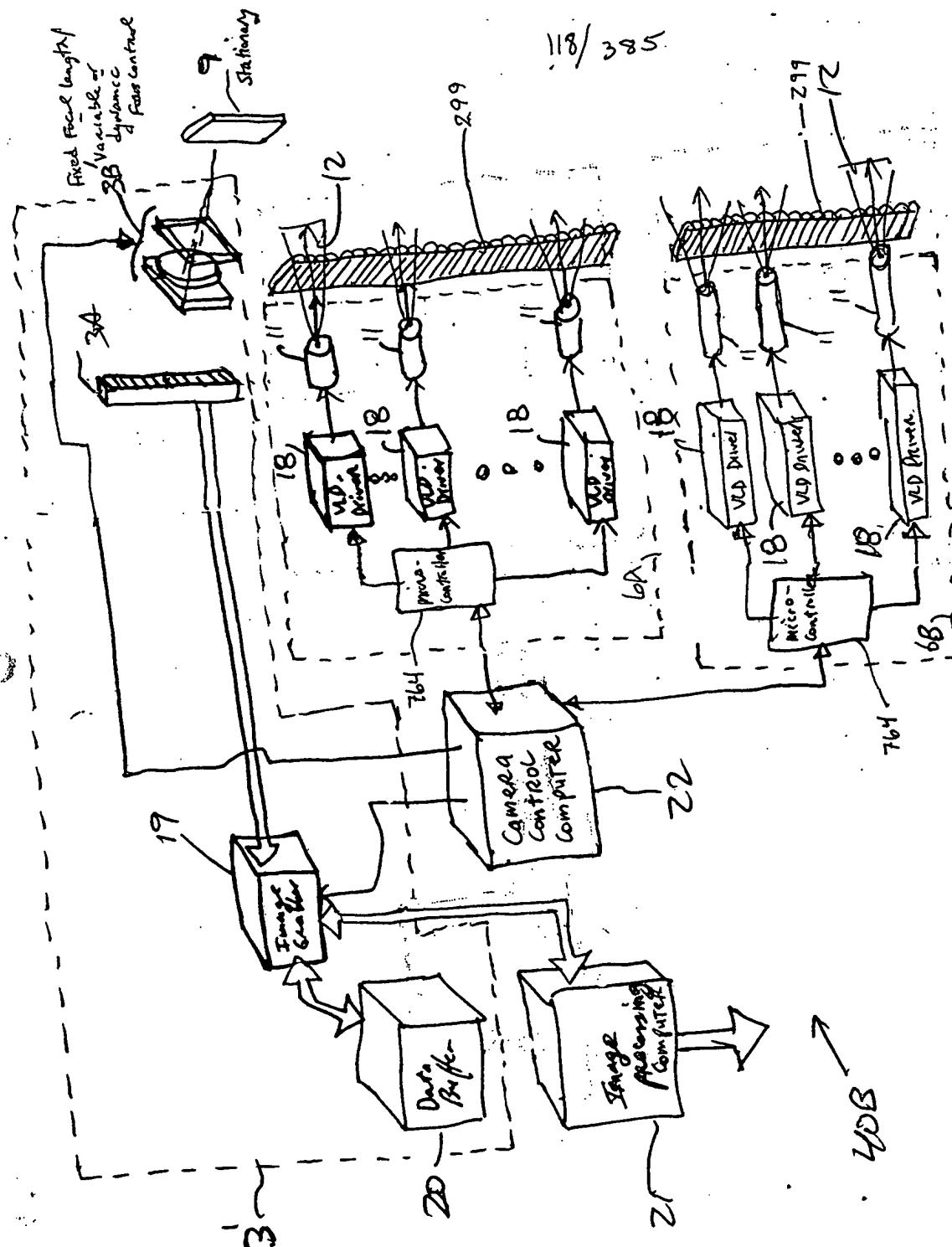


FIG. 2D1

[illegible]

AG. 2D2

119/385

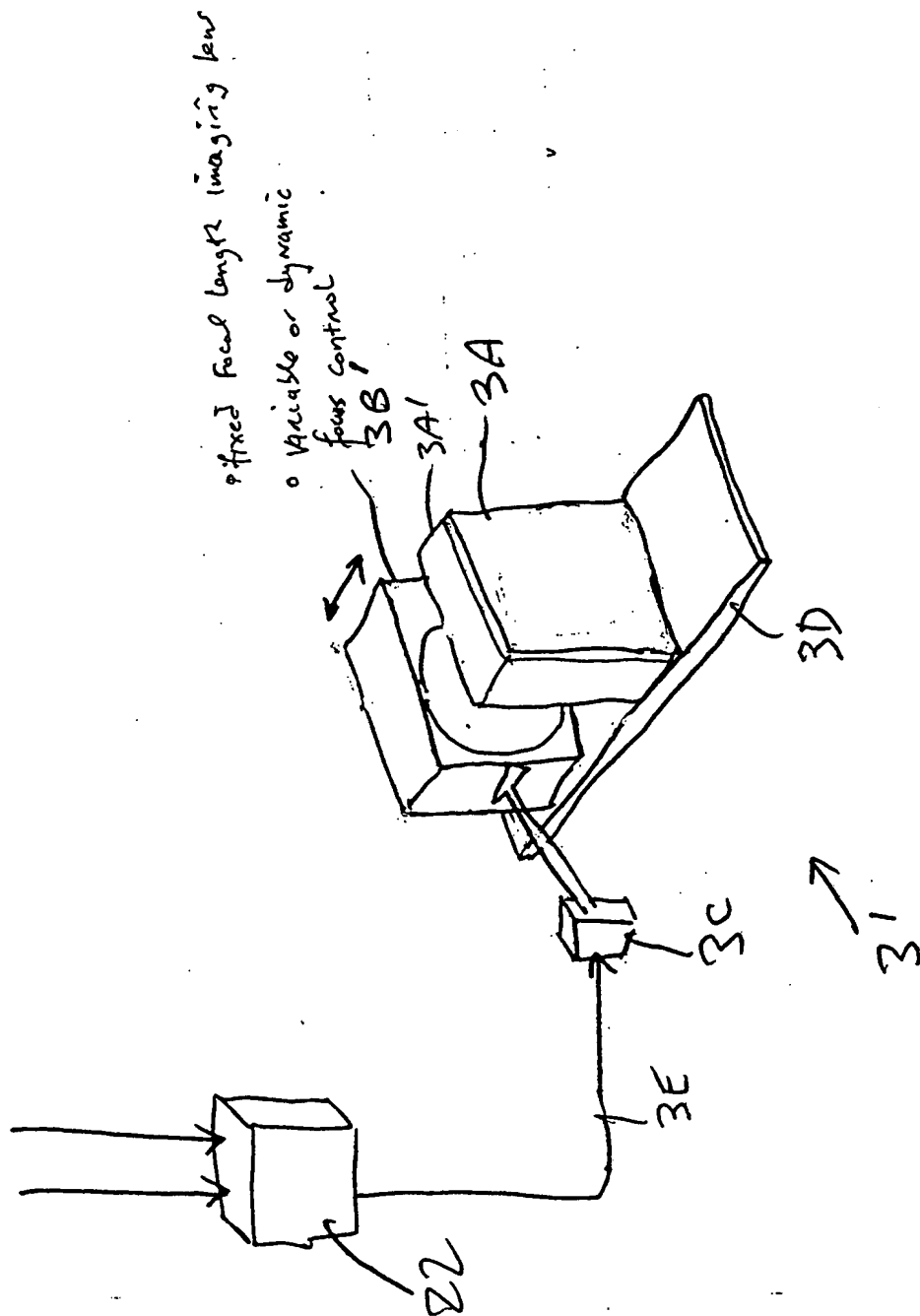


FIG. 2D3

00000505 12101

120/385

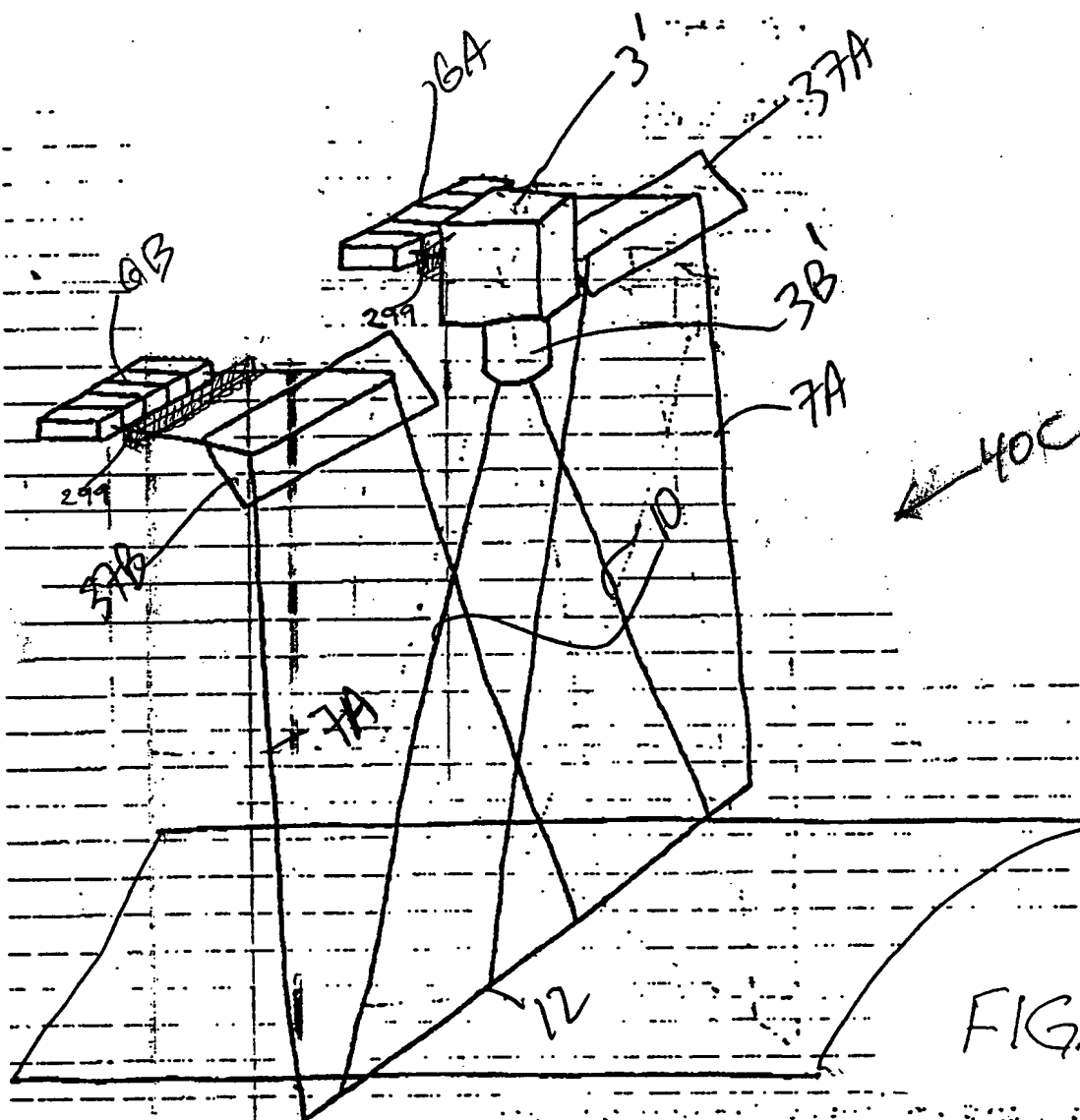


FIG. 2E1

FIG. 2E2

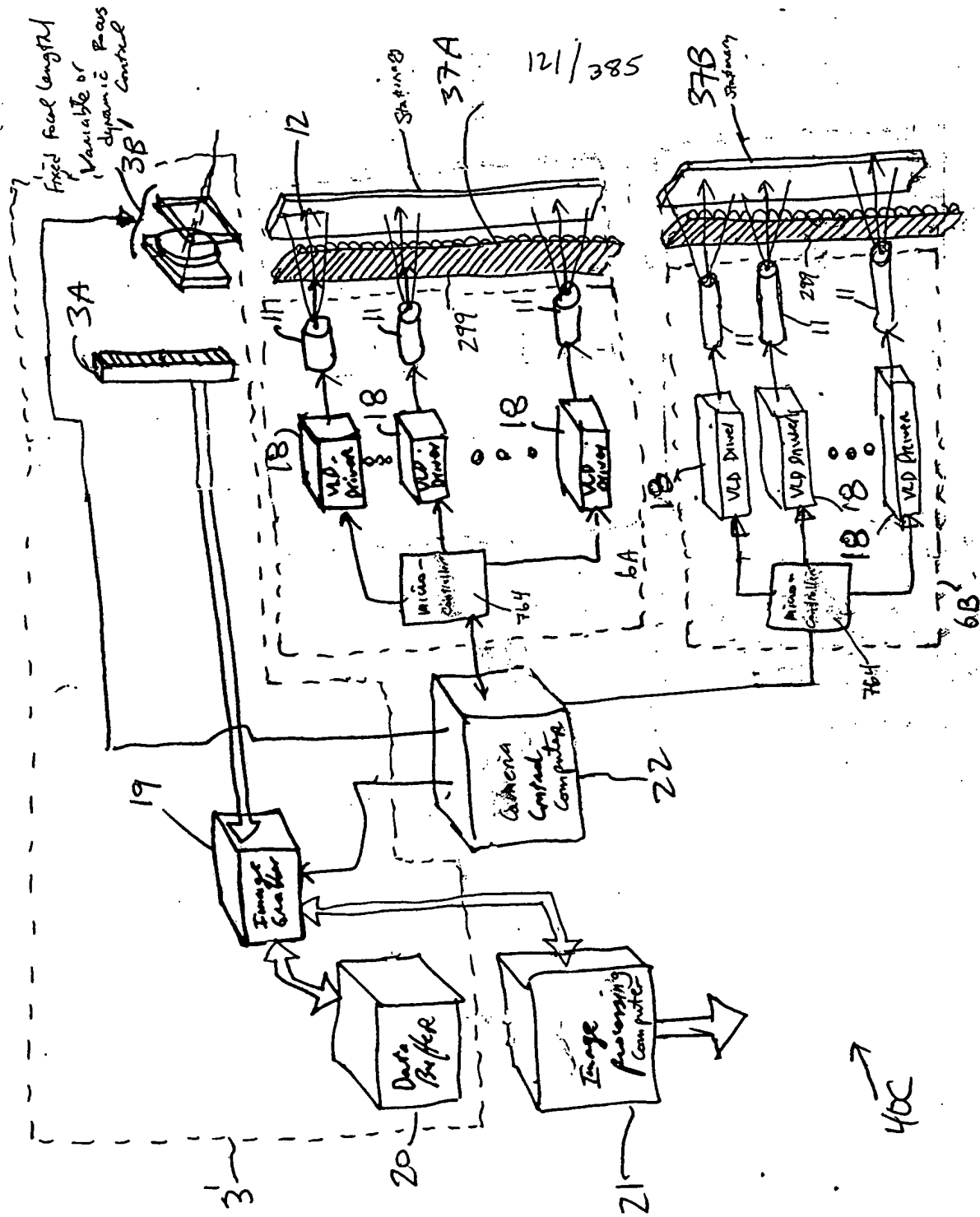


FIG. 2E2

122/385-

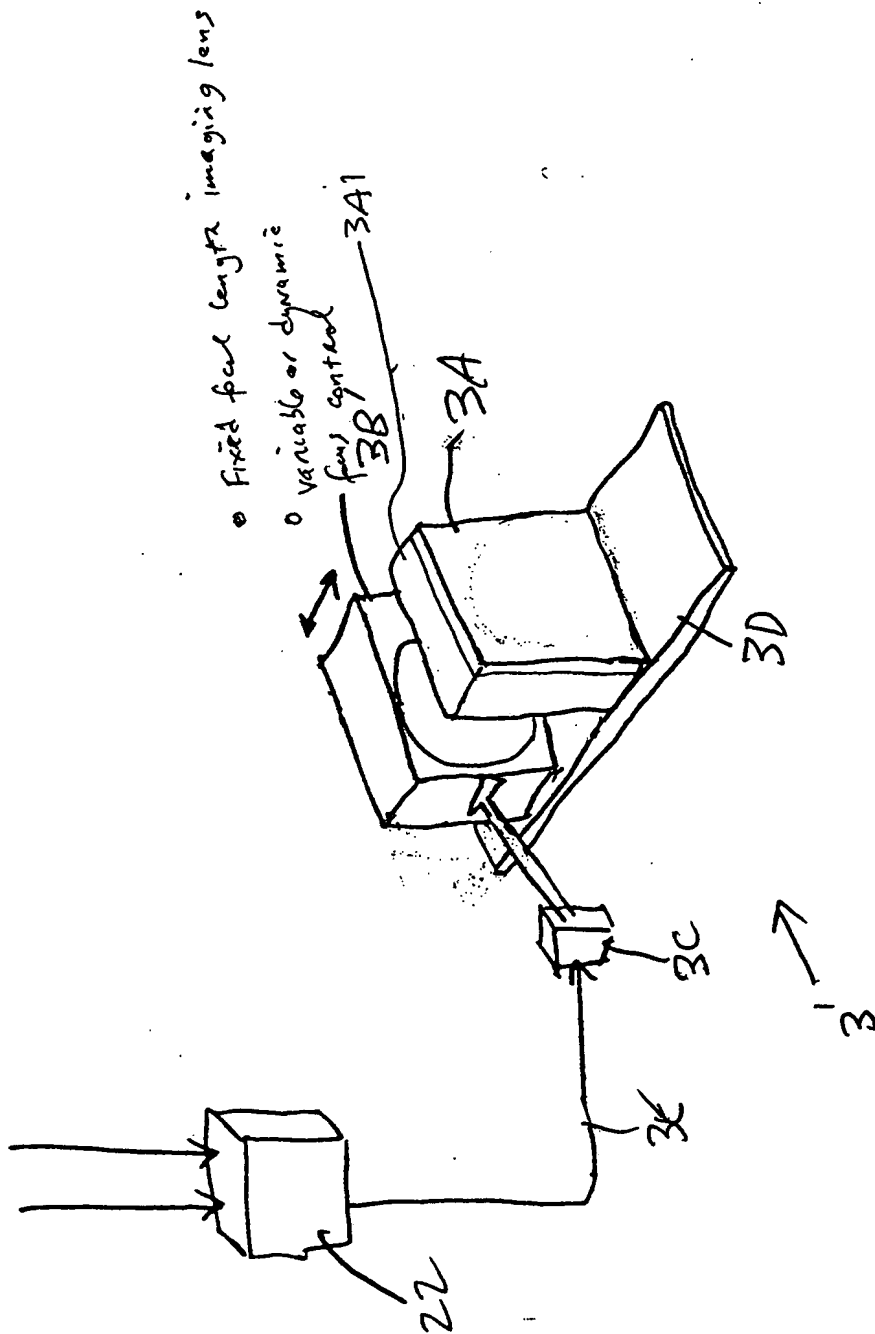


FIG. 2E3

FIG. 2F2

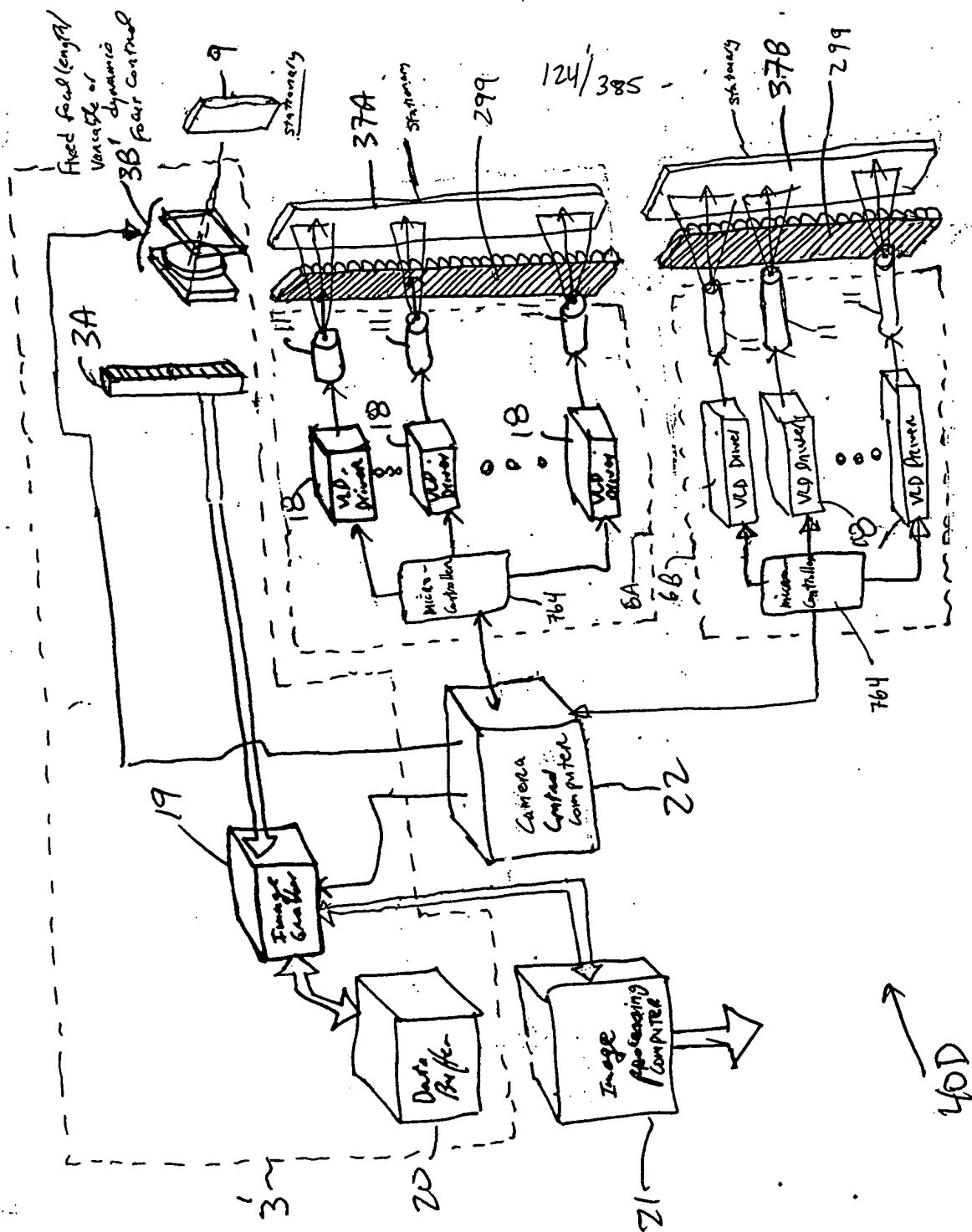
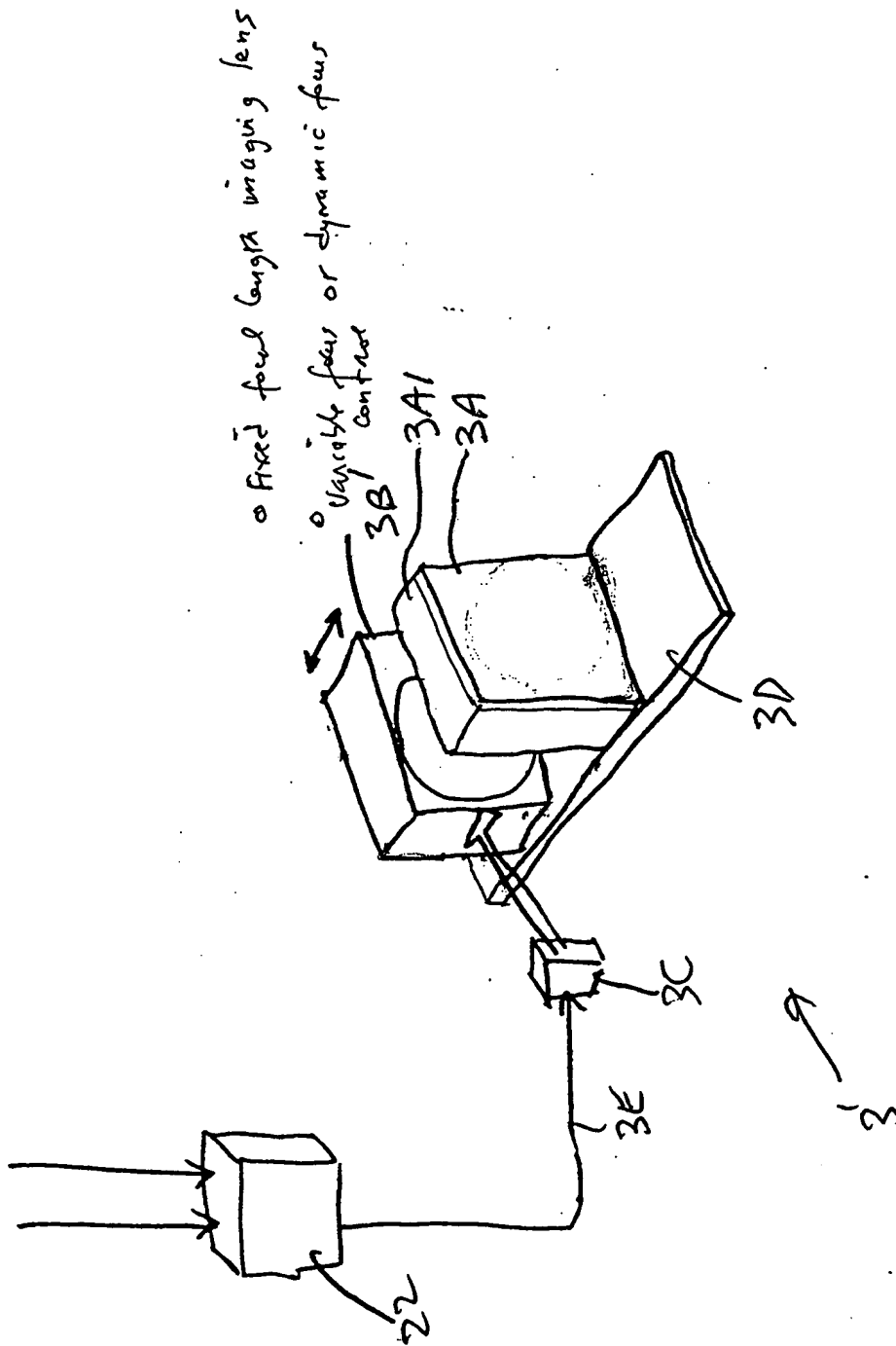


FIG. 2F2

125/385



126/385

00000585 112101

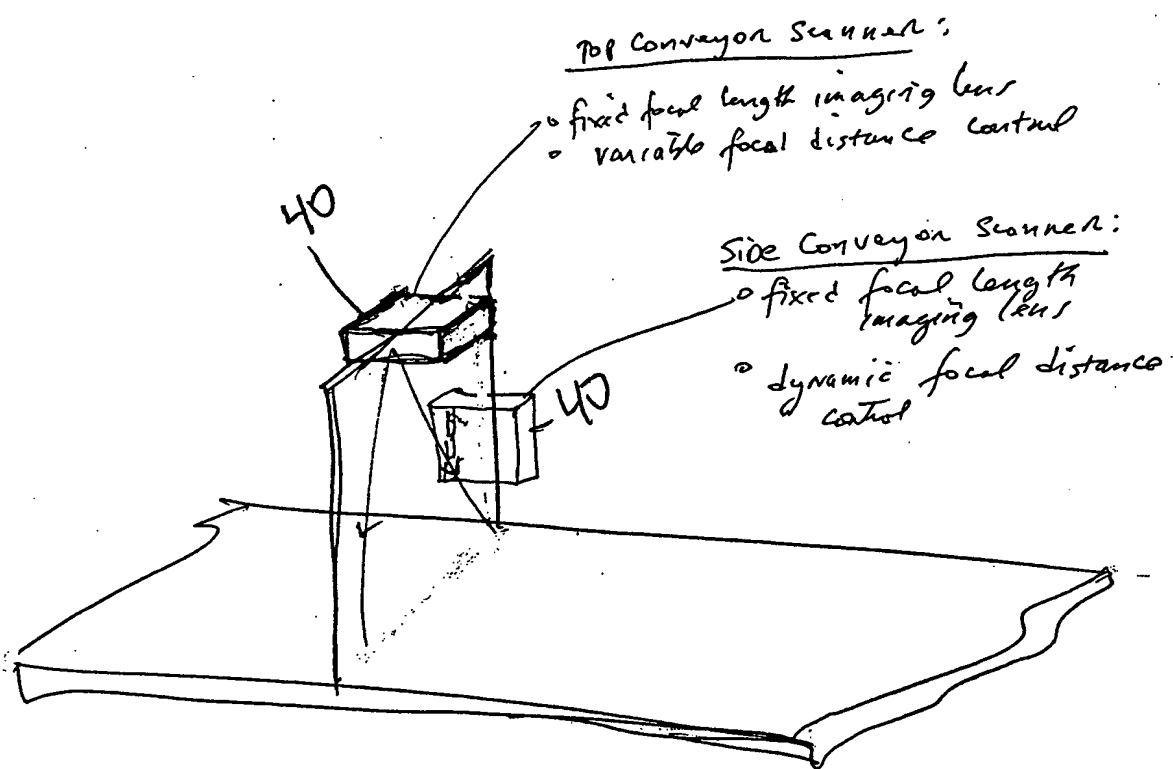


FIG. 2G

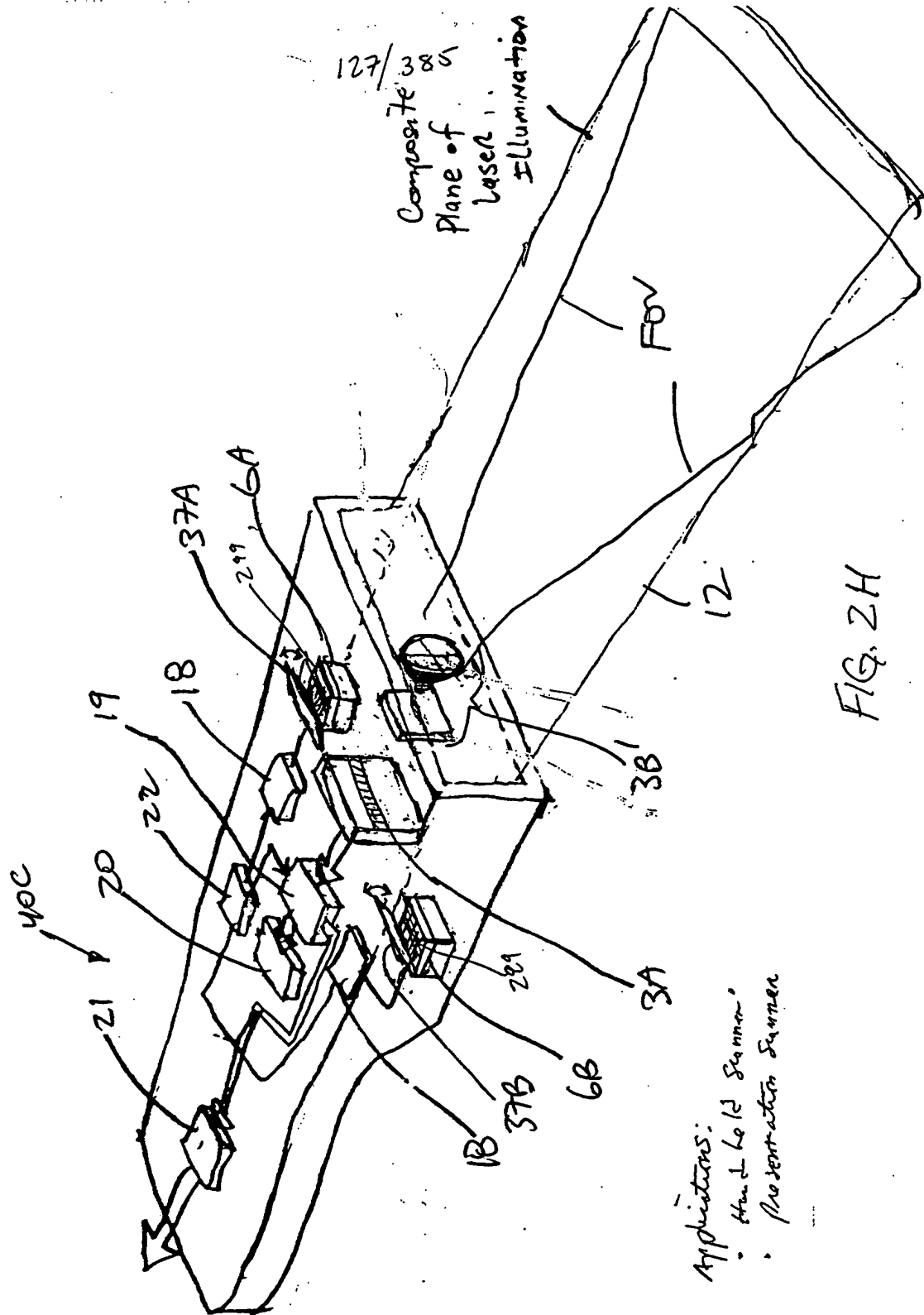


FIG. 2H

Applications:
• Hand Held Scanner
• Presentation Scanner

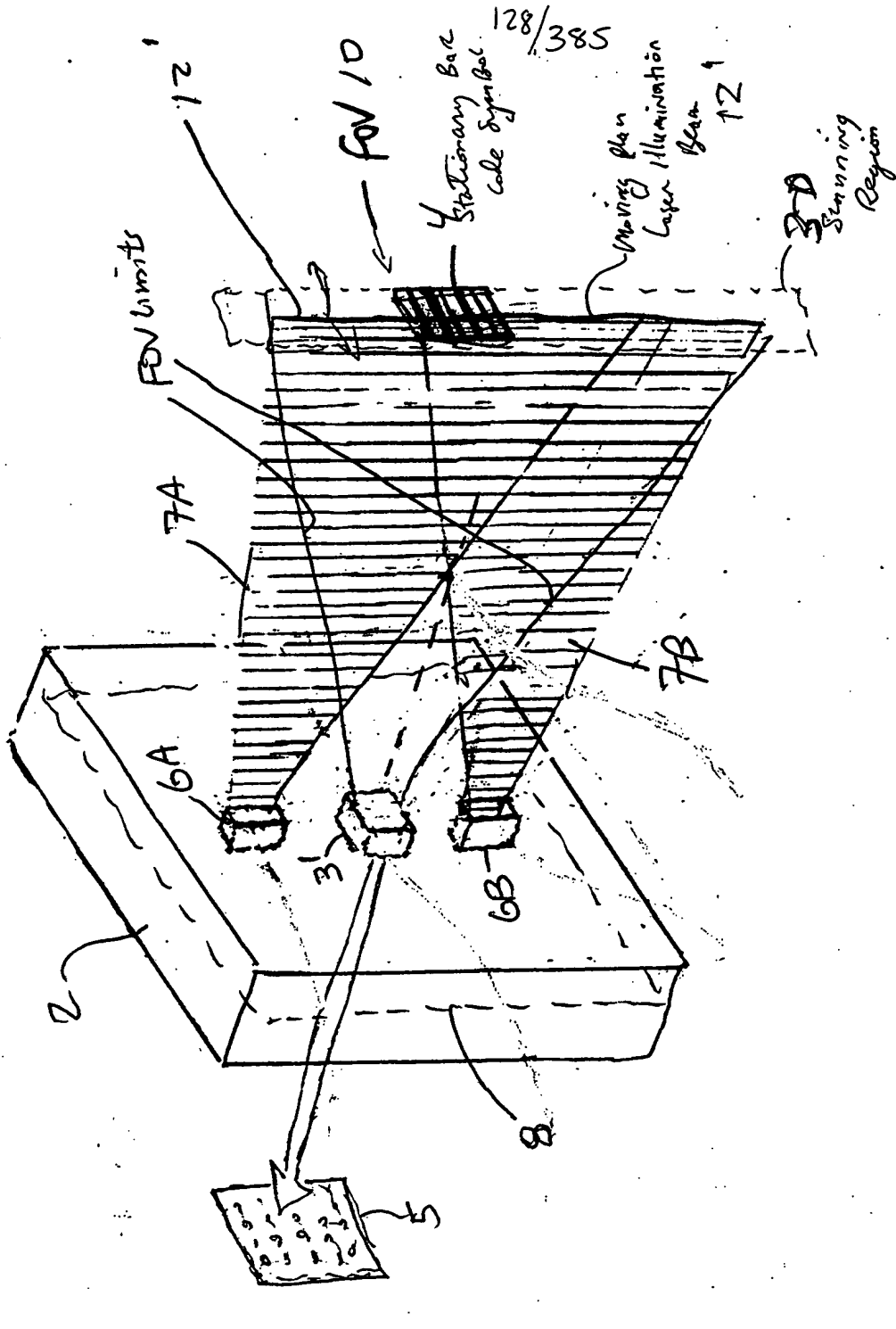
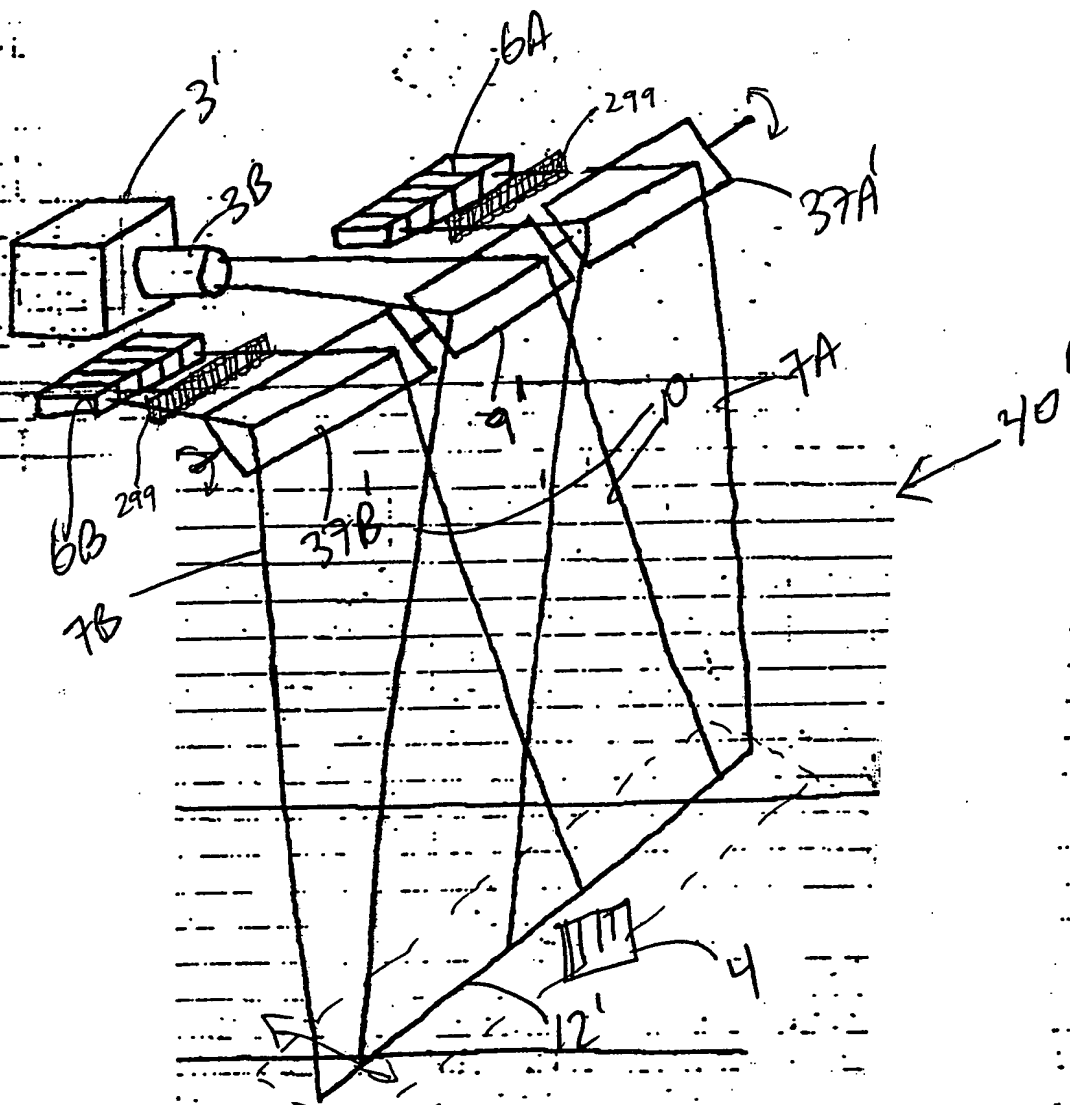


FIG. 2II

00000585 1101 58506660

129/385



3-D
Scanning
Region

FIG 2I2

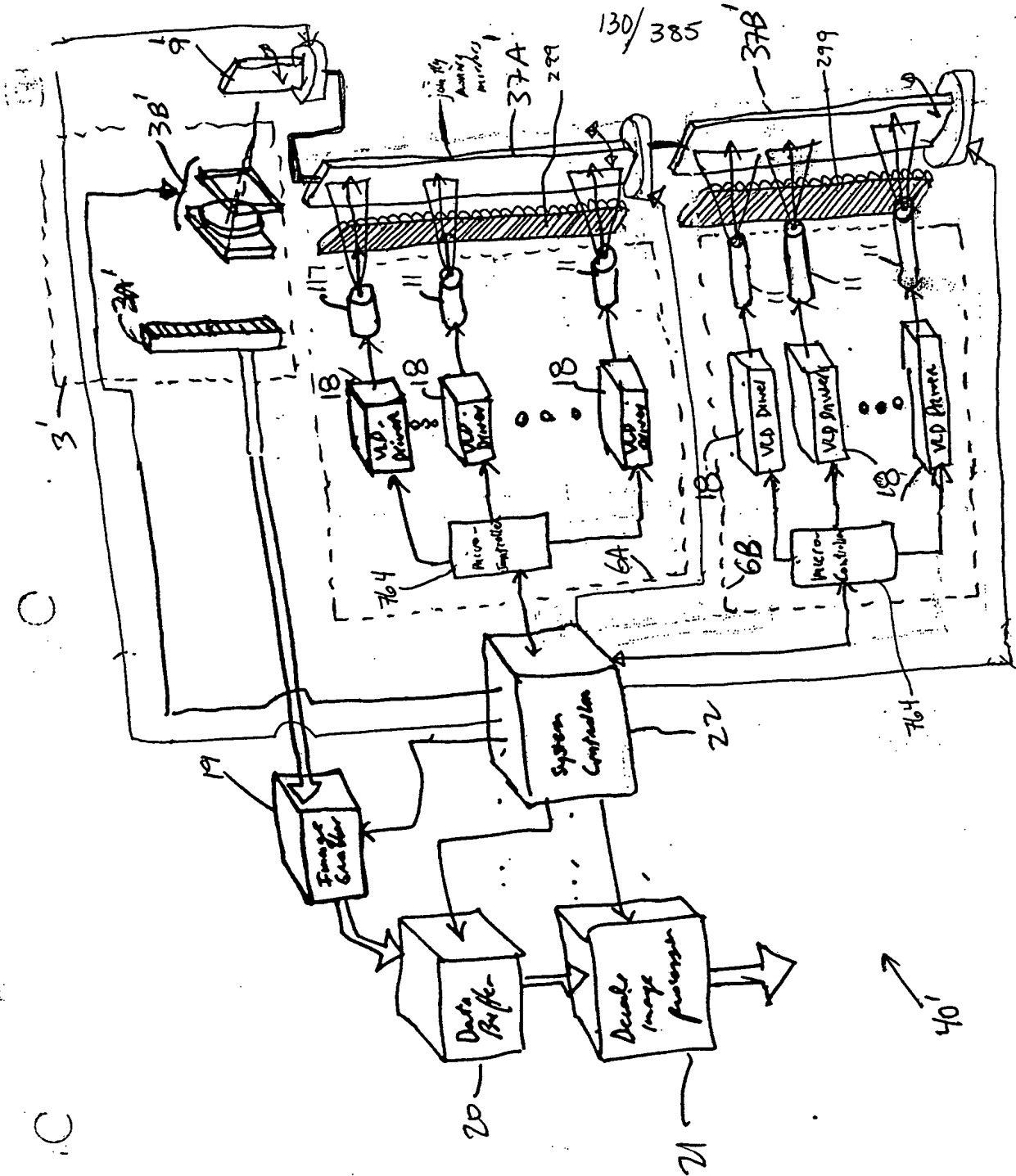


FIG. 2I3

131/385

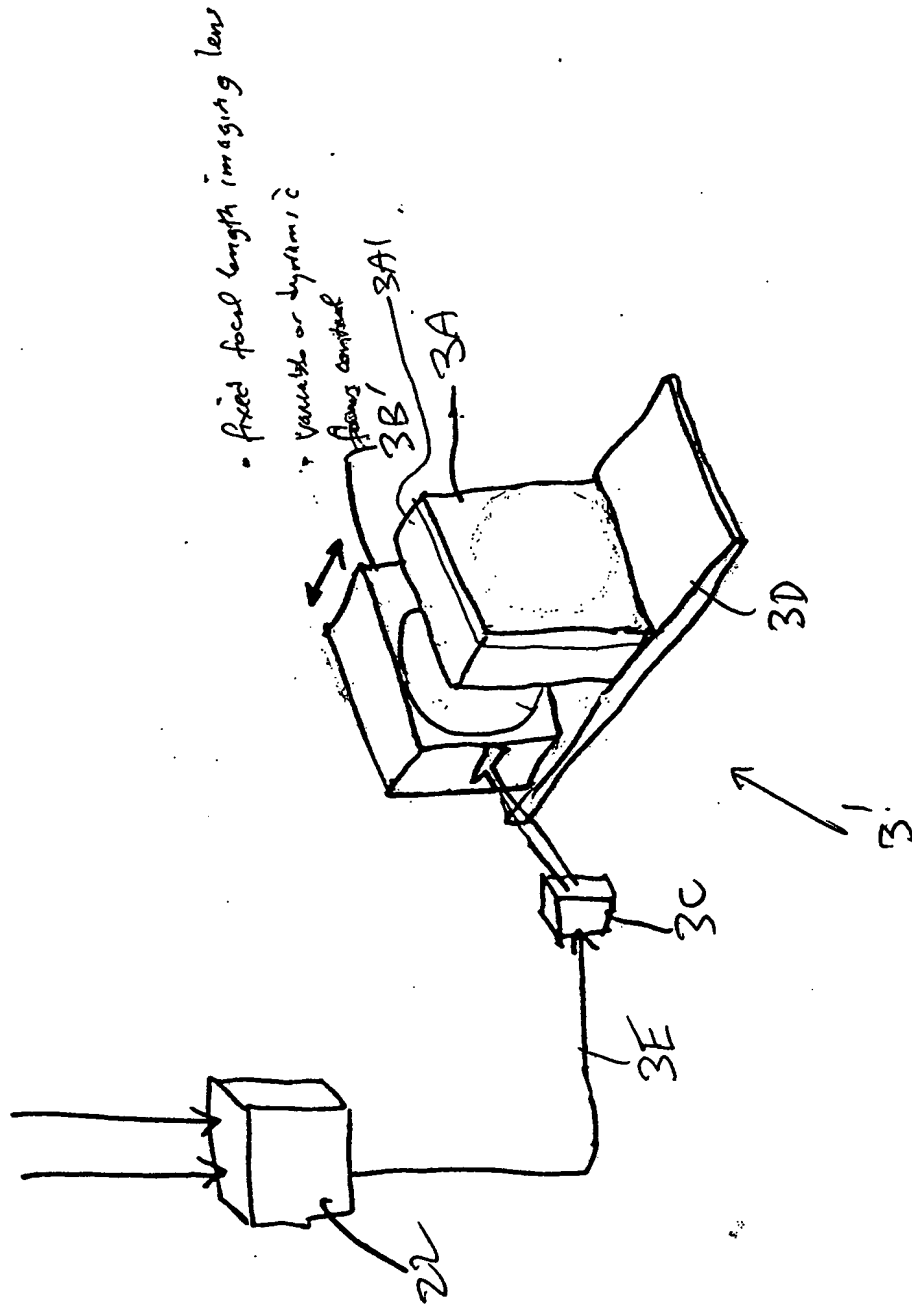
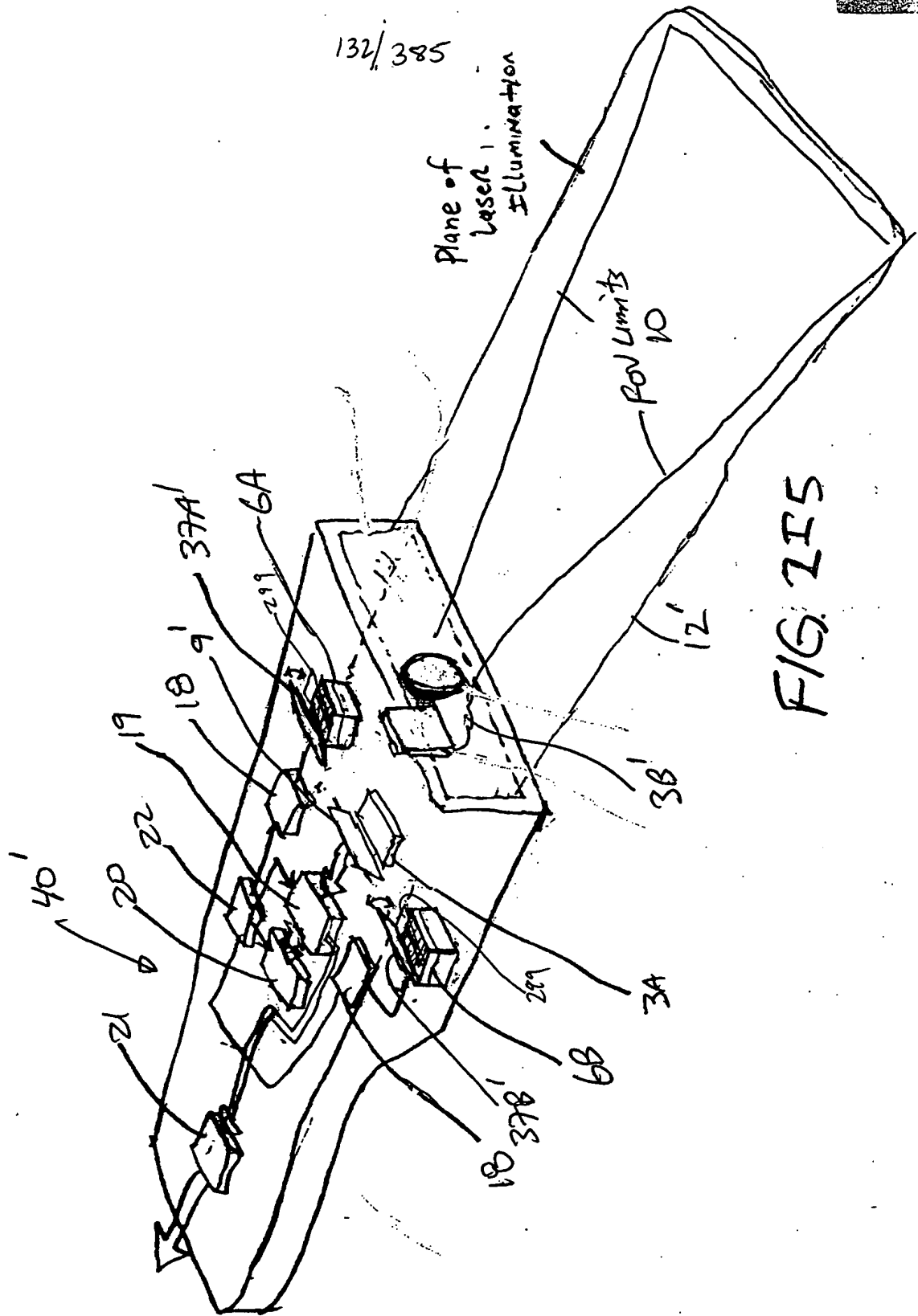


FIG. 2I4



133/385

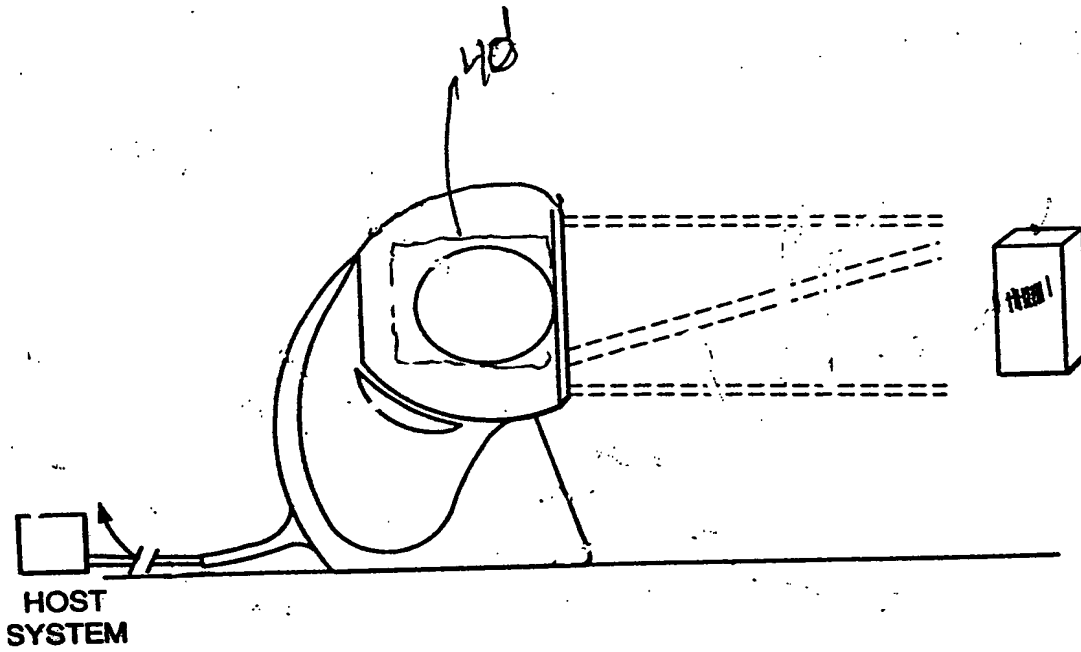


FIG. 2I6

TOTAL 58506660

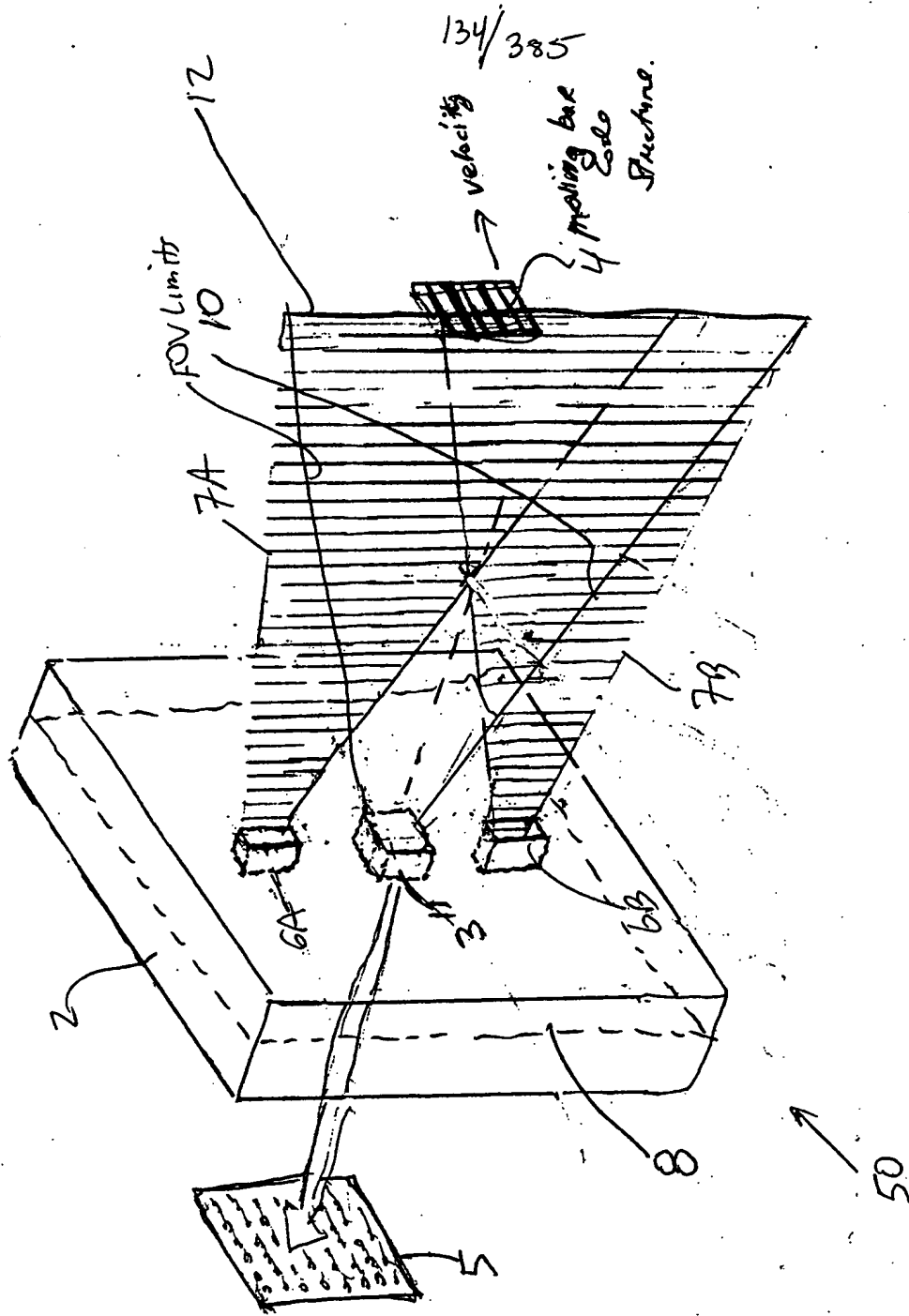


FIG 3A

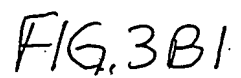
[illegible]

FIG. 3B1.

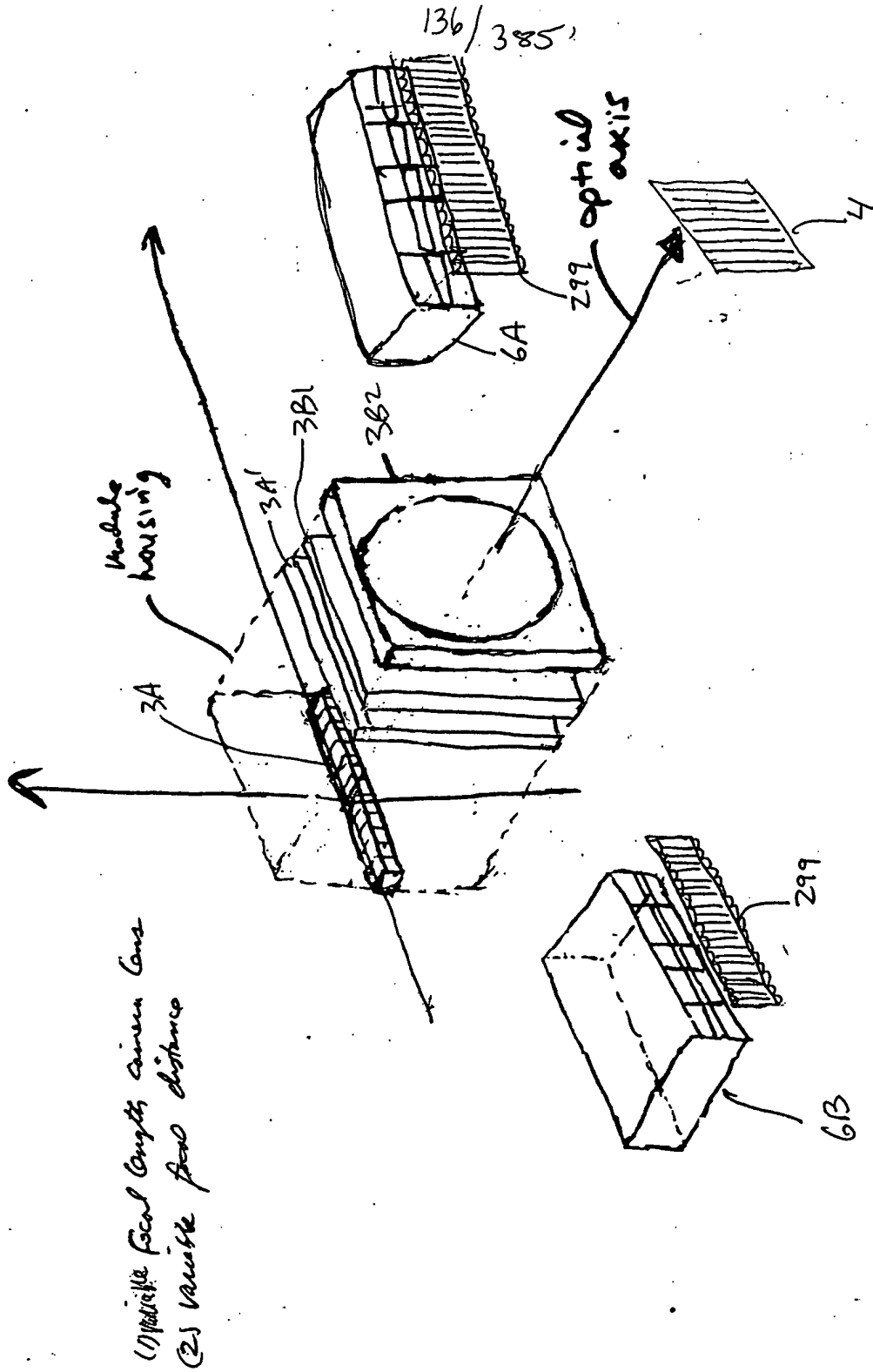


FIG. 3B2

| SEASON | WINTER | SPRING | SUMMER | FALL | YEAR |
|---------|--------|--------|--------|------|------|
| 1951-52 | 100 | 100 | 100 | 100 | 100 |
| 1952-53 | 100 | 100 | 100 | 100 | 100 |
| 1953-54 | 100 | 100 | 100 | 100 | 100 |
| 1954-55 | 100 | 100 | 100 | 100 | 100 |
| 1955-56 | 100 | 100 | 100 | 100 | 100 |
| 1956-57 | 100 | 100 | 100 | 100 | 100 |
| 1957-58 | 100 | 100 | 100 | 100 | 100 |
| 1958-59 | 100 | 100 | 100 | 100 | 100 |
| 1959-60 | 100 | 100 | 100 | 100 | 100 |
| 1960-61 | 100 | 100 | 100 | 100 | 100 |
| 1961-62 | 100 | 100 | 100 | 100 | 100 |
| 1962-63 | 100 | 100 | 100 | 100 | 100 |
| 1963-64 | 100 | 100 | 100 | 100 | 100 |
| 1964-65 | 100 | 100 | 100 | 100 | 100 |
| 1965-66 | 100 | 100 | 100 | 100 | 100 |
| 1966-67 | 100 | 100 | 100 | 100 | 100 |
| 1967-68 | 100 | 100 | 100 | 100 | 100 |
| 1968-69 | 100 | 100 | 100 | 100 | 100 |
| 1969-70 | 100 | 100 | 100 | 100 | 100 |
| 1970-71 | 100 | 100 | 100 | 100 | 100 |
| 1971-72 | 100 | 100 | 100 | 100 | 100 |
| 1972-73 | 100 | 100 | 100 | 100 | 100 |
| 1973-74 | 100 | 100 | 100 | 100 | 100 |
| 1974-75 | 100 | 100 | 100 | 100 | 100 |
| 1975-76 | 100 | 100 | 100 | 100 | 100 |
| 1976-77 | 100 | 100 | 100 | 100 | 100 |
| 1977-78 | 100 | 100 | 100 | 100 | 100 |
| 1978-79 | 100 | 100 | 100 | 100 | 100 |
| 1979-80 | 100 | 100 | 100 | 100 | 100 |
| 1980-81 | 100 | 100 | 100 | 100 | 100 |
| 1981-82 | 100 | 100 | 100 | 100 | 100 |
| 1982-83 | 100 | 100 | 100 | 100 | 100 |
| 1983-84 | 100 | 100 | 100 | 100 | 100 |
| 1984-85 | 100 | 100 | 100 | 100 | 100 |
| 1985-86 | 100 | 100 | 100 | 100 | 100 |
| 1986-87 | 100 | 100 | 100 | 100 | 100 |
| 1987-88 | 100 | 100 | 100 | 100 | 100 |
| 1988-89 | 100 | 100 | 100 | 100 | 100 |
| 1989-90 | 100 | 100 | 100 | 100 | 100 |
| 1990-91 | 100 | 100 | 100 | 100 | 100 |
| 1991-92 | 100 | 100 | 100 | 100 | 100 |
| 1992-93 | 100 | 100 | 100 | 100 | 100 |
| 1993-94 | 100 | 100 | 100 | 100 | 100 |
| 1994-95 | 100 | 100 | 100 | 100 | 100 |
| 1995-96 | 100 | 100 | 100 | 100 | 100 |
| 1996-97 | 100 | 100 | 100 | 100 | 100 |
| 1997-98 | 100 | 100 | 100 | 100 | 100 |
| 1998-99 | 100 | 100 | 100 | 100 | 100 |
| 1999-00 | 100 | 100 | 100 | 100 | 100 |
| 2000-01 | 100 | 100 | 100 | 100 | 100 |
| 2001-02 | 100 | 100 | 100 | 100 | 100 |
| 2002-03 | 100 | 100 | 100 | 100 | 100 |
| 2003-04 | 100 | 100 | 100 | 100 | 100 |
| 2004-05 | 100 | 100 | 100 | 100 | 100 |
| 2005-06 | 100 | 100 | 100 | 100 | 100 |
| 2006-07 | 100 | 100 | 100 | 100 | 100 |
| 2007-08 | 100 | 100 | 100 | 100 | 100 |
| 2008-09 | 100 | 100 | 100 | 100 | 100 |
| 2009-10 | 100 | 100 | 100 | 100 | 100 |
| 2010-11 | 100 | 100 | 100 | 100 | 100 |
| 2011-12 | 100 | 100 | 100 | 100 | 100 |
| 2012-13 | 100 | 100 | 100 | 100 | 100 |

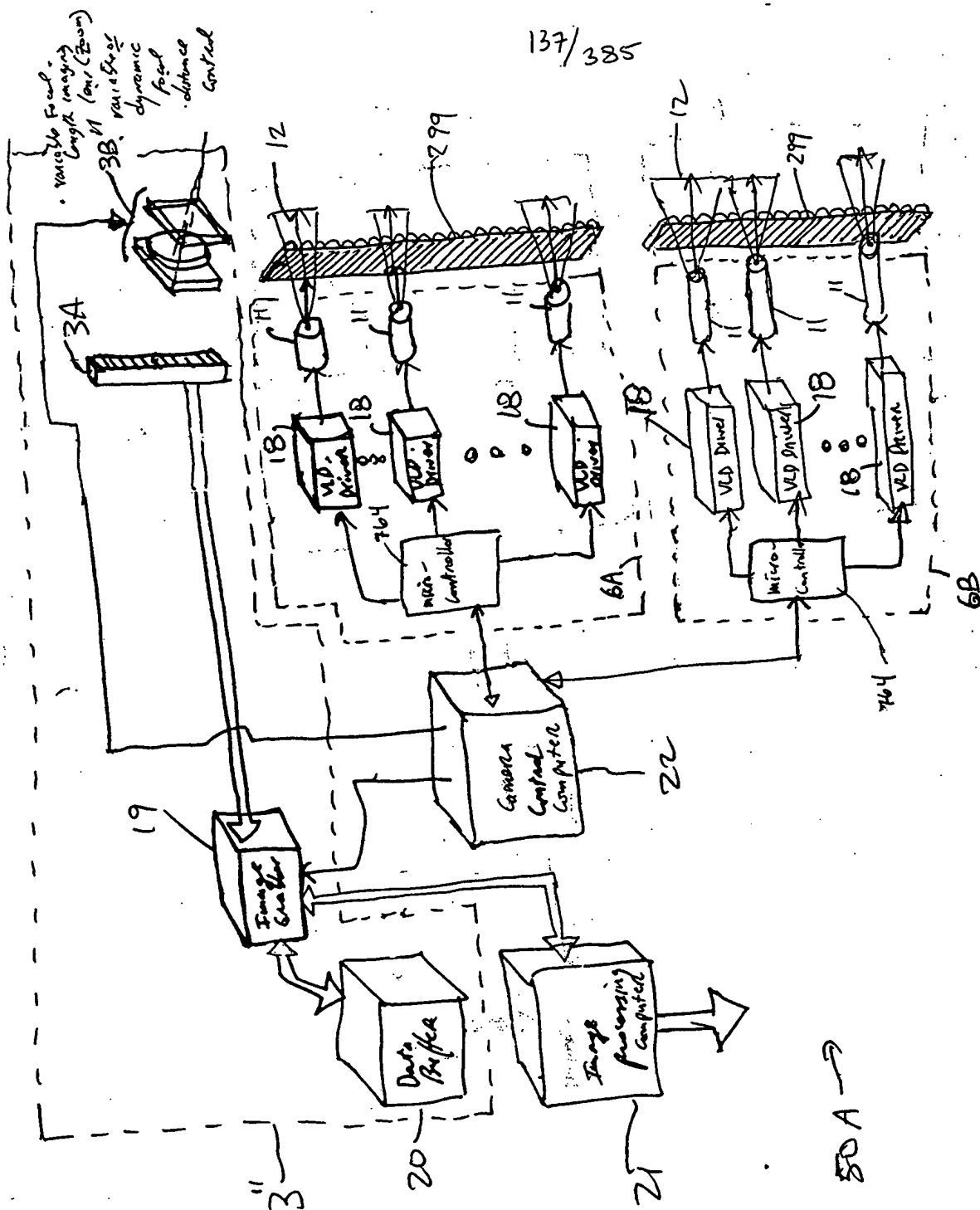
$$137 \overline{) 385}$$


Fig 3C

50A

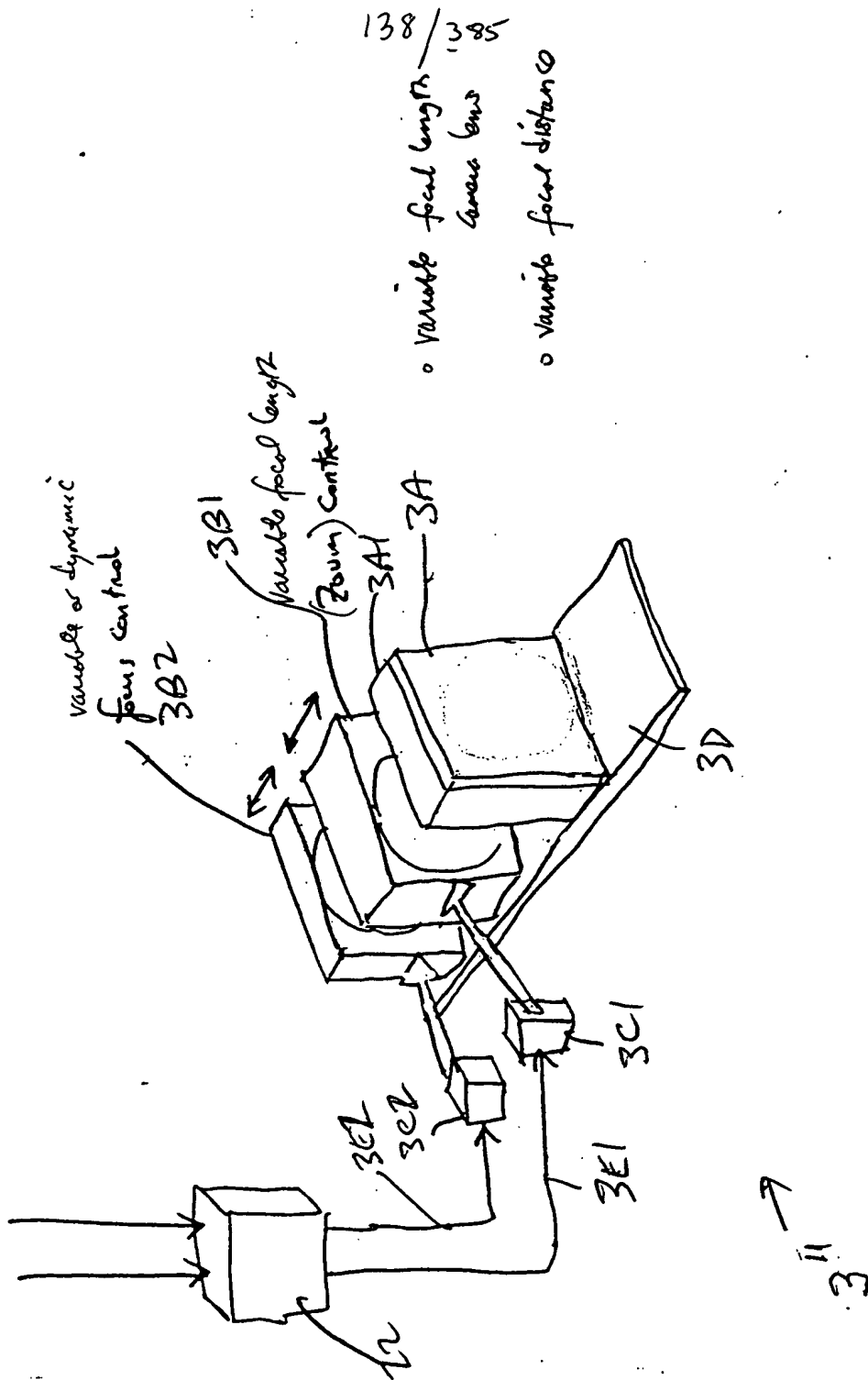
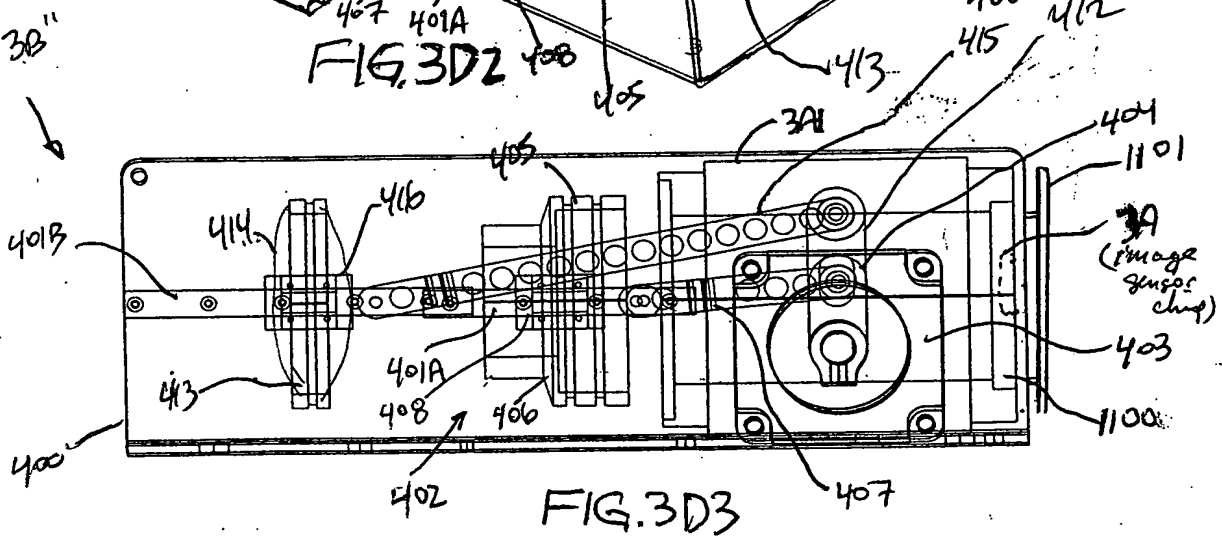
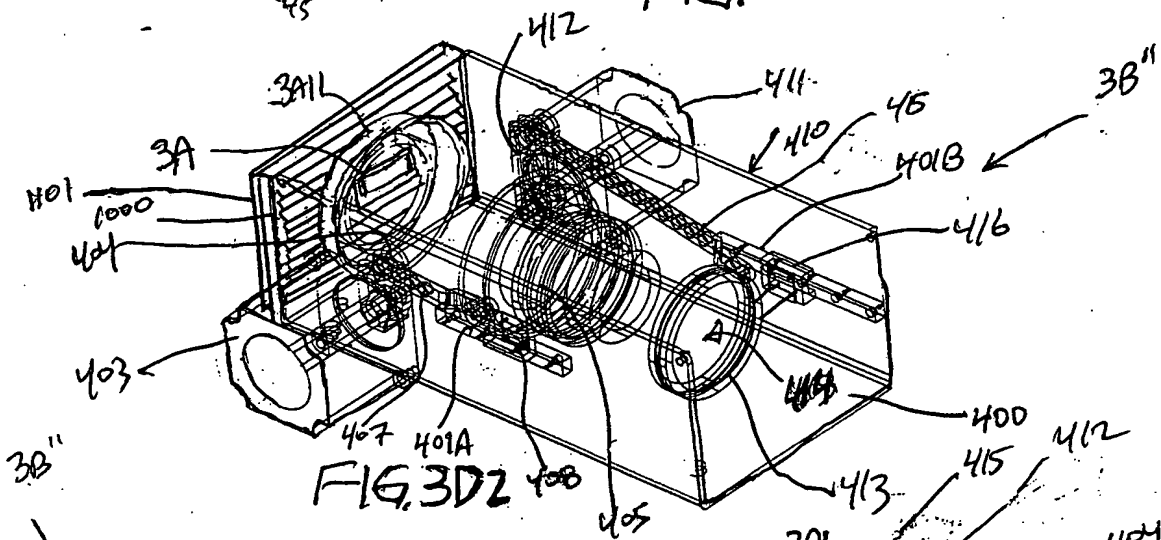
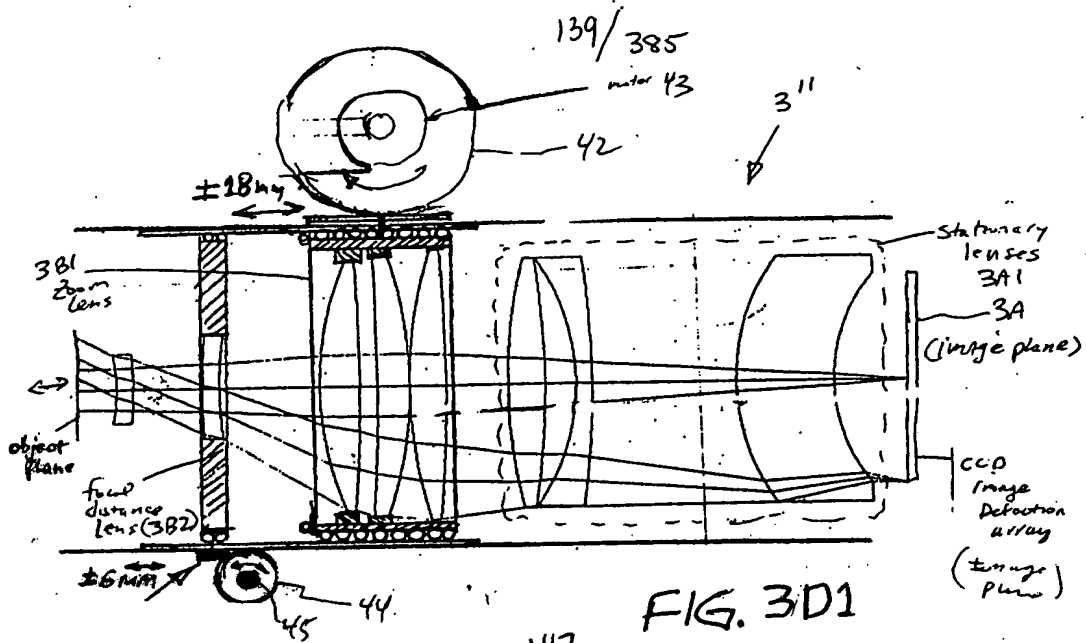


FIG. 3CZ

00000555 1101



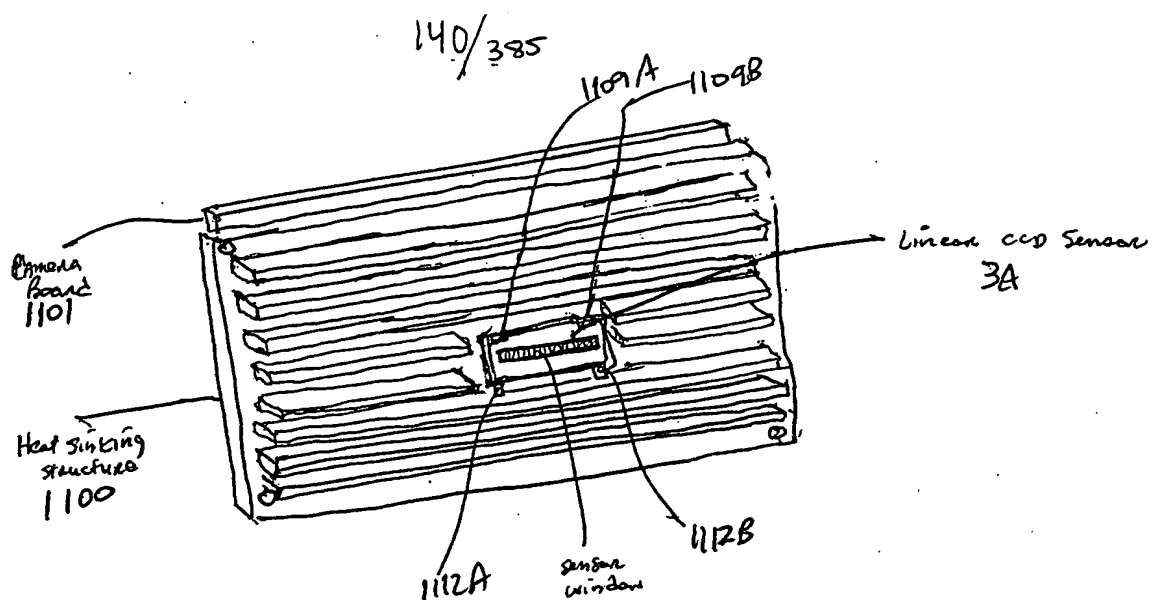
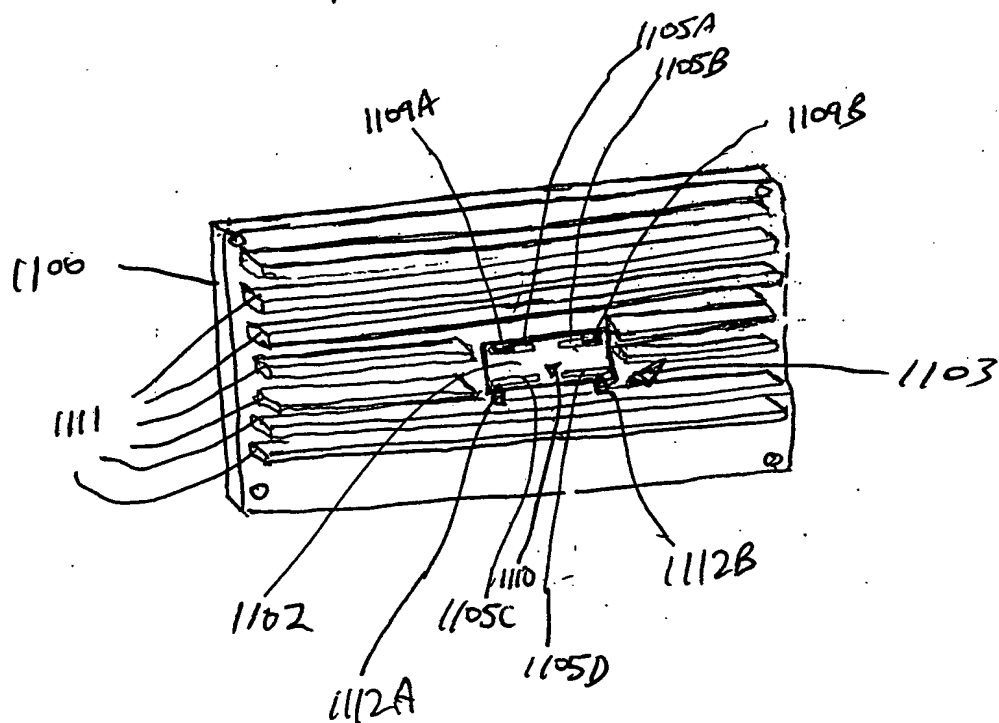
[illegible]

FIG. 3D4



F1 G. 3D5

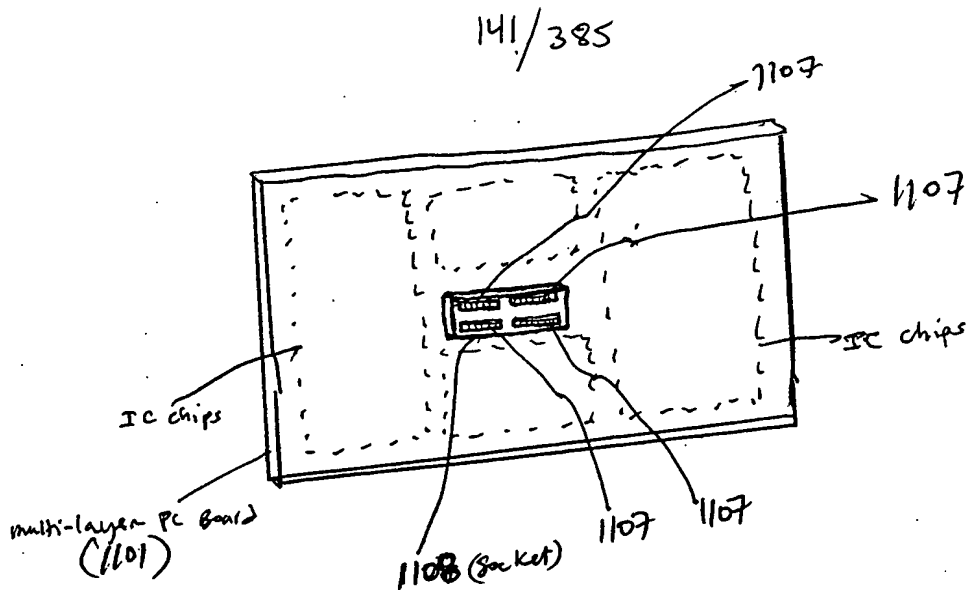


FIG. 3D6

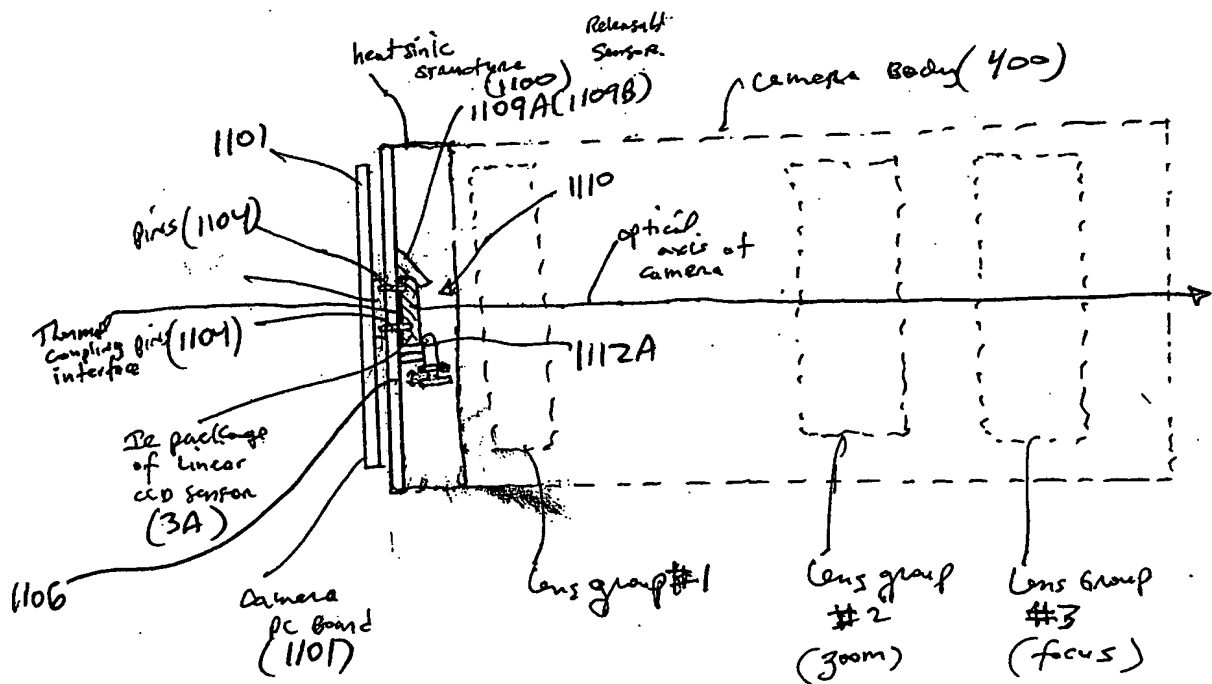


FIG. 3D7

142/385

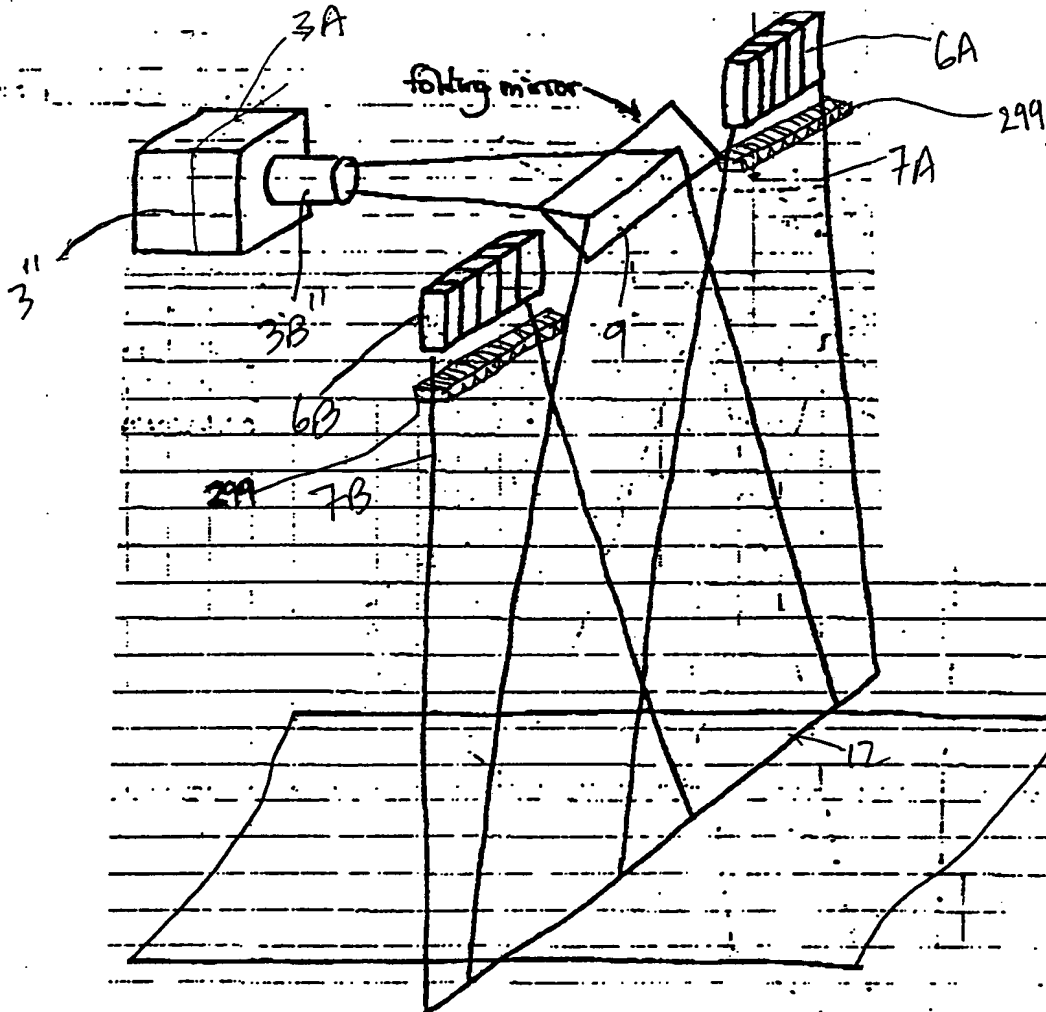


FIG 3E1

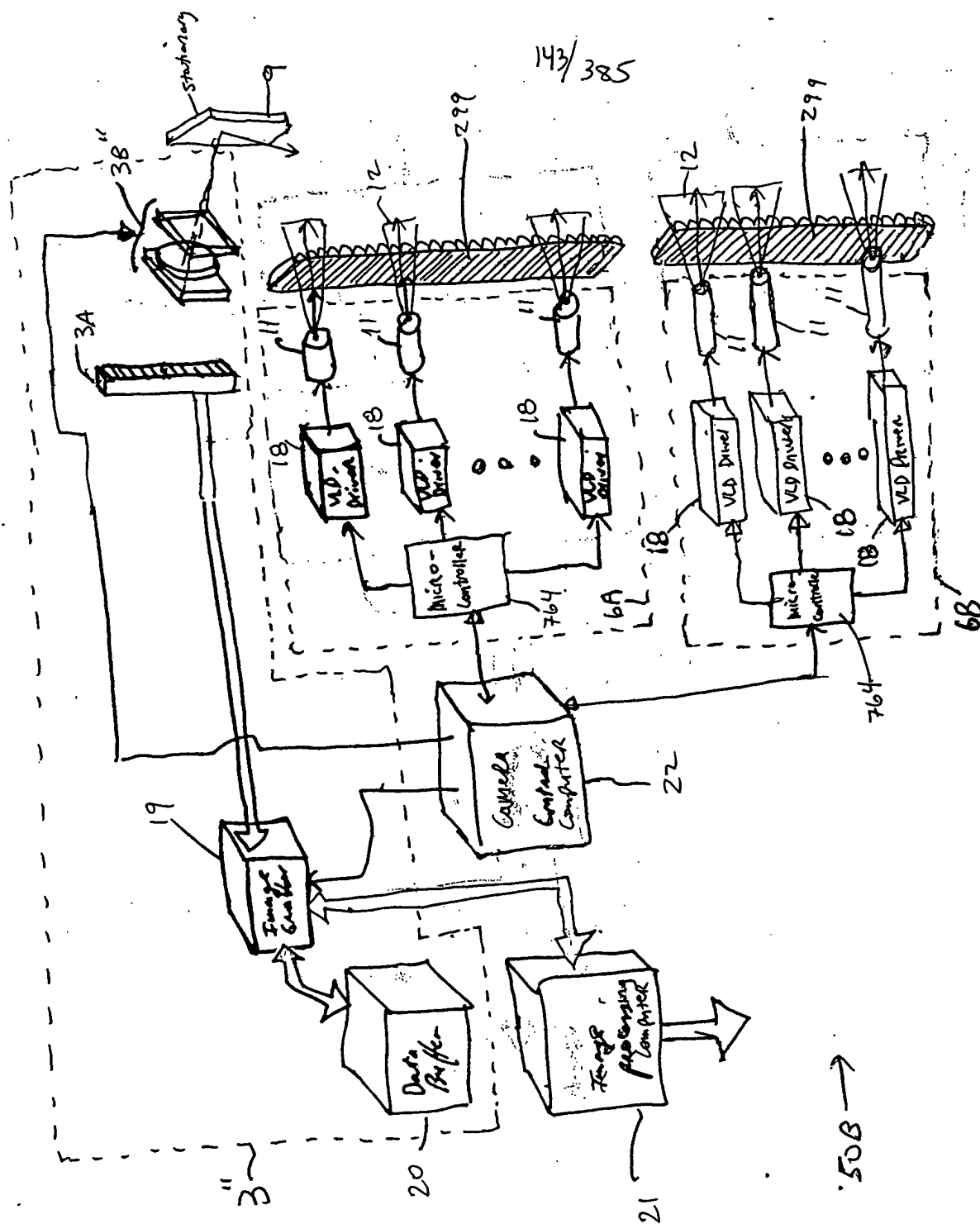
[illegible]

FIG. 3E2

TOP SECRET

144/385

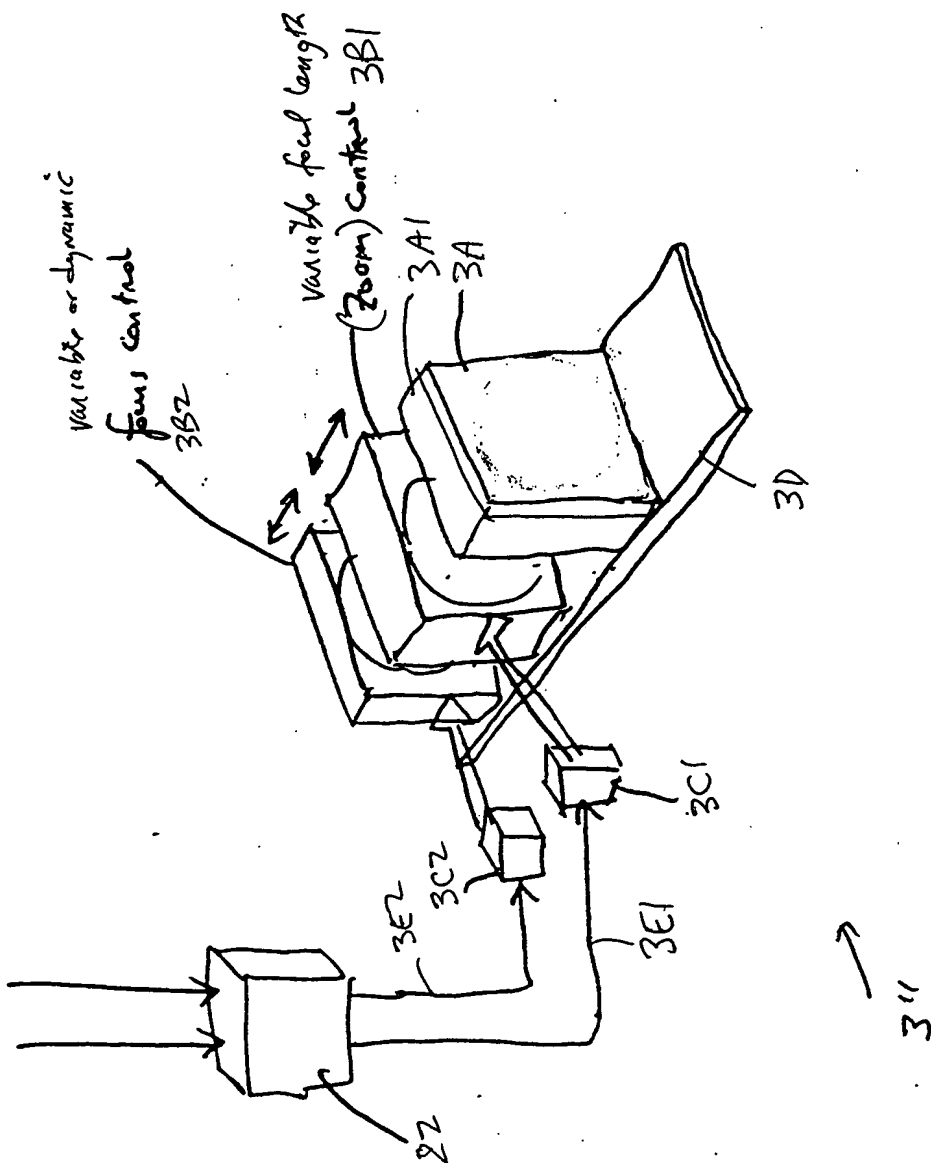


FIG. 3E3

145/385)

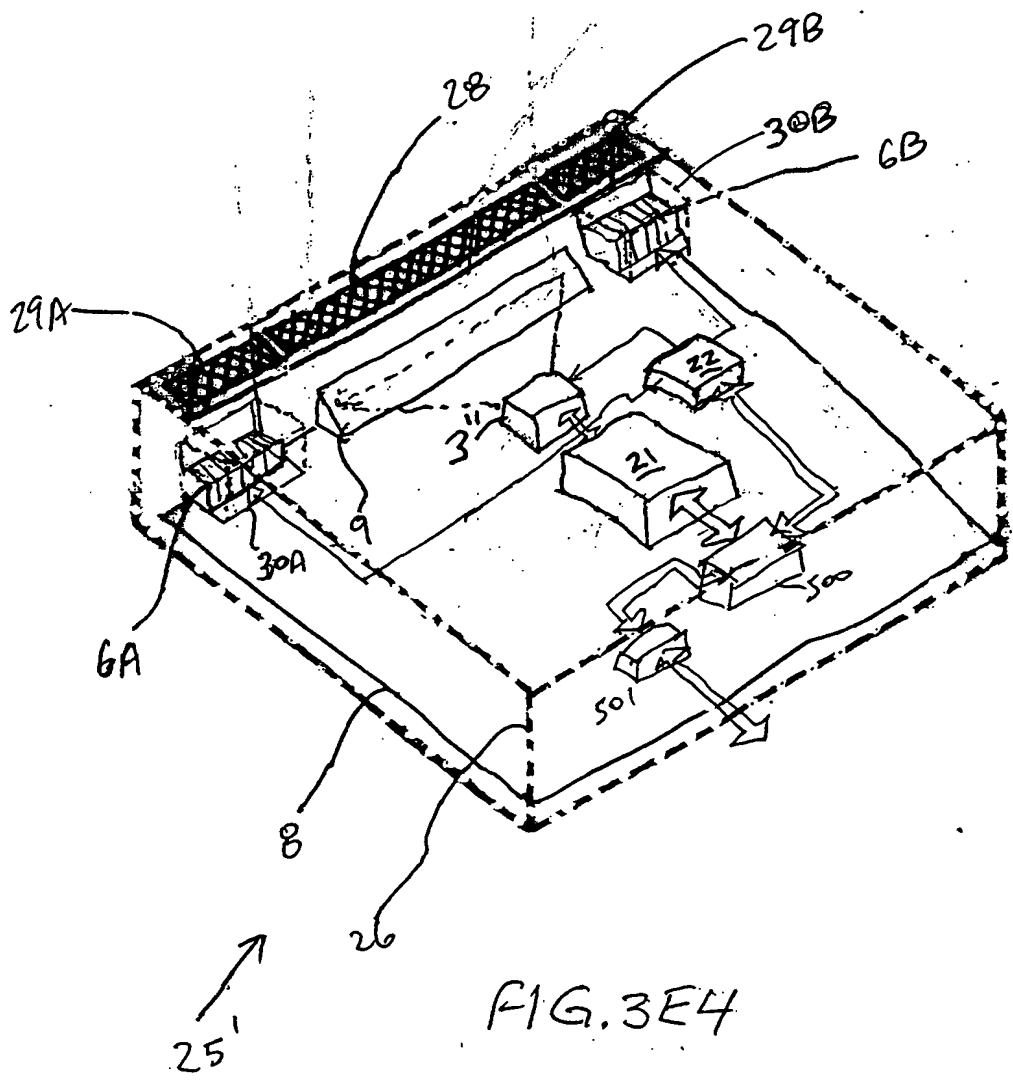


FIG. 3E4

146/385

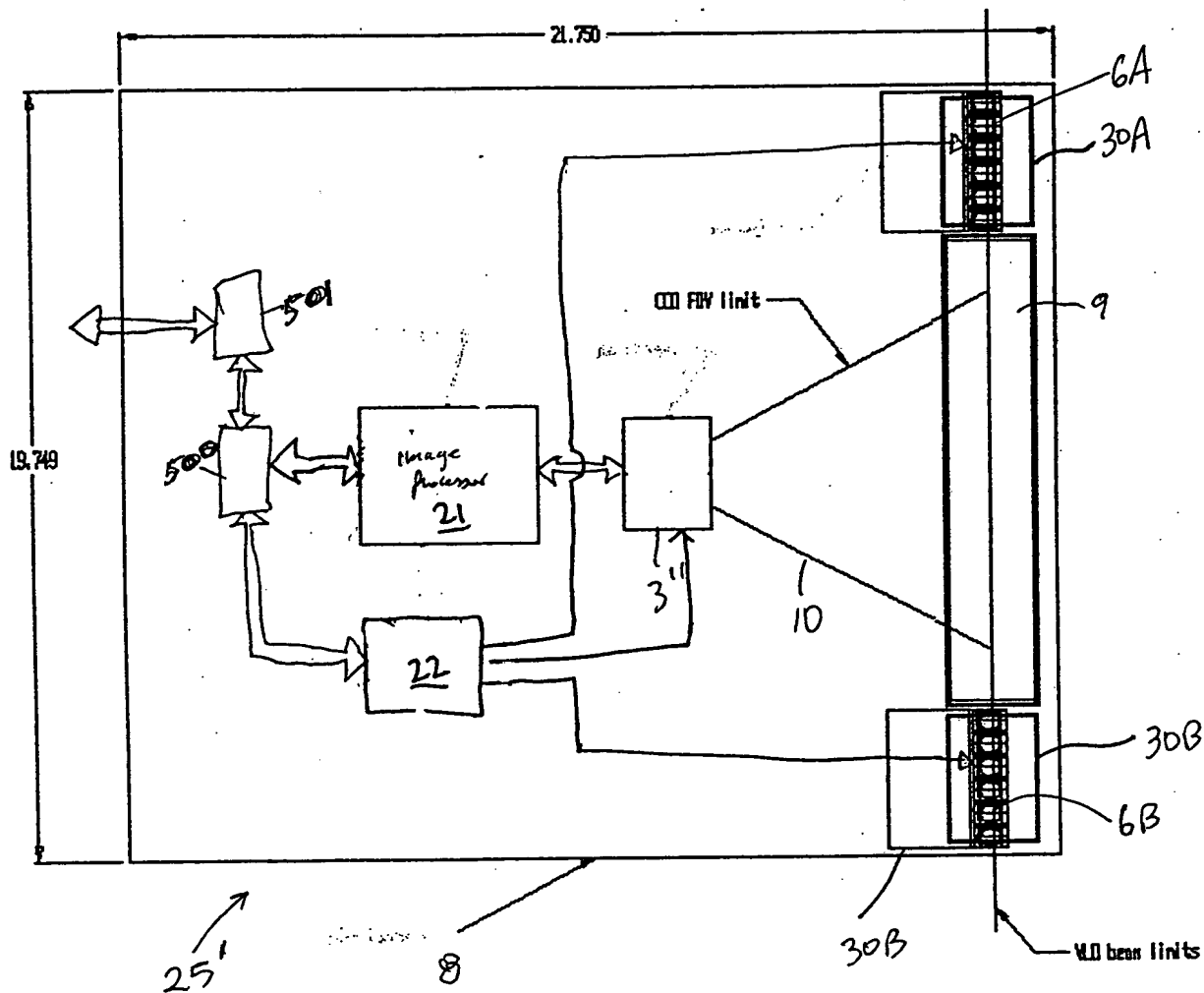


FIG. 3E5

147/385

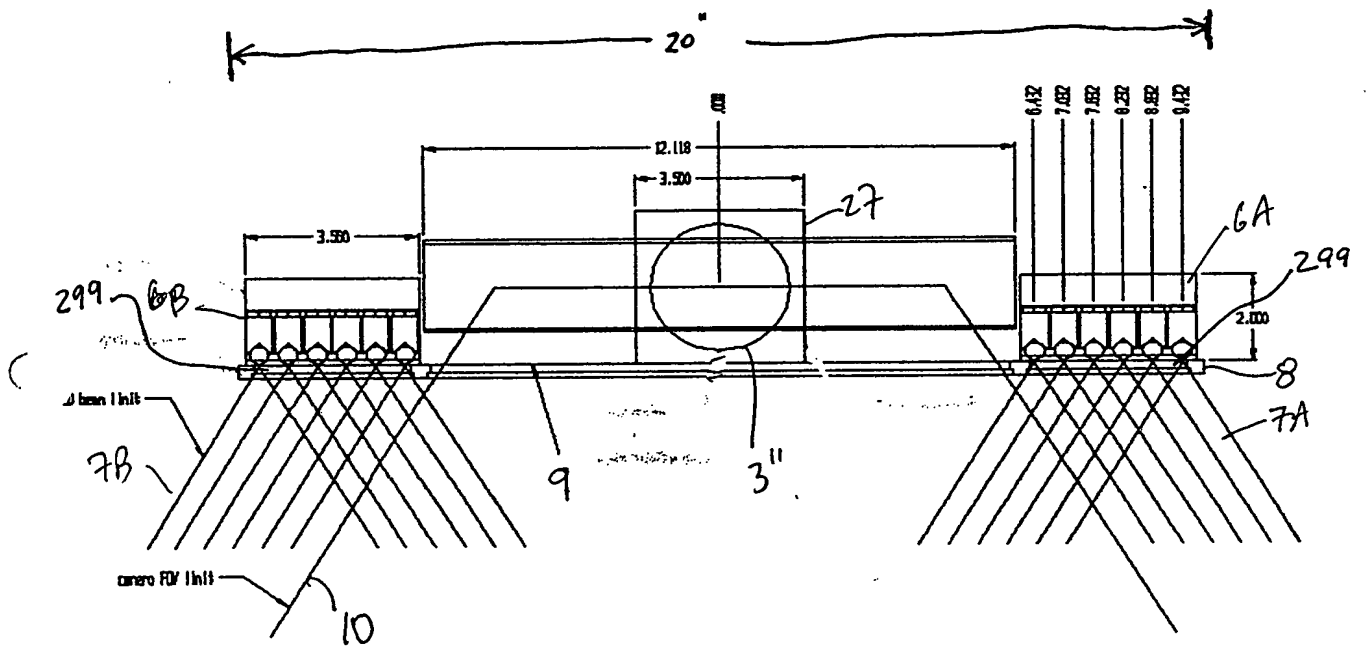


FIG. 3E6

148/385

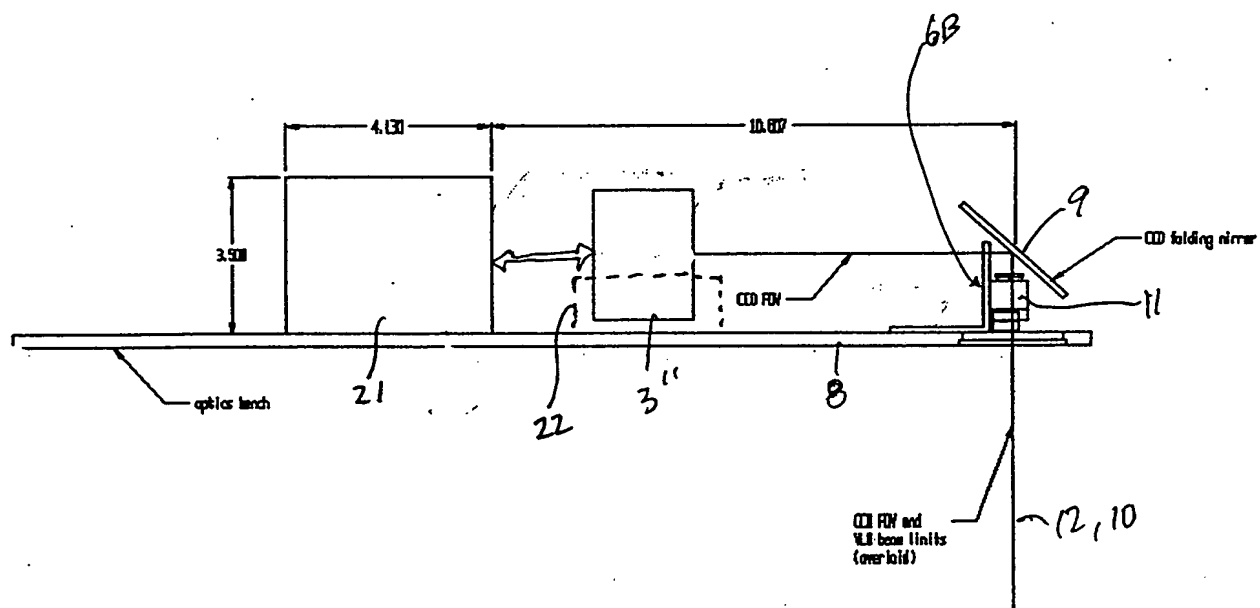


FIG. 3E7

149/385

*Variable FOV

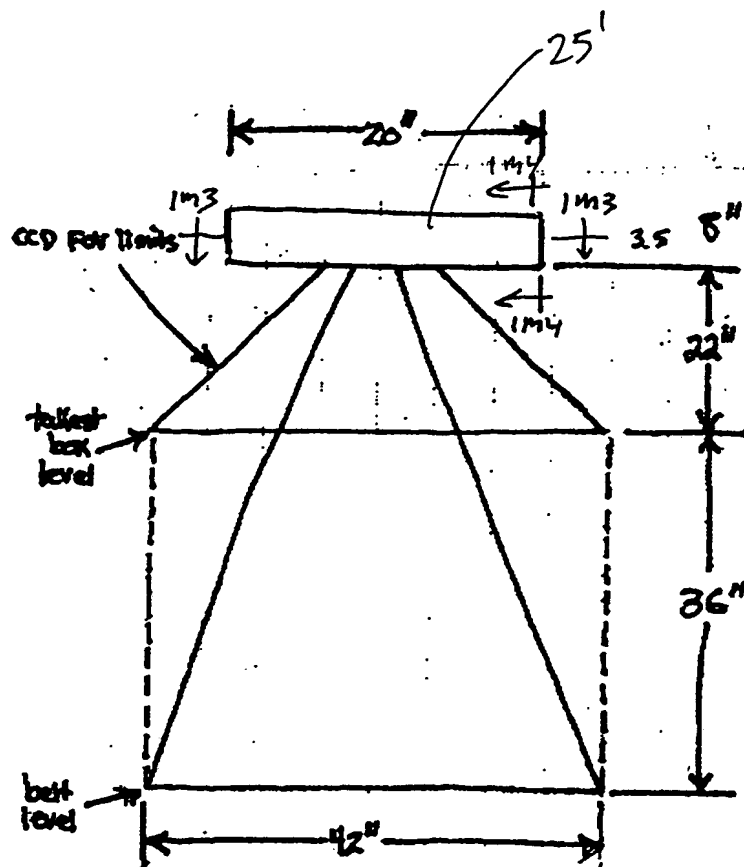


FIG. 3E8

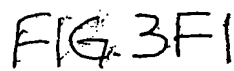
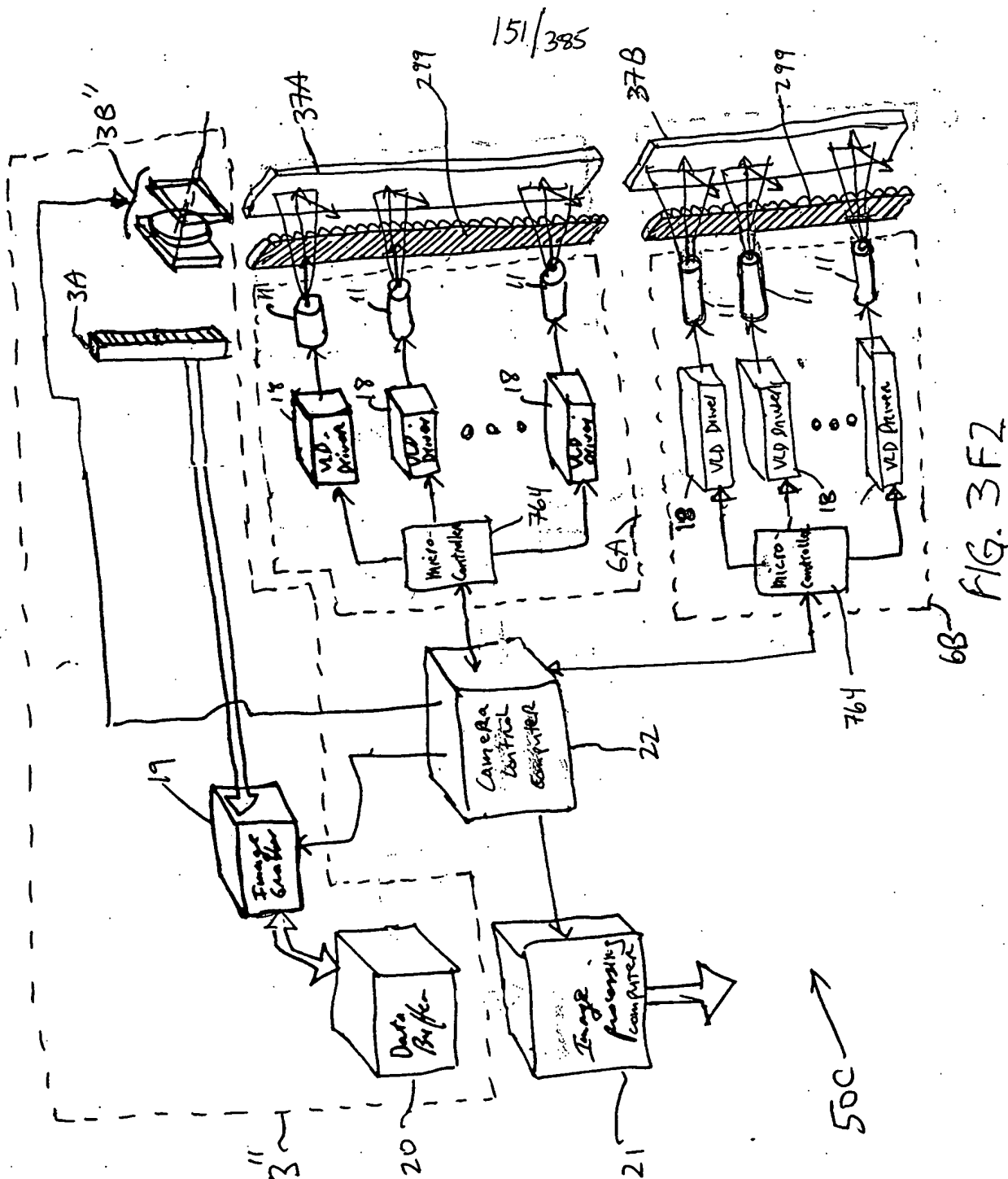
[illegible]

FIG. 3F1

THE **WORLD'S** **LARGEST** **BOOKSTORE**



| Station | Time | Lat. | Long. | Alt. | Wind | Temp. | Hum. | Press. | Clouds | Remarks |
|---------|------|-----------|------------|------|------|-------|------|--------|--------|---------|
| 1000 | 0000 | 34° 15' N | 122° 00' W | 10 | 000 | 50.0 | 85 | 30.00 | 000 | Clear |
| 1001 | 0100 | 34° 15' N | 122° 00' W | 10 | 000 | 50.0 | 85 | 30.00 | 000 | Clear |
| 1002 | 0200 | 34° 15' N | 122° 00' W | 10 | 000 | 50.0 | 85 | 30.00 | 000 | Clear |
| 1003 | 0300 | 34° 15' N | 122° 00' W | 10 | 000 | 50.0 | 85 | 30.00 | 000 | Clear |
| 1004 | 0400 | 34° 15' N | 122° 00' W | 10 | 000 | 50.0 | 85 | 30.00 | 000 | Clear |
| 1005 | 0500 | 34° 15' N | 122° 00' W | 10 | 000 | 50.0 | 85 | 30.00 | 000 | Clear |
| 1006 | 0600 | 34° 15' N | 122° 00' W | 10 | 000 | 50.0 | 85 | 30.00 | 000 | Clear |
| 1007 | 0700 | 34° 15' N | 122° 00' W | 10 | 000 | 50.0 | 85 | 30.00 | 000 | Clear |
| 1008 | 0800 | 34° 15' N | 122° 00' W | 10 | 000 | 50.0 | 85 | 30.00 | 000 | Clear |
| 1009 | 0900 | 34° 15' N | 122° 00' W | 10 | 000 | 50.0 | 85 | 30.00 | 000 | Clear |
| 1010 | 1000 | 34° 15' N | 122° 00' W | 10 | 000 | 50.0 | 85 | 30.00 | 000 | Clear |
| 1011 | 1100 | 34° 15' N | 122° 00' W | 10 | 000 | 50.0 | 85 | 30.00 | 000 | Clear |
| 1012 | 1200 | 34° 15' N | 122° 00' W | 10 | 000 | 50.0 | 85 | 30.00 | 000 | Clear |
| 1013 | 1300 | 34° 15' N | 122° 00' W | 10 | 000 | 50.0 | 85 | 30.00 | 000 | Clear |
| 1014 | 1400 | 34° 15' N | 122° 00' W | 10 | 000 | 50.0 | 85 | 30.00 | 000 | Clear |
| 1015 | 1500 | 34° 15' N | 122° 00' W | 10 | 000 | 50.0 | 85 | 30.00 | 000 | Clear |
| 1016 | 1600 | 34° 15' N | 122° 00' W | 10 | 000 | 50.0 | 85 | 30.00 | 000 | Clear |
| 1017 | 1700 | 34° 15' N | 122° 00' W | 10 | 000 | 50.0 | 85 | 30.00 | 000 | Clear |
| 1018 | 1800 | 34° 15' N | 122° 00' W | 10 | 000 | 50.0 | 85 | 30.00 | 000 | Clear |
| 1019 | 1900 | 34° 15' N | 122° 00' W | 10 | 000 | 50.0 | 85 | 30.00 | 000 | Clear |
| 1020 | 2000 | 34° 15' N | 122° 00' W | 10 | 000 | 50.0 | 85 | 30.00 | 000 | Clear |
| 1021 | 2100 | 34° 15' N | 122° 00' W | 10 | 000 | 50.0 | 85 | 30.00 | 000 | Clear |
| 1022 | 2200 | 34° 15' N | 122° 00' W | 10 | 000 | 50.0 | 85 | 30.00 | 000 | Clear |
| 1023 | 2300 | 34° 15' N | 122° 00' W | 10 | 000 | 50.0 | 85 | 30.00 | 000 | Clear |
| 1024 | 0000 | 34° 15' N | 122° 00' W | 10 | 000 | 50.0 | 85 | 30.00 | 000 | Clear |
| 1025 | 0100 | 34° 15' N | 122° 00' W | 10 | 000 | 50.0 | 85 | 30.00 | 000 | Clear |
| 1026 | 0200 | 34° 15' N | 122° 00' W | 10 | 000 | 50.0 | 85 | 30.00 | 000 | Clear |
| 1027 | 0300 | 34° 15' N | 122° 00' W | 10 | 000 | 50.0 | 85 | 30.00 | 000 | Clear |
| 1028 | 0400 | 34° 15' N | 122° 00' W | 10 | 000 | 50.0 | 85 | 30.00 | 000 | Clear |
| 1029 | 0500 | 34° 15' N | 122° 00' W | 10 | 000 | 50.0 | 85 | 30.00 | 000 | Clear |
| 1030 | 0600 | 34° 15' N | 122° 00' W | 10 | 000 | 50.0 | 85 | 30.00 | 000 | Clear |
| 1031 | 0700 | 34° 15' N | 122° 00' W | 10 | 000 | 50.0 | 85 | 30.00 | 000 | Clear |
| 1032 | 0800 | 34° 15' N | 122° 00' W | 10 | 000 | 50.0 | 85 | 30.00 | 000 | Clear |
| 1033 | 0900 | 34° 15' N | 122° 00' W | 10 | 000 | 50.0 | 85 | 30.00 | 0 | |



FIG. 3F2

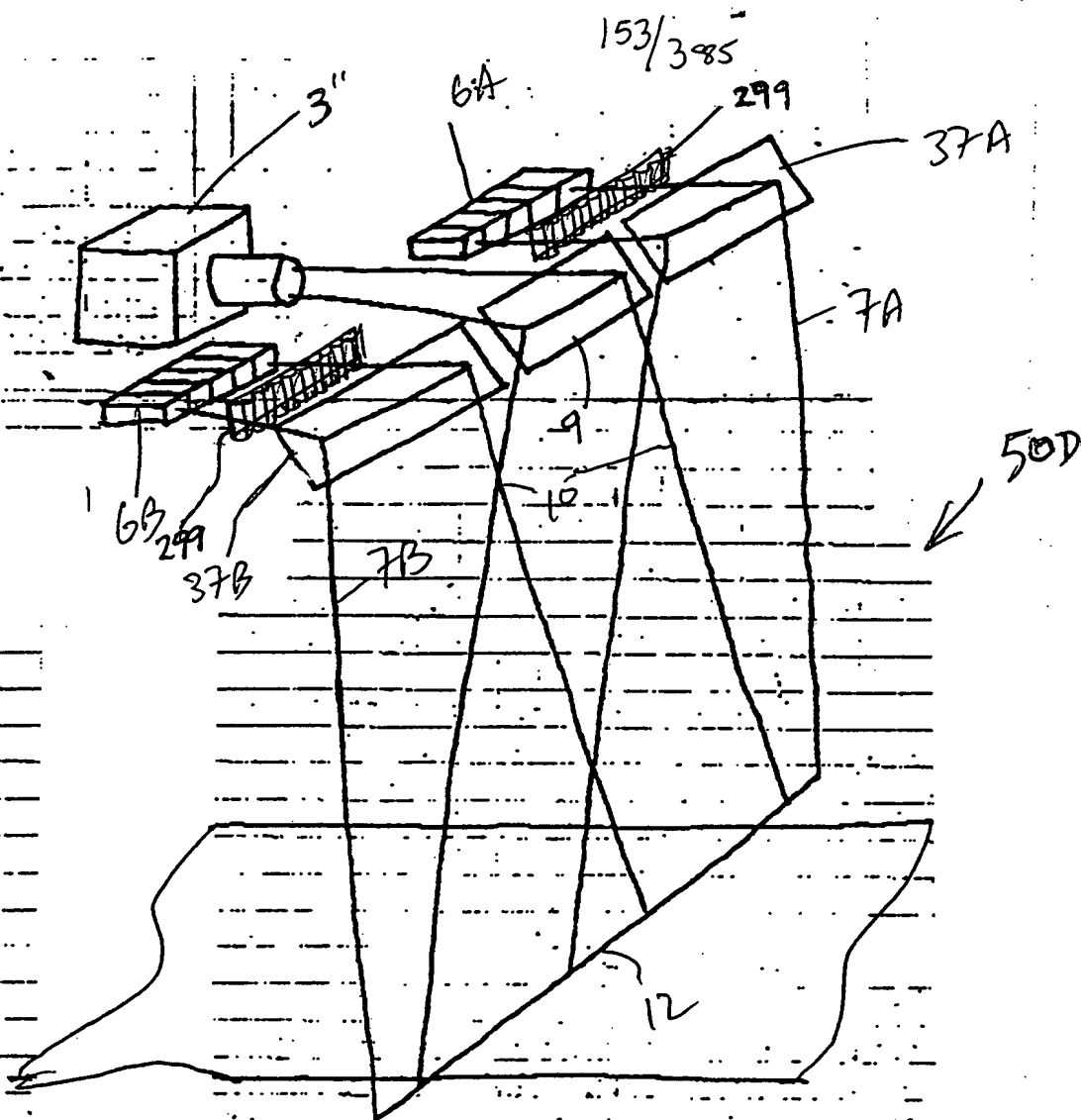
[illegible]

FIG. 3G1

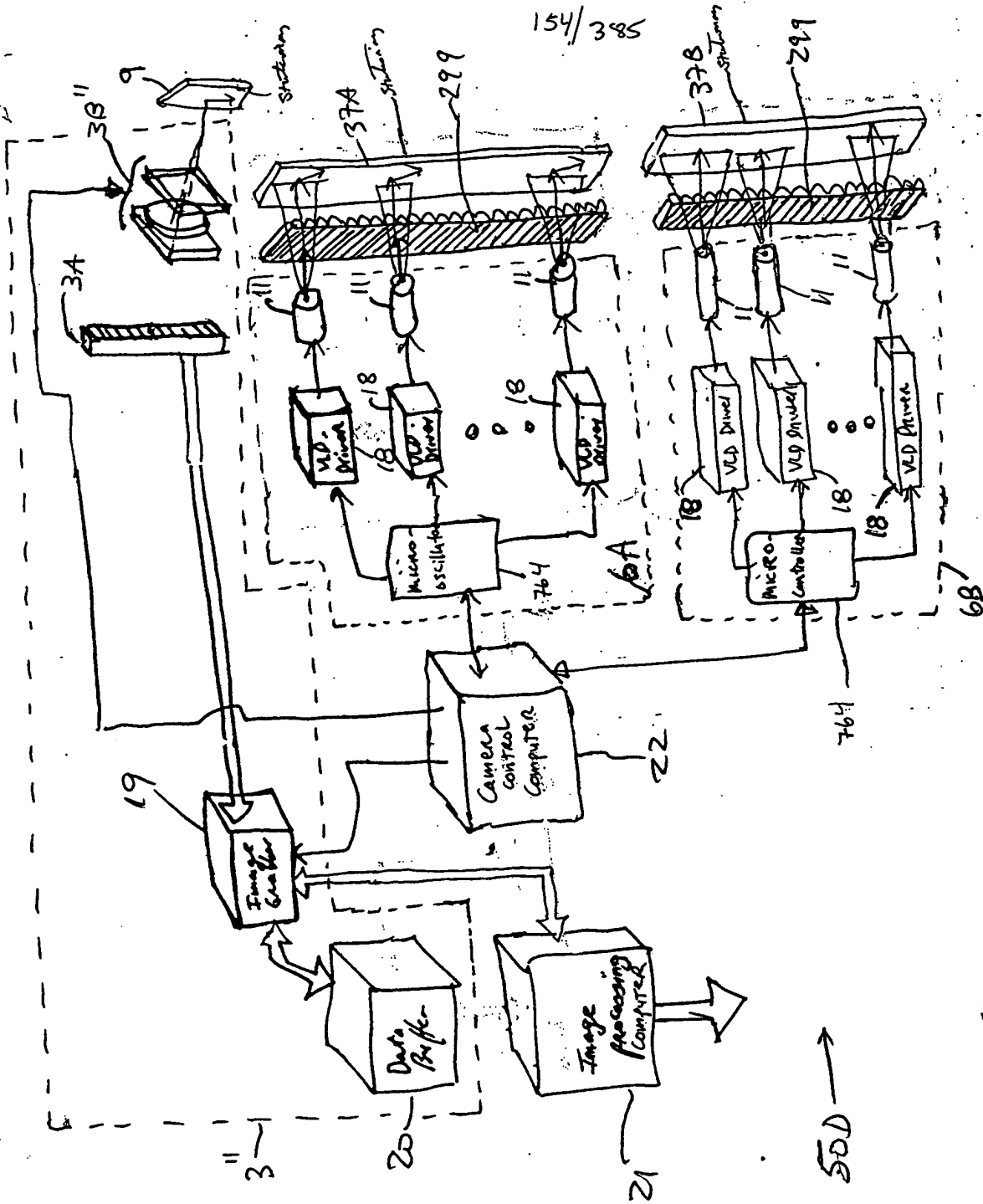


FIG. 362

155/385

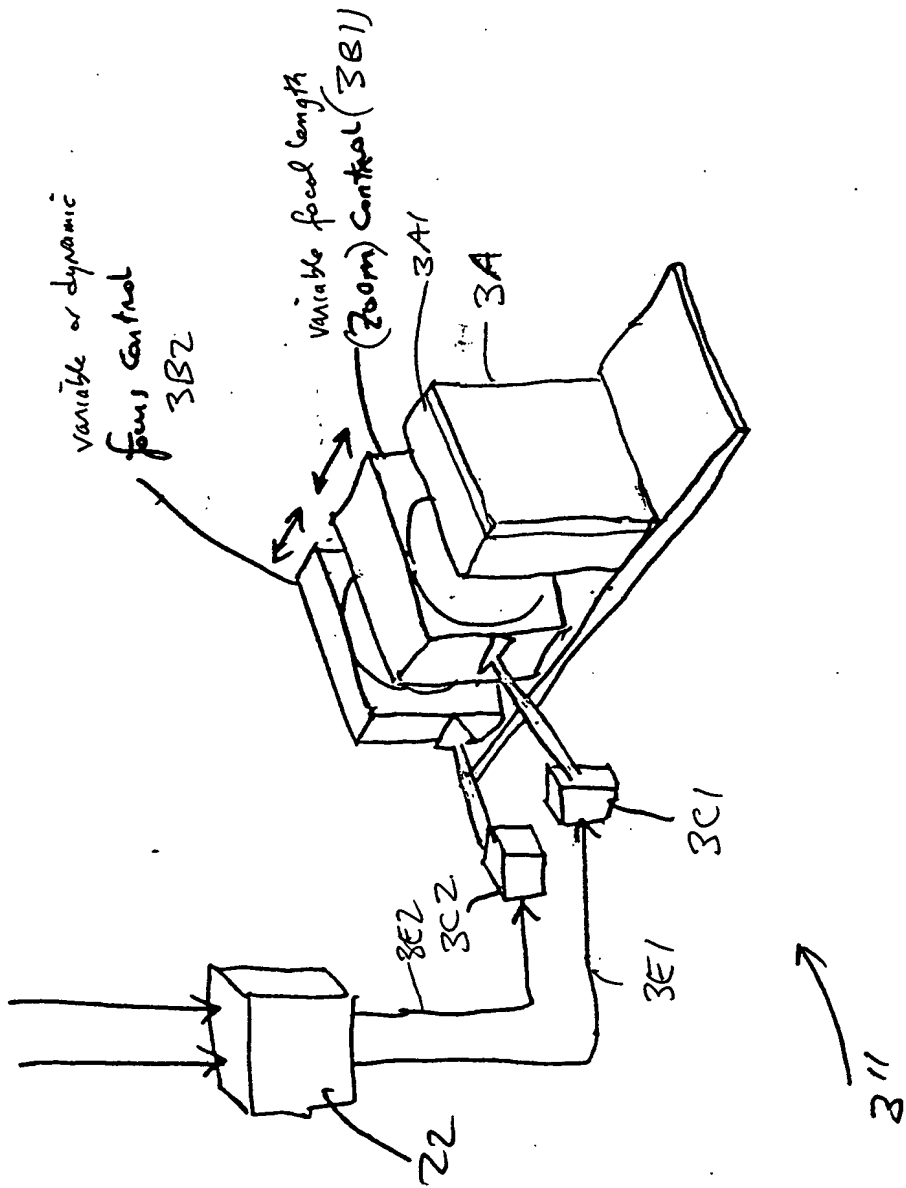


FIG. 3Q3

156/385

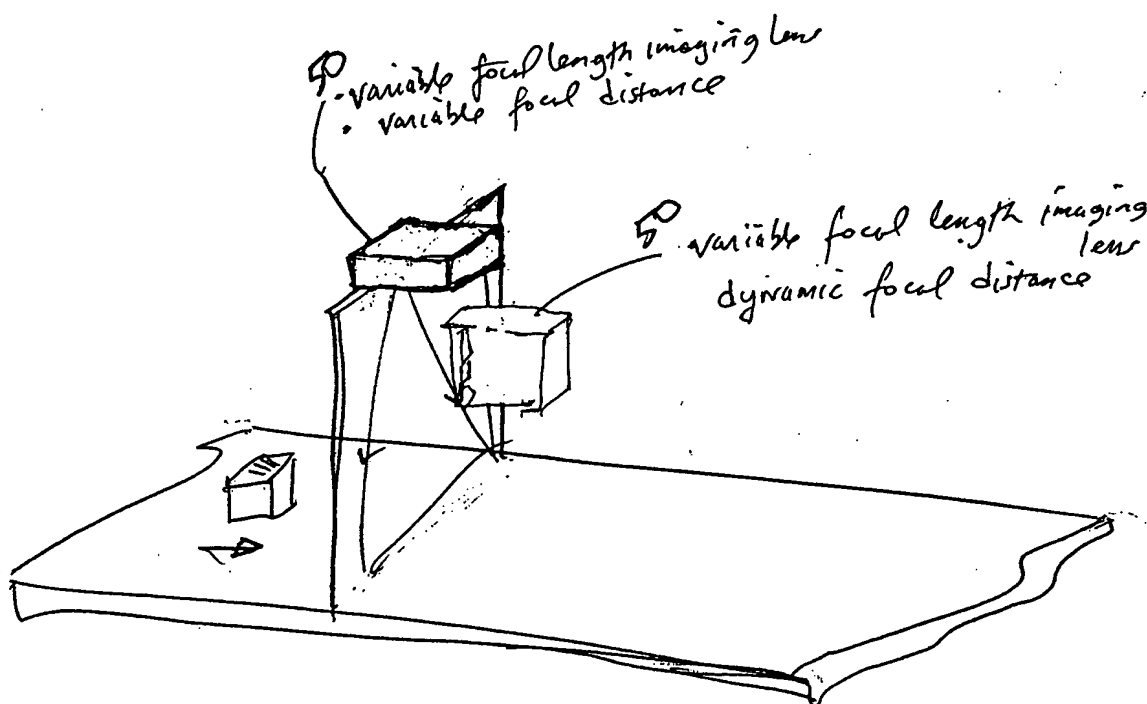
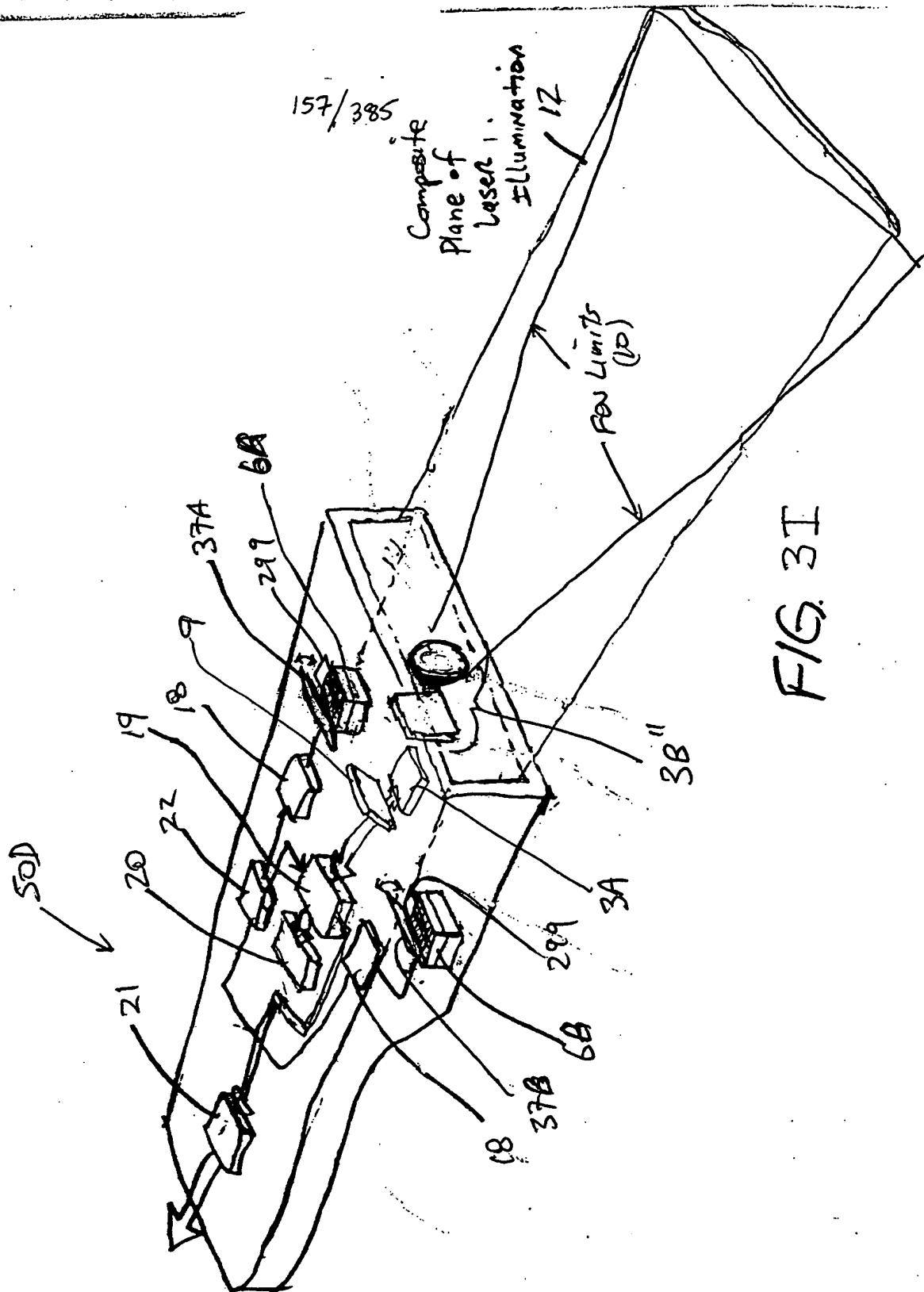


FIG. 3H

FIG. 3I



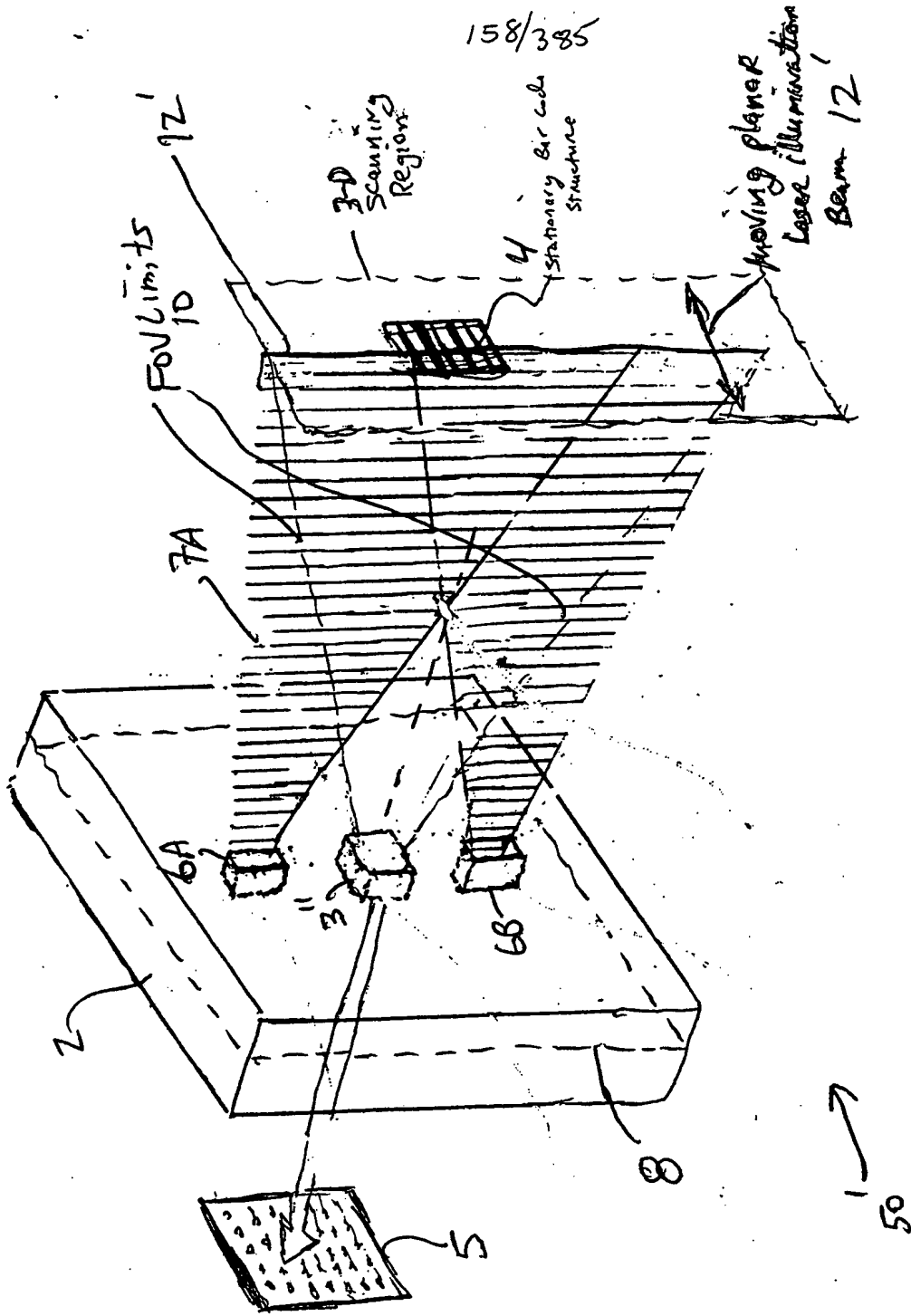


FIG. 3J1

09900585 43404
TOTAL 5250560

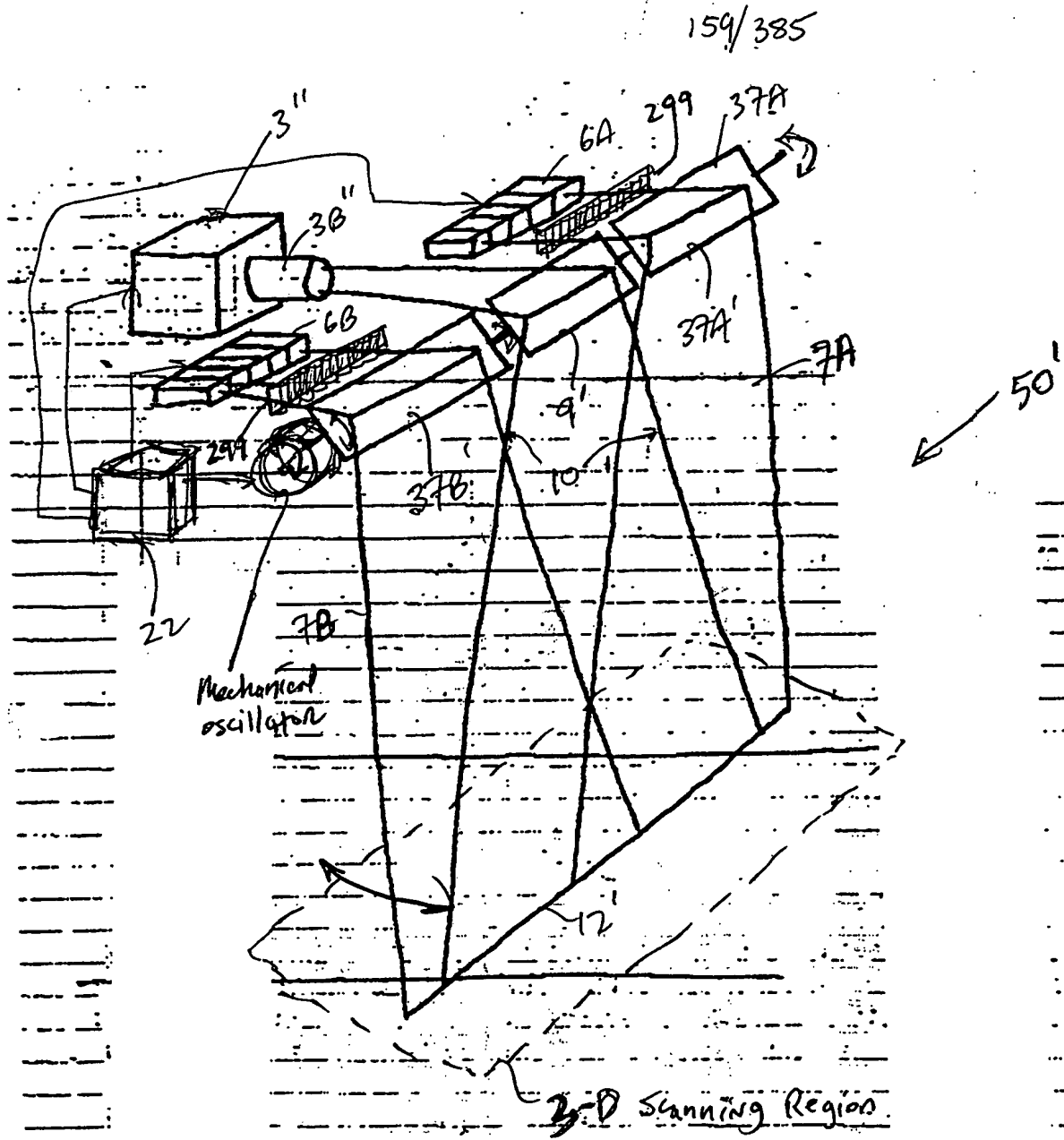


FIG 3J2

TOP SECRET

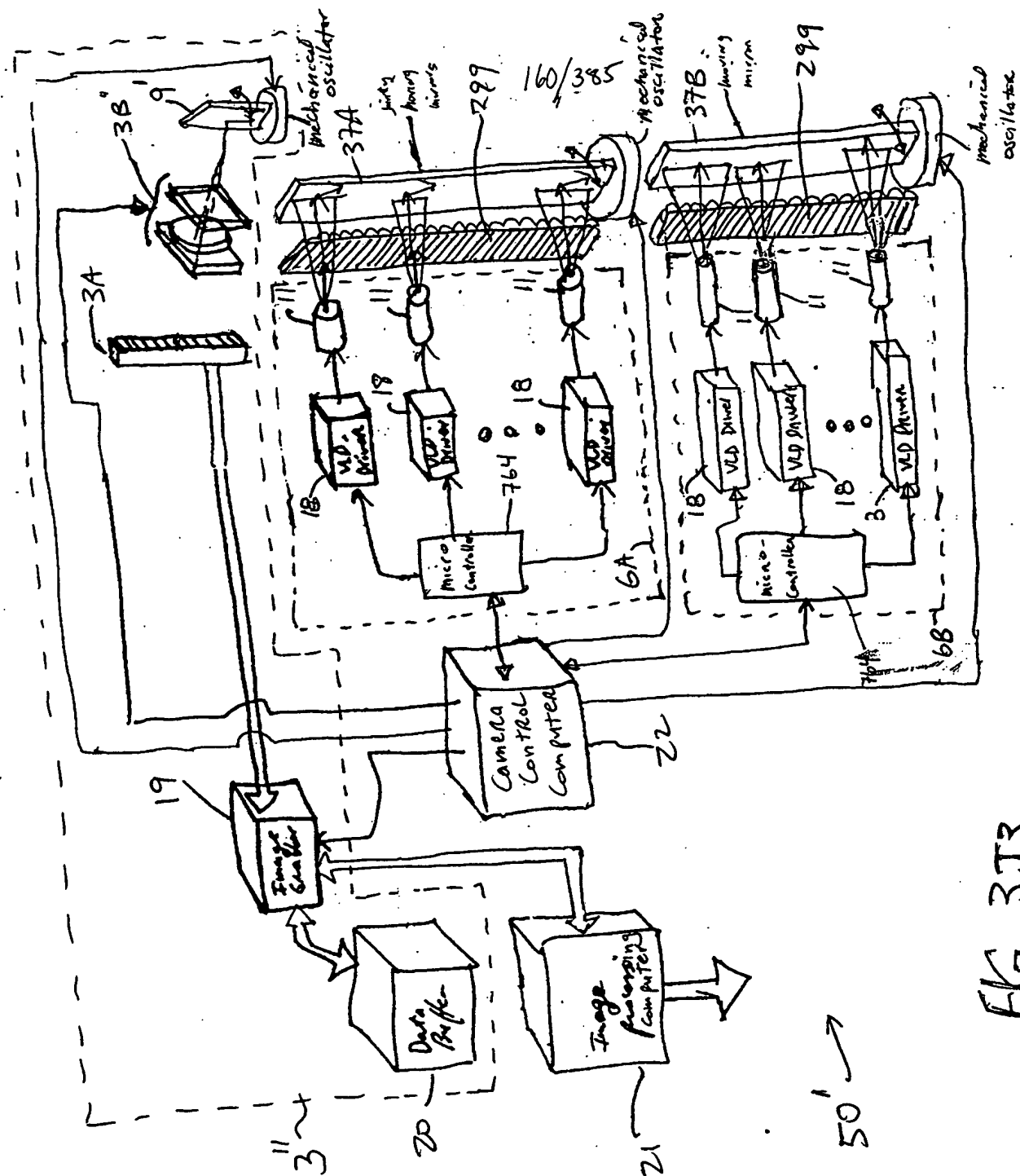


FIG. 3J3

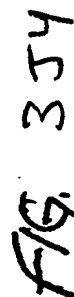
[illegible]

FIG. 354

FIG. 3B

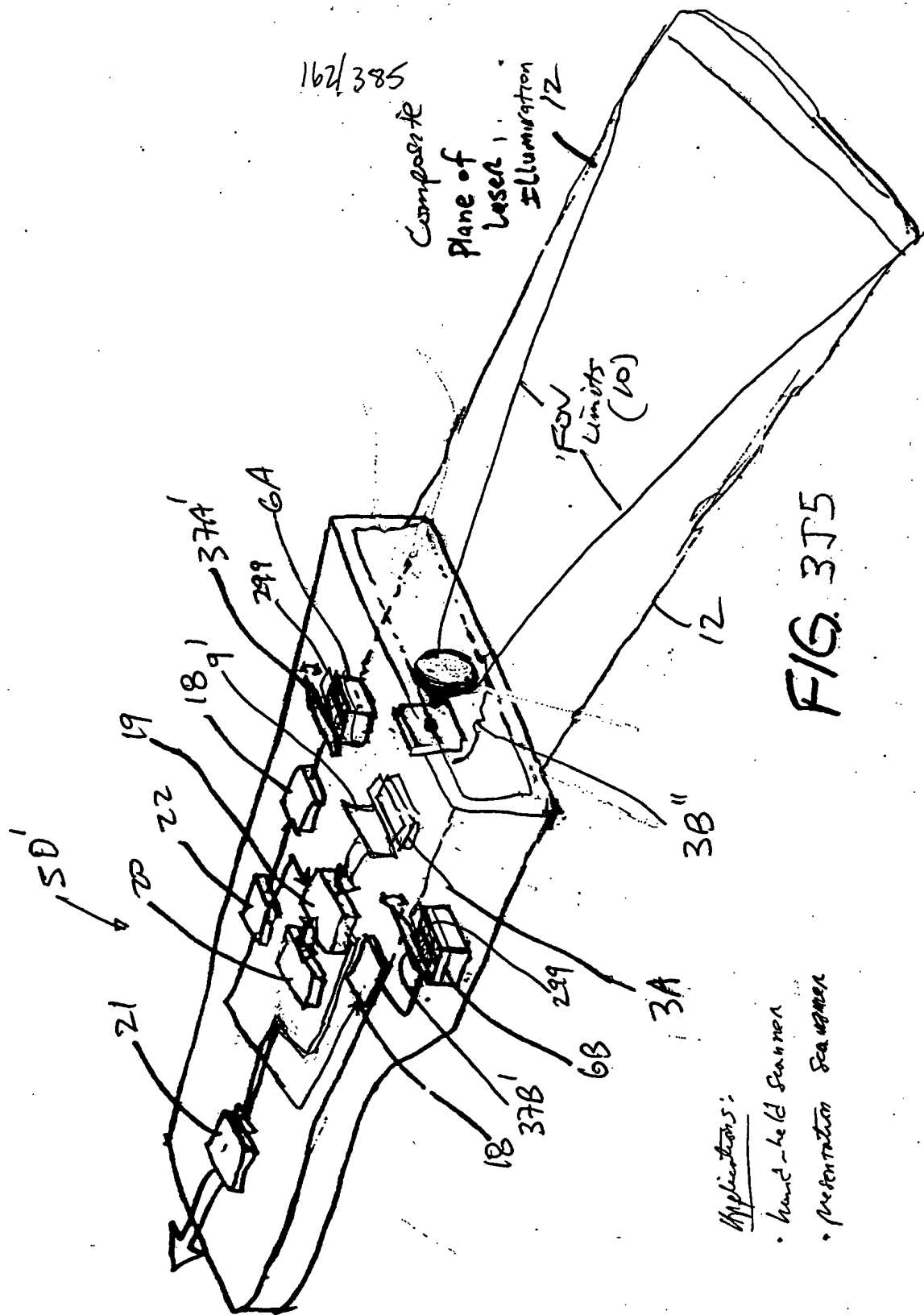
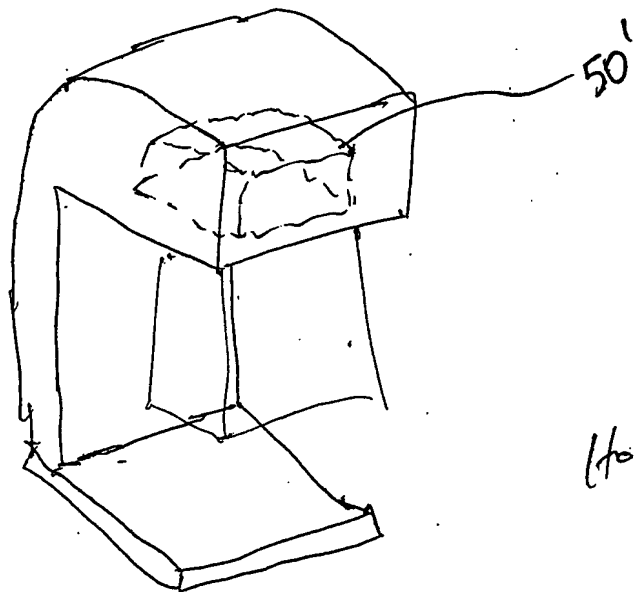


FIG. 3B

- Applications:
- hand-held scanner
 - presentation scanner

163/385

09090585 42104



2-D
Hold-up der
Scanner

FIG-3J6

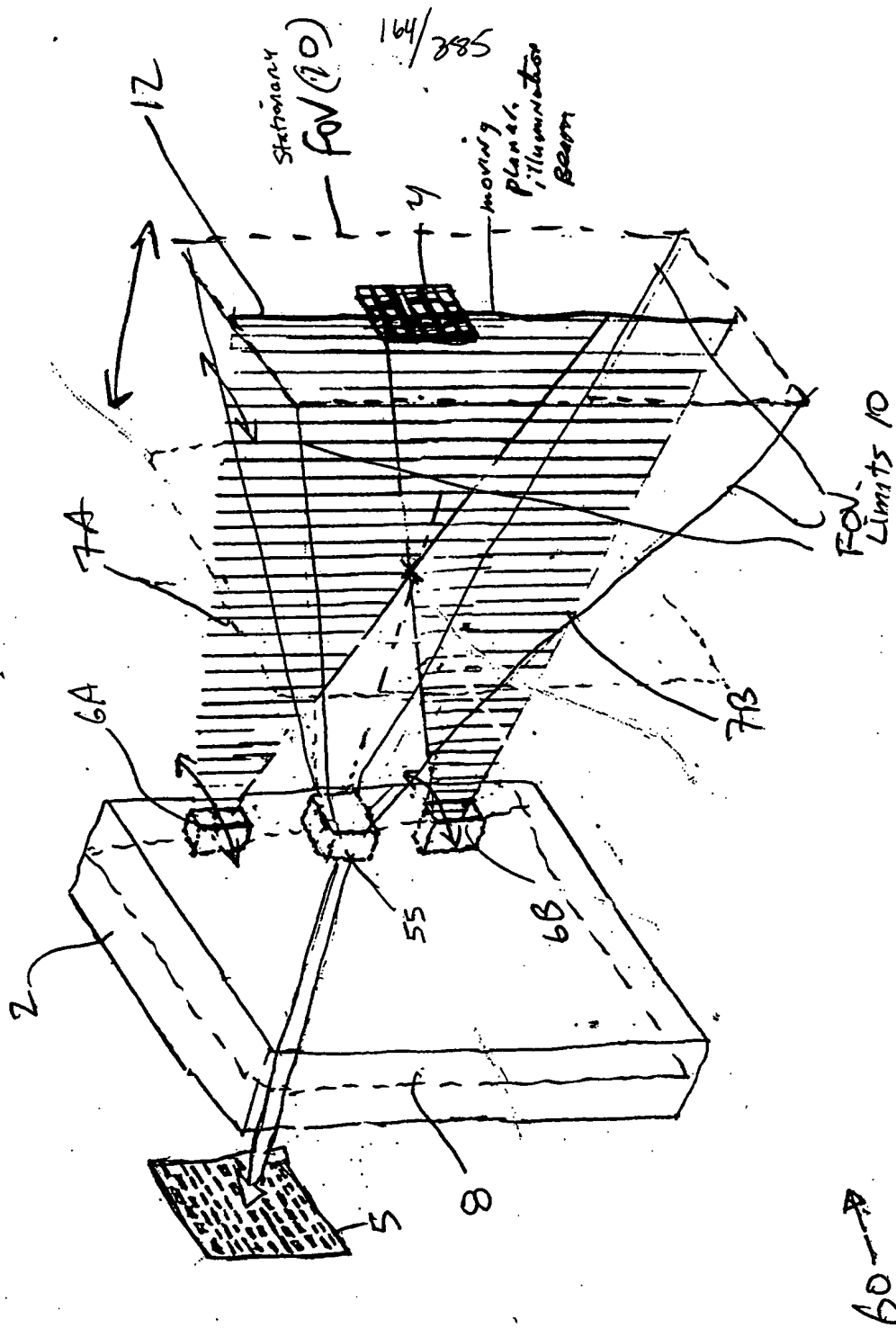
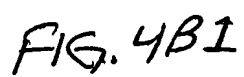


FIG 4A

| Station | Time | Lat. | Long. | Alt. | Wind | Temp. | Hum. | Clouds | Remarks |
|---------|------|-----------|------------|------|------|-------|------|--------|---------|
| 1 | 0000 | 34° 15' N | 122° 00' W | 10 | 000 | 50 | 80 | 000 | Clear |
| 2 | 0100 | 34° 15' N | 122° 00' W | 10 | 000 | 50 | 80 | 000 | Clear |
| 3 | 0200 | 34° 15' N | 122° 00' W | 10 | 000 | 50 | 80 | 000 | Clear |
| 4 | 0300 | 34° 15' N | 122° 00' W | 10 | 000 | 50 | 80 | 000 | Clear |
| 5 | 0400 | 34° 15' N | 122° 00' W | 10 | 000 | 50 | 80 | 000 | Clear |
| 6 | 0500 | 34° 15' N | 122° 00' W | 10 | 000 | 50 | 80 | 000 | Clear |
| 7 | 0600 | 34° 15' N | 122° 00' W | 10 | 000 | 50 | 80 | 000 | Clear |
| 8 | 0700 | 34° 15' N | 122° 00' W | 10 | 000 | 50 | 80 | 000 | Clear |
| 9 | 0800 | 34° 15' N | 122° 00' W | 10 | 000 | 50 | 80 | 000 | Clear |
| 10 | 0900 | 34° 15' N | 122° 00' W | 10 | 000 | 50 | 80 | 000 | Clear |
| 11 | 1000 | 34° 15' N | 122° 00' W | 10 | 000 | 50 | 80 | 000 | Clear |
| 12 | 1100 | 34° 15' N | 122° 00' W | 10 | 000 | 50 | 80 | 000 | Clear |
| 13 | 1200 | 34° 15' N | 122° 00' W | 10 | 000 | 50 | 80 | 000 | Clear |
| 14 | 1300 | 34° 15' N | 122° 00' W | 10 | 000 | 50 | 80 | 000 | Clear |
| 15 | 1400 | 34° 15' N | 122° 00' W | 10 | 000 | 50 | 80 | 000 | Clear |
| 16 | 1500 | 34° 15' N | 122° 00' W | 10 | 000 | 50 | 80 | 000 | Clear |
| 17 | 1600 | 34° 15' N | 122° 00' W | 10 | 000 | 50 | 80 | 000 | Clear |
| 18 | 1700 | 34° 15' N | 122° 00' W | 10 | 000 | 50 | 80 | 000 | Clear |
| 19 | 1800 | 34° 15' N | 122° 00' W | 10 | 000 | 50 | 80 | 000 | Clear |
| 20 | 1900 | 34° 15' N | 122° 00' W | 10 | 000 | 50 | 80 | 000 | Clear |
| 21 | 2000 | 34° 15' N | 122° 00' W | 10 | 000 | 50 | 80 | 000 | Clear |
| 22 | 2100 | 34° 15' N | 122° 00' W | 10 | 000 | 50 | 80 | 000 | Clear |
| 23 | 2200 | 34° 15' N | 122° 00' W | 10 | 000 | 50 | 80 | 000 | Clear |
| 24 | 2300 | 34° 15' N | 122° 00' W | 10 | 000 | 50 | 80 | 000 | Clear |
| 25 | 0000 | 34° 15' N | 122° 00' W | 10 | 000 | 50 | 80 | 000 | Clear |



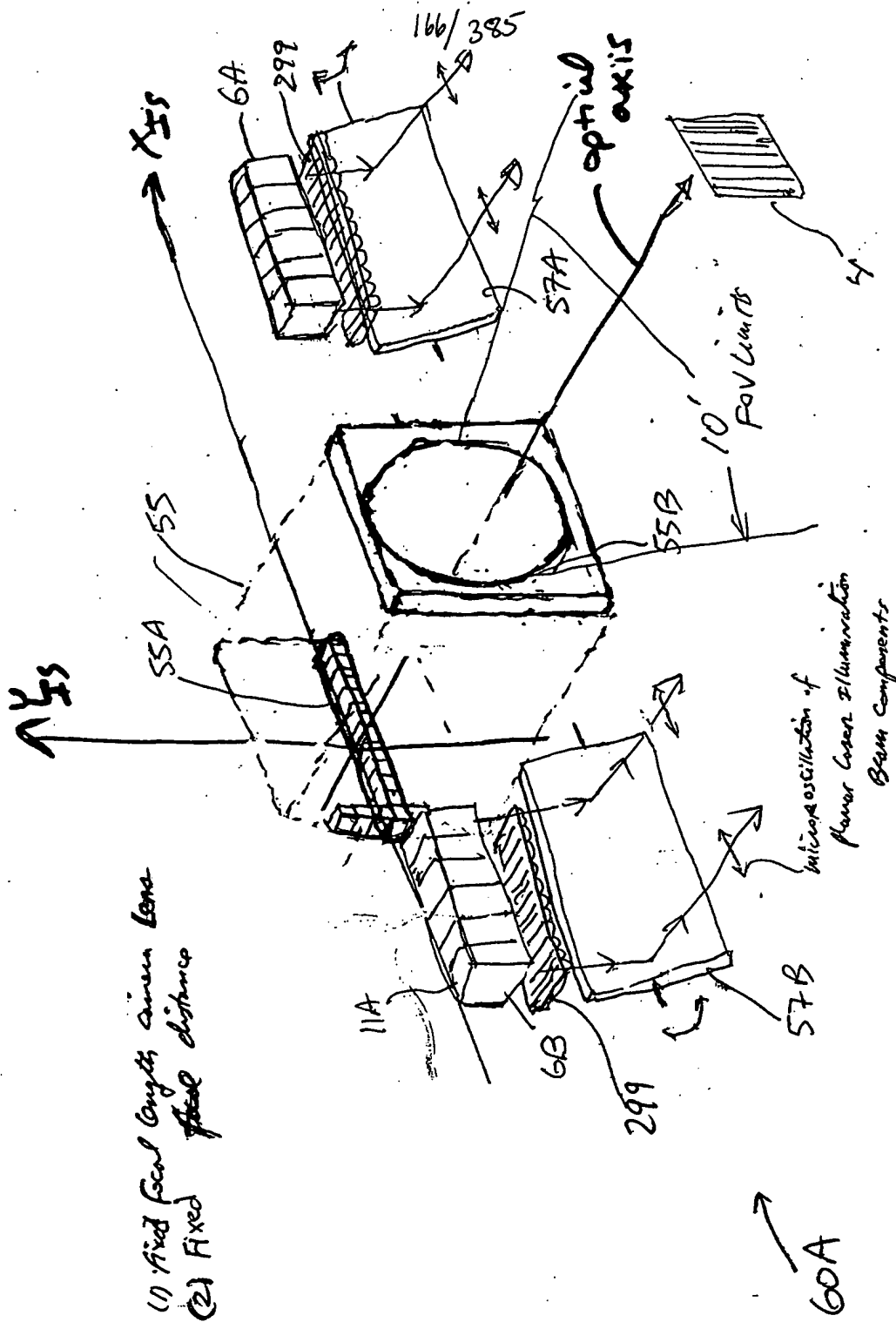


FIG. 4B.Z

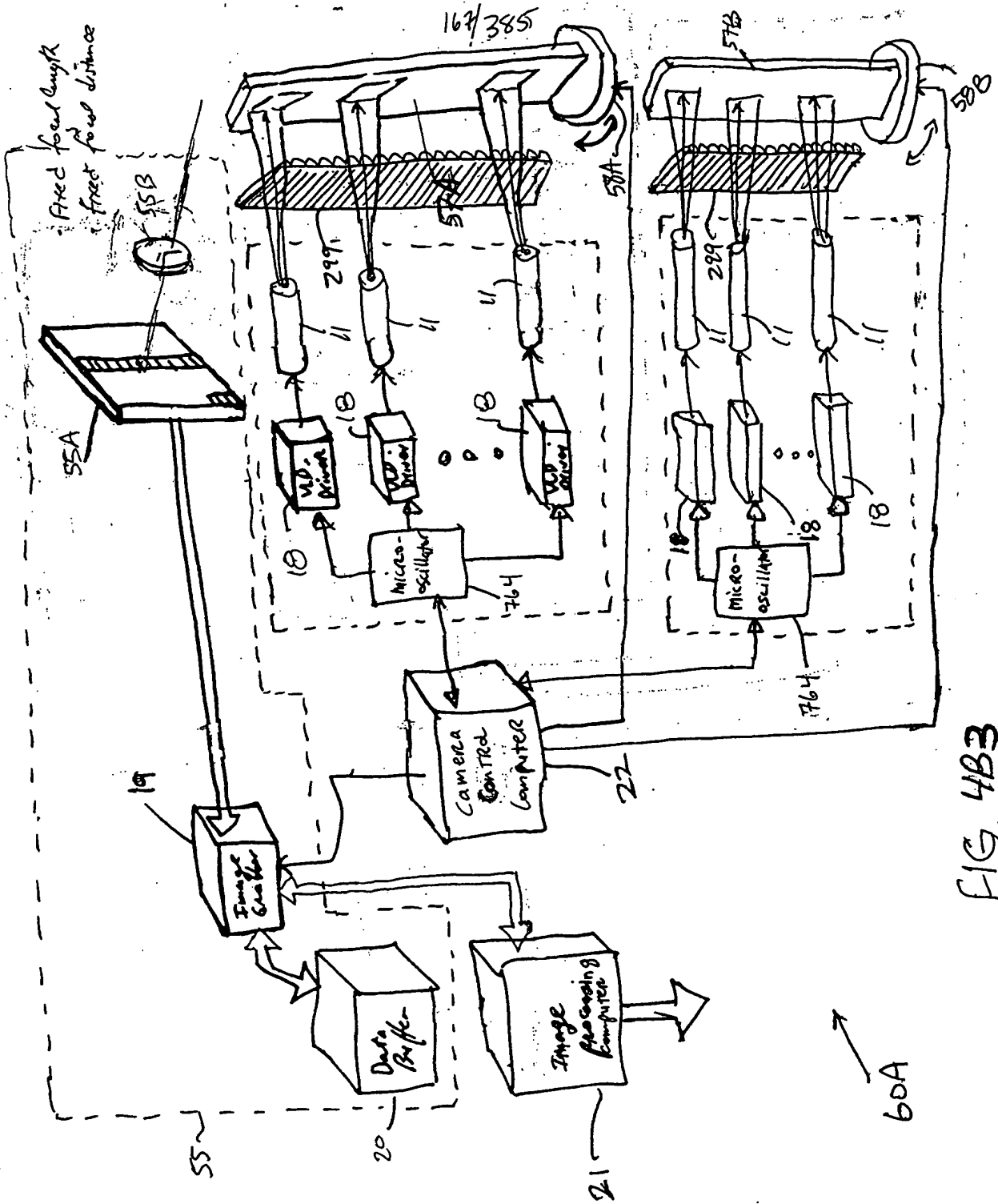


FIG. 4B3

| Time | Temperature | Pressure | Humidity | Wind | Clouds | Visibility | Remarks |
|------|-------------|----------|----------|------|--------|------------|---------|
| 0000 | 50.0 | 1013.2 | 65 | 0.0 | 0.0 | 10.0 | Clear |
| 0100 | 49.5 | 1013.1 | 64 | 0.0 | 0.0 | 10.0 | Clear |
| 0200 | 49.0 | 1013.0 | 63 | 0.0 | 0.0 | 10.0 | Clear |
| 0300 | 48.5 | 1012.9 | 62 | 0.0 | 0.0 | 10.0 | Clear |
| 0400 | 48.0 | 1012.8 | 61 | 0.0 | 0.0 | 10.0 | Clear |
| 0500 | 47.5 | 1012.7 | 60 | 0.0 | 0.0 | 10.0 | Clear |
| 0600 | 47.0 | 1012.6 | 59 | 0.0 | 0.0 | 10.0 | Clear |
| 0700 | 46.5 | 1012.5 | 58 | 0.0 | 0.0 | 10.0 | Clear |
| 0800 | 46.0 | 1012.4 | 57 | 0.0 | 0.0 | 10.0 | Clear |
| 0900 | 45.5 | 1012.3 | 56 | 0.0 | 0.0 | 10.0 | Clear |
| 1000 | 45.0 | 1012.2 | 55 | 0.0 | 0.0 | 10.0 | Clear |
| 1100 | 44.5 | 1012.1 | 54 | 0.0 | 0.0 | 10.0 | Clear |
| 1200 | 44.0 | 1012.0 | 53 | 0.0 | 0.0 | 10.0 | Clear |
| 1300 | 43.5 | 1011.9 | 52 | 0.0 | 0.0 | 10.0 | Clear |
| 1400 | 43.0 | 1011.8 | 51 | 0.0 | 0.0 | 10.0 | Clear |
| 1500 | 42.5 | 1011.7 | 50 | 0.0 | 0.0 | 10.0 | Clear |
| 1600 | 42.0 | 1011.6 | 49 | 0.0 | 0.0 | 10.0 | Clear |
| 1700 | 41.5 | 1011.5 | 48 | 0.0 | 0.0 | 10.0 | Clear |
| 1800 | 41.0 | 1011.4 | 47 | 0.0 | 0.0 | 10.0 | Clear |
| 1900 | 40.5 | 1011.3 | 46 | 0.0 | 0.0 | 10.0 | Clear |
| 2000 | 40.0 | 1011.2 | 45 | 0.0 | 0.0 | 10.0 | Clear |
| 2100 | 39.5 | 1011.1 | 44 | 0.0 | 0.0 | 10.0 | Clear |
| 2200 | 39.0 | 1011.0 | 43 | 0.0 | 0.0 | 10.0 | Clear |
| 2300 | 38.5 | 1010.9 | 42 | 0.0 | 0.0 | 10.0 | Clear |

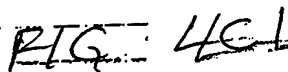
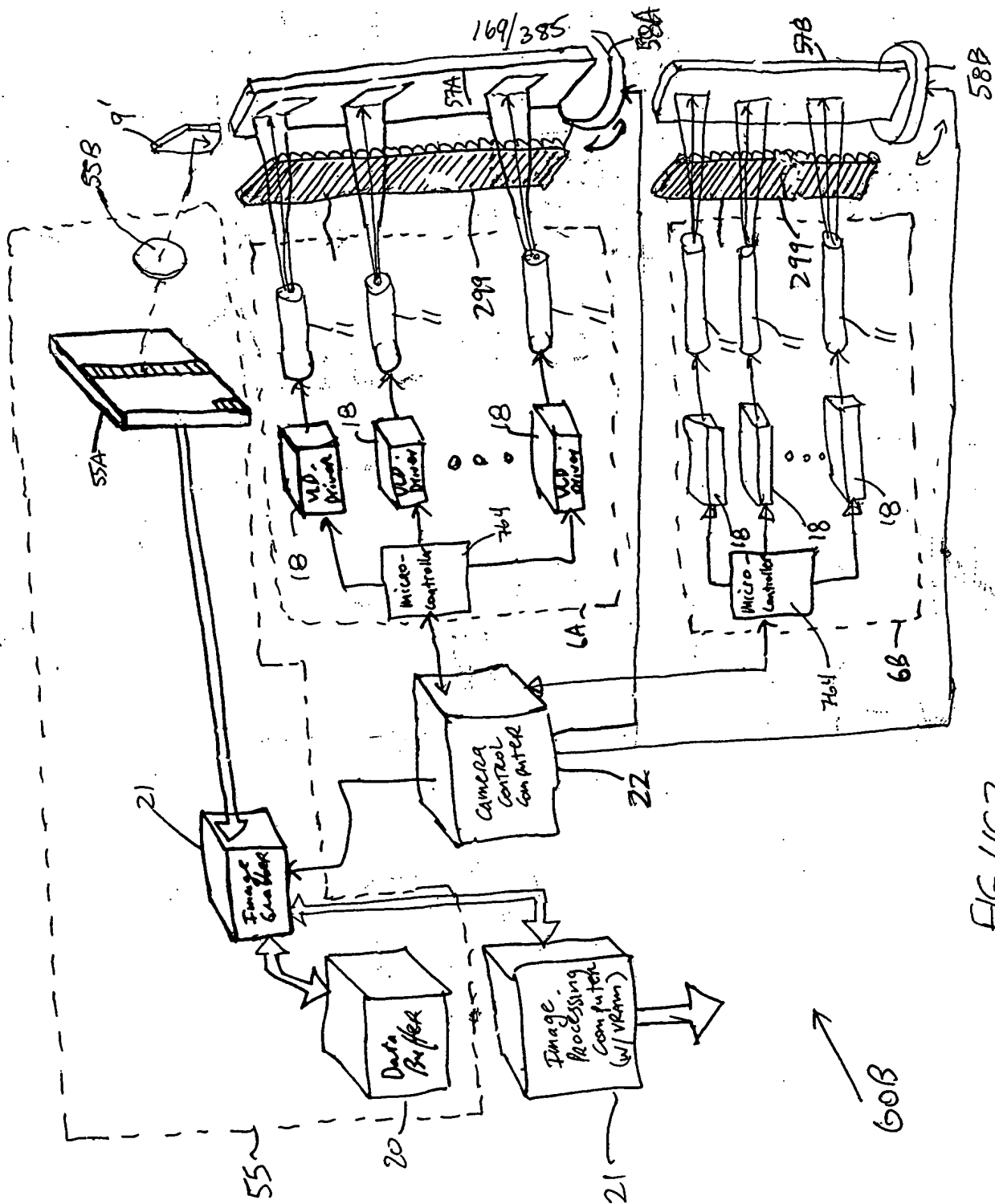


FIG. 4C1



170/385

TOP SECRET

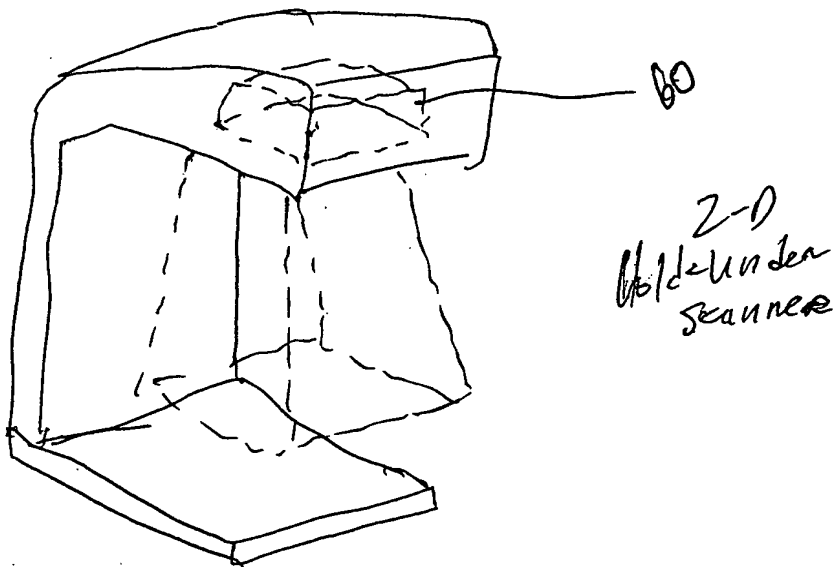


FIG. 4D

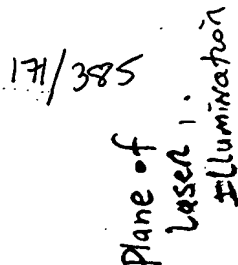
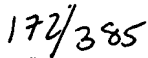


FIG 4E

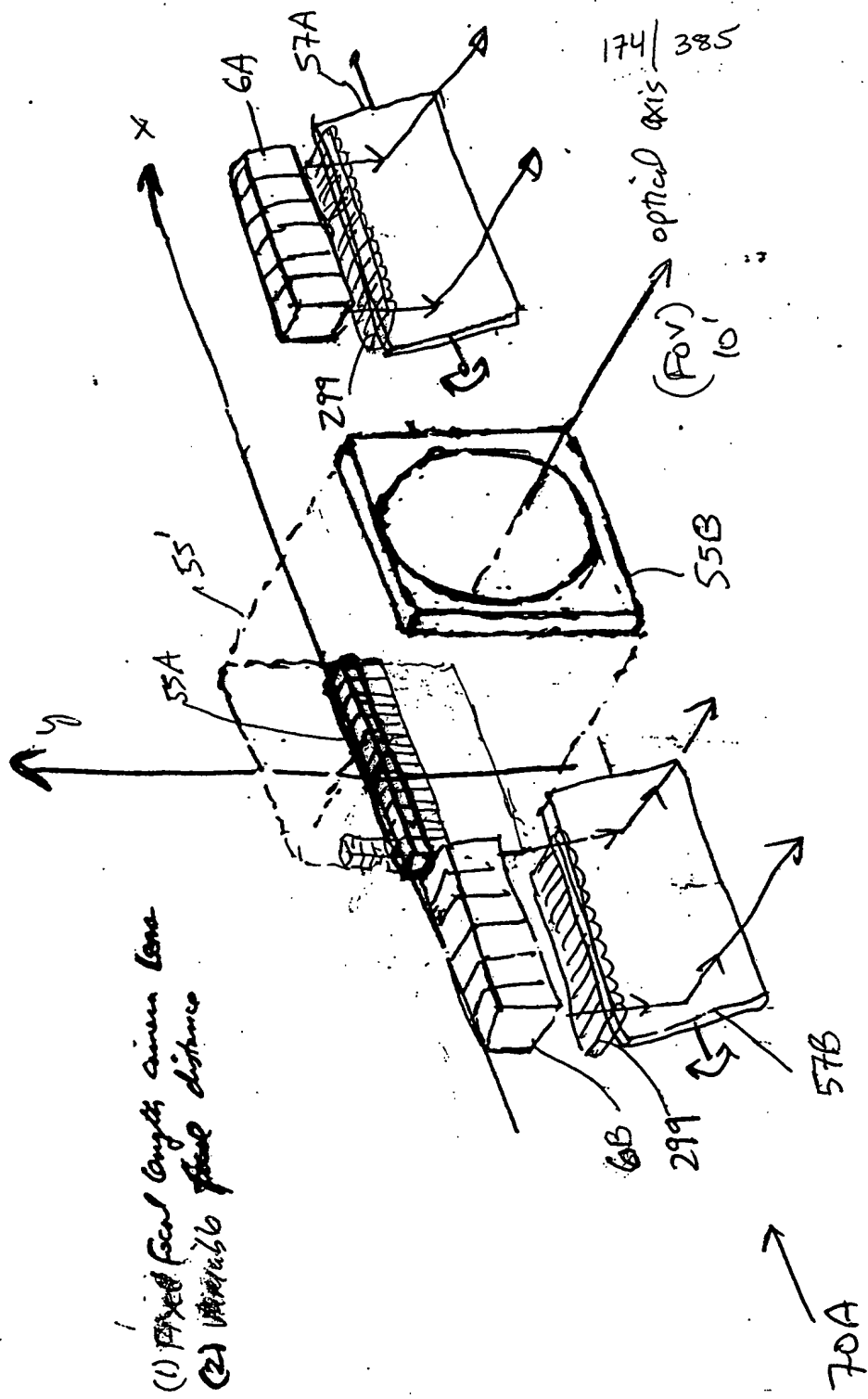
Applications:

- Hand-held Scanner
- Presentation Scanner



AG 5A

of



- (1) Fixed focal length lens
- (2) Variable focal distance

FIG. 5B1

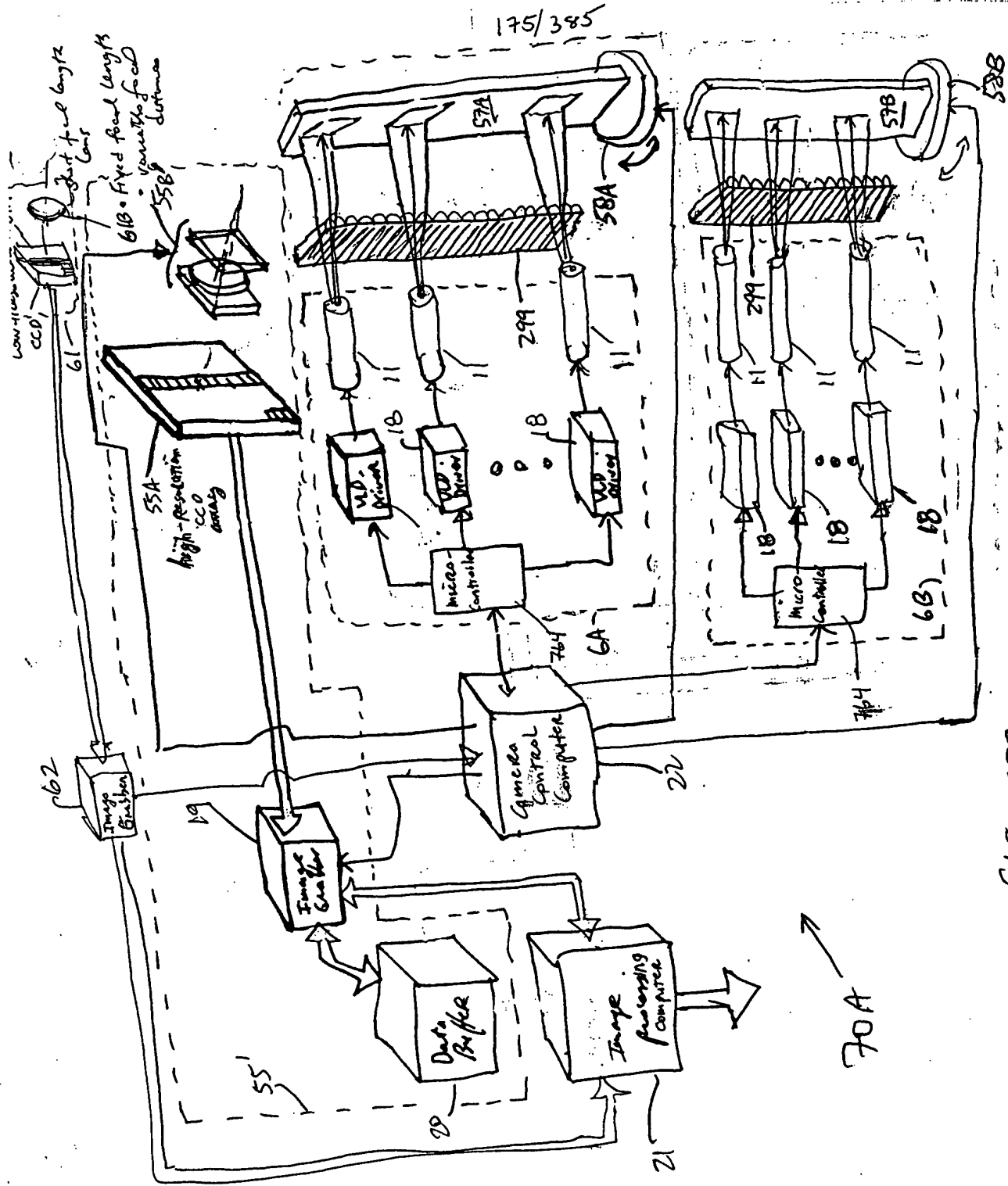


FIG. 5B3

176/385

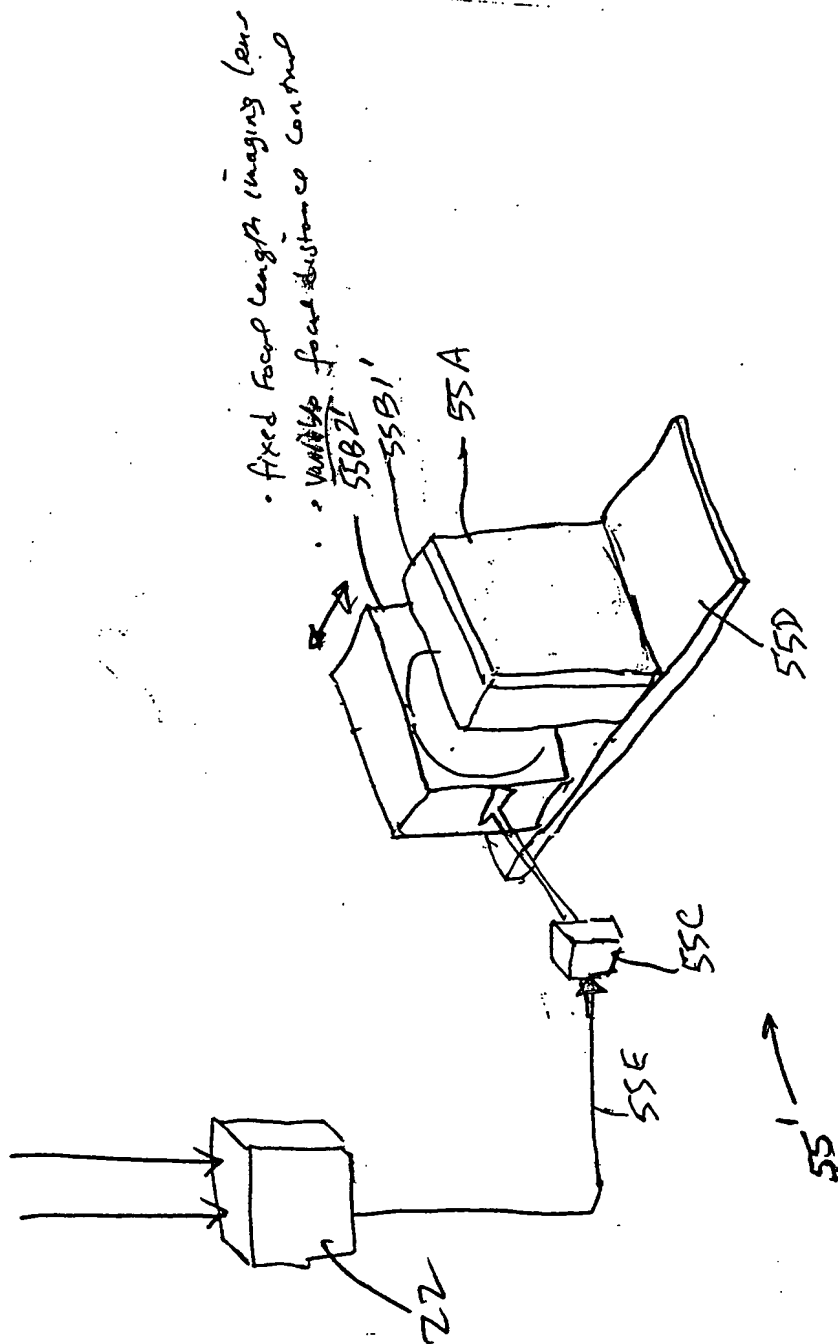
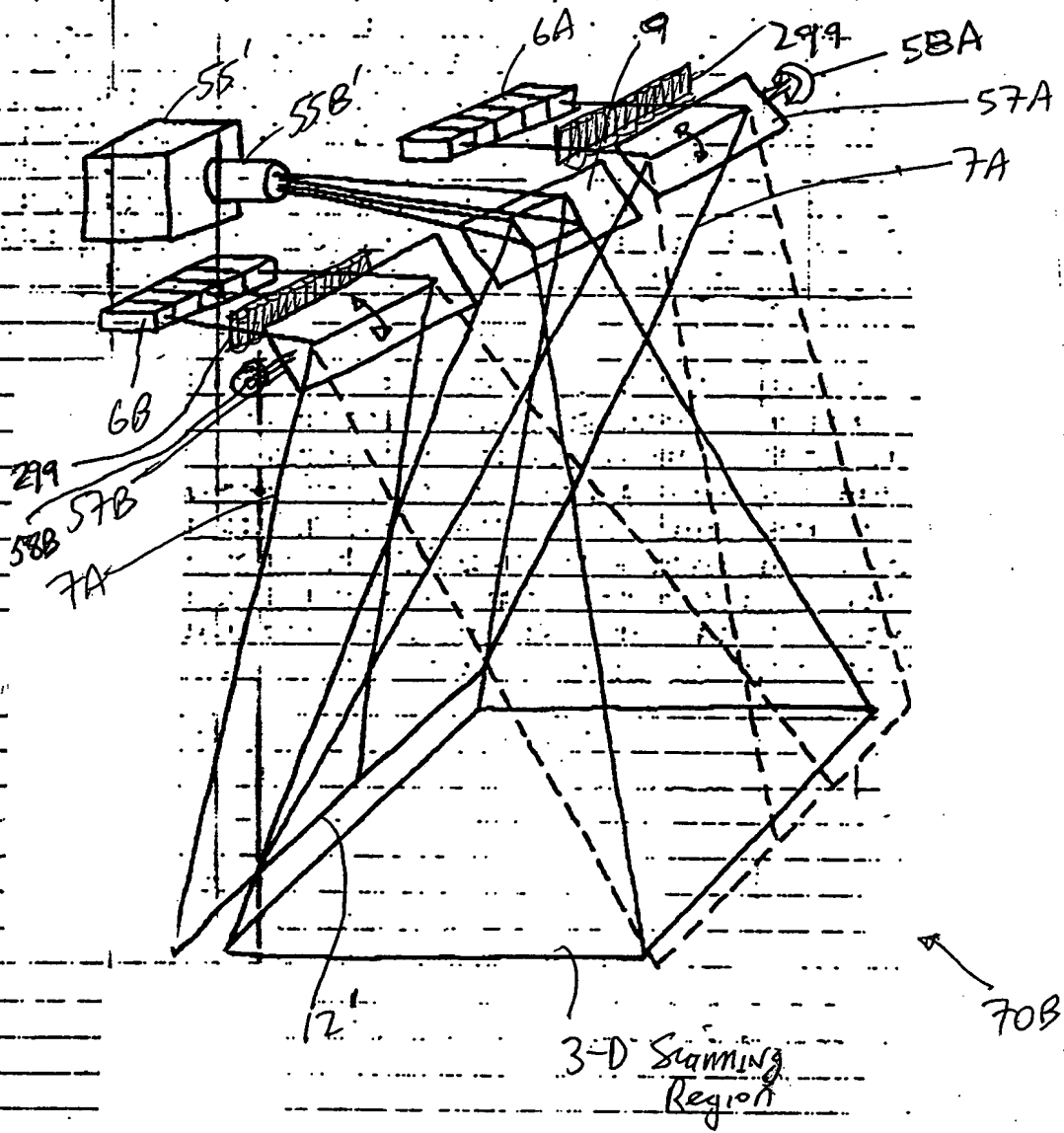


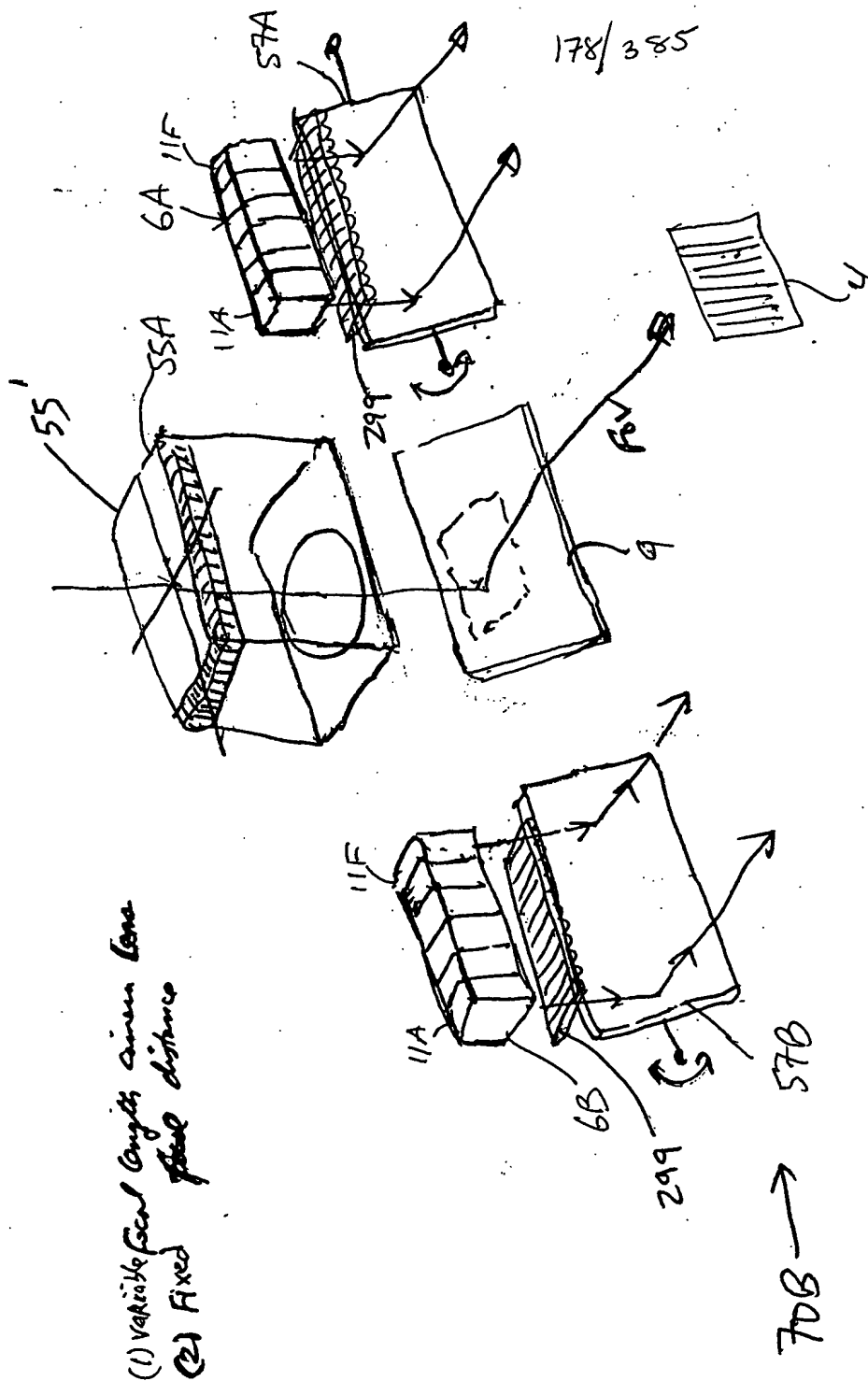
FIG. 5B4

TOP SECRET

177/385



\therefore Fig. 5C1



(1) Variable focal length lens
(2) Fixed focal distance

FIG. 50

FIG. 5C3

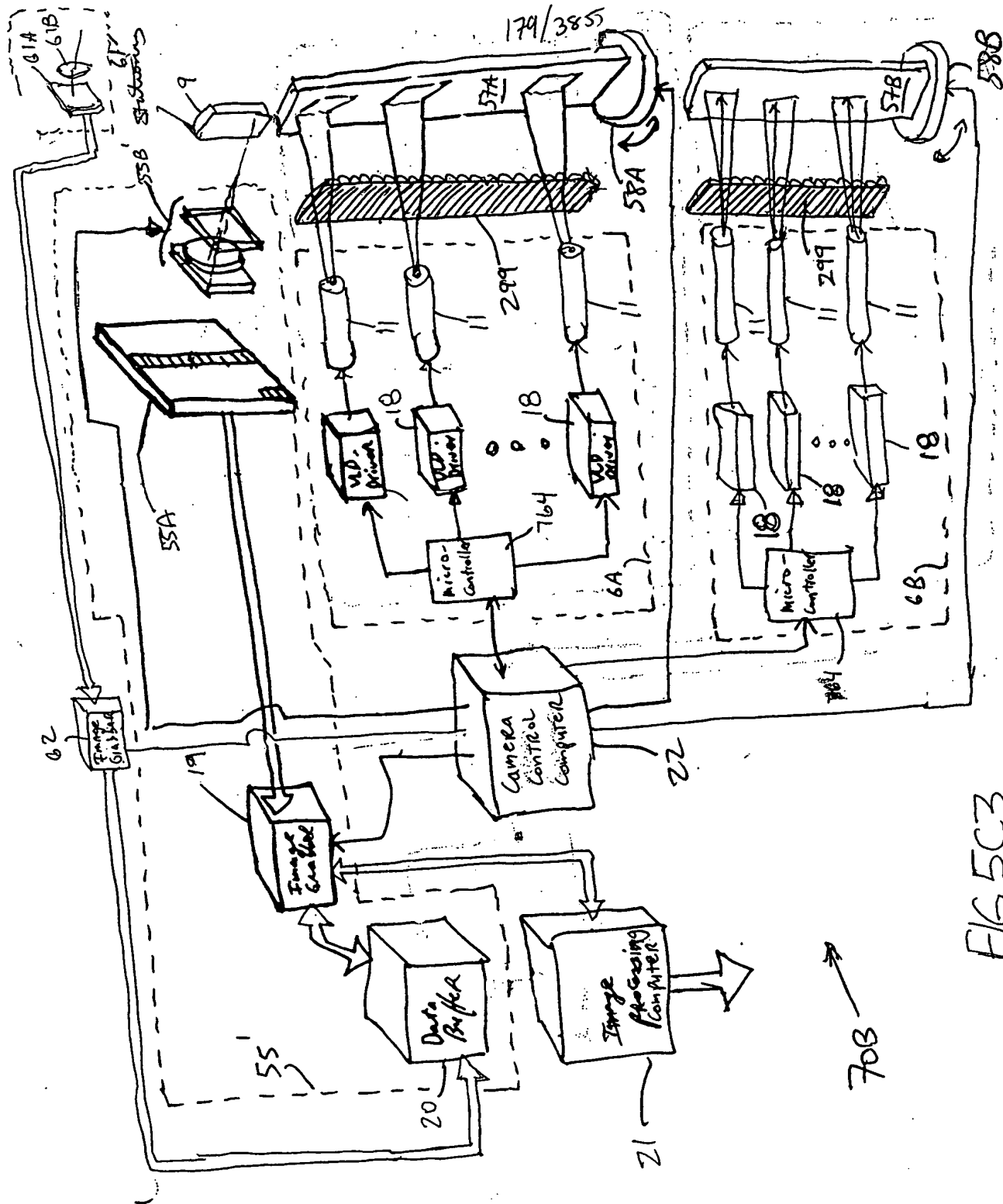


FIG. 5C3

FIG. 5C

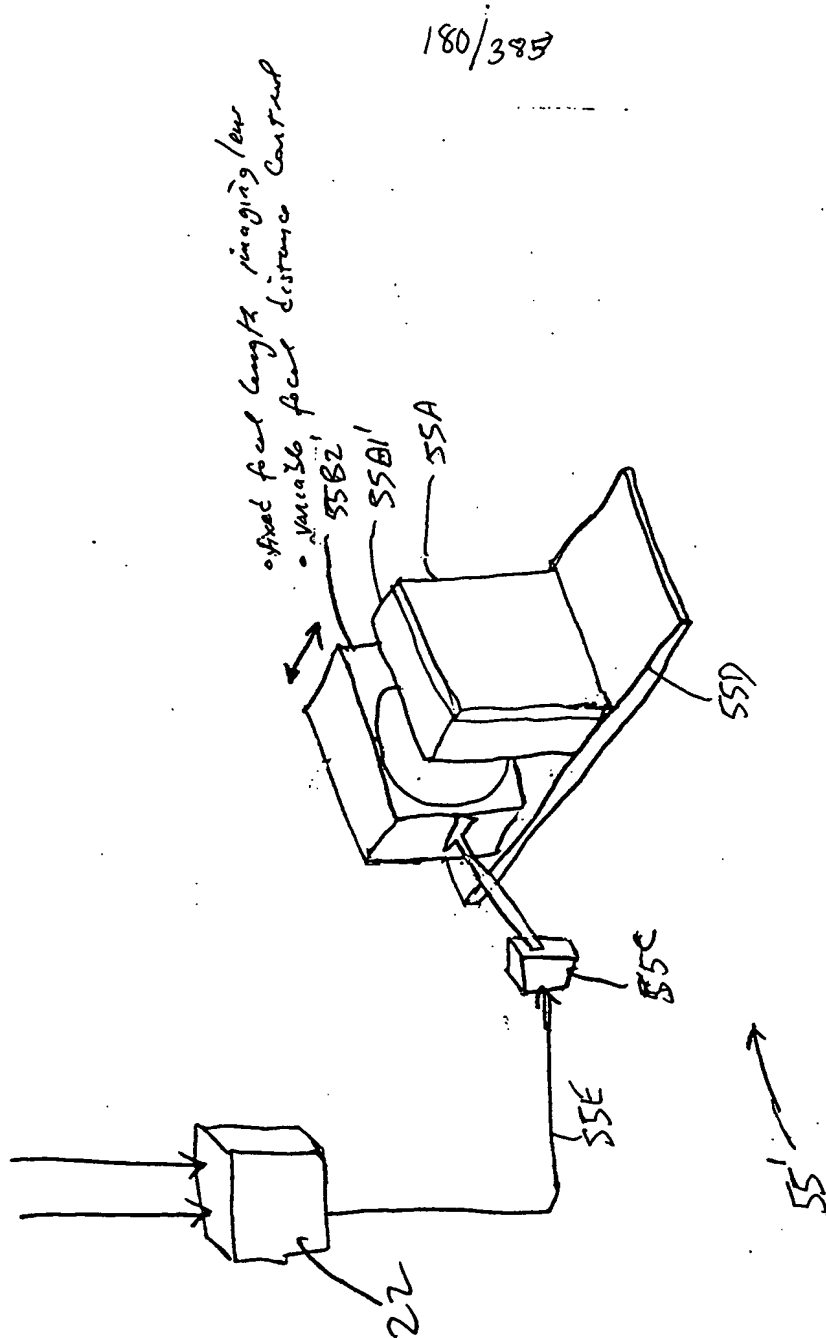


FIG. 5C4



709638 from New York
709639 from New York
709640 from New York
709641 from New York
709642 from New York
709643 from New York
709644 from New York
709645 from New York
709646 from New York
709647 from New York
709648 from New York
709649 from New York
709650 from New York
709651 from New York
709652 from New York
709653 from New York
709654 from New York
709655 from New York
709656 from New York
709657 from New York
709658 from New York
709659 from New York
709660 from New York
709661 from New York
709662 from New York
709663 from New York
709664 from New York
709665 from New York
709666 from New York
709667 from New York
709668 from New York
709669 from New York
709670 from New York
709671 from New York
709672 from New York
709673 from New York
709674 from New York
709675 from New York
709676 from New York
709677 from New York
709678 from New York
709679 from New York
709680 from New York
709681 from New York
709682 from New York
709683 from New York
709684 from New York
709685 from New York
709686 from New York
709687 from New York
709688 from New York
709689 from New York
709690 from New York
709691 from New York
709692 from New York
709693 from New York
709694 from New York
709695 from New York
709696 from New York
709697 from New York
709698 from New York
709699 from New York
709700 from New York

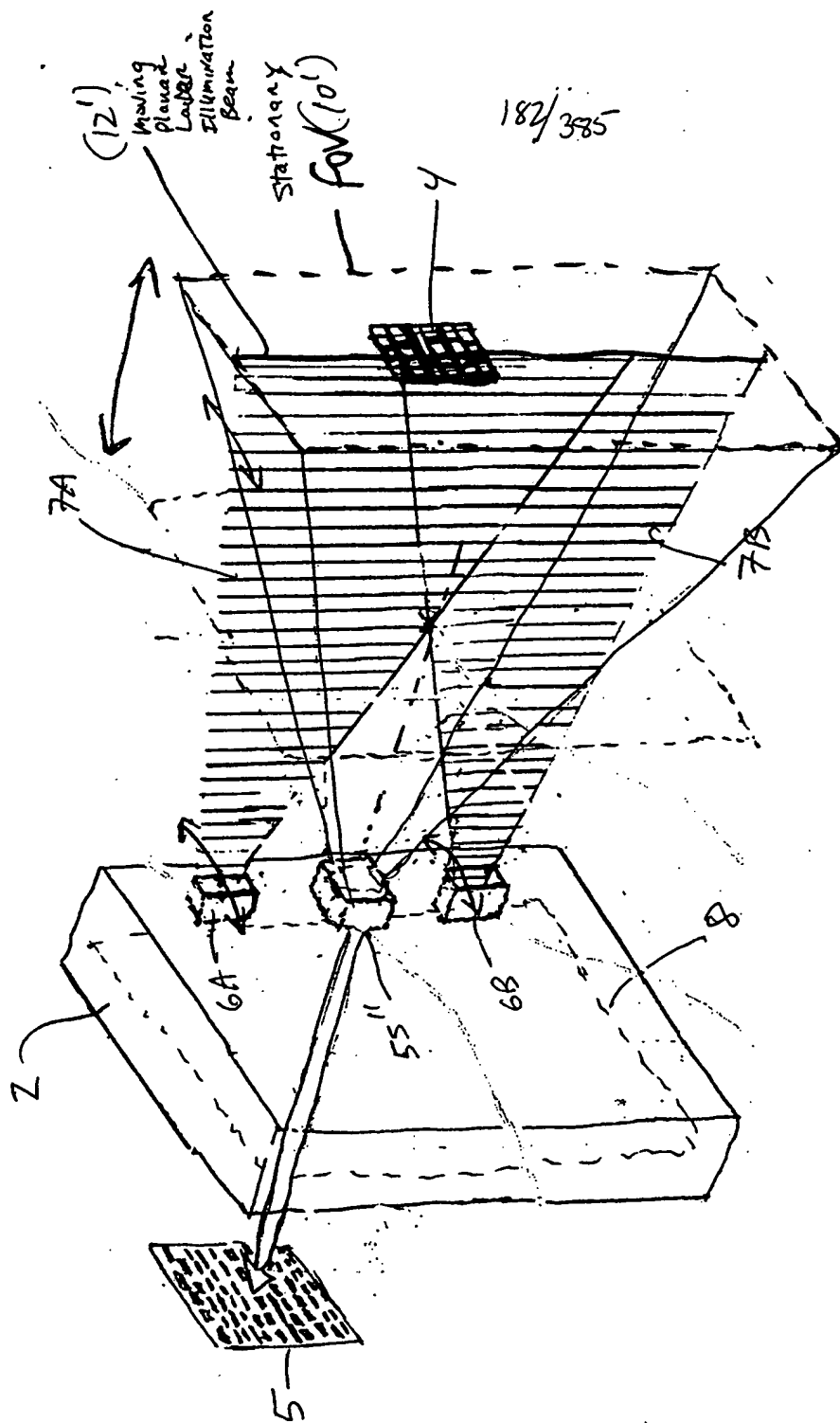


FIG. 6A

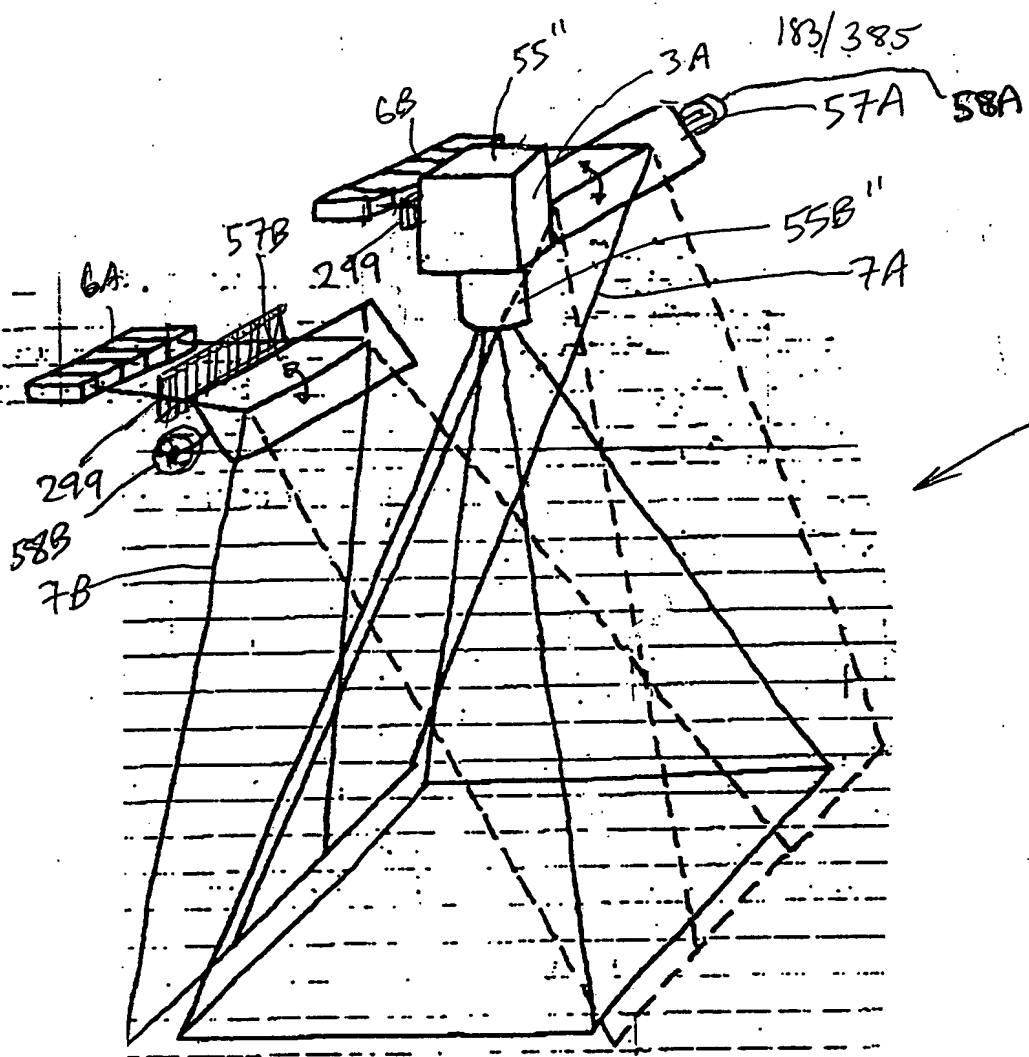
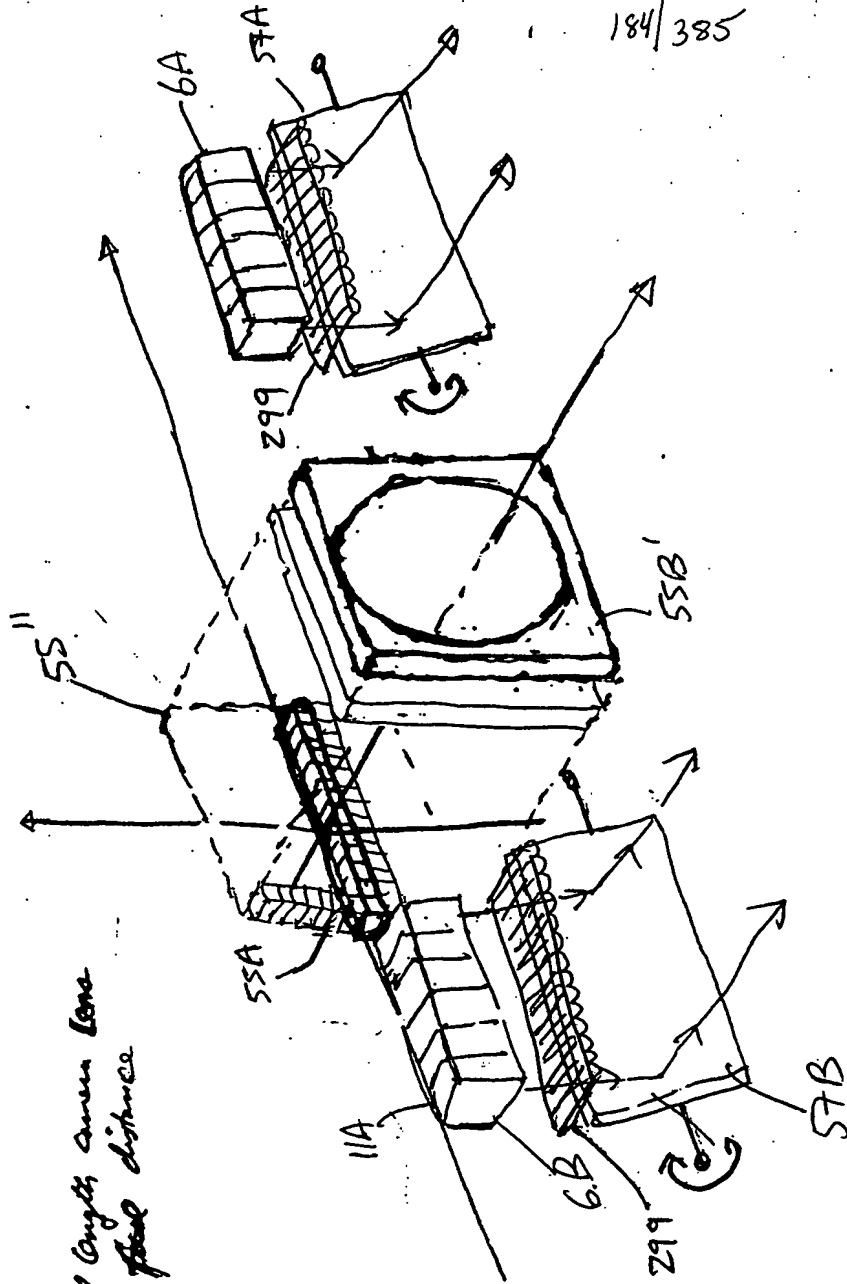


FIG. 6B1

184/385



- (1) Variable focal length camera lens
- (2) Variable focal distance

80A

FIG. 6B2

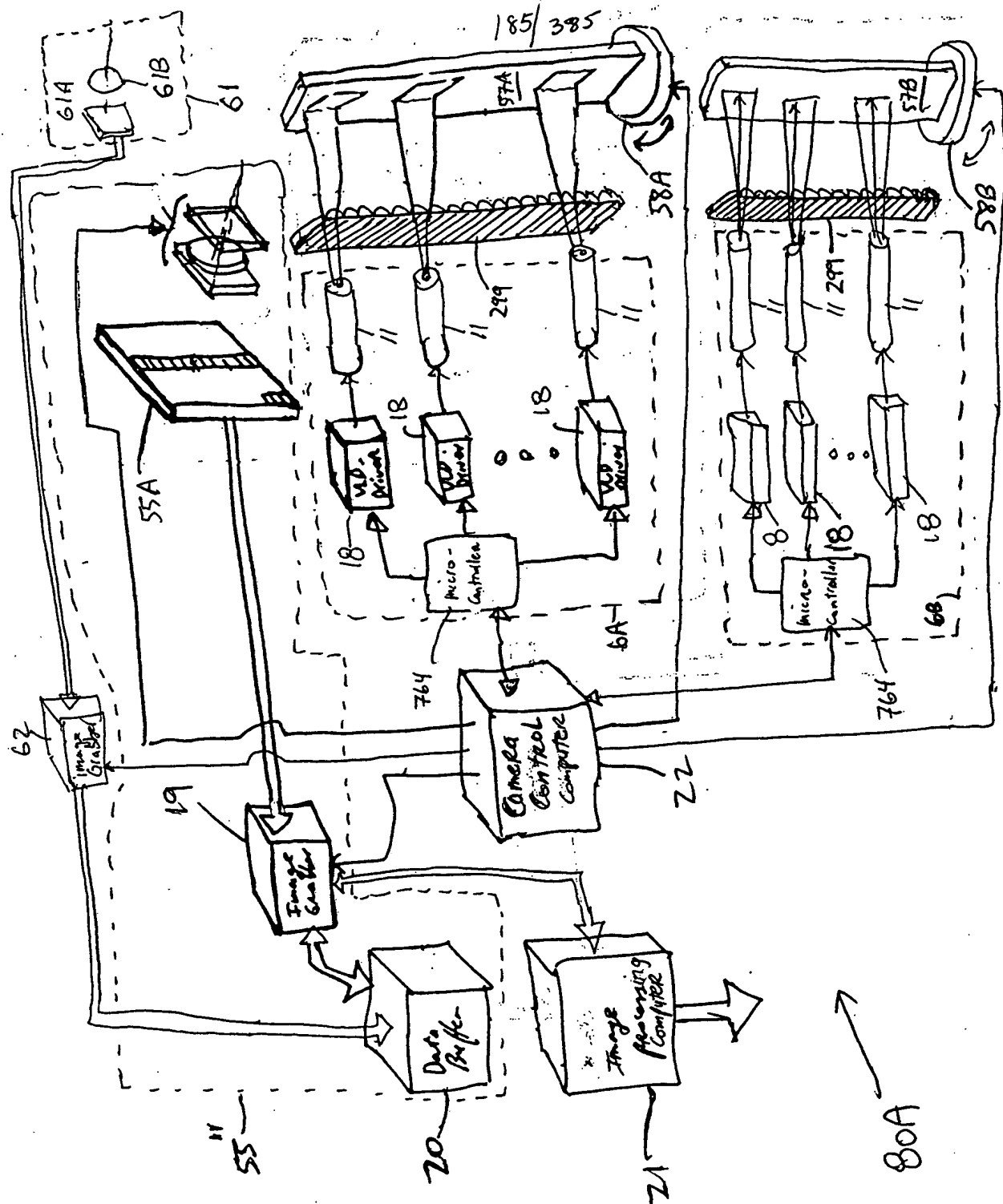
[illegible]

FIG. 6B3

187/385

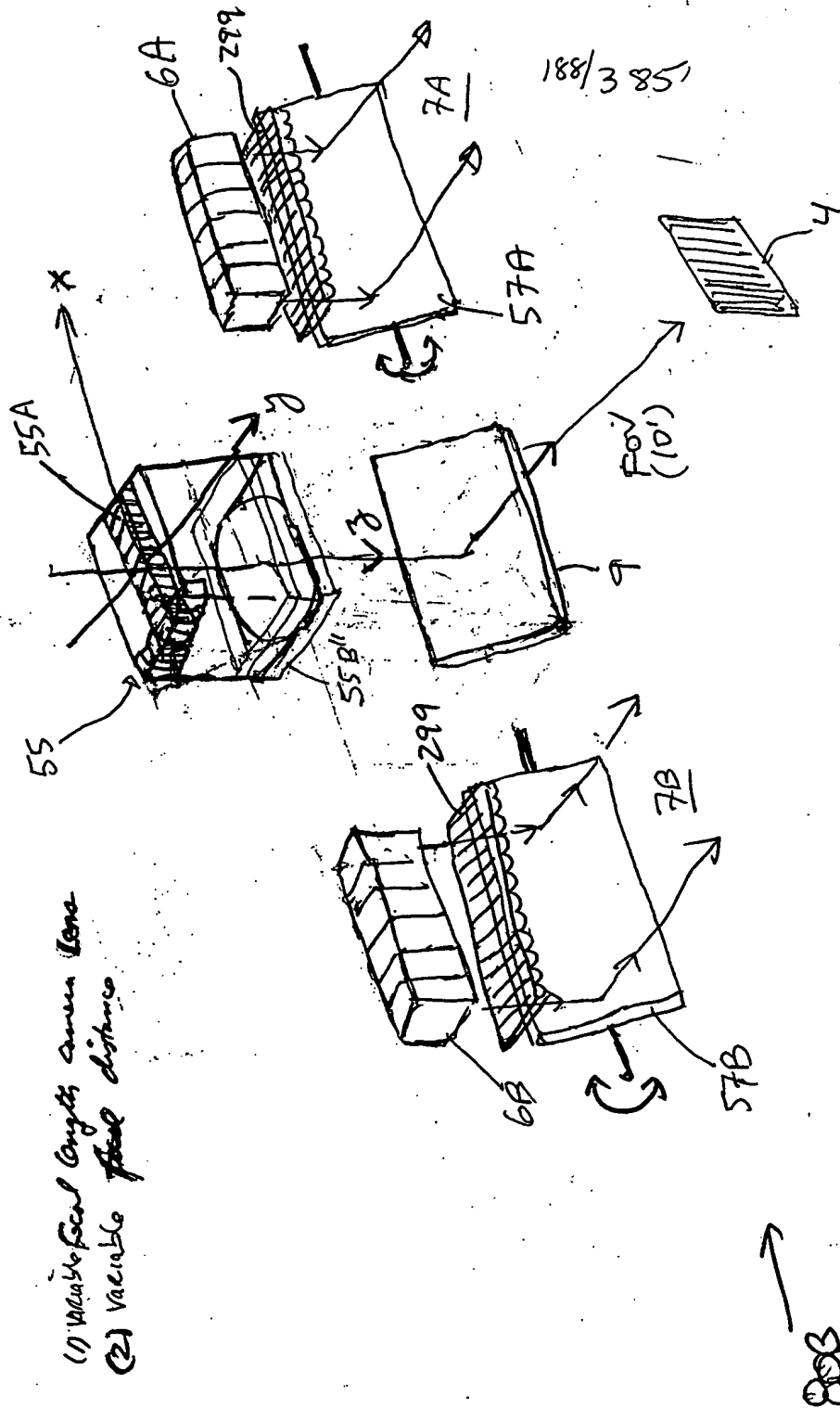


FIG. 6C2

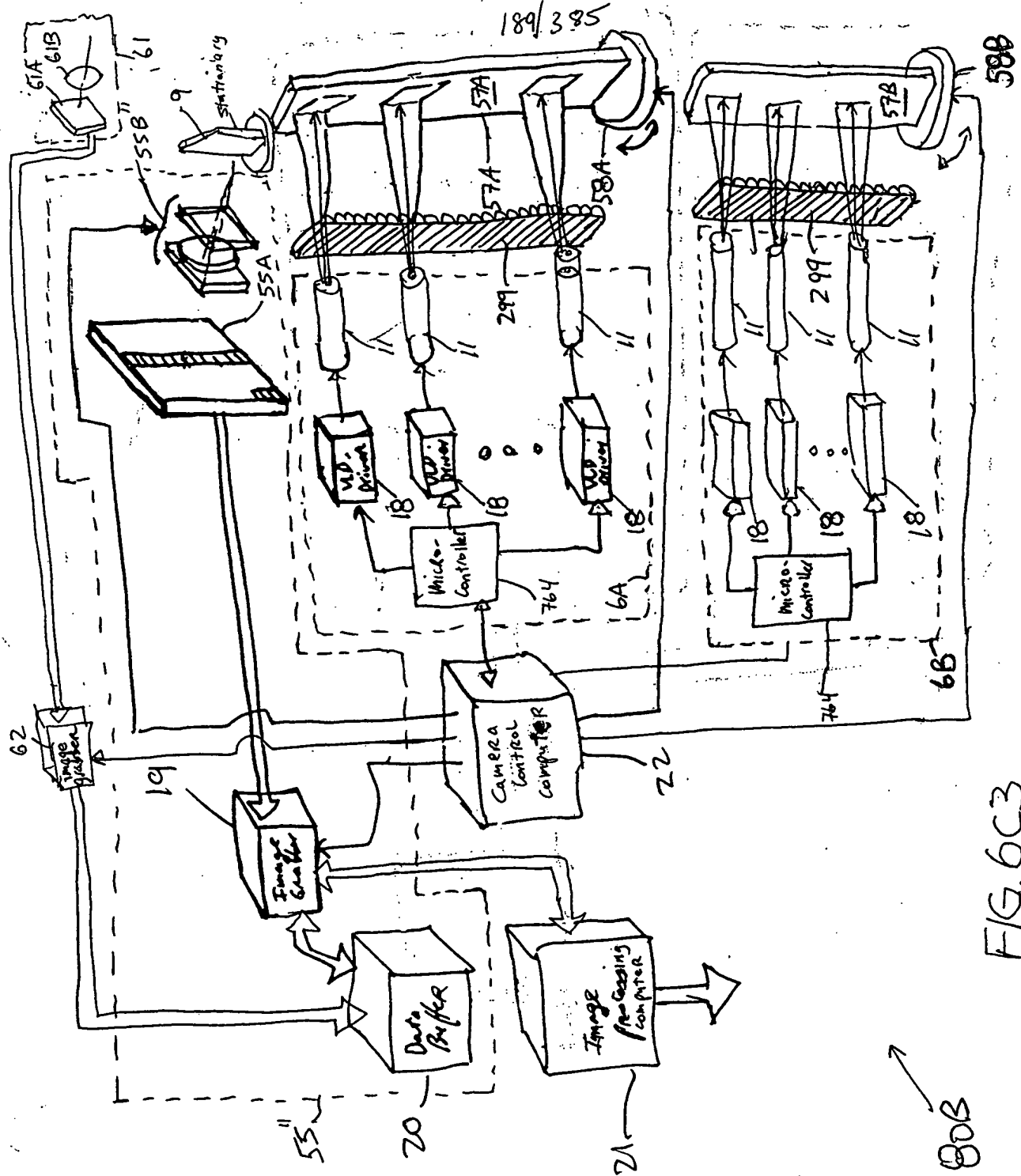


FIG. 6C3

[illegible]

FIG. 6C4

191/385

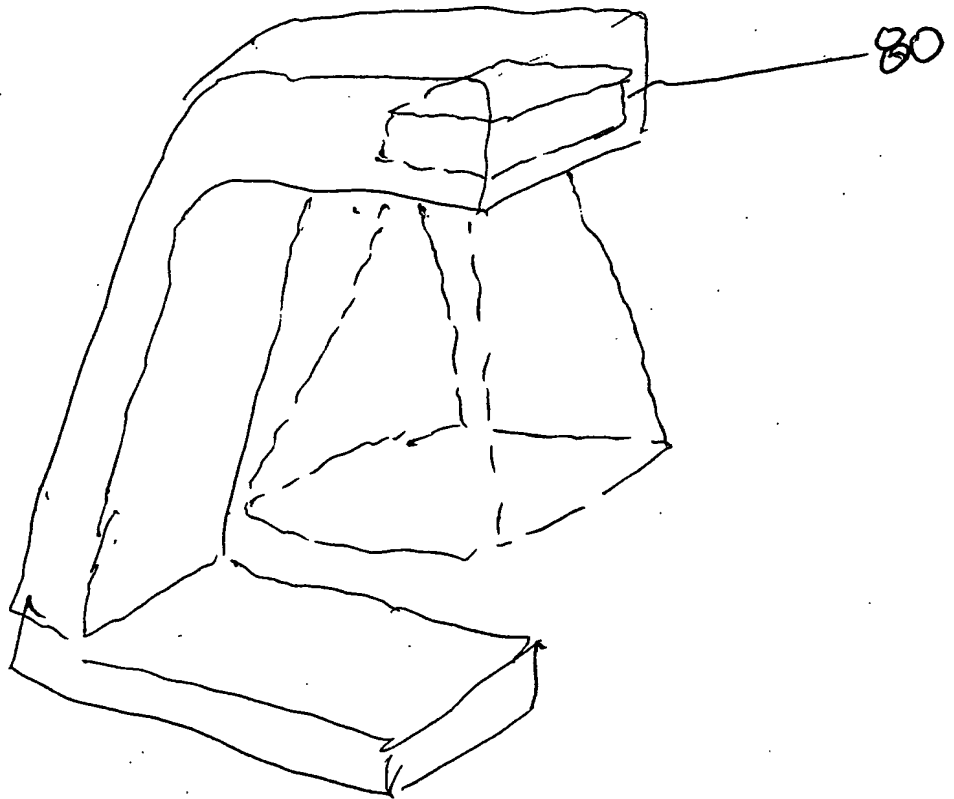


FIG. 6C5

00000000 112101

00000585 442404

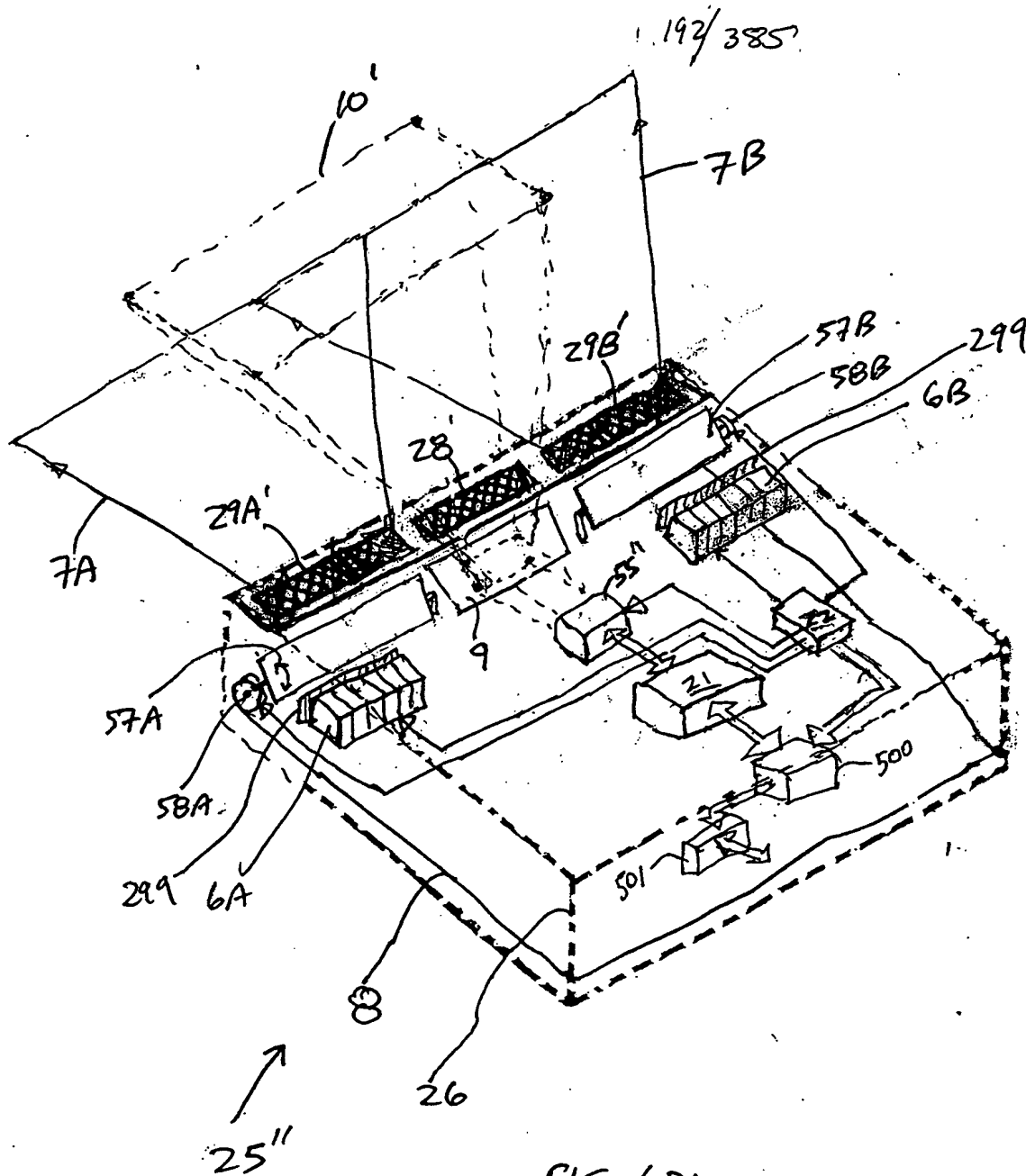


FIG. 6D1

193/385

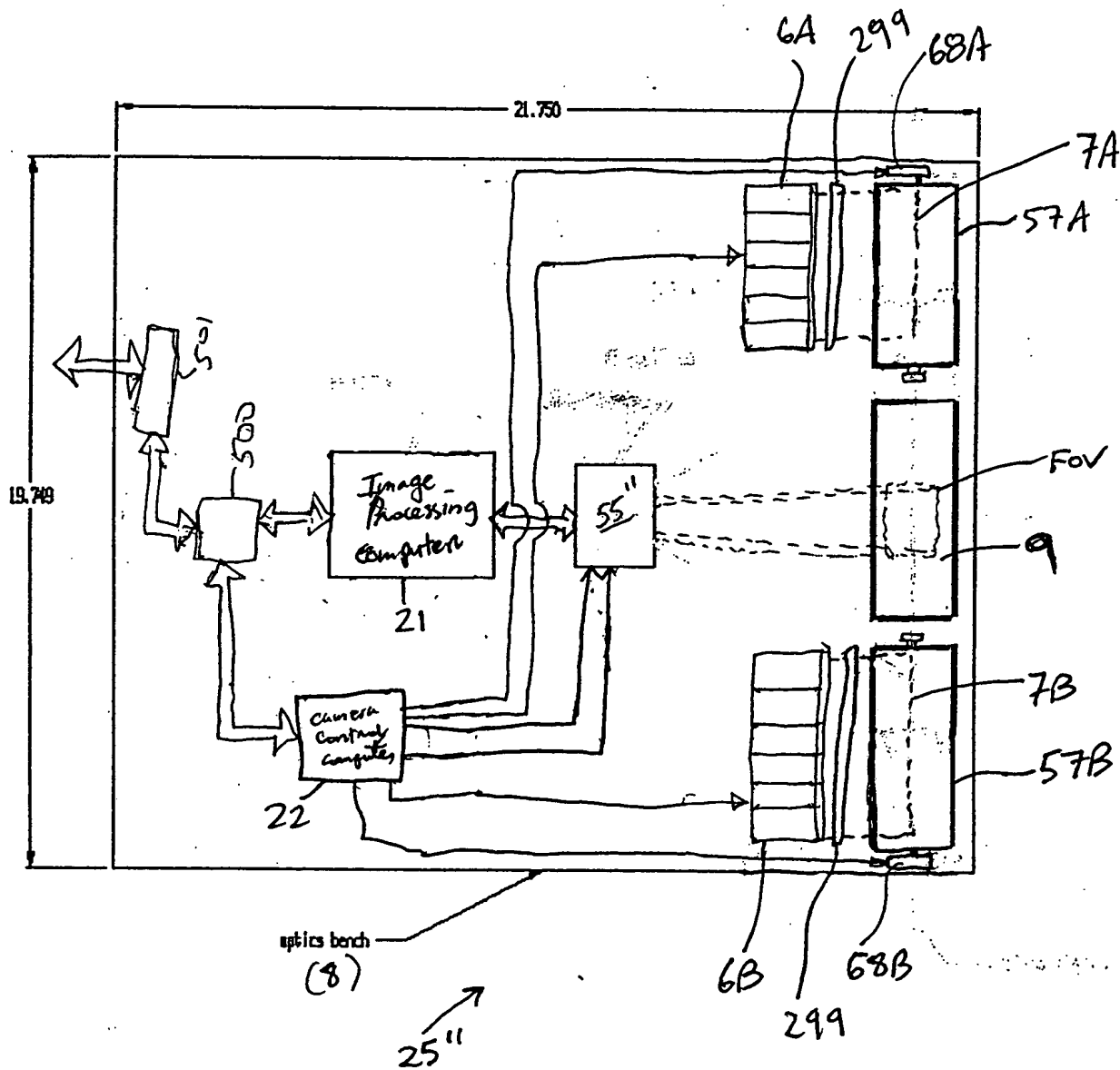


FIG. 6DZ

194/385

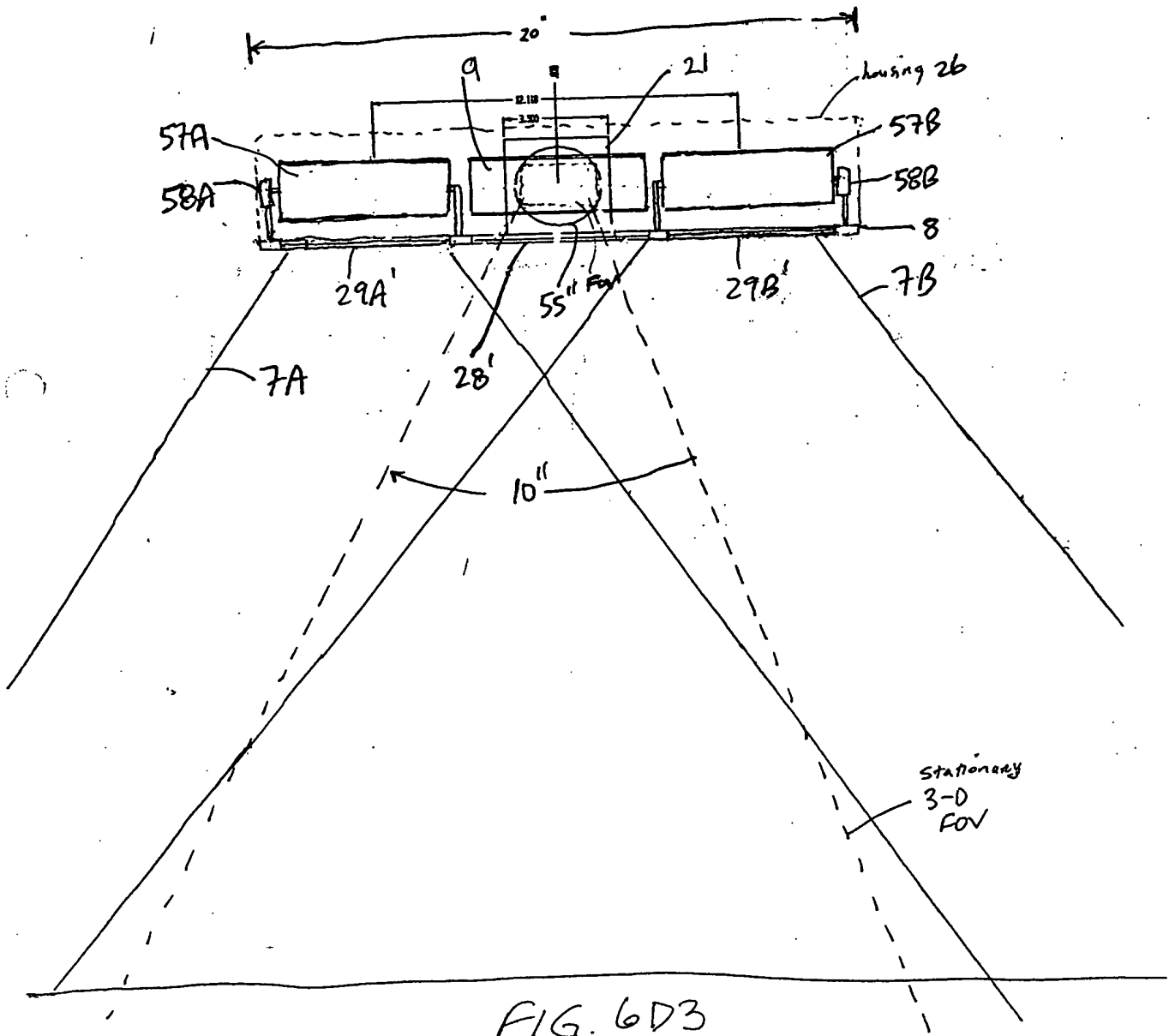


FIG. 6D3

TOP SECRET

195/385

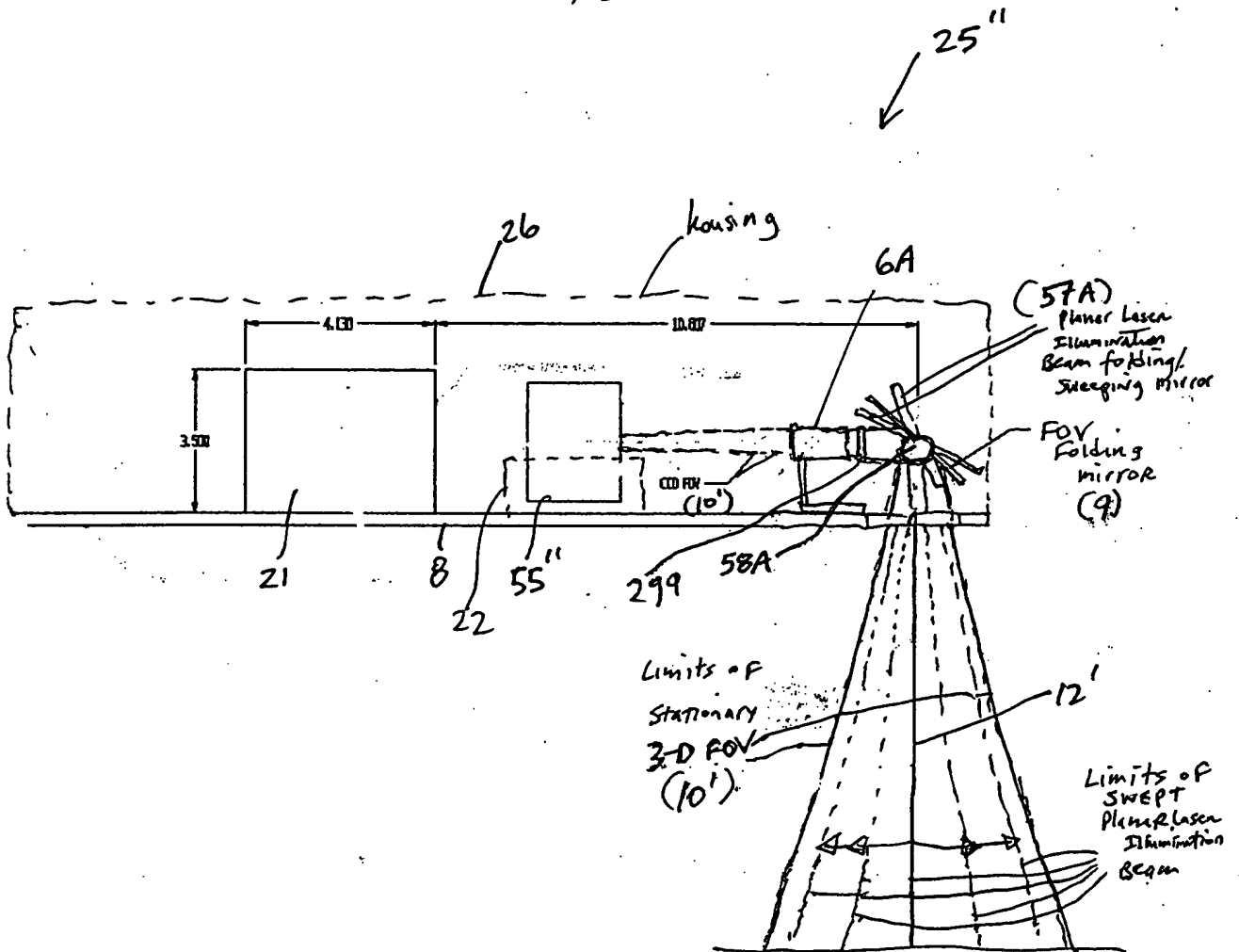


FIG. 6D4

196/385

variable FOV

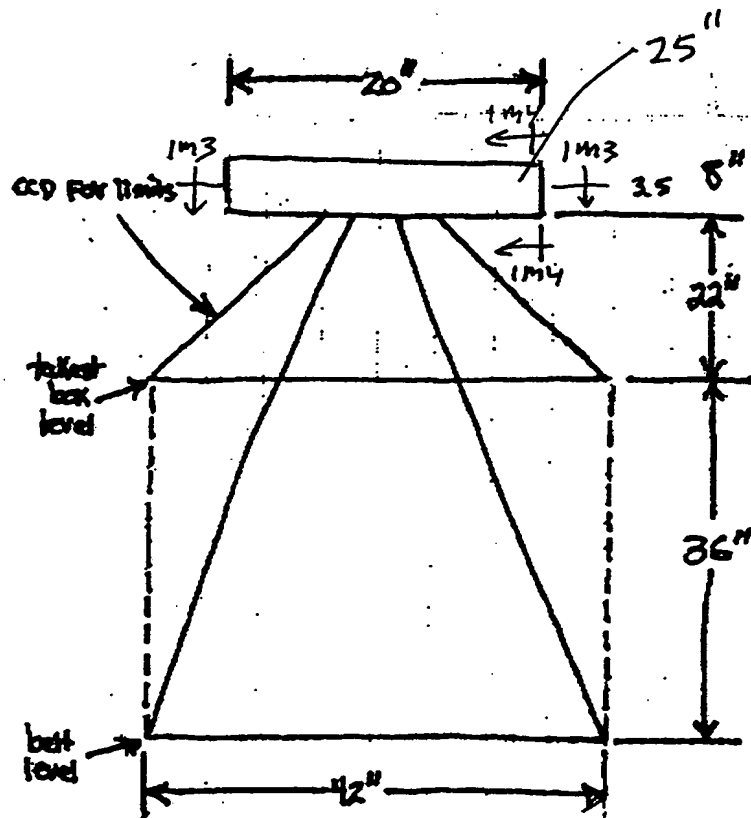


FIG. 6D5

0000555 11210

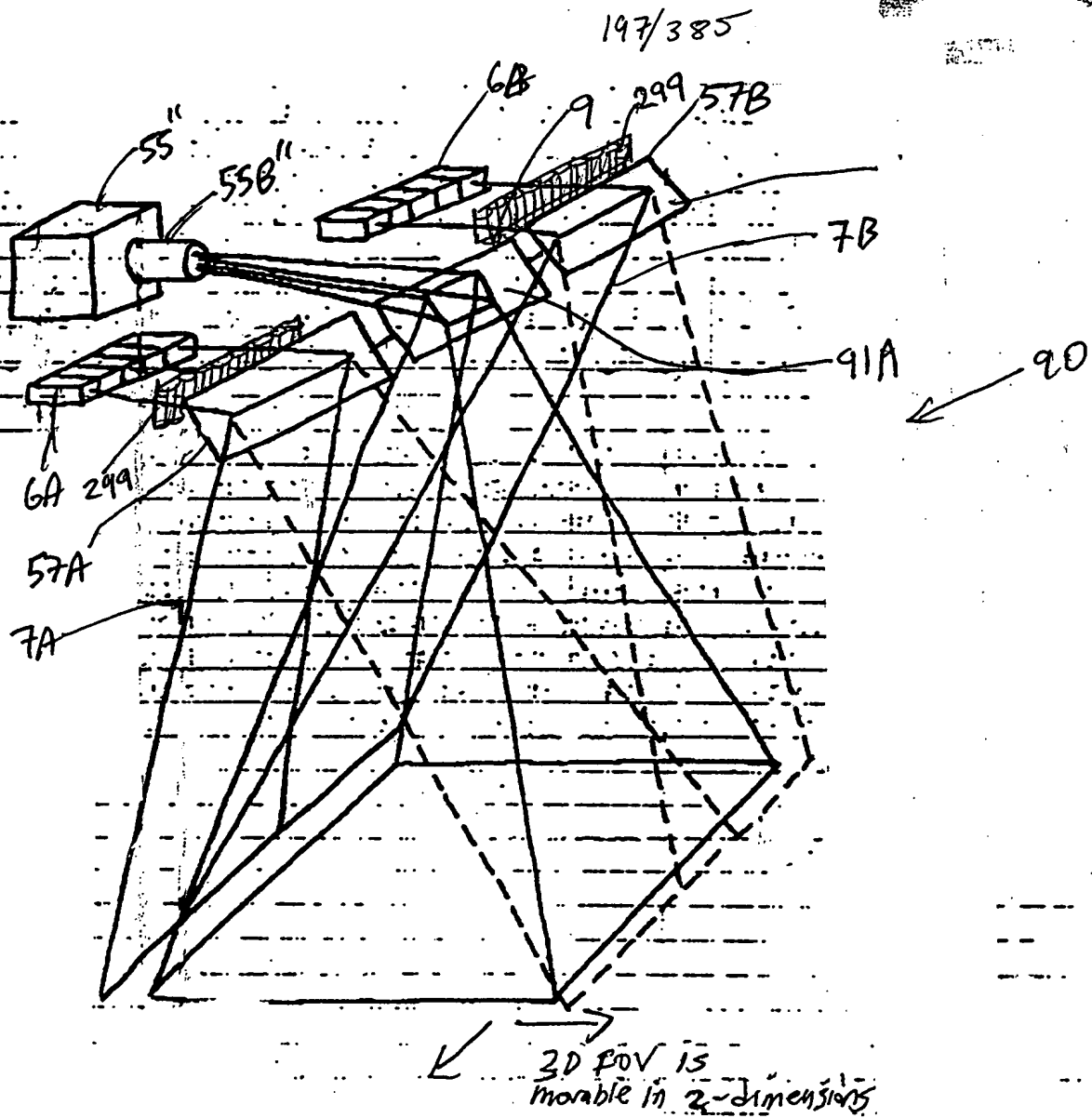


FIG 6E1

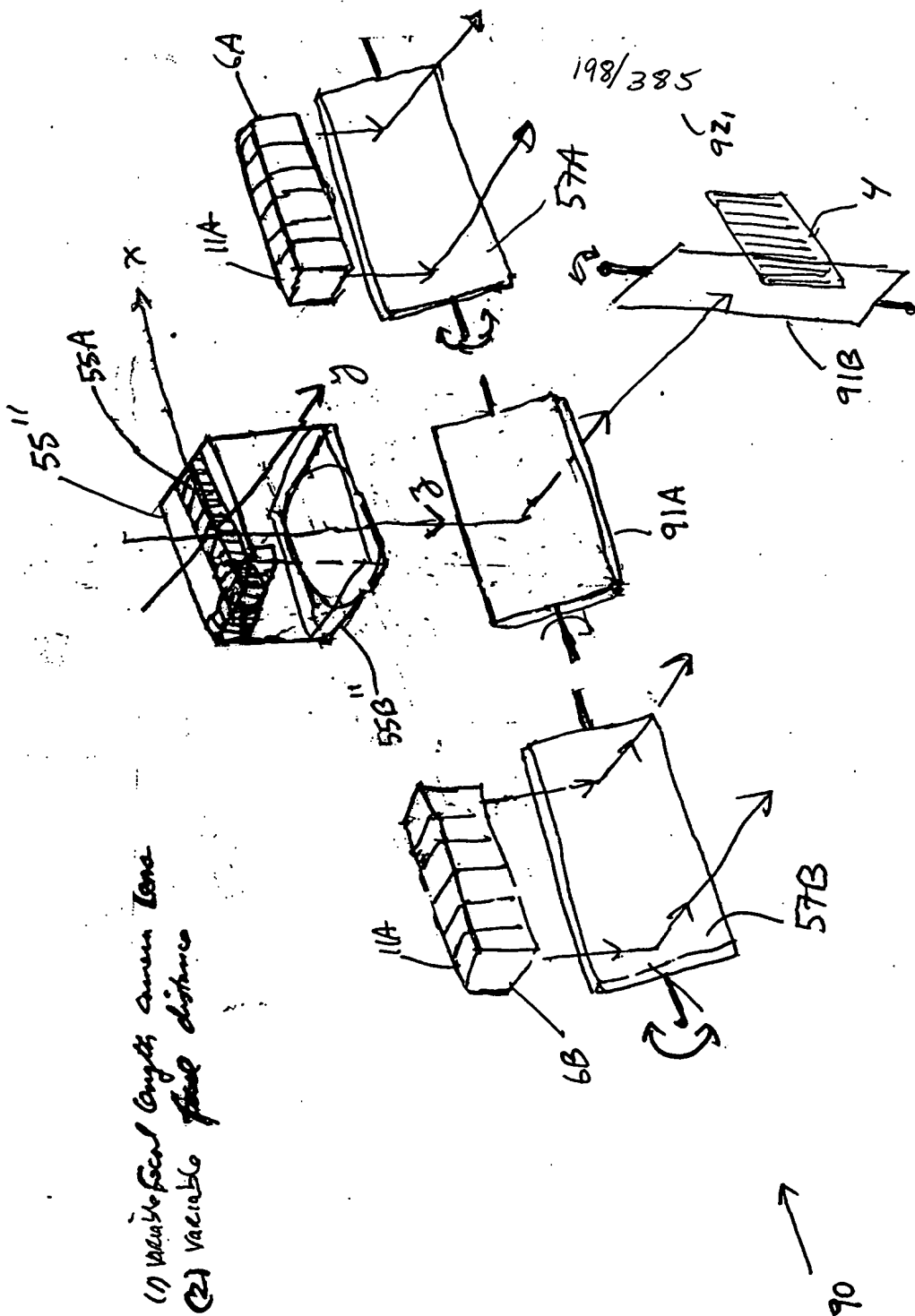


FIG. 6E2

(1) Variable fluid distance
(2) Variable fluid distance

199/385

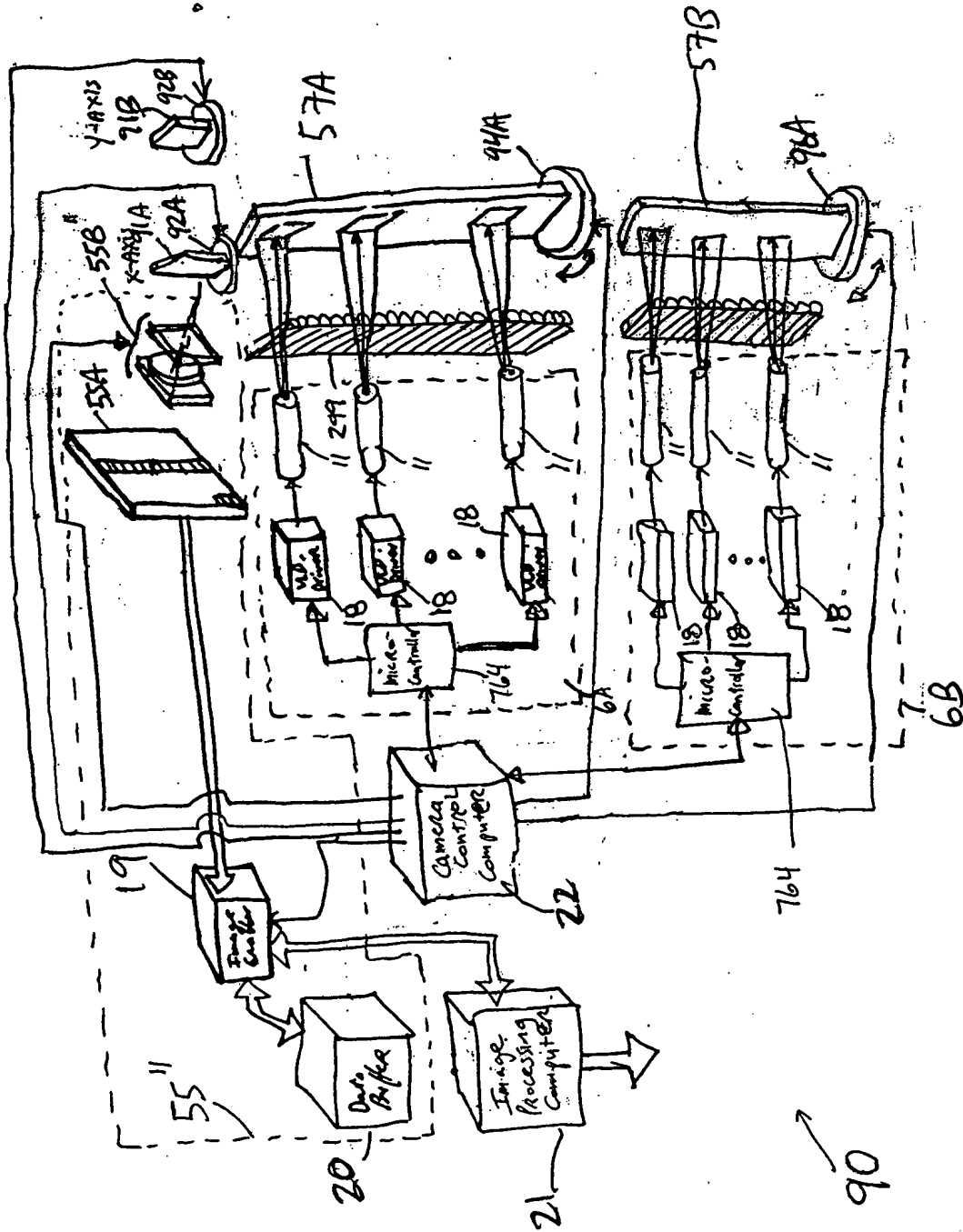


FIG. 6E3

200/385

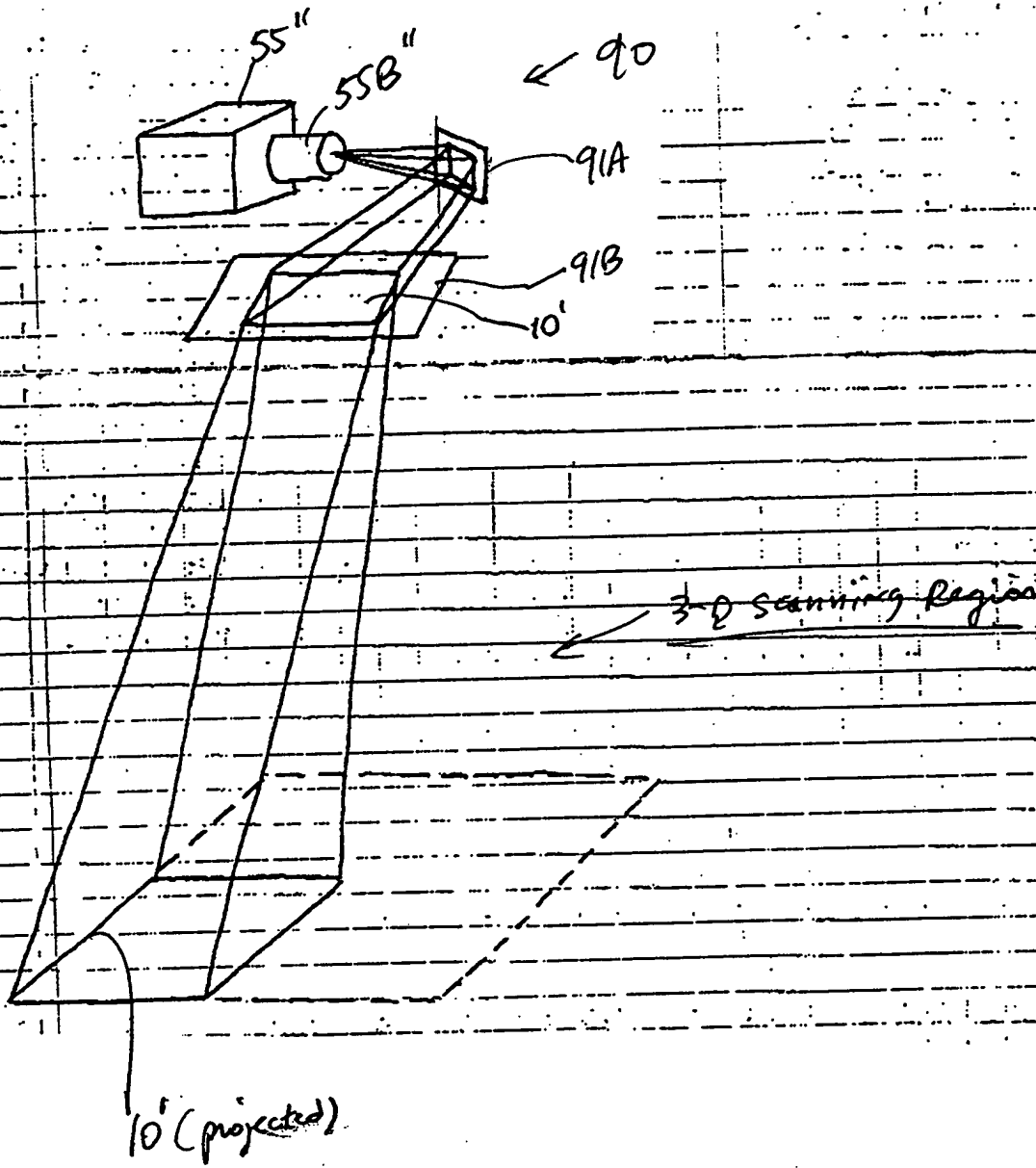
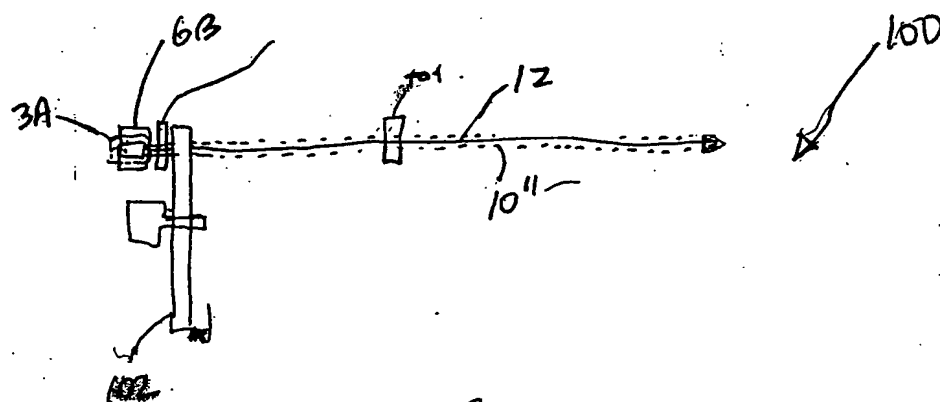
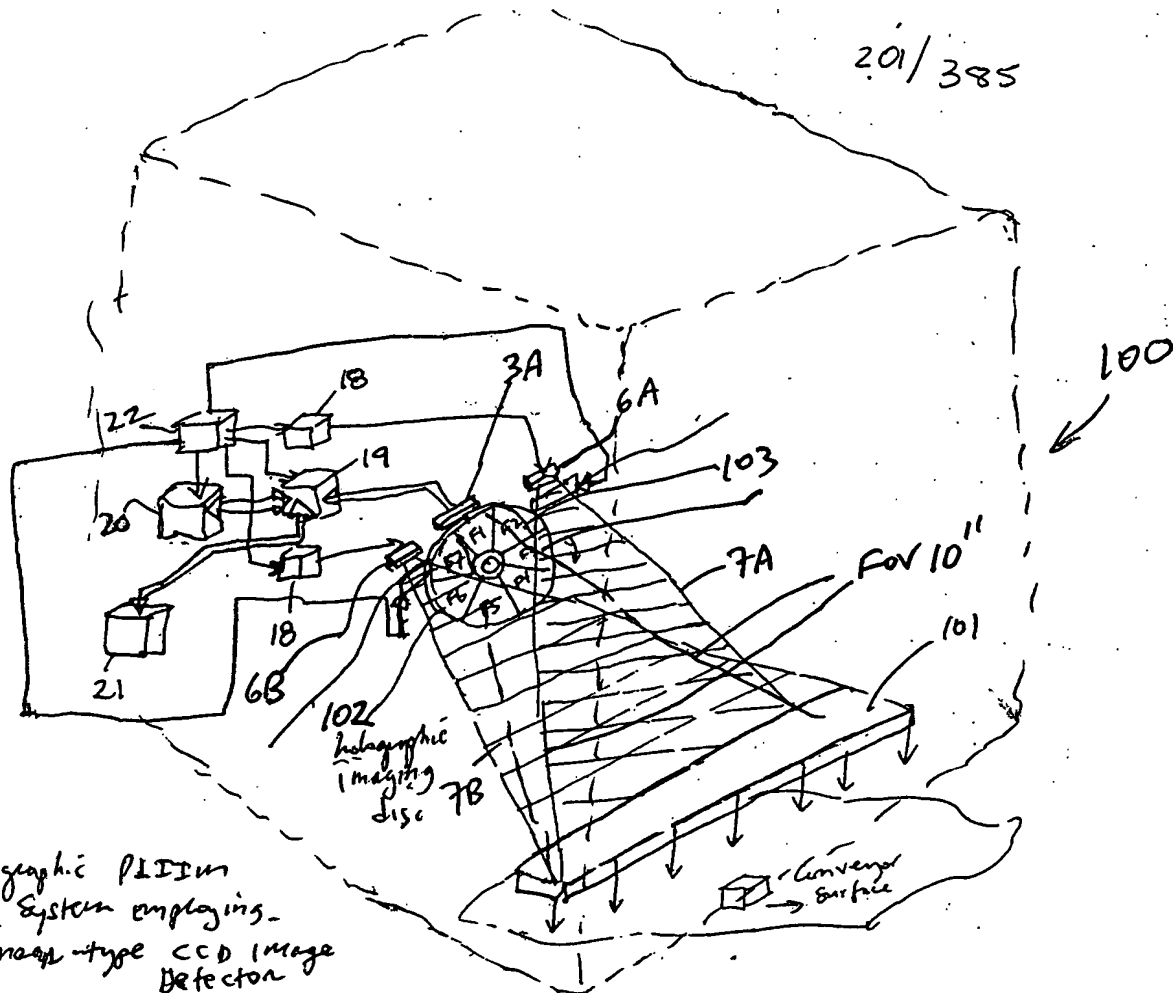


FIG. 6E4

Holographic PLIIM
System employing
Linac-type CCD image
Detector



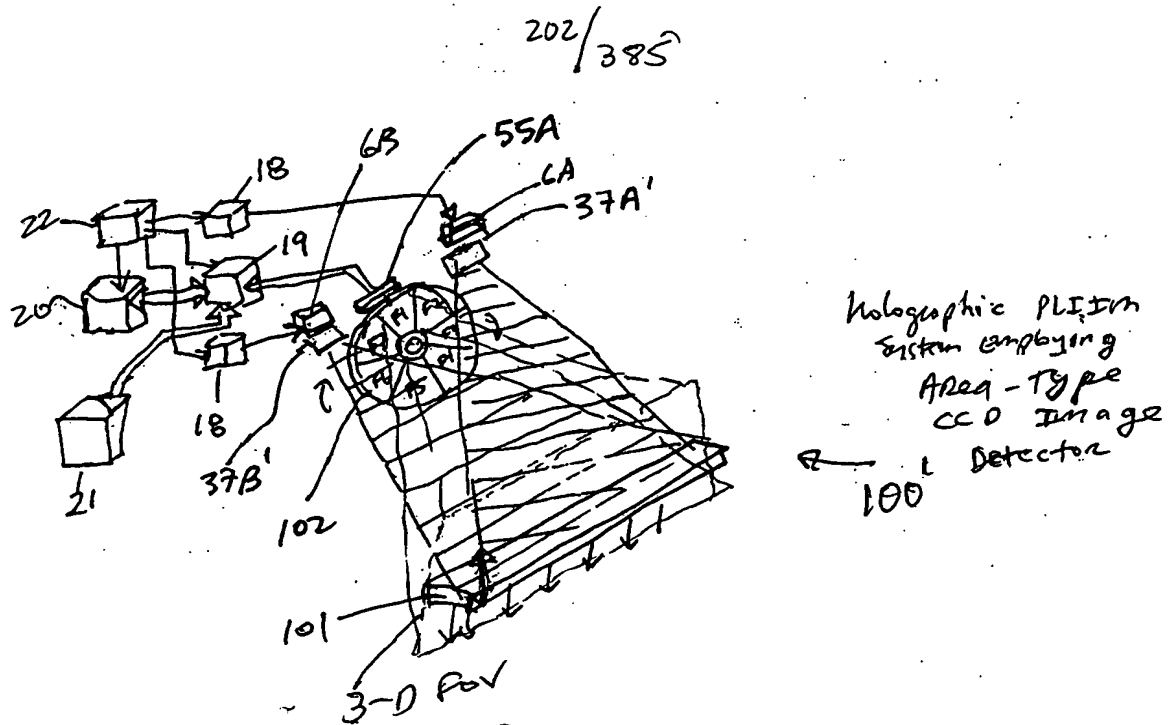


FIG. 8A

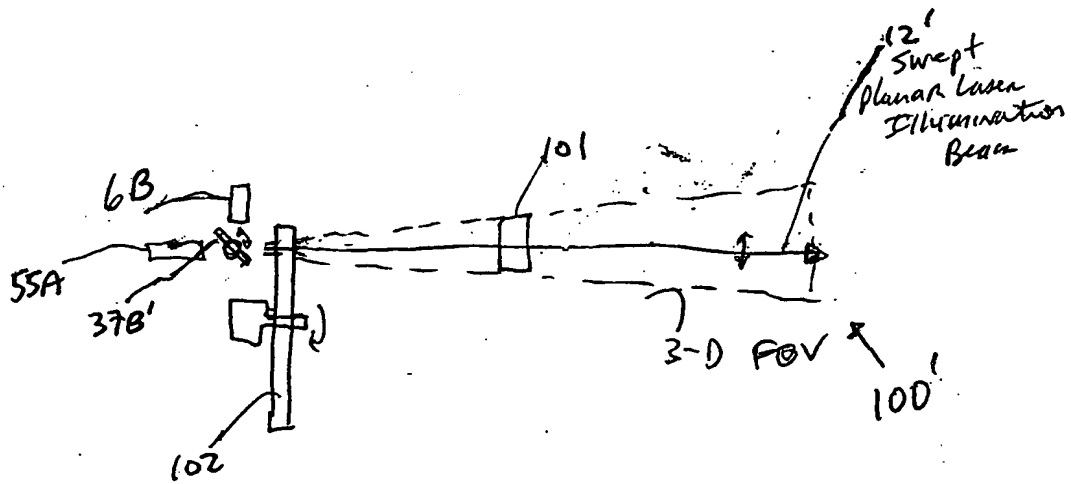


FIG. 8B

C



FIG. 9

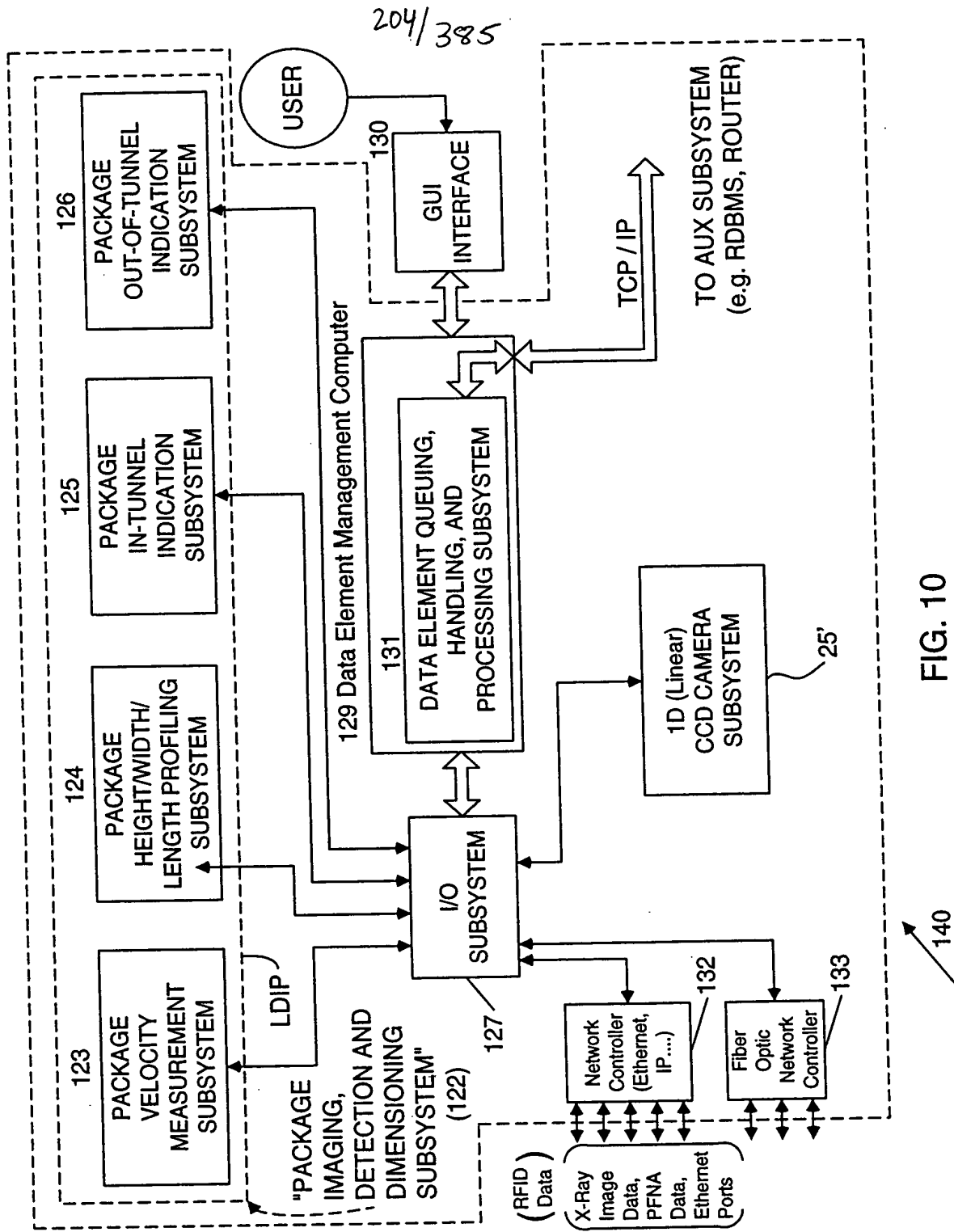


FIG. 10

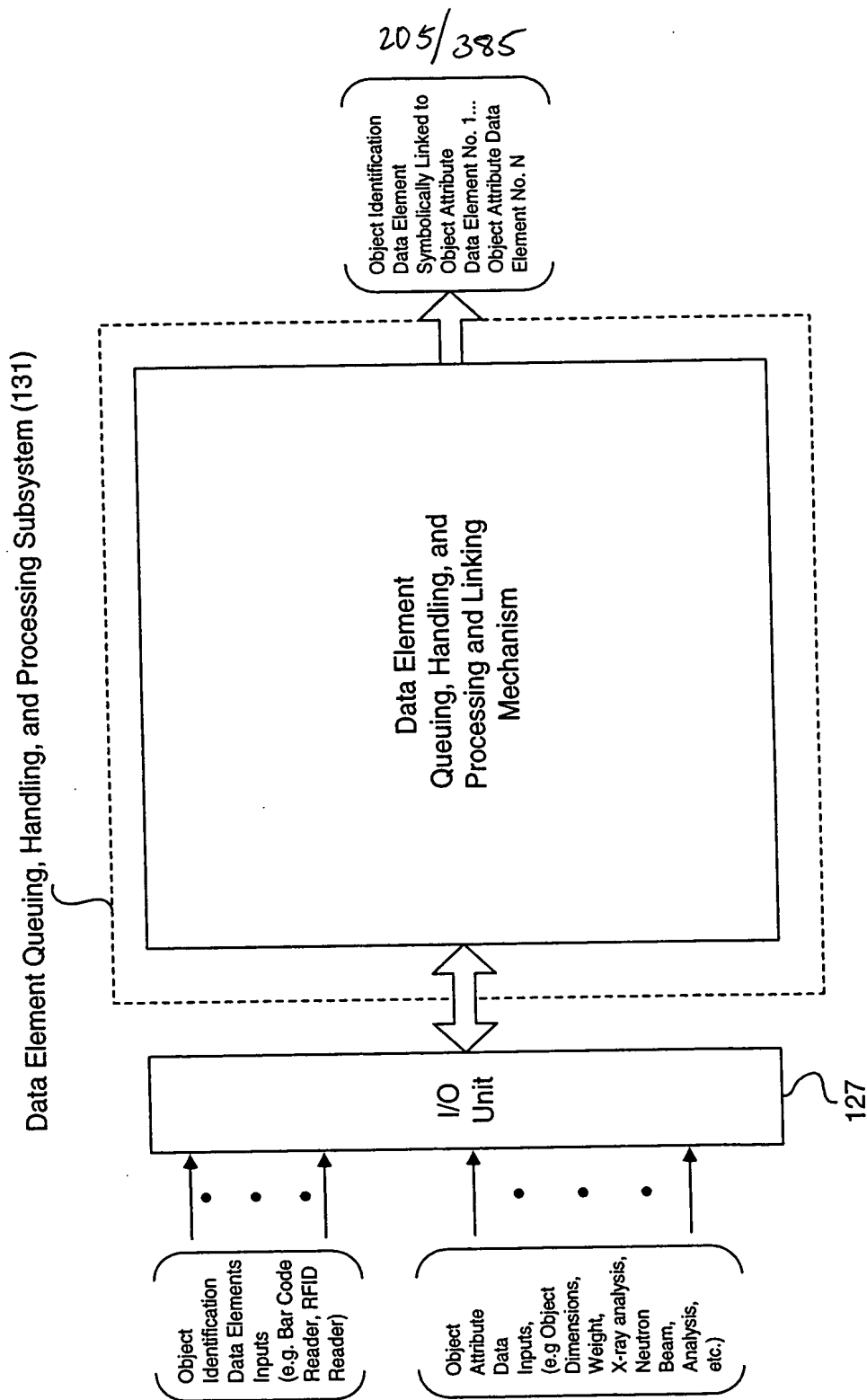


FIG. 10A

206/385

Primary Network
and/or System
Functions:

A.
Specification of Object
Detection and
Tracking Capability of
System

B.
Specification of Object
Identification
Capability of System

C.
Specification of
Object Attribute
Acquisition Capability
of System

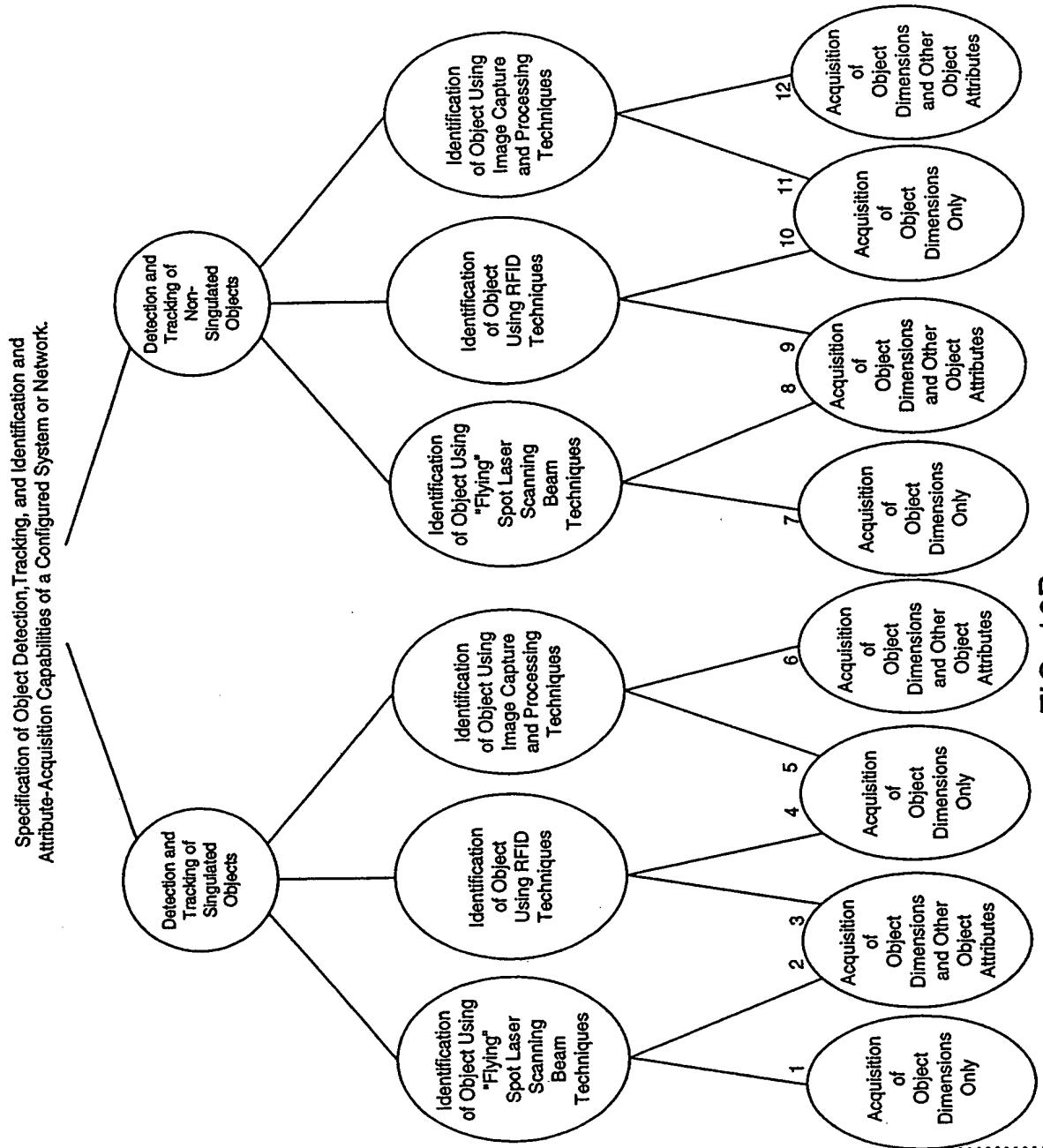


FIG. 10B

207/385

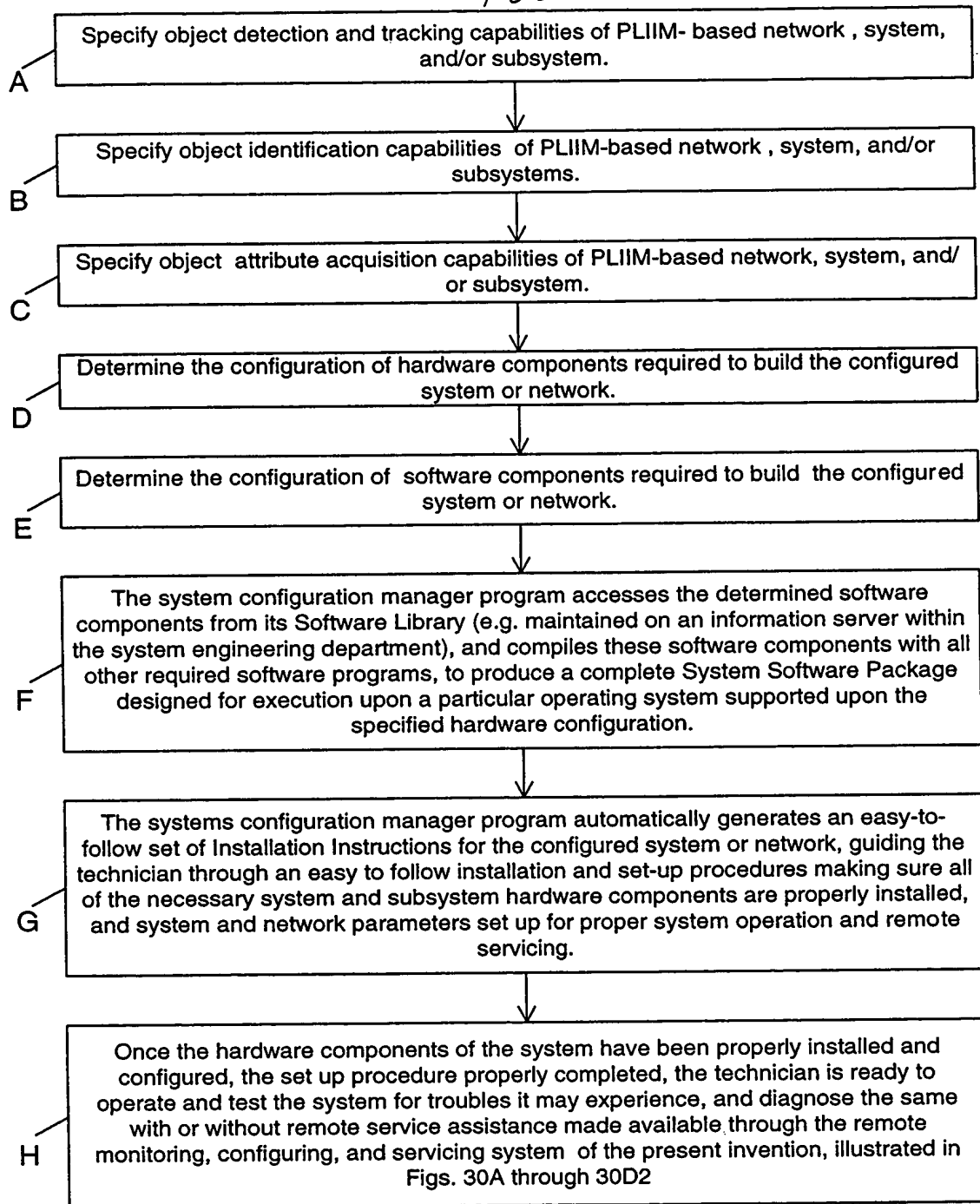


FIG. 10C

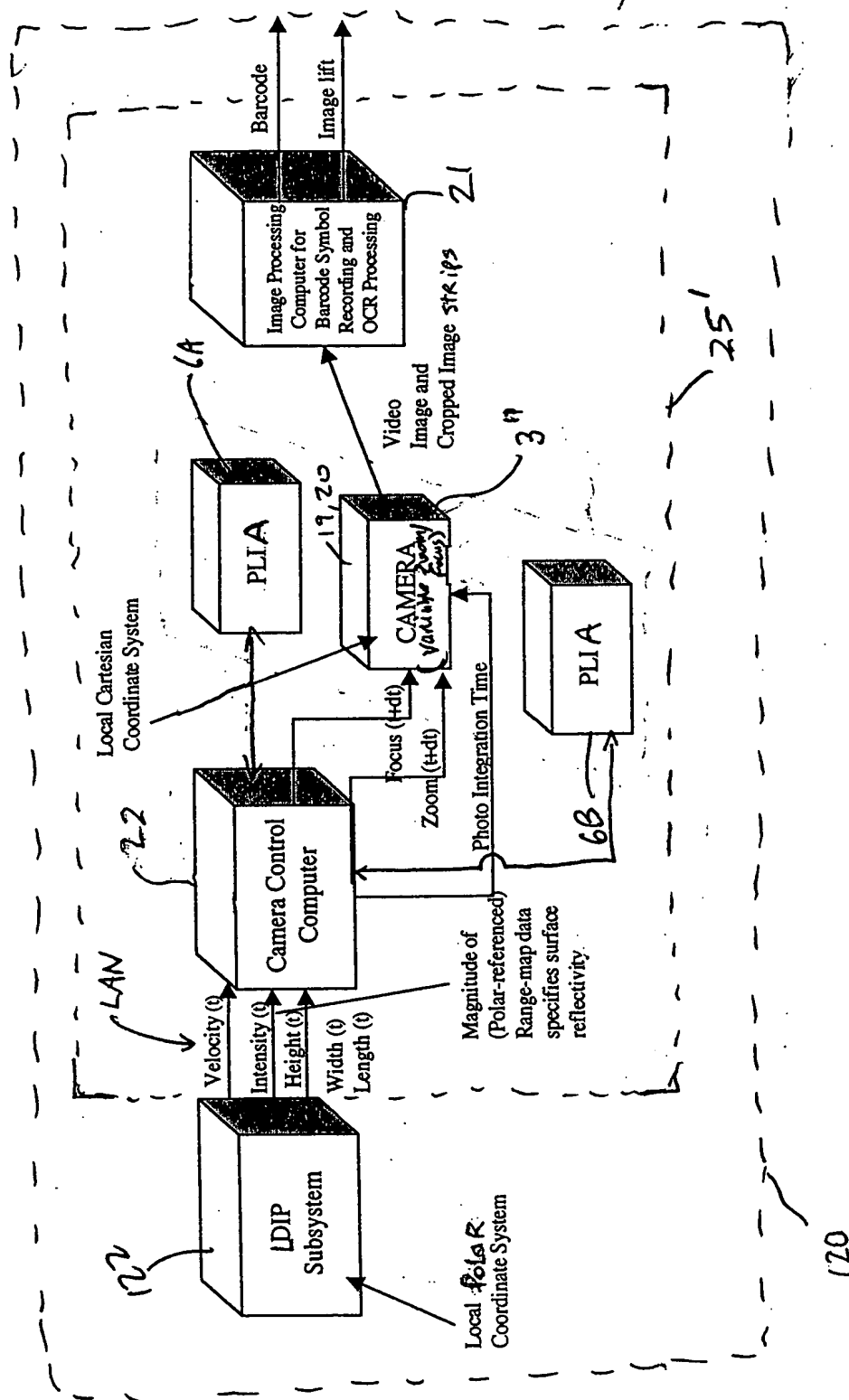


FIG. 11

FIG. 12A

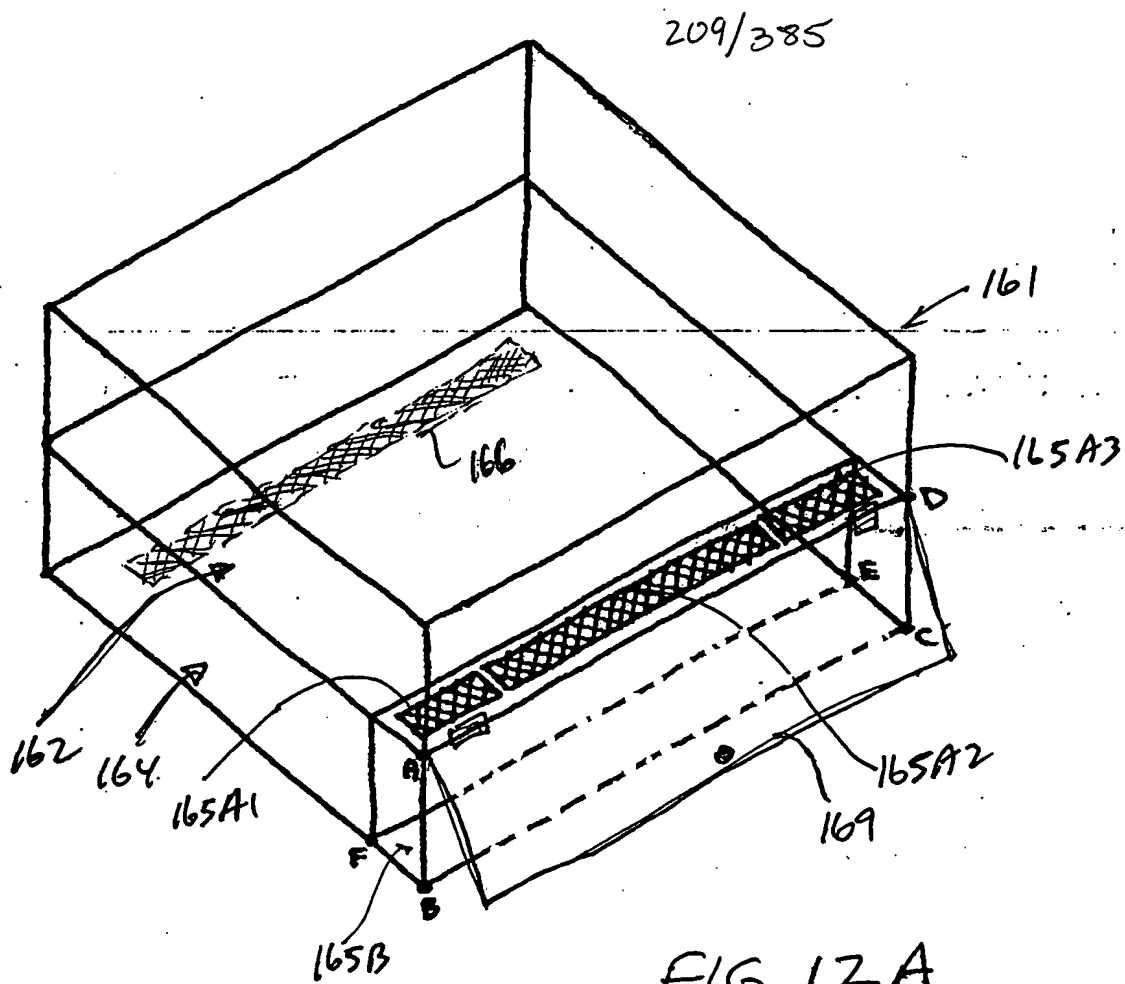


FIG. 12A

210/385

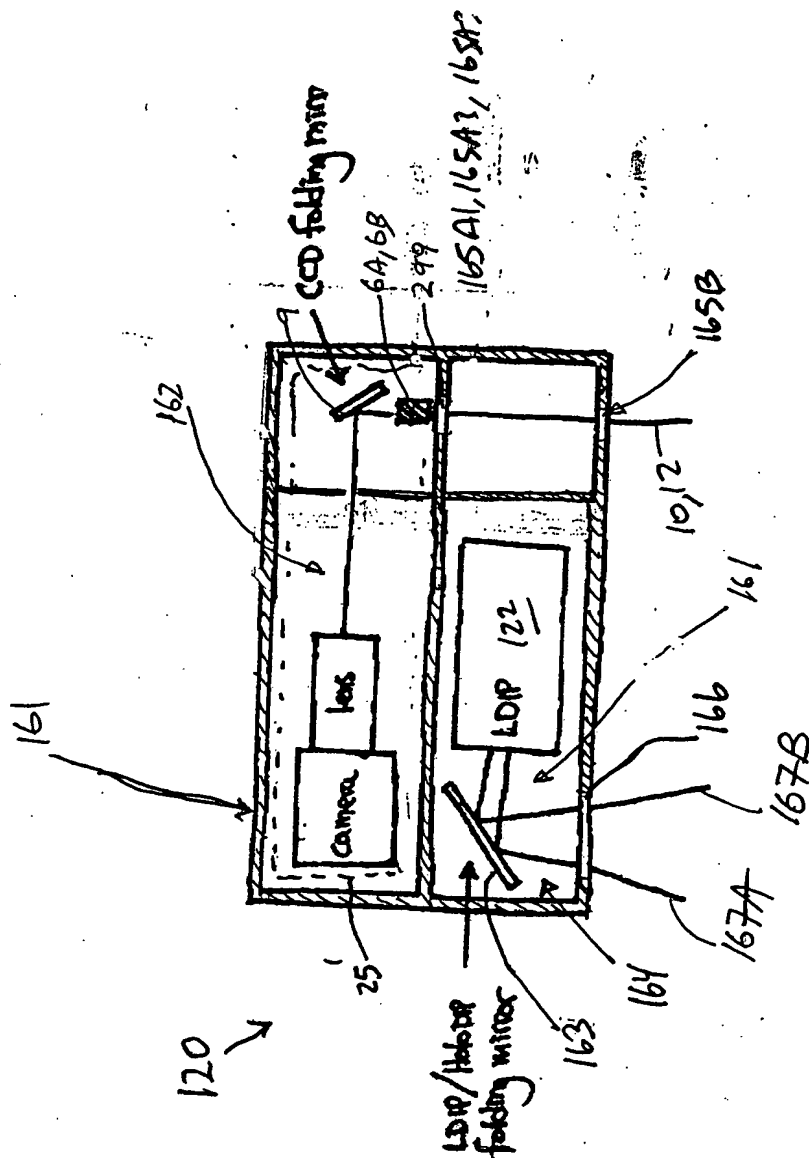


FIG. 12B

211/385

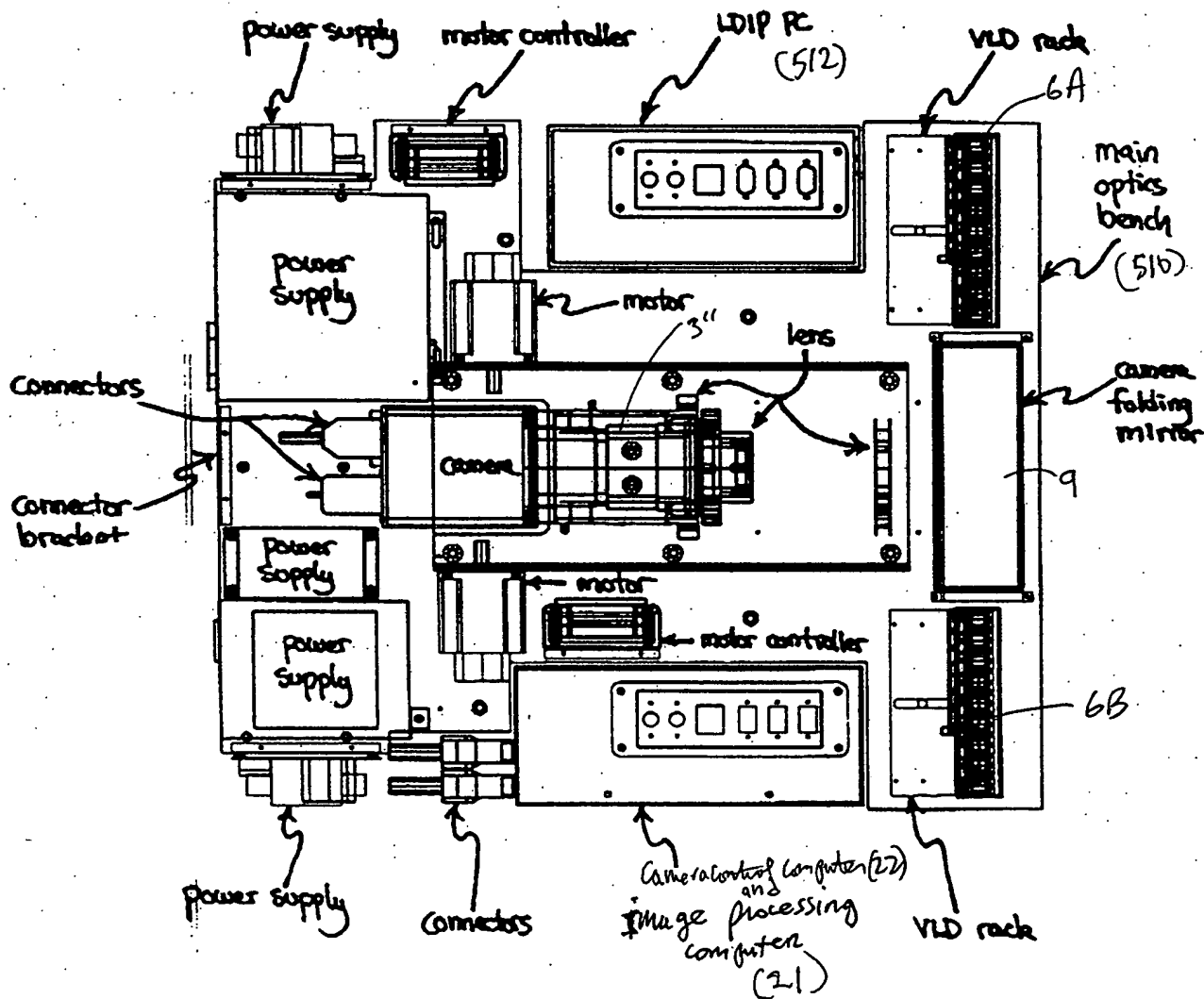


FIG. 12C

212/385

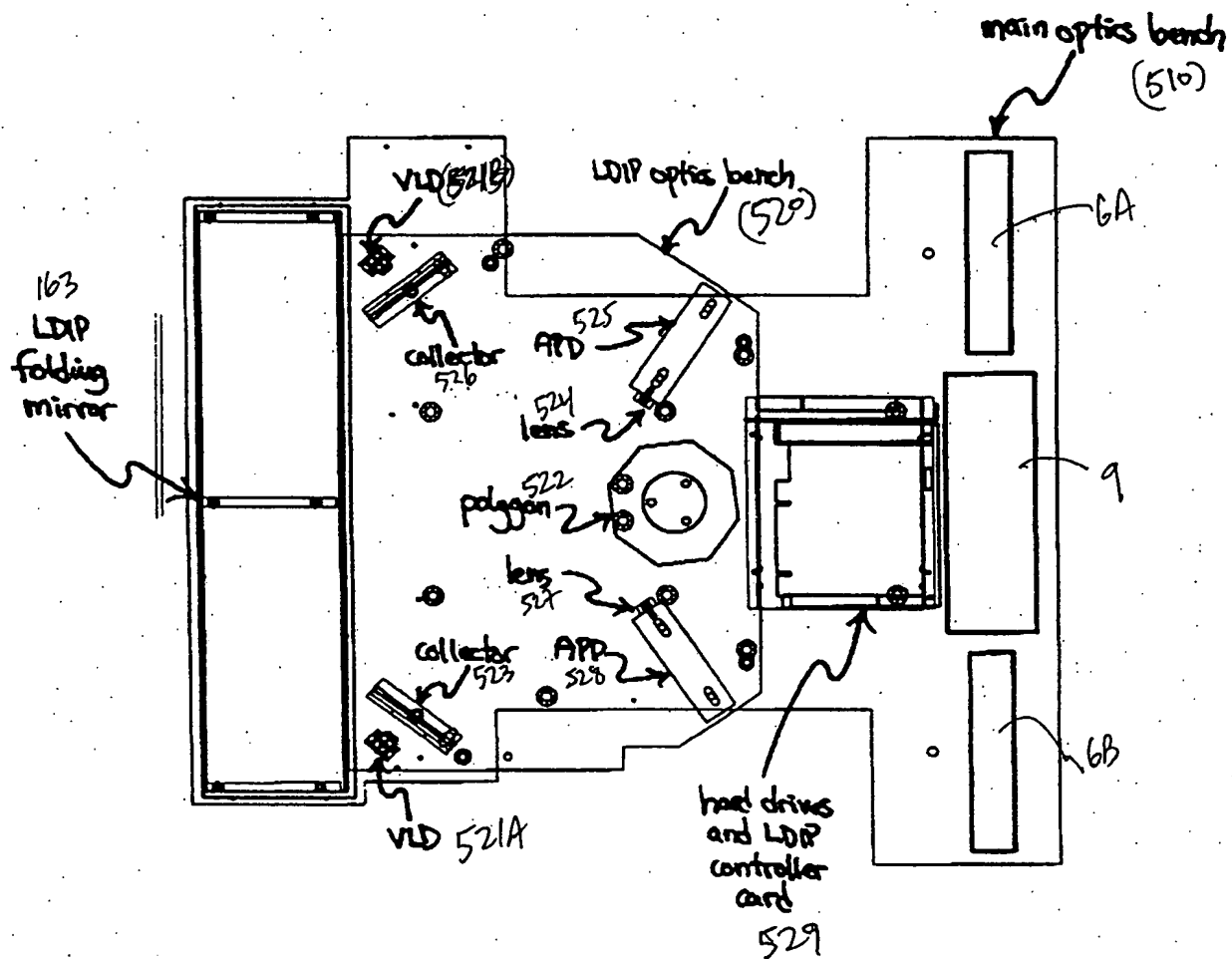
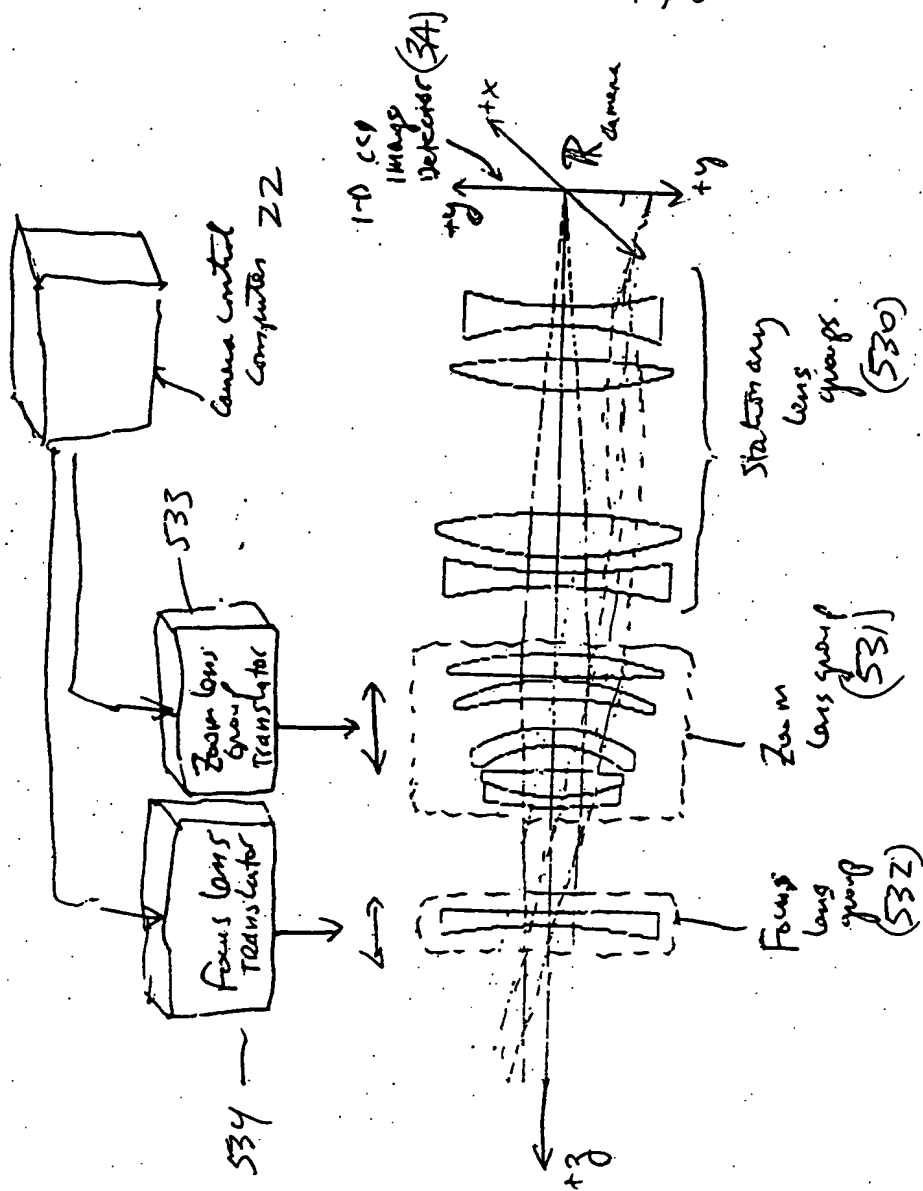


FIG. 12D

213/385



(main optics)
(lens groups)

FIG. 12E

214/385

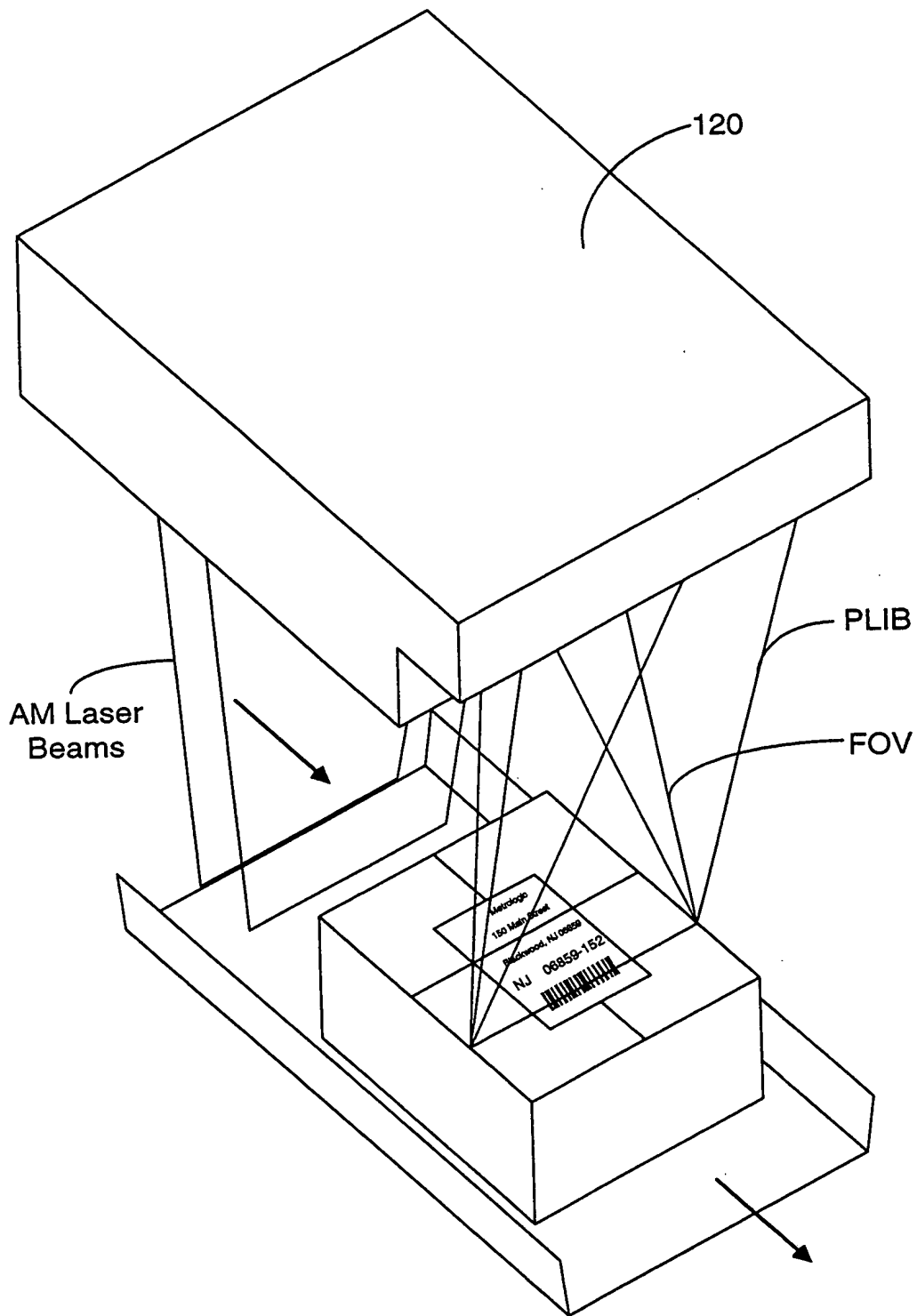


FIG. 13A

215/385

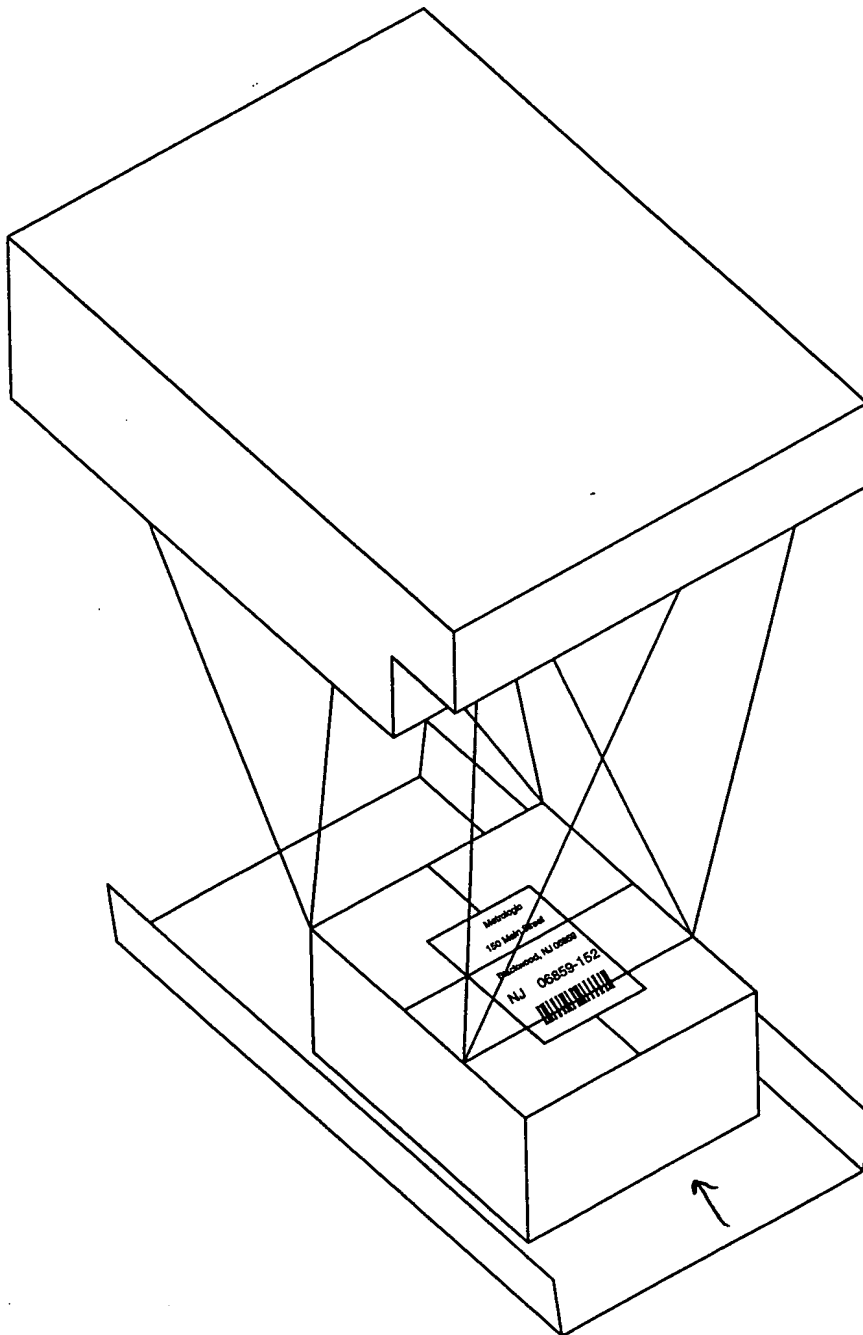


FIG. 13A

216/385

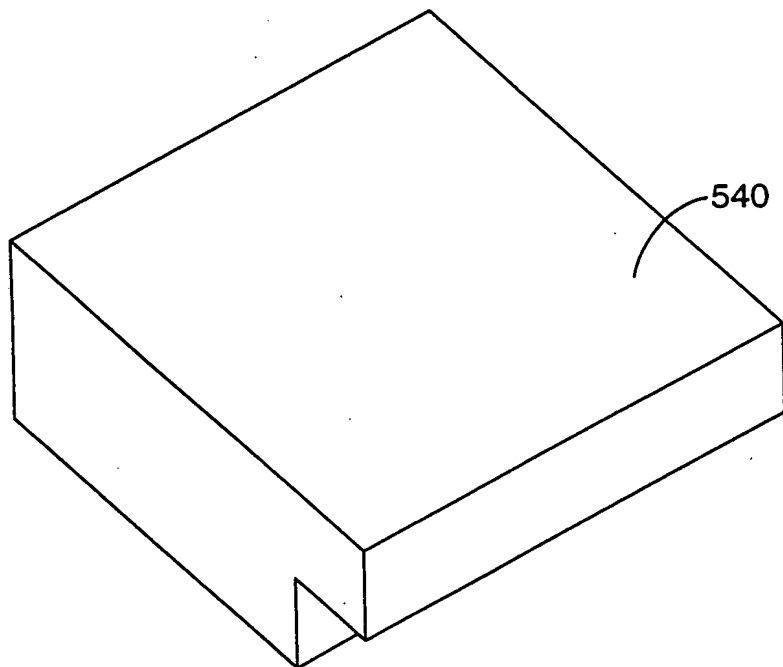


FIG. 13B

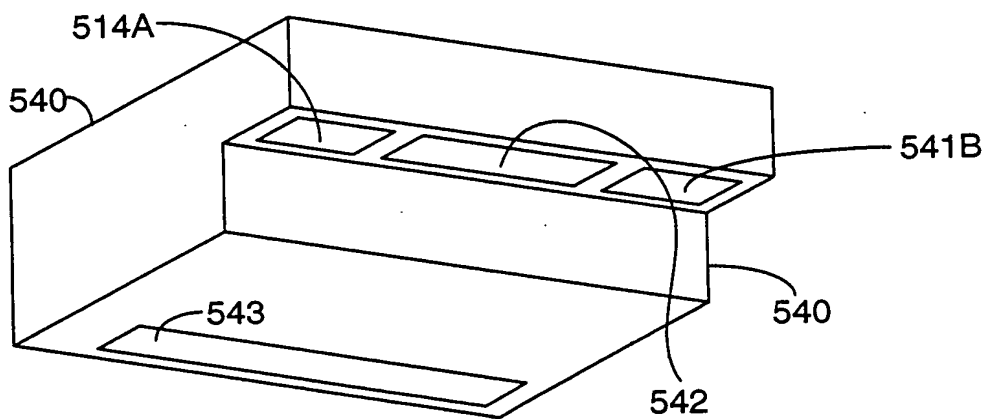


FIG. 13C

Patent 6,666,666

27/ 385
 PLLIM-BASED PACKAGE IDENTIFICATION AND
 DIMENSIONING (PID) SYSTEM

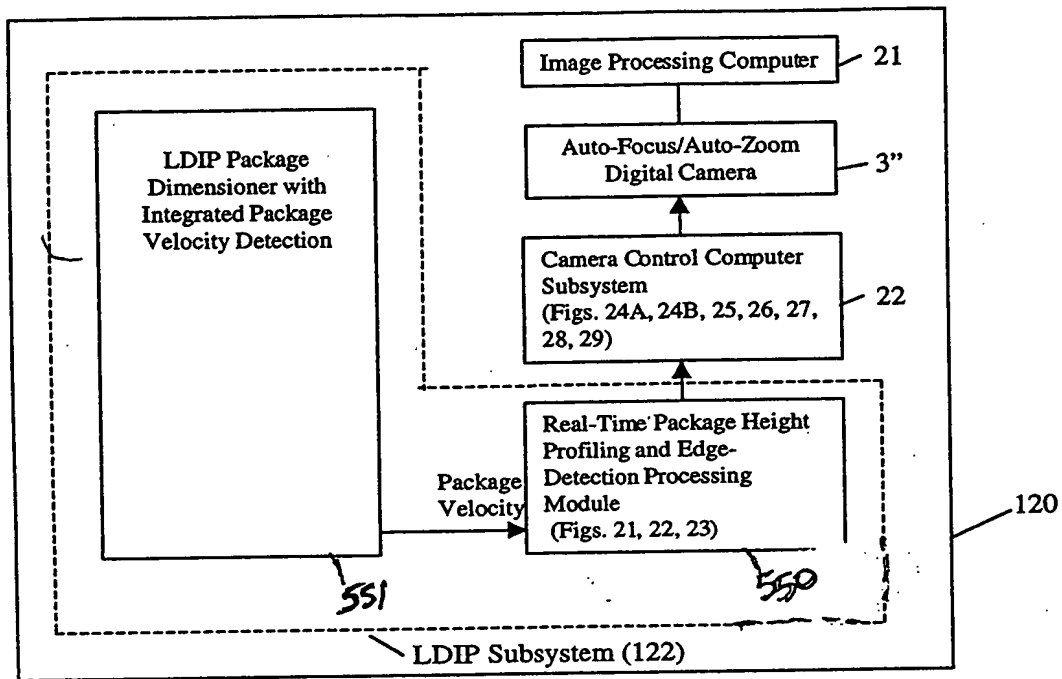


FIG. 14

218/395

LDIP REAL-TIME PACKAGE HEIGHT PROFILE AND EDGE DETECTION METHOD

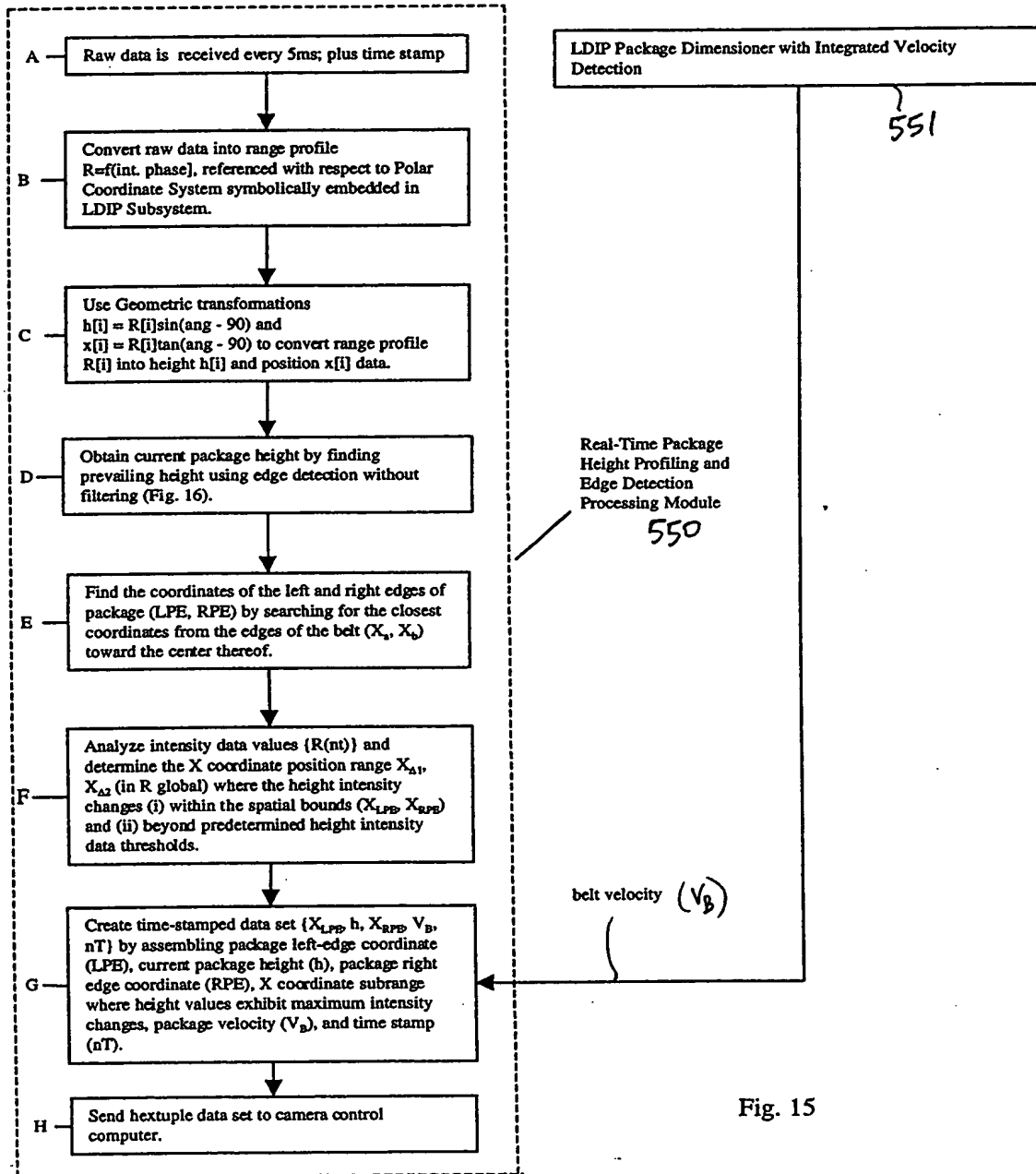
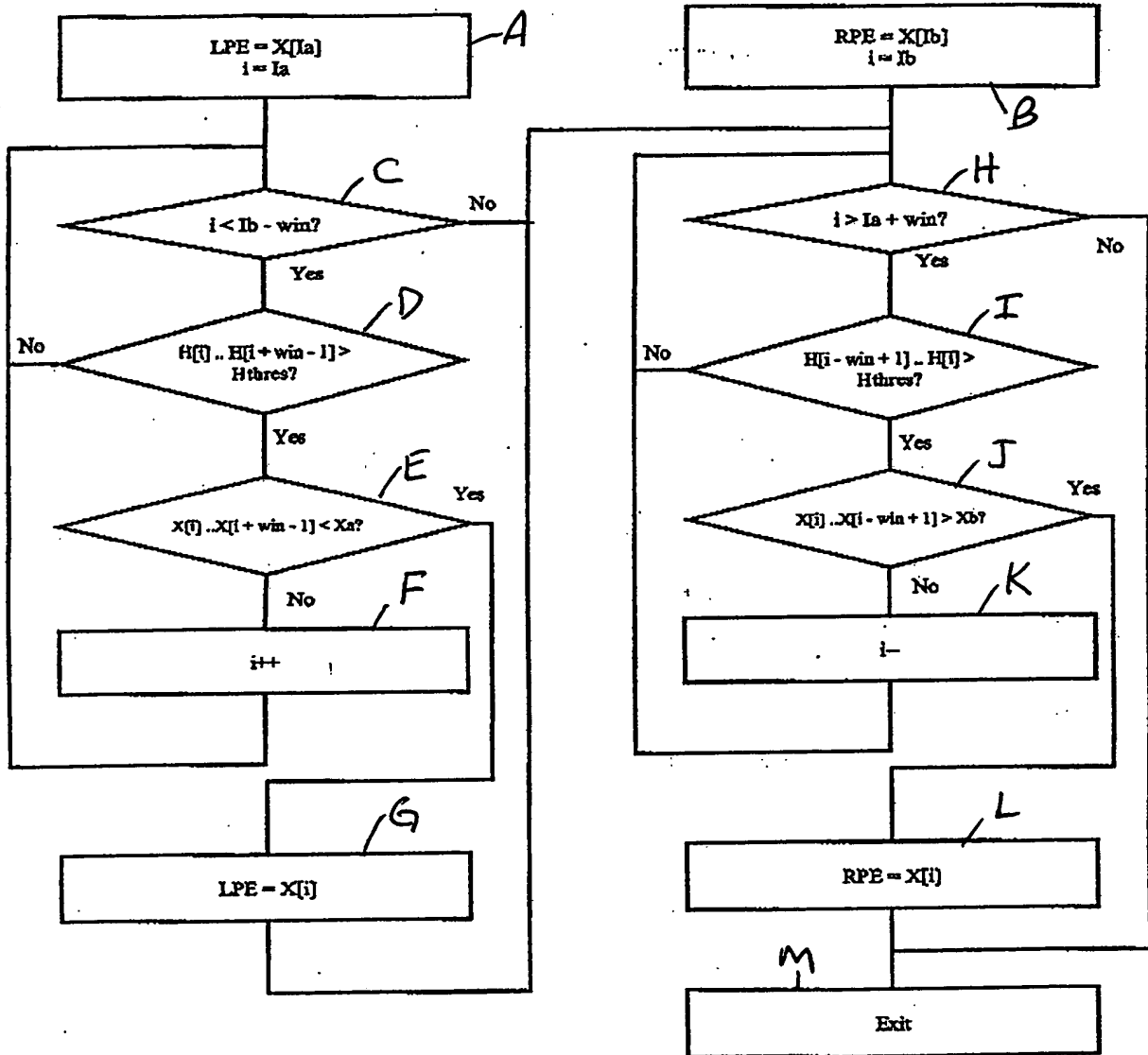


Fig. 15

219/385

LDIP Real Time Package Edge Detection



Xa = location of belt left edge; Xb = location of belt right edge
 Ia = belt edge edge pixel; Ib = belt right edge pixel
 LPE = Left package edge; RPE = Right package edge
 $H[]$ = Pixel height array; $X[]$ = Pixel location array
 win = package detection window

FIG. 16

220/385

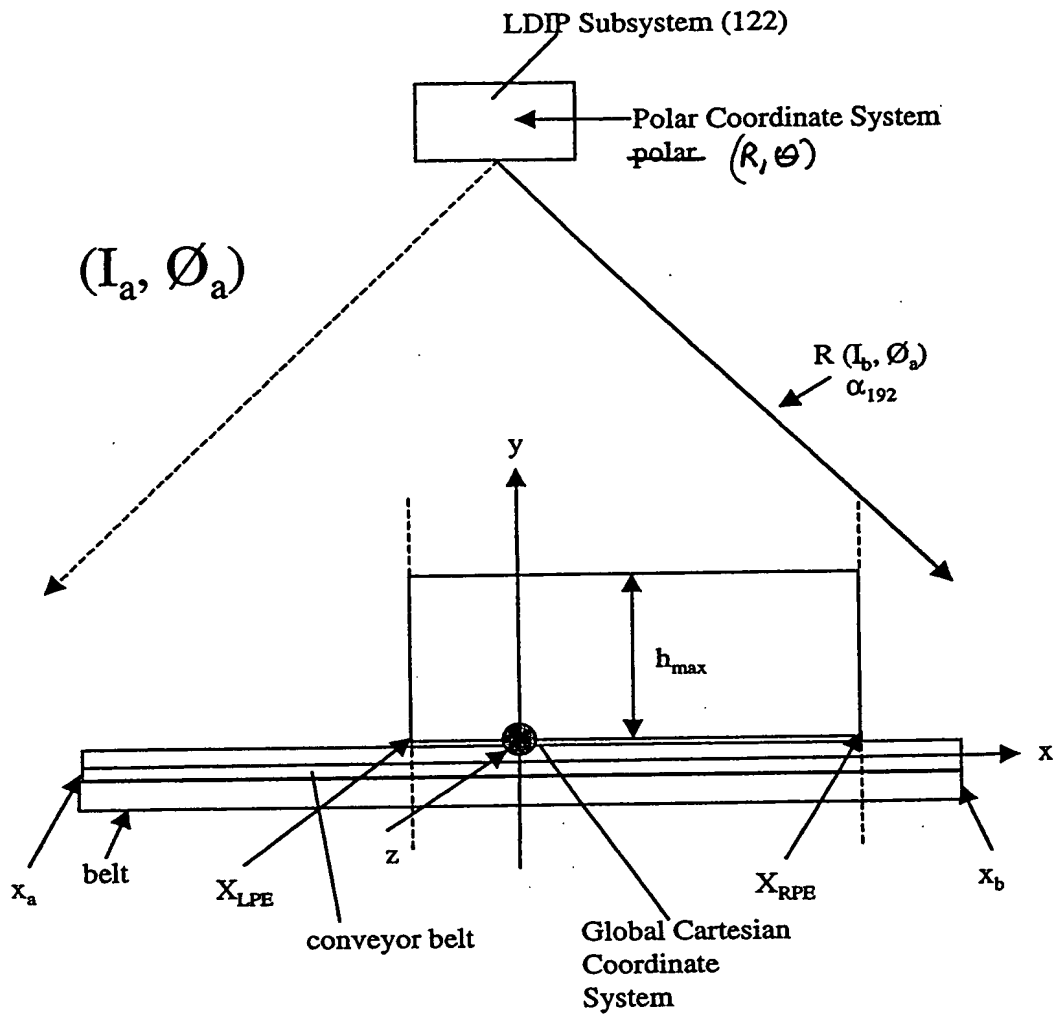


Fig. 17

224/385

INFORMATION MEASURED AT SCAN ANGLES BEFORE COORDINATE TRANSFORMS

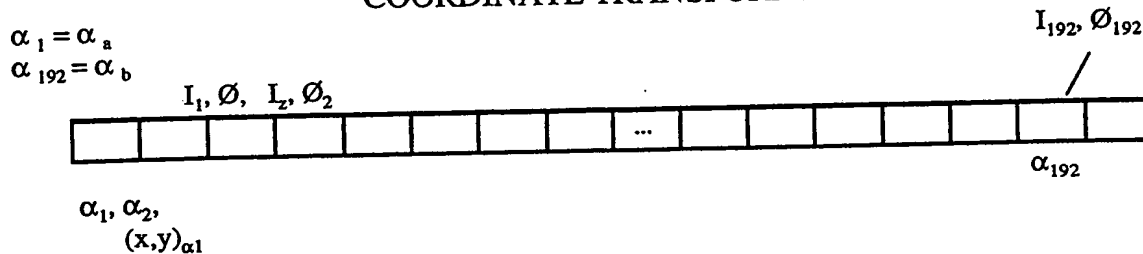


Fig. 17A

RANGE AND POLAR ANGLE MEASURES TAKEN AT SCAN ANGLE α BEFORE COORDINATE TRANSFORMS

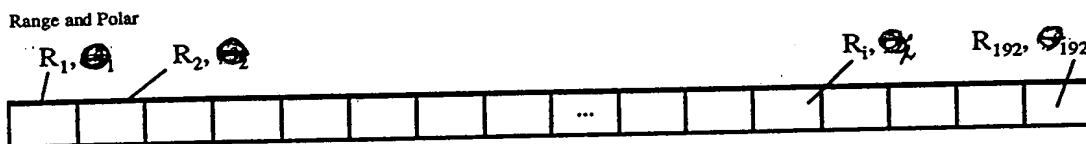


Fig. 17B

MEASURED PACKAGE HEIGHT AND POSITION VALUES AFTER COORDINATE TRANSFORMS

H []
Input height after
coordinate transforms

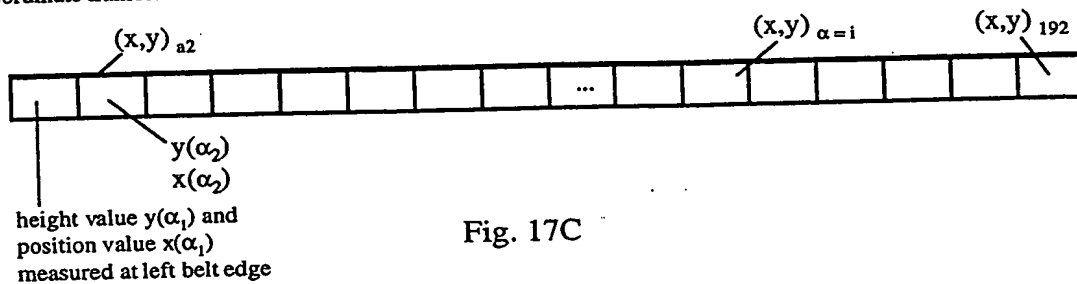


Fig. 17C

FORM 3850-6-60

222/385

CAMERA CONTROL PROCESS CARRIED OUT WITHIN THE CAMERA CONTROL SUBSYSTEM OF EACH OBJECT IDENTIFICATION AND ATTRIBUTE ACQUISITION SYSTEM OF PRESENT INVENTION

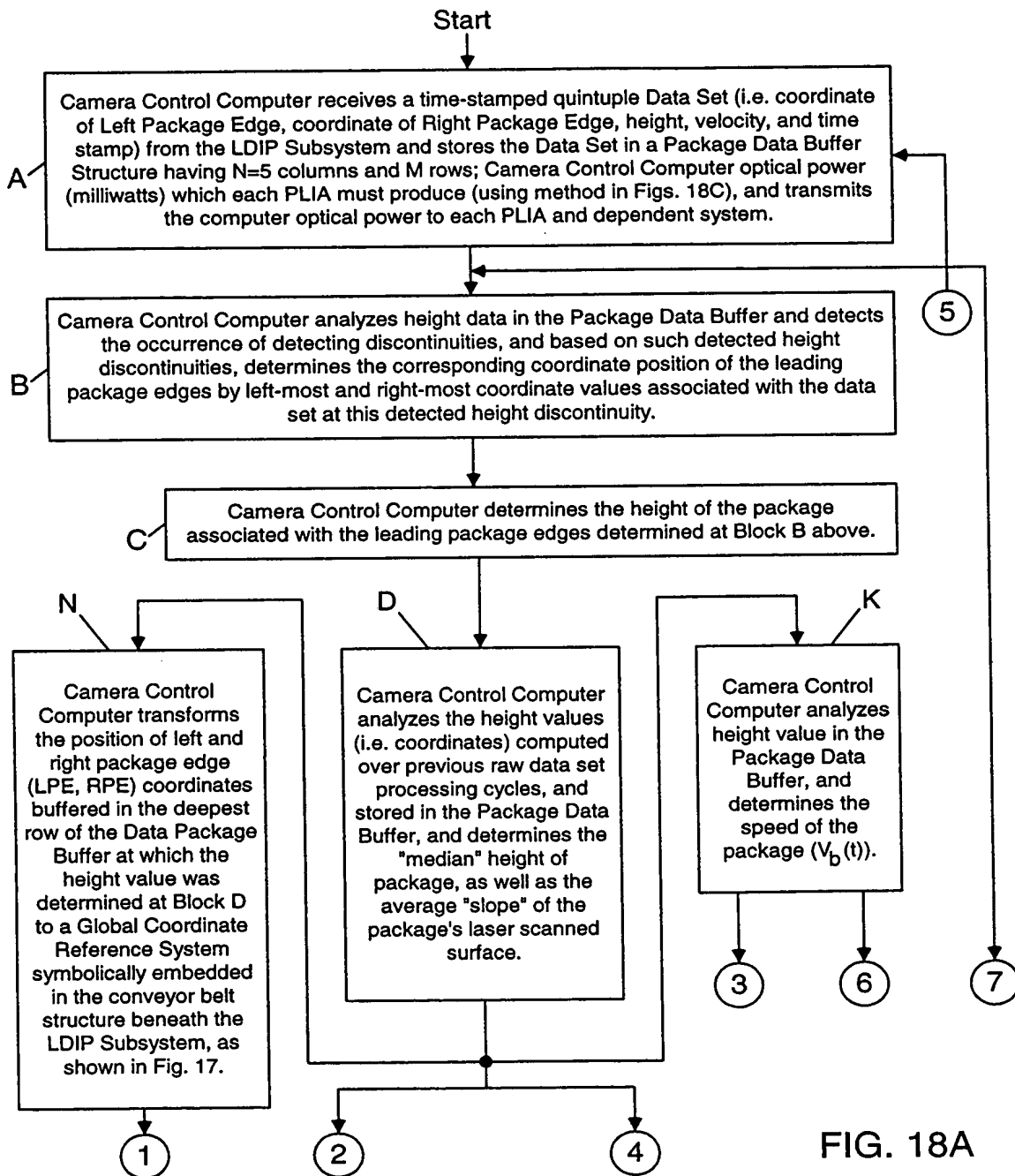
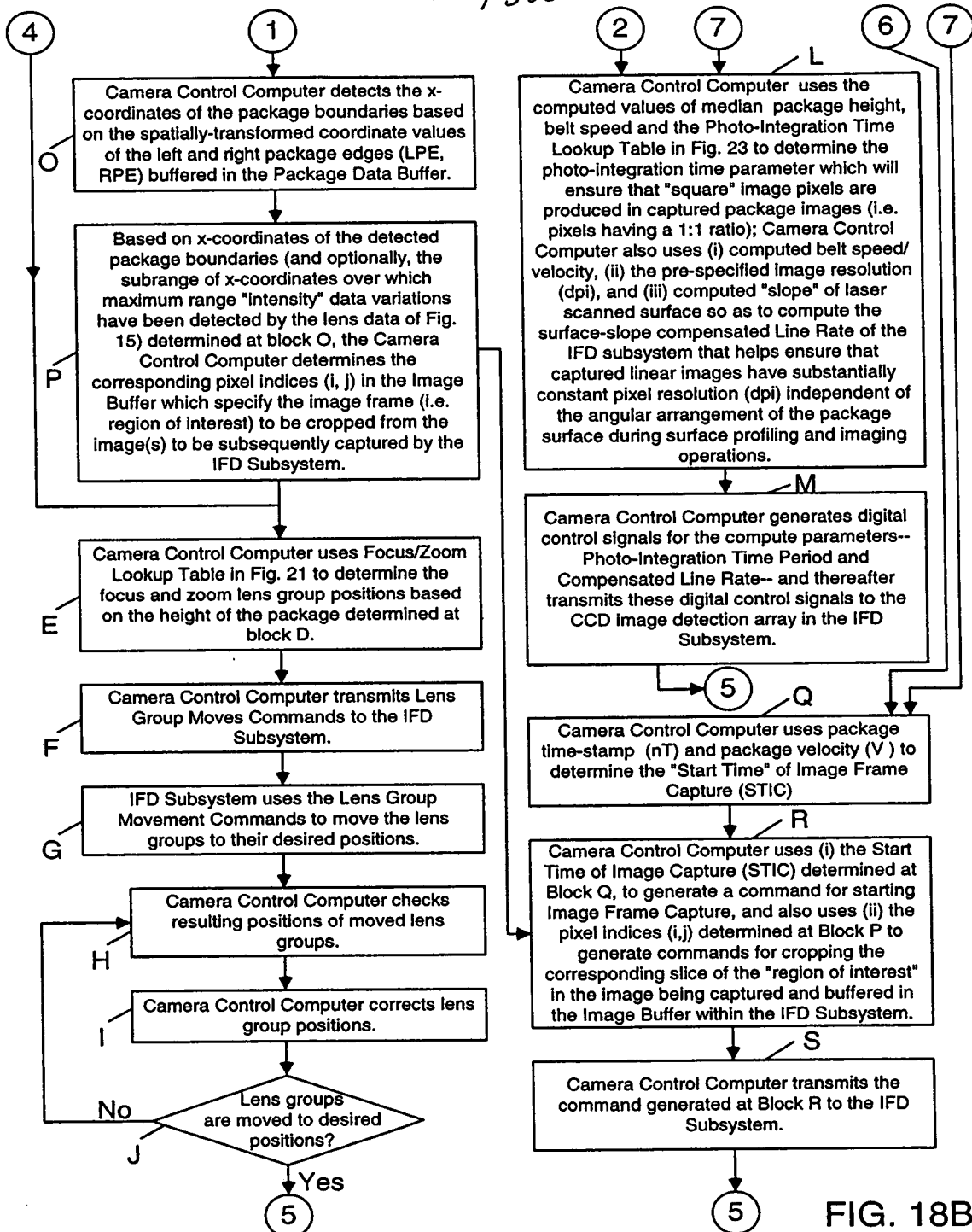


FIG. 18A

223/385



224/ 385

METHOD OF COMPUTING OPTICAL OUTPUT POWER FROM CASE
DIODES IN PLANAR LASER ILLUMINATION ARRAY (PLIA) FOR
CONTROLLING CONSTANT WHITE LEVEL IN IMAGE PIXELS CAPTURED
BY PLIIM-BASED LINEAR IMAGER

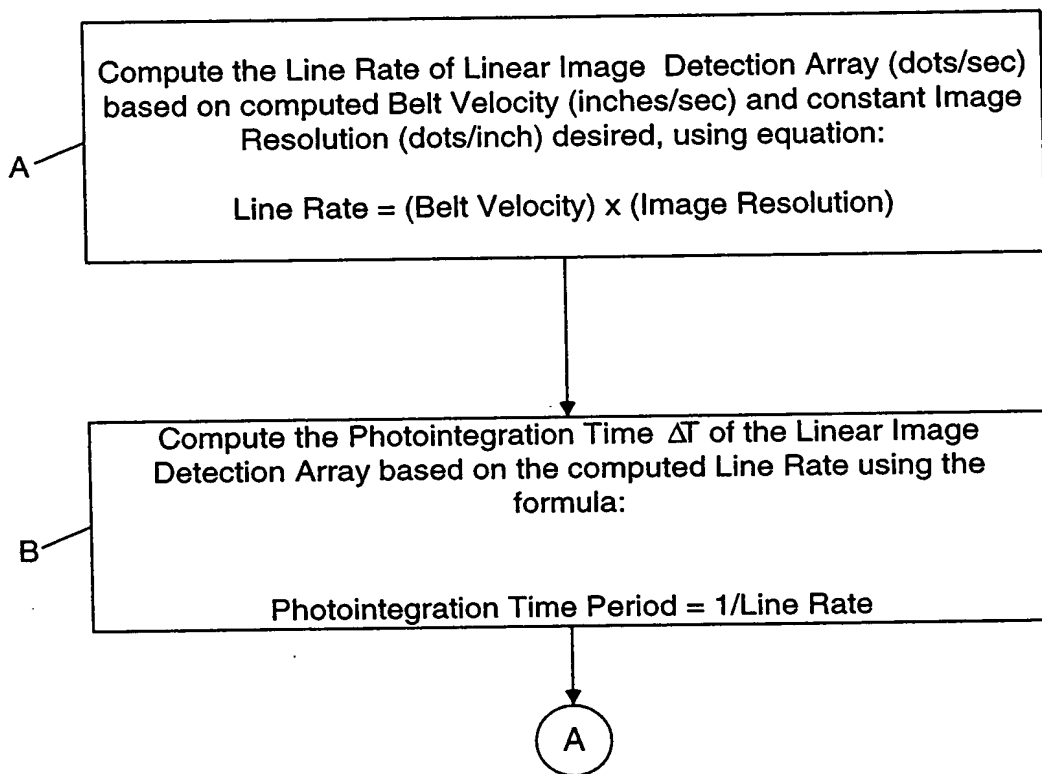


FIG. 18C1

225/385

A

Compute the Optical Power (milliwatts) of each PLIA based on computed Photointegration Time Period (ΔT) using the following formula:

$$\text{Optical Power of VLD (milliwatts)} = \frac{\text{constant}}{\text{Photointegration Time Period } \Delta T}$$

FIG. 18C2

226/325

METHOD OF COMPUTING COMPENSATED LINE RATE FOR CORRECTING
VIEWING-ANGLE DISTORTION OCCURING IN IMAGES OF OBJECT
SURFACES CAPTURED AS OBJECT SURFACES MOVE PAST PLIIM-
BASED LINEAR IMAGER AT NON-ZERO SKEWED ANGLE

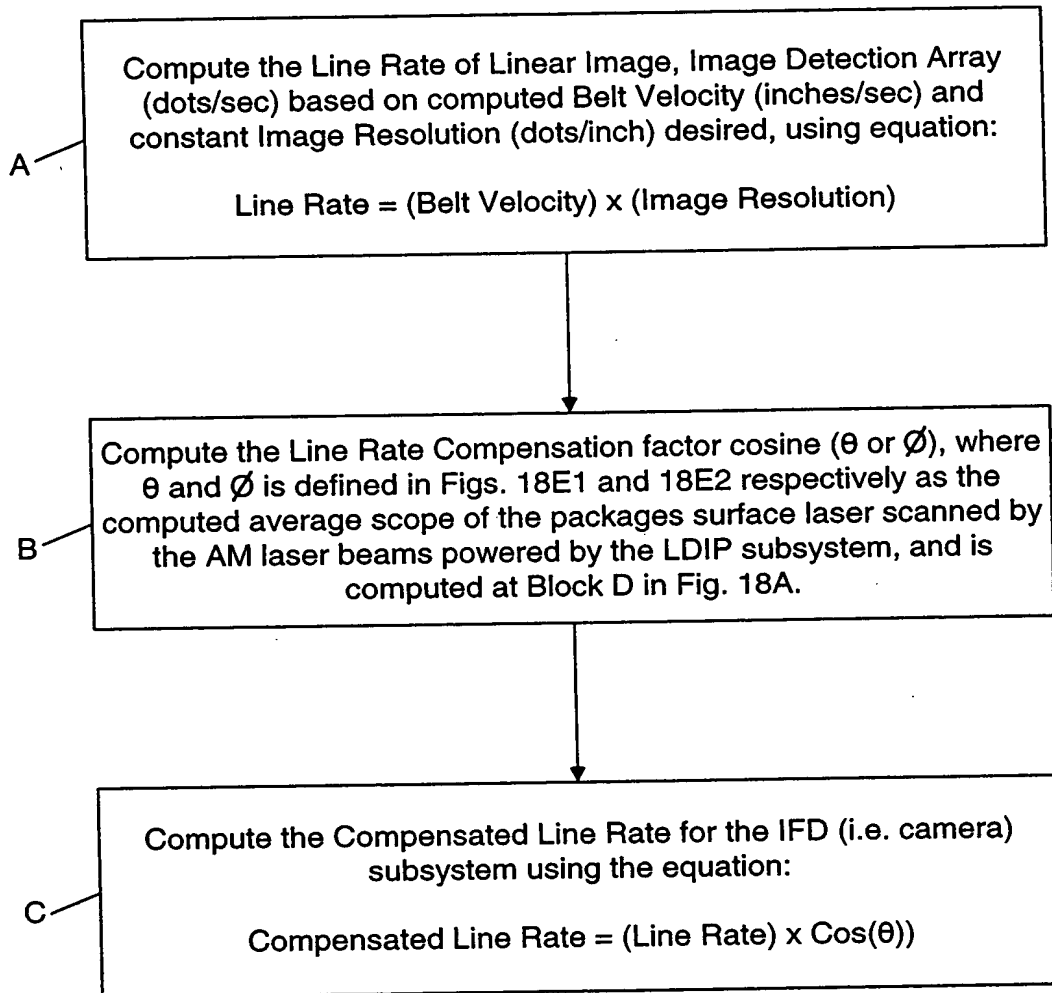


FIG. 18D

227/385

CASE 1:
Top Down Imaging

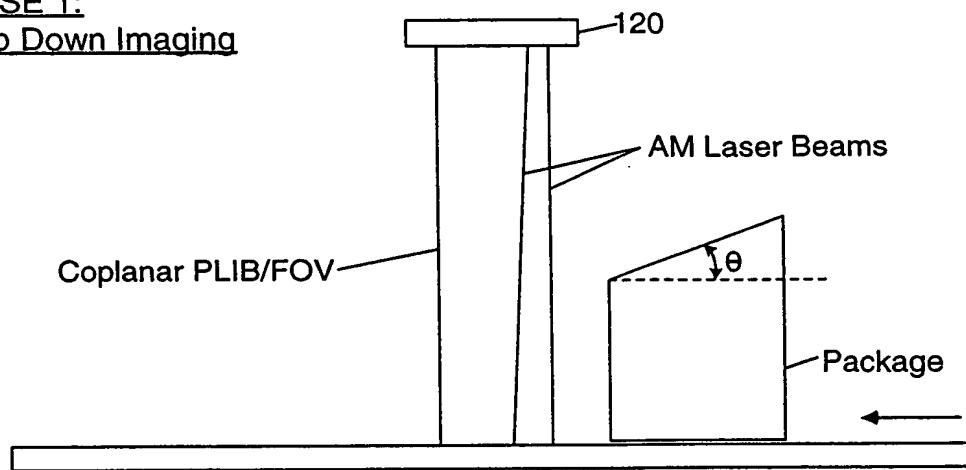


FIG. 18E1

CASE 2:
Side Imaging

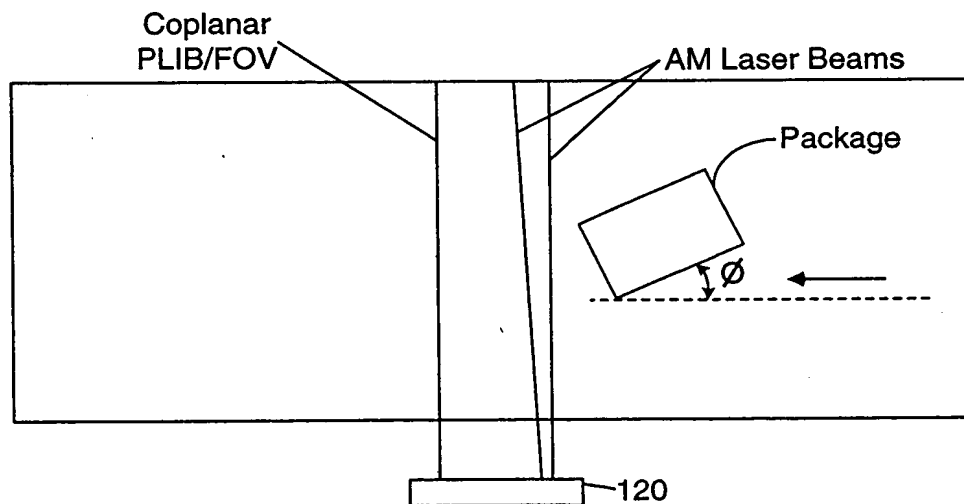


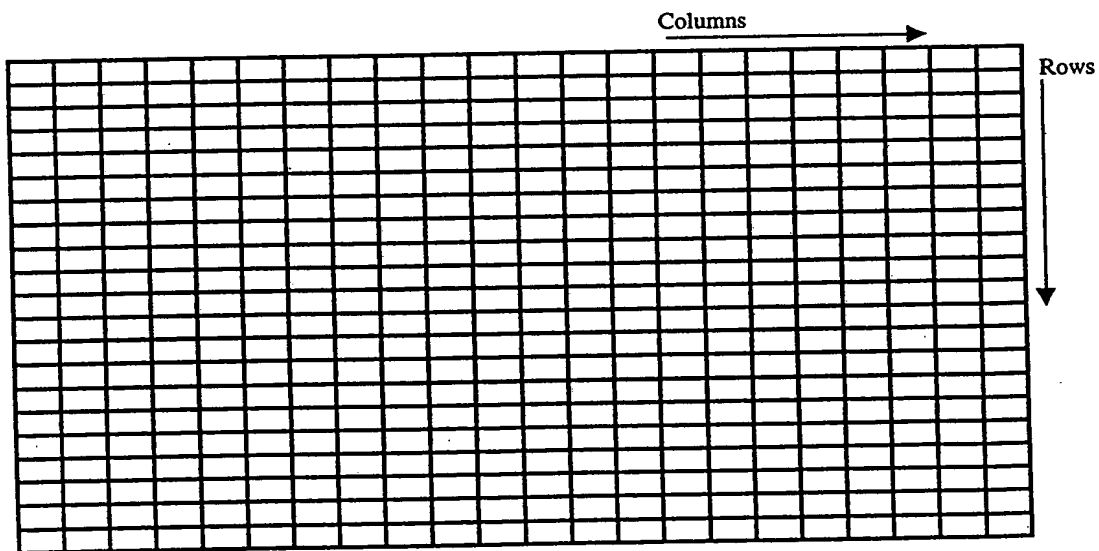
FIG. 18E2

228/385

X coordinate subrange where
maximum range "intensity"
variations have been detected

| Left Package Edge (LDE) | Package Height (h) | Right Package Edge (RPE) | Package Velocity | Time-stamp (nT) | |
|----------------------------|--------------------|-----------------------------|---------------------|--------------------|-------|
| | | | | | Row 1 |
| | | | | | Row 2 |
| | | | | | Row 3 |
| | | | | | Row 4 |
| | | | | | Row 5 |
| | | | | | Row M |
| Package Data Buffer (FIFO) | | | | | |
| | | | | | |
| | | | | | |

Fig. 19



Camera Pixel Data Buffer
pixel indices (i,j.)

Fig. 20

TOP SECRET

229/385

Zoom and Focus Lens Group Position
Look-up Table

| Distance from Camera H (mm) | Zoom group distance (mm) Y (Zoom) | Focus group distance (mm) Y (Focus) |
|--------------------------------|--------------------------------------|----------------------------------------|
| 1000 | 21.57489228 | 2.47E-05 |
| 1100 | 19.38089696 | 10.99009783 |
| 1200 | 17.10673434 | 20.65783177 |
| 1300 | 14.77137314 | 29.10917002 |
| 1400 | 12.39153565 | 36.47312595 |
| 1500 | 9.979114358 | 42.87845436 |
| 1600 | 7.540639114 | 48.44003358 |
| 1700 | 5.078794775 | 53.25495831 |
| 1800 | 2.595989366 | 57.40834303 |
| 1900 | 0.099972739 | 60.98883615 |

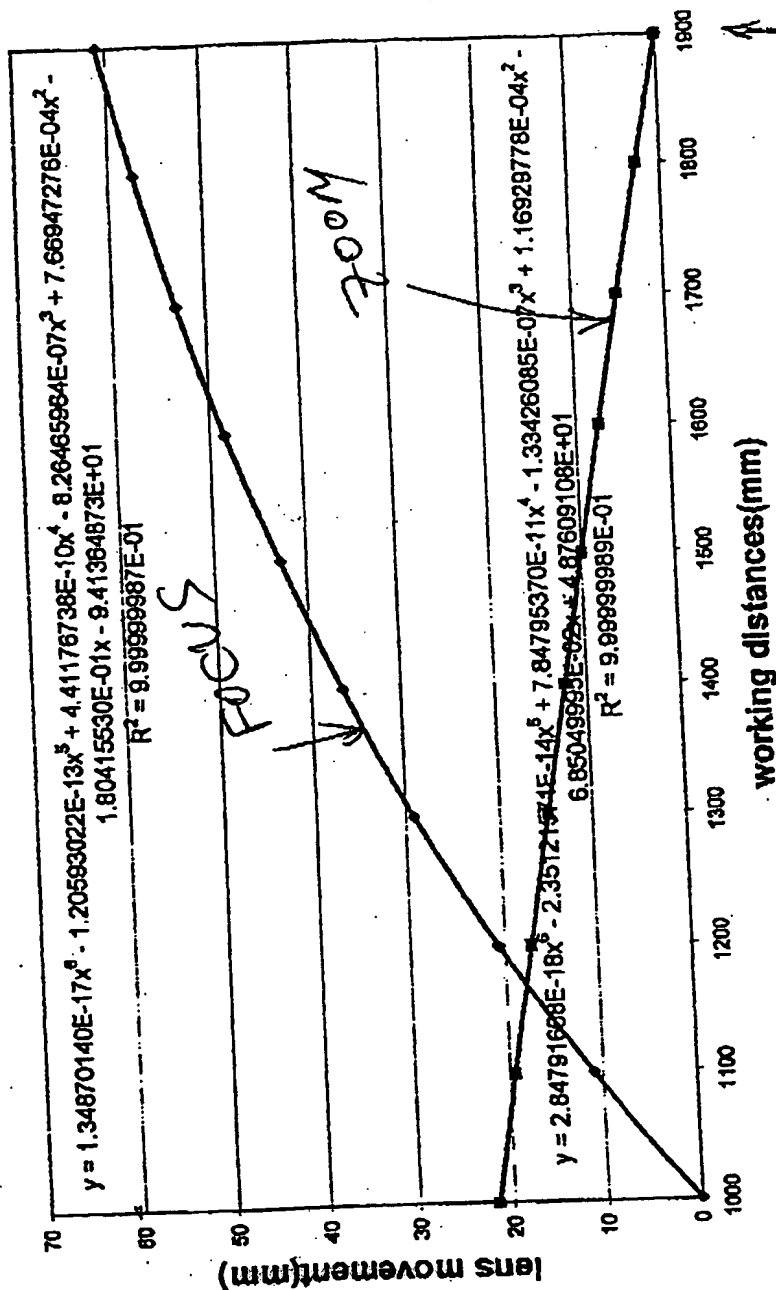
(use interpolation techniques for walking distances between listed points in table)

FIG. 21.

TTTTT 53506660

* Note: On feed distance & zoom (left hand graph) of camera lens are coupled (inter-dependent) in camera has a fixed aperture F5.6

Focus and Zoom lens movement vs. working distances



—•— zoom 1 —•— zoom 2 — Poly. (zoom 1) — Poly. (zoom 2)

↑ (inches) 30 above conveyor belt
 ← package height above conveyor
 conveyor-belt surface

FIG. 22A

230/385

231/385

TOP SECRET

Photo-Integration Time Look-Up Table

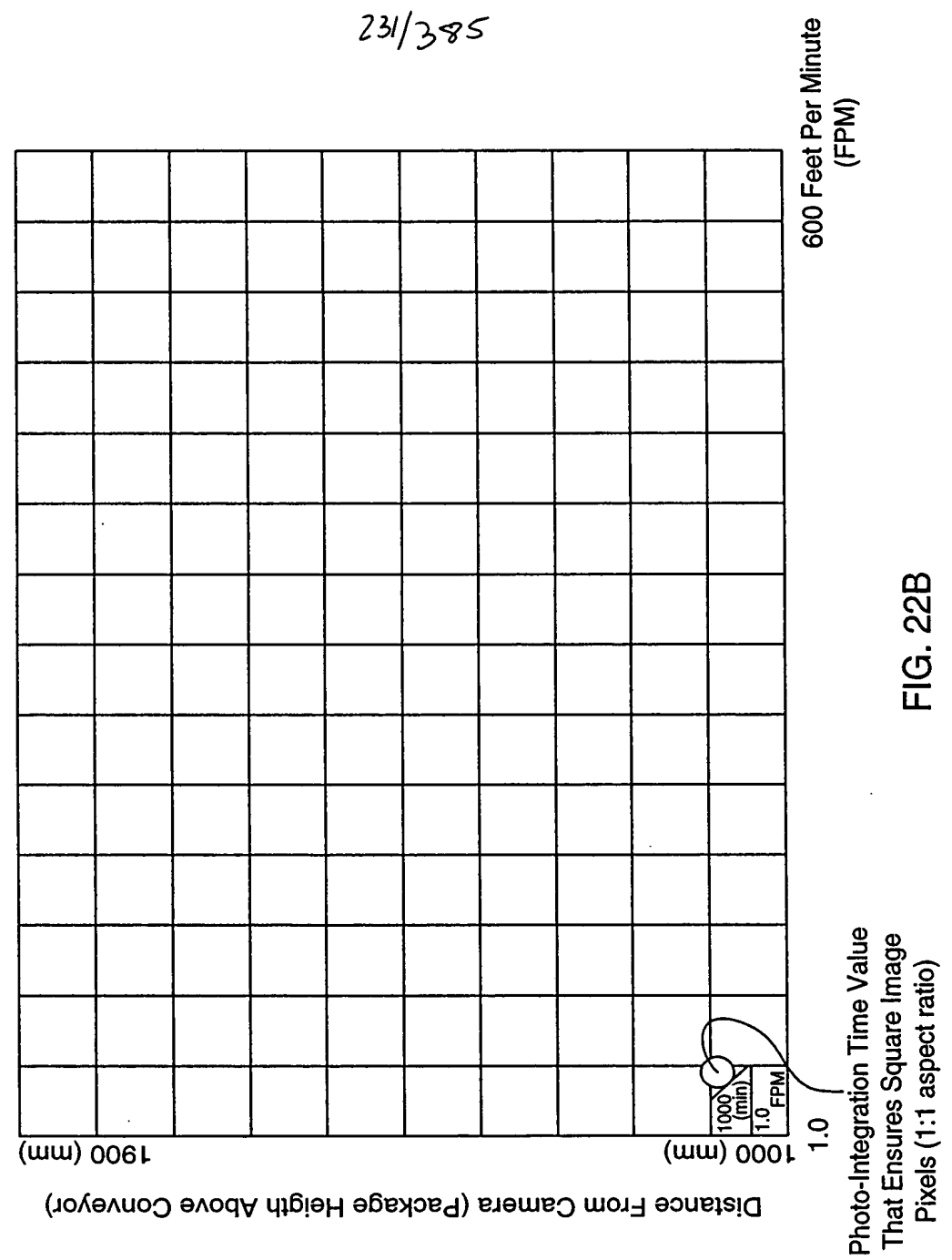


FIG. 22B

Geometrical Modelling Of Arbitrary 3-D Object Surface

At Image Processing Computer

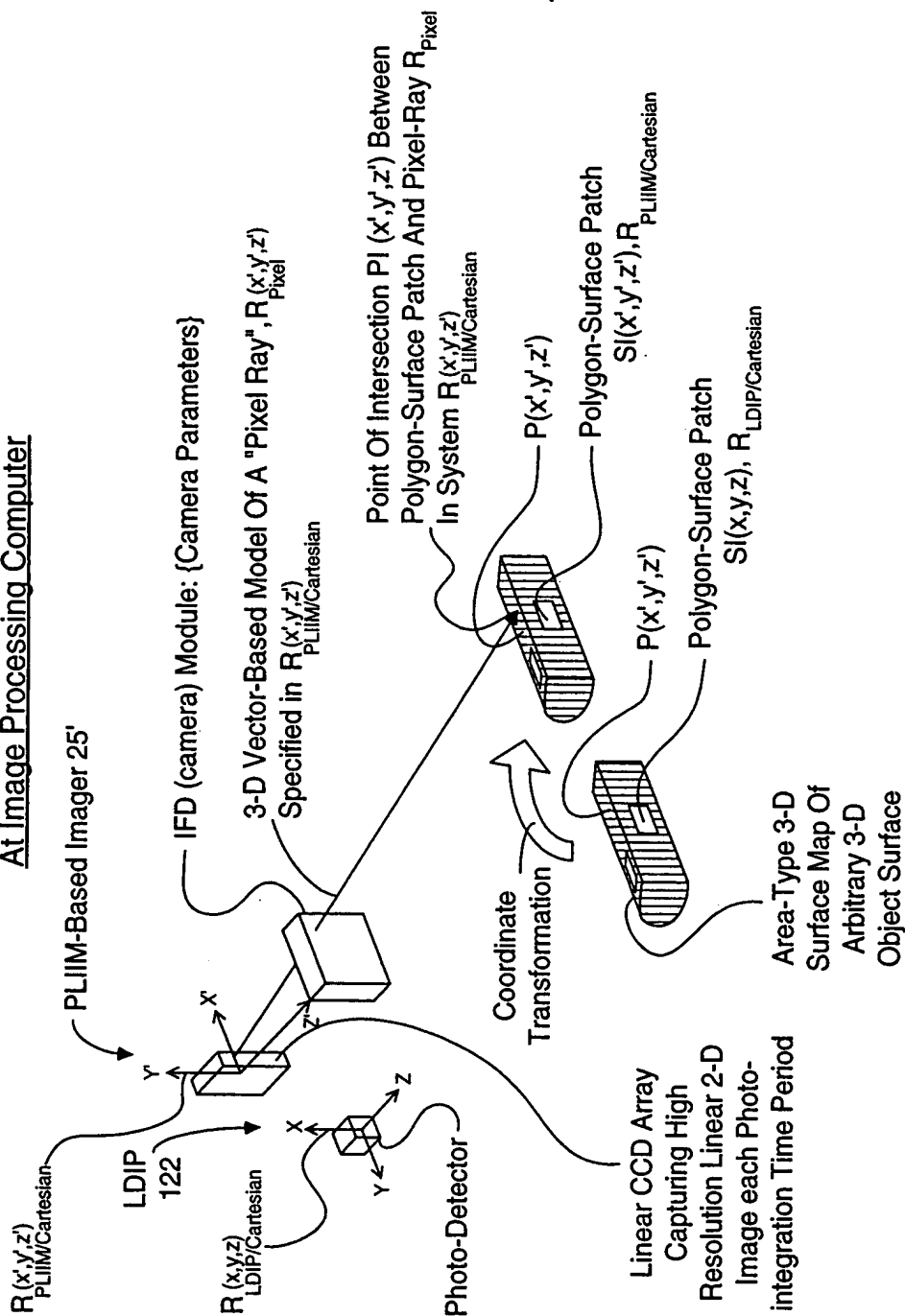


FIG. 23B

234/385

METHOD OF AND APPARATUS FOR PERFORMING AUTOMATIC
RECOGNITION OF GRAPHICAL INTELLIGENCE CONTAINED IN 2-D
IMAGES CAPTURED FROM ARBITRARY 3-D OBJECT SURFACES

STEP 1: At the unitary PLIIM-based object imaging and profiling system, use the laser doppler imaging and profiling (LDIP) subsystem employed therein to (i) consecutively capture a series of linear 3-D surface profile maps on a targeted arbitrary (e.g. non-planar or planar) 3-D object surface bearing forms of graphical intelligence and (ii) measure the velocity of the arbitrary 3-D object surface, wherein the polar coordinates of each point in the captured linear 3-D surface profile map are specified in a local polar coordinate system $R_{LDIP/polar}$, symbolically embedded within the LDIP subsystem.

A

STEP 2: At the unitary PLIIM-based object imaging and profiling system, use coordinate transforms to automatically convert the polar coordinates of each point $p(\alpha, R)$ in the captured linear 3-D surface profile map into x, y, z Cartesian coordinates specified as $p(x, y, z)$ in a local Cartesian coordinate system $R_{LDIP/Cartesian}$, symbolically embedded within the LDIP subsystem.

B

STEP 3: At the unitary PLIIM-based object imaging and profiling system, use the PLIIM-based imager employed therein to consecutively capture high-resolution linear 2-D images of the arbitrary 3-D object surface bearing forms of graphical intelligence (e.g. symbol character strings), wherein (i) the x', y' coordinates of each pixel in each said captured high-resolution linear 2-D image is specified in local Cartesian coordinate system $R_{PLIIM/Cartesian}$ symbolically embedded within the PLIIM-based imager, and (ii) the intensity value of the pixel $I(x', y')$ is associated with the x', y' Cartesian coordinates of the image detection element in the linear image detection array at which the pixel is detected, and (iii) wherein also the planar laser illumination beam (PLIB) of the PLIIM-based imager is spaced from the amplitude modulated (AM) laser scanning beam of the LDIP subsystem is about D centimeters.

C

A

FIG. 23C1

TOP SECRET

235/385
A

STEP 4: At the unitary PLIIM-based object imaging and profiling system, capture and buffer the camera (IFD) parameters used to form and detect each linear high-resolution 2-D image captured during the corresponding photo-integration time period ΔT_K , by the PLIIM-based imager.

STEP 5: At the end of each photo-integration time period ΔT_K , use the unitary PLIIM-based object imaging and profiling system to transmit the following information elements to the Image Processing Computer for data storage and subsequent information processing:

(1) the converted coordinates x, y, z , of each point in the linear 3-D surface profile map of the arbitrary 3-D object surface captured during photo-integration time period ΔT_K ;

(2) the measured velocity(ies) of the arbitrary 3-D object surface during photo-integration time period ΔT_K ;

(3) the x', y' coordinates and intensity value $I(x', y')$ of each pixel in each high-resolution linear 2-D image captured during photo-integration time period ΔT_K and specified in the local Cartesian coordinate system $R_{PLIIM/Cartesian}$; and

(4) the captured camera (IFD) parameters used to form and detect each linear high-resolution 2-D image captured during the photo-integration time period ΔT_K

STEP 6: At the Image Processing Computer, receive the data elements transmitted from the PLIIM-based profiling and imaging system during Step 5, buffer data elements (1) and (2) in a first FIFO buffer memory structure, and data elements (3) and (4) in a second FIFO buffer memory structure.

B

FIG. 23C2

236/ 385

(B)

STEP 7: At the Image Processing Computer, use the x, y, z coordinates associated with a consecutively captured series of linear 3-D surface profile maps (i.e. stored in first FIFO memory storage structure) in order to construct a 3-D polygon-mesh surface representation of said arbitrary 3-D object surface, represented by $S_{LDIP}(x, y, z)$ and having (i) vertices specified by x, y, z in local coordinate reference system $R_{PLIIM/Carthesian}$, and (ii) planar polygon surface patches $s_i(x, y, z)$ and being defined by a set of said vertices.

G

STEP 8: At the Image Processing Computer, convert the x', y', z' coordinates of each vertex in the 3-D polygon-mesh surface representation into the local Cartesian coordinate reference system $R_{PLIIM/Carthesian}$ symbolically embedded within the PLIIM-based imager.

H

STEP 9: At the Image Processing Computer, specify the x', y', z' coordinates of each i -th planar polygon surface patch $s(x, y, z)$ represented in the local Cartesian coordinate reference system $R_{PLIIM/Carthesian}$, so as to produce a set of corresponding polygon surface patch $\{s_i(x', y', z')\}$ represented in system $R_{PLIIM/Carthesian}$

I

STEP 10: At the Image Processing Computer, for a selected linear high-resolution 2-D image captured at photo-integration time period ΔT_K , and spatially corresponding to one of the linear 3-D surface profile maps employed at Step 7, use the camera (IFD) parameters used and recorded (i.e. captured) during the corresponding photo-integration time period in order to construct a 3-D vector-based "pixel ray" model specifying the optical formation of each pixel in the linear 2-D image, wherein a pixel ray reflected off a point on the arbitrary 3-D object surface is focused through the camera's image formation optics (i.e. configured by the camera parameters) and is detected at the pixel's detection element in the linear image detection array of the IFD (camera) subsystem.

J

(C)

FIG. 23C3

(C)

237/385

STEP 11: At the Image Processing Computer, for each laser beam ray (producing one of the pixels in said selected linear 2-D image), (i) determine which polygon surface patch $s_i(x, y, z)$ the pixel ray intersects, (ii) compute the x, y, z coordinates of the point of intersection (POI) between the pixel ray and the polygon surface patch represented in Cartesian coordinate reference system $R_{PLIIM/Cartesian}$, and (iii) designate the computed set of points of intersection as $\{p_i(x, y, z)\}$.

K

STEP 12: At the Image Processing Computer, for each laser beam ray passing through a determined polygon surface patch $s(x', y', z')$ at a computed point of intersection $p_i(x, y, z)$, assign the intensity value $I(x', y')$ of the pixel ray to the x', y', z' coordinates of the point of intersection, thereby producing a linear high-resolution 3-D image comprising a 2-D array of pixels, each said pixel pixel having as its attributes (i) an Intensity value $I(x', y', z')$ and (ii) coordinates x', y', z' specified in the local Cartesian coordinate reference system $R_{PLIIM/Cartesian}$.

L

STEP 13: Put the computed linear high-resolution 3-D image in a third FIFO memory storage structure in the image processing computer.

M

STEP 14: Repeat Steps 1-6 to update the first and second FIFO data queues maintained in the image processing computer, and Steps 7-13 to update the consecutively computed linear high-resolution 3-D image stored in the third FIFO memory storage structure.

N

STEP 15: Assemble in an image buffer in the image processing computer, a set of consecutively computed linear high-resolution 3-D images retrieved from the third FIFO data storage device so as to construct an "area-type" high-resolution 3-D image of said arbitrary 3-D object surface.

O

(D)

FIG. 23C4

238/385
(D)

STEP 16: At the Image Processing Computer, map the intensity value $I(x', y', z')$ of each pixel in the computed area-type 3-D image onto the x', y', z' coordinates of the points on a uniformly-spaced apart "grid" positioned perpendicular to the optical axis of the camera subsystem (i.e. to model the 2-D planar substrate on which the forms of graphical intelligence was originally rendered), wherein said mapping process involves using an intensity weighing function based on the x', y', z' coordinate values of each pixel in the area-type high-resolution 3-D image, thereby producing an area-type high-resolution 2-D image of the 2-D planar substrate surface bearing said forms of graphical intelligence (e.g. symbol character strings).

P

STEP 17: At the Image Processing Computer, use said OCR algorithm to perform automated recognition of graphical intelligence contained in said area-type high-resolution 2-D image of said 2-D planar substrate surface so as to recognize said graphical intelligence and generate symbolic knowledge structures representative thereof.

Q

STEP 18: Repeat Steps 1-17 as often as required to recognize changes in graphical intelligence on the arbitrary moving 3-D object surface.

R

FIG. 23C5

TTTTTSSSSSS

239/385

Photo-Integration Time Look-up Table

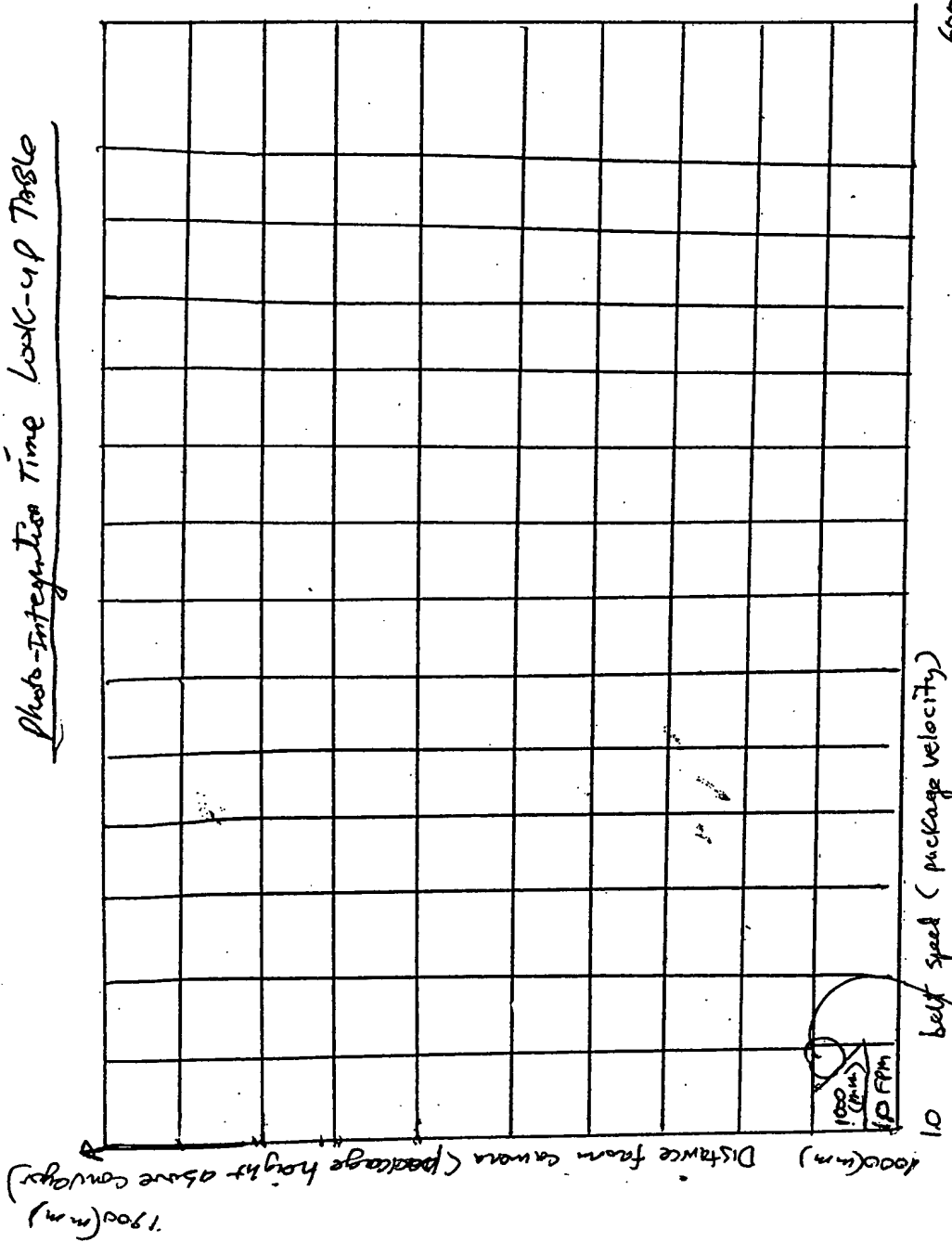


FIG. 22B

Photo-integration time value that ensures square image pixels (1:1 aspect ratio)

FIG. 24

LOW RESOLUTION 2D CCD CAMERA (61)
HIGH RESOLUTION 2D CCD CAMERA (55")

LDIP (122)

25"

140

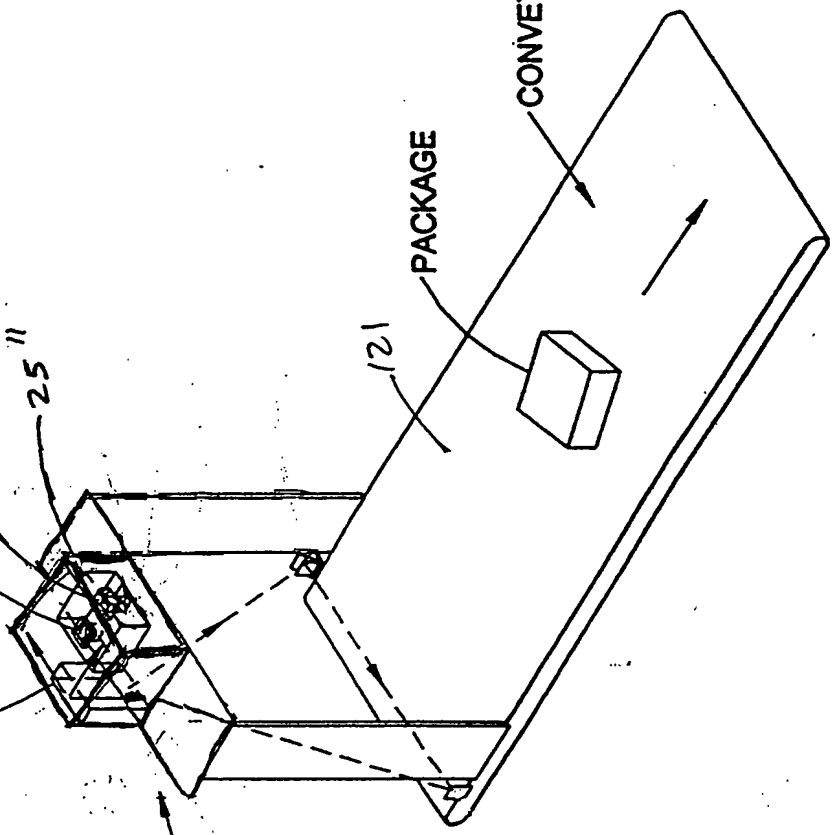
240/385

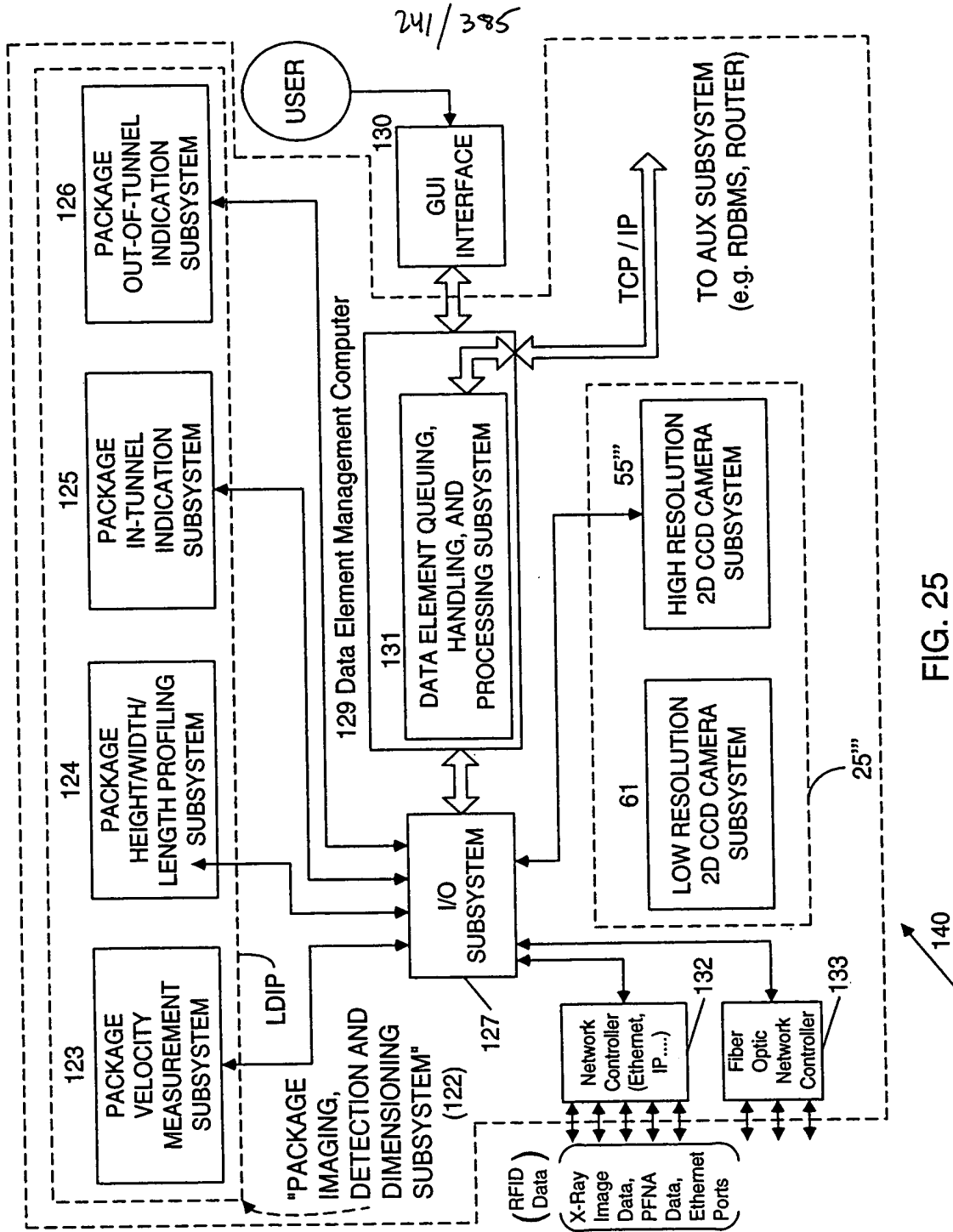
PACKAGE

CONVEYOR BELT

121

FIG 24





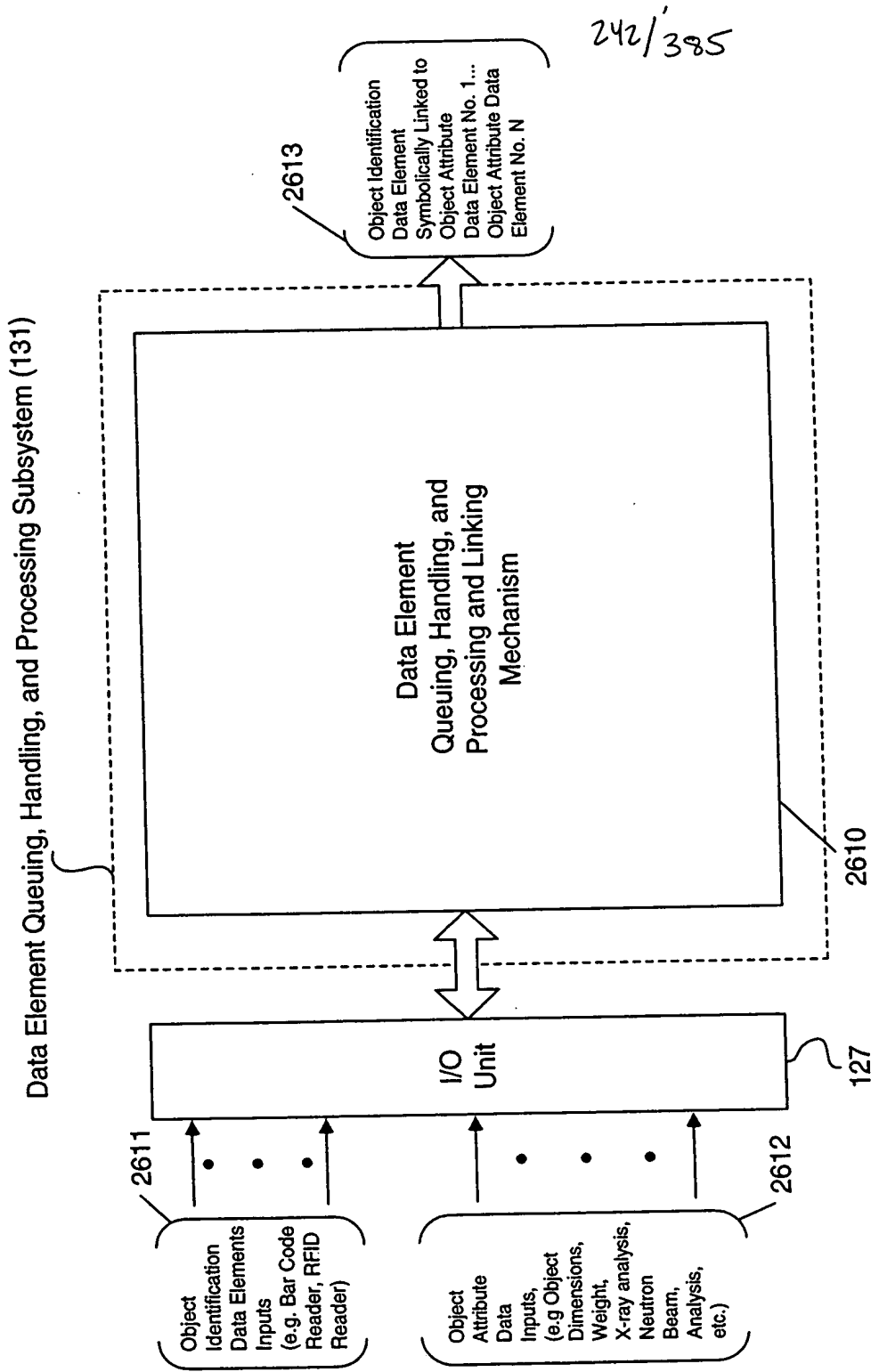
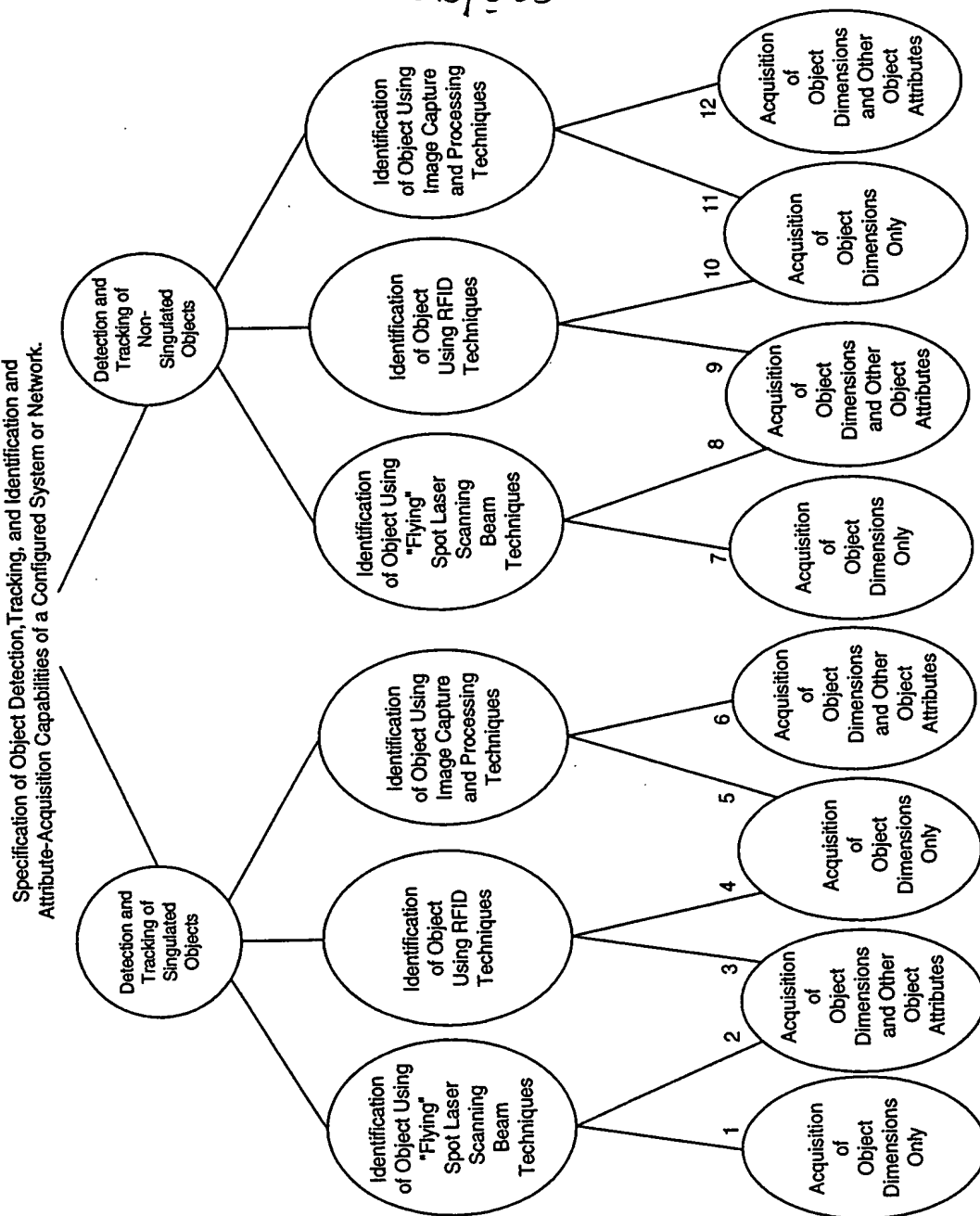


FIG. 25A

743/385



**Primary Network:
and/ or System
Functions:**

A. Specification of Object Detection and Tracking Capability of System

B. Specification of Object Identification Capability of System

C. Specification of Object Attribute Acquisition Capability of System

FIG. 25B

24/385

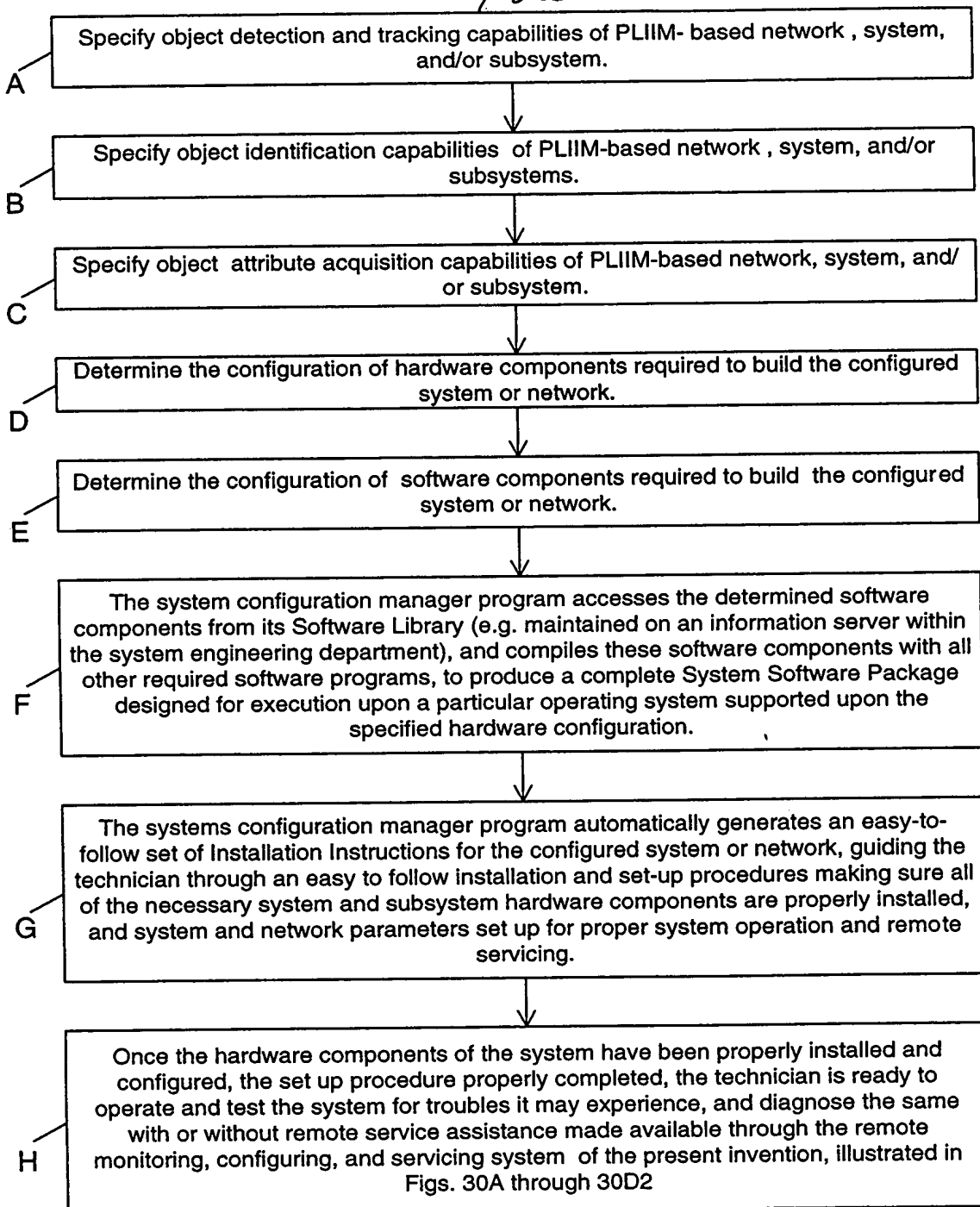


FIG. 25C

245/385

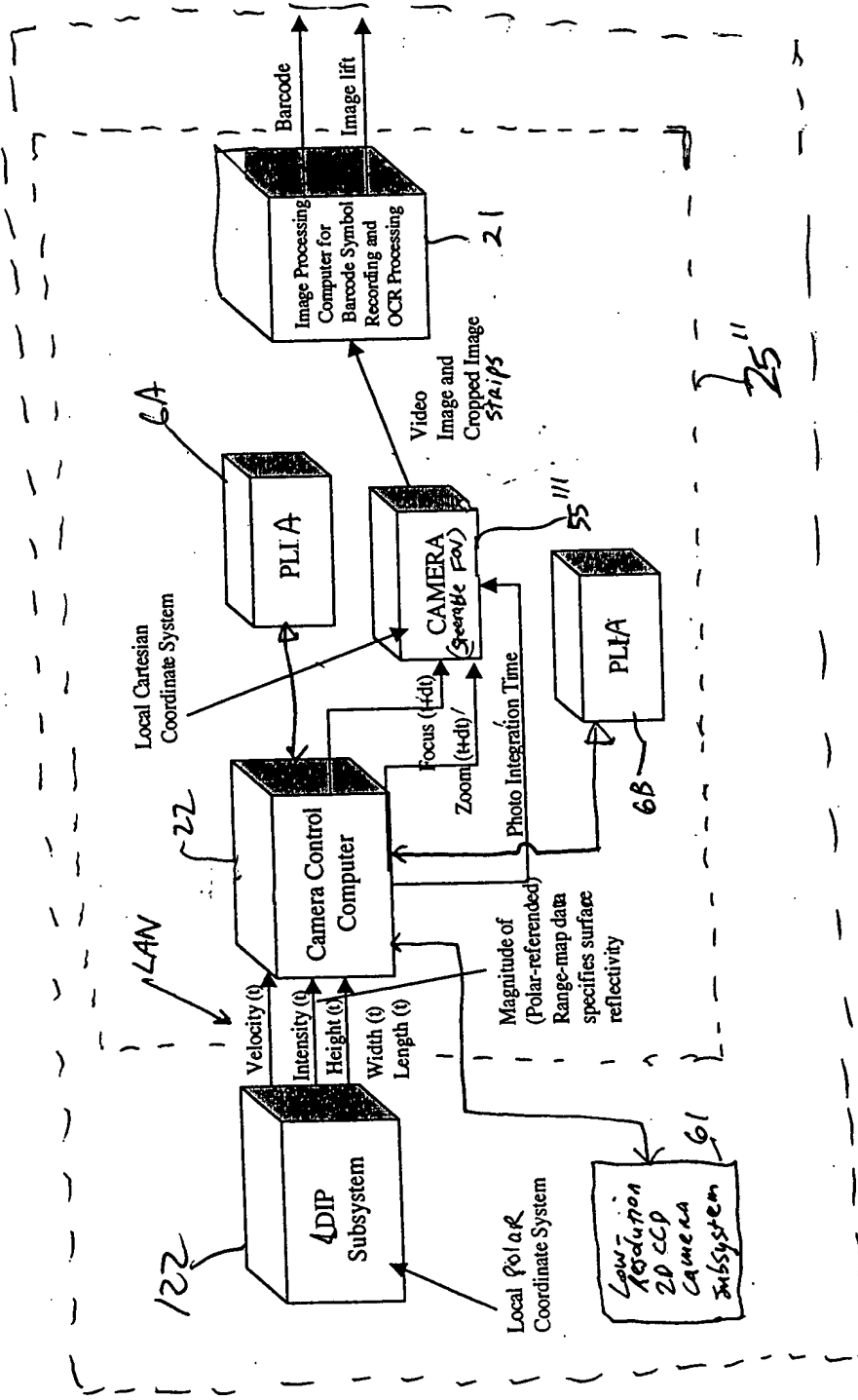


FIG. 26

140

0990585-112101
TOTAL 580660

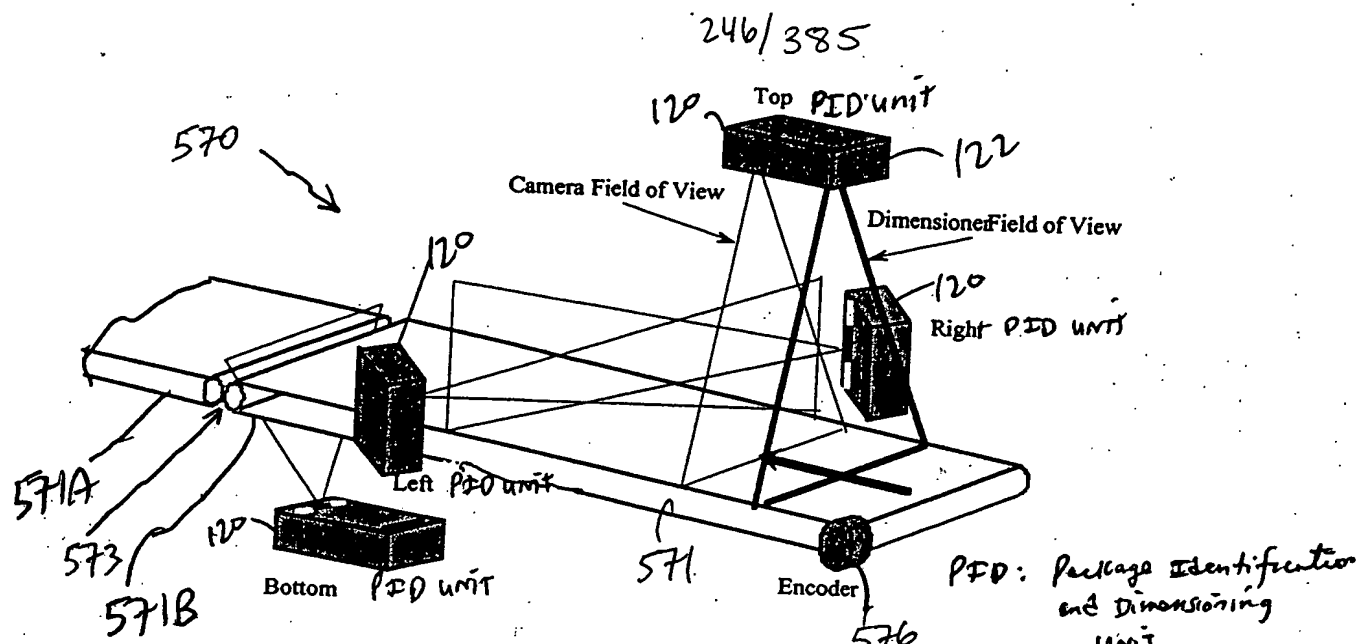


FIG 27

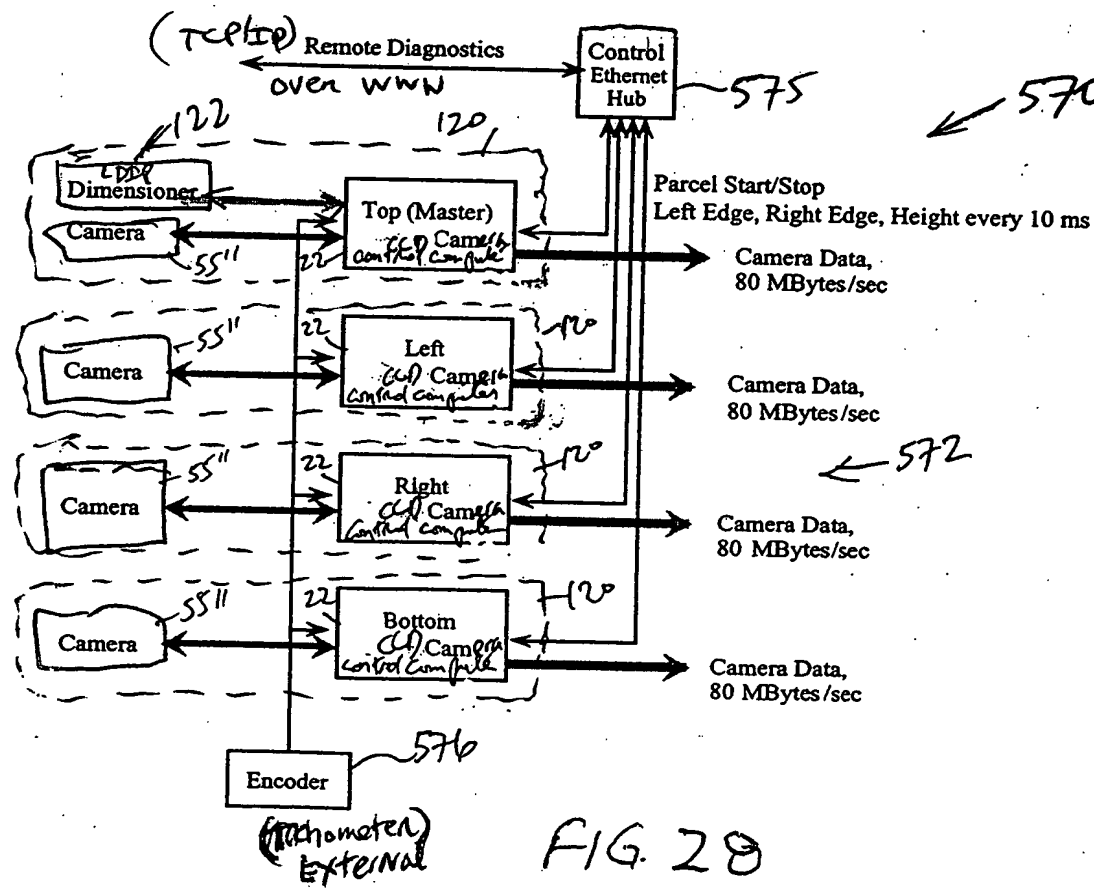


FIG 28

FOI b6 b7C

247/3851

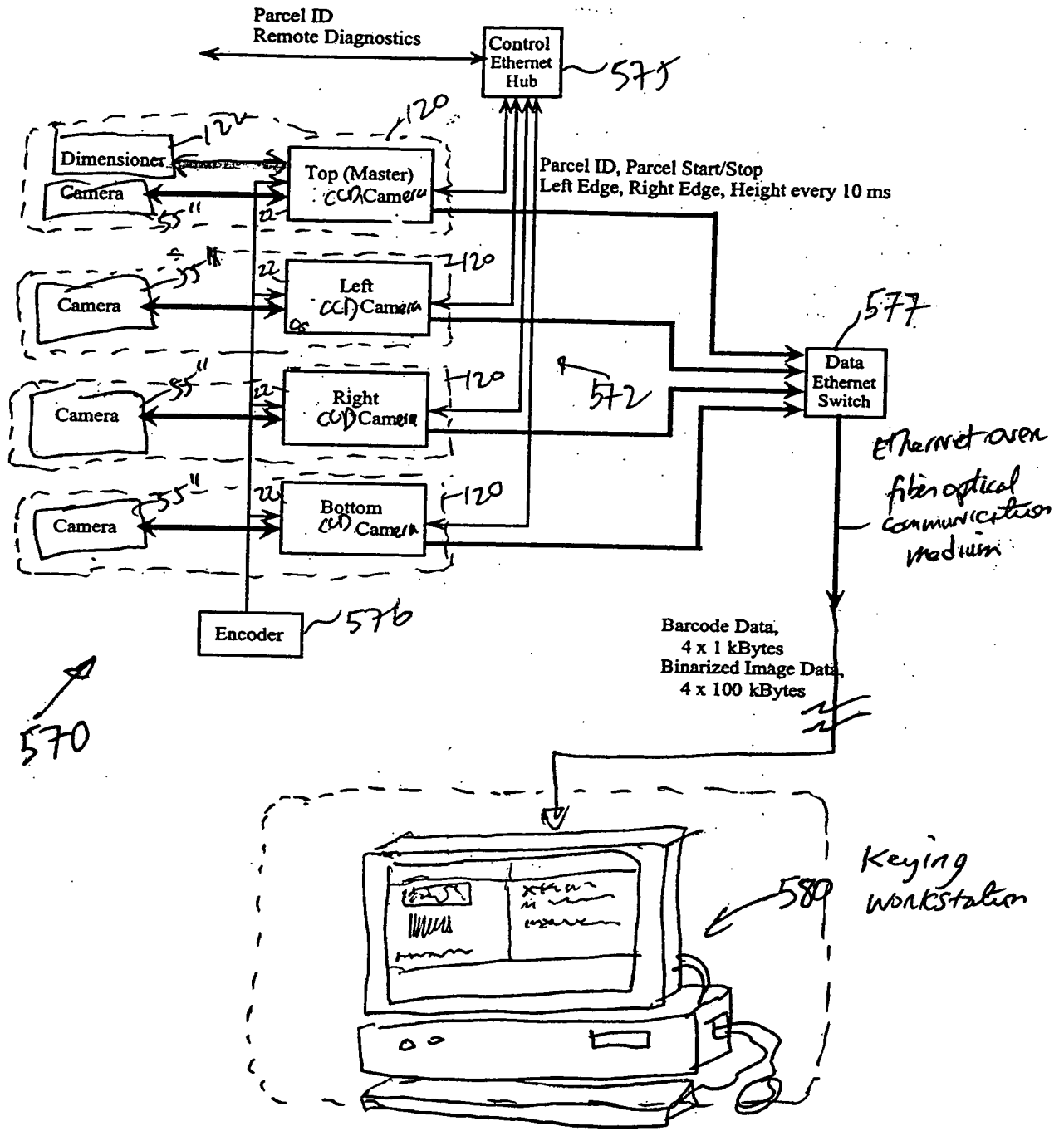
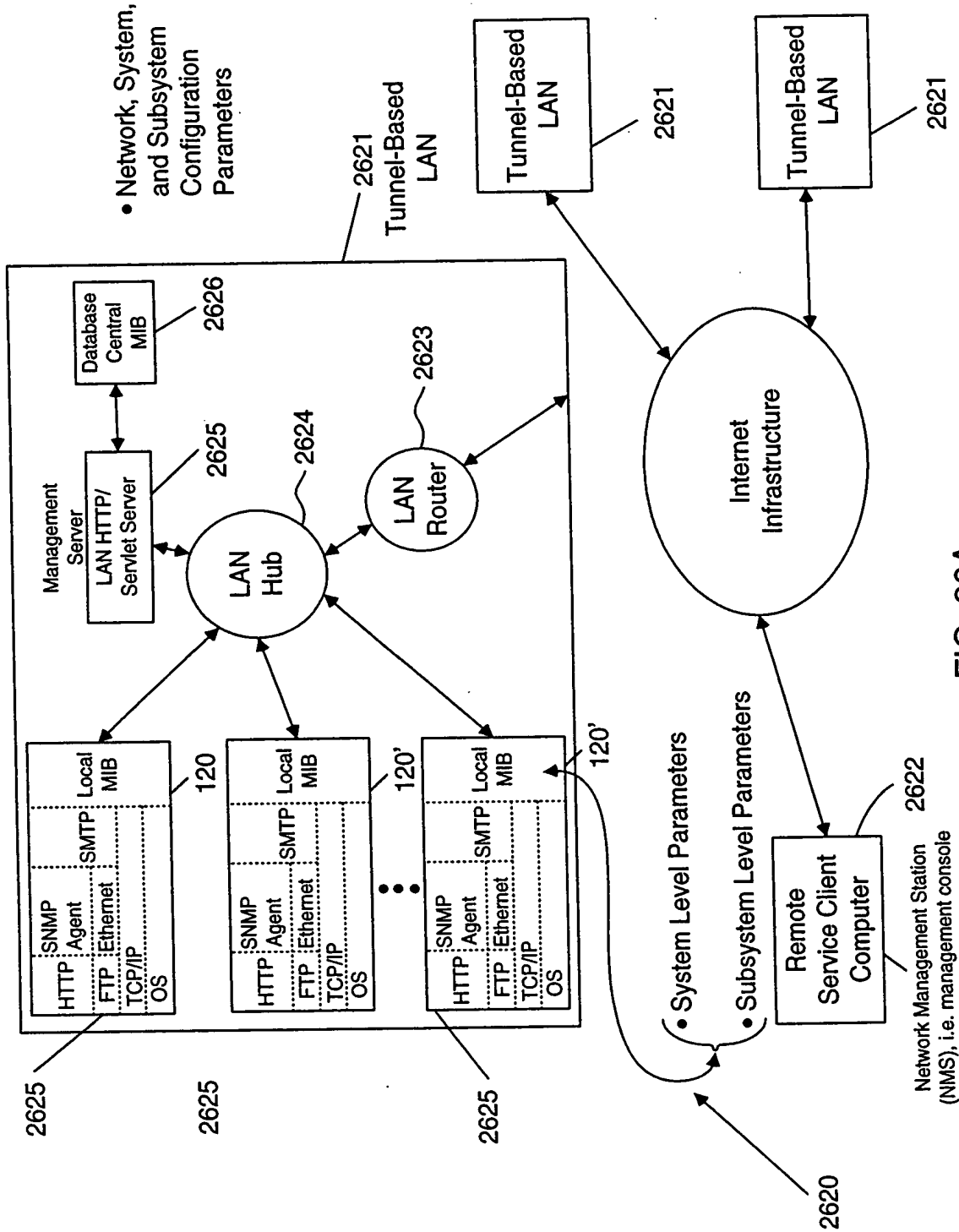


FIG. 29



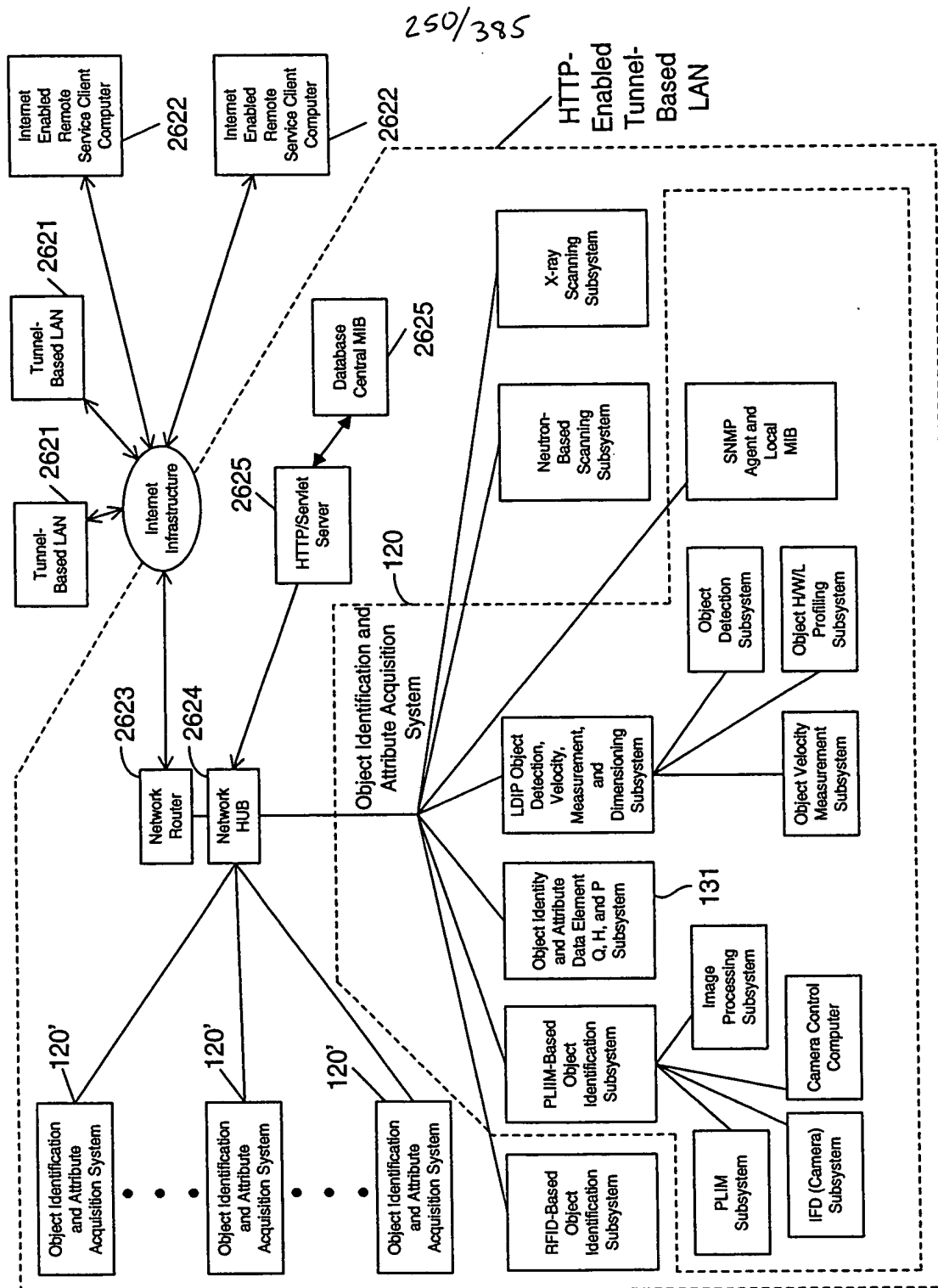


FIG. 30B

Network Configuration Parameters:

[Router IP address; no. of nodes (i.e. systems) in LAN; passwords, LAN location; name of customer facility; technical contact; phone no.; domain name; object identity codes; object attribute acquisition codes;....]

System Configuration Parameters:

[System IP Address; passwords; object identity codes; object attribute acquisition codes;....]

Monitorable and/or Configurable Parameters for Subsystems Within Each System:

- | | |
|----------------------------------------------------------------------------------------------------------------------------------------------------------------------------------------|-------------------------------------------------------------------------------------------------------------------------------------------------------------------------------------------------------------------------------------------------------------------------------------------------------------------------------------------------------------------------------------------------------------------------------------------------------------------------------------------------------------------------------------------------------------------------------------------------------------------------------------------------------------------------------------------|
| <p>These subsystems generate object identity parameters</p> | <p><input type="checkbox"/> PLIM-based object identification subsystem: [object identity code; object attribute acquisition codes;....]</p> <p><input type="checkbox"/> PLIM Subsystem: [VLD status; power VLD; TIM function; temp.;....]</p> <p><input type="checkbox"/> IFD (Camera) Subsystem: [sensor temp;]</p> <p><input type="checkbox"/> Image Processing Subsystem (Computer): [processor load history; system up time; # of frames (pgs); barcode read rate; current line rate;....]</p> <p><input type="checkbox"/> Camera Contact Subsystem (Computer): [number of frames dropped; number of focused zoom commands; number and kinds of motor control errors;....]</p> |
| <p>This system links object attribute data element parameters (i.e. object identity data element) to corresponding object identity parameters (i.e. object attribute data element)</p> | <p><input type="checkbox"/> RFID-based object identification subsystem: [....]</p> <p><input type="checkbox"/> Object identity and attribute data element queuing, handling and processing subsystem: [....]</p> |
| <p>These subsystems generate object attribute parameters</p> | <p><input type="checkbox"/> LDIP object identification, velocity-measurement, and dimensioning subsystem: [....]</p> <p><input type="checkbox"/> Object velocity measurement subsystem: [polygon RPM; polygon laser output X; channel X drift; channel X noise; trigger error events; instant lock reference drift; temperature]</p> <p><input type="checkbox"/> Object H/W/L profiling subsystem</p> <p><input type="checkbox"/> Object detection subsystem: [non- singulation/ singulation code;....]</p> <p><input type="checkbox"/> X-ray scanning subsystem: [....]</p> <p><input type="checkbox"/> Neutron-beam scanning subsystem: [....]</p> |

FIG. 30C

252/385

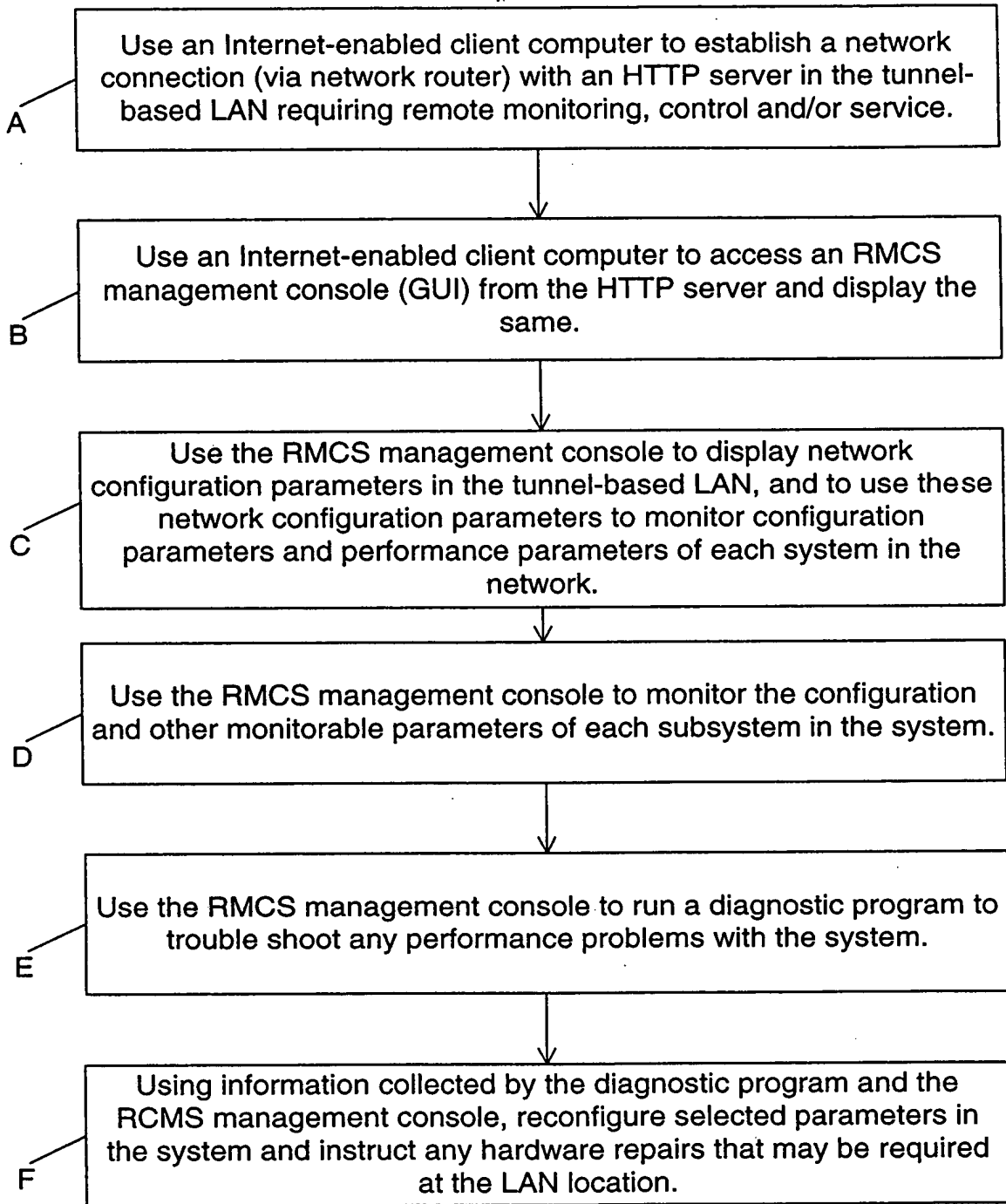


FIG. 30D1

253/385 (A)

G

Use the RMCS management console to rerun diagnostic programs on troubled systems and subsystems in the LAN after parameter reconfiguration and/or hardware repair at the LAN location, so as to test the performance of such systems and subsystems and the overall tunnel based LAN.

H

Use the RMCS management console to monitor parameters of the system and subsystems in the tunnel based LAN, from time to time, to determine whether or not the system and/or network tunnel is required.

I

Use the RMCS management console to record all monitored parameter records and result of diagnostic programs in a customer service database for future reference, and access during subsequent remote service calls over the Internet.

FIG. 30D2

CCD Camera-Based Tunnel System
Employing Package Coordinate Data
Driven Method of Automatic Camera
Zoom and Focus Control

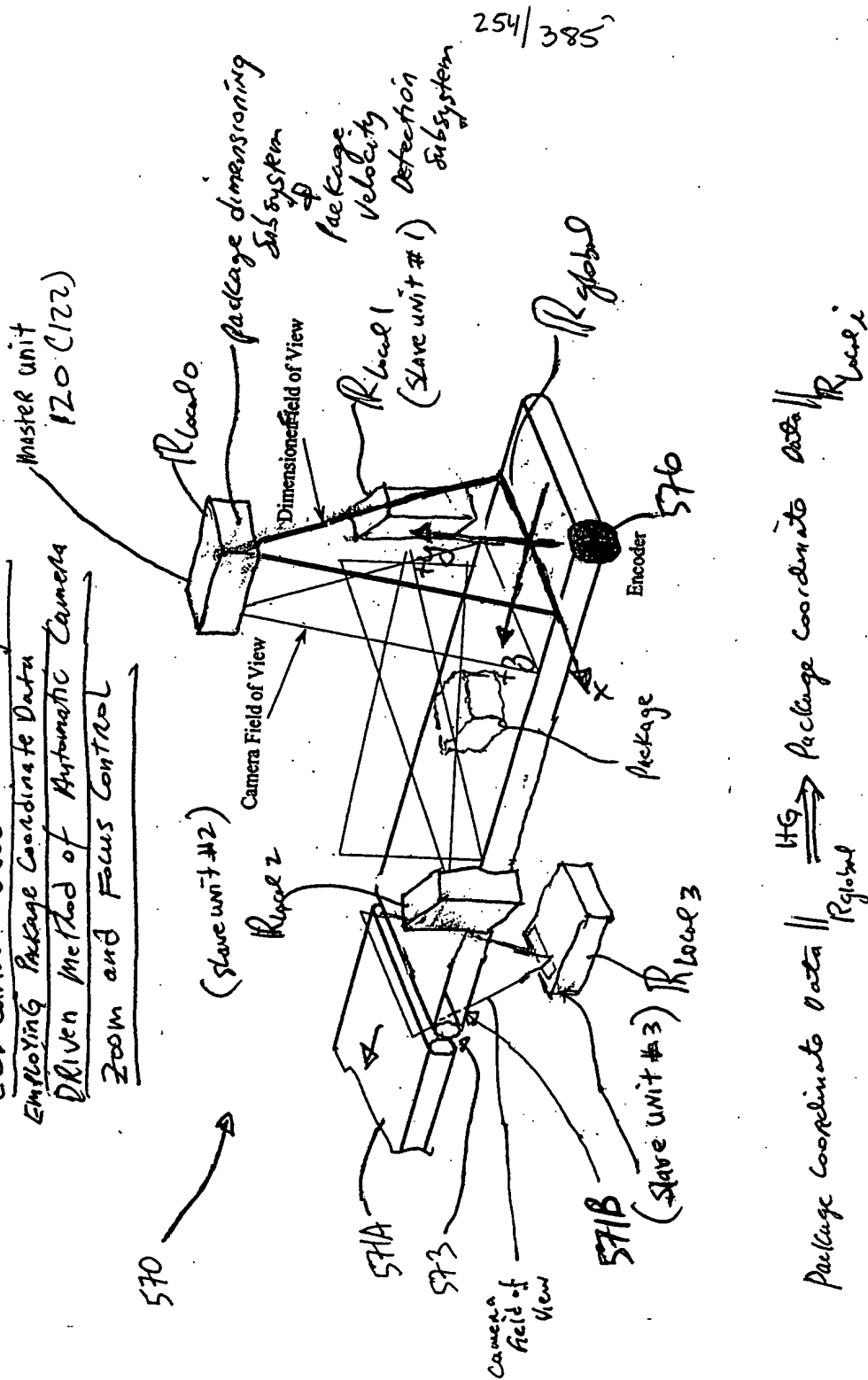


FIG. 31

255/385

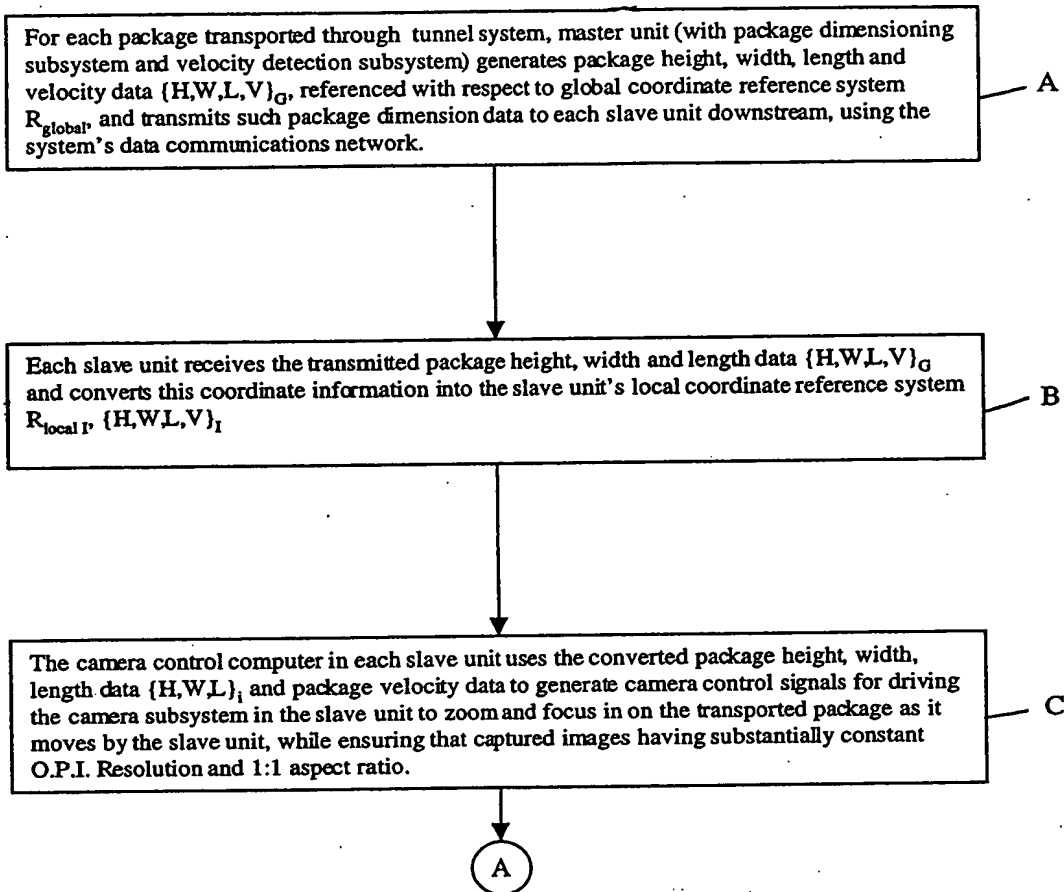


FIG. 32A

00000585-13104
FIG. 32A

256/385
A

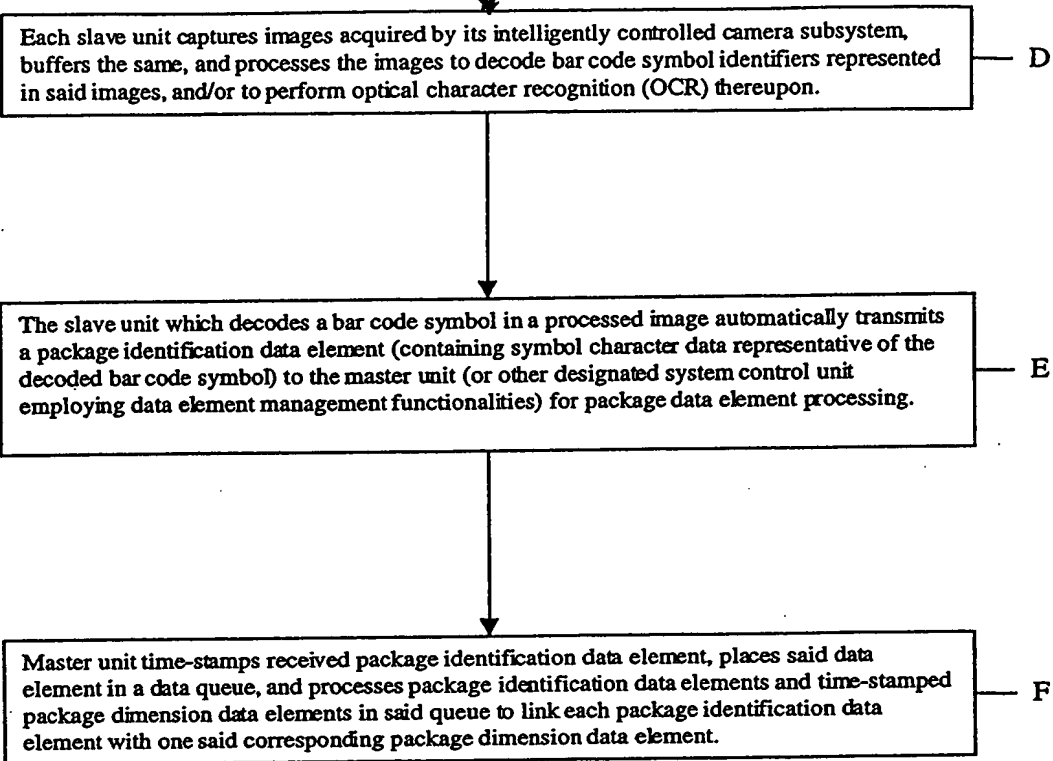


FIG. 32B

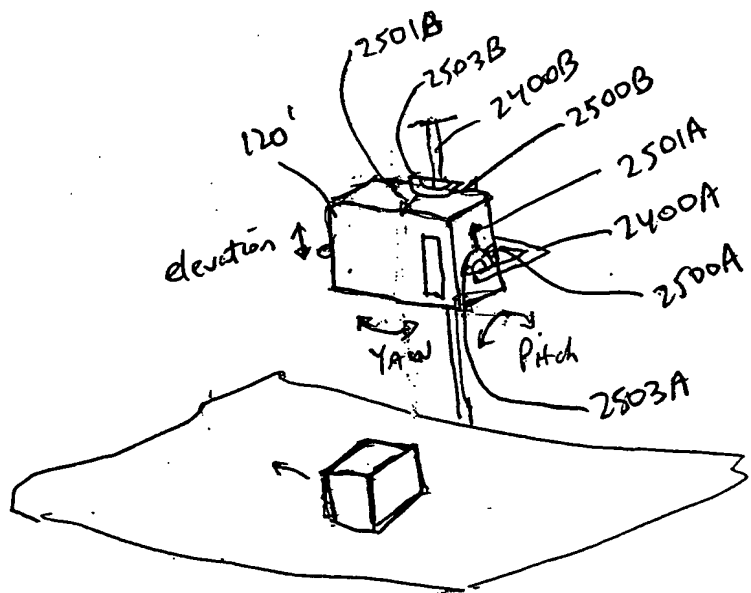
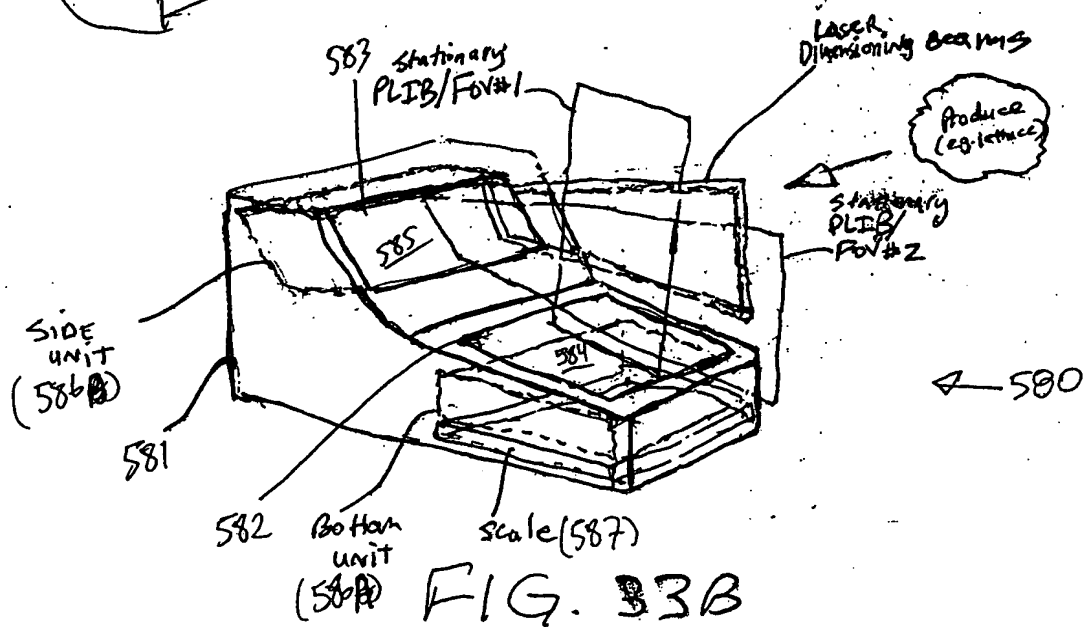
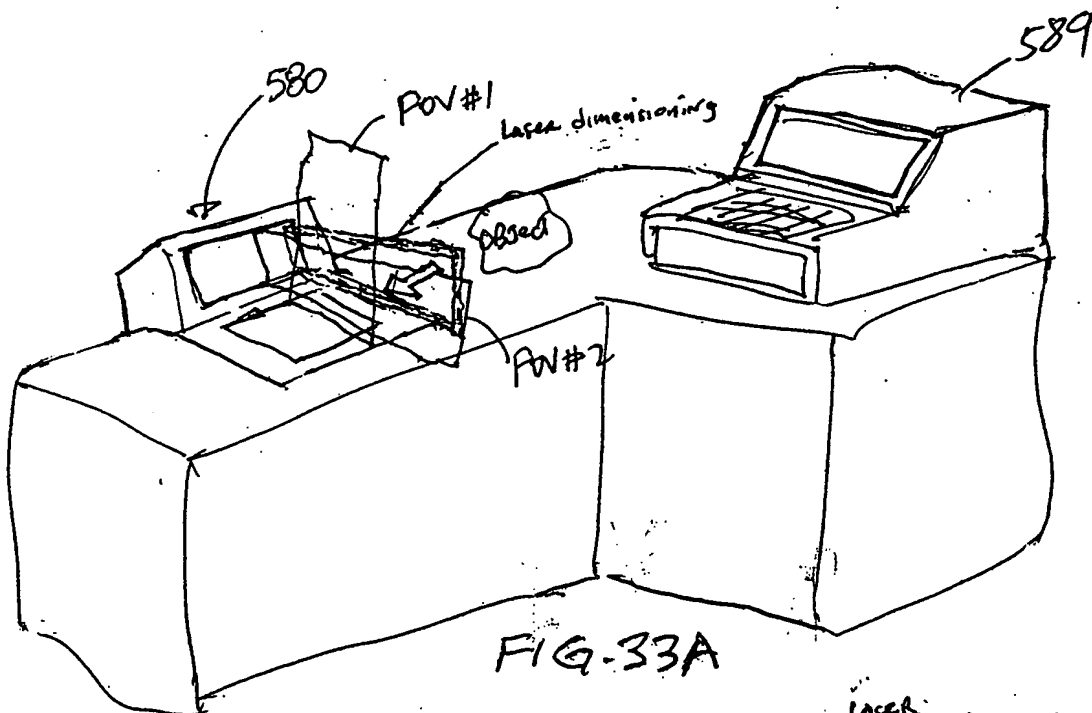


FIG. 31A

257/385



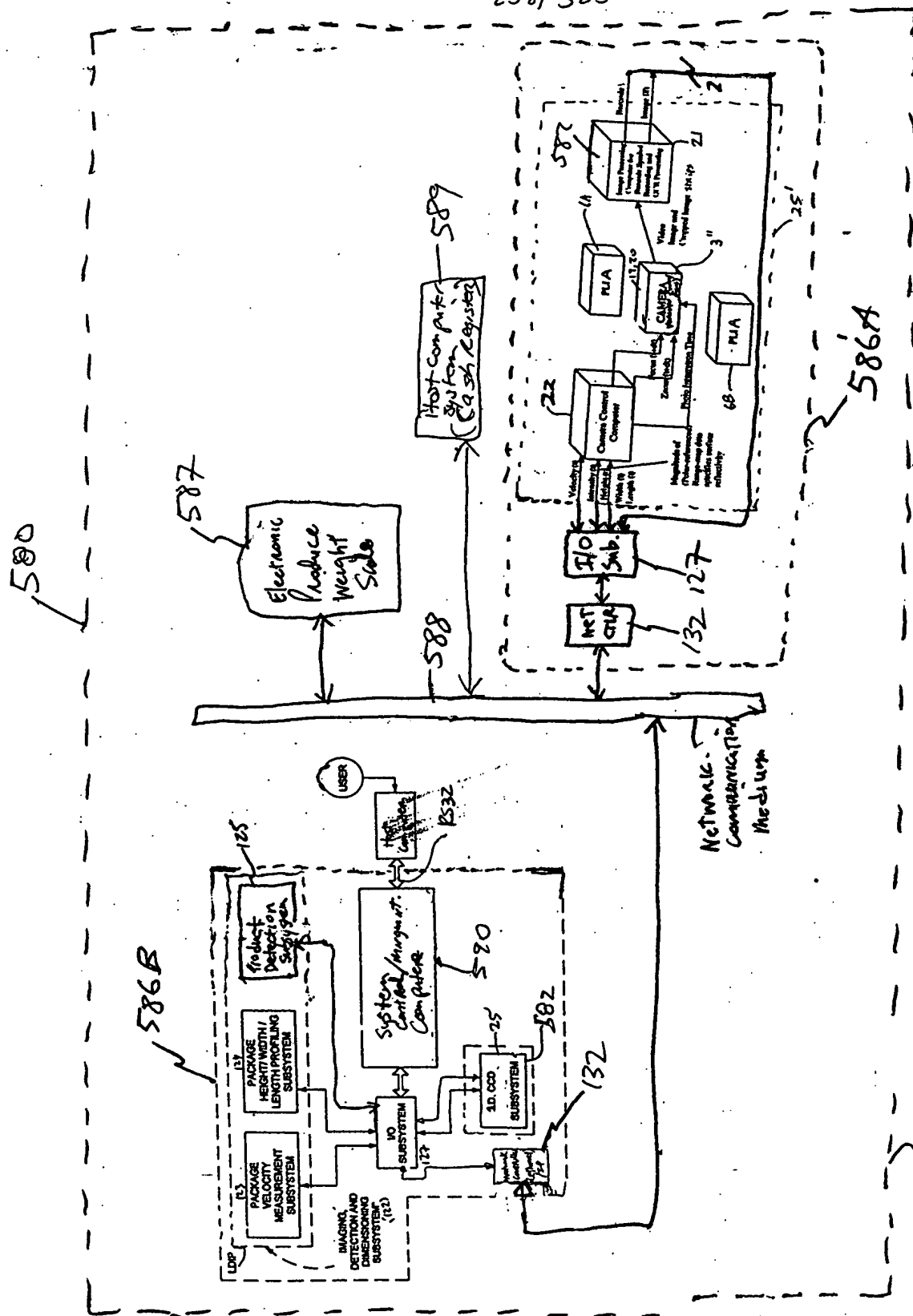


FIG. 33C

259/385

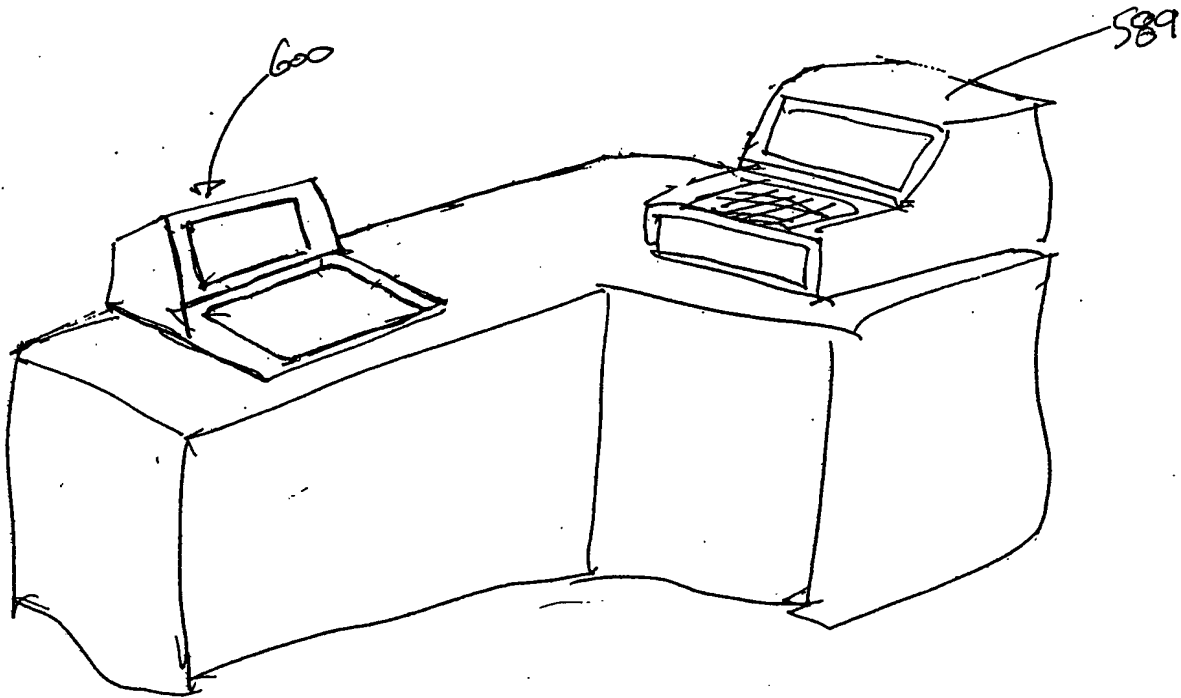


FIG. 34A

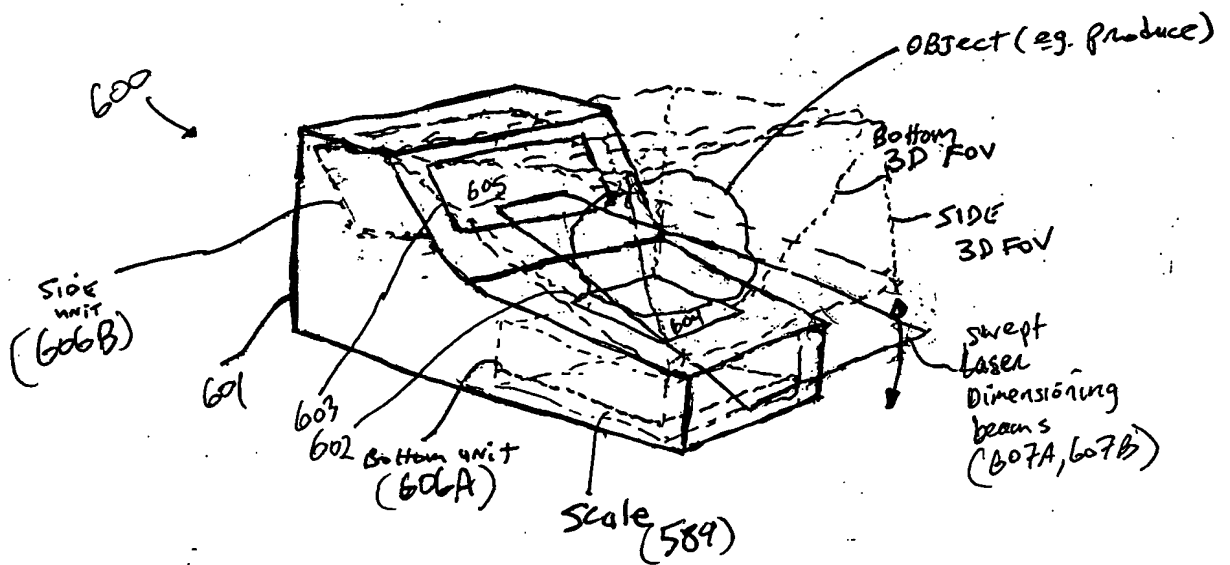


FIG. 34B

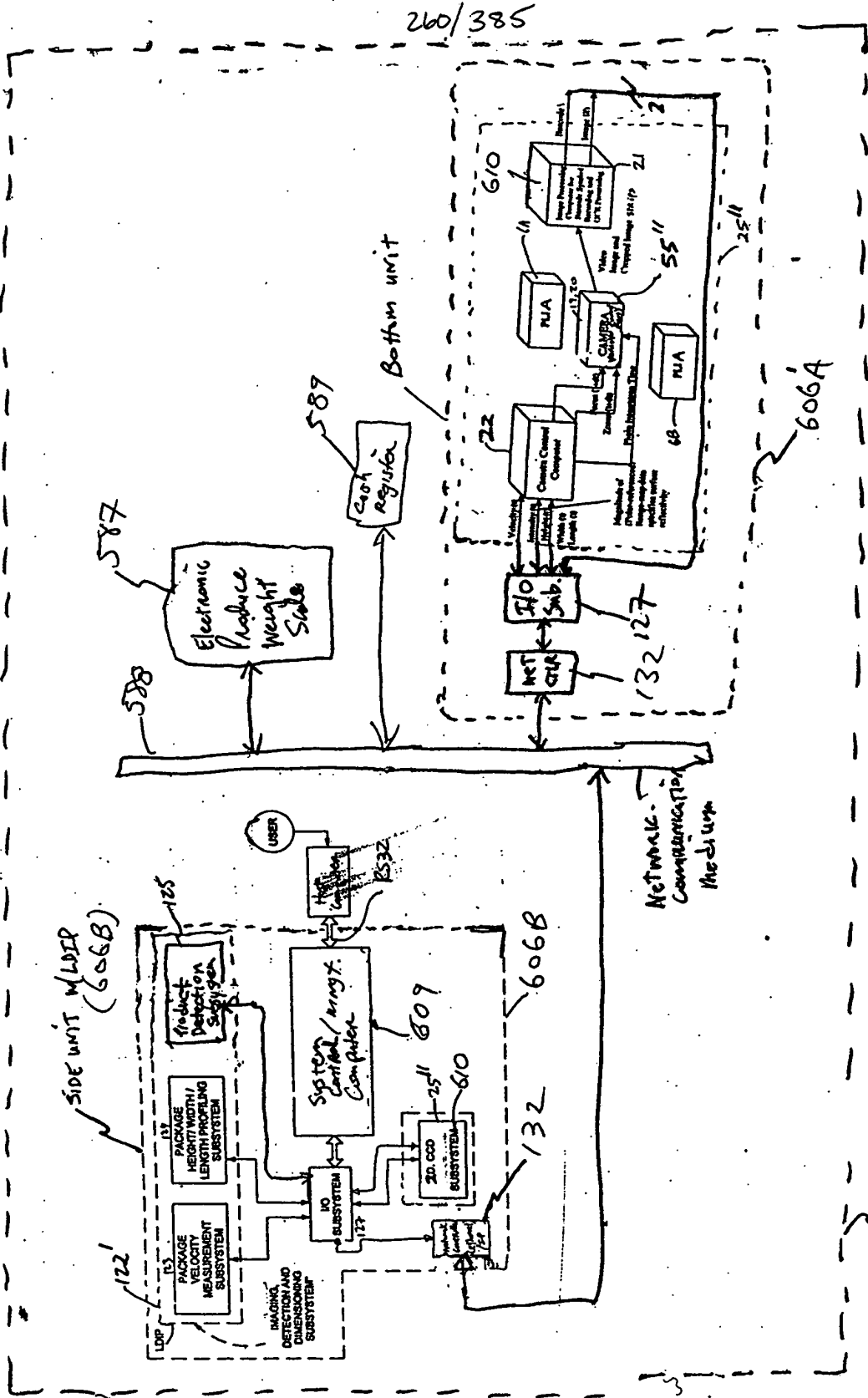
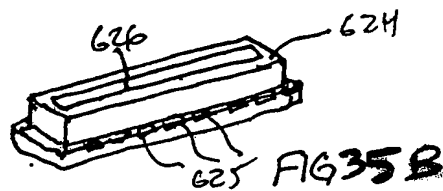
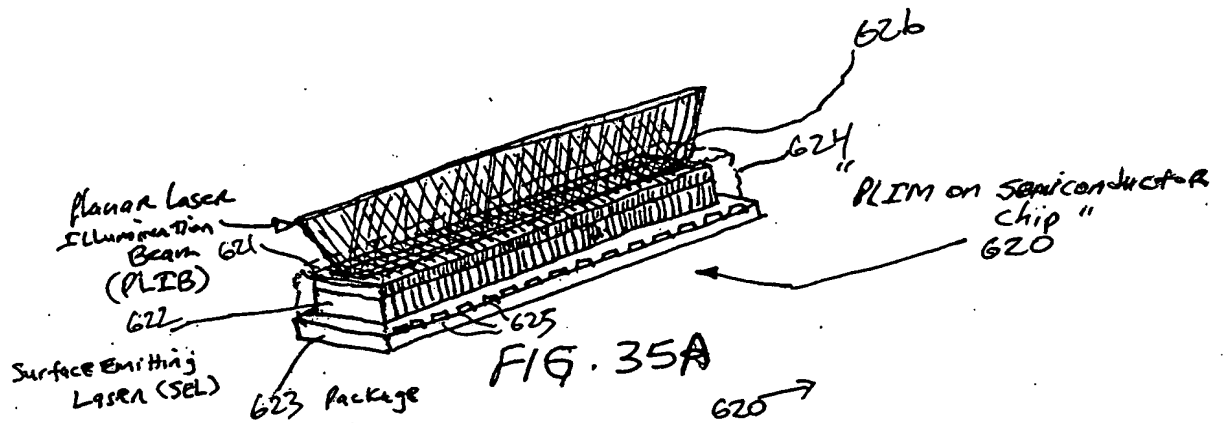
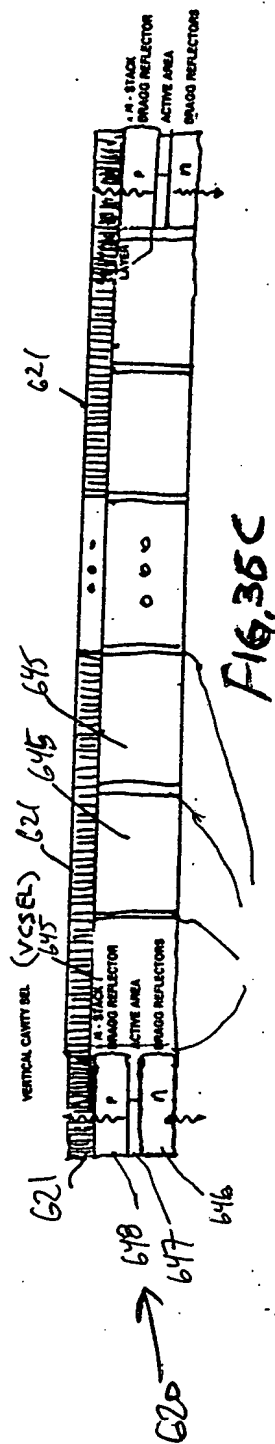
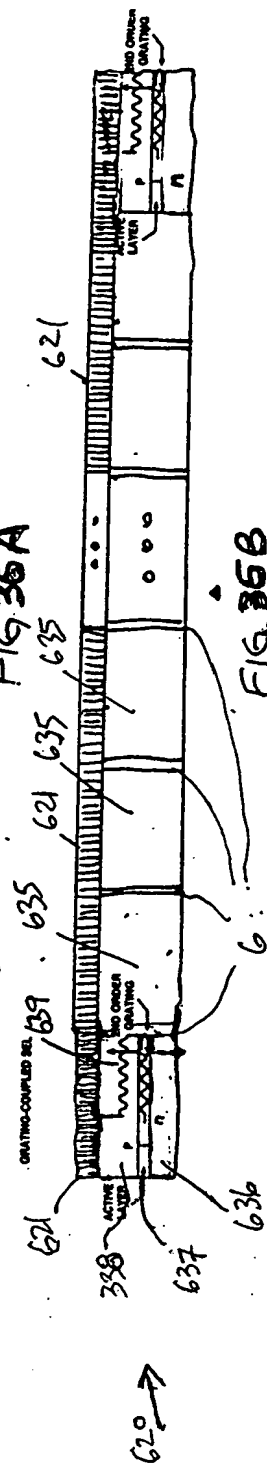
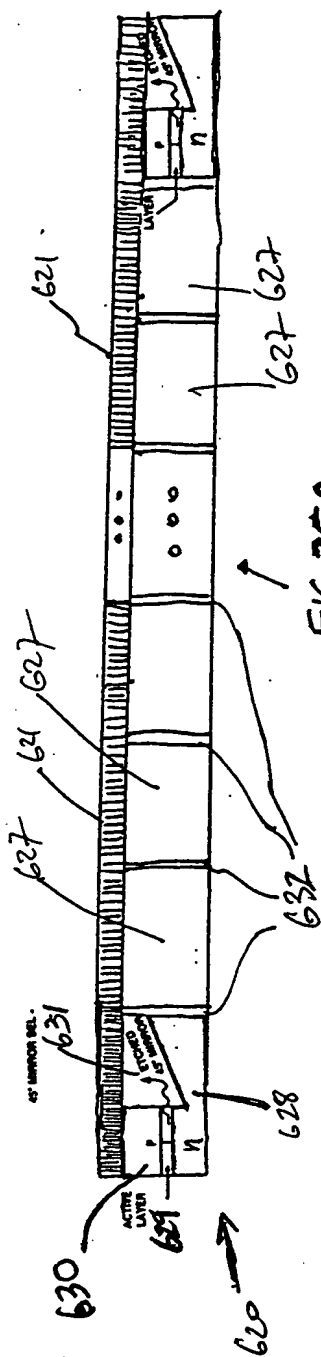


FIG. 34C

261/385



00000000 112101 58506660



2 63/3857

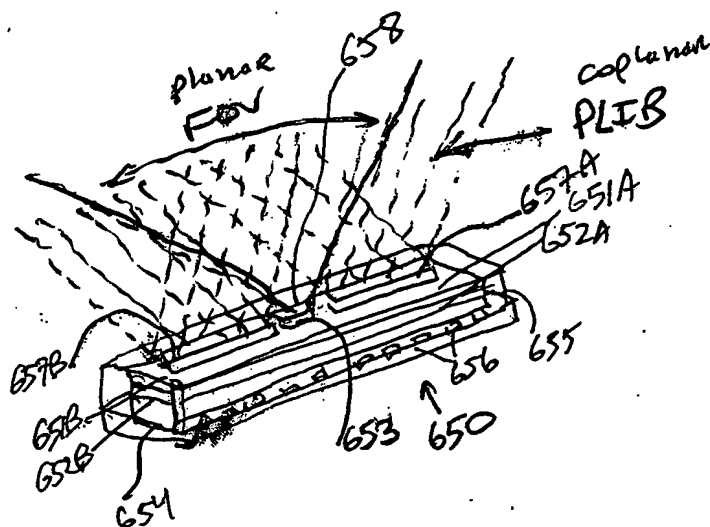


FIG. 37

00000585 4404
FOFF 58506660

09900585 142101

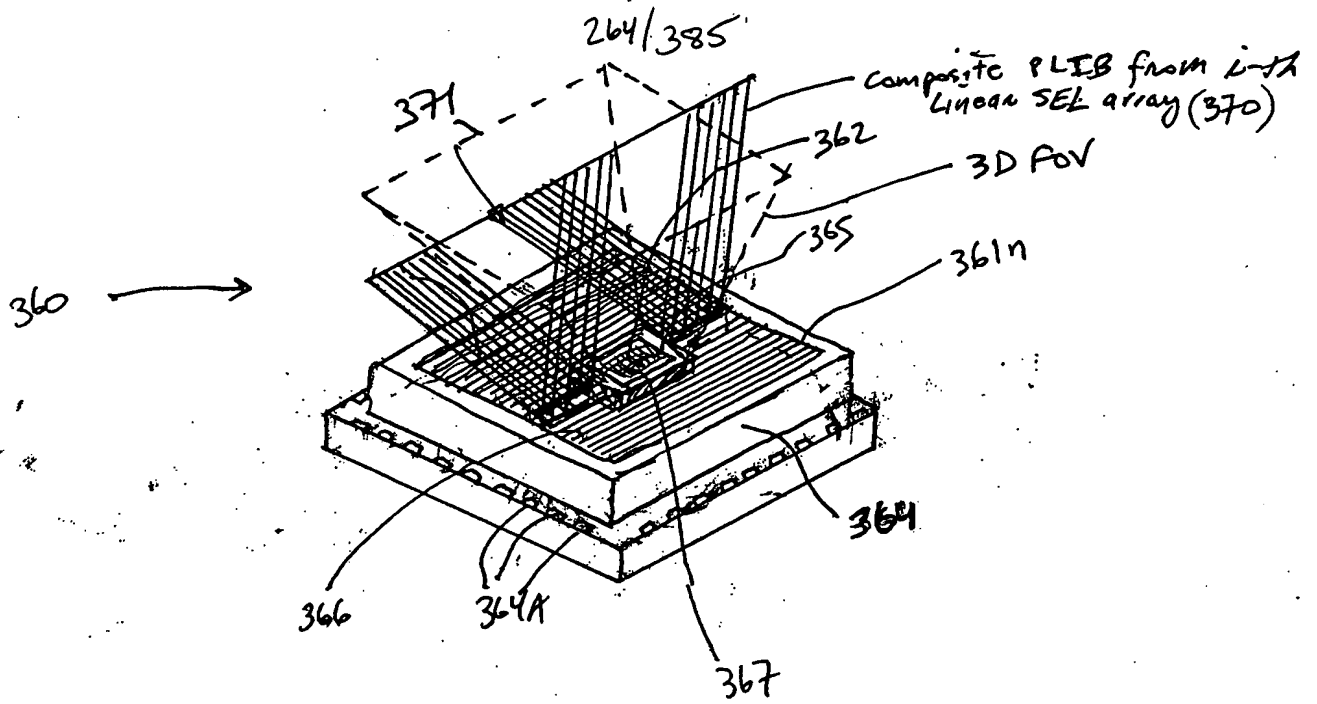


FIG. 38A

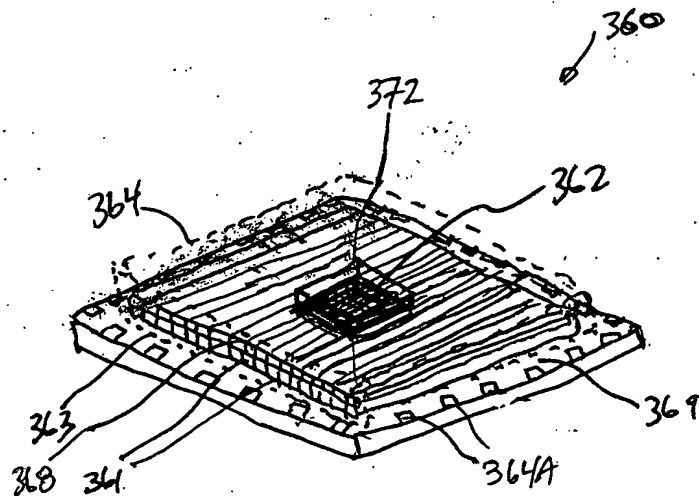
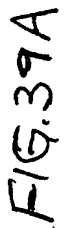


FIG. 38B

Y



00000585 112101
FOI b7E b7C b7D

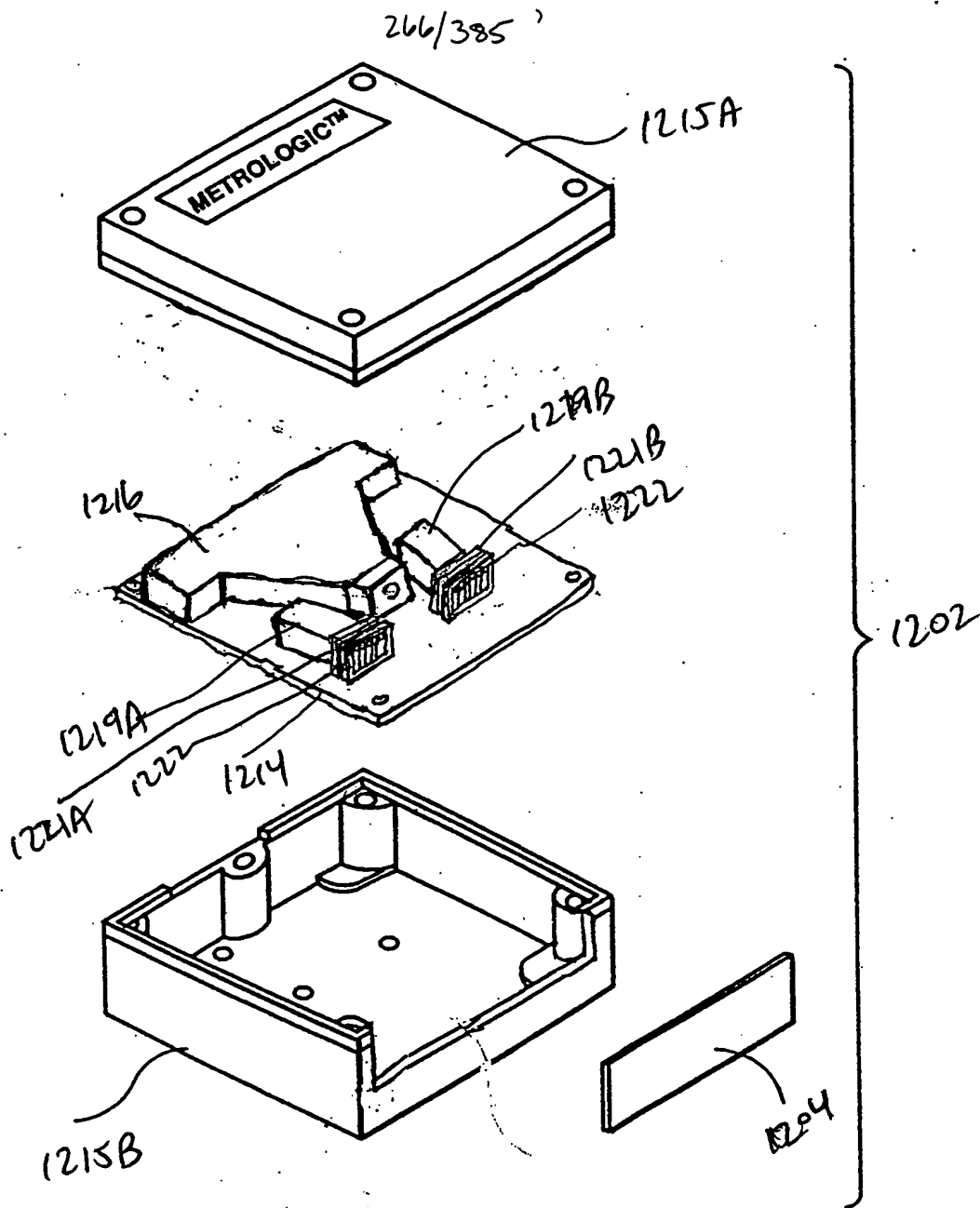


FIG. 39B

268/385

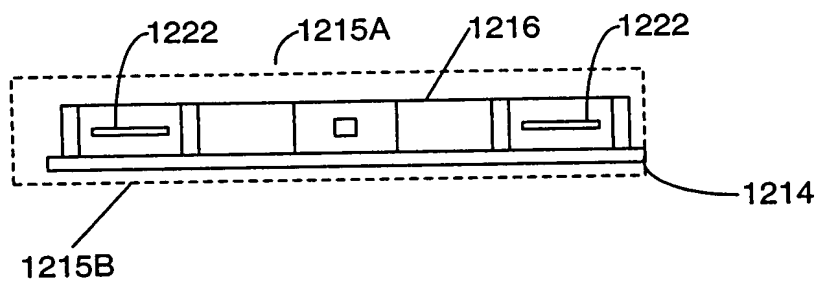


FIG. 39D

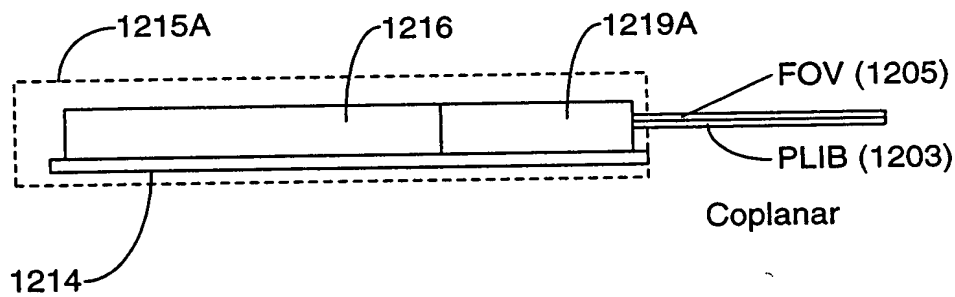


FIG. 39E

FIG. 39D

269/385

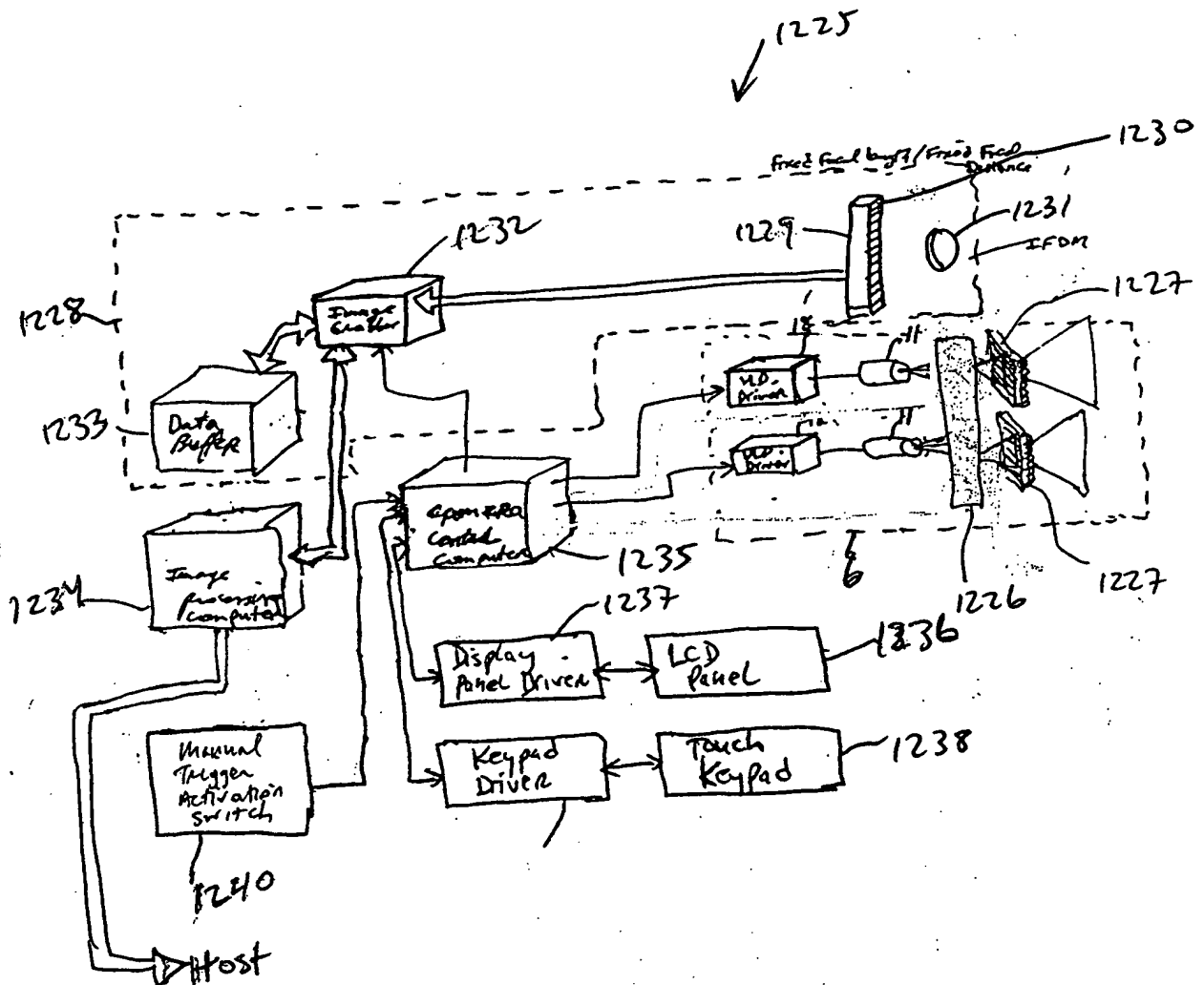
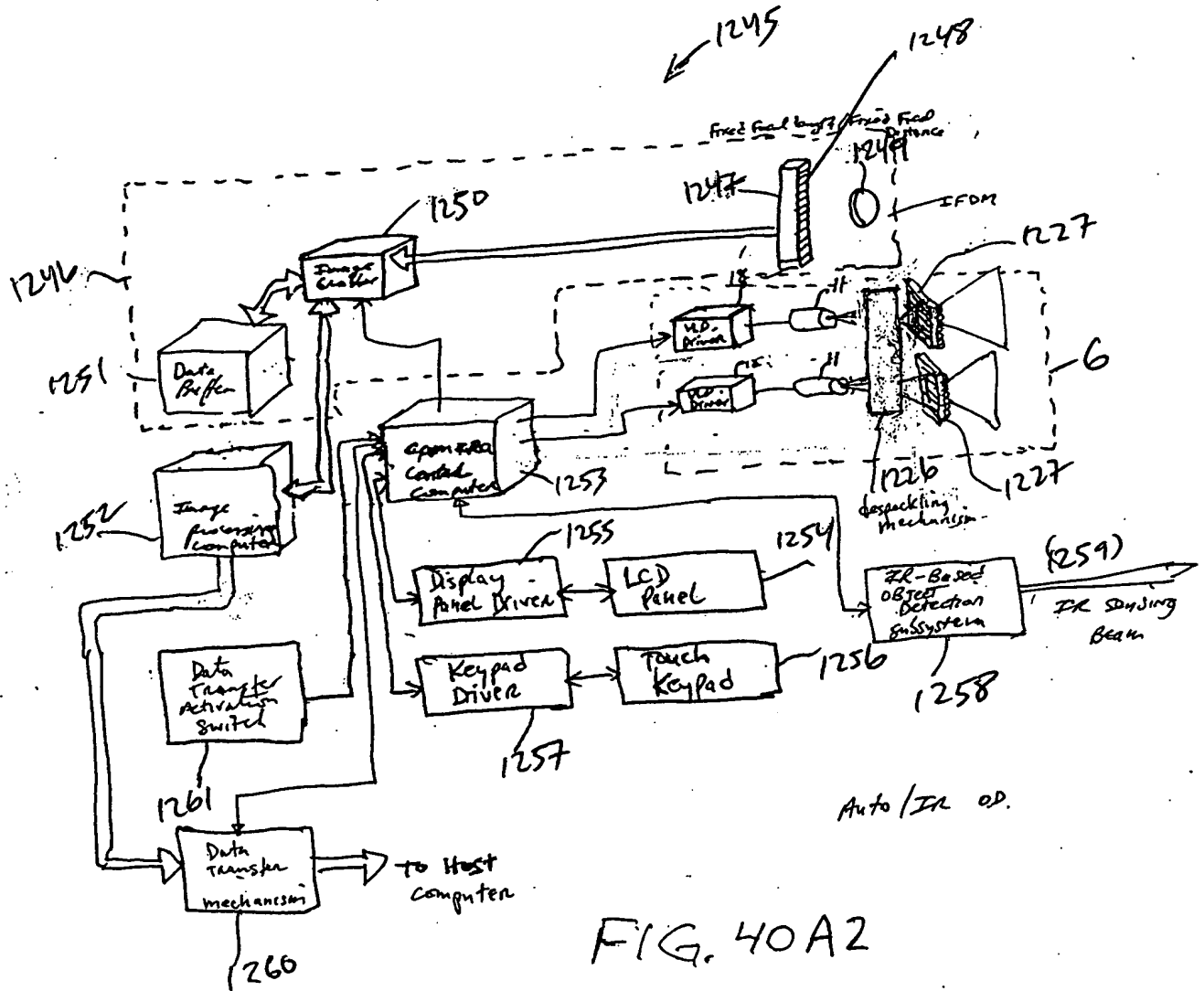
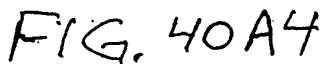


FIG. 40A1

$$270/385$$


[illegible]

273/385

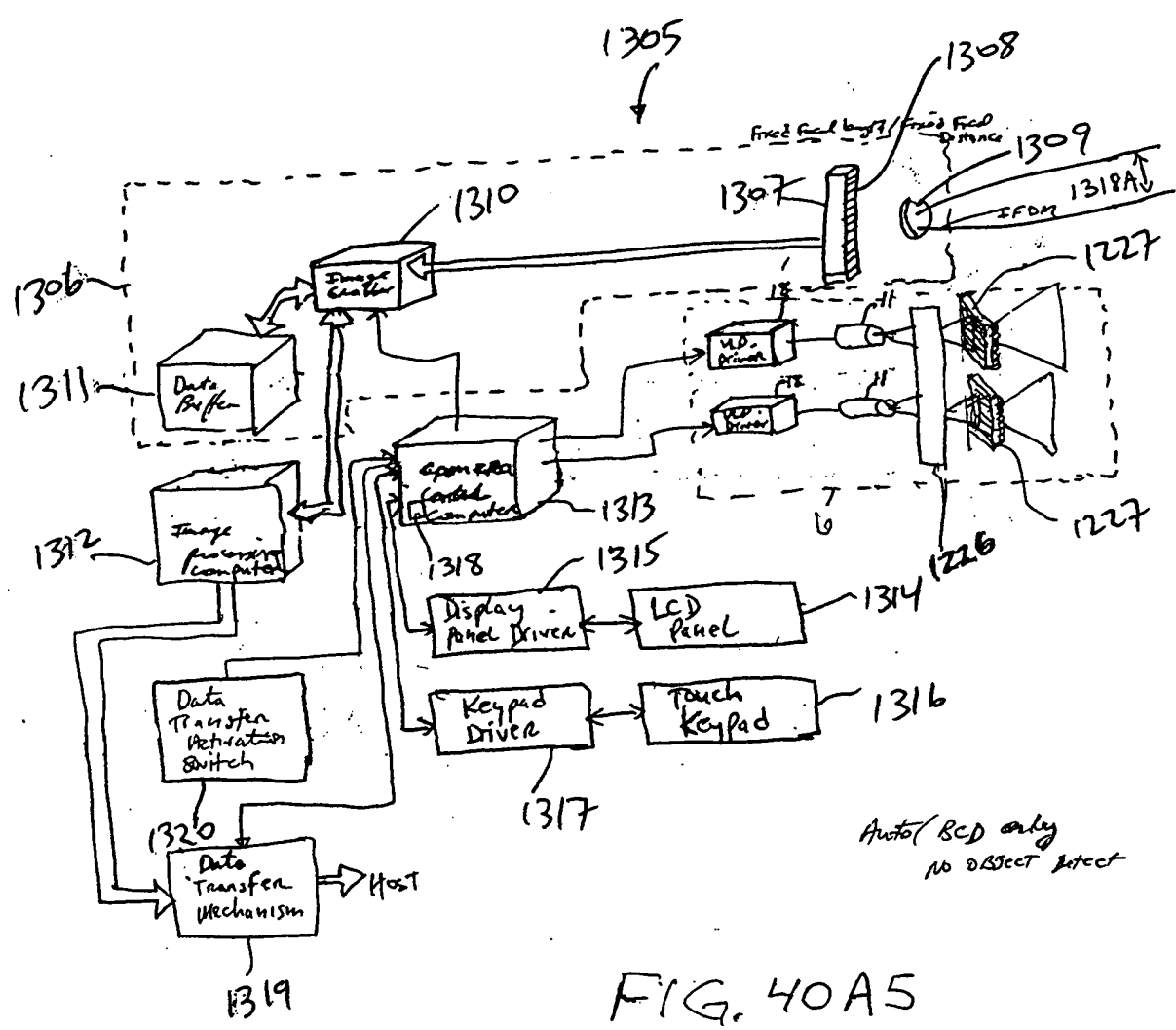


FIG. 40A5

274/385

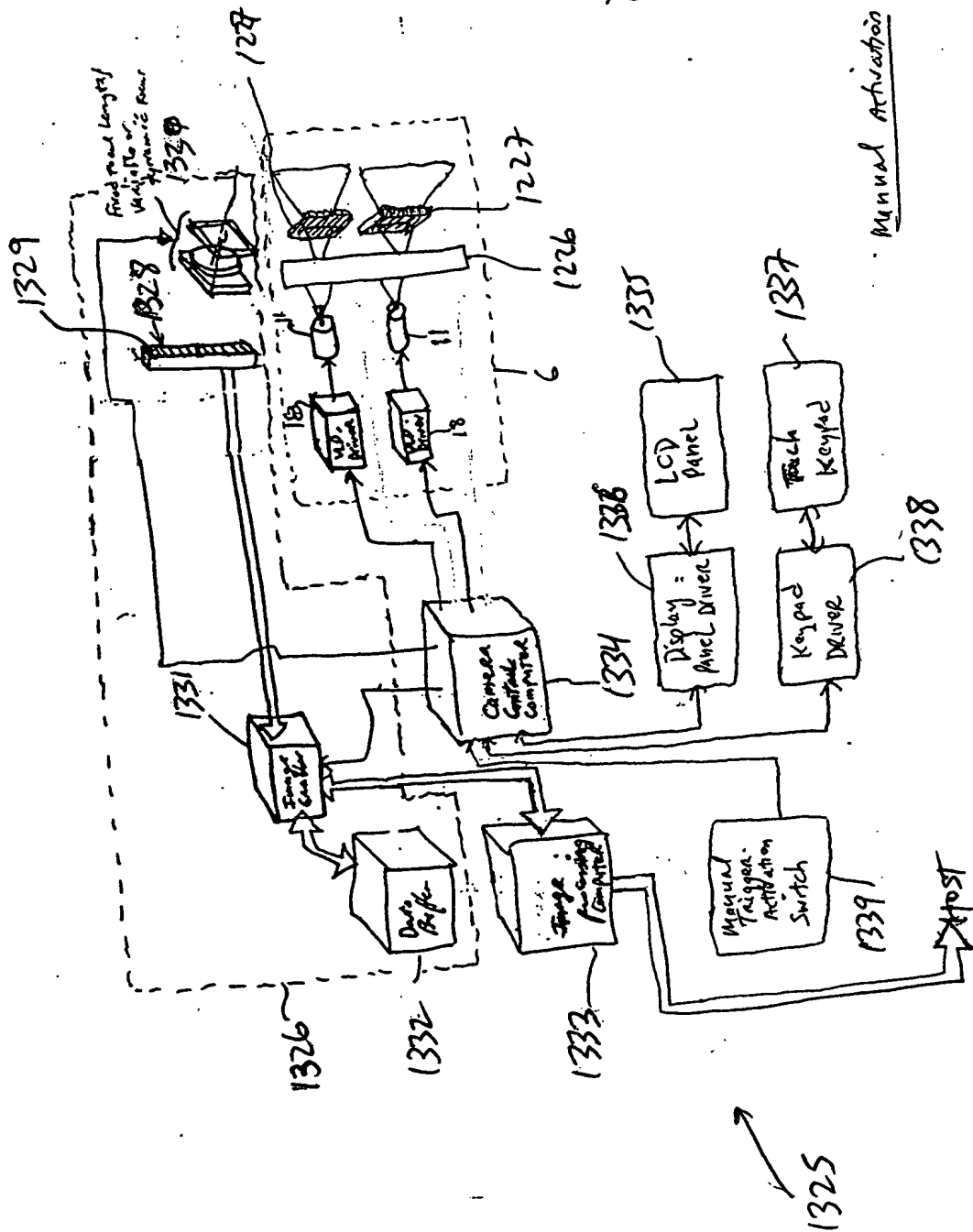
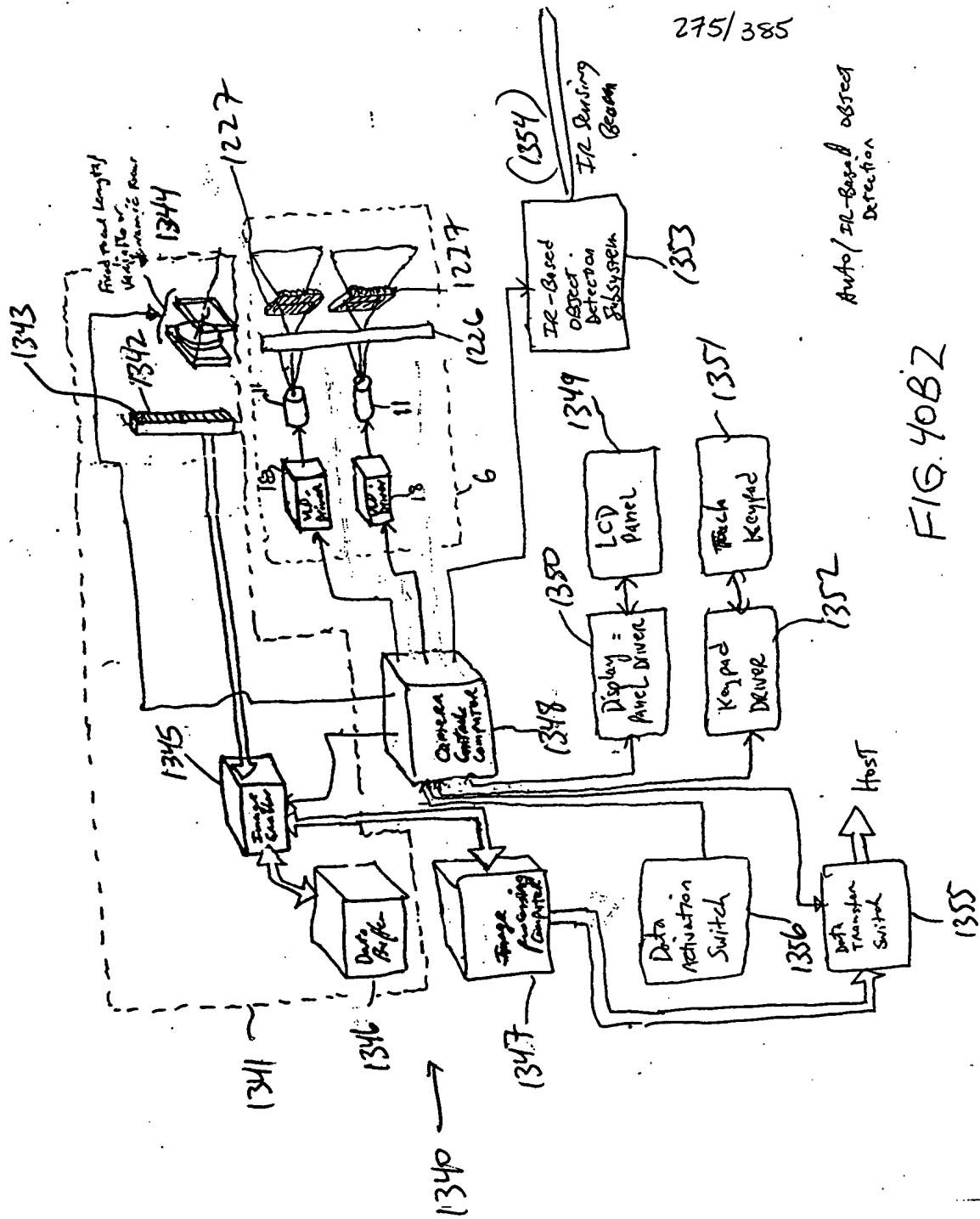


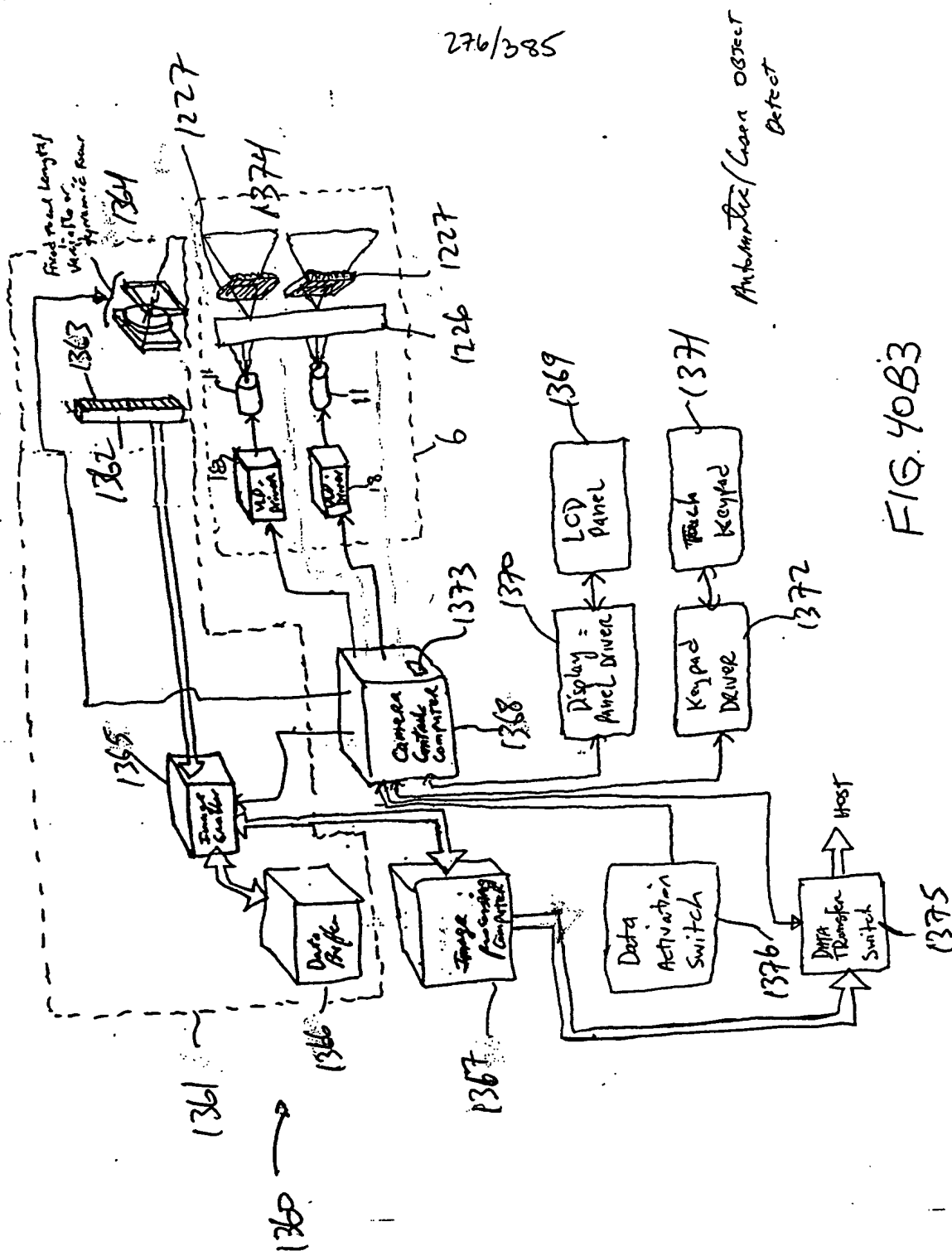
FIG. 40B

| Time | Temperature | Pressure | Humidity | Wind | Clouds | Visibility | Remarks |
|------|-------------|----------|----------|------|--------|------------|---------|
| 0000 | 50.0 | 1013.2 | 65 | 000 | 000 | 10 | Clear |
| 0100 | 50.0 | 1013.2 | 65 | 000 | 000 | 10 | Clear |
| 0200 | 50.0 | 1013.2 | 65 | 000 | 000 | 10 | Clear |
| 0300 | 50.0 | 1013.2 | 65 | 000 | 000 | 10 | Clear |
| 0400 | 50.0 | 1013.2 | 65 | 000 | 000 | 10 | Clear |
| 0500 | 50.0 | 1013.2 | 65 | 000 | 000 | 10 | Clear |
| 0600 | 50.0 | 1013.2 | 65 | 000 | 000 | 10 | Clear |
| 0700 | 50.0 | 1013.2 | 65 | 000 | 000 | 10 | Clear |
| 0800 | 50.0 | 1013.2 | 65 | 000 | 000 | 10 | Clear |
| 0900 | 50.0 | 1013.2 | 65 | 000 | 000 | 10 | Clear |
| 1000 | 50.0 | 1013.2 | 65 | 000 | 000 | 10 | Clear |
| 1100 | 50.0 | 1013.2 | 65 | 000 | 000 | 10 | Clear |
| 1200 | 50.0 | 1013.2 | 65 | 000 | 000 | 10 | Clear |
| 1300 | 50.0 | 1013.2 | 65 | 000 | 000 | 10 | Clear |
| 1400 | 50.0 | 1013.2 | 65 | 000 | 000 | 10 | Clear |
| 1500 | 50.0 | 1013.2 | 65 | 000 | 000 | 10 | Clear |
| 1600 | 50.0 | 1013.2 | 65 | 000 | 000 | 10 | Clear |
| 1700 | 50.0 | 1013.2 | 65 | 000 | 000 | 10 | Clear |
| 1800 | 50.0 | 1013.2 | 65 | 000 | 000 | 10 | Clear |
| 1900 | 50.0 | 1013.2 | 65 | 000 | 000 | 10 | Clear |
| 2000 | 50.0 | 1013.2 | 65 | 000 | 000 | 10 | Clear |
| 2100 | 50.0 | 1013.2 | 65 | 000 | 000 | 10 | Clear |
| 2200 | 50.0 | 1013.2 | 65 | 000 | 000 | 10 | Clear |
| 2300 | 50.0 | 1013.2 | 65 | 000 | 000 | 10 | Clear |



[illegible]

276/385



277/385

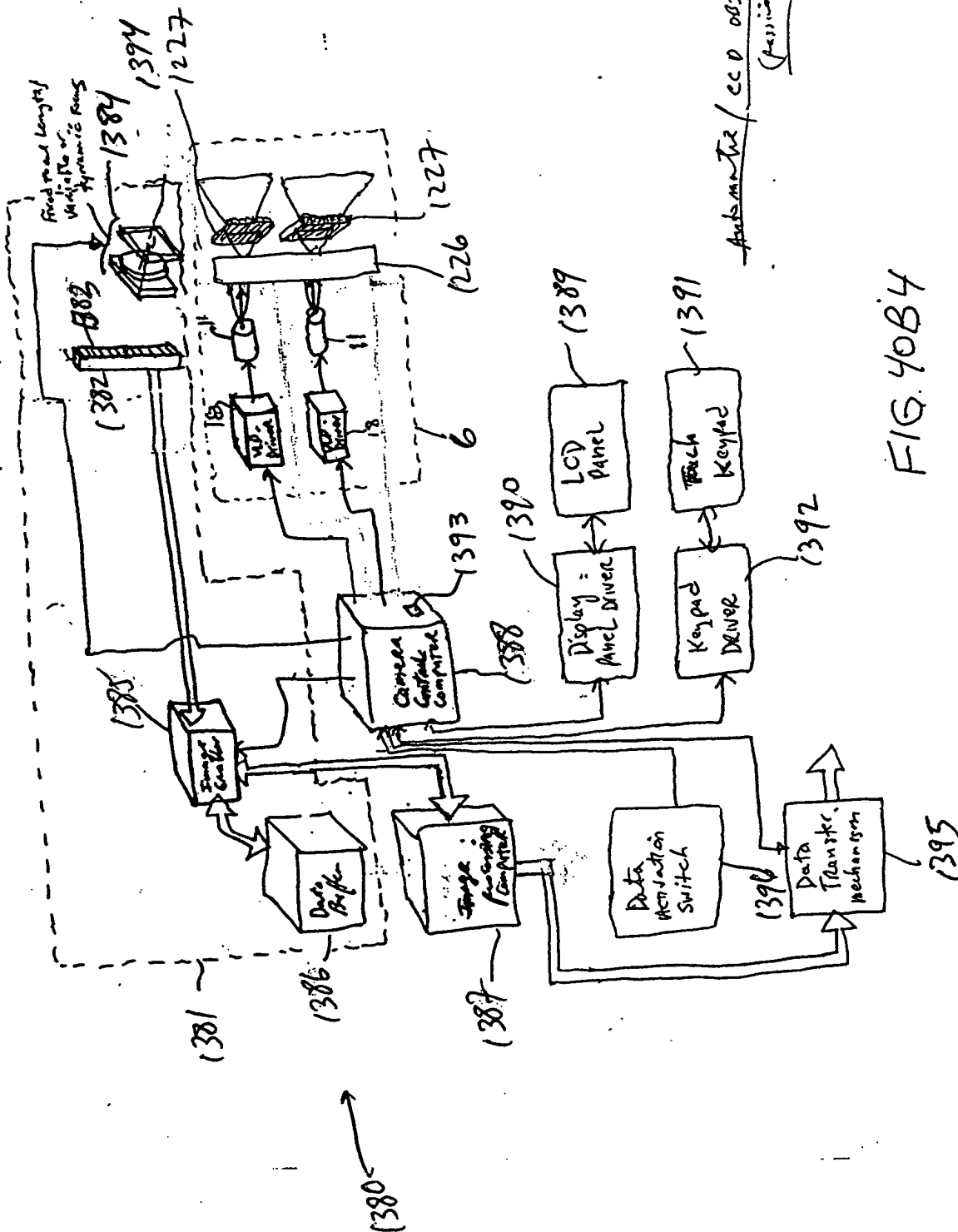
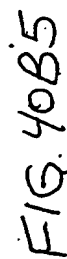


FIG. 40B4

278/385



[illegible]

279/385

maximal detritation

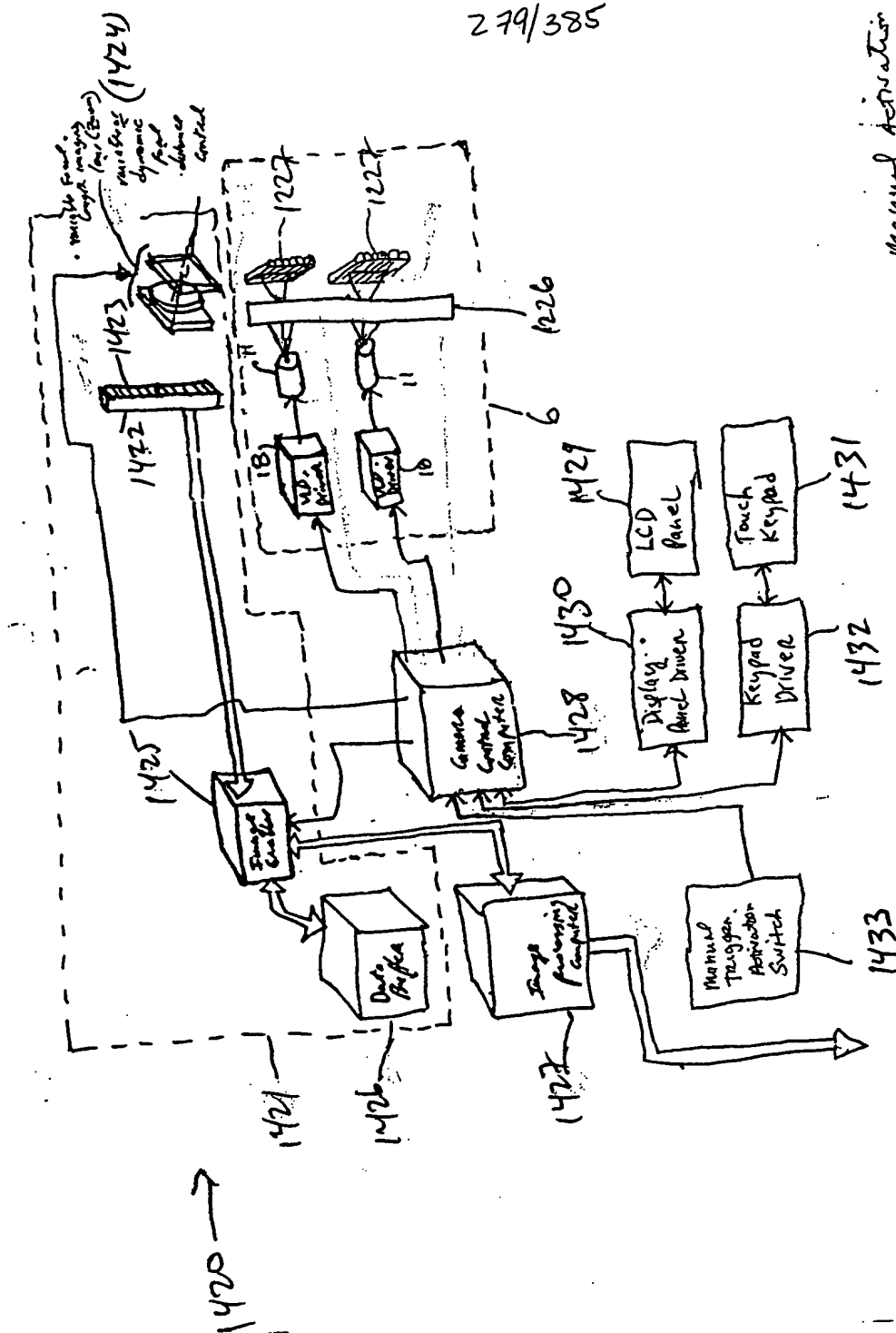


FIG. 40C1

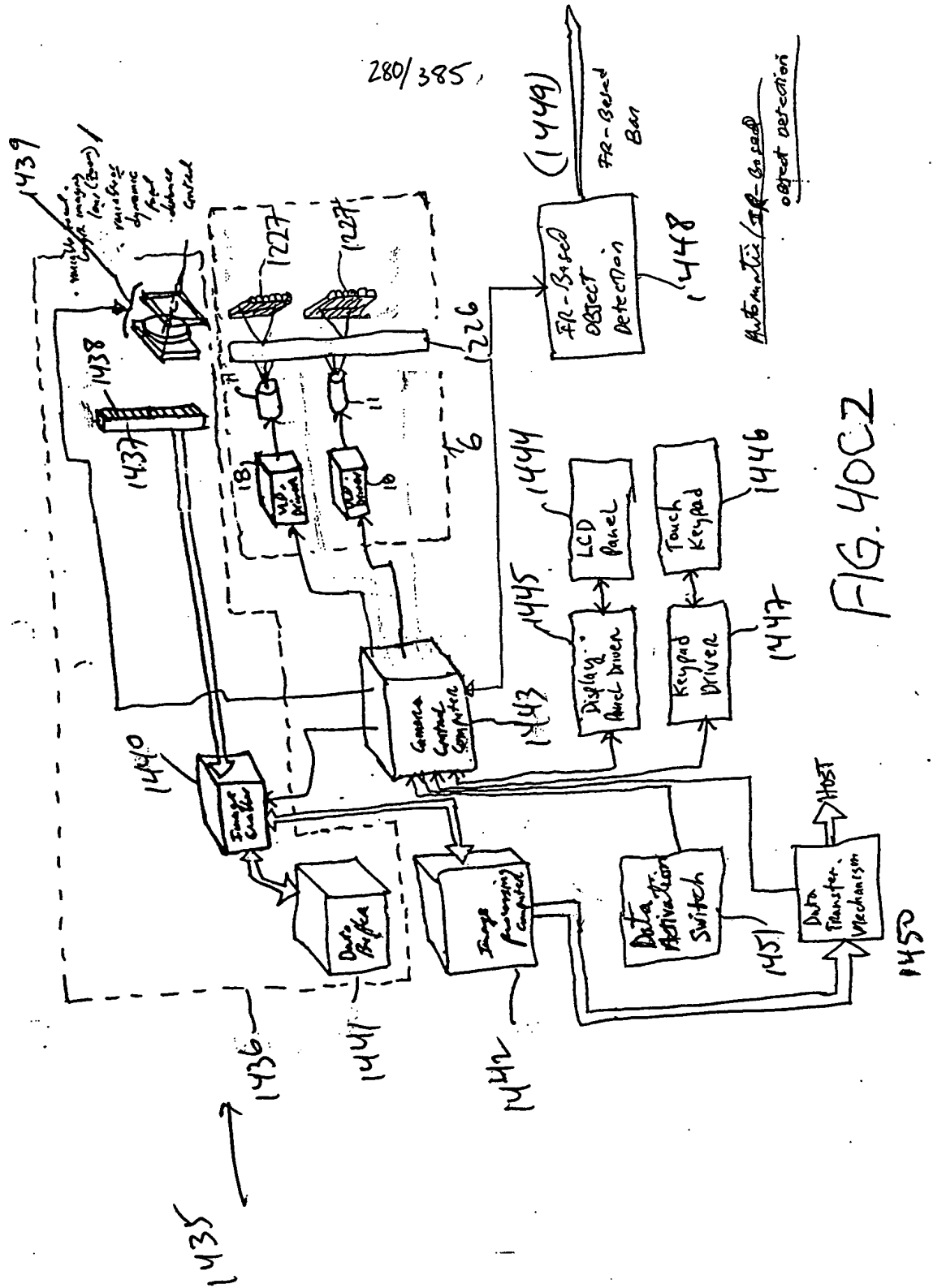
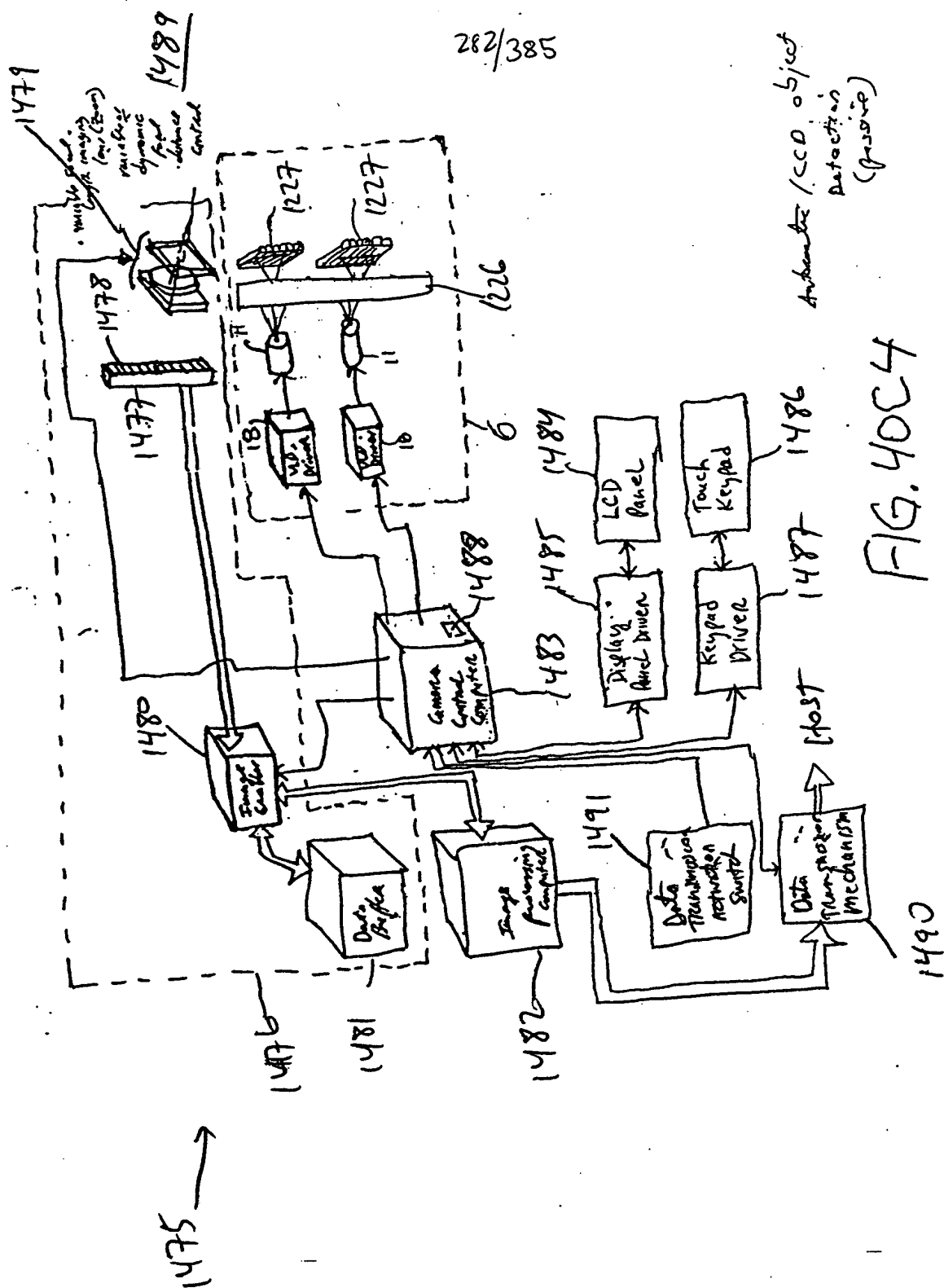


FIG. 400CZ



[illegible]
$$283/385$$

Autotrophic/BCP only
-No object trace

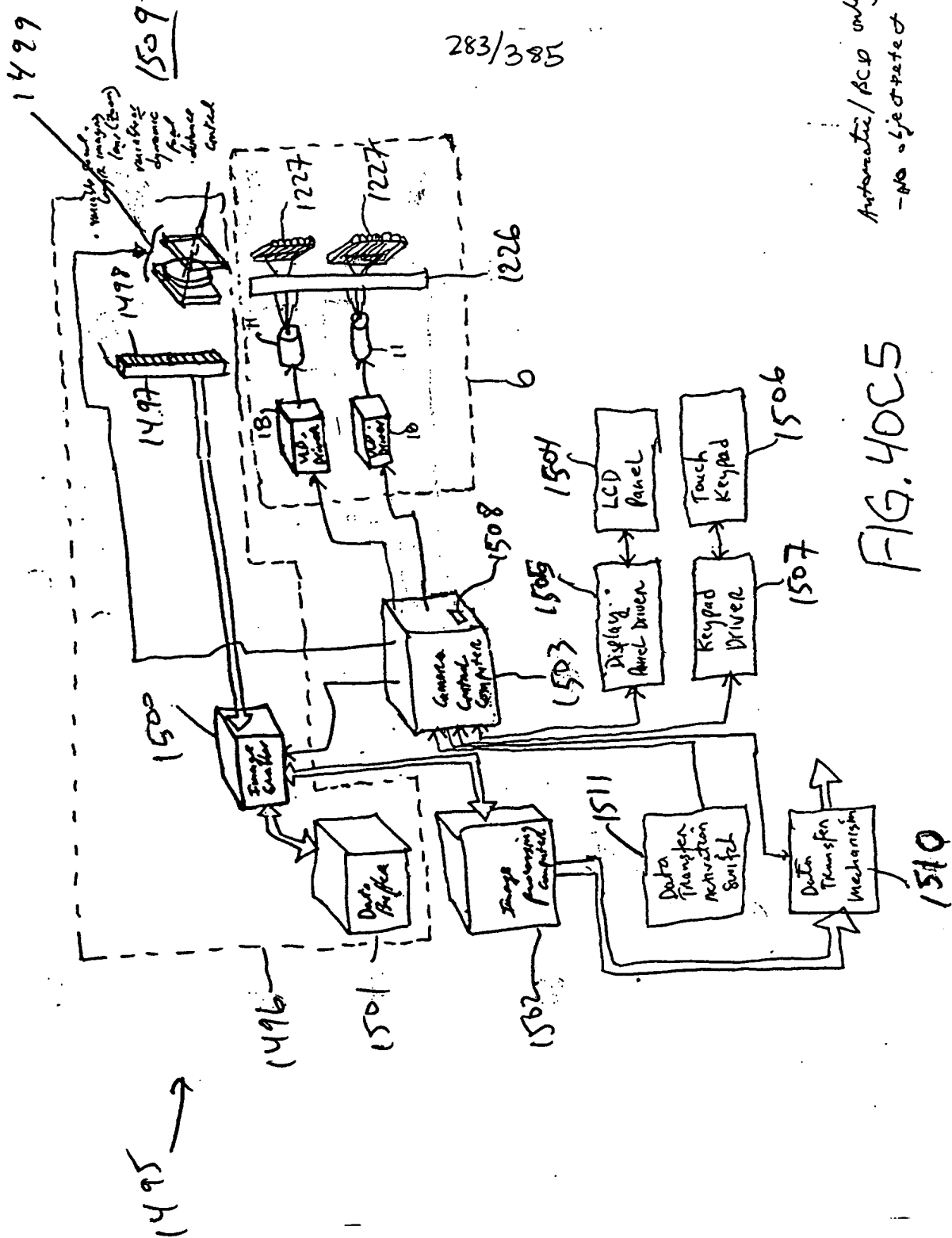


FIG. 40C5

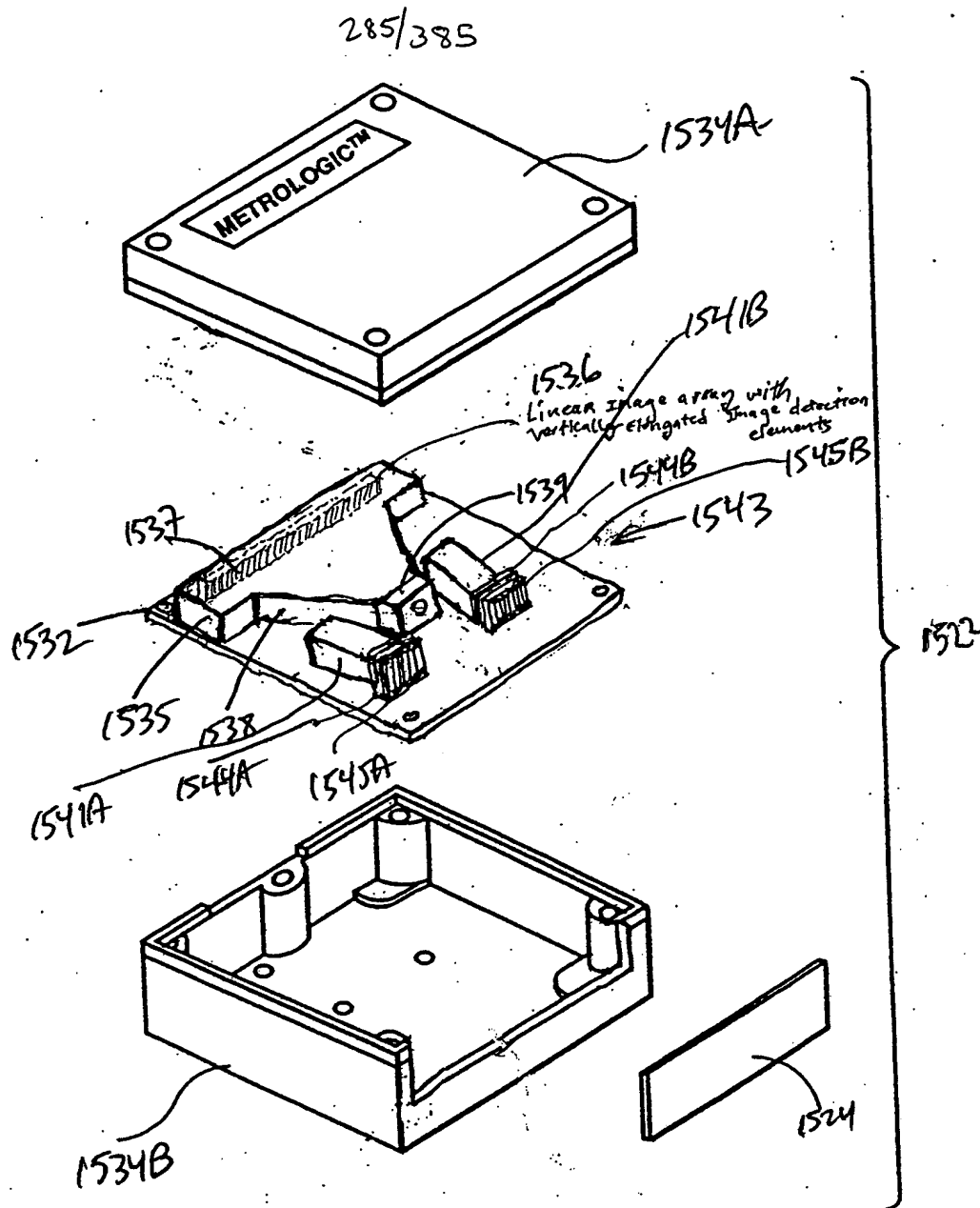


FIG. 41B

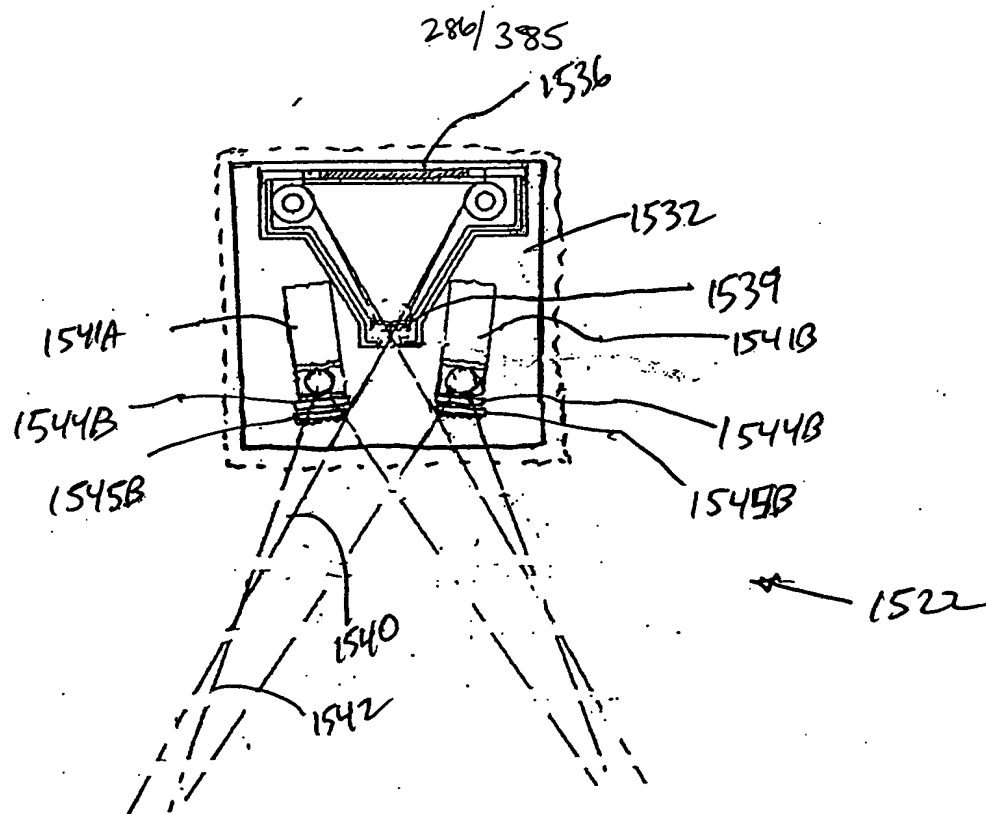


FIG. 41C

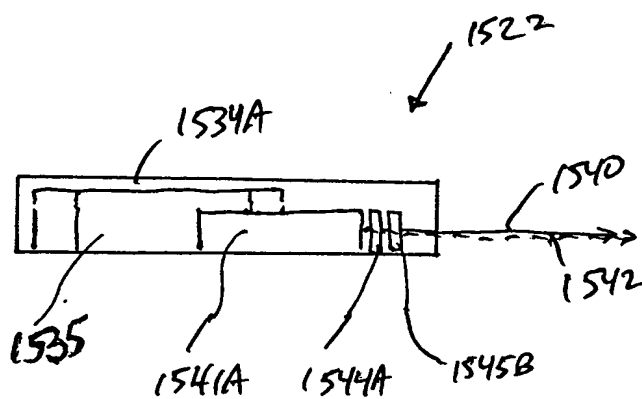


FIG. 41D

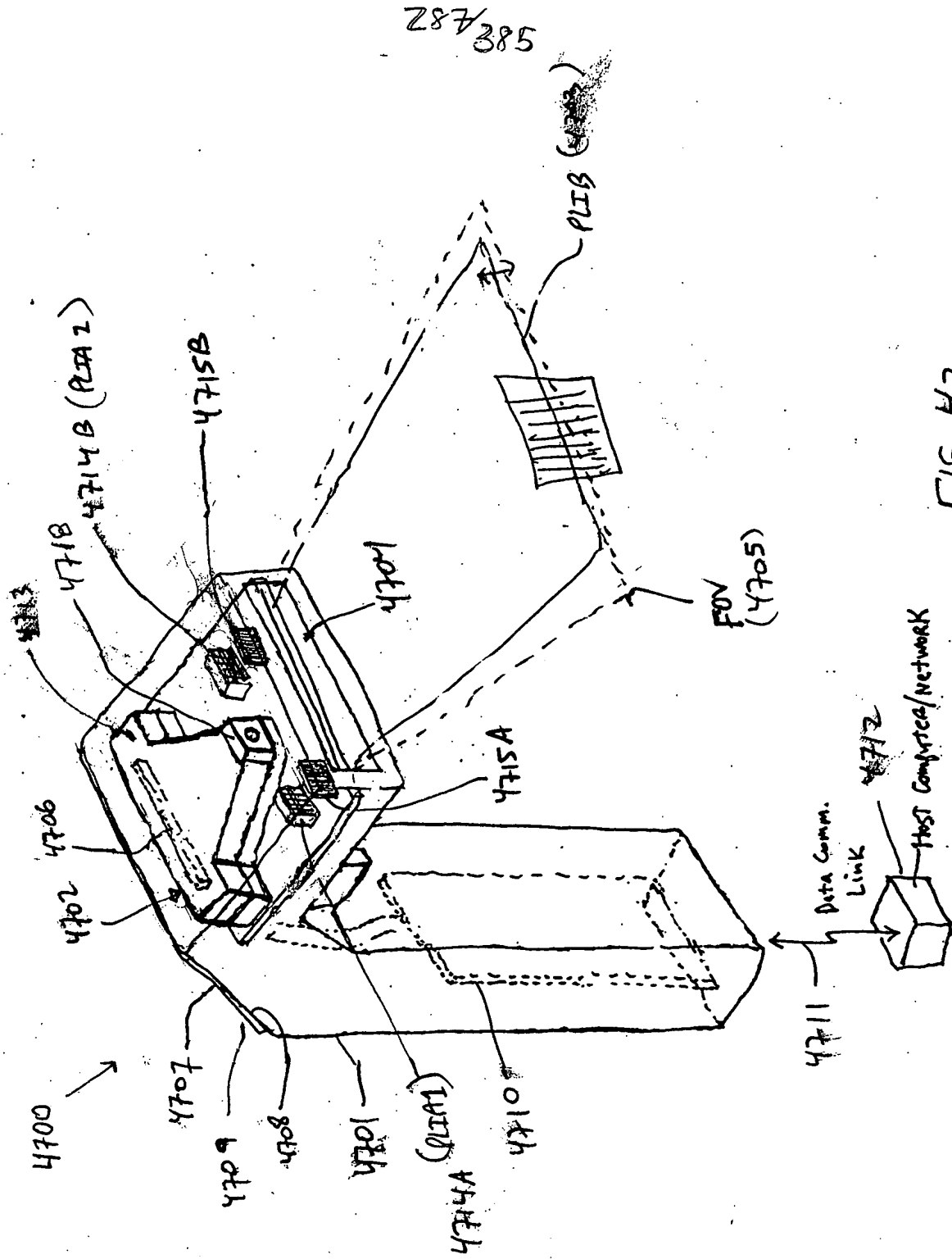
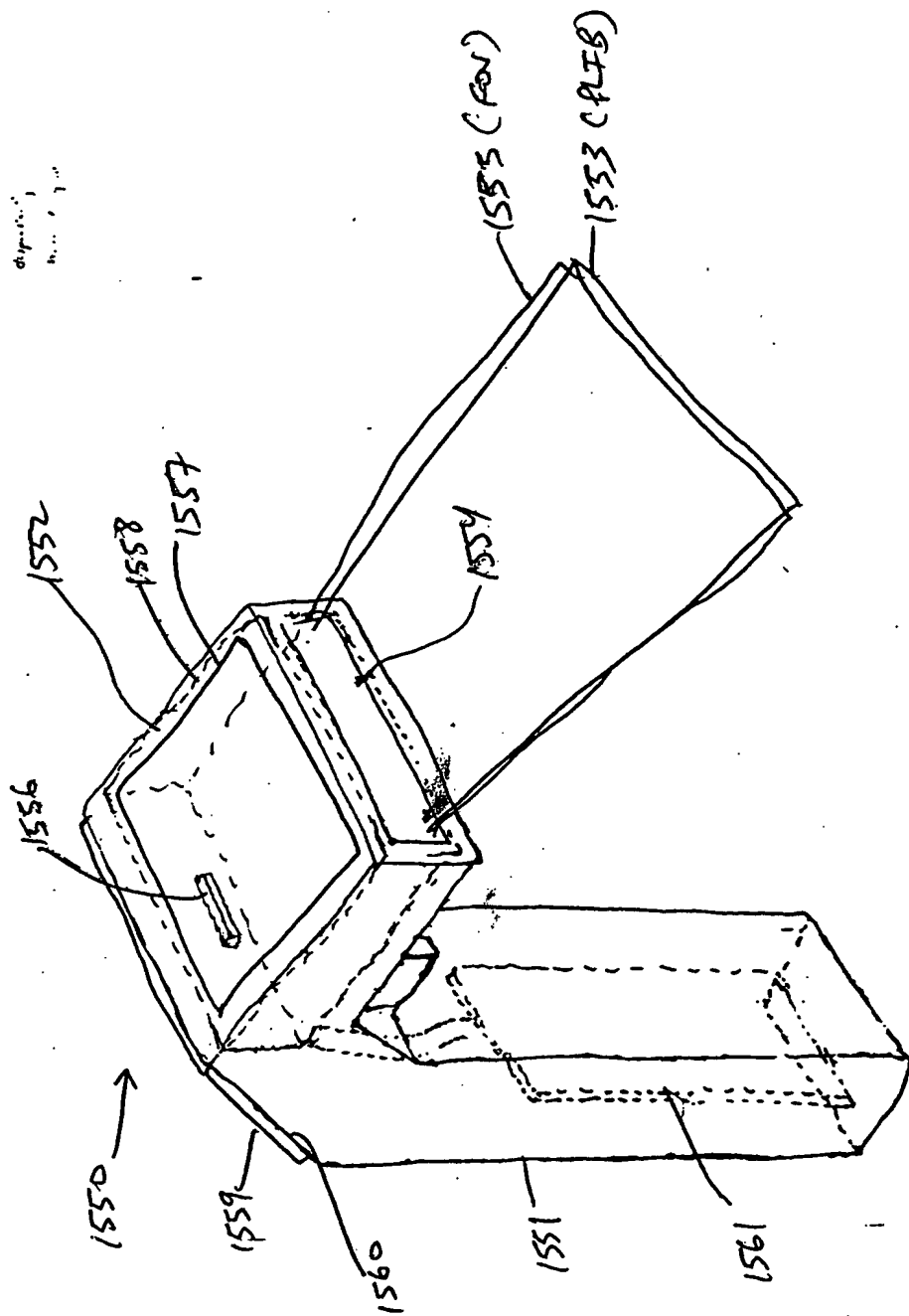


FIG 42

1-D
display
...



288/385

FIG. 42A

289/385

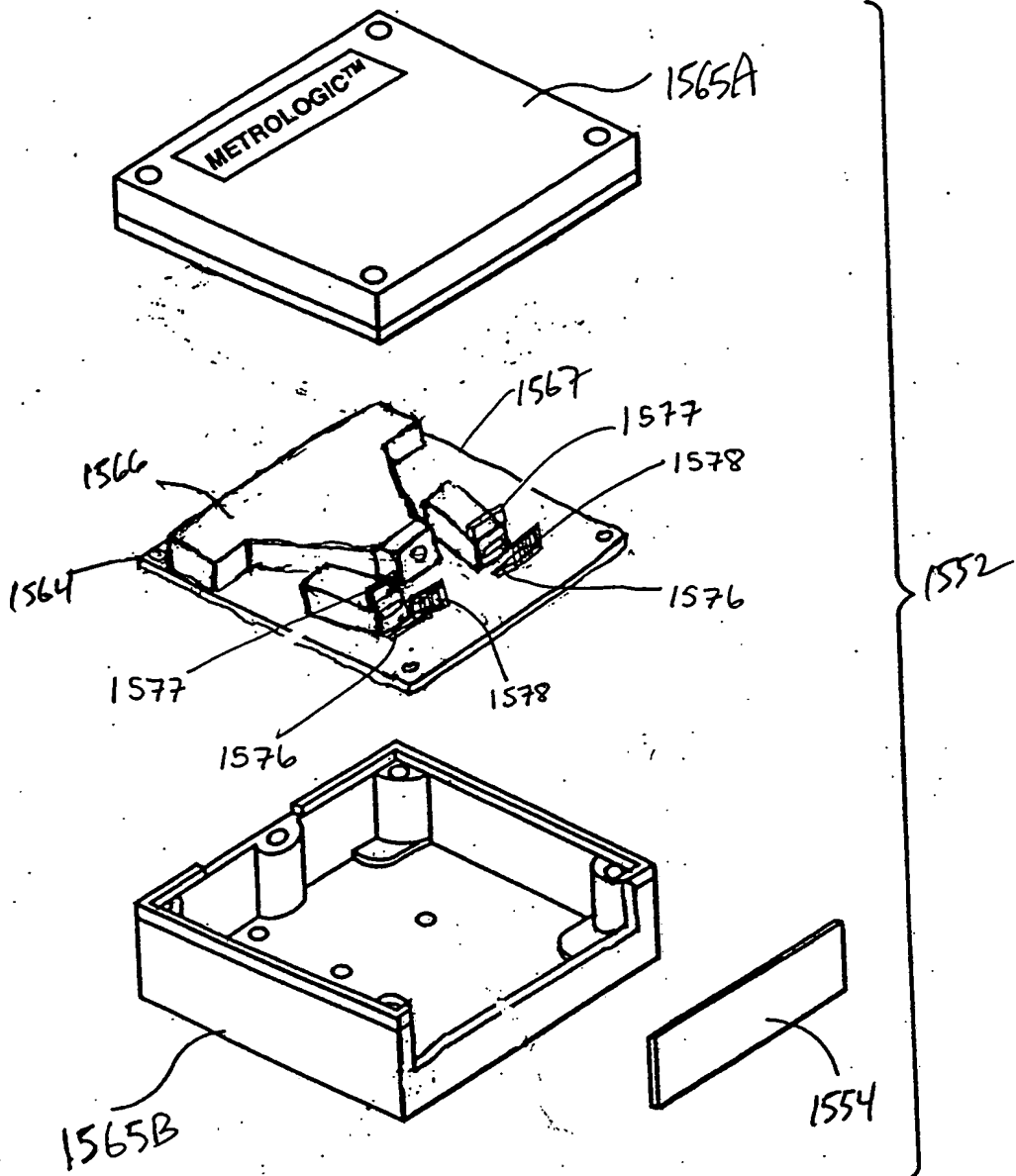


FIG. 42B

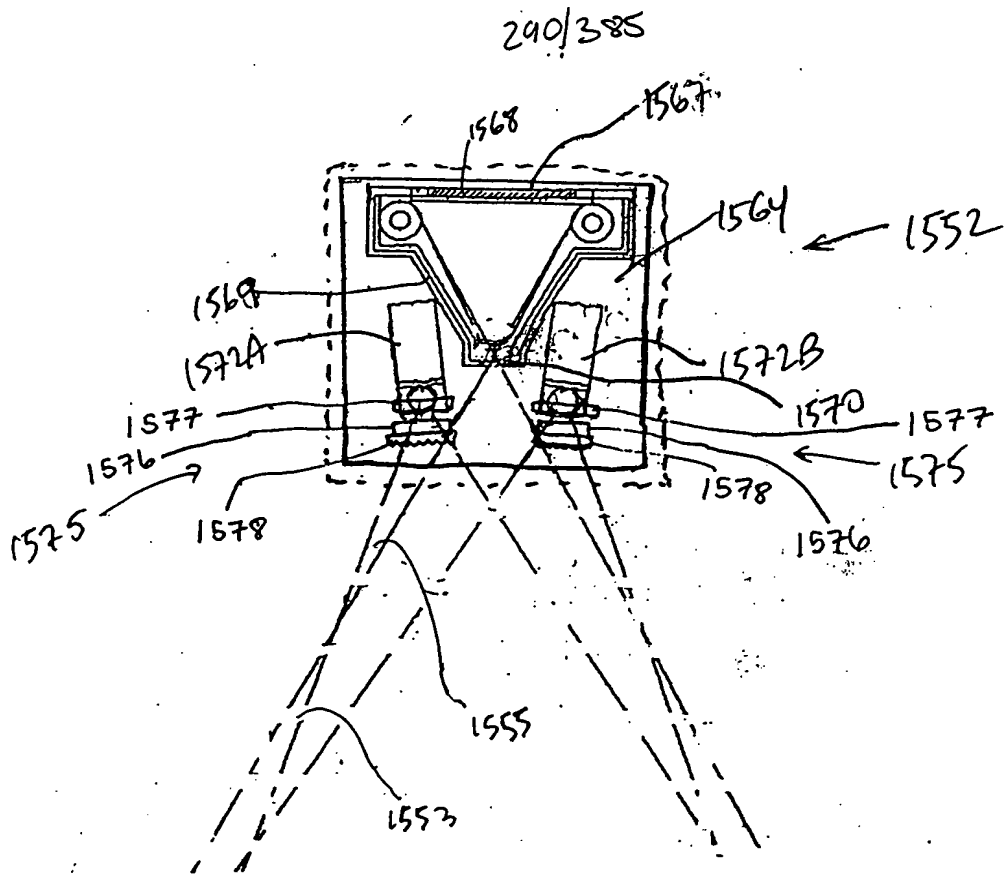


FIG. 42C

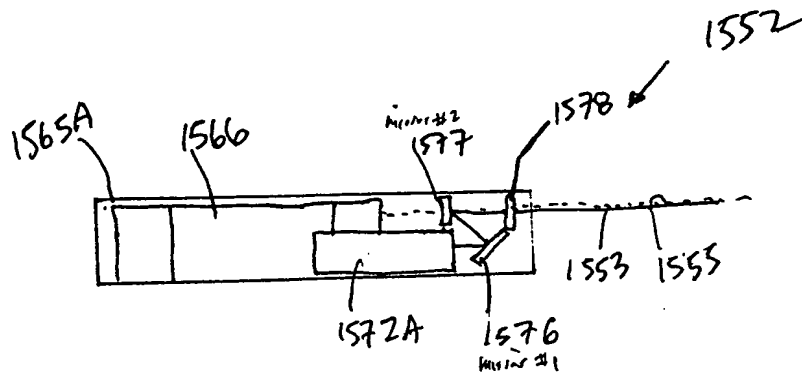


FIG. 42D

TOTET 58506660

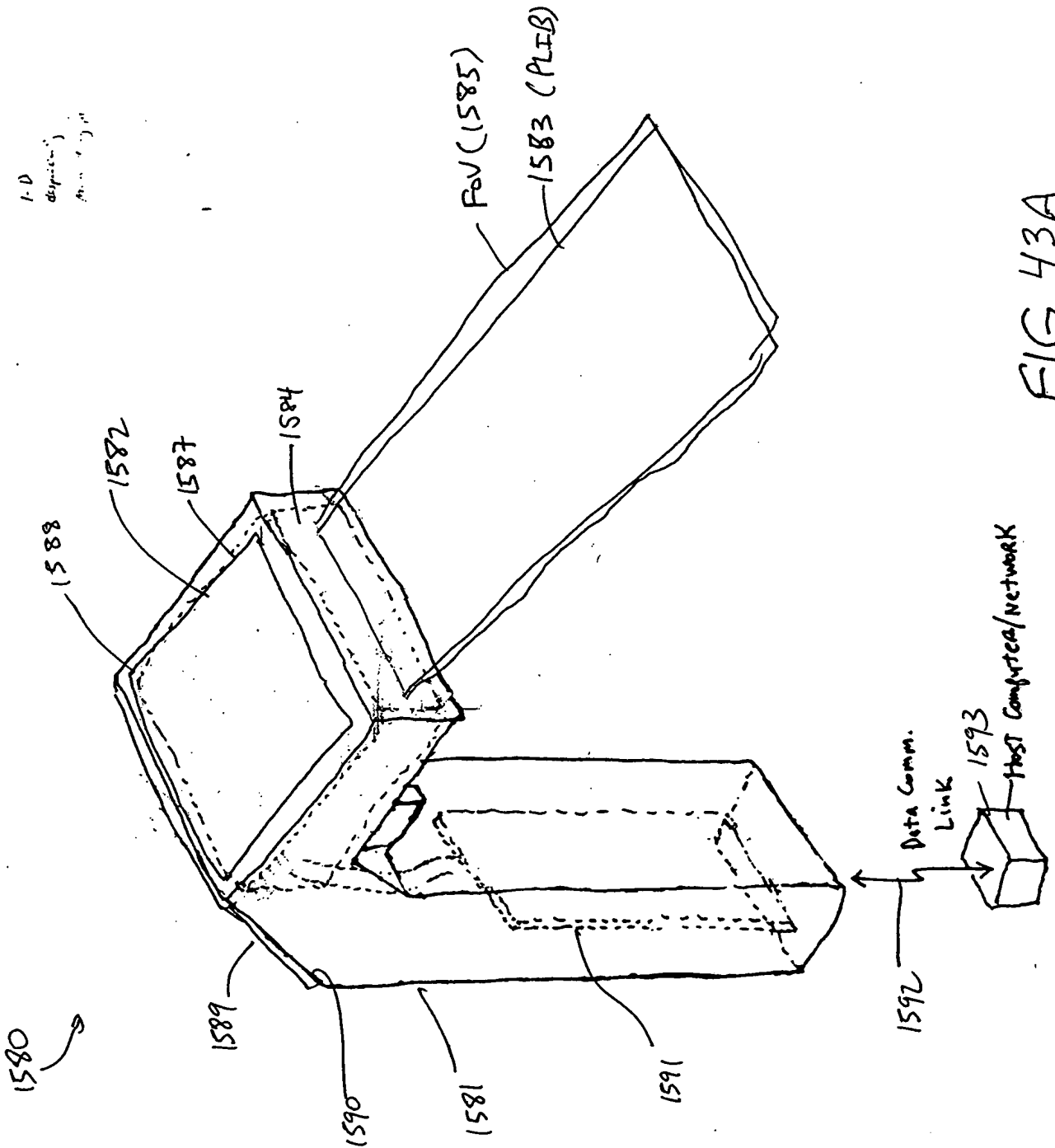


FIG. 43A

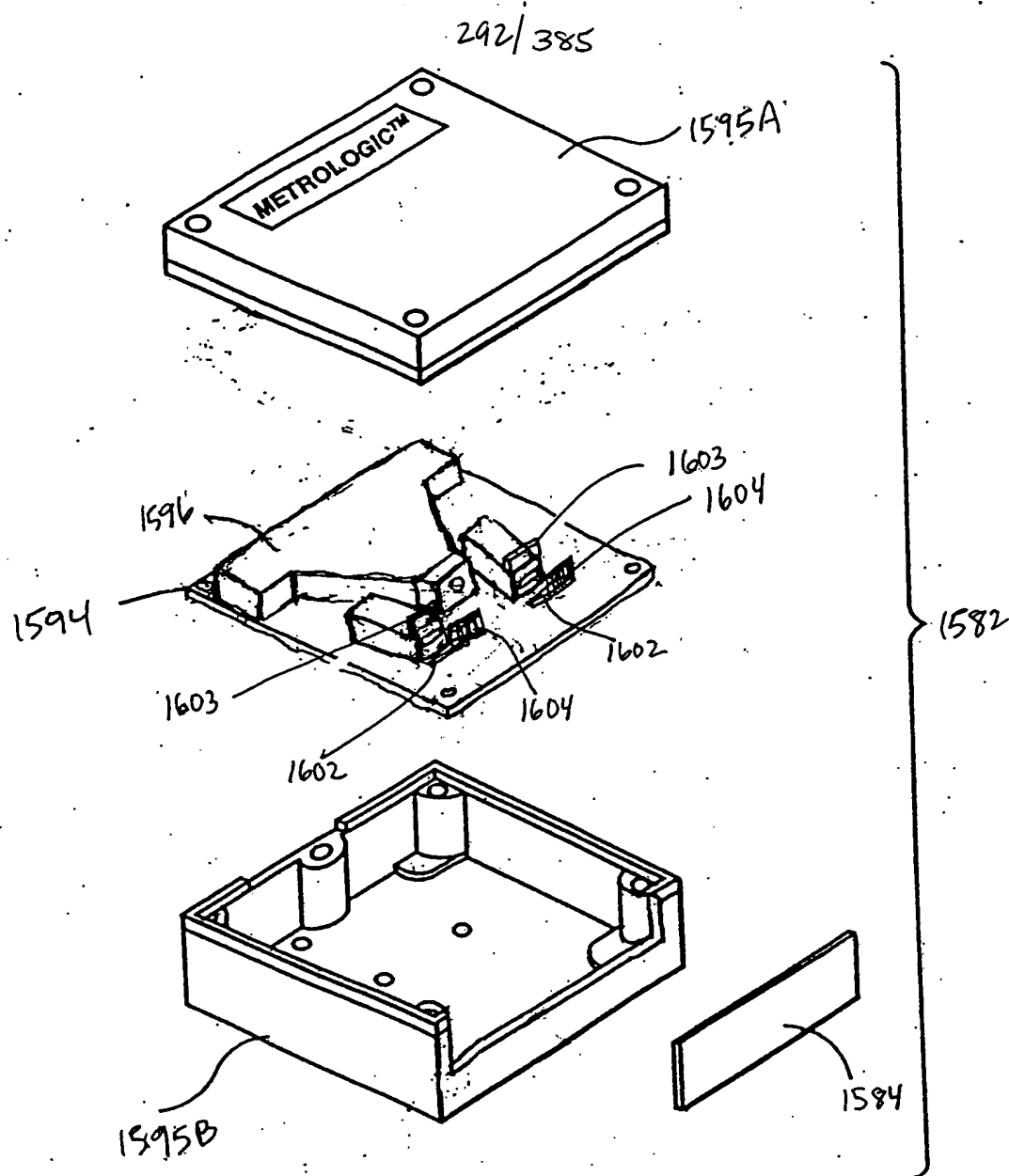
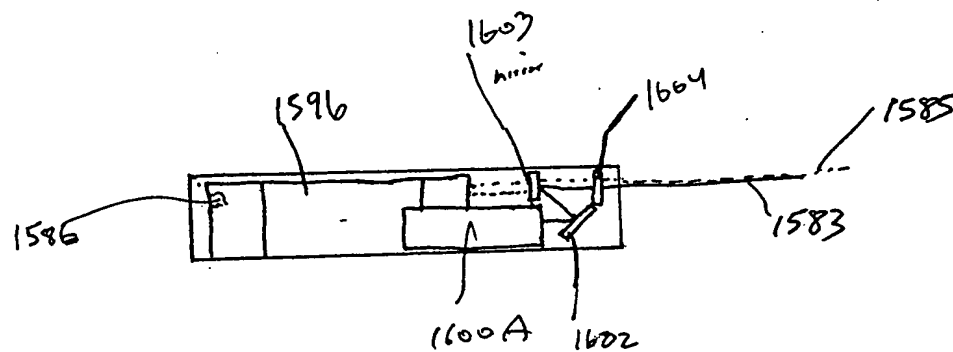
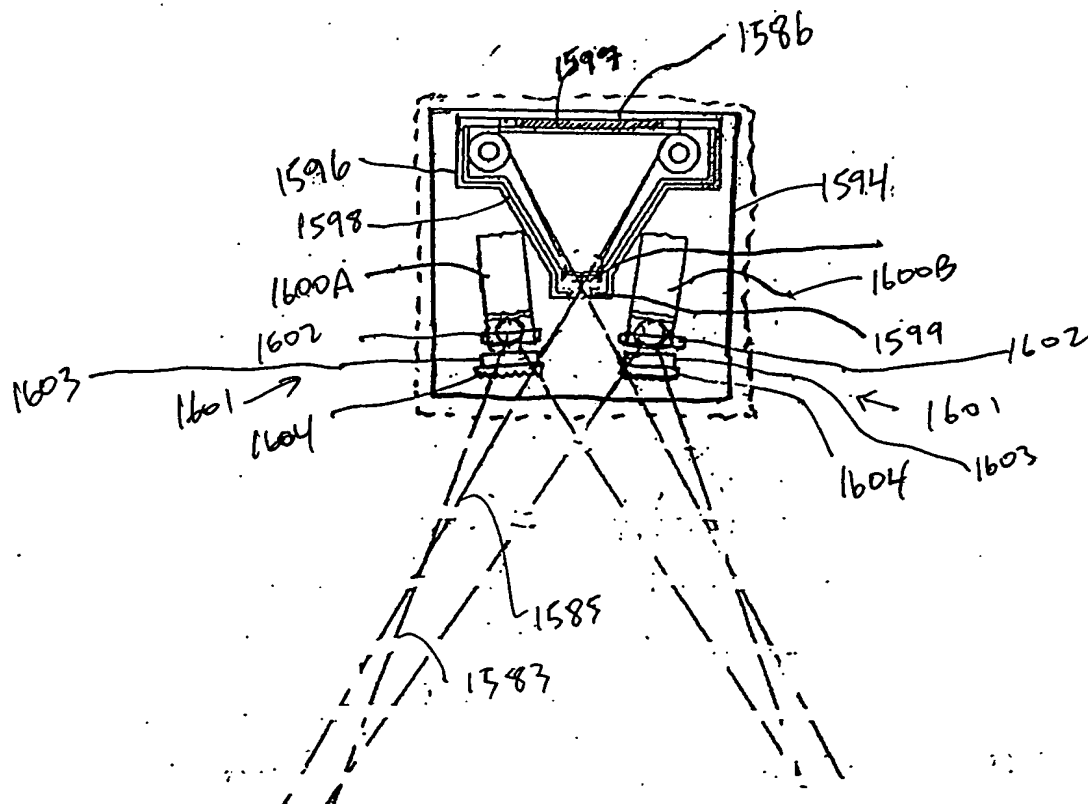


FIG. 43B



TOTAL: 53506660

1-D
display

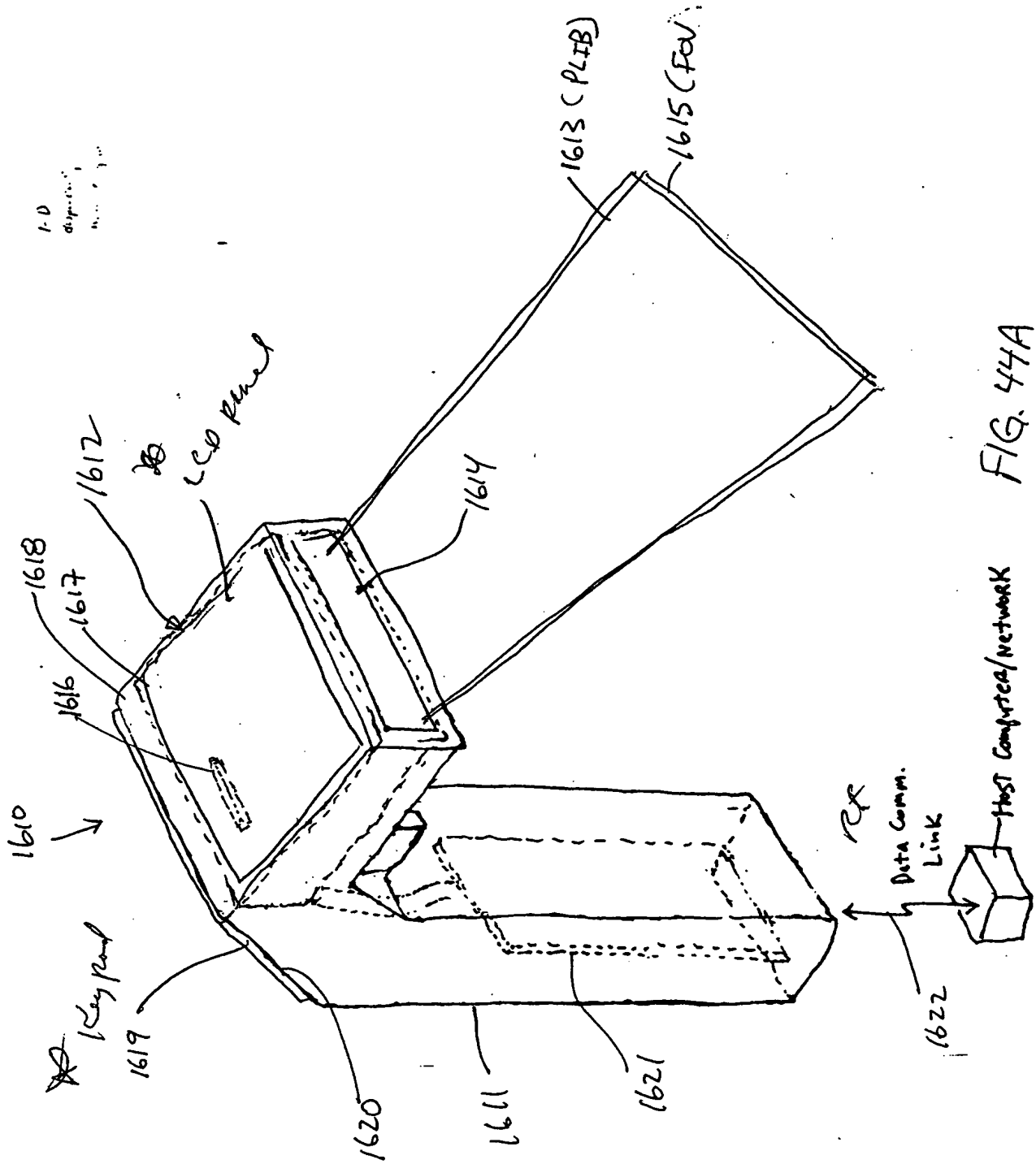


FIG. 44A

294/285

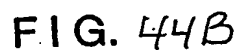
[illegible]

FIG. 44B

00000585, 442104
TOP SECRET

296/3857

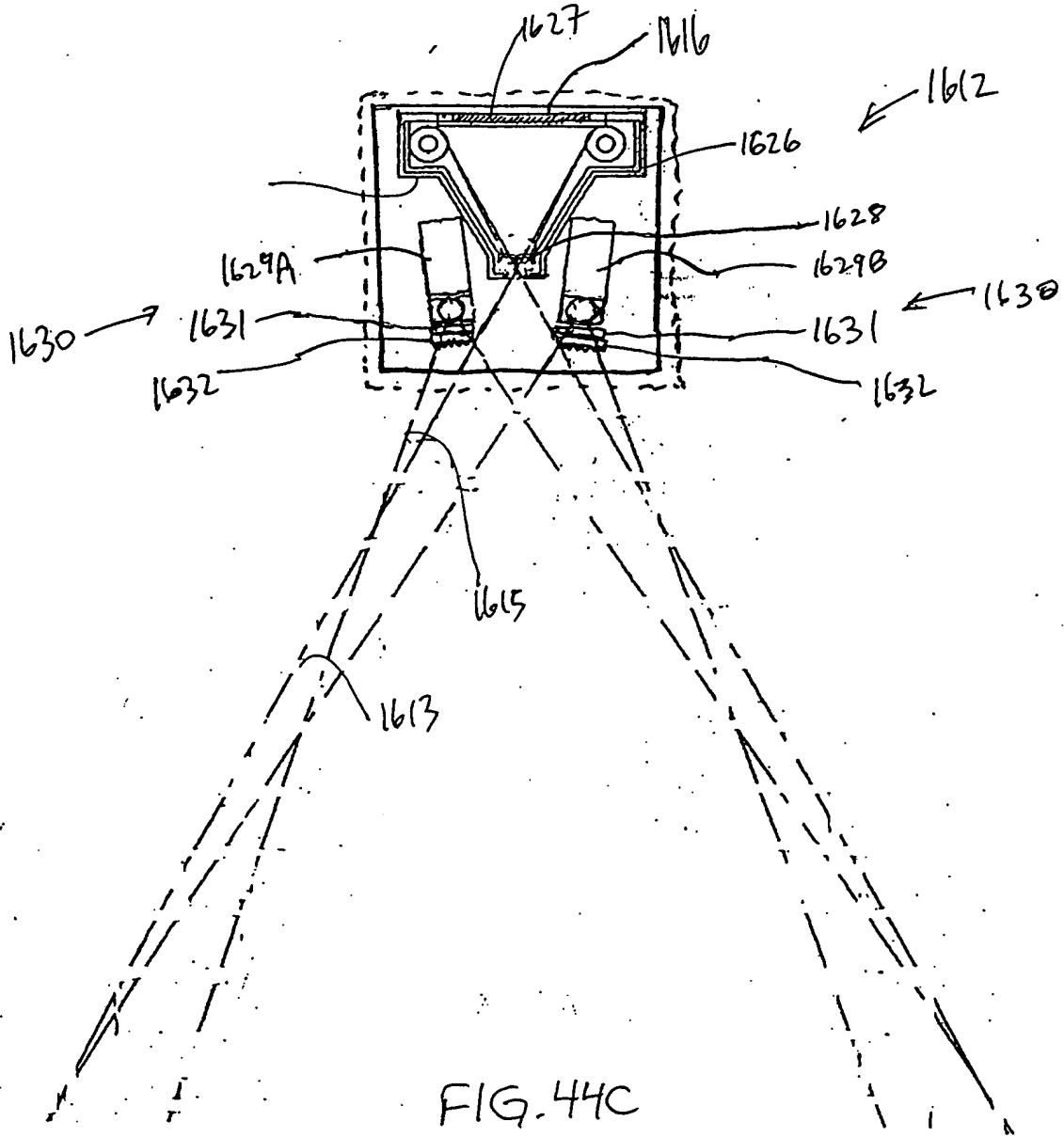


FIG. 44C

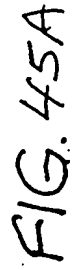


FIG. 45A

00000585.112101

298/385

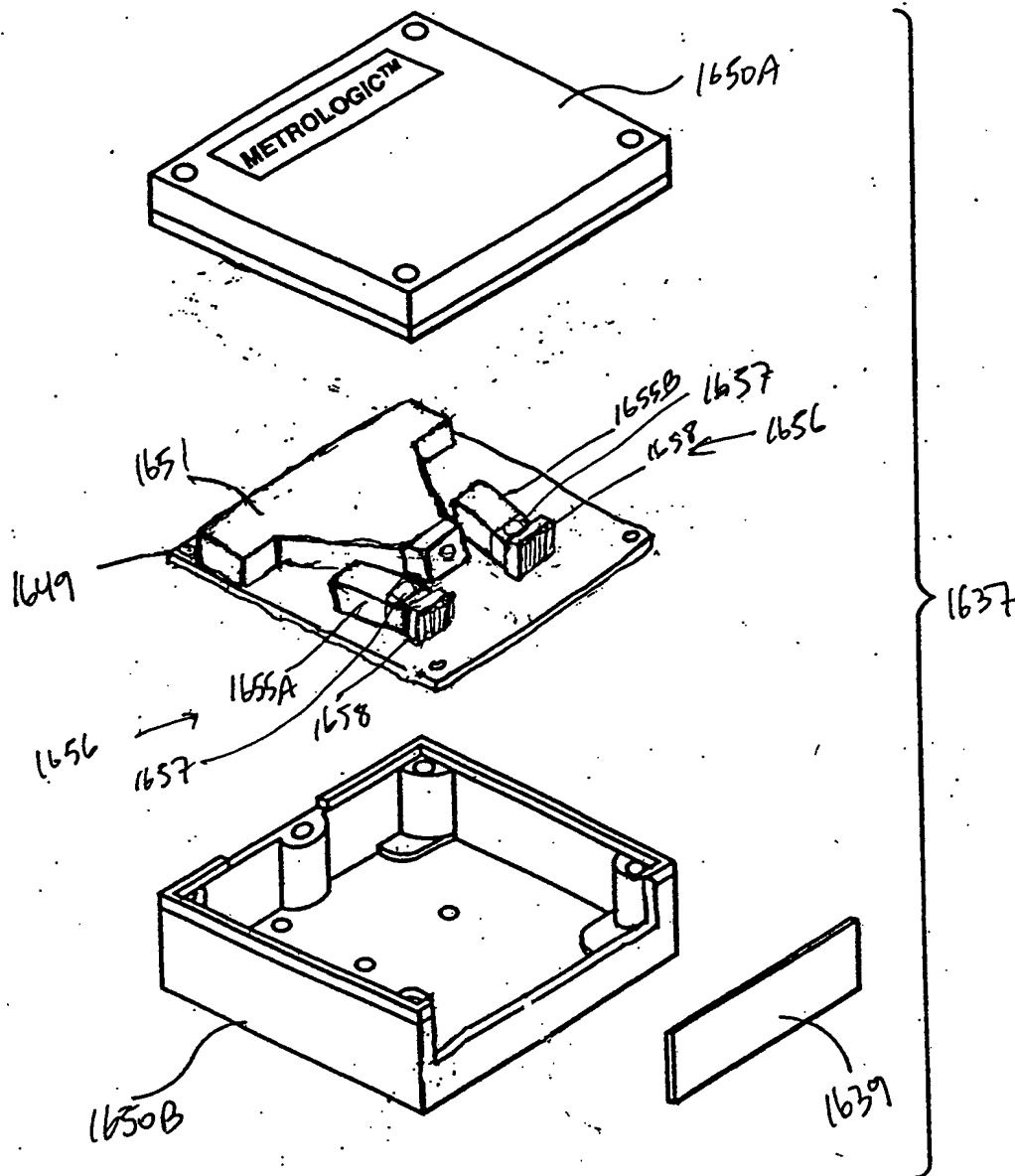
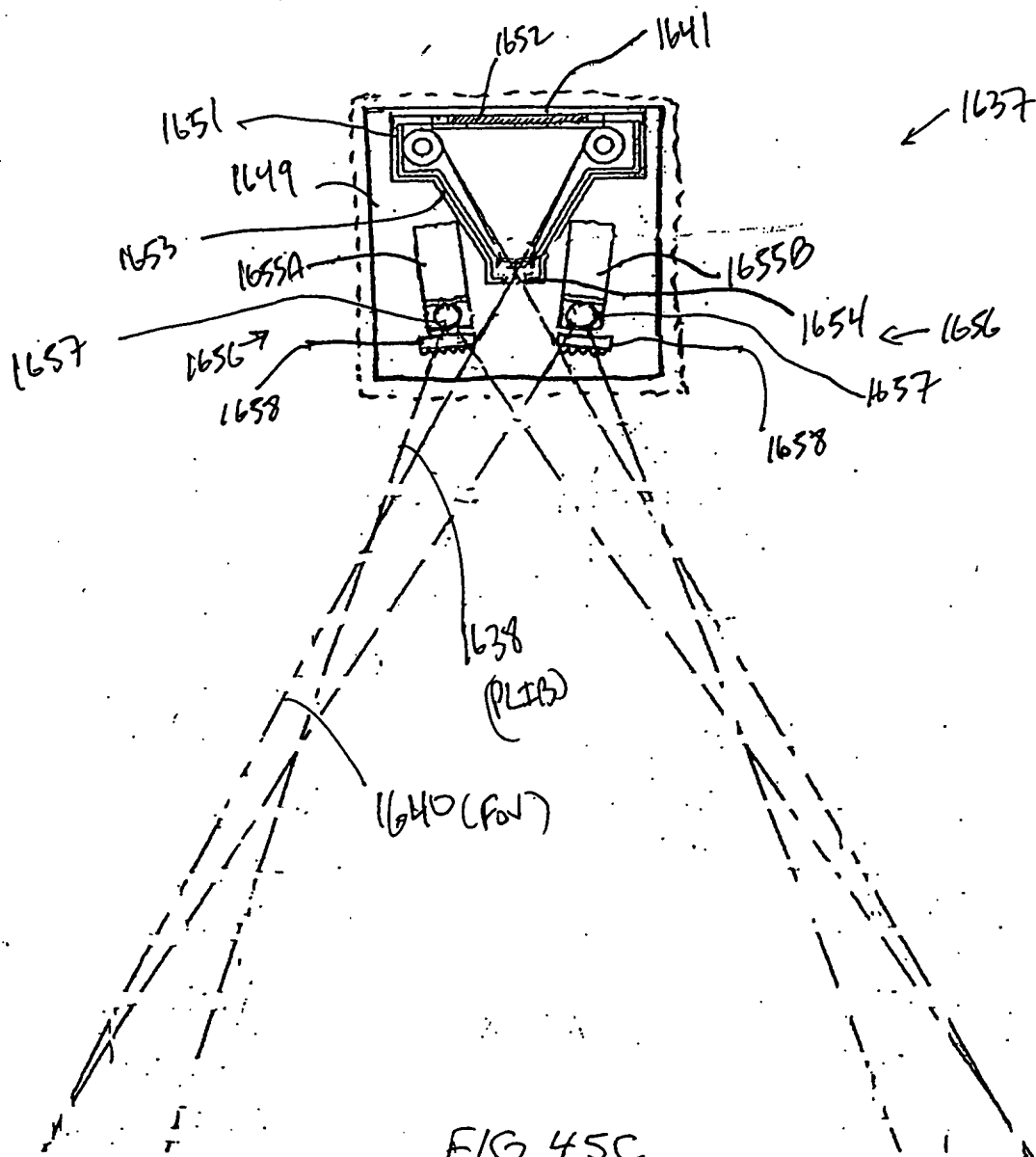


FIG. 45B

09990585 12101

299/385



10121-33306660

300/385

1-D
display
unit

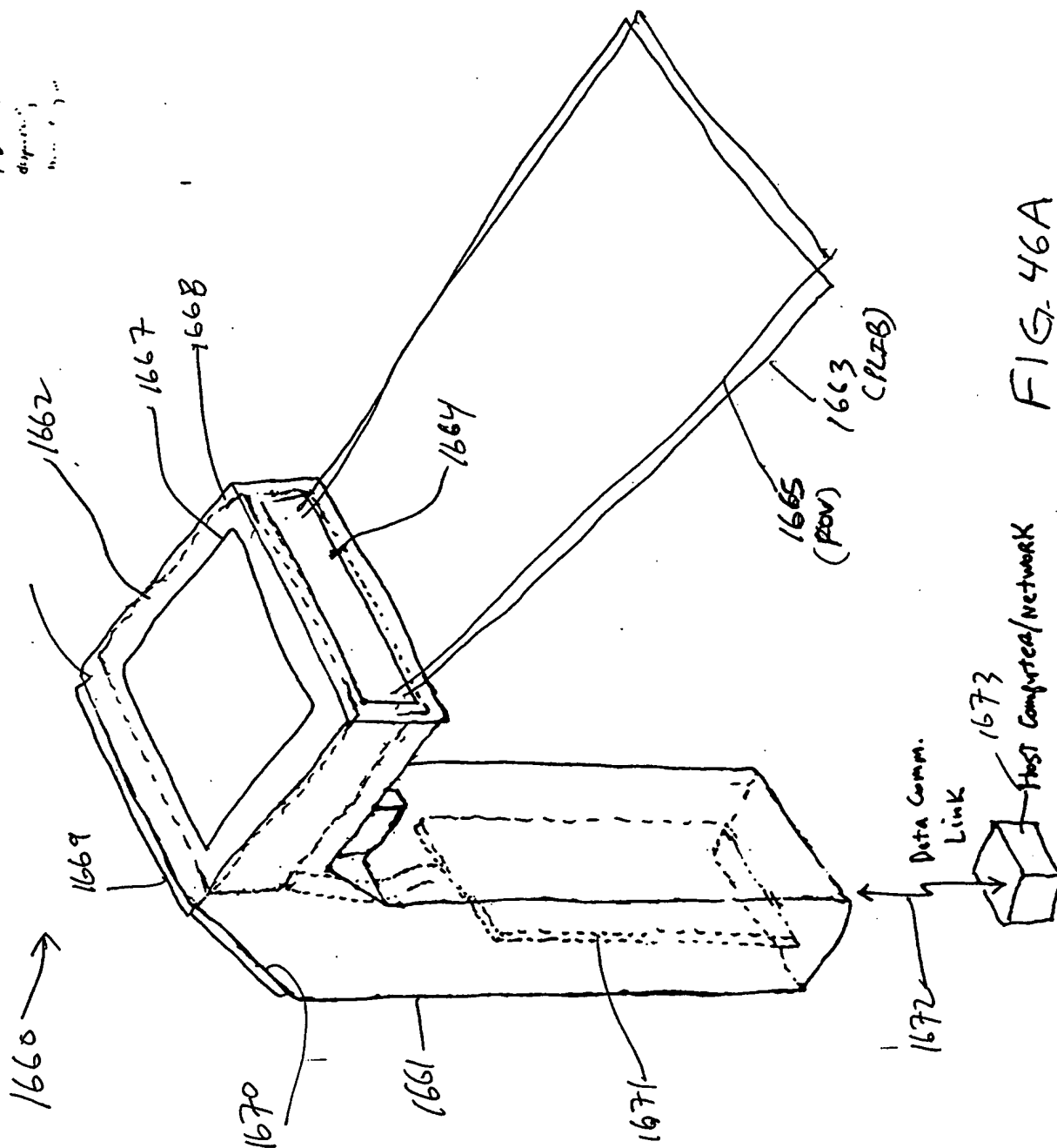


FIG. 46A

0990555-112101

301/385

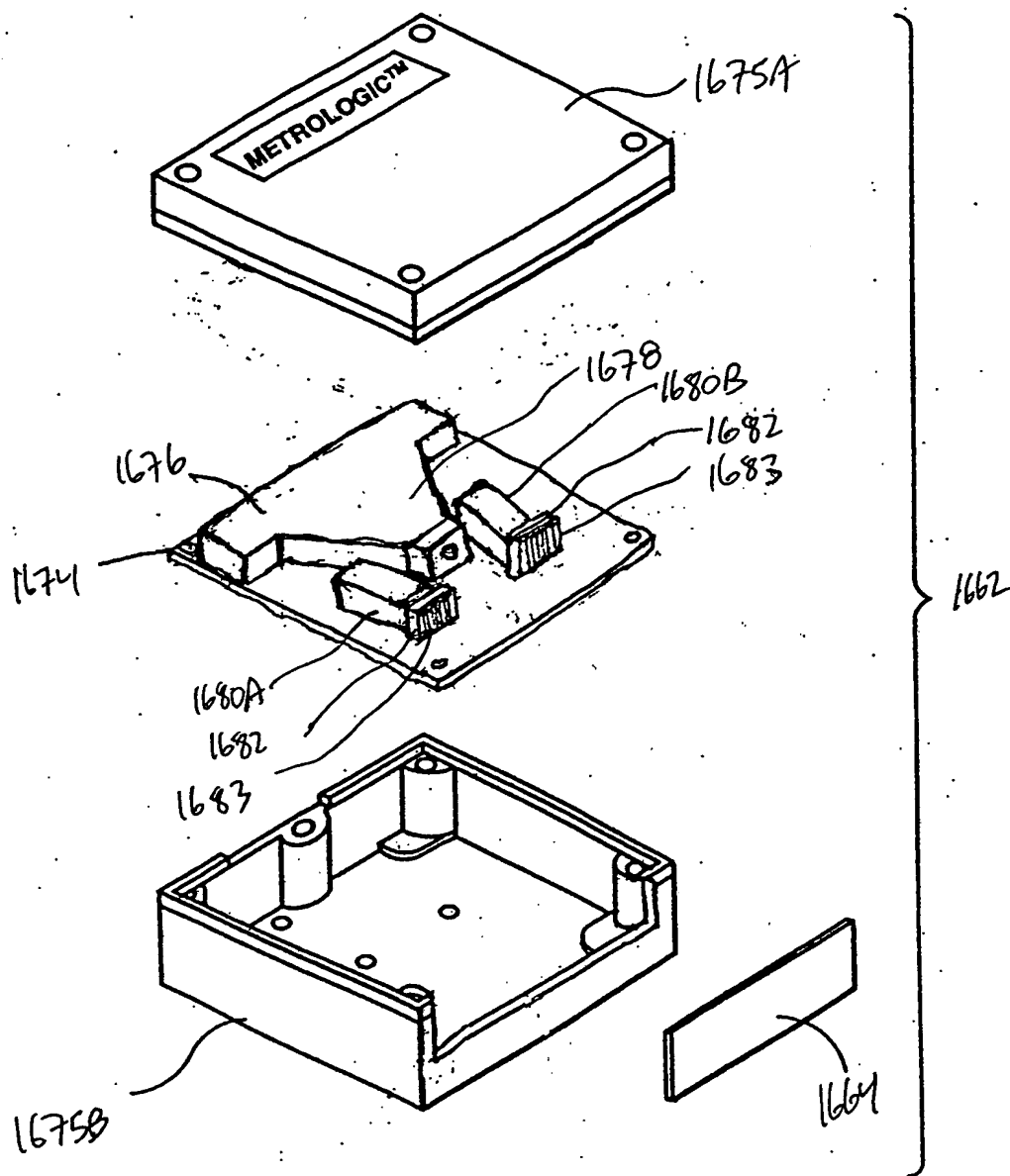
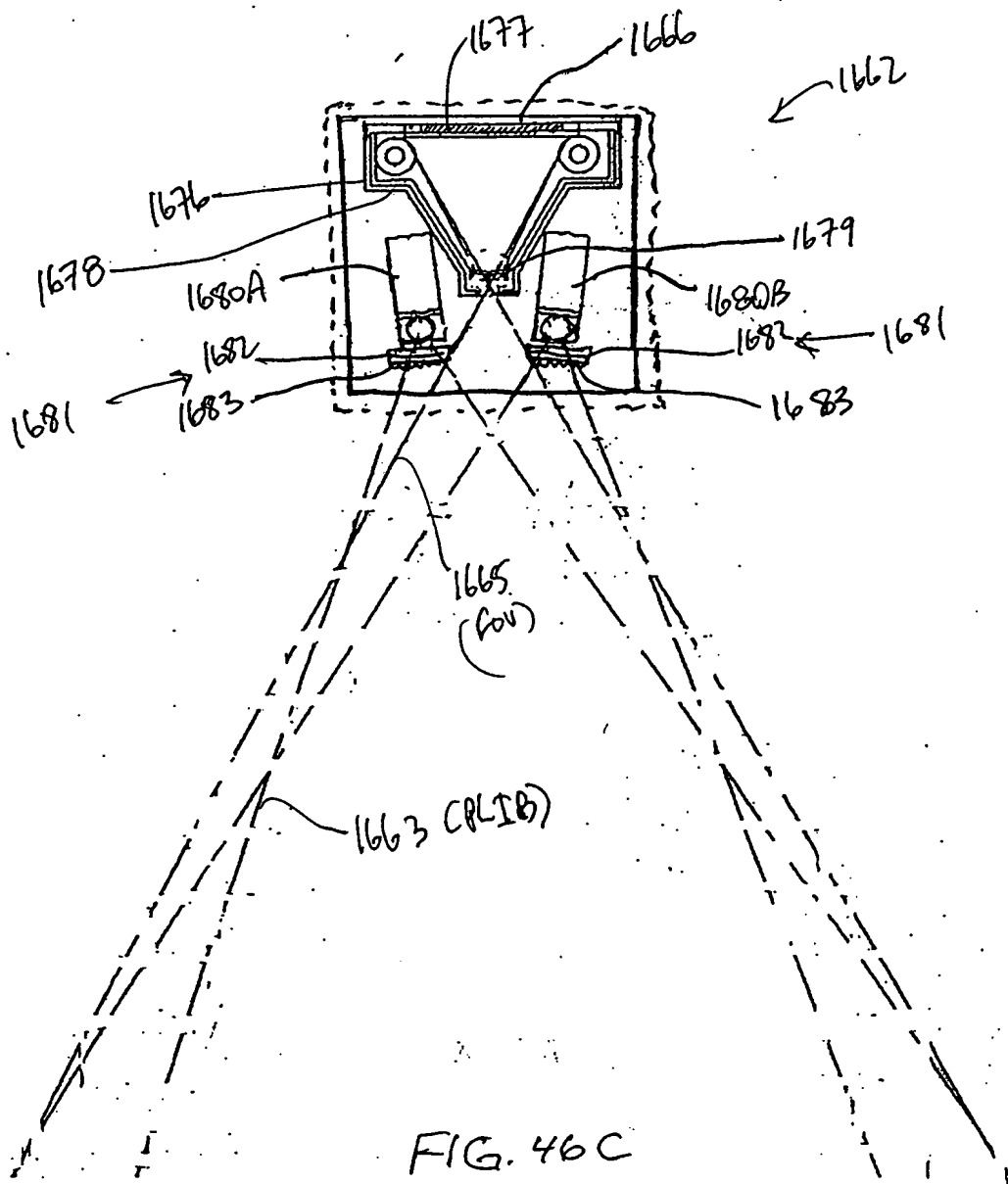


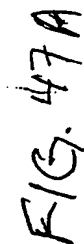
FIG. 46B

000055-1101

302/385



1-D
disposition;
nature, ...



000055-1114
10121 5350660

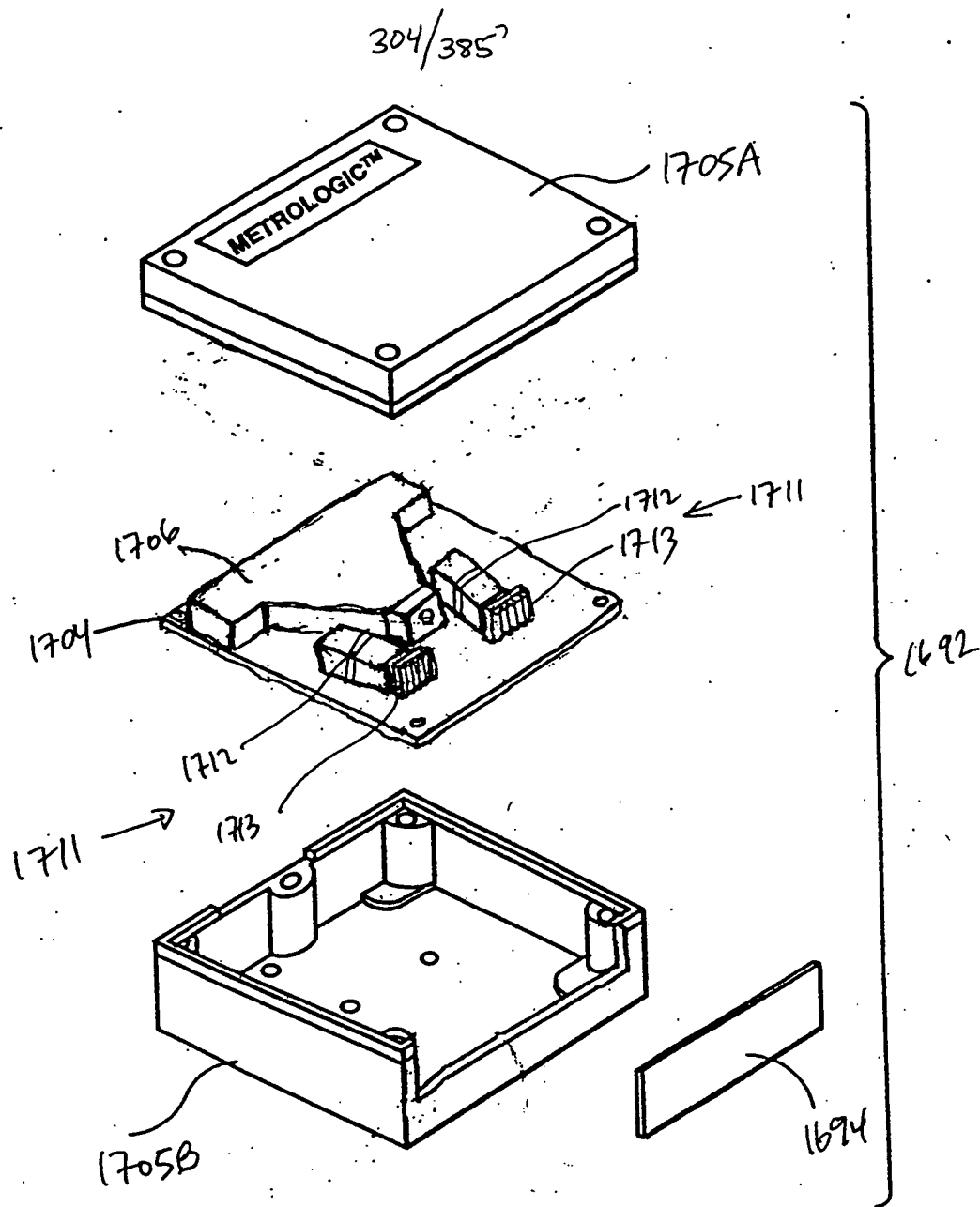
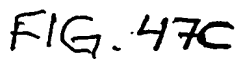


FIG. 47B

[illegible]

00000585-12101

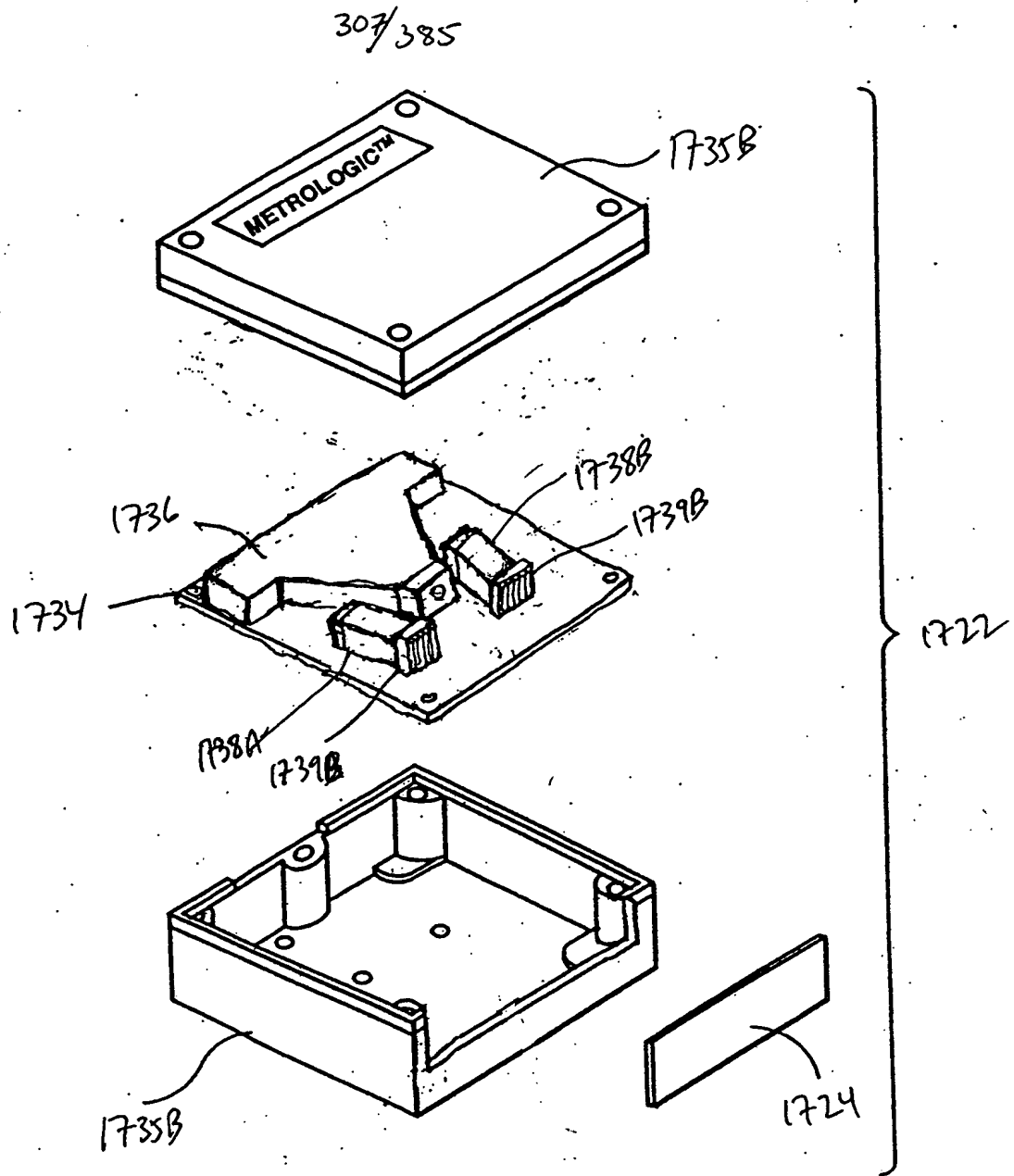


FIG. 4aB

000055-11101
FOR 5850660

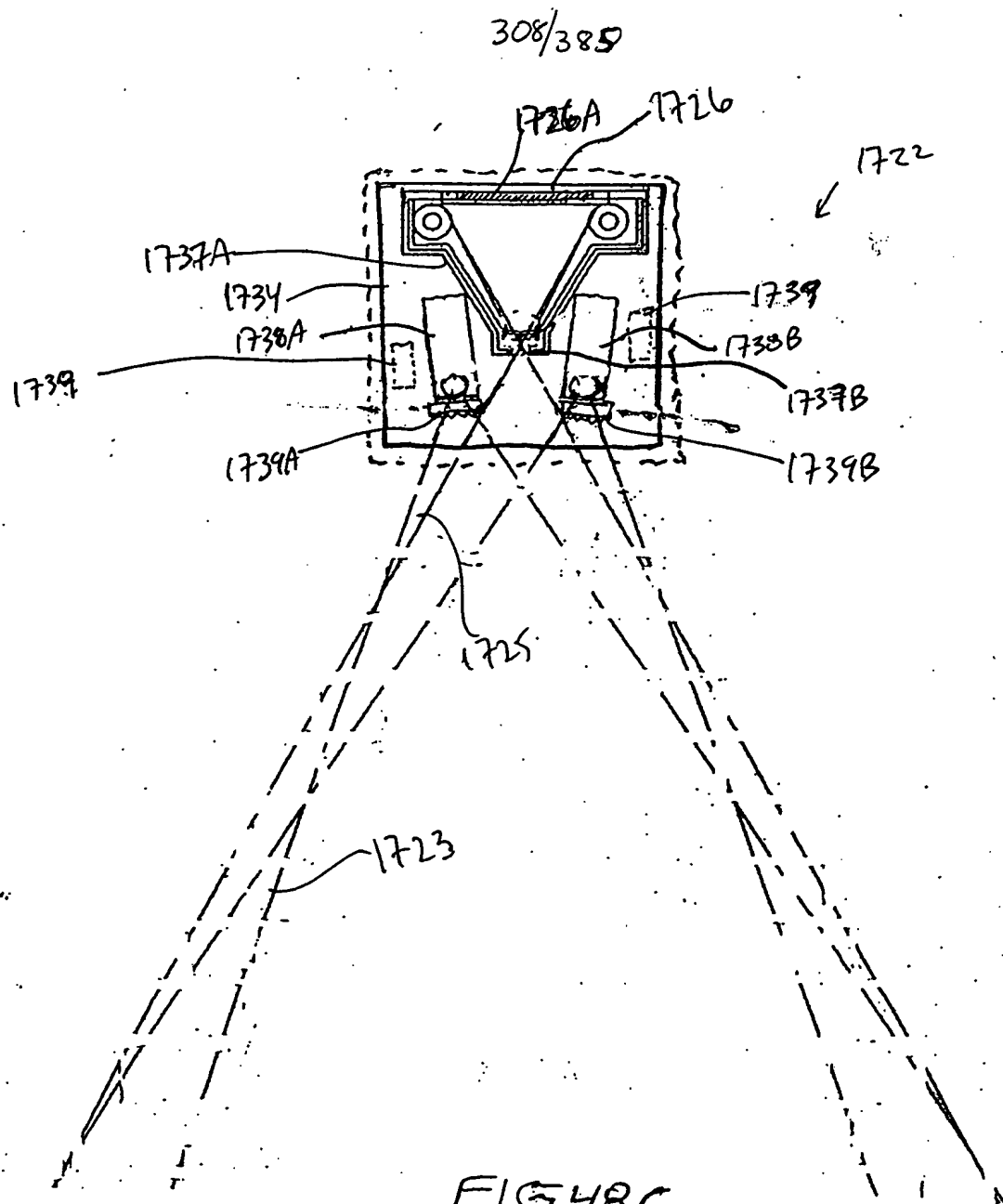
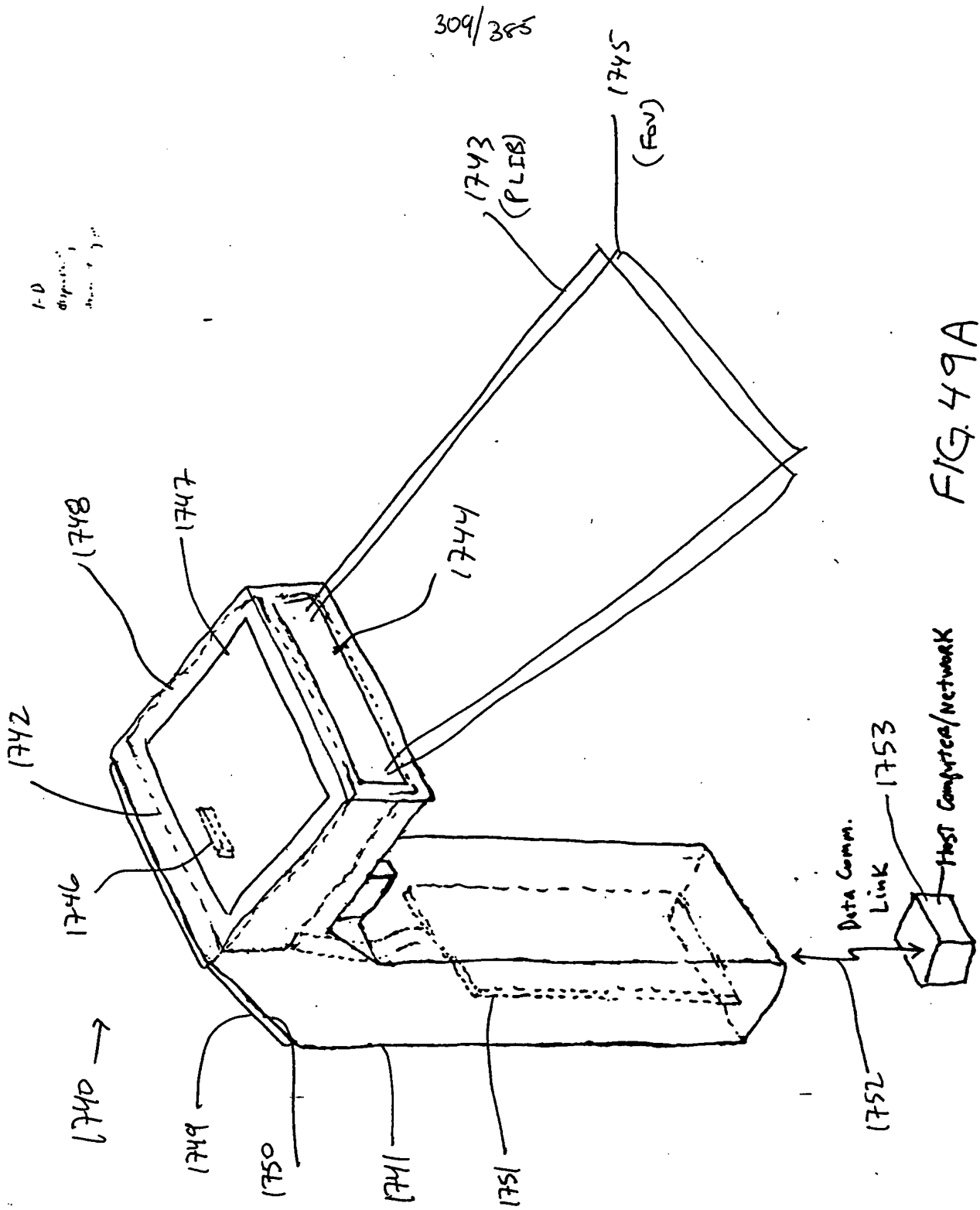


FIG. 48C

FIG. 49A



310/385

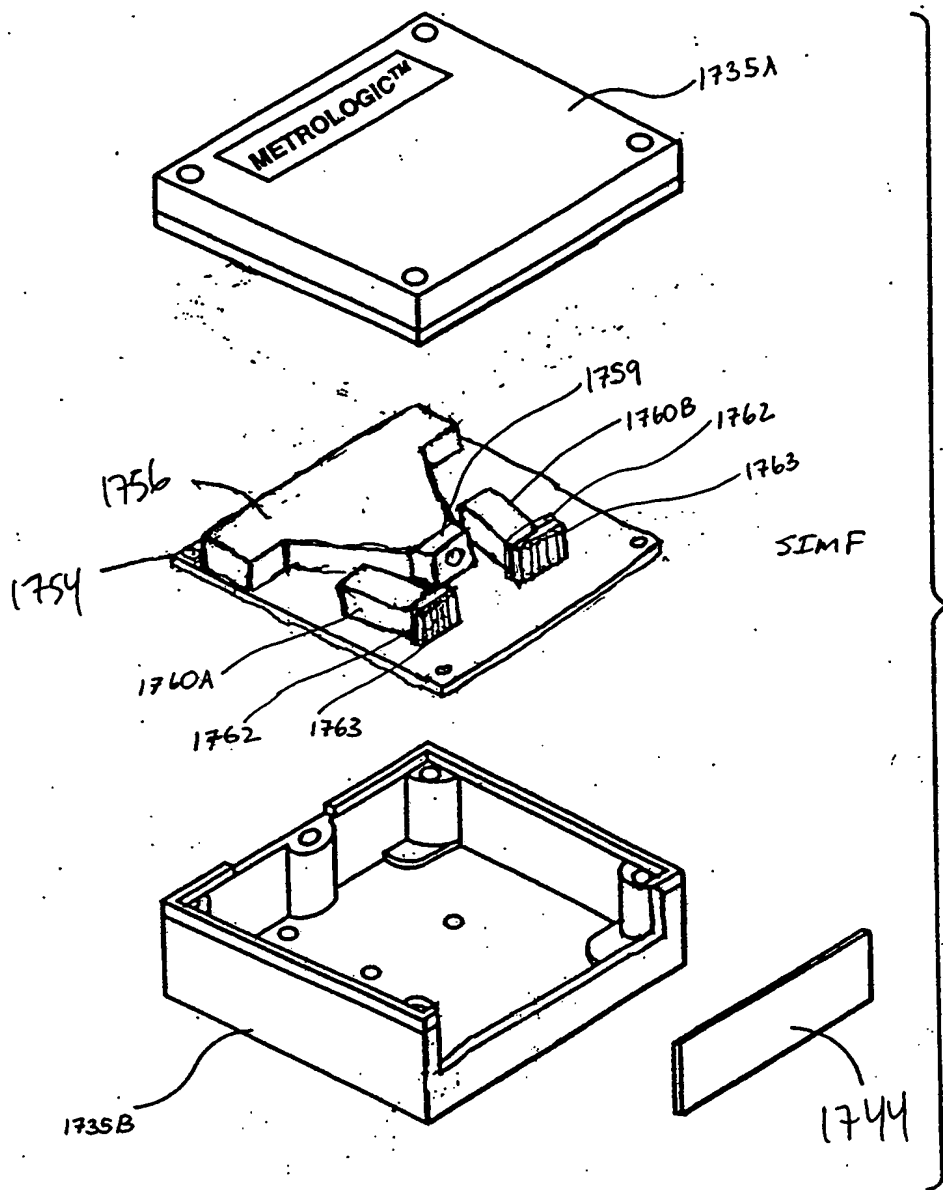


FIG. 49B

0000585-112101

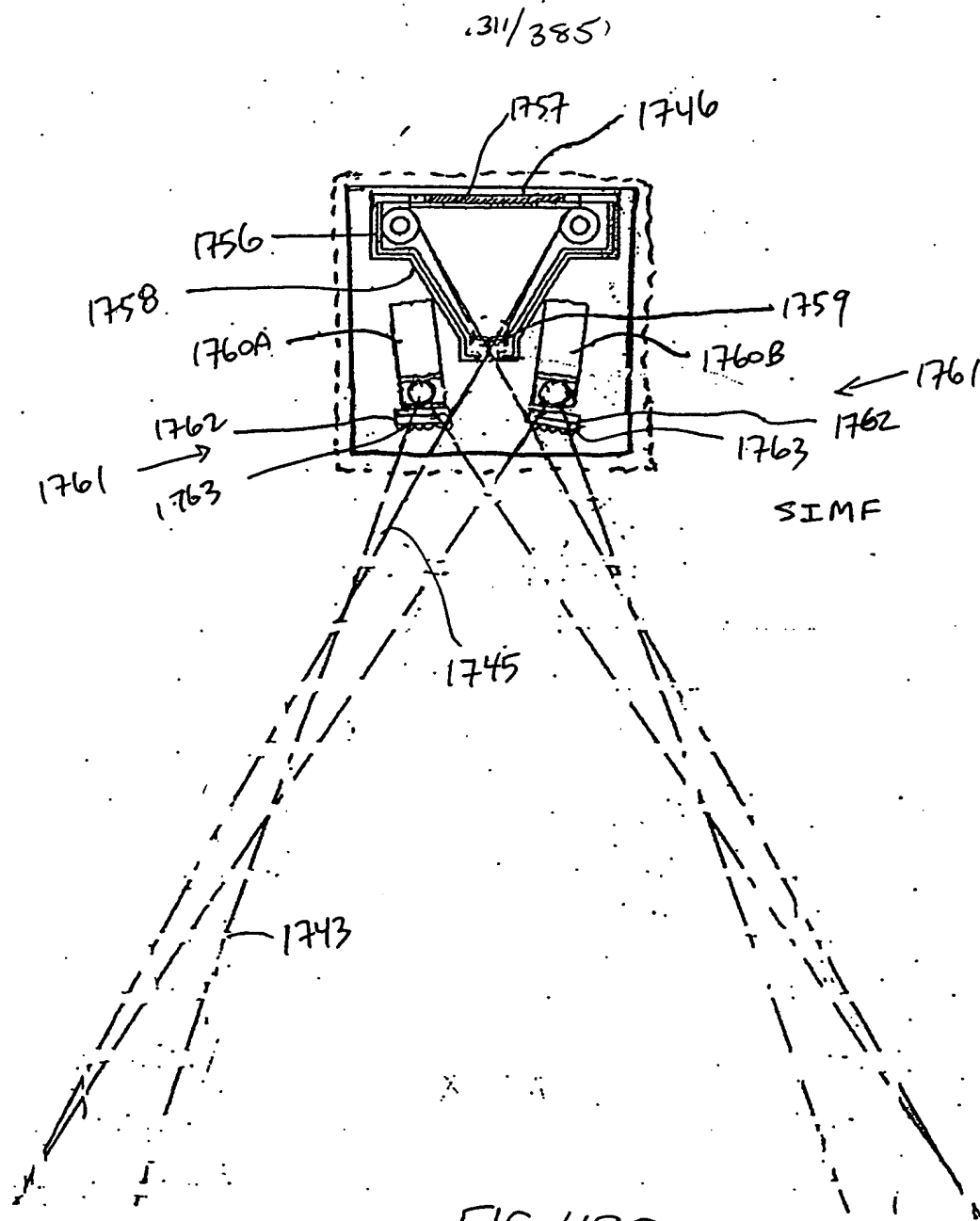
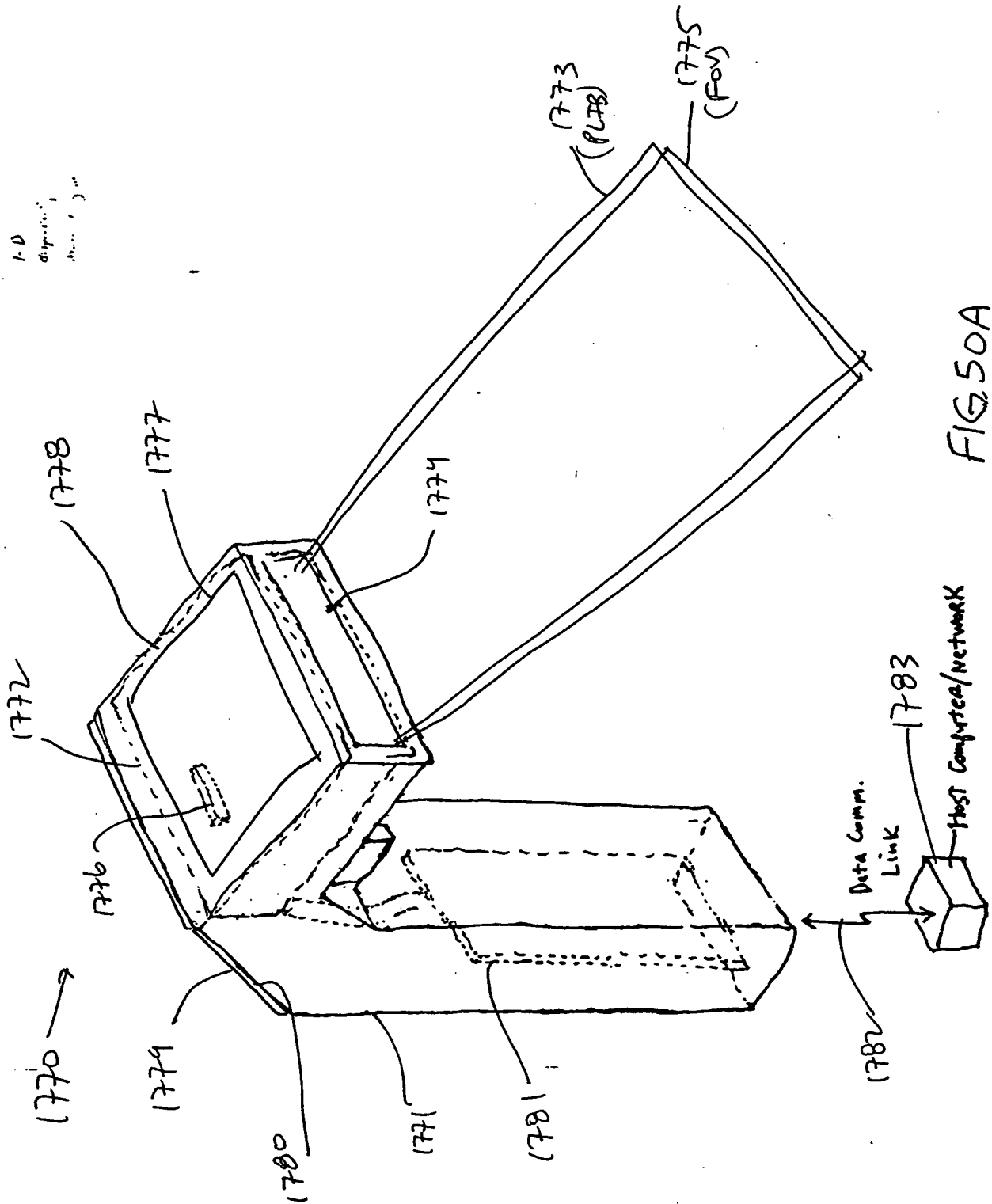


FIG.49C

312/385



313/ 385

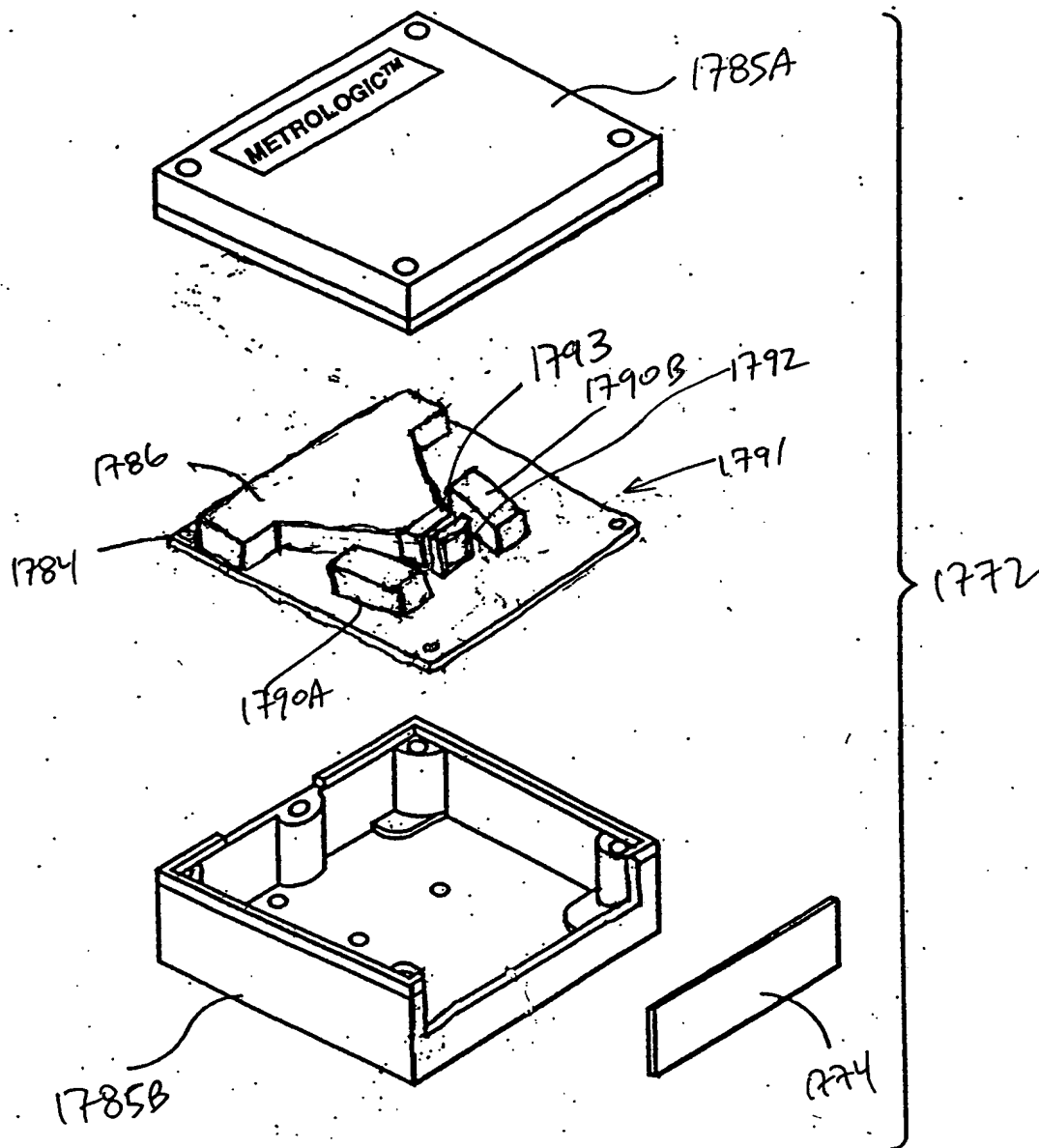


FIG. 50B

0090585 112104

314/385

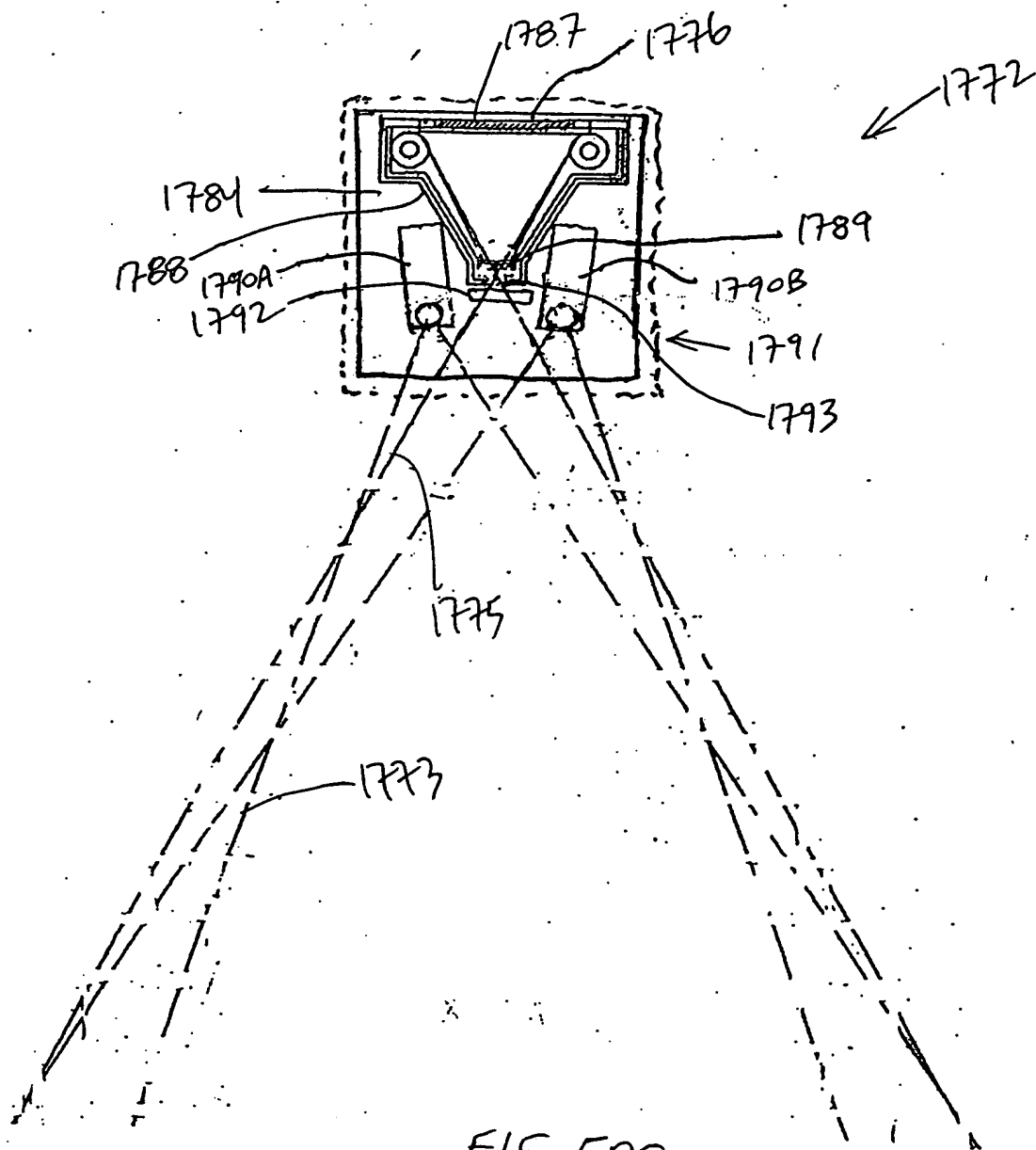


FIG. 50C

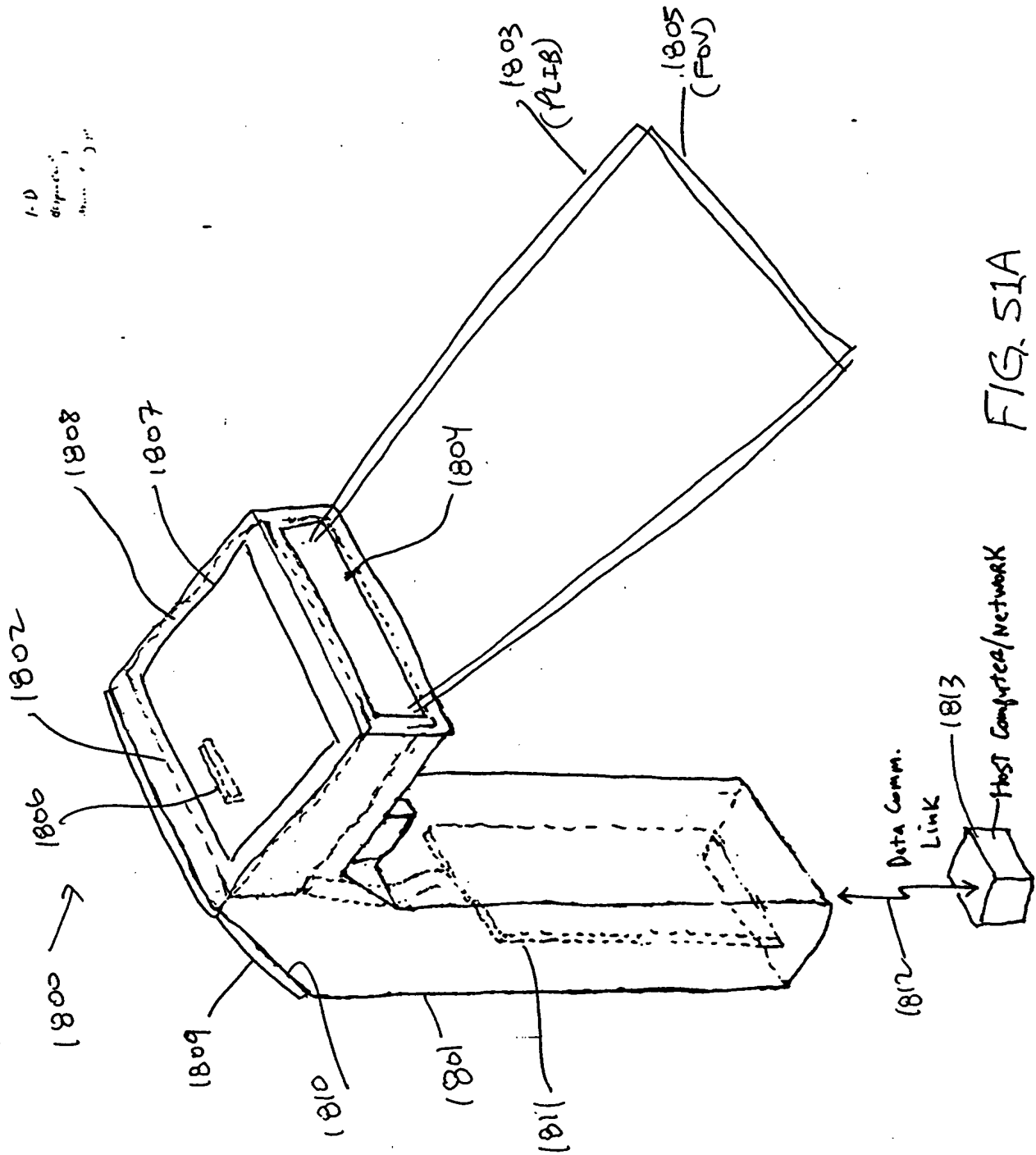


FIG. 51A

0000555 112101

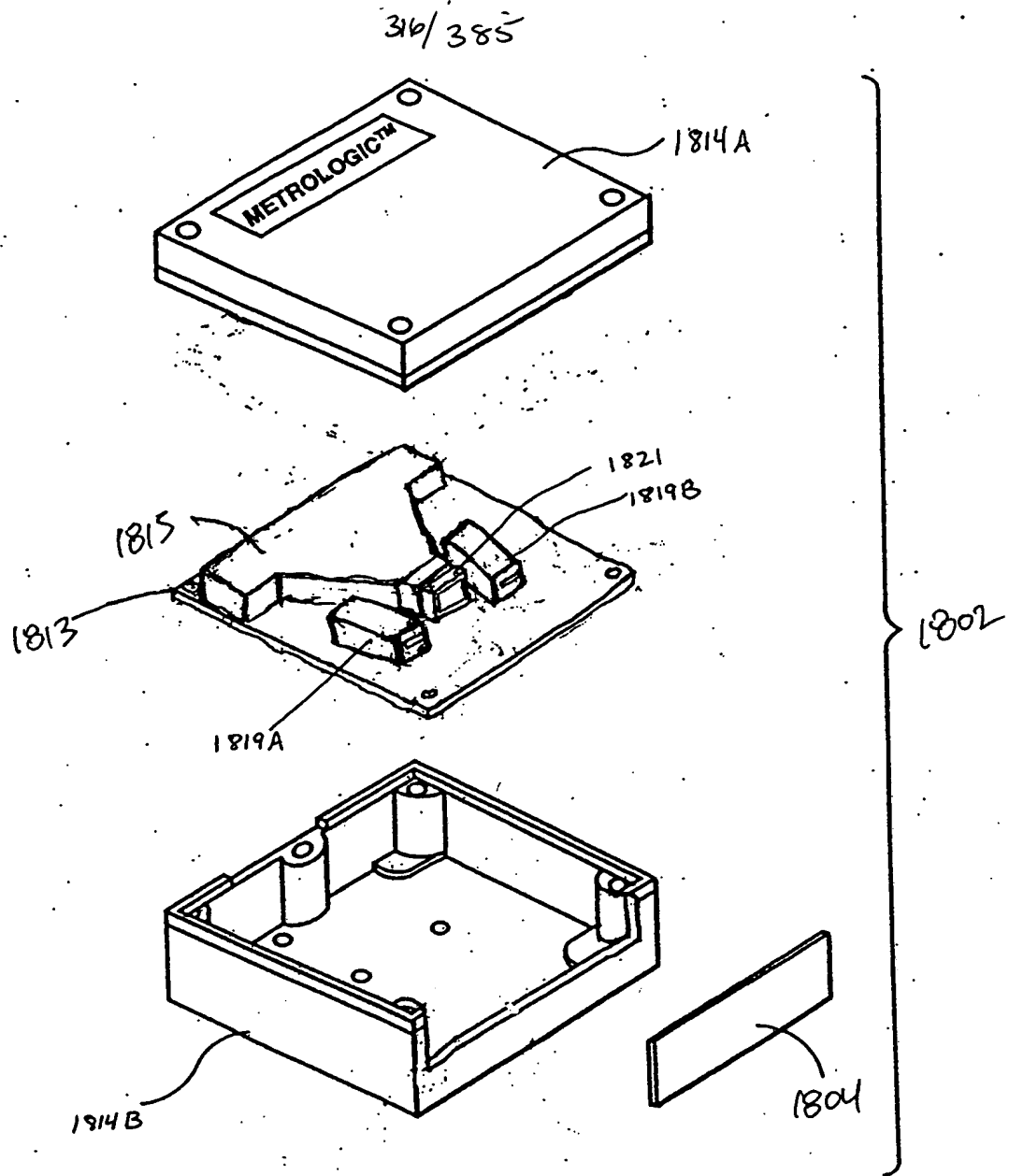
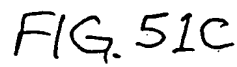
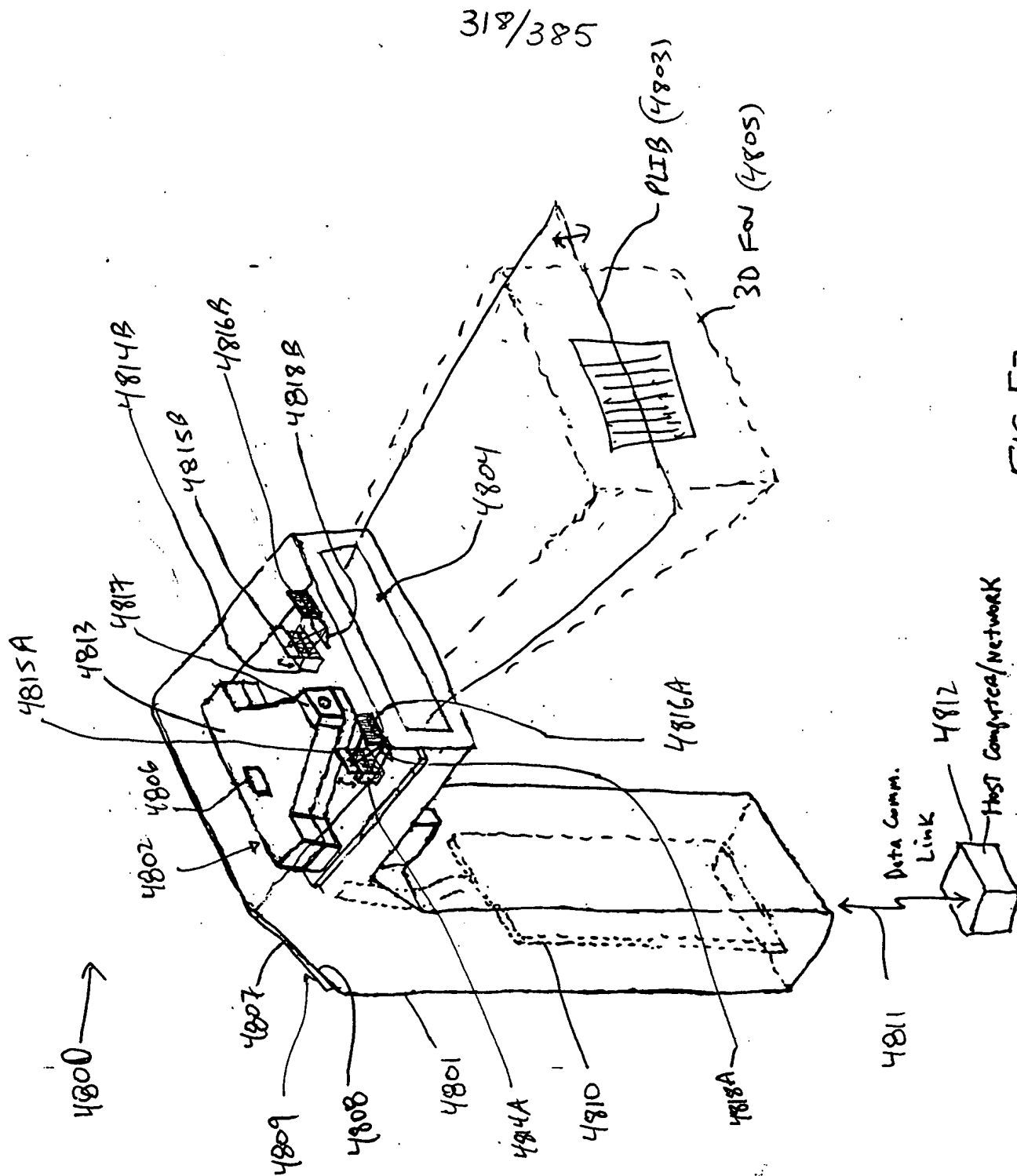


FIG. 51B

[illegible]



319/385

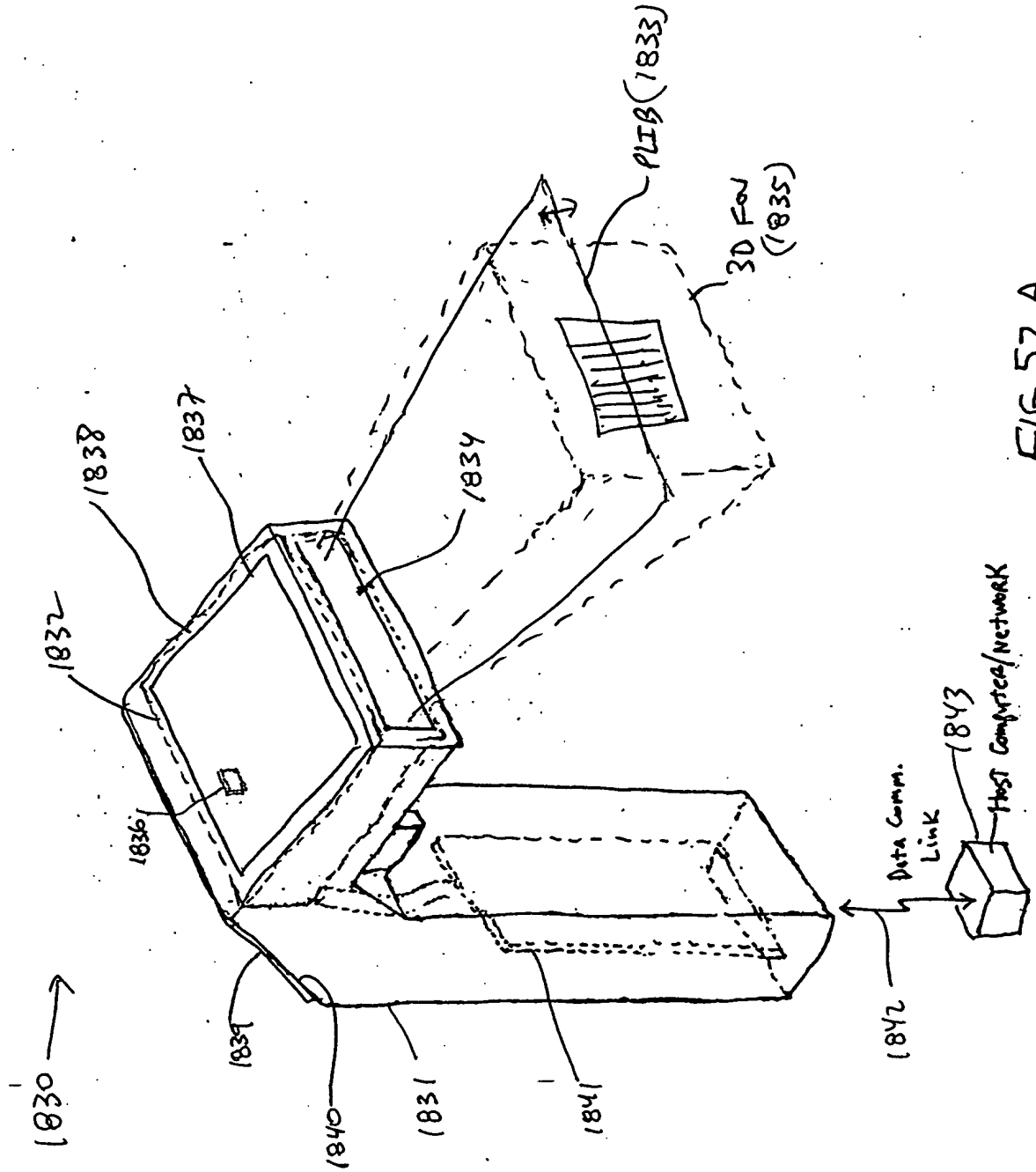


FIG. 52A

000055 413401 10221 53505550

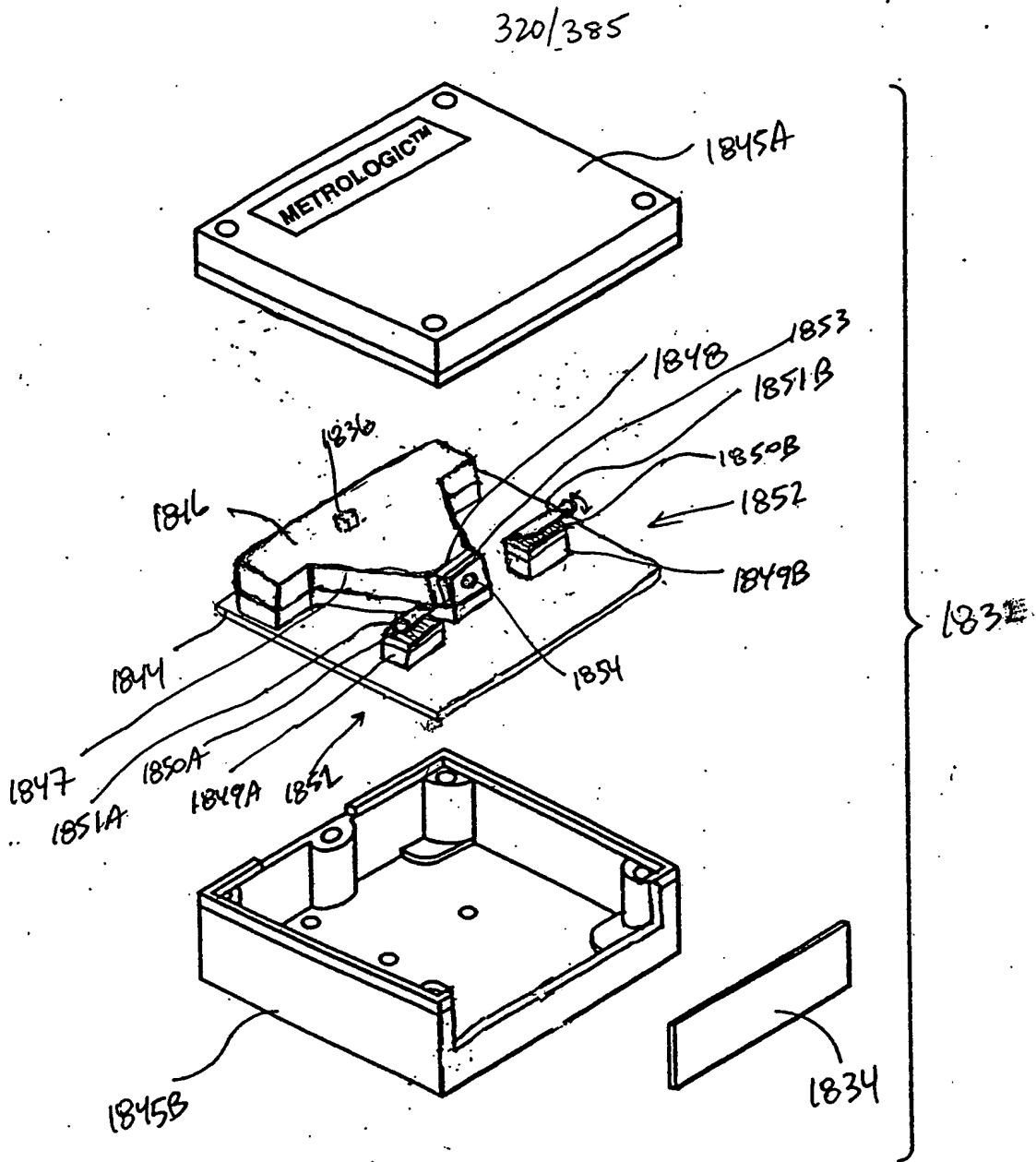
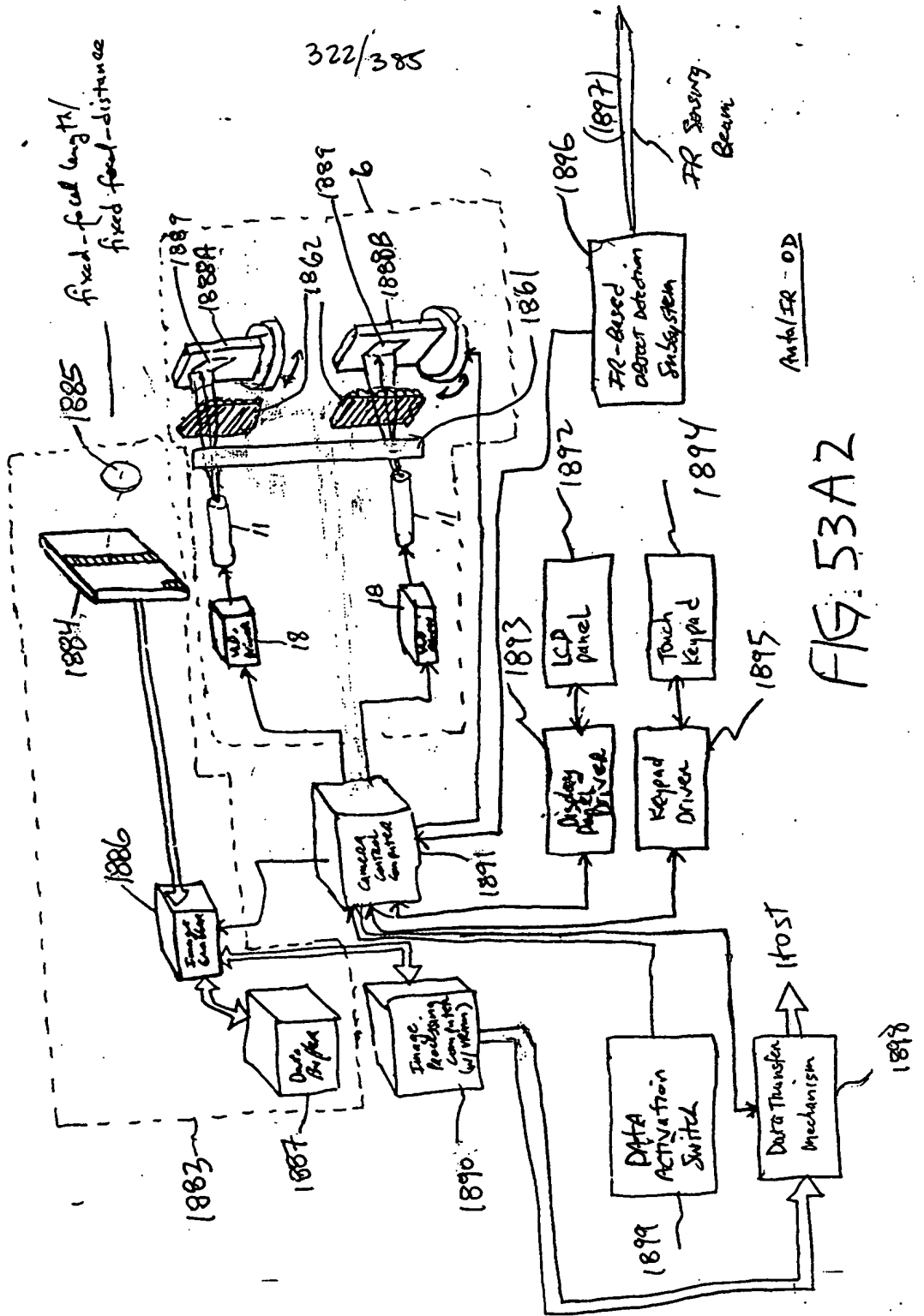


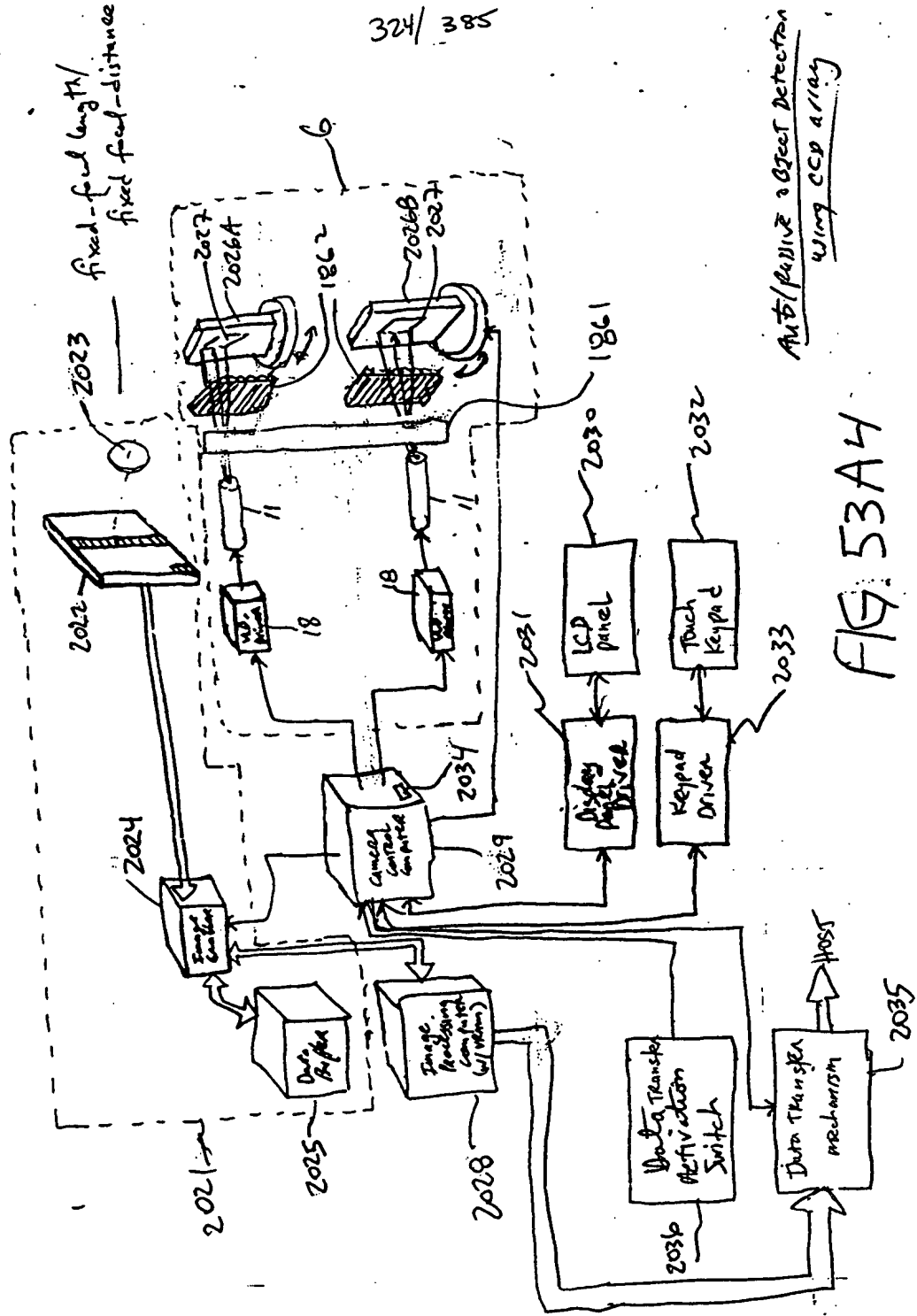
FIG. 52B

Fig. 1I 3A-3B

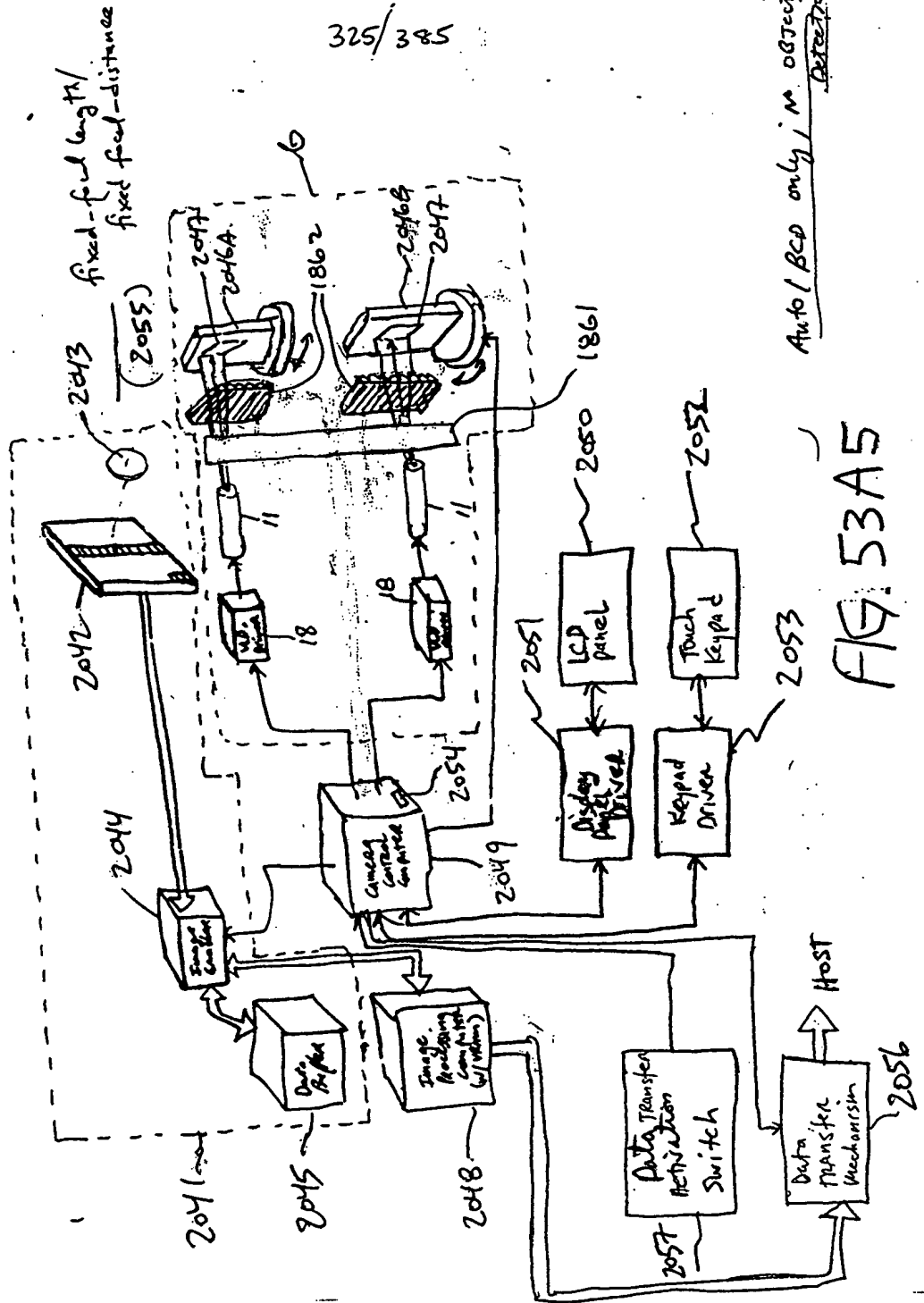
1880



2022 →



2040



325/385

Auto / BCD only / no object detection

FIG. 53A5

2080 →

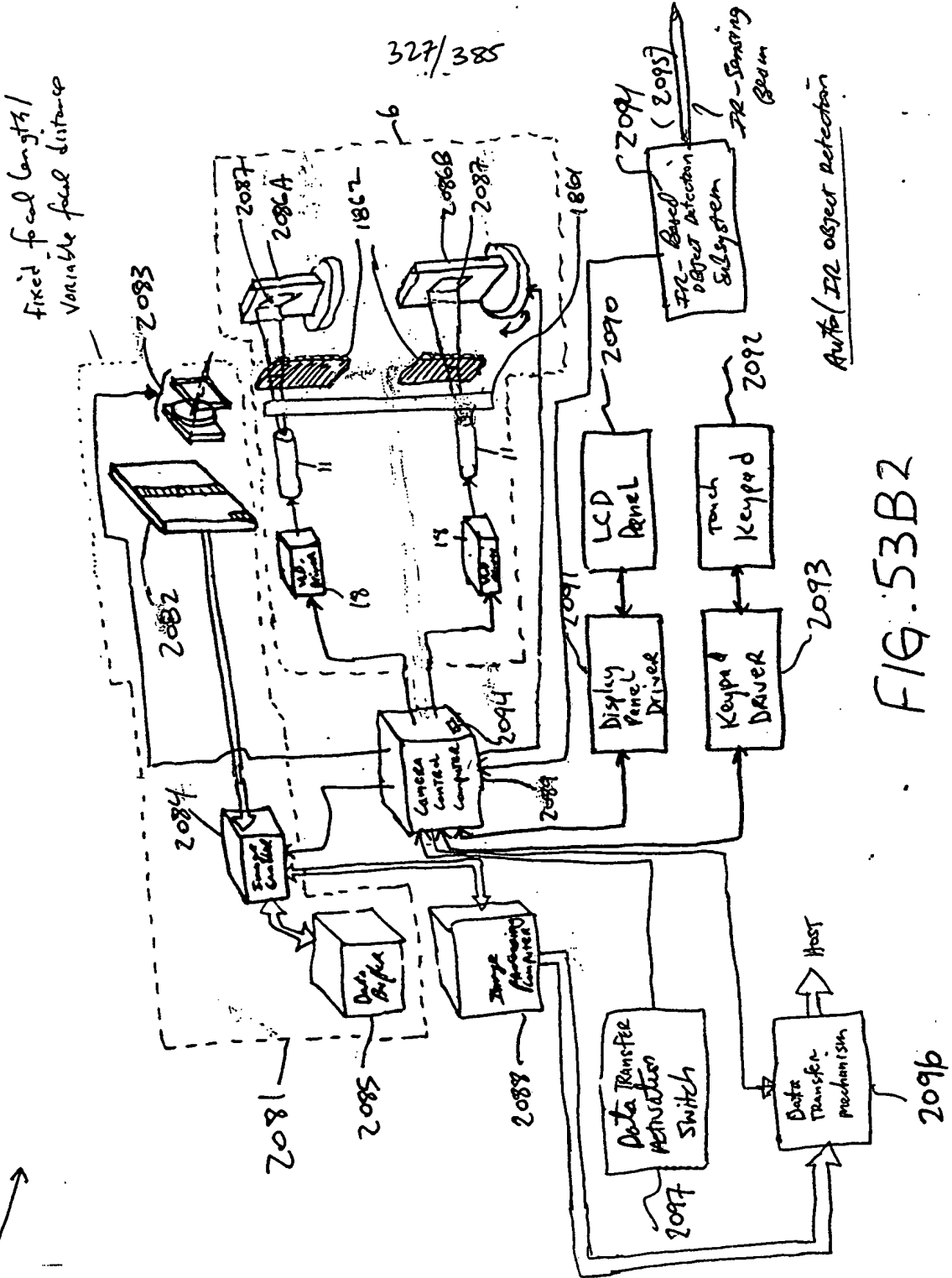
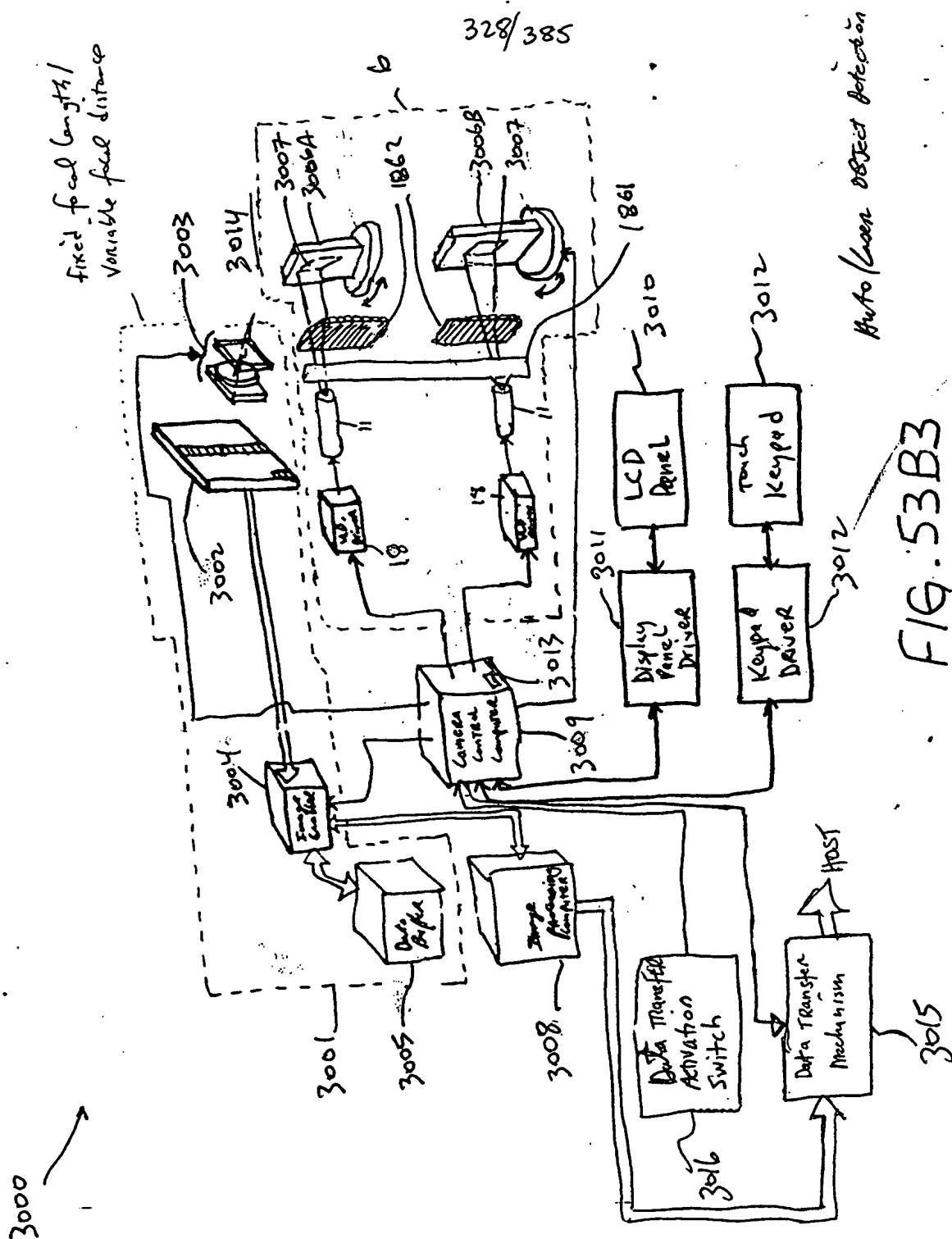
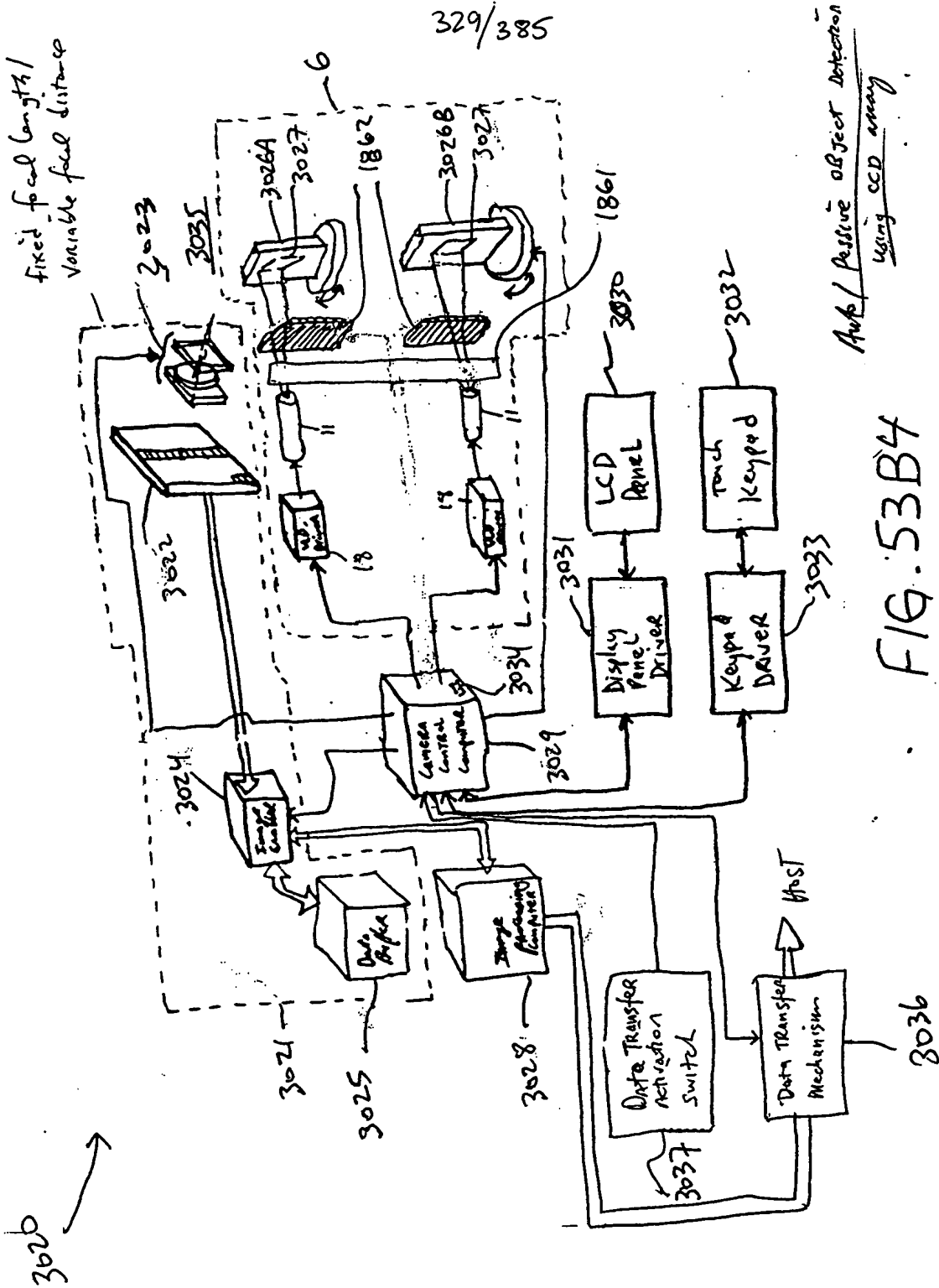


FIG. 53B2

[illegible]



3049c

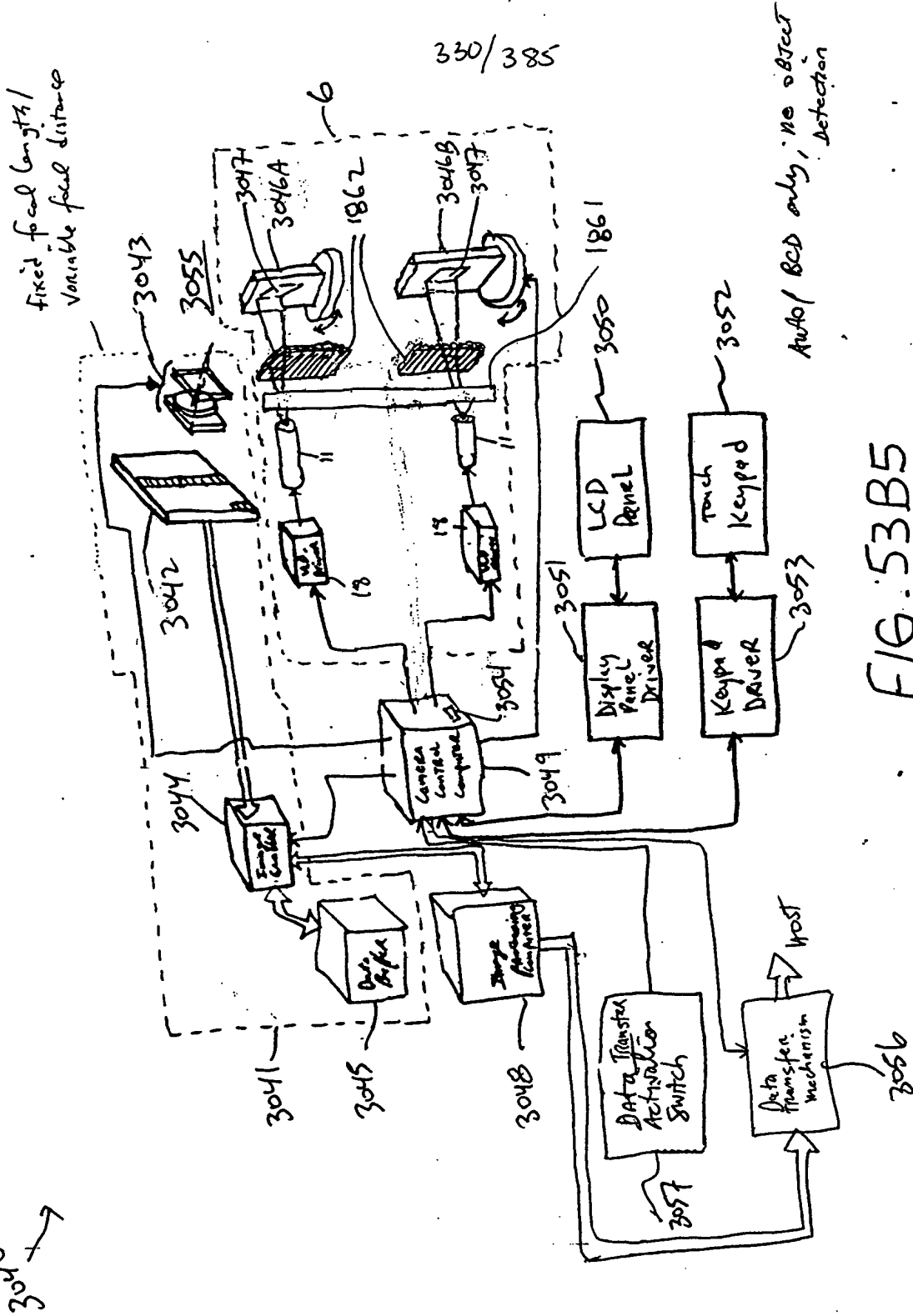


FIG. 53B5

330/385

Auto/BCD only, no object detection

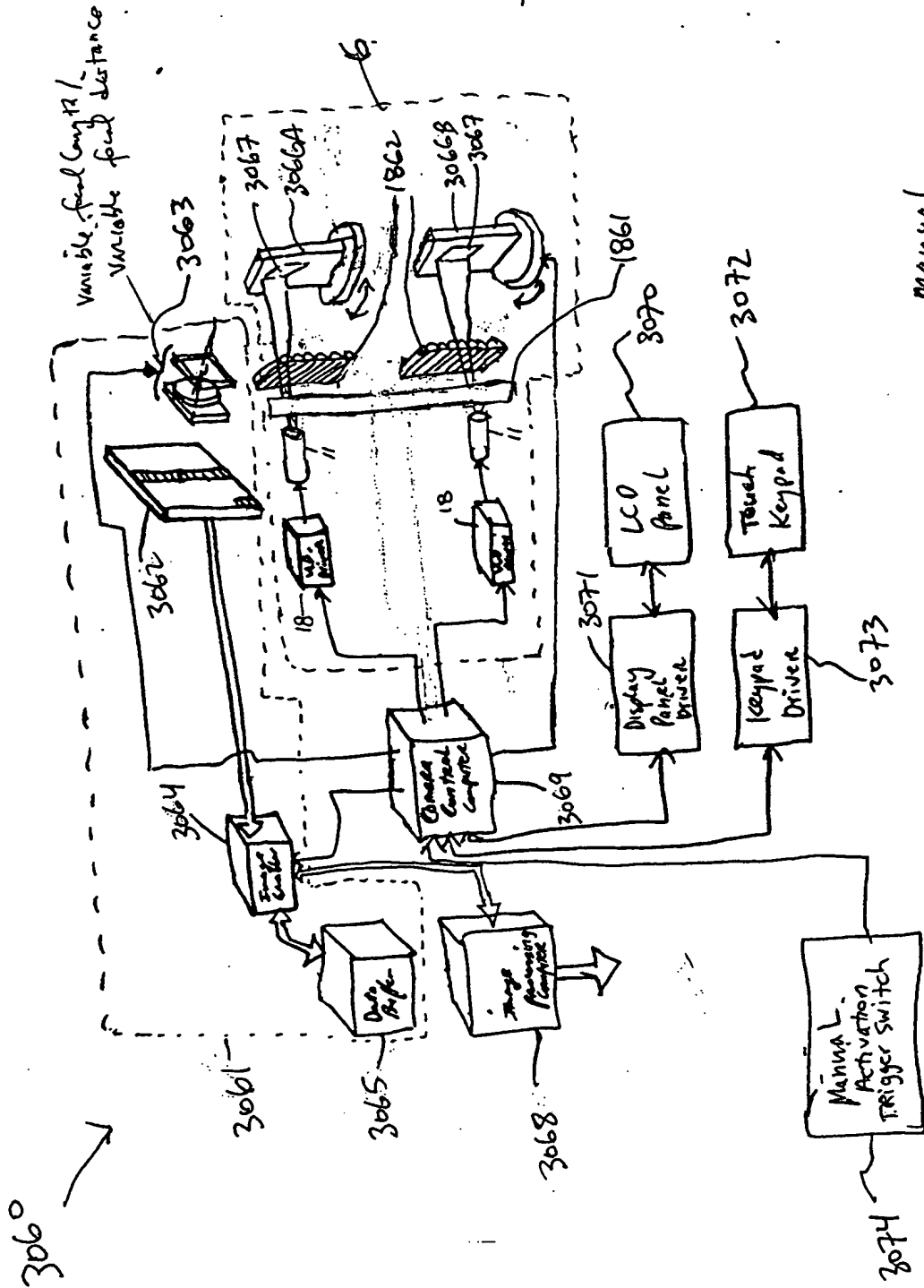
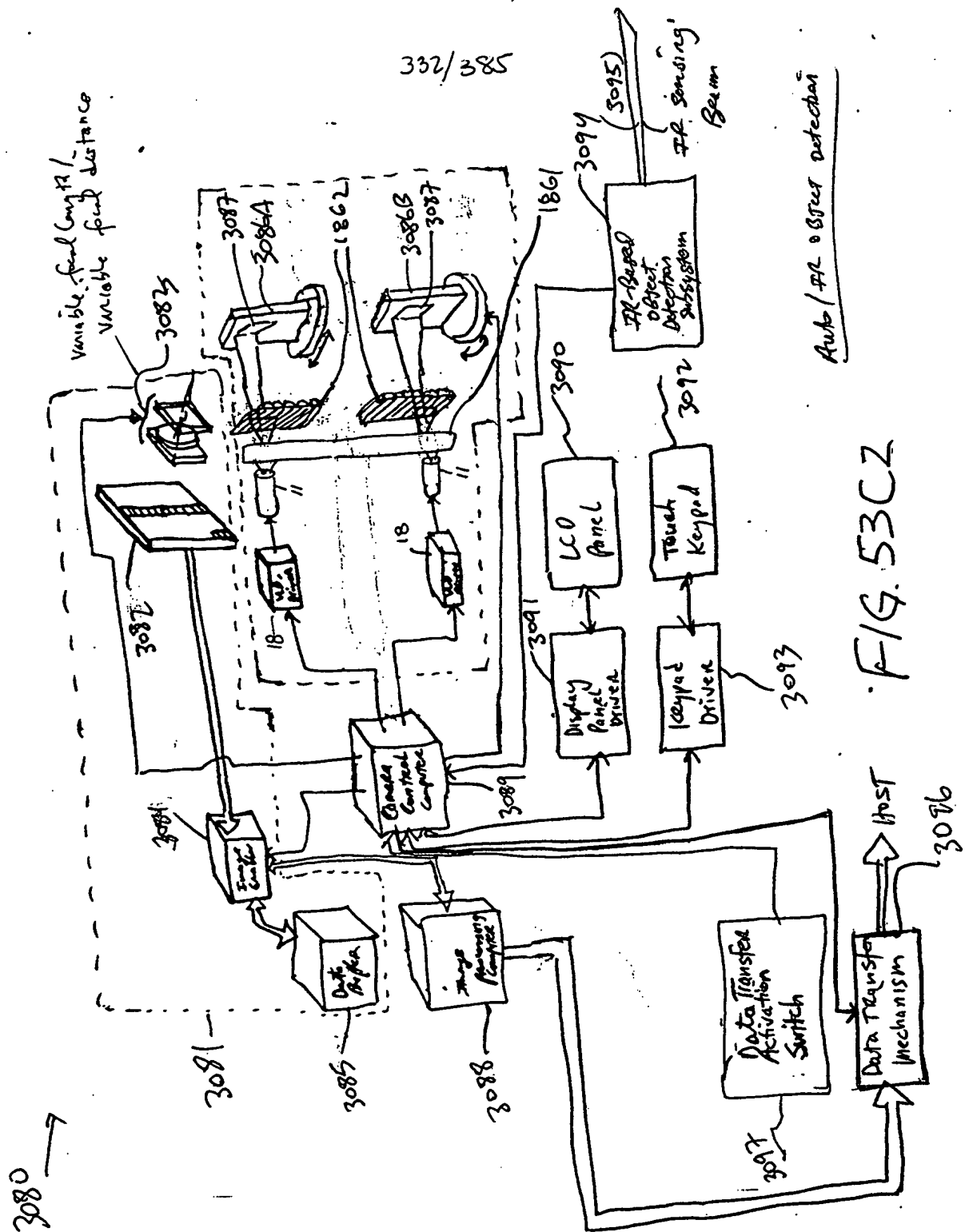


FIG. 53C1

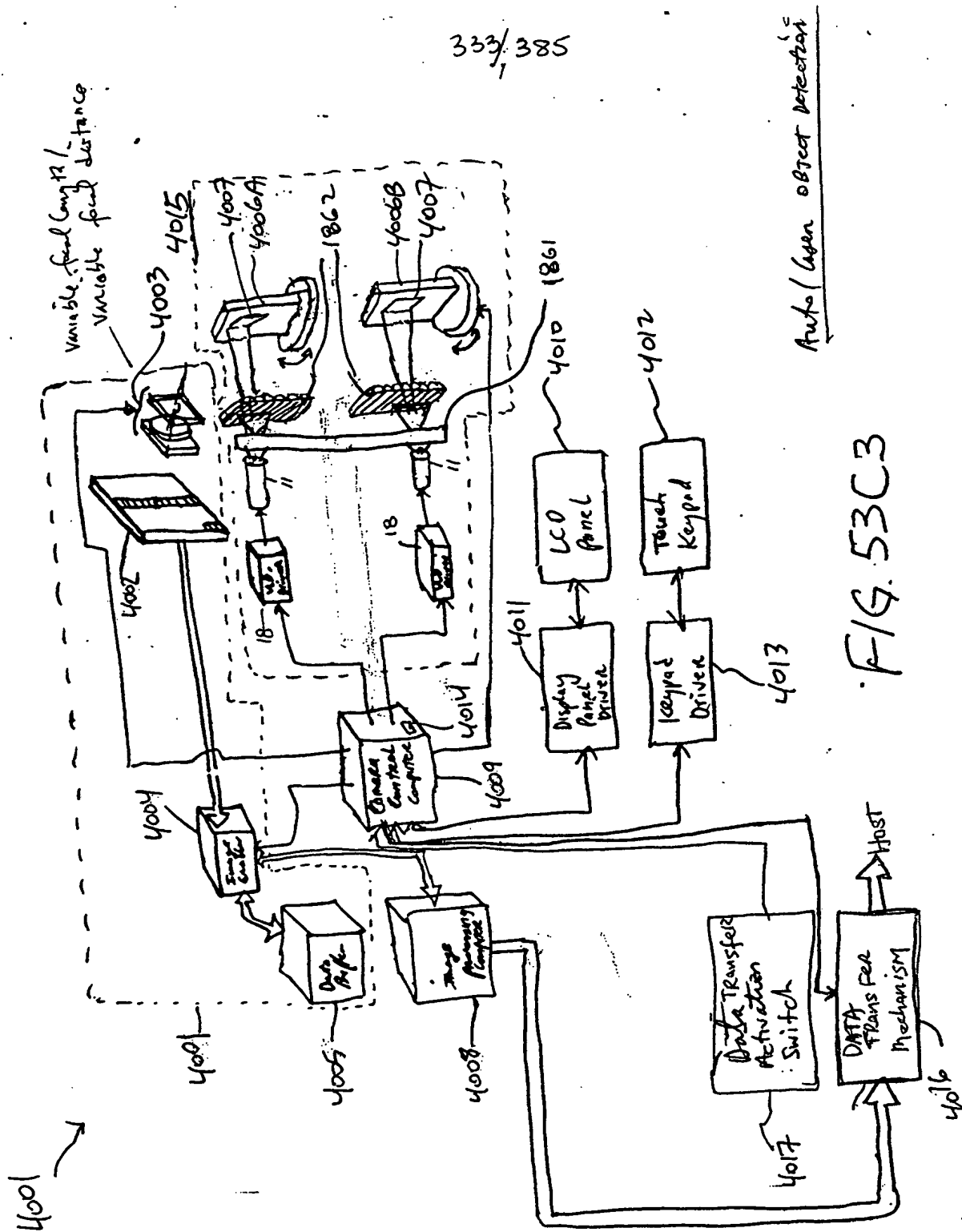
[illegible]

332/385

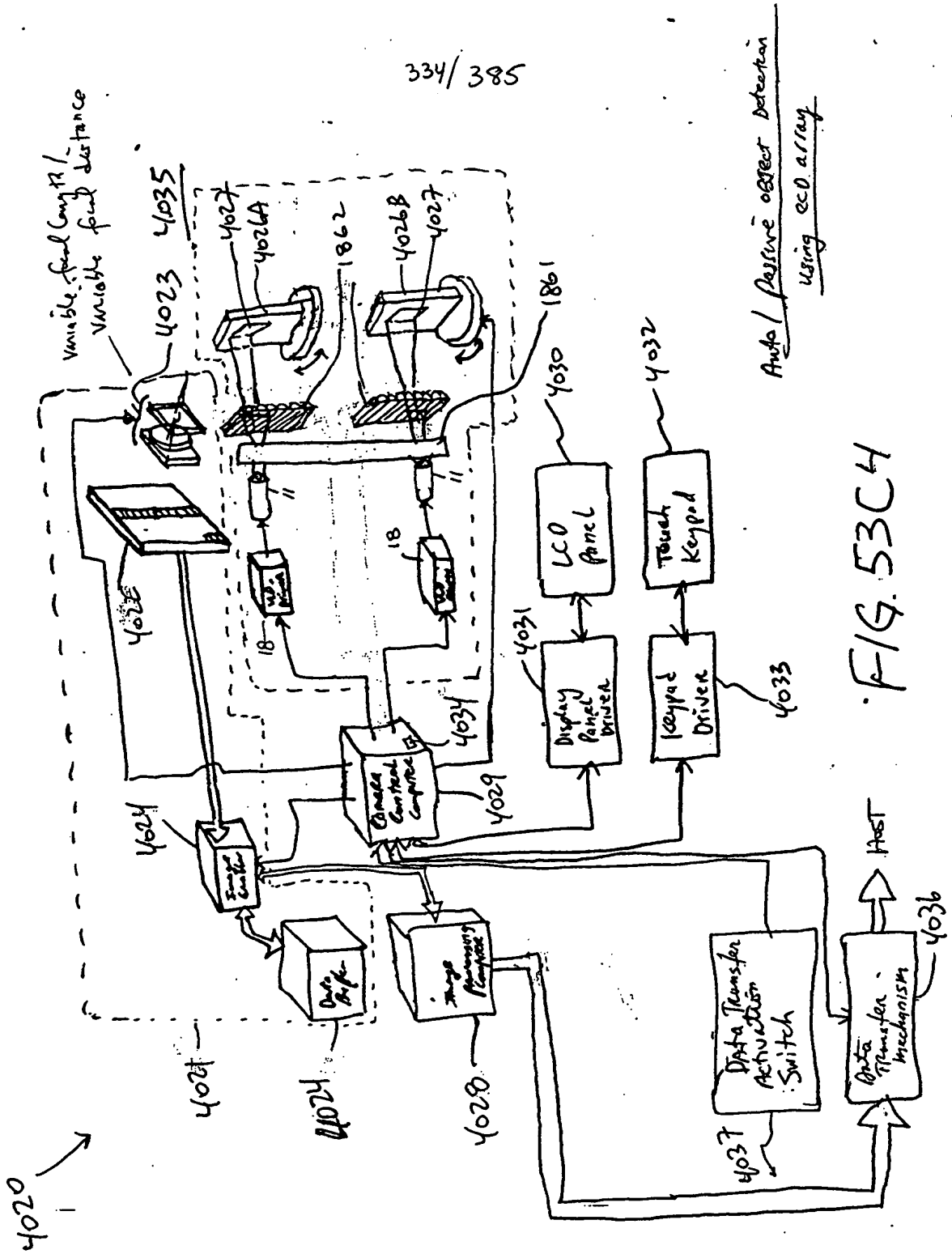
Aut / FR object detection

FIG. 53C2

333/385



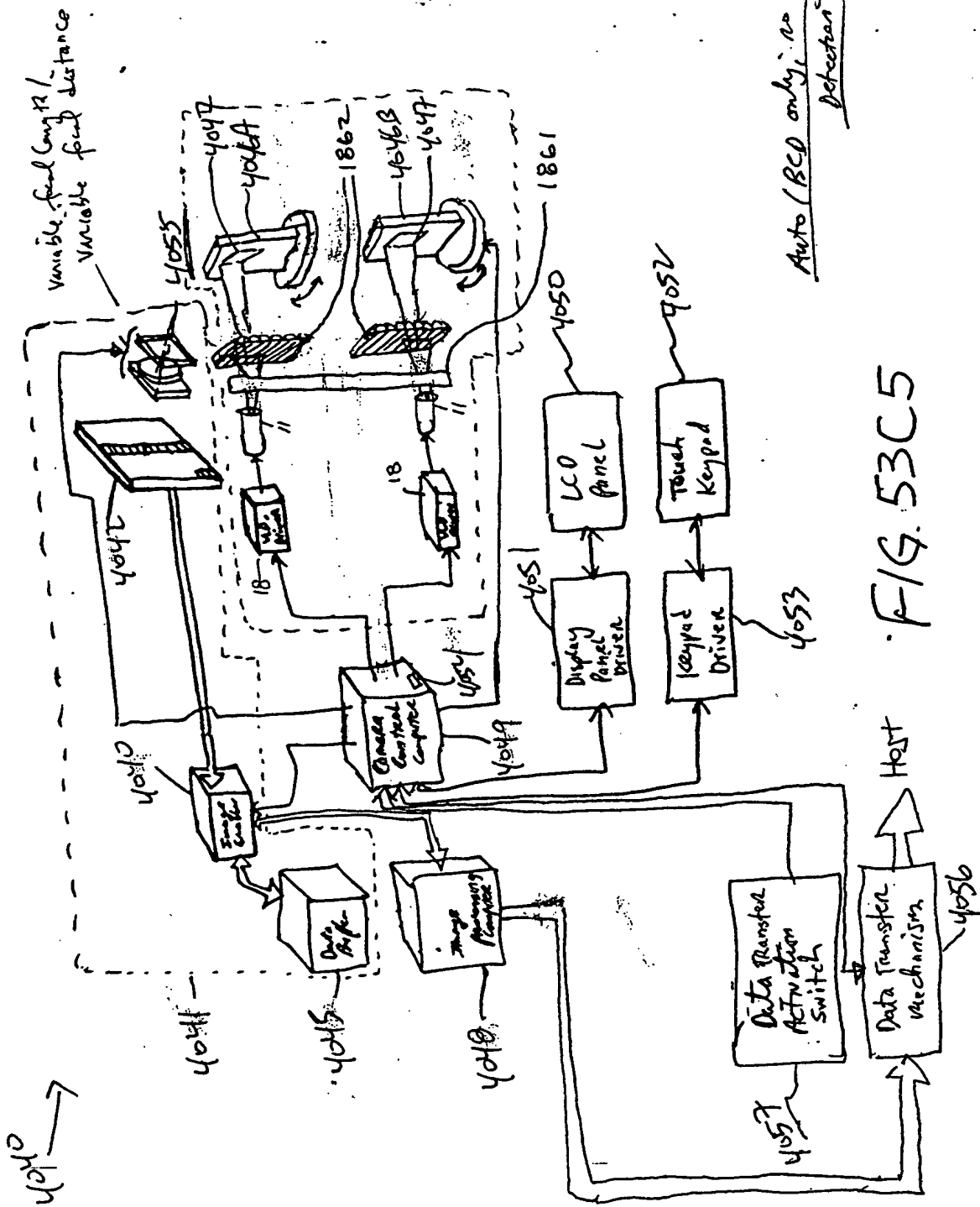
334/385



Auto / Passive object detection
using ECO array

FIG. 53C4

335/385



Auto (BCD only) no object detection

FIG. 53C5

337/385

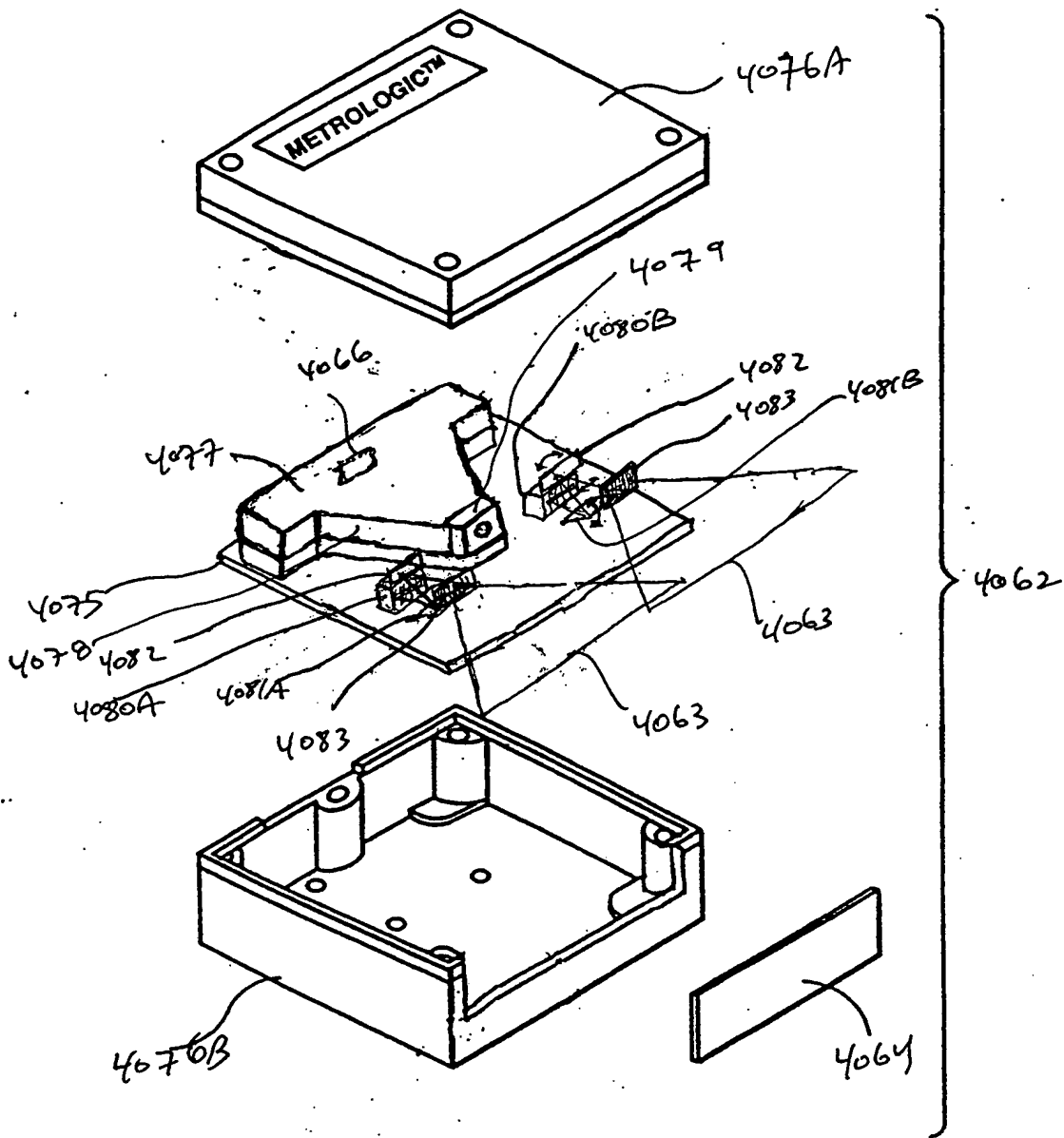


FIG. 54B

(dual mirrors)

Fig. 175A-SP1

338/385

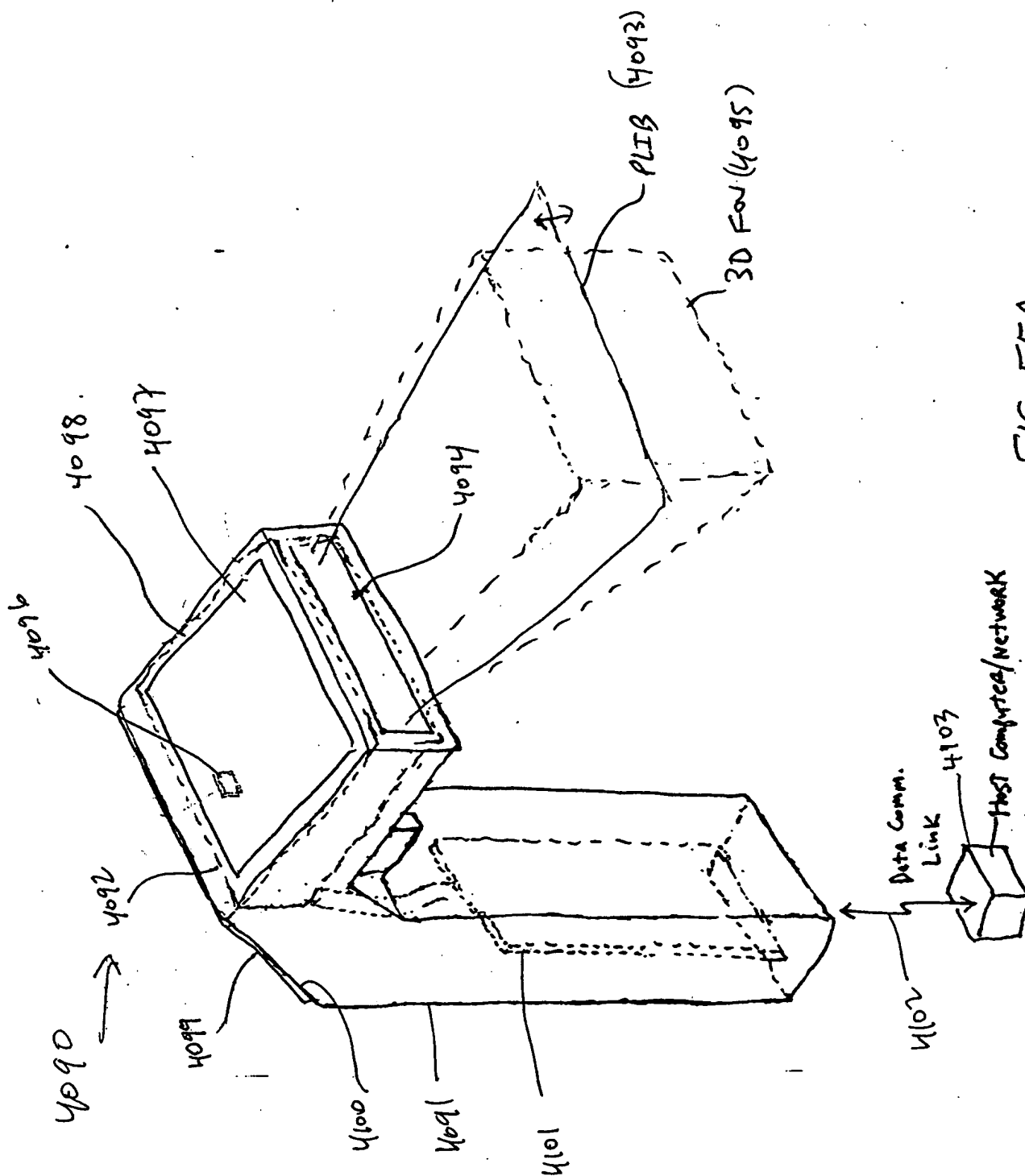


FIG. 55A

339/385

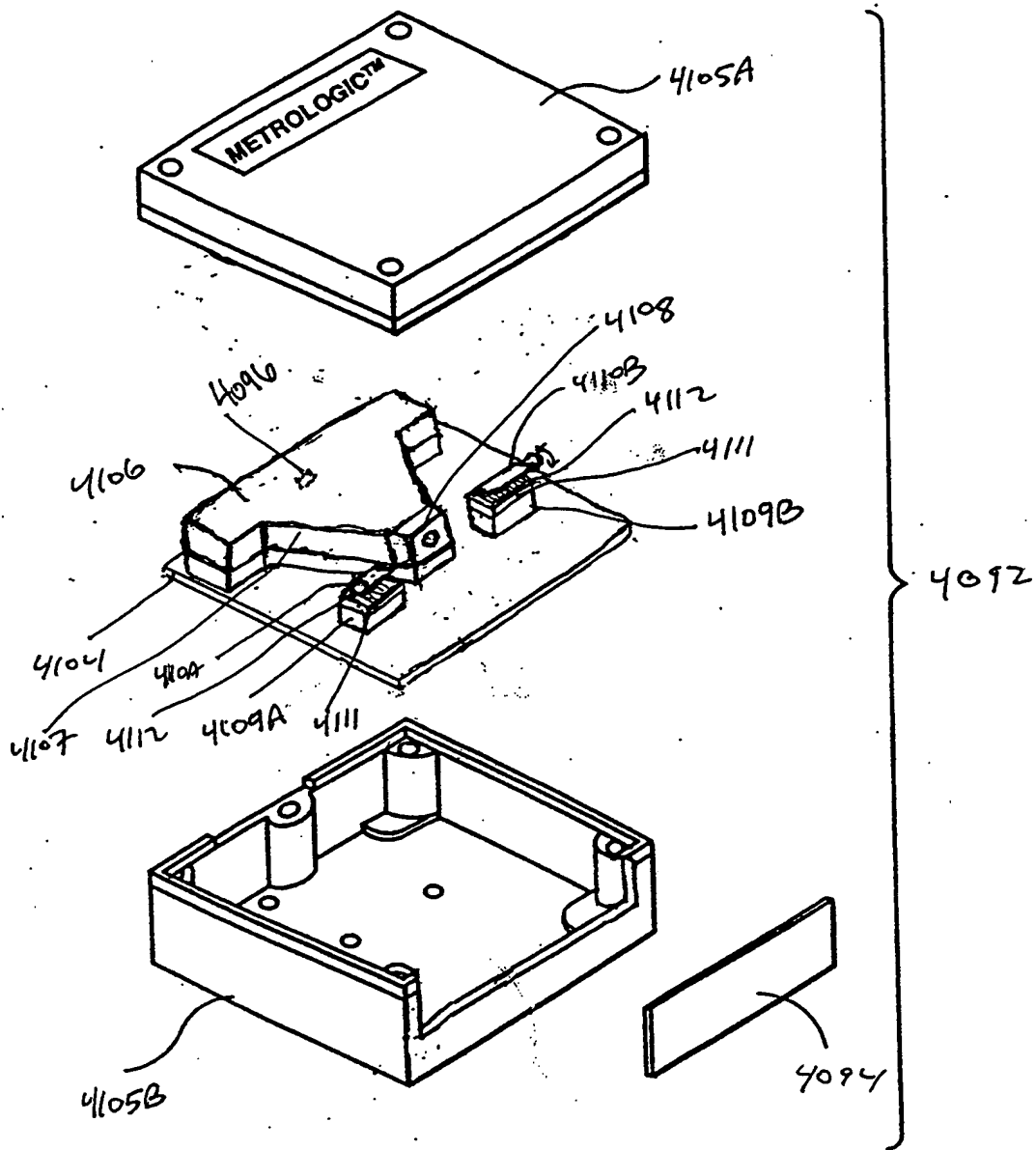


FIG. 55B

Brogg cell
Fig. 1A-6B

090055-4204
FOR 5850550

340/385

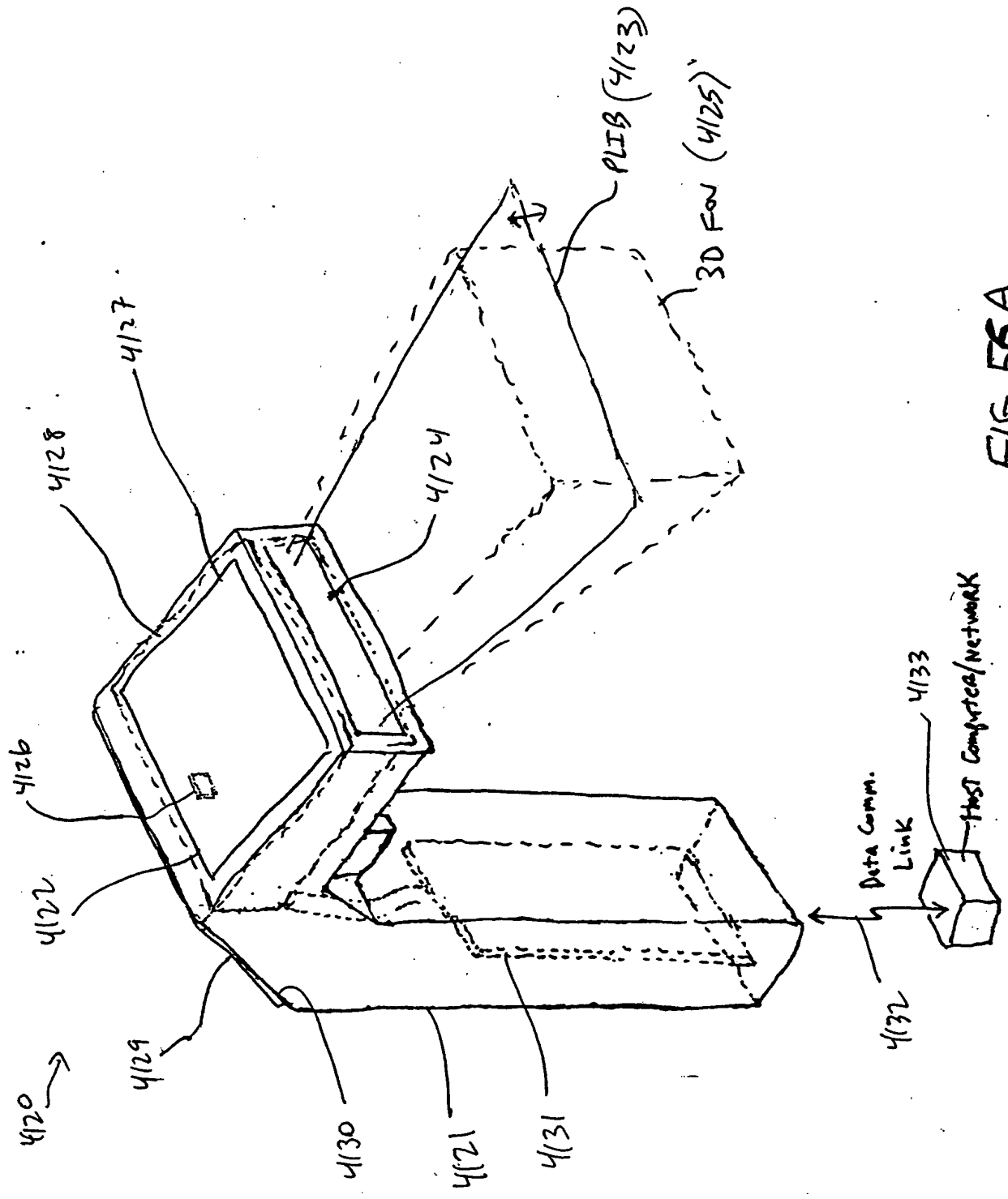


FIG. 56A

342/385

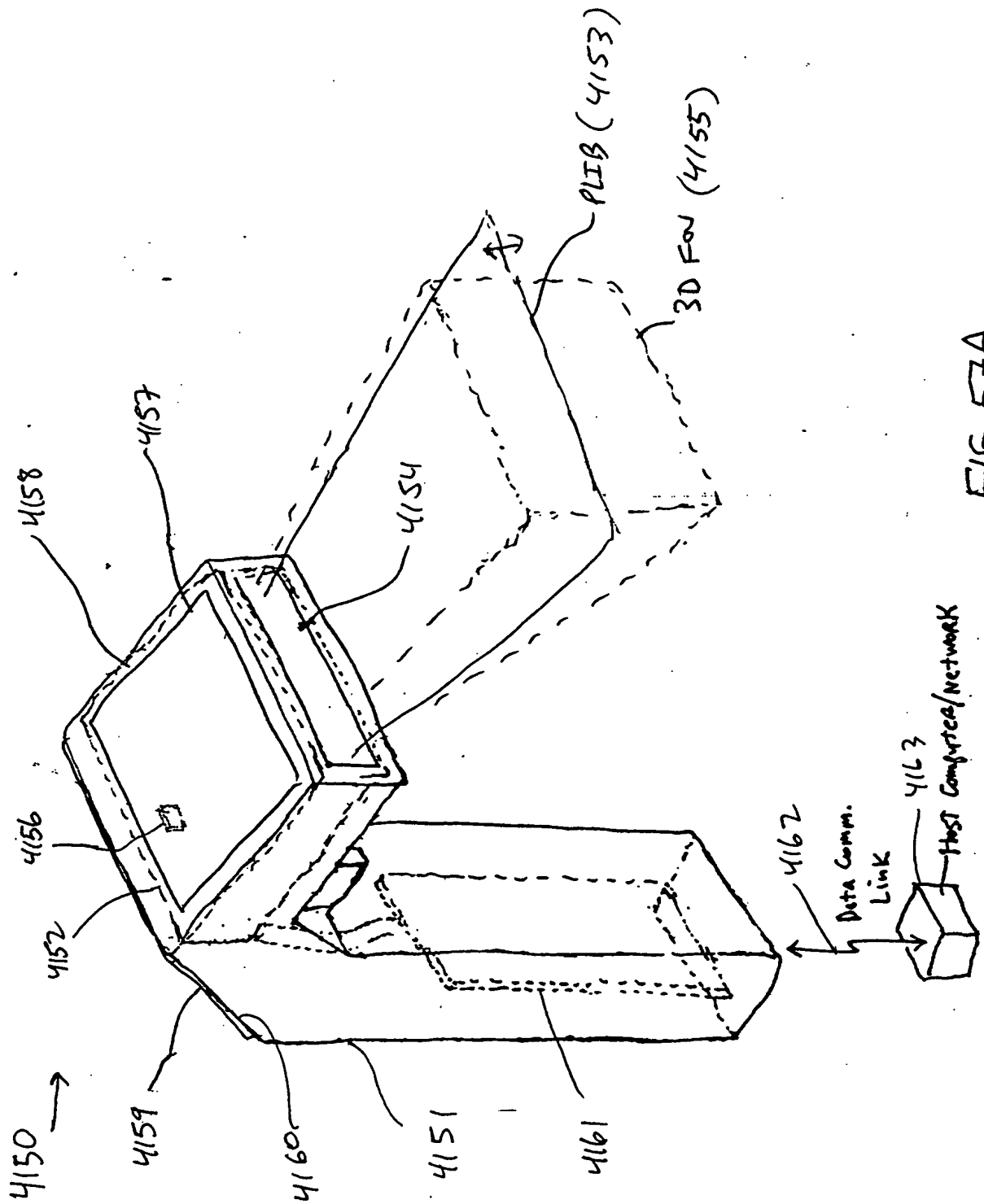


FIG. 57A

344/385

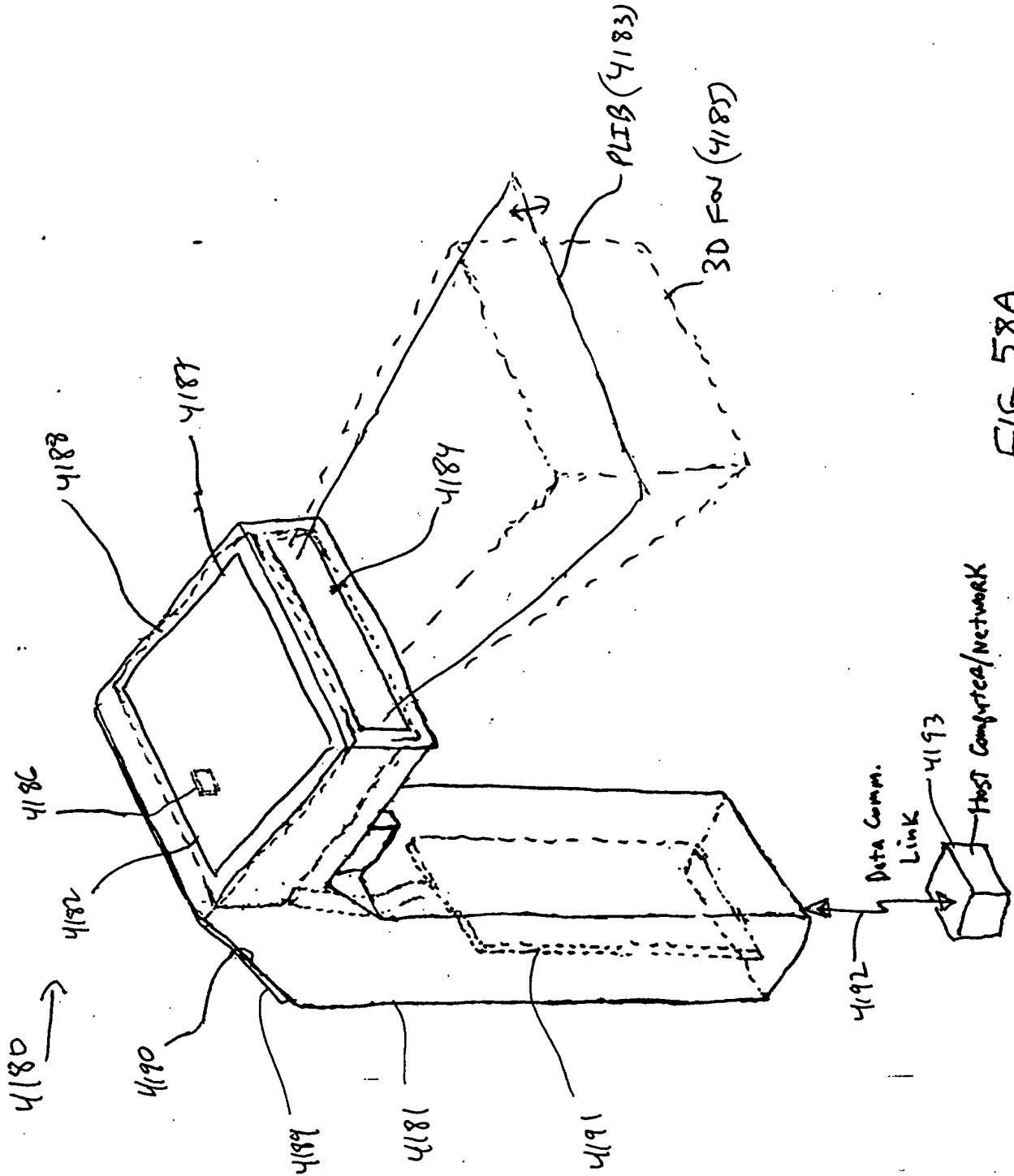


FIG. 58A

TOTAL 58505560

346/385

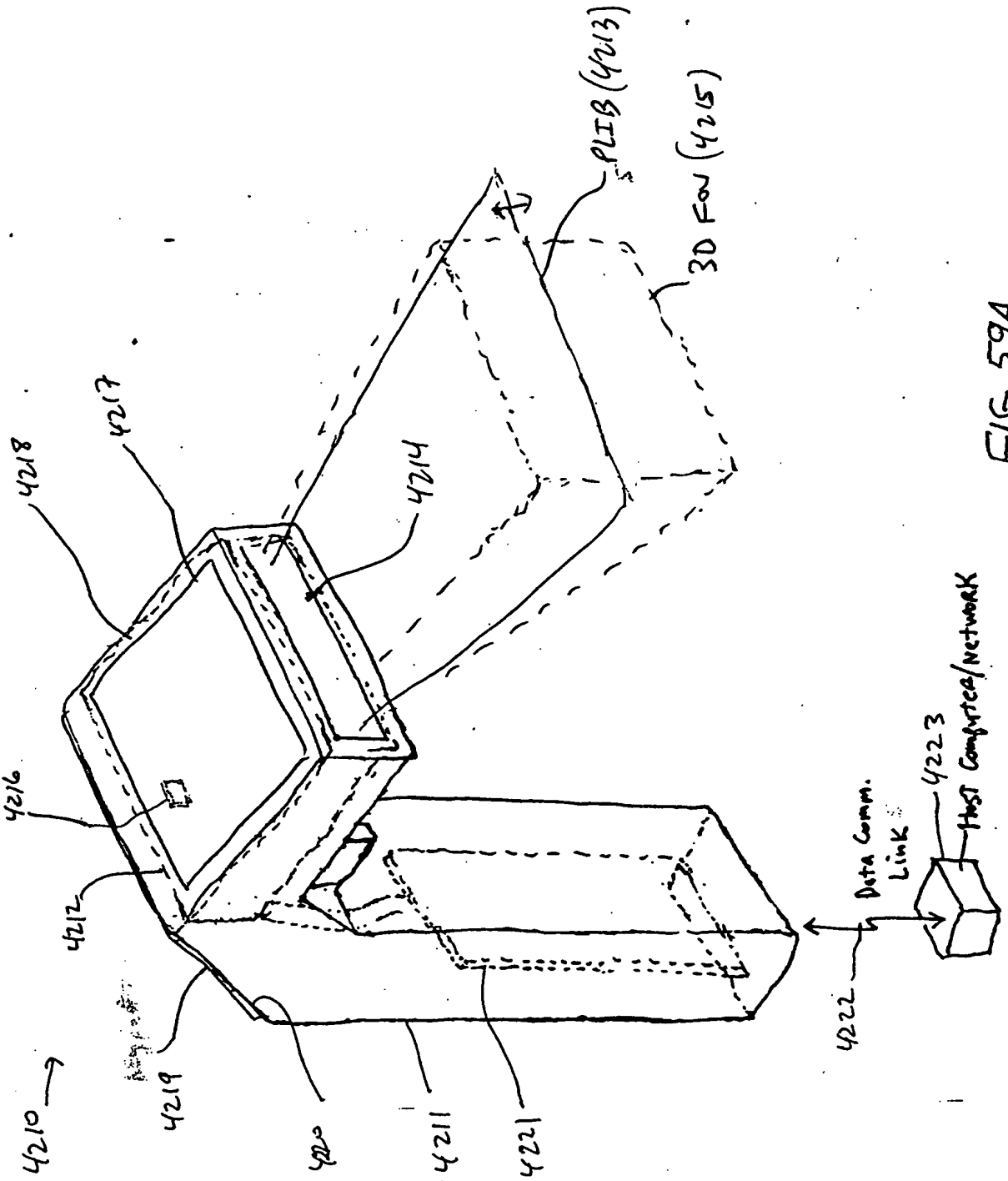


FIG. 59A

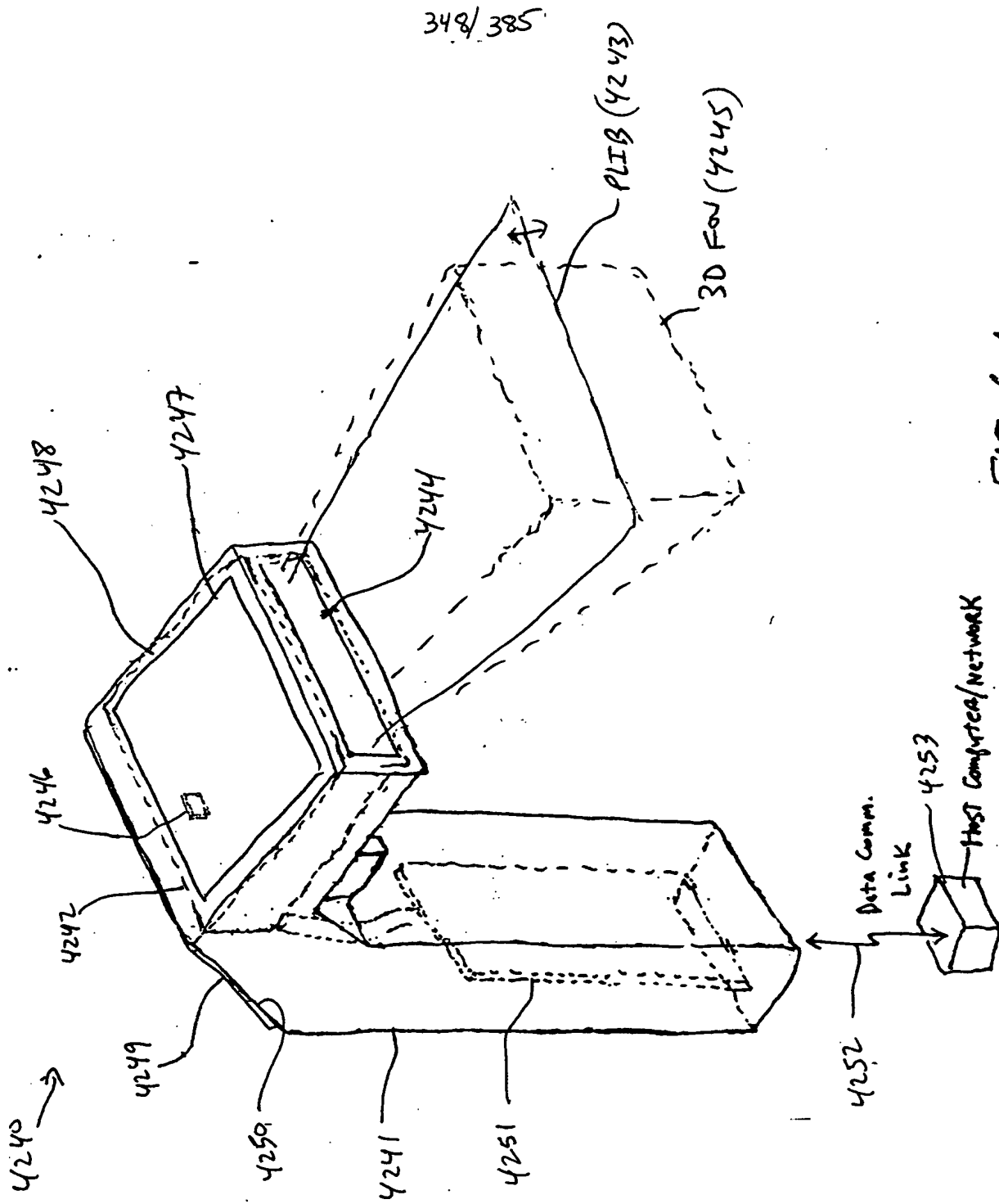


FIG. 60A

349/385

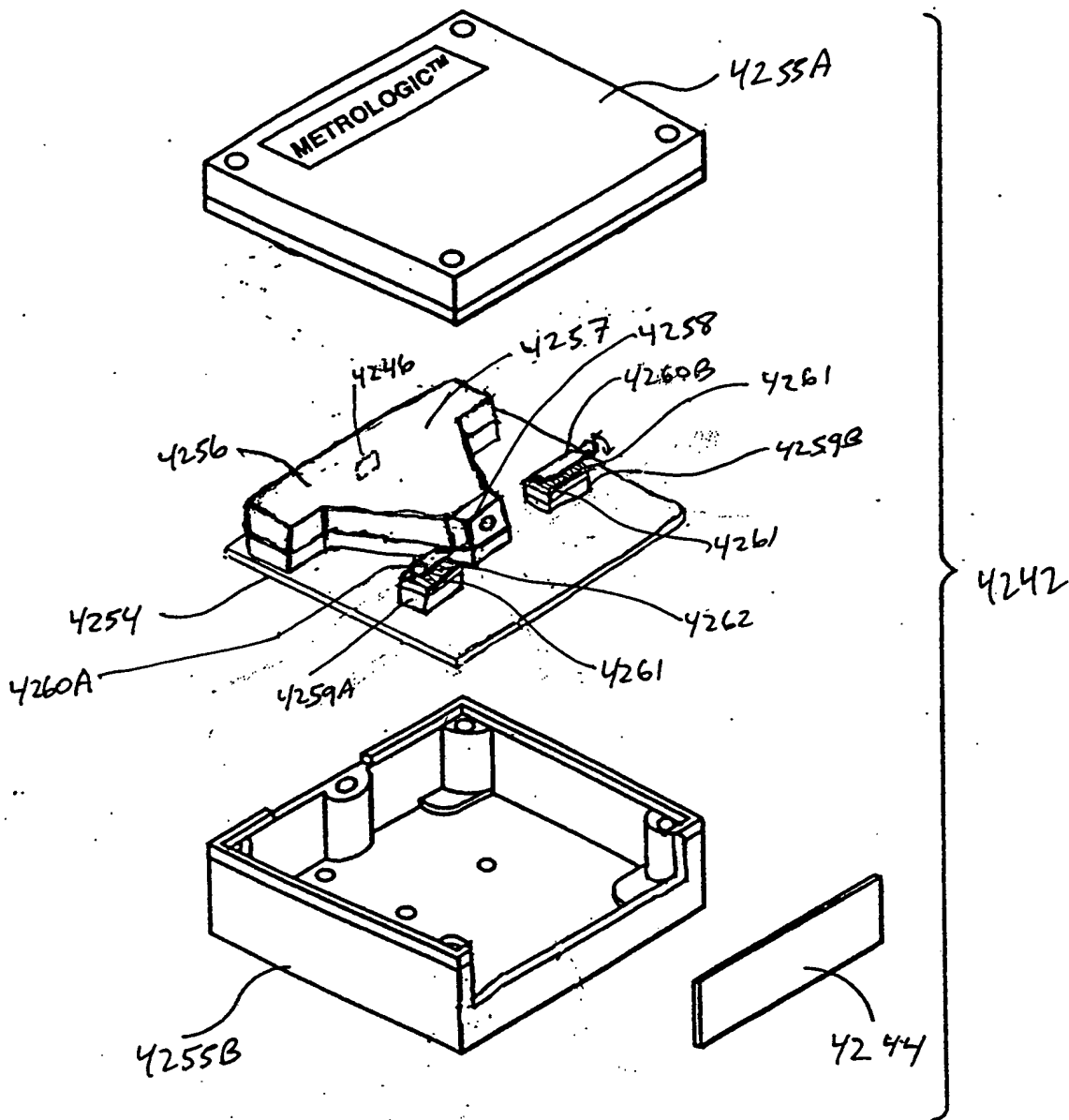


FIG. 60B

Bthalon (Tang. phase mod.)
Fig. 1 I 17A-17B

0090555-1101
10121-5350660

Y

7



00000585-112101

351/385

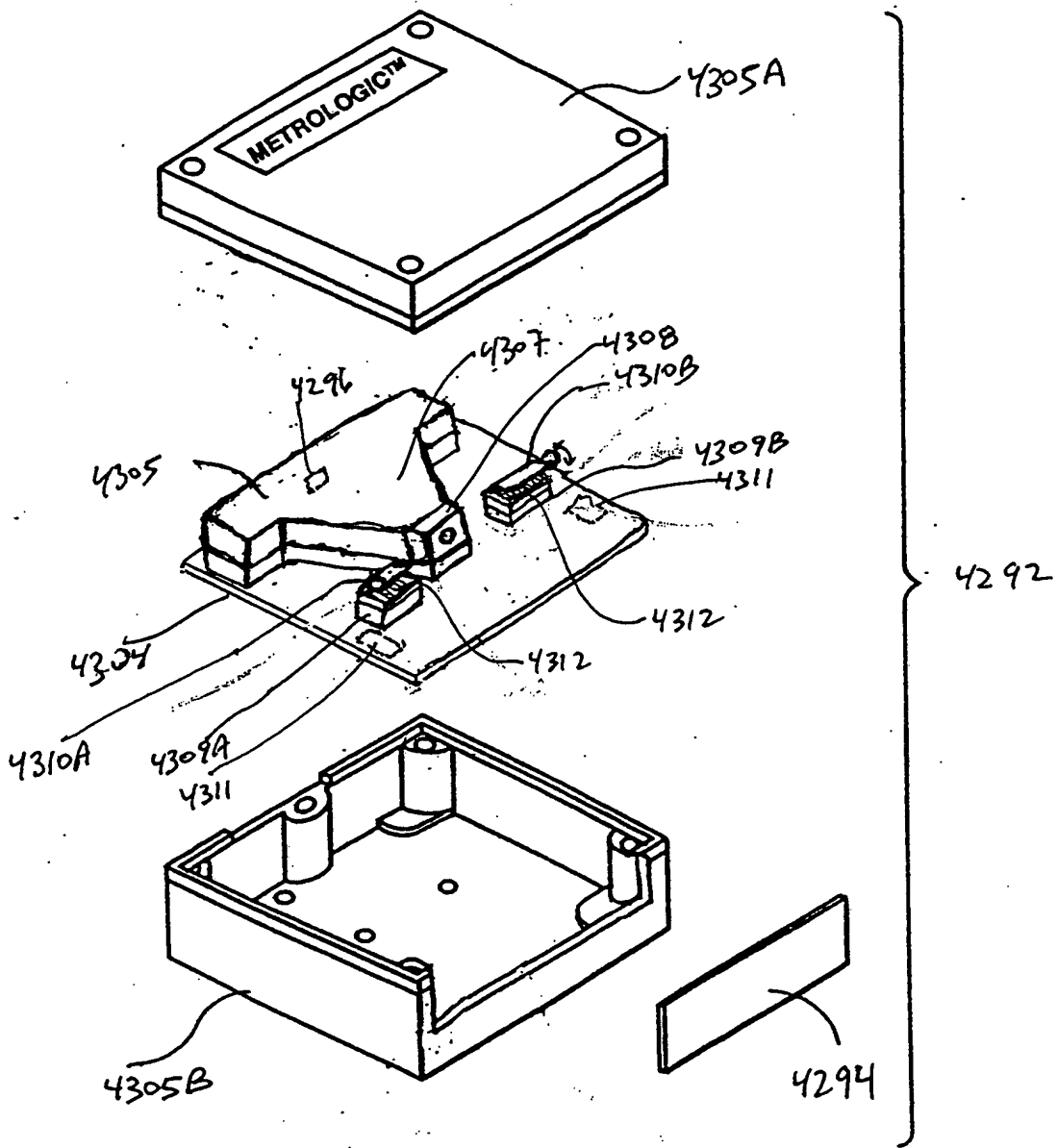


FIG. 61B

Mod. hugging

Fig. 1A-19B

352/885

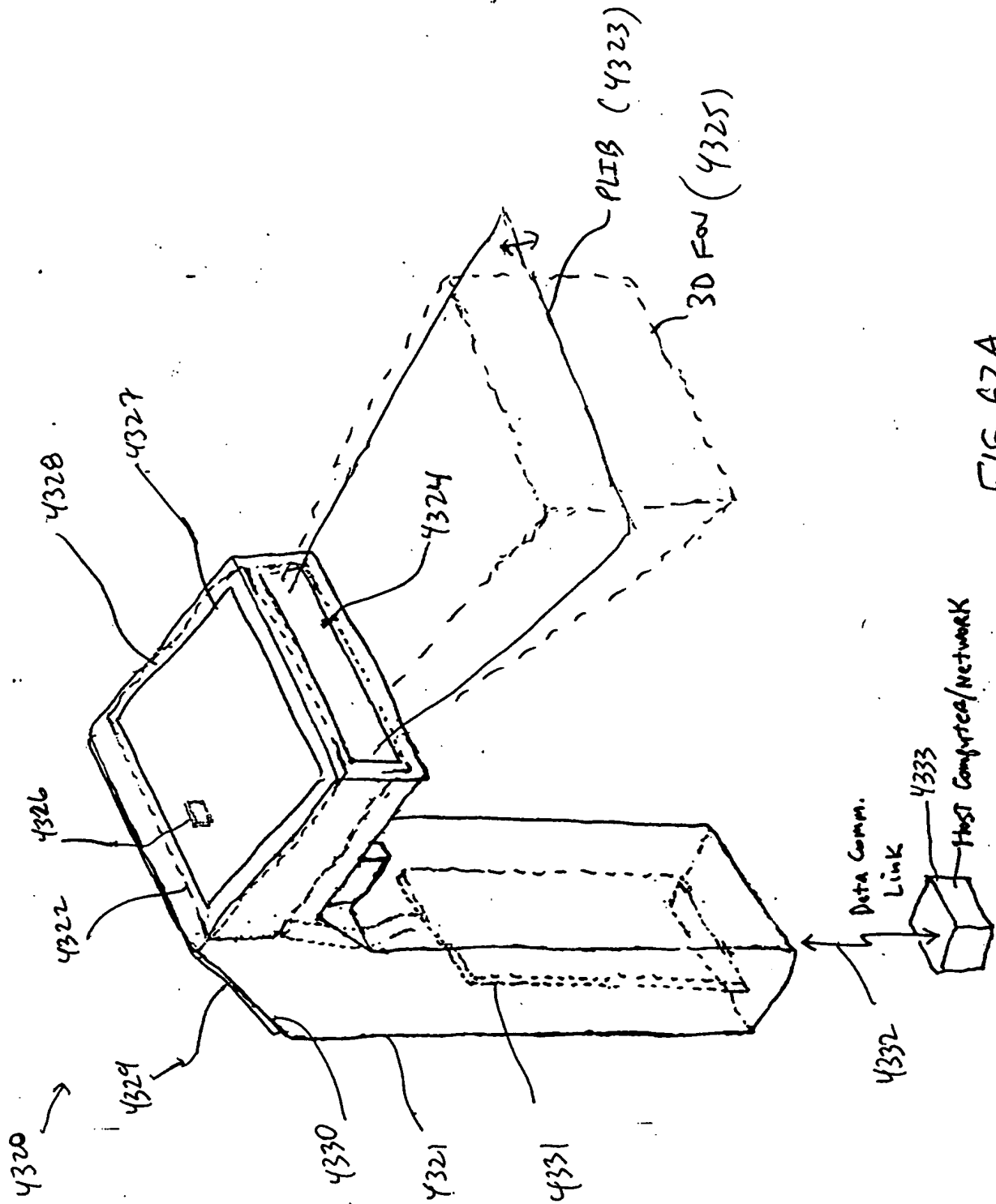


FIG. 62A

353/ 385

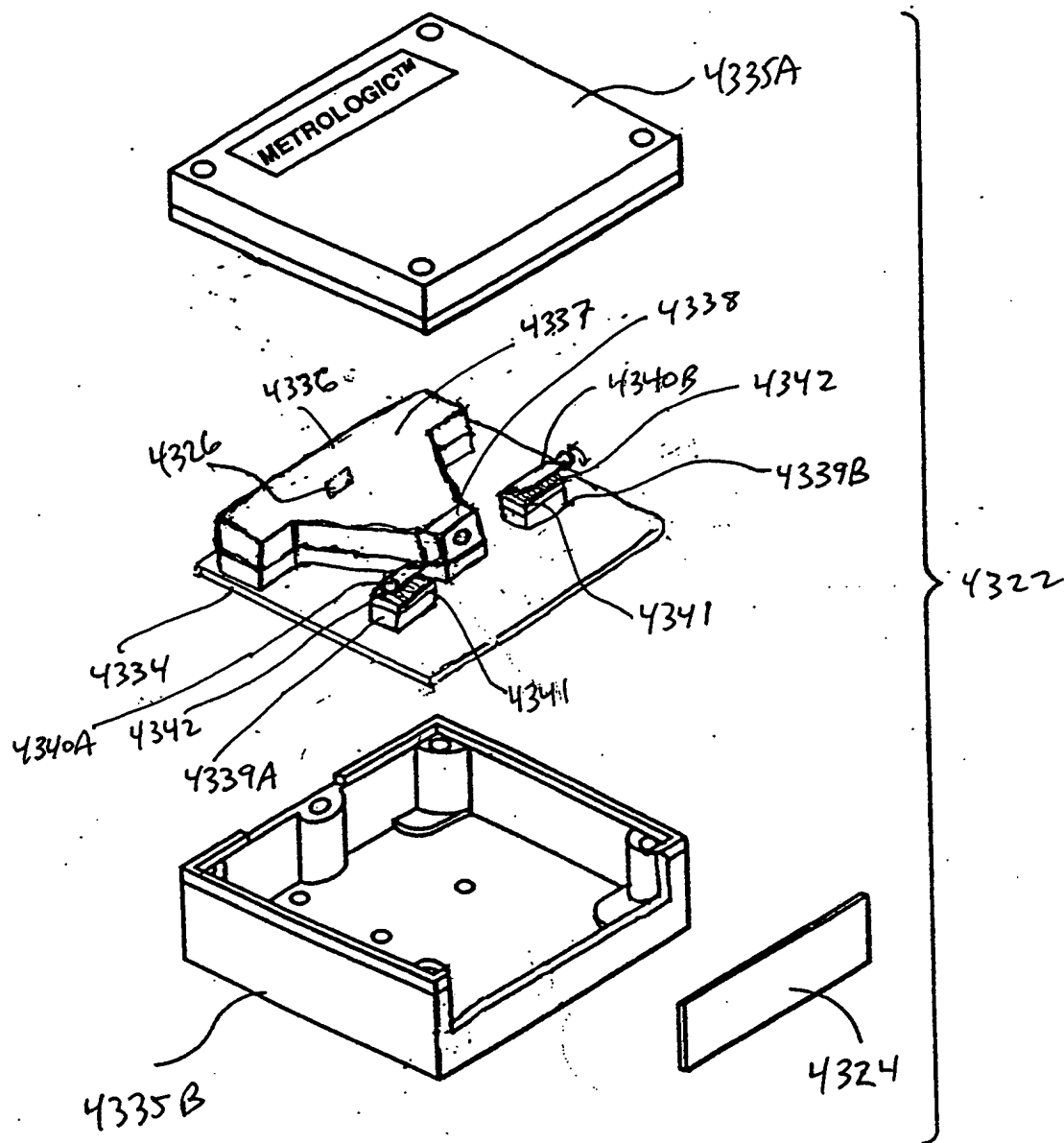


FIG. 62B

measuring
spot intensity
mod. panel

Fig. 1F21A-21D

0000055440
TOP SECRET

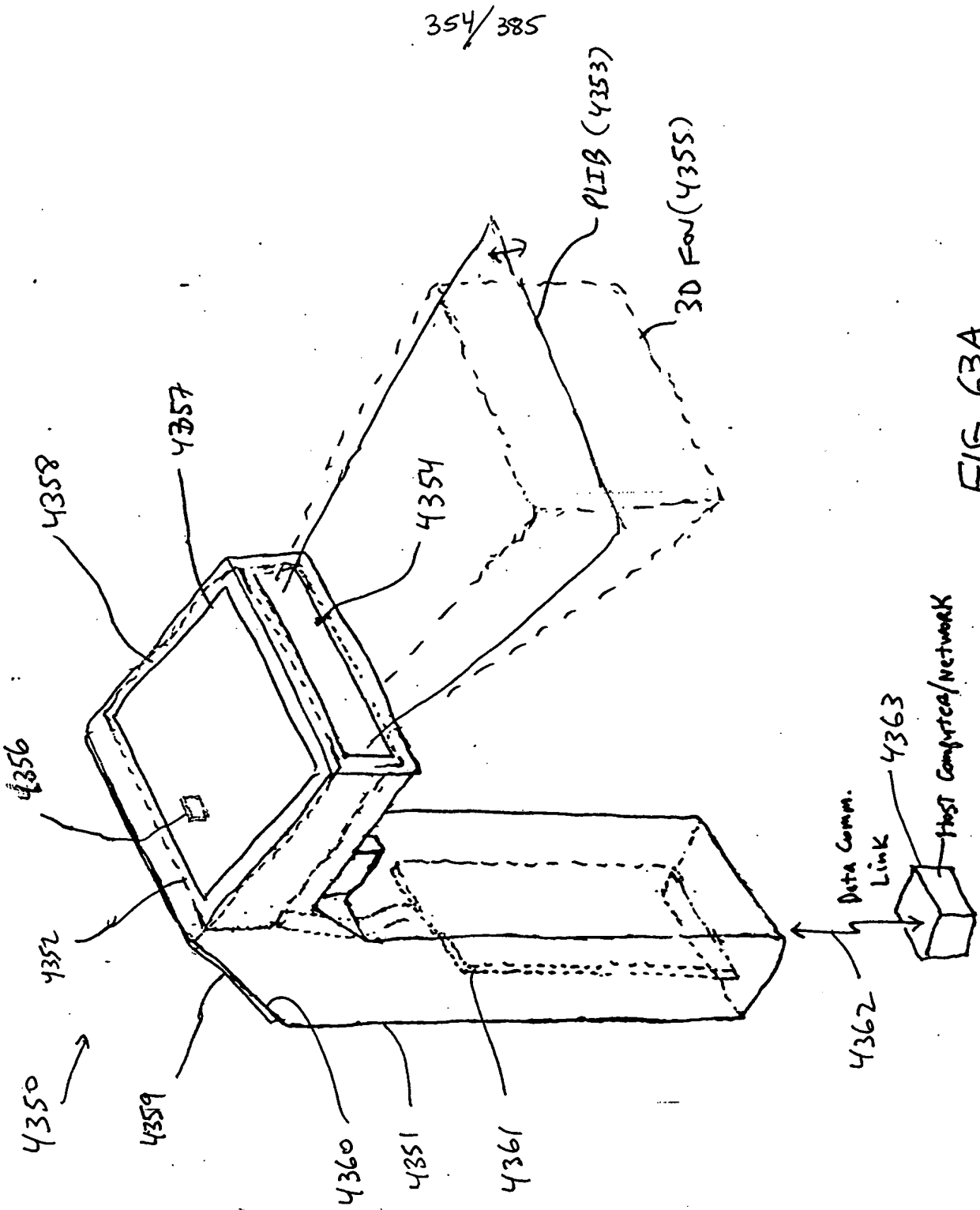


FIG. 63A

355/385

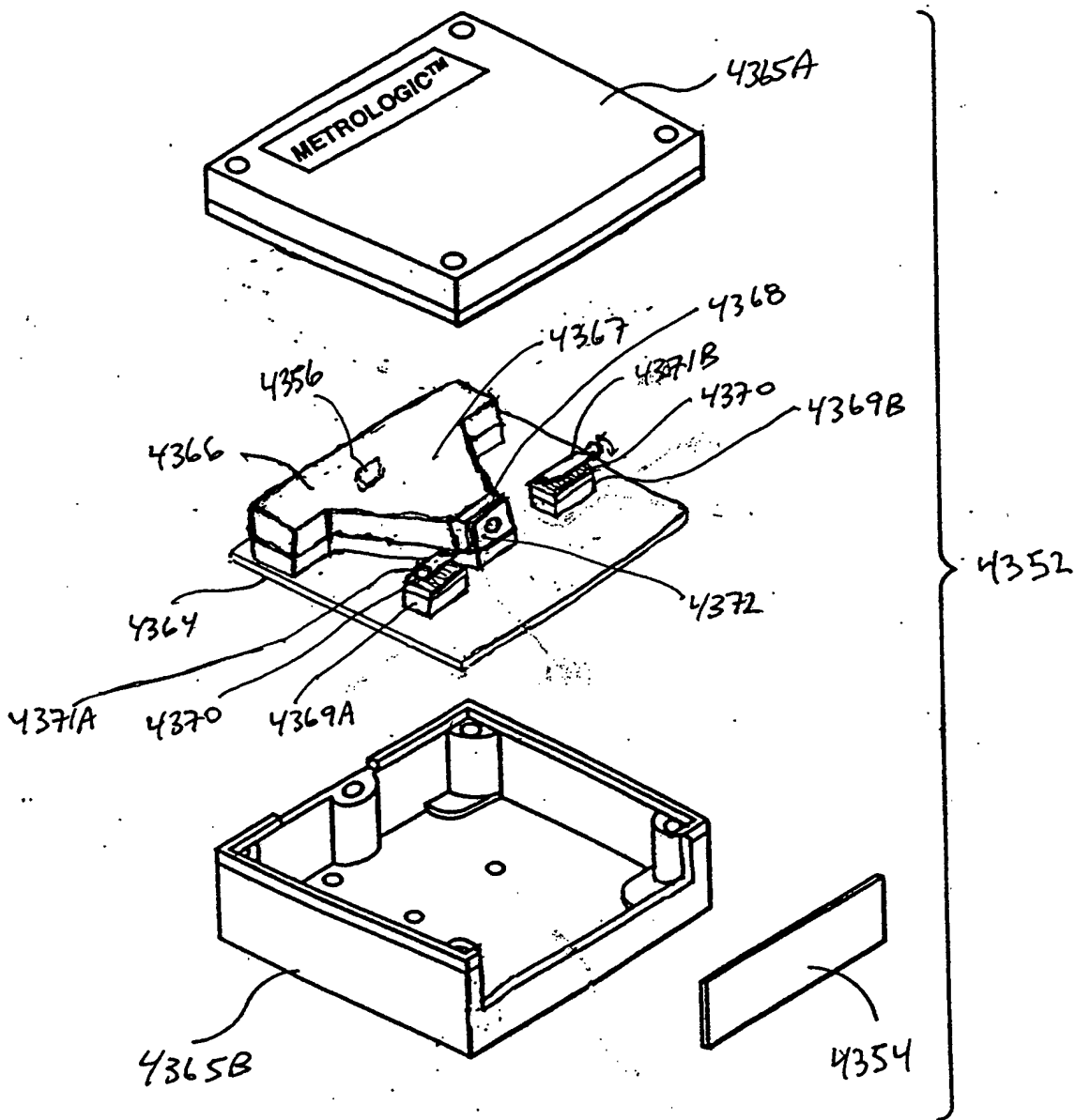


FIG. 63B

ED 01.
Mechanical Rotating Iris
Fig. 1E
23A-23B

356/385

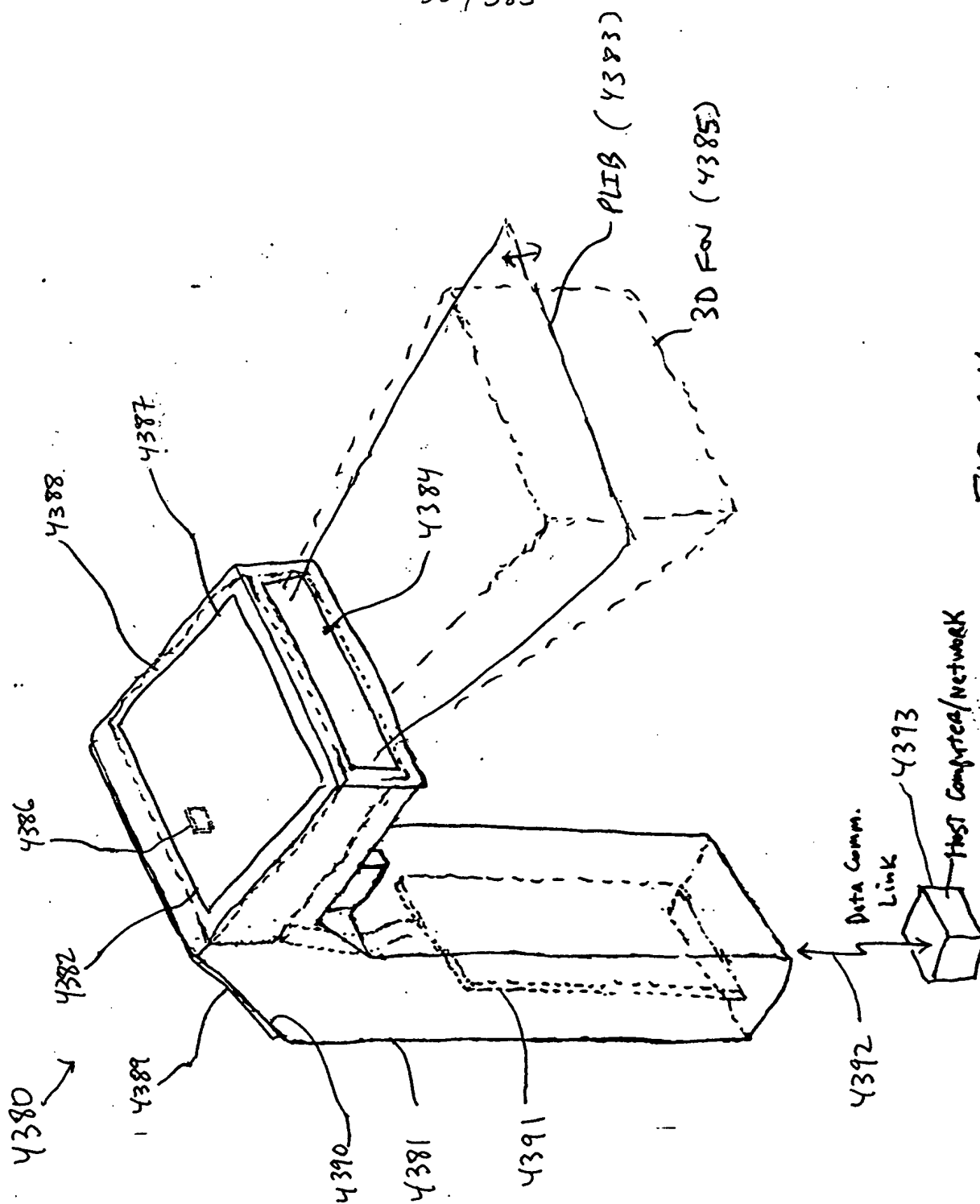


FIG. 64A

00990825-1201
TOTAL 52505650

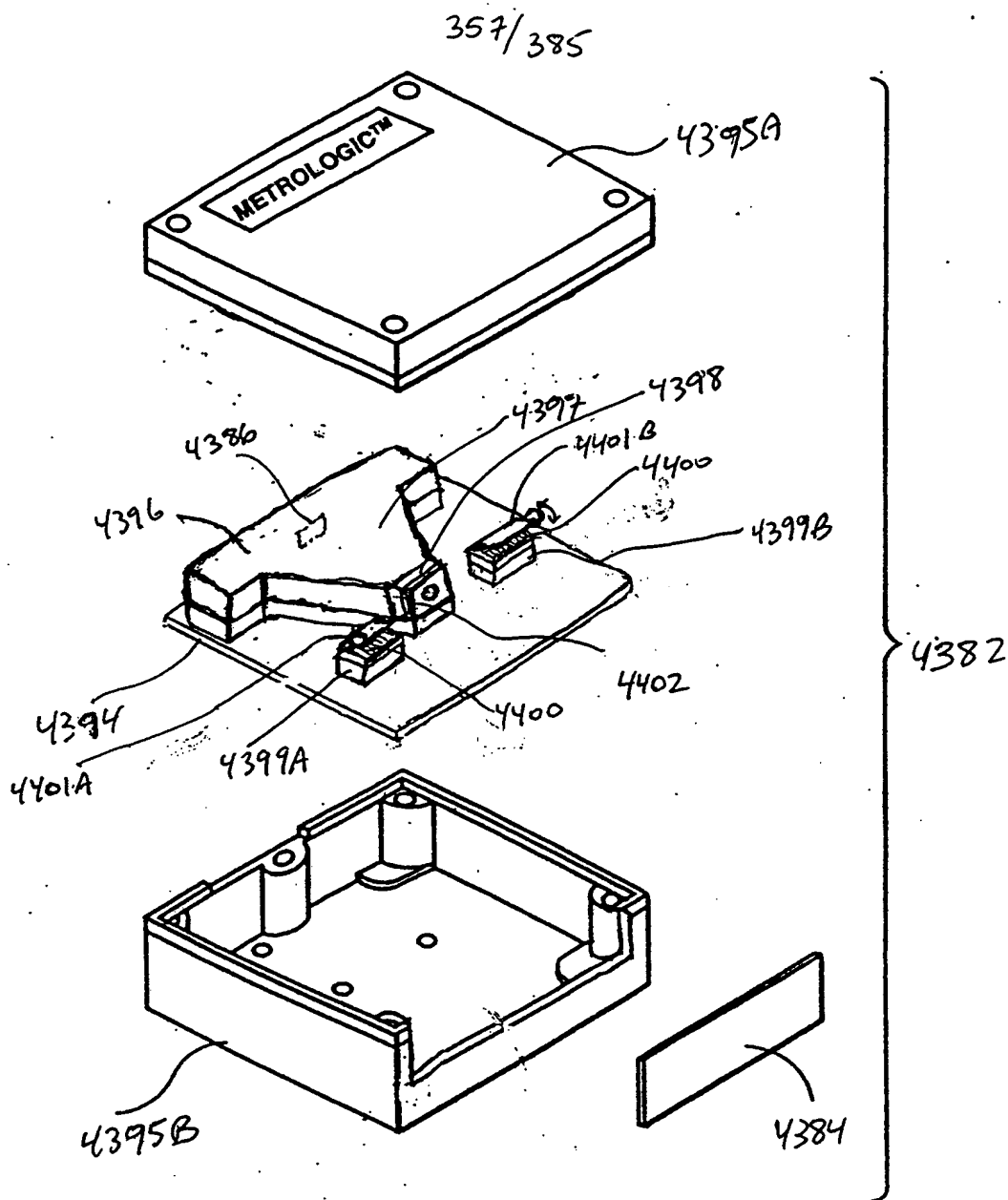


FIG. 64B

* E-optical
Shutter Before
EP Lens
Cg-124A

358/285

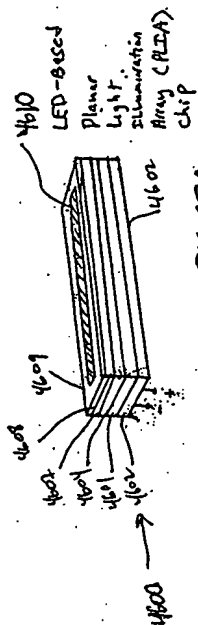


FIG. 67A

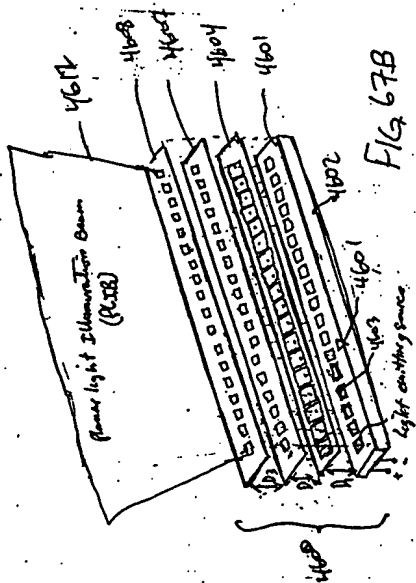


FIG. 67B

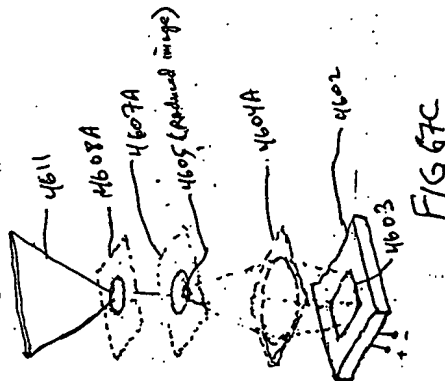


FIG. 67C

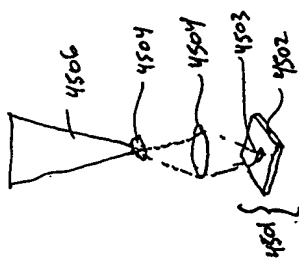


FIG. 65B

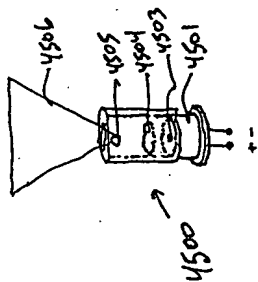


FIG. 65A

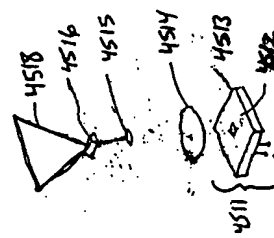


FIG. 66B

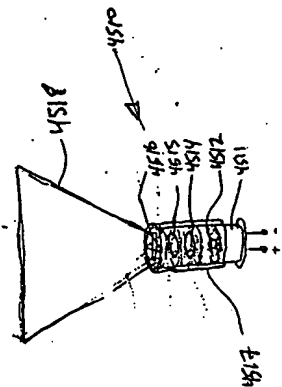
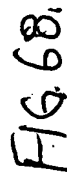


FIG. 66A



360/385

101211 58506660

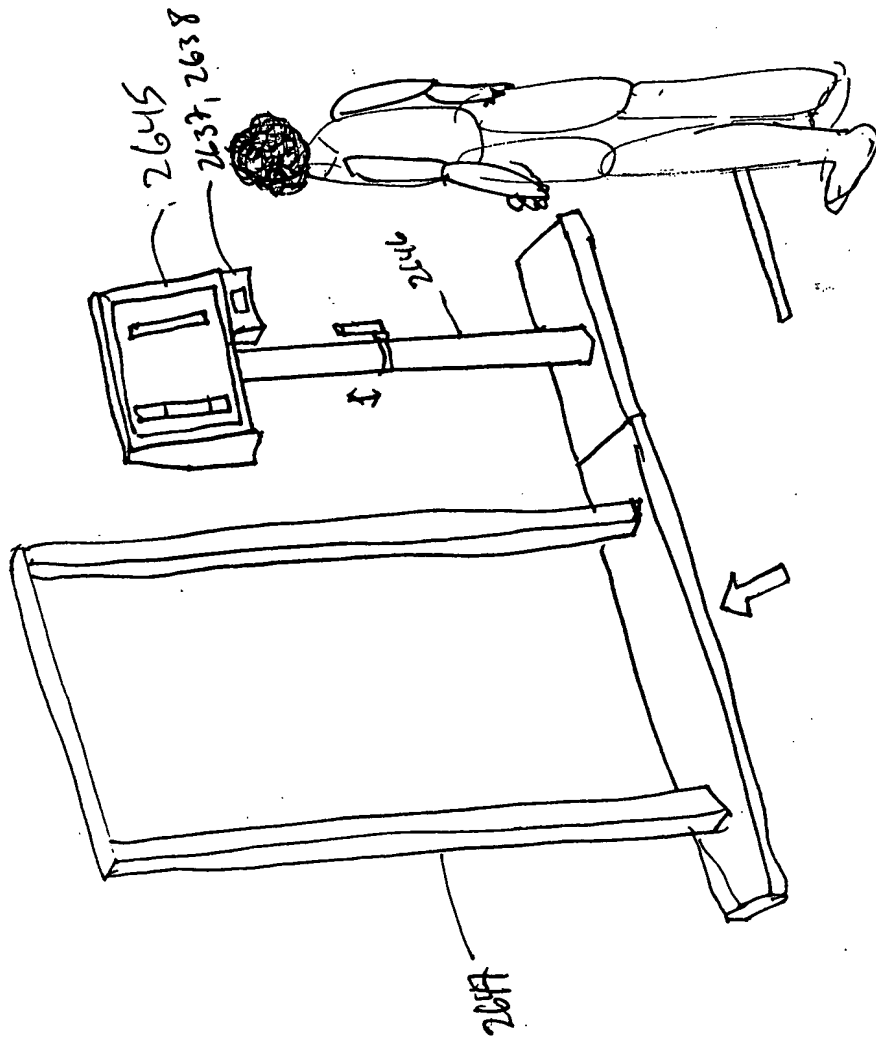


FIG. 68A

361/385

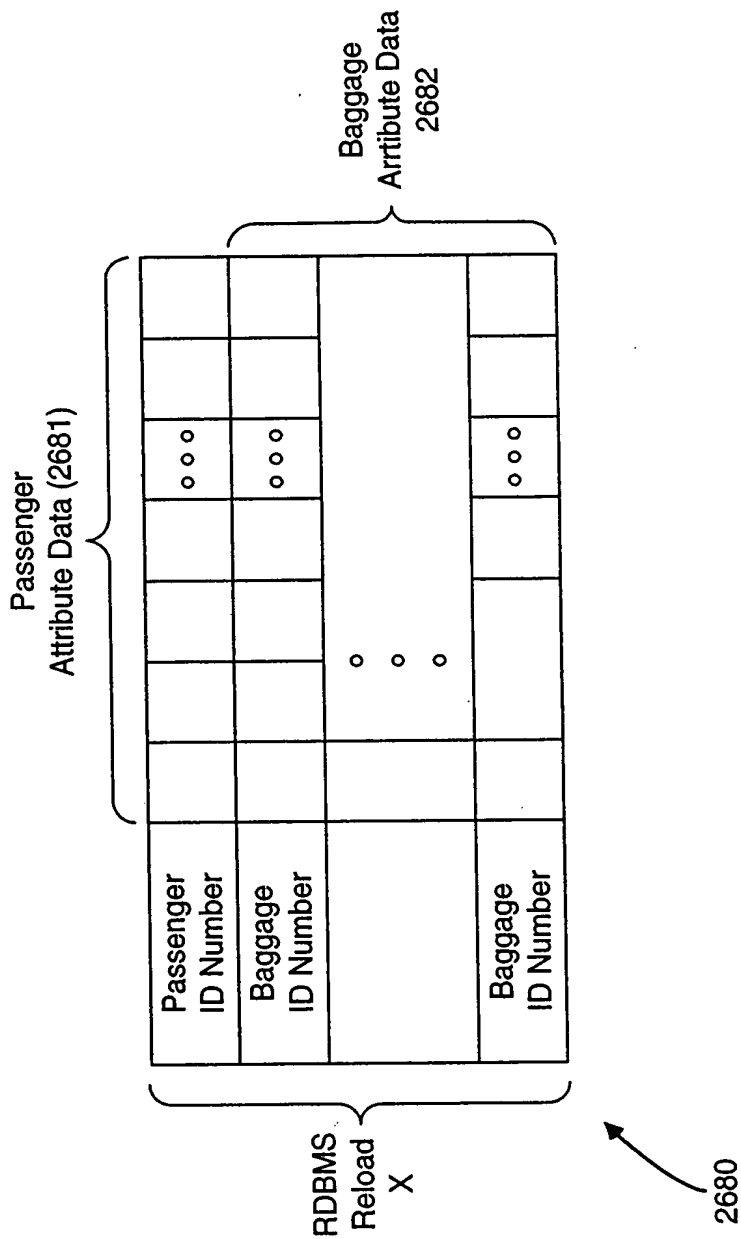


FIG. 68B

0000050660

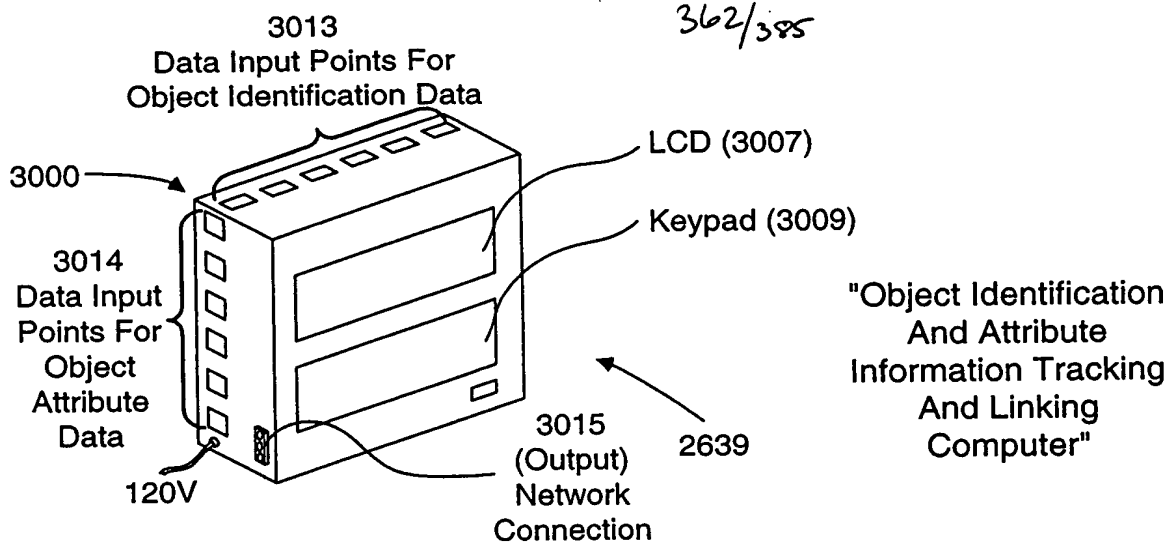


FIG. 68C1

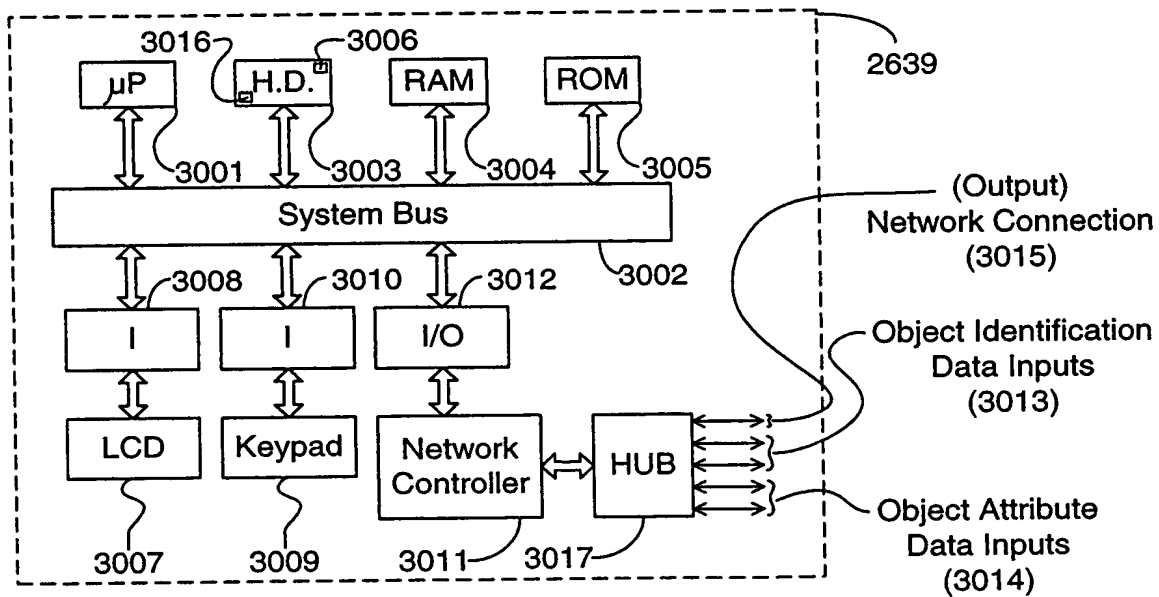


FIG. 68C2

Object Identification And Attribute Information Tracking And Linking Computer System.

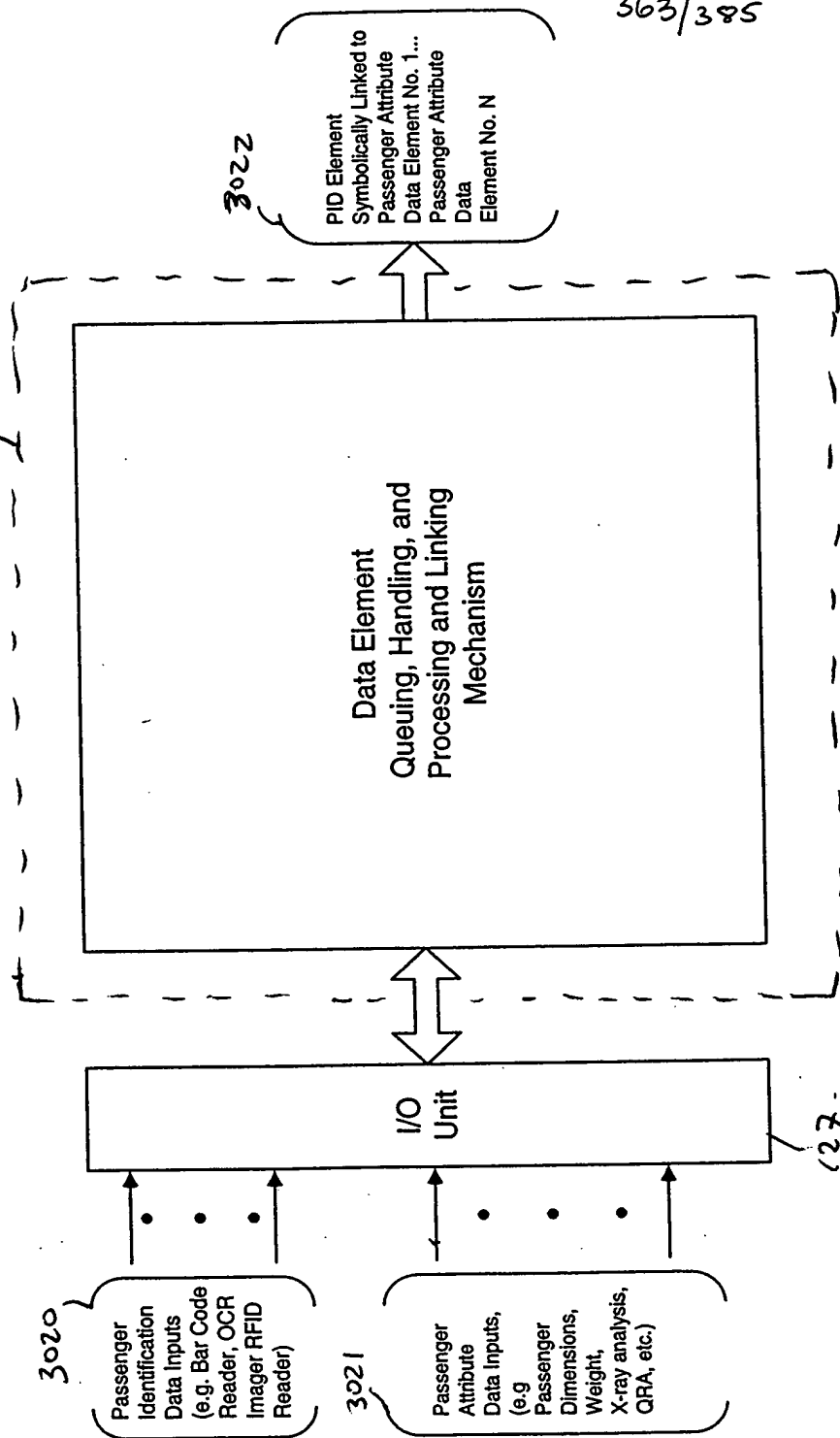


FIG. 68C3

Data Element Queuing, Handling, and Processing Subsystem Employed In The Object Identification And Attribute Acquisition System Of The Present Invention. (131)

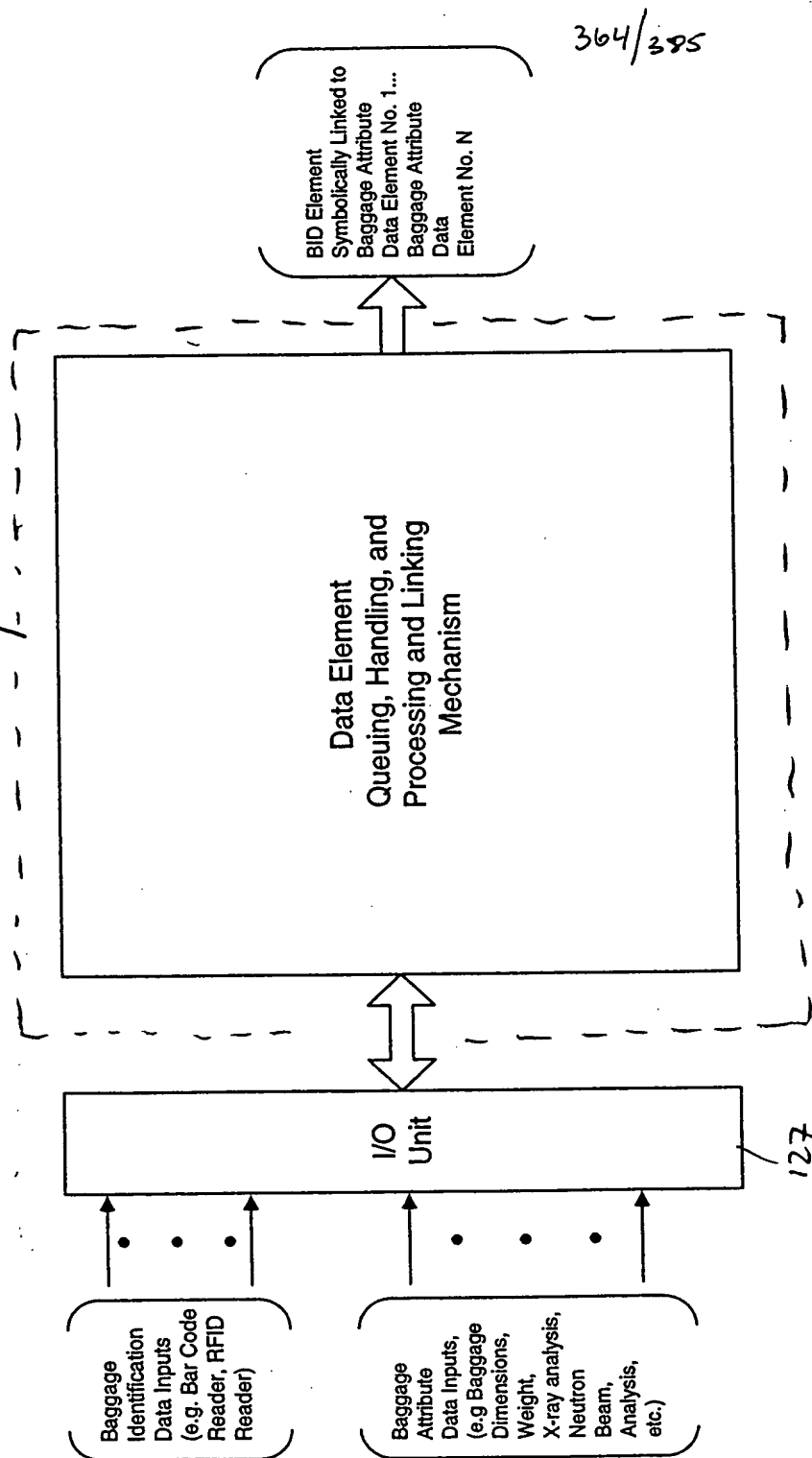


FIG. 68C4

365/385

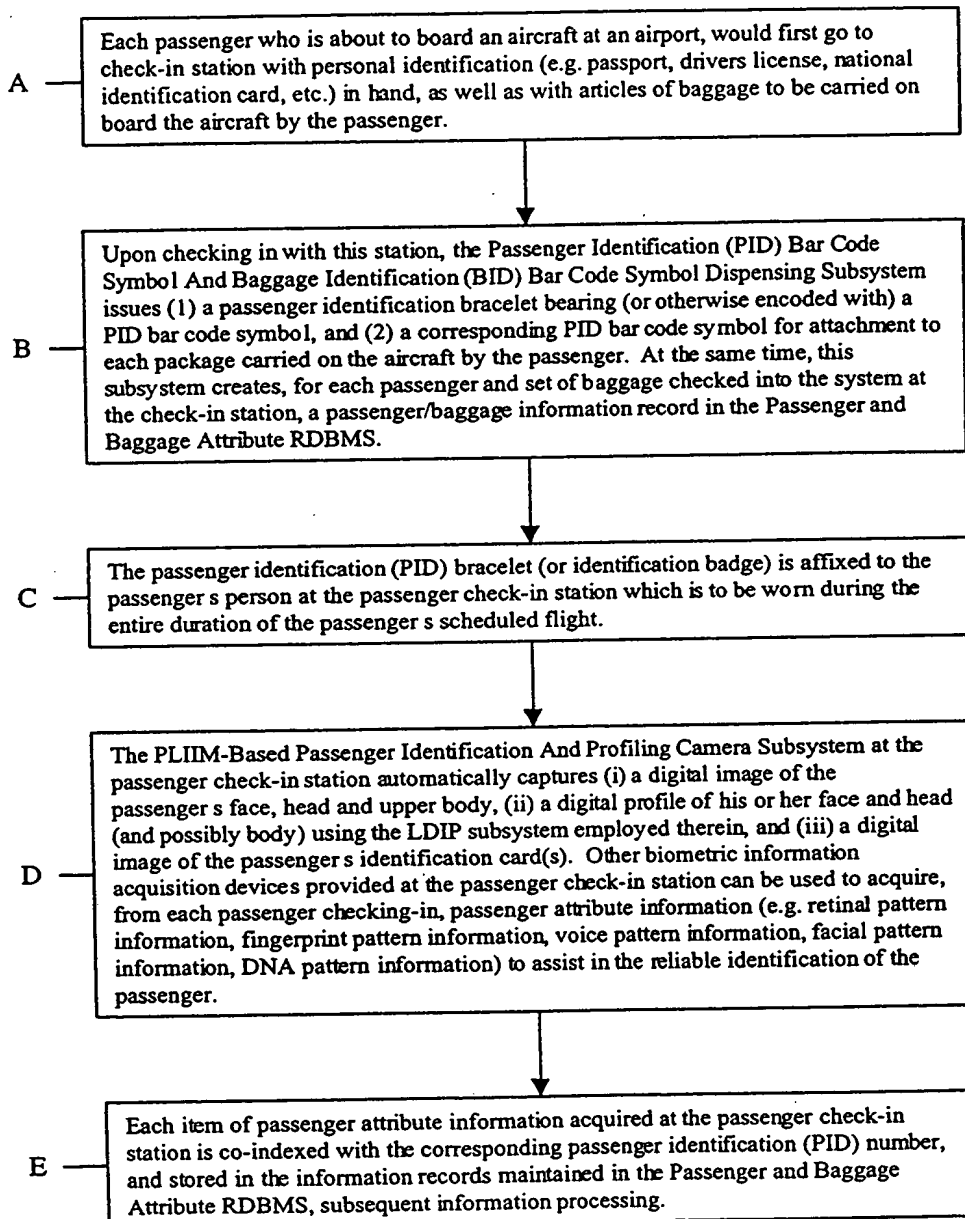


FIG. 68D1

367/385

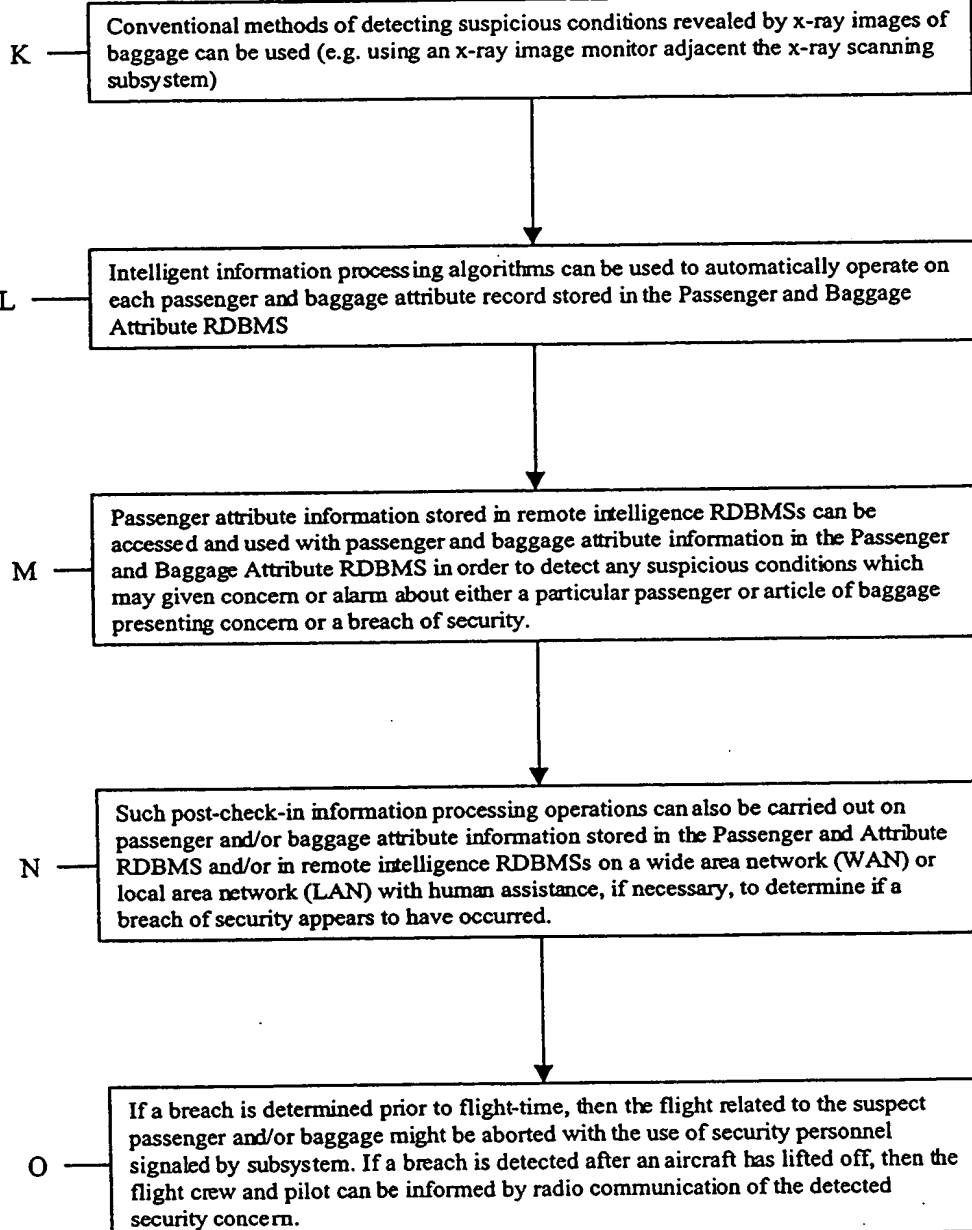
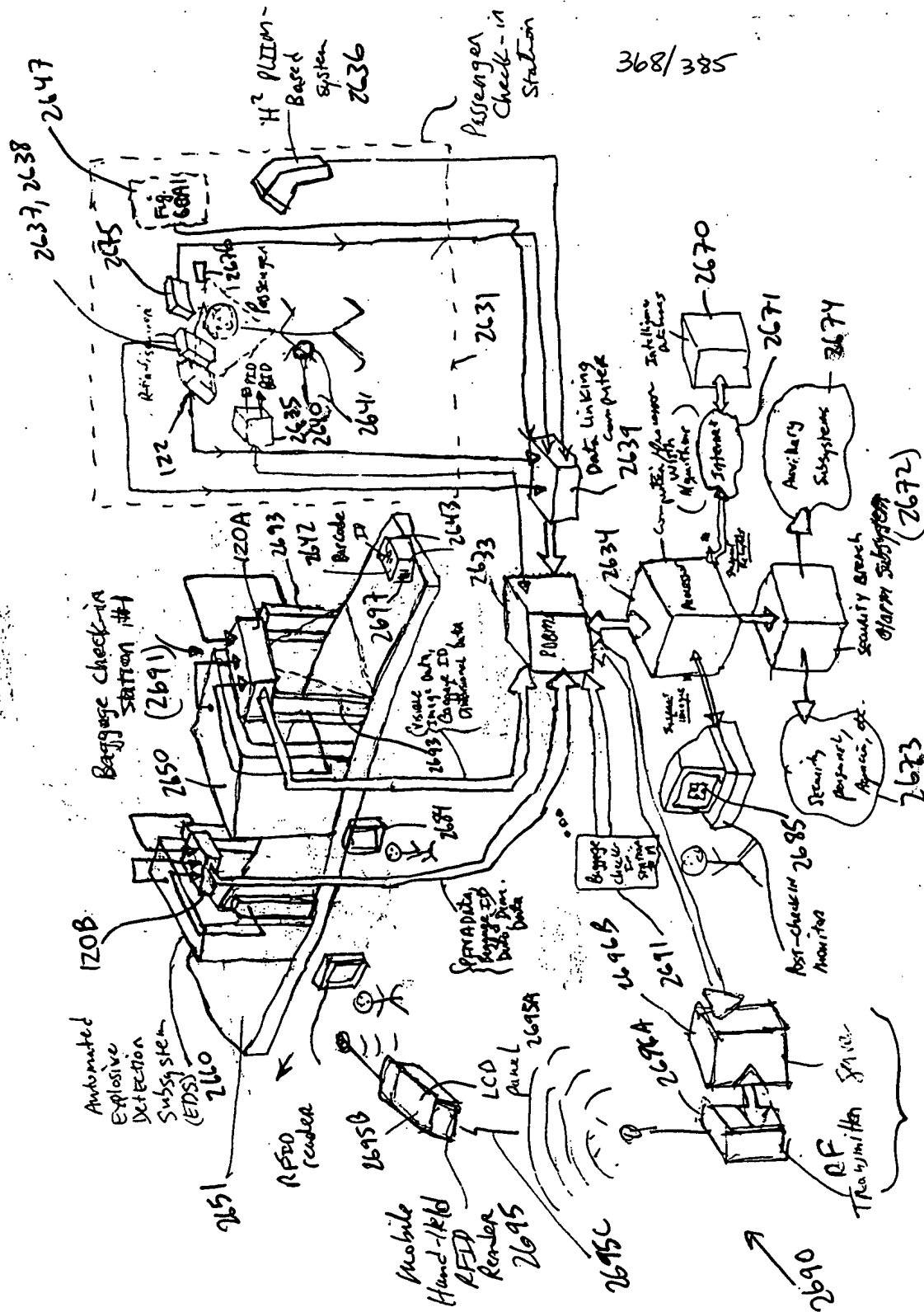


FIG. 68D3



369/385

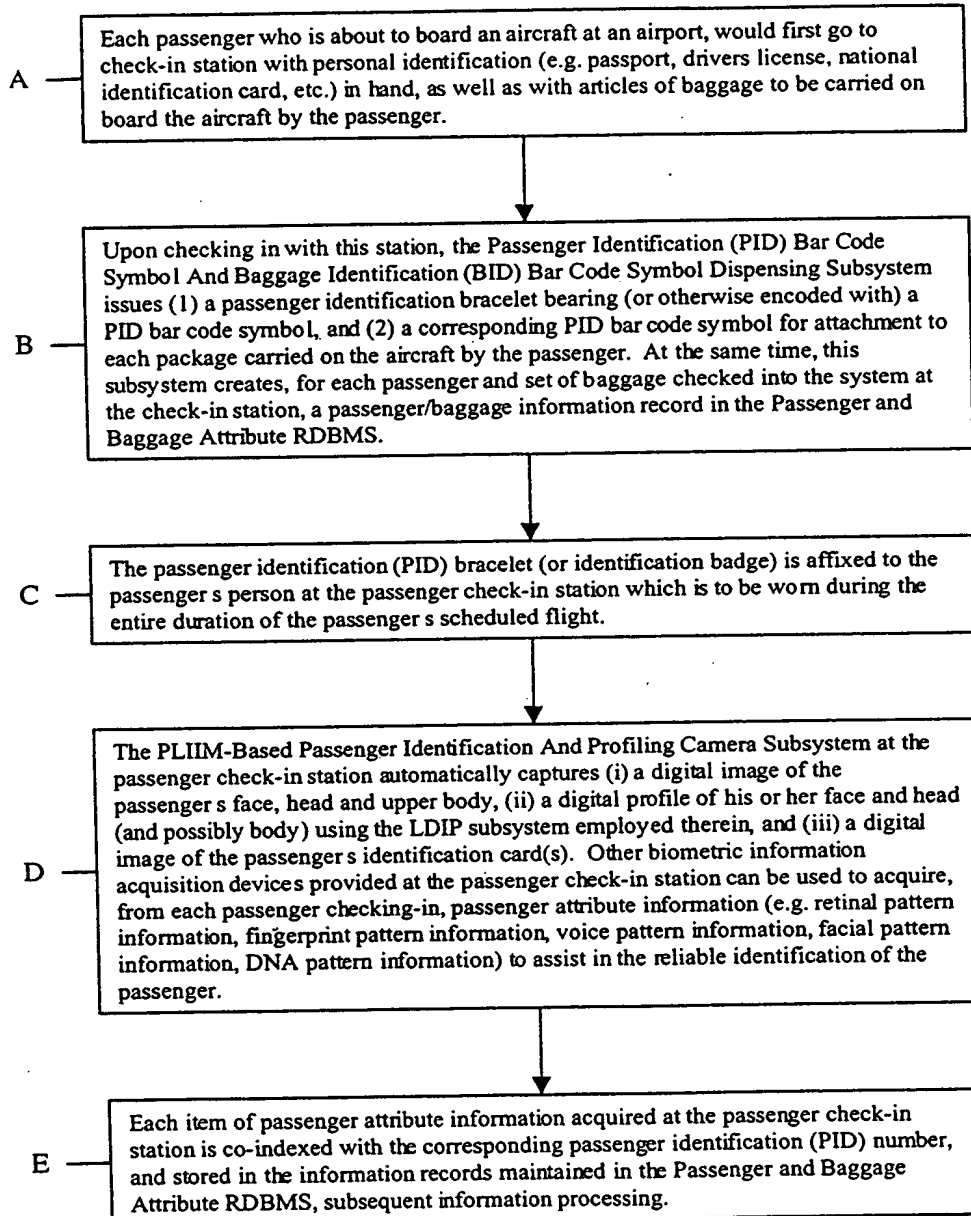


FIG. 69B1

371/385

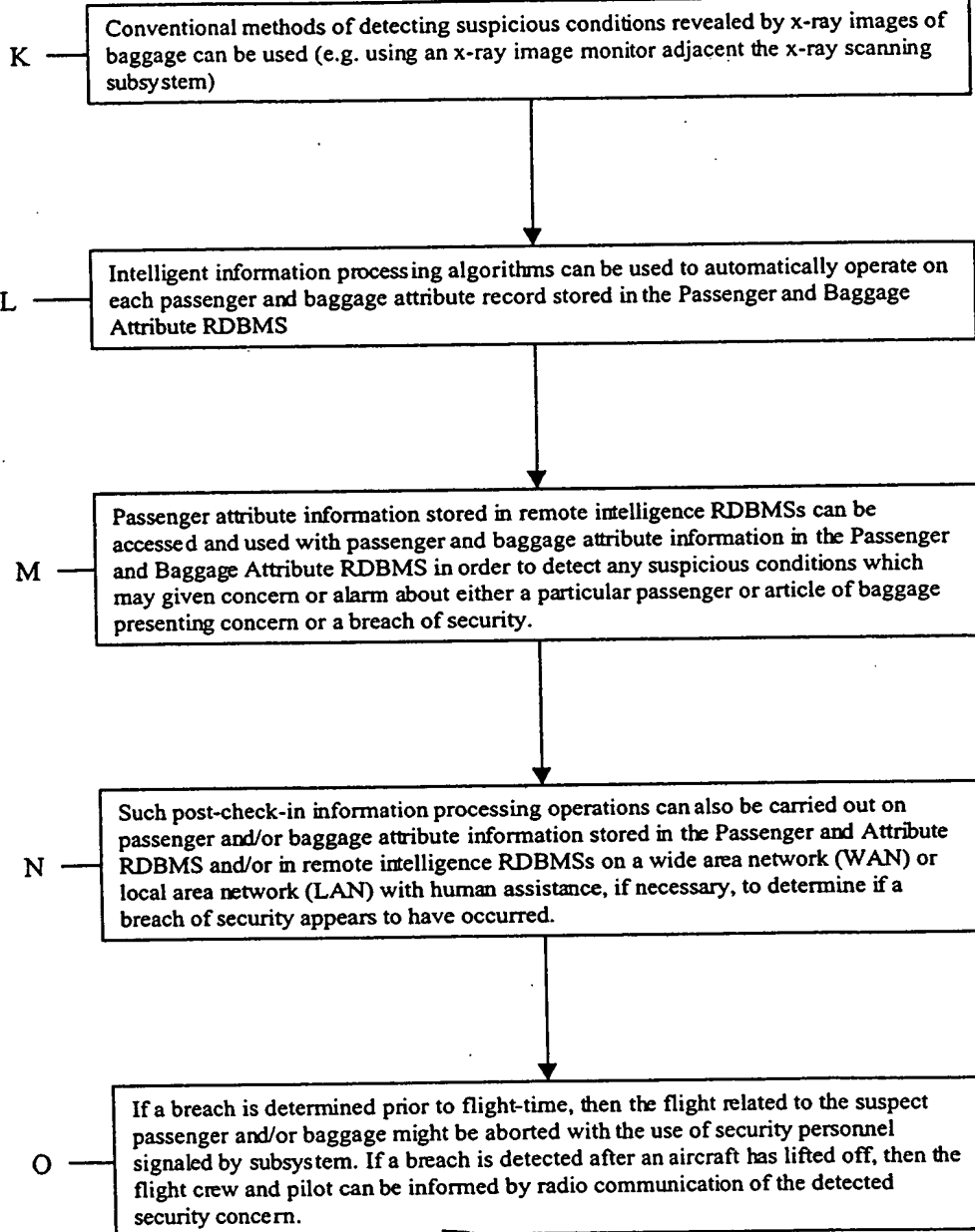


FIG. 69B3

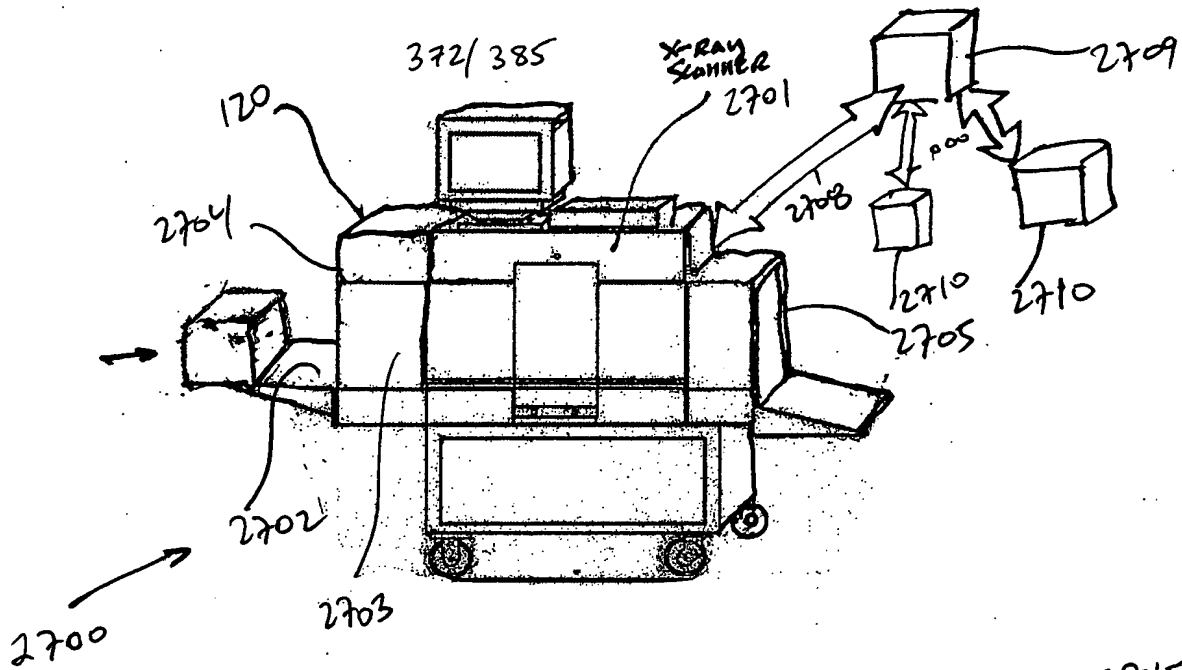


FIG 70A

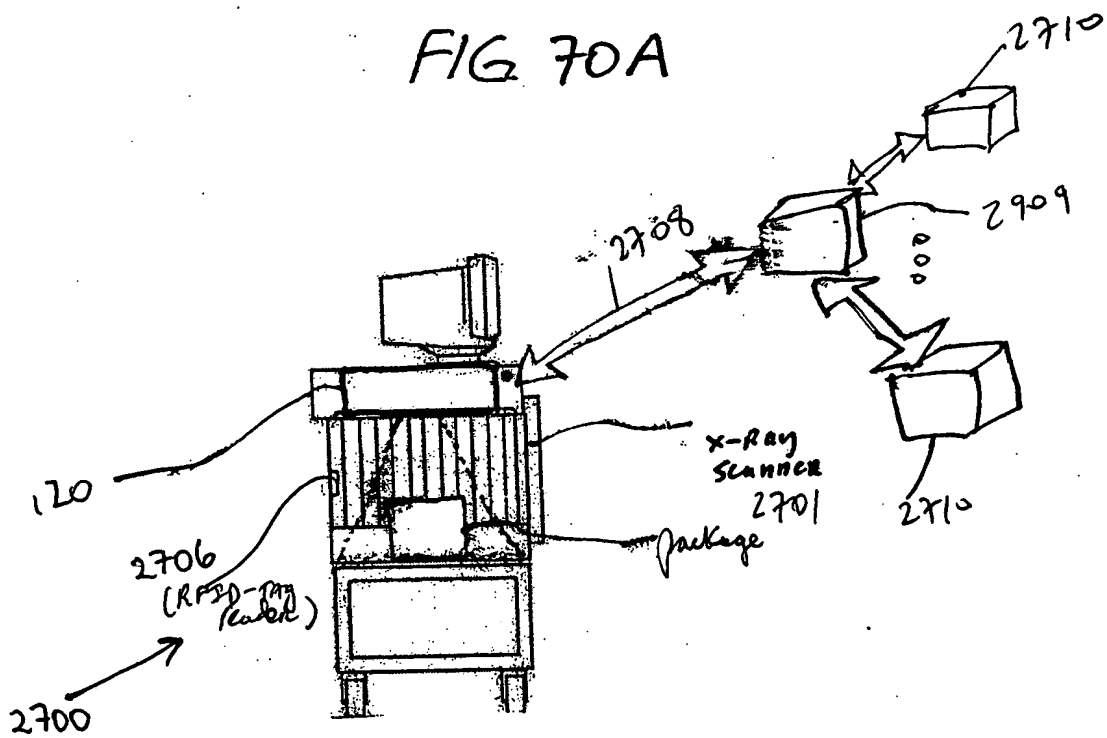


FIG. 70B

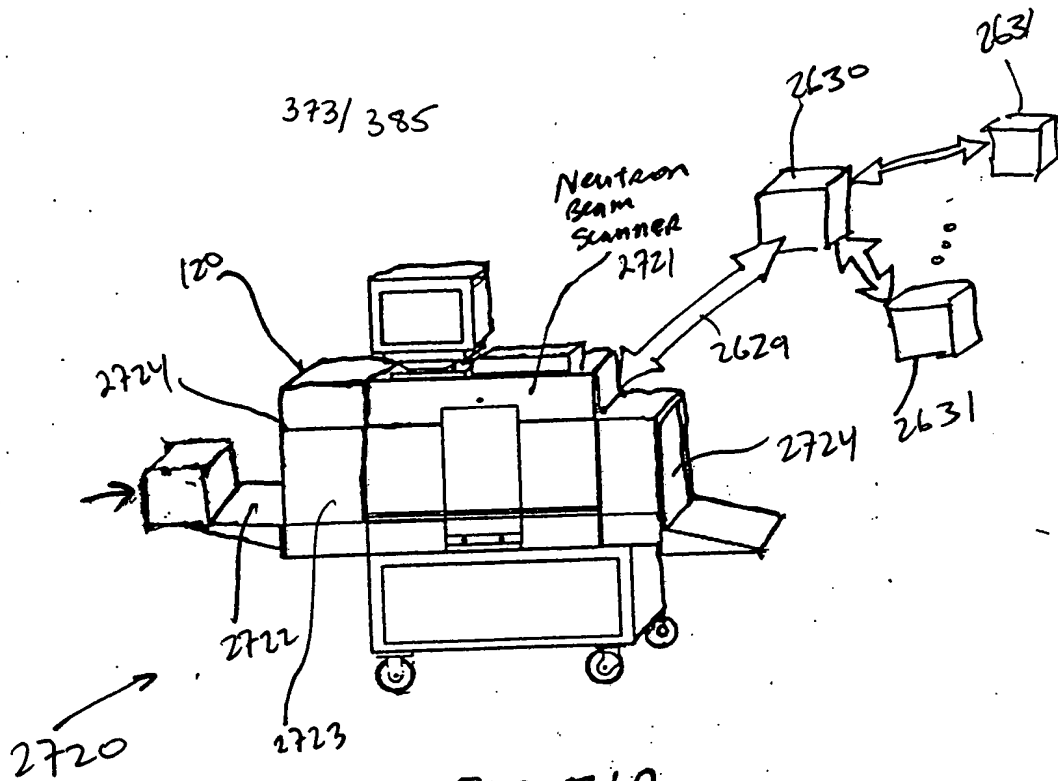


FIG. 7A

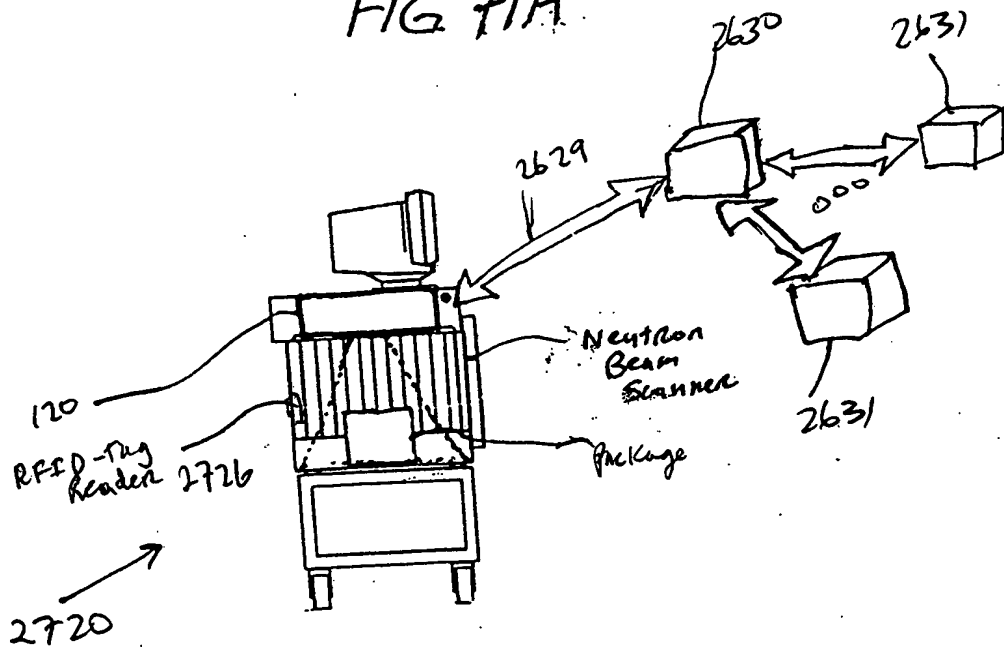


FIG. 7B

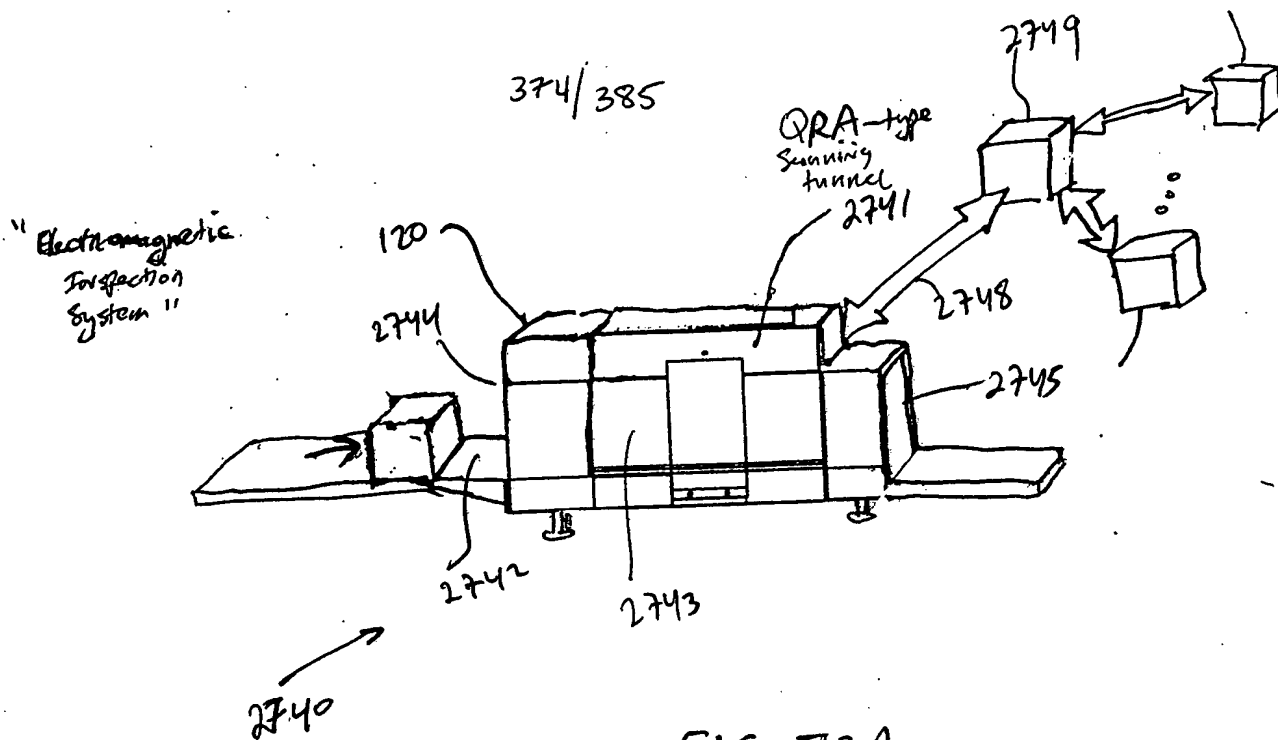


FIG 72A

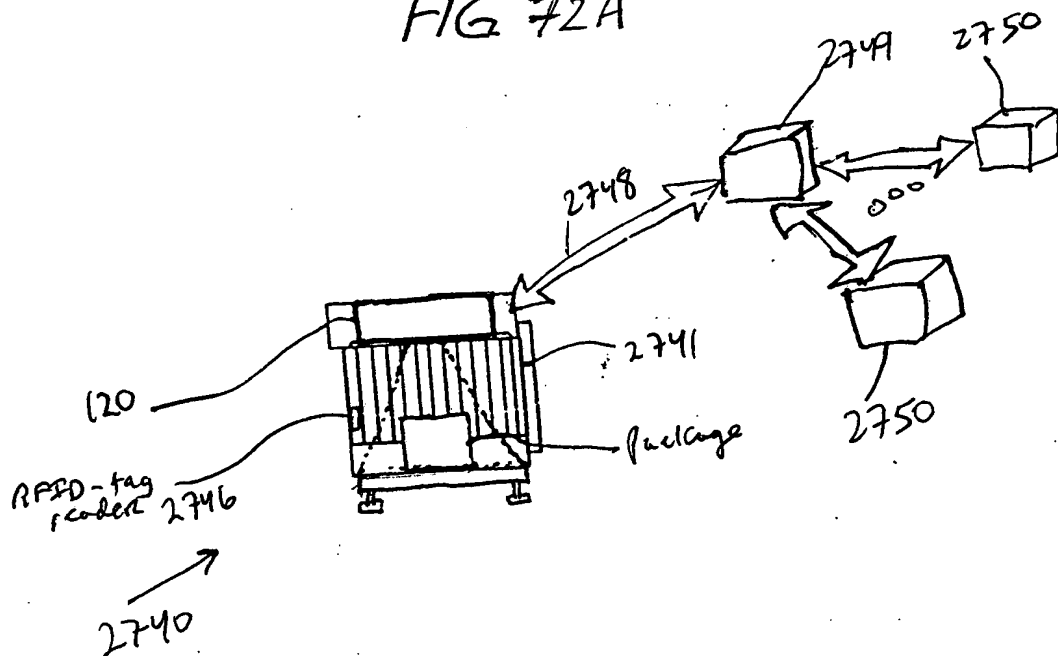


FIG. 72B

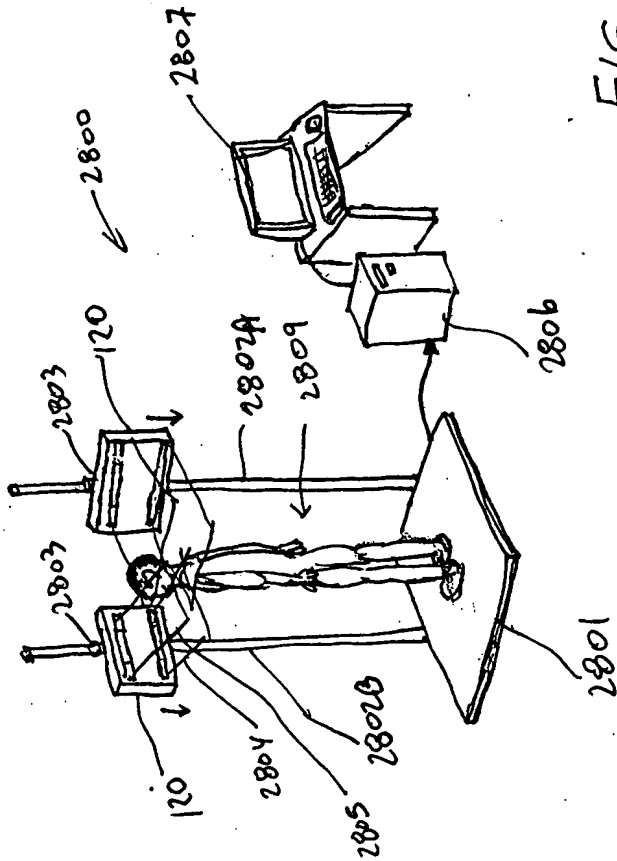


FIG. 76

377/385

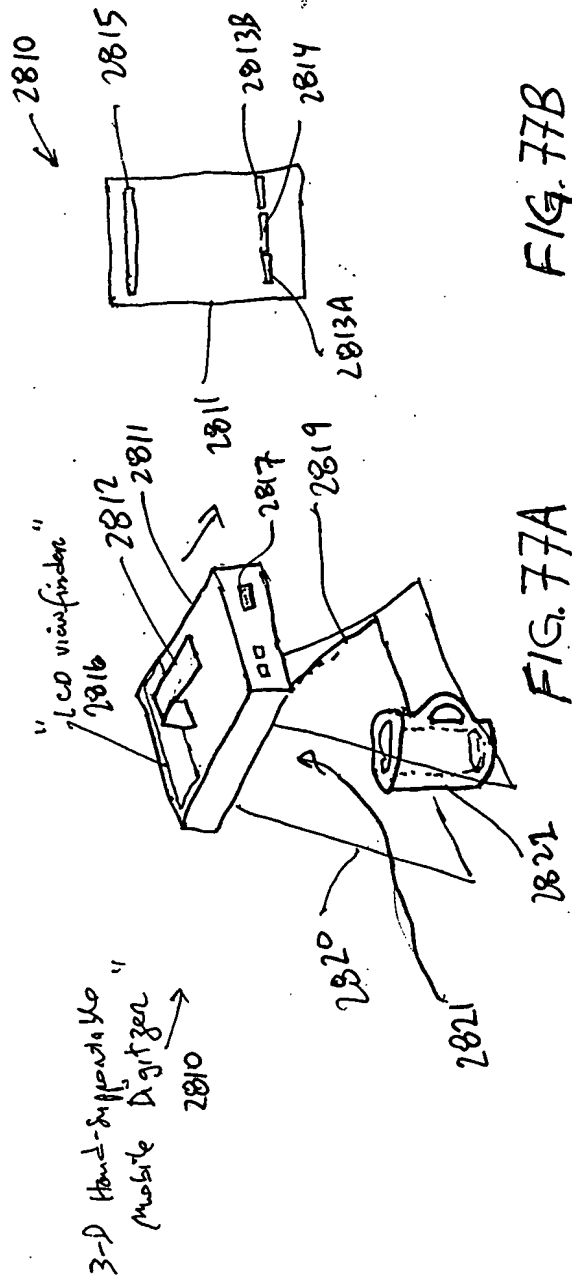
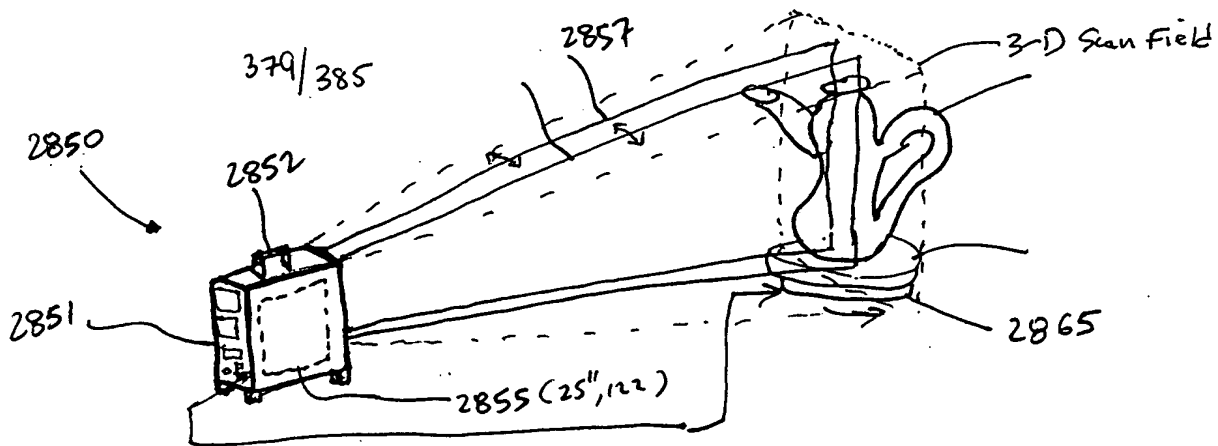
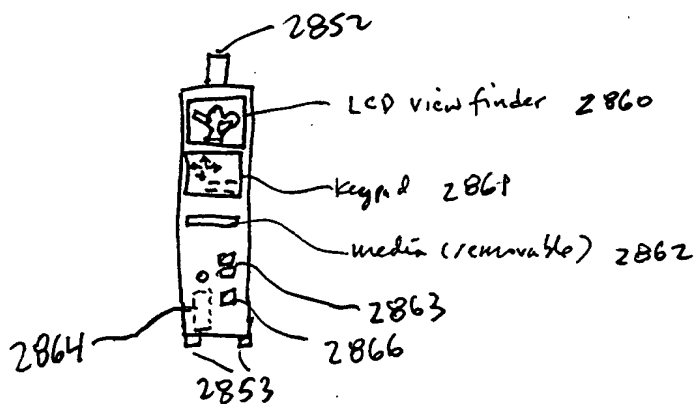
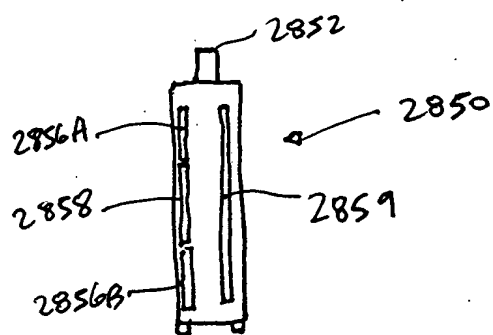


FIG. 77A

FIG. 77B



Z-D(Area) sensor



Automatic Vehicle Identification (AVI)
System of Present Invention

* Employing overhead profiling
and imaging during
license plate image capture

2870 →

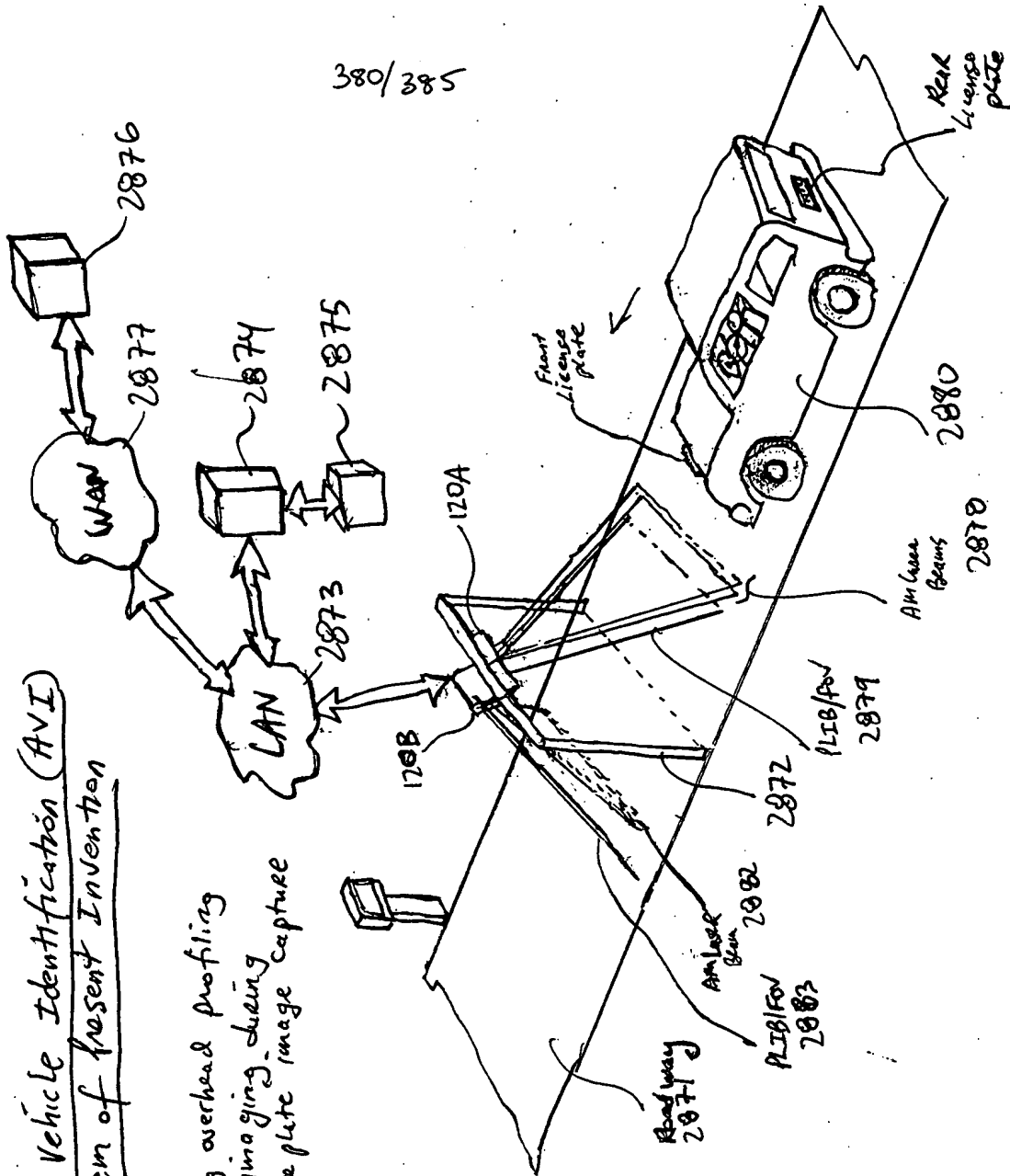
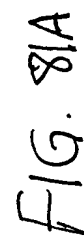


FIG. 80

- Employing overhead profiling and imaging techniques during license plate image capture



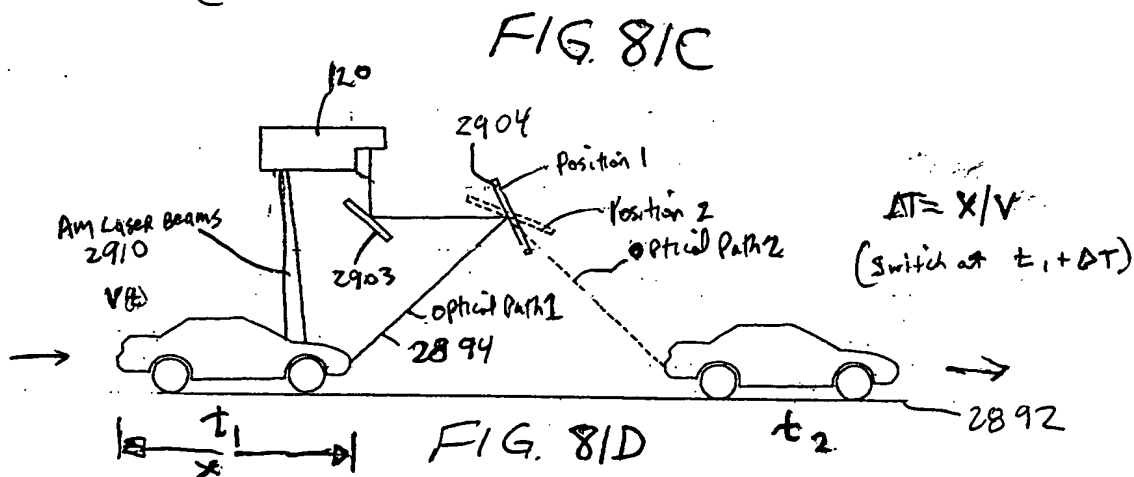
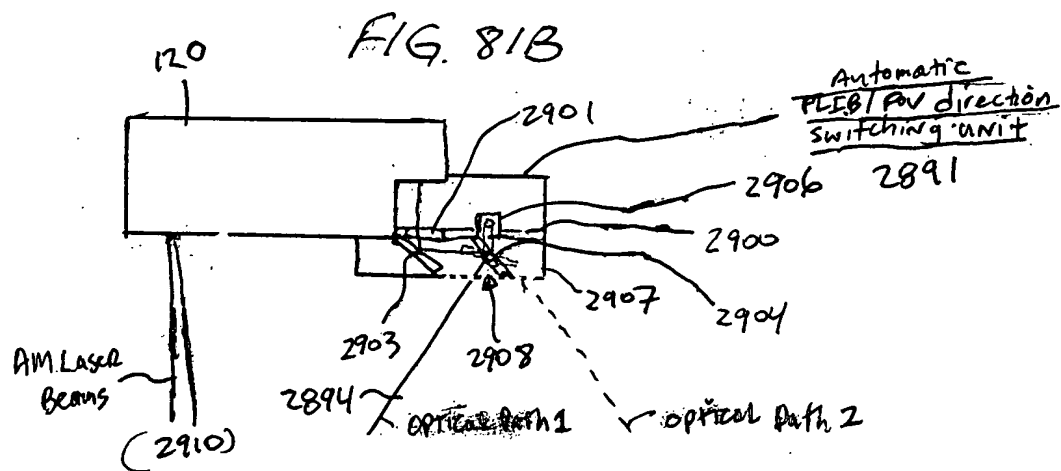
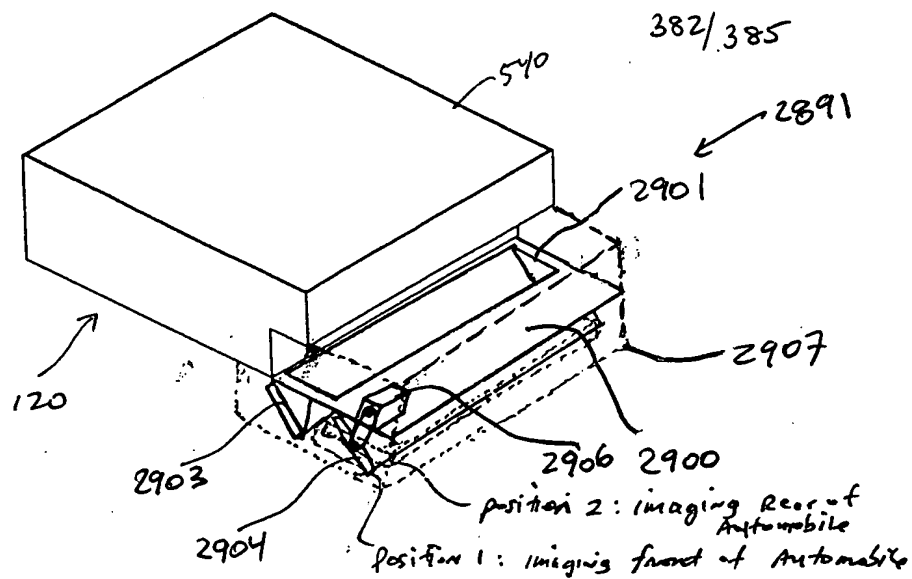
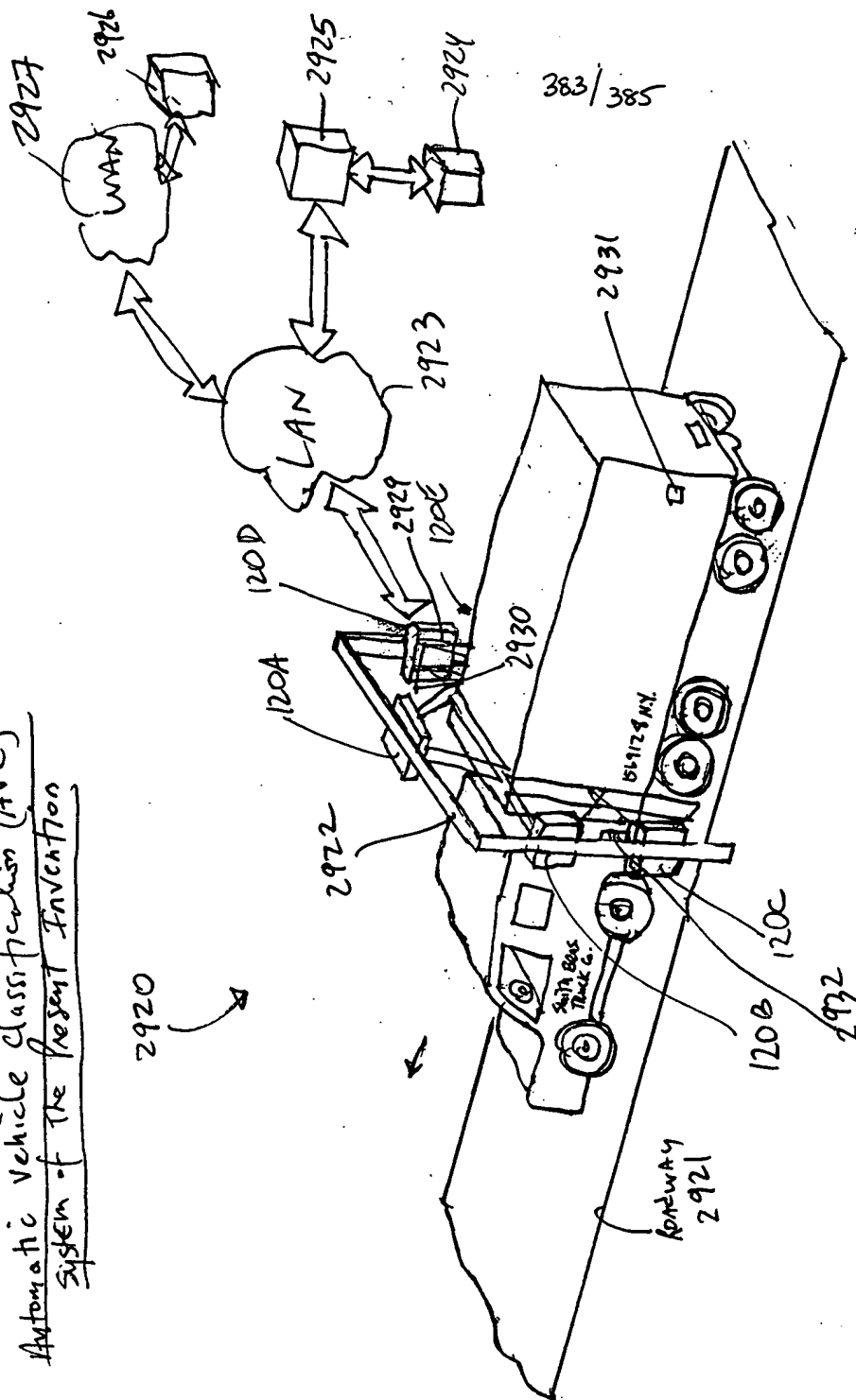


FIG. 8D

Automatic Vehicle Classification (AVC)
System of the present Invention



Employing overhead and lateral
Profiling and imaging
Techniques

FIG. 82

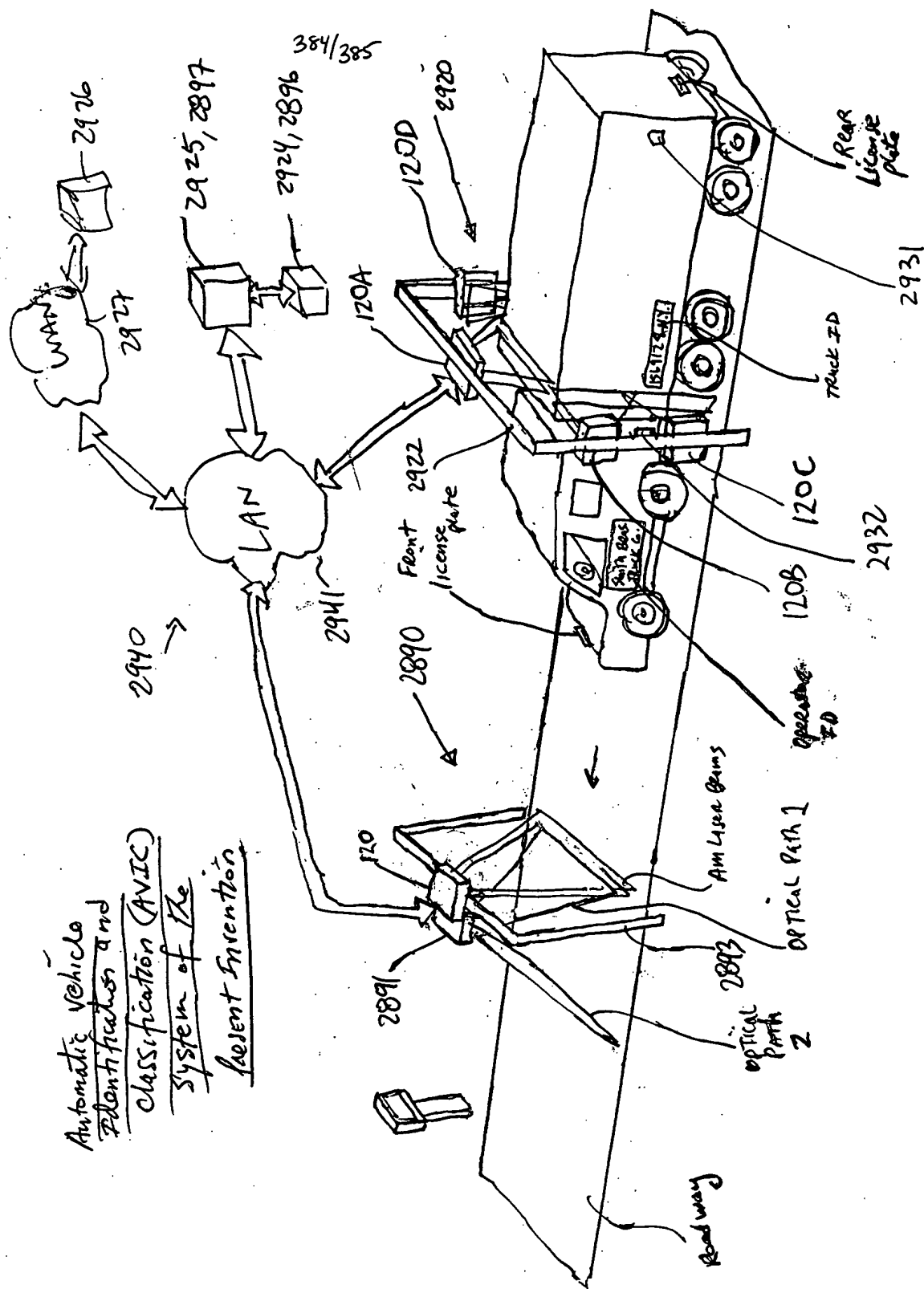


FIG. 83

385/385

